CONTENTS

4. DESCRIPTION AND ENVIRONMENTAL CHARACTERIZATION OF THE STUDY AREA 15

4.1 ABIOTIC MEDIUM 15

4.1.1 GEOLOGY 15

4.1.1.1 REGIONAL GEOLOGY 15

4.1.1.1.1 Metamorphic Rocks 16

4.1.1.1.2 Igneous rocks 18

4.1.1.1.3 Sedimentary rocks 19

4.1.1.2 REGIONAL STRUCTURAL GEOLOGY 20

4.1.1.3 LOCAL GEOLOGY 21

4.1.1.4 LOCAL STRUCTURAL GEOLOGY 24

4.1.1.5 INDIRECT EXPLORATION 25

4.1.1.6 DIRECT EXPLORATION 26

4.1.1.6.1 Geochemistry 26

4.1.1.6.2 Trench and hoof digging 27

4.1.1.6.3 Existing wells and exploratory galleries 28

4.1.2 GEOMORPHOLOGY 32

4.1.2.1 REGIONAL GEOMORPHOLOGY 32

4.1.2.2 LOCAL GEOMORPHOLOGY 32

4.1.2.2.1 Geomorphological Units 32

4.1.2.2.2 Morphometry 40

4.1.2.2.3 Morph dynamic processes 42

4.1.3 GEOTECHNICAL ENGINEERING 49

4.1.3.1 INDIRECT EXPLORATION, SEISMIC METHODS 49

4.1.3.2 DIRECT EXPLORATION 58

4.1.3.2.1 Field penetration test results (spt) 60

4.1.3.2.2 Geotechnical laboratory test results 64

4.1.3.2.3 Stability analysis 66

4.1.3.3 GEOLOGICAL GEOTECHNICAL PROFILES (GEOLOGICAL - GEOTECHNICAL MODEL) 69

4.1.3.3.1 Results of stability analysis 74

4.1.4 SOILS 75

4.1.4.1 SOIL MAPPING UNITS 75

4.1.4.1.1 Typic Hapludox - LCOT 82

4.1.4.1.2 Spolic Tecnosol - LCT 88

4.1.4.1.3 Typic Hapludox - LVAOT Terraces Association 92

4.1.4.1.4 Alluvial alluvial deposit association (LVAD) 97

4.1.4.2 AGROLOGICAL CLASSIFICATION AND POTENTIAL LAND USES 101

4.1.4.2.1 Subclass IIs 102

4.1.4.2.2. Subclass IVse 104

4.1.4.2.3 Subclass VIpe 105

4.1.4.2.4 Soils in conservation 110

4.1.4.2.5 Soils in use Production-Protection Forestry (Fcpp) 111

4.1.4.2.6 Soils in extensive grazing (Gpe) 111

4.1.4.2.7 Agricultural Soils 111

4.1.4.2.8. Soils in Transitional semi-intensive crops for own consumption (Act) 111

4.1.4.2.9 Soils in semi-intensive perennial crops (Acp) 111

4.1.4.2.10 Soils in Opencast Mining and Associated Lands (Ma) ... 111
4.1.4.3 LAND USE CONFLICT ... 111
4.1.4.3.1 Land use conflict due to moderate overuse ... 113
4.1.4.3.2 Land use conflict due to severe overuse ... 114
4.1.4.3.3 Land without conflict of use ... 116
4.1.4.4 HYDROLOGY ... 116
4.1.4.4.1 Hydrography ... 116
4.1.4.4.2 Drainage patterns ... 116
4.1.4.4.3 Morphology of the basin ... 121
4.1.4.5 HYDROLOGICAL REGIME ... 123
4.1.4.5.1 Precipitation and evapotranspiration regime ... 123
4.1.4.5.2 Flow Regime ... 127
4.1.4.5.3 Average flow rates ... 127
4.1.4.5.4 Water balance ... 127
4.1.4.5.5 Monthly water balances ... 129
4.1.4.5.6 Ecological Flow ... 130
4.1.4.5.7 Rainfall intensity ... 140
4.1.4.6 SEDIMENTOLOGICAL REGIME ... 142
4.1.4.6.1 Estimate of the annual denudation of the study area ... 142
4.1.4.6.2 Flood temporal and spatial relationship ... 146
4.1.4.7 WATER SUPPLY ... 146
4.1.4.8 WATER USES AND USERS (WATER DEMAND) ... 150
4.1.4.8.1 Calculation of the overall water demand of the SN#1 basin ... 153
4.1.4.9 SCARCE INDEX ... 163
4.1.4.9.1 Water quality ... 164
4.1.4.9.2 Interpretation of results ... 169
4.1.4.9.3 Total Suspended Solids (TSS) ... 169
4.1.4.9.4 Total Dissolved Solids (TDS) ... 170
4.1.4.9.5 Sediment solids (SSED) ... 171
4.1.4.9.6 Total Solids (TS) ... 171
4.1.4.10 ELECTRICAL CONDUCTIVITY ... 172
4.1.4.10.1 Hydrogen potential (pH) ... 173
4.1.4.10.2 Ambient temperature ... 174
4.1.4.10.3 Water temperature ... 174
4.1.4.10.4 Turbidity ... 175
4.1.4.10.5 Dissolved Oxygen (DO) ... 176
4.1.4.10.6 Percentage of dissolved oxygen saturation (% Sat) ... 177
4.1.4.11 PHYSICAL-CHEMICAL AND MICROBIOLOGICAL INDICES ... 195
4.1.5 HYDROGEOLOGY ... 200
4.1.5.1 REGIONAL HYDROGEOLOGY ... 200
4.1.5.2 INVENTORY OF WATER POINTS ... 202
4.1.5.3 HYDROGEOLOGICAL UNITS ... 204
4.1.5.3.1 Hydrogeological Unit 1 (UH1 - Aquitard) ... 206
4.1.5.3.2 Hydrogeological Unit 2 (UH2 - Aquifuge) ... 206
4.1.5.4 INFILTRATION ANALYSIS ... 207
4.1.5.5 INDIRECT GROUNDWATER EXPLORATION (GEOPHYSICS) ... 210
4.1.5.6 CONCEPTUAL HYDROGEOLOGICAL MODEL ... 230
4.1.5.7 OTHER CONSIDERATIONS ON HYDROGEOLOGY ... 235
4.1.5.7.1 Hydrochemical analysis of groundwater ... 235
4.1.5.7.2 Intrinsic vulnerability of the aquifer to pollution ... 235
4.1.5.7.3 Pumping test and determination of hydraulic parameters ... 235
4.1.5.7.4 Numerical hydrogeological model ... 235
4.1.5.7.5 Monitoring Wells network ... 235

4.1.6 ATMOSPHERE 236
4.1.6.1 WEATHER 236
4.1.6.1.1 Precipitation 236
4.1.6.1.2 Evapotranspiration 238
4.1.6.1.3 Relative humidity 240
4.1.6.1.4 Temperature 240
4.1.6.1.5 Solar Brightness 241
4.1.6.1.6 Solar radiation 242
4.1.6.1.7 Atmospheric pressure 243
4.1.6.1.8 Cloud cover 244
4.1.6.1.9 Aridity index 245
4.1.6.2 AIR QUALITY 246
4.1.6.2.1 Results and Analysis 246
4.1.6.2.2 Wind Rose 256
4.1.6.2.3 Conclusions 257
4.1.6.3 NOISE 259
4.1.6.3.1 Sampling Sites 259
4.1.6.3.2 Presentation of results and analysis 260
4.1.6.3.3 Conclusions 288
4.1.7 LANDSCAPE 289
4.1.7.1 LANDSCAPE UNITS 289
4.1.7.2 LANDSCAPE ELEMENTS 294
4.1.7.3 VISUAL LANDSCAPE ANALYSIS 296
4.1.7.3.1 Visual quality of the landscape 303
4.1.7.3.2 Overall aesthetic potential of the landscape 306

ILLUSTRATIONS

Illustration 4.1-1. Regional Geology. 17
Illustration 4.1-2. Structure formation diagram with the 3 main events. 21
Illustration 4.1-3. Granodiorite hand sample, left weathered, right cooler. 22
Illustration 4.1-4. Local geology. 23
Illustration 4.1-5. Structural local geology. 24
Illustration 4.1-6. Geophysical measurement scheme with the pole-to-pole array (left); field work for electrode placement (right). 25
Illustration 4.1-7. Soil sampling procedure. 26
Illustration 4.1-8. Trench T39. 27
Illustration 4.1-9. Electrical tomography 28
Illustration 4.1-10. Drilling platform. 29
Illustration 4.1-11. Drilling cores ready for the logging process. 29
Illustration 4.1-12. Logging zone. 30
Illustration 4.1-13. Location of perforations (in green). 30
Illustration 4.1-14. Samples packaged for analysis after cutting. 31
Illustration 4.1-15. Quartz vein with sulphides, an outcrop material in the sector. 31
Illustration 4.1-16. Visual points and control points. 33
Illustration 4.1-17. Geomorphological units of the study area, scale 1:10000. 34
Illustration 4.1-18. The hill (Dc) surrounded by an alluvial terrace. 35
Illustration 4.1-19. Ridges (Dl), composed of residual soil in the western part of the study area (PV 12). 35
Illustration 4.1-20. Moderate slopes (Dlm), on residual soil (PV 11) 36
Illustration 4.1-21. Craggy slope (Dle), covered by pastures and forests (PV 14). 36
Illustration 4.1-22. Structural Ridges (Sle), the dotted red line indicates the direction of the line (PV 03). 37
Illustration 4.1-23. Terrace (Ft), the black line indicates the alluvial terrace located on the right bank of a tributary of the El Pescado stream (PV 06). 38
Illustration 4.1-24. Active channel (Fca), photograph taken in a tributary of the El Pescado stream. 39
Illustration 4.1-25. Full of debris (All), found in the south-west part of the study area. 39
Illustration 4.1-26. Yard Sidehill (Ale), current project infrastructure located in the northwest zone (PV 12). 40
Illustration 4.1-27. Slope map of the study area, scale 1:10000. 41
Illustration 4.1-28. Histogram number of pixels Vs range of slopes. 41
Illustration 4.1-29. The main parts of a slide. 43
Illustration 4.1-30. Morph dynamic processes map, study area, scale 1:10000. 43
Illustration 4.1-31. The red lines indicate some of the crowns of the movements found in the study area (PV 15). 44
Illustration 4.1-32. Lateral undermining located on the right bank of a tributary of El Pescado Creek with a crown measuring approximately 50m. 45

Illustration 4.1-33. The white lines indicate the terracotta on the slopes. PV 06, own register. 45
Illustration 4.1-34. The red circle indicates the laminar erosion present on the moderate slopes of the study area (PV 11). 46
Illustration 4.1-35. Detail of the areas with no green line vegetation, the yellow polygon approaching the mining concession 5969. 47
Illustration 4.1-36. Detail of the areas with no red line vegetation, purple circle laminar erosion zone and the yellow polygon mining concession 5969..... 48
Illustration 4.1-37. Reading instruments. 50
Illustration 4.1-38. Detail of seismic refraction line J. 50
Illustration 4.1-39. Location of the lines of simian refraction. 51
Illustration 4.1-40. Vs variation with respect to depth, seismic refraction line LA (LPS-1). 52
Illustration 4.1-41. Vs variation with respect to depth, seismic refraction line LB (LPS-2)..... 52
Illustration 4.1-42. Vs variation with respect to depth, seismic refraction line LC (LPS-3)..... 53
Illustration 4.1-43. Vs variation with respect to depth, seismic refraction line LD (LPS-4). 53
Illustration 4.1-44. Vs variation with respect to depth, seismic refraction line LE (LPS-5)..... 54
Illustration 4.1-45. Vs variation with respect to depth, seismic refraction line LF (LPS-6)..... 54
Illustration 4.1-46. Vs variation with respect to depth, seismic refraction line LG (LPS-7). 55
Illustration 4.1-47. Vs Variation relative to depth, seismic refraction line LH (LPS-8)..... 55
Illustration 4.1-48. Vs variation with respect to depth, seismic refraction line LI (LPS-9)..... 56
Illustration 4.1-49. Vs variation with respect to depth, seismic refraction line LJ (LPS-10). 56
Illustration 4.1-50. Location of geotechnical boreholes, mining title 5969. 59
Illustration 4.1-51. Detail of the execution of the SPT test in the field. Survey No. 4. 60
Illustration 4.1-52. Seismic Threat Zones applicable to buildings for NSR-10 at function of Aa and Av. The red dot indicates approximately where the municipality of Segovia Antioquia is located.. 67
Illustration 4.1-53. Location of the sections, from which the geological-geotechnical profiles were obtained. 69
Illustration 4.1-54. Geotechnical geological profile of section AA. 70
Illustration 4.1-55. Geotechnical geological profile of section BB. 70
Illustration 4.1-56. Geotechnical geological profile of the CC section. 71
Illustration 4.1-57. Geotechnical geological profile of the DD. 71
Illustration 4.1-58. Geotechnical geological profile of the U.S. section 72
Illustration 4.1-59. Geotechnical geological profile of section FF. 72
Illustration 4.1-60. Geotechnical geological profile of section GG..... 73
Illustration 4.1-61. Geotechnical geological profile of section HH. 73
Illustration 4.1-62. Location of control points for lifting floor units, 1: 10,000..... 76
Illustration 4.1-63. Soil associations in the study area. 78
Illustration 4.1-64. Distribution of soil associations 79
Illustration 4.1-65. Distribution of soil phases in the study area 80
Illustration 4.1-66. Soil phases in the study area. 81
Illustration 4.1-67. DLM Profile, YANO-DL Replica. 83
Illustration 4.1-68 YANO-DL infiltration curve. 84
Illustration 4.1-69. Minerals in circles, present in the soil LCOT, 1: Hyaline abundant quartz..... 87

Illustration 4.1-70. Minerals in circles, present in the soil LCOT, 1: Very Weathered Rock, 2: Sericite and 3: Quartz 87
Illustration 4.1-71. Informal exploitation aspect. 88
Illustration 4.1-72. Informal exploitation aspect. 88
Illustration 4.1-73. Modal profile FHYP-CA. 89
Illustration 4.1-74. Anthropic material. 89
Illustration 4.1-75. Horizons extracted. 89
Illustration 4.1-76. Infiltration curve FHYP-CA. 90
Illustration 4.1-77. Terrace with alluvial deposit. 92
Illustration 4.1-78. Lithological discontinuity. 92
Illustration 4.1-79. Modal profile YANO FT. 93
Illustration 4.1-80. Infiltration curve YANO-FT. 94
Illustration 4.1-81. In mineral circles present in the YANO-FT profile: 1. Hyaline quartz. 2. Meteorite Metamorphic Rock 4. Albita 6. Garnet 8. Epidot and Actinolite. 96
Illustration 4.1-82. Alluvial deposit site. 97
Illustration 4.1-83. Alluvial deposit profile (PB-FT). 98
Illustration 4.1-84. Horizon detail B1. 98
Illustration 4.1-85. Detail of horizon B2. 98
Illustration 4.1-86 Infiltration curve LVAD 99
Illustration 4.1-87. Comparison of water infiltrations in the soil for the study area associations. .. 101
Illustration 4.1-88. Agrologic classes in the study area. 103
Illustration 4.1-89. Aspect of category IIs land. 104
Illustration 4.1-90. Logging and burning of forest, conflict over severe overuse. 106
Illustration 4.1-91. Distribution of agrological classes. 106
Illustration 4.1-92. Potential land use. 107
Illustration 4.1-93. Distribution of land use vocation 107
Illustration 4.1-94. Current land use. 109
Illustration 4.1-95. Distribution of current land use. 110
Illustration 4.1-96. Land use conflicts. 113
Illustration 4.1-97. Distribution of conflicts in the area of study. 114
Illustration 4.1-98. Soil intervened with anthropogenic deposits. 115
Illustration 4.1-99. Underground Mining 115
Illustration 4.1-100. Soil erosion processes 115
Illustration 4.1-101. Moderate and steep slopes. 115
Illustration 4.1-102. Location of the drainage network. 117
Illustration 4.1-103. Drainage network inside the study area. 118
Illustration 4.1-104. Hierarchical order of the drainage network of the study area. 119
Illustration 4.1-105. Hierarchical order of the drainage network of the study area. 120
Illustration 4.1-106. Monthly precipitation values. 123
Illustration 4.1-107. Spatial distribution of precipitation 124
Illustration 4.1-108. Monthly evaporation values. 125
Illustration 4.1-109. Spatial distribution of evapotranspiration. 126
Illustration 4.1-110. Hydrological balance scheme 127

Illustration 4.1-111. Monthly water balances. 129
Illustration 4.1-112. Minimum flow rates for the basin of the unnamed stream #1. 131
Illustration 4.1-113. Minimum flows for the basin of the unnamed stream #9. 132
Illustration 4.1-114. Minimum flow rates for the basin of the unnamed #2 stream. 132
Illustration 4.1-115. Minimum flow rates for the basin of the unnamed stream #3. 133
Illustration 4.1-116. Minimum flows for the basin of the unnamed stream #4. 133
Illustration 4.1-117. Minimum flows for the basin of the unnamed stream #5. 134
Illustration 4.1-118. Minimum flows for the basin of the unnamed stream #8. 134
Illustration 4.1-119. Minimum flows for the basin of the unnamed stream #6. 135
Illustration 4.1-120. Minimum flows for the basin of the unnamed stream #7. 135
Illustration 4.1-121. Intensity - frequency - duration curve for the Palma de Coco season. 141
Illustration 4.1-122. Morphological classification of currents. 144
Illustration 4.1-123. Laminar erosion map in the study area. 147
Illustration 4.1-124. Probabilistic density curve. 149
Illustration 4.1-125. Dimensionless flow duration curve. 150
Illustration 4.1-126. Quantitative inventory of uses and users. 151
Illustration 4.1-127. Percentage distribution of water demands in the SN#1 basin. 155
Illustration 4.1-128. Percentage distribution of water demand by sub-basin over 100% of demand of the SN#1 basin 159
Illustration 4.1-129. Components of the water footprint within the microbasin 160
Illustration 4.1-130. Distribution of current water demand, available water supply and ecological flow. 162
Illustration 4.1-131. Location of water quality monitoring stations. 165
Illustration 4.1-132. Total suspended solids values. 170
Illustration 4.1-133. Total dissolved solids values. 171
Illustration 4.1-134. Total solids values. 172
Illustration 4.1-135. Electrical conductivity values. 172
Illustration 4.1-136. pH values. 173
Illustration 4.1-137. Ambient temperature values. 174
Illustration 4.1-138. Water temperature values. 175
Illustration 4.1-139. Turbidity results. 175
Illustration 4.1-140. Dissolved Oxygen Results 176
Illustration 4.1-141. Results of % dissolved oxygen saturation. 177
Illustration 4.1-142. Total organic carbon (TOC) results. 179
Illustration 4.1-143. Total alkalinity results. 180
Illustration 4.1-144. Acidity results. 181
Illustration 4.1-145. Total hardness results. 182
Illustration 4.1-146. Bicarbonate results 182
Illustration 4.1-147. Result of inorganic phosphorus. 185
Illustration 4.1-148. Result of total match. 186
Illustration 4.1-149. Result of total iron. 187
Illustration 4.1-150. Calcium result. 187
Illustration 4.1-151. Magnesium result. 188

Illustration 4.1-152. Total sodium result. 189
Illustration 4.1-153. Total Potassium Result. 190
Illustration 4.1-154. Result of fats and oils. 191
Illustration 4.1-155. Result of phenols. 192
Illustration 4.1-156. Total cyanide result 193
Illustration 4.1-157. Result of total coliforms. 194
Illustration 4.1-158. Result of fecal coliforms 195
Illustration 4.1-159. Water quality index (WQI) values. 196
Illustration 4.1-160. Pollution index values (ICO). 197
Illustration 4.1-161. IACAL at mid-year conditions for 309 hydrographic sub-areas 199
Illustration 4.1-162. Map of homogeneous hydrogeological zones in Antioquia. 200
Illustration 4.1-163. Inventory of surface water sources. 203
Illustration 4.1-164. Local geology. 204
Illustration 4.1-165. Profile of hydrogeological units (W-E orientation). 206
Illustration 4.1-166. Scenarios that favor infiltration. 208
Illustration 4.1-167. Potential infiltration in mm/year 209
Illustration 4.1-168. Histogram of infiltration potential (mm/year) 210
Illustration 4.1-169. Location of the electrical tomography lines 211
Illustration 4.1-170. Ohm's Law 212
Illustration 4.1-171. Acquisition diagram with the Dipole-Dipole type configuration. 213
Illustration 4.1-172. Resistivity values for different lithologies 214
Illustration 4.1-173. Zones of loss or acquisition of information associated with the separation between electrodes. 215
Illustration 4.1-174. Profile No. 29 iso-resistivity. 216
Illustration 4.1-175. Profile No. 30 iso-resistivity. 216
Illustration 4.1-176. Profile No. 31 iso-resistivity. 217
Illustration 4.1-177. Profile No. 32 iso-resistivity. 217
Illustration 4.1-178. Profile No. 33 iso-resistivity. 218
Illustration 4.1-179. Profile No. 34 iso-resistivity. 218
Illustration 4.1-180. Profile No. 35 iso-resistivity. 219
Illustration 4.1-181. Profile No. 36 iso-resistivity. 219
Illustration 4.1-182. Iso-resistivity profile No. 37. 220
Illustration 4.1-183. Profile No 38 iso-resistivity. 220
Illustration 4.1-184. Profile No. 39 iso-resistivity. 221
Illustration 4.1-185. Profile No. 40 iso-resistivity. 221
Illustration 4.1-186. Profile No. 42 iso-resistivity. 222
Illustration 4.1-187. Iso-resistivity profile No 44. 222
Illustration 4.1-188. Profile No 46 iso-resistivity. 223
Illustration 4.1-189. Profile No 48 iso-resistivity. 223
Illustration 4.1-190. Profile No. 29 iso-resistivity, interpreted applied to hydrogeology. 224
Illustration 4.1-191. Profile No. 30 iso-resistivity, interpreted applied to hydrogeology. 224
Illustration 4.1-192. Profile No. 31 iso-resistivity, interpreted applied to hydrogeology. 224
Illustration 4.1-193. Profile No. 32 iso-resistivity, interpreted applied to hydrogeology. 225

Illustration 4.1-194. Profile No. 33 iso-resistivity, interpreted applied to hydrogeology. 225
Illustration 4.1-195. Profile No. 34 iso-resistivity, interpreted applied to hydrogeology. 225
Illustration 4.1-196. Profile No. 35 iso-resistivity, interpreted applied to hydrogeology. 226
Illustration 4.1-197. Profile No. 36 iso-resistivity, interpreted as applied to hydrogeology. 226
Illustration 4.1-198. Profile No. 37 iso-resistivity, interpreted as applied to hydrogeology 226
Illustration 4.1-199. Profile No. 38 iso-resistivity, interpreted applied to hydrogeology. 227
Illustration 4.1-200. Profile No. 39 iso-resistivity, interpreted as applied to hydrogeology 227
Illustration 4.1-201. Profile No. 40 iso-resistivity, interpreted applied to hydrogeology. 227
Illustration 4.1-202. Profile No. 42 iso-resistivity, interpreted applied to hydrogeology 228
Illustration 4.1-203. Profile No. 44 iso-resistivity, interpreted as applied to hydrogeology 228
Illustration 4.1.204. Profile No. 46 iso-resistivity, interpreted as applied to hydrogeology 228
Illustration 4.1-205. Profile No. 48 iso-resistivity, interpreted as applied to hydrogeology 229
Illustration 4.1-206. Block diagrams of the geo-electric interpretation of the terrain, view No. 1.. 229
Illustration 4.1-207. Block diagrams of the geo-electric interpretation of the terrain, view No. 2.. 230
Illustration 4.1-208. Detail of the execution of the SPT test in the field, sounding No. 1. 231
Illustration 4.1-209. Detail of dry saprolite, sounding No. 1. 231
Illustration 4.1-210. Detail of the execution of the SPT test in the field, sounding No. 6. 232
Illustration 4.1-211. Detail of dry saprolite, sounding No. 6. 232
Illustration 4.1-212. Dry residual soil or without underground water in an artisanal mining tunnel, in (UH1 - Aquitard). 232
Illustration 4.1-213. Dry residual soil from artisanal mining tunnel without underground water (UH1 - Aquitard)..... 232
Illustration 4.1-214. Artisanal mining tunnel, transfer of residual soil to saprolite (UH1 - Aquitard). 233
Illustration 4.1-215. Artisanal mining tunnel, transfer of residual soil to saprolite (UH1 - Aquitard). 233
Illustration 4.1-216. Schematic profile of the water flow system in the waste soil. 234
Illustration 4.1-217. Block diagram of the water flow system in the waste soil. 234
Illustration 4.1-218. Monthly precipitation values..... 236
Illustration 4.1-219. Spatial distribution of precipitation. 237
Illustration 4.1-220. Monthly evaporation values. 238
Illustration 4.1-221. Spatial distribution of evapotranspiration 239
Illustration 4.1-222. Monthly relative humidity values. 240
Illustration 4.1-223. Spatial temperature variation 241
Illustration 4.1-224. Monthly values of solar brightness. 242
Illustration 4.1-225. Monthly solar radiation values. 243
Illustration 4.1-226. Monthly values of atmospheric pressure. 244
Illustration 4.1-227. Monthly cloud cover values. 244
Illustration 4.1-228. Spatial variation of the aridity index. 245
Illustration 4.1-229. Concentration of PM_{10} vs. standard Point 1 248
Illustration 4.1-230. SO_2 vs Standard Comparison Point 1 250
Illustration 4.1-231. NO_2 Comparison Standard Point 1 251
Illustration 4.1-232. Comparison PM_{10} vs Standard Point 2 253

Illustration 4.1-233. SO_2 vs Standard Comparison Point 2. 254
Illustration 4.1-234. Comparison NO_2 vs Standard point 2 255
Illustration 4.1-235. Wind speed distribution. 256
Illustration 4.1-236. Wind Rose Sampling Point Segovia 257
Illustration 4.1-237. PM_{10} comparison between evaluated points 258
Illustration 4.1-238. Comparison of SO_2 between evaluated points. 258
Illustration 4.1-239. Comparison of NO_2 between evaluated points. 259
Illustration 4.1-240. Location Sampling points, within the mining project "El Pescado". 260
Illustration 4.1-241. Environmental Noise Assessment Daytime Point 1. 261
Illustration 4.1-242. Environmental Noise Assessment Daytime Point 2. 262
Illustration 4.1-243. Environmental Noise Assessment Daytime Point 3. 263
Illustration 4.1-244. Environmental Noise Assessment Daytime Point 4. 264
Table 4.1-117. Environmental Noise Results Corrected Point 1 Daytime Week. 268
Illustration 4.1-245. Frequency sweep Average Point 1 Daytime Week. 268
Illustration 4.1-246. Hue Adjustments Point 1 Daytime Week. 269
Table 4.1-126. Environmental Noise Results Corrected Point 2 Daytime Week 273
Illustration 4.1-247. Frequency sweep Average Point 2 Daytime Week. 274
Illustration 4.1-248. Hue Adjustments Point 2 Daytime Week. 275
Table 4.1-135. Environmental Noise Results Corrected Point 3 Daytime Week 279
Illustration 4.1-249. Frequency sweep Average Point 3 Daytime Week. 280
Illustration 4.1-250. Hue Adjustments Point 3 Daytime Week. 281
Table 4.1-144. Environmental Noise Results Corrected Point 4 Daytime Week 285
Illustration 4.1-251. Frequency sweep Average Point 4 Daytime Week. 286
Illustration 4.1-252. Hue Adjustments Point 4 Daytime Week. 287
Illustration 4.1-253. Landscape units. 290
Illustration 4.1-254. No. of plant coverings by geomorphological units 291
Illustration 4.1-255. No. of replicability of vegetation cover areas by geomorphological units. 291
Illustration 4.1-256. Percentage of vegetative cover area by geomorphological units. 292
Illustration 4.1-257. Percentage distribution of anthropism and dense underground forest. 293
Illustration 4.1-258. No. of replicability by UP 293
Illustration 4.1-259. Percentage distribution of areas by UP. 294
Illustration 4.1.260. Landscape elements and percentage distributions. 295
Illustration 4.1-261. Landscape elements. 295
Illustration 4.1-262. Landscape visibility. 298
Illustration 4.1-263. Percentage distribution of landscape visibility. 299
Illustration 4.1-264. Percentage distribution of visual fragility or absorption capacity. 302
Illustration 4.1-265. Fragility or visual absorption capacity of the landscape 302
Illustration 4.1-266. Landscape visual quality. 305
Illustration 4.1-267. Percentage distribution of landscape visual quality. 306

TABLES

Table 4.1-1. Land slope categories and ranges. 40
Table 4.1-2. Percentage each of the ranges. 42
Table 4.1-3. Land slope categories and ranges. 46
Table 4.1-4. Seismic characterization of soils, NEHRP 2003. 57
Table 4.1-5. Detail of the soil profile to which the subsoil materials correspond. 57
Table 4.1-6. Values from Ø' equivalent using Kishida and JRB Vs depth. Drilling 1. 60
Table 4.1-7. Values from Ø' equivalent using Kishida and JRB Vs depth. Drilling 2. 61
Table 4.1-8. Values from Ø' equivalent using Kishida and JRB Vs depth. Drill hole 3. 61
Table 4.1-9. Values from Ø' equivalent using Kishida and JRB Vs depth. Drill hole 4. 61
Table 4.1-10. Values from Ø' equivalent using Kishida and JRB Vs depth. Drill hole 5. 62
Table 4.1-11. Values from Ø' equivalent using Kishida and JRB Vs depth. Drill hole 6. 62
Table 4.1-12. Values from Ø' equivalent using Kishida and JRB Vs depth. Drilling 7. 62
Table 4.1-13. Values from Ø' equivalent using Kishida and JRB Vs depth. Drill hole 8. 63
Table 4.1-14. Values from Ø' equivalent using Kishida and JRB Vs depth. Drill 9. 63
Table 4.1-15. Values from Ø' equivalent using the expressions of Kishida and JRB, for each of the materials. 63
Table 4.1-16. Expressions of the linear regression proposed by González 64
Table 4.1-17. Tests executed on the samples taken from the different soundings 64
Table 4.1-18. Results of geotechnical classification tests. 65
Table 4.1-19. Soil mechanical parameters for materials identified in the field work 65
Table 4.1-20. Basic safety factors Table H.2.4-1 NSR-10. 68
Table 4.1-21. Safety factor rating ranges for the static and dynamic case (US Army Corps of Engineers, October 2003). 68
Table 4.1-22. Safety factor values for each of the conditions evaluated. 74
Table 4.1-23. Geographical location of observation and sampling sites. 75
Table 4.1-24. Identification of phases of soil associations. 77
Table 4.1-25. Taxonomy and other characteristics of the soils characterized in the study area. 77
Table 4.1-26. Distribution of soil associations in the study area. 79
Table 4.1-27. Distribution of soil phases in the study area. 80
Table 4.1-28. Taxonomic classification of Typic Hapludox soil. 82
Table 4.1-29. Description of horizons. 83
Table 4.1-30. Physico-chemical results of the YANO-DL soil profile. 84
Table 4.1-31. Mineral count on horizon App. 86
Table 4.1-32. Mineral count on horizon B. 86
Table 4.1-33. Description of horizons. 89
Table 4.1-34. Physico-chemical laboratory results of the soil profile FHYP-CA. 90
Table 4.1-35 Description of horizons. 93
Table 4.1-36. Physico-chemical results of the YANO-FT soil profile. 94
Table 4.1-37. Mineral count on Ap horizon. 95

Table 4.1-38. Mineral count in horizon Bw. ... 96
Table 4.1-39. Description by horizons. ... 98
Table 4.1-40. Physical results of the PB-FT soil profile. ... 99
Table 4.1-41. Potential land use. ... 102
Table 4.1-42. Distribution of agrological classes. ... 106
Table 4.1-43. Distribution of potential land uses. ... 108
Table 4.1-44. Land use classification factors. ... 108
Table 4.1-45. Current land use. ... 108
Table 4.1-46. Distribution of current land use. ... 110
Table 4.1-47. Land use conflicts. ... 112
Table 4.1-48 Distribution of conflicts in the area of study. ... 112
Table 4.1-49. Current order for basins in the study area. ... 121
Table 4.1-50. Geomorphological parameters of the SN #1, SN#9, SN#2, SN #3, SN #4, SN #5, SN #8, #6 and #7 basins. ... 121
Table 4.1-51. Other geomorphological parameters of basins N #1, SN#9, SN#2, SN #3, SN #4, SN #5, SN #8, #6 and #7. ... 121
Table 4.1-52. Multiannual mean rainfall for nearby stations. ... 123
Table 4.1-53. Monthly evaporation values for nearby stations. ... 124
Table 4.1-54. Average flows of the basins of the study area. ... 128
Table 4.1-55. Yields of the basins intervened in the AID and AII of the mining concession 5969. ... 129
Table 4.1-56. Monthly average flow rates for the unnamed current #1, #6 and #7 ... 130
Table 4.1-57. Concentration times for the unnamed current #1. ... 138
Table 4.1-58. Concentration times for unnamed current #9. ... 138
Table 4.1-59. Concentration times for the unnamed current #2. ... 138
Table 4.1-60. Concentration times for unnamed current #3. ... 139
Table 4.1-61. Concentration times for the unnamed current #4. ... 139
Table 4.1-62. Concentration times for the unnamed current #5. ... 139
Table 4.1-63. Concentration times for the unnamed current #8. ... 139
Table 4.1-64. Concentration times for the unnamed current #6. ... 140
Table 4.1-65. Concentration times for the unnamed current #7. ... 140
Table 4.1-66. Intensities for different return periods. ... 141
Table 4.1-67. Runoff coefficients. ... 142
Table 4.1-68. Maximum flow rates. ... 142
Table 4.1-69. Values assigned to P according to the slope. ... 145
Table 4.1-70. Laminar erosion in each of the currents. ... 145
Table 4.1-71. Scale of reductions for temporary irregularity in water supply. ... 149
Table 4.1-72. Water supply of the currents under study. ... 150
Table 4.1-73. Hydrographic location of catchments and user dumping. ... 151
Table 4.1-74. Inventory of uses and users. ... 152
Table 4.1-75. Basin water demand SN#1. ... 153
Table 4.1-76. Total water demand within the SN#1 watershed. ... 154
Table 4.1-77. Net provision according to the level of complexity of the system. ... 156
Table 4.1-78. Effect of climate on net provisioning. ... 156

Table 4.1-79. Maximum daily consumption coefficient, k1, according to the System Complexity Level 157
Table 4.1-80. Maximum hourly consumption coefficient, k2, depending on the System Complexity Level and the distribution network type..... 157
Table 4.1-81. Water demand by basin..... 159
Table 4.1-82. Water supply available for new activities. 161
Table 4.1-83. Water supply of the currents under study..... 163
Table 4.1-84. Geographic location of the sampling stations..... 164
Table 4.1-85. Maximum permissible limits of variables evaluated. 166
Table 4.1-86. Results of monitored physicochemical parameters..... 168
Table 4.1-87. Dissolved oxygen concentration ranges and frequent ecosystem consequences. 177
Table 4.1-88. ICAs and ICOs by sampling stations..... 195
Table 4.1-89. Points of birth of water currents..... 202
Table 4.1-90. Theoretical permeability values..... 206
Table 4.1-91. Multiannual mean rainfall for nearby stations..... 236
Table 4.1-92. Monthly evaporation values for nearby stations. 238
Table 4.1-93. Monthly relative humidity values for nearby stations. 240
Table 4.1-94. Monthly solar radiation values for the NCEP/NCAR point. 242
Table 4.1-95. Monthly atmospheric pressure values at NCEP/NCAR point. 243
Table 4.1-96. Monthly cloudiness values for the reanalysis point..... 244
Table 4.1-97. Exposure limit values for evaluated contaminants. 246
Teble 4.1-98. Equipment PM_{10} Point 1 calibration 247
Table 4.1-99 PM_{10} Point 1 results..... 248
Table 4.1-100. RAC3 fumes calibration Point 1 249
Table 4.1-101. SO_2 Concentrations Point 1..... 249
Table 4.1-102. NO_2 Concentrations Point 1..... 250
Table 4.1-103. PM_{10} Point 2 Calibration 251
Table 4.1-104. PM_{10} Point 2 Results. 252
Table 4.1-105. Calibration data RAC3 fumes Point 2..... 253
Table 4.1-106. SO_2 Concentrations Point 2..... 254
Table 4.1-107. NO_2 Concentrations Point 2..... 255
Table 4.1-108. Location Monitoring Points..... 259
Table 4.1-109. Weather Conditions Daytime Week 260
Table 4.1-110. Frequency Sweep for LAeq, 1h Point 1 North Daytime Week 265
Table 4.1-111. Frequency Sweep for LAeq, 1h Point 1 South Daytime Week 265
Table 4.1-112. Frequency Sweep for LAeq, 1h Point 1 East Daytime Week 266
Table 4.1-113. Frequency Sweep for LAeq, 1h Point 1 West Daytime Week 266
Table 4.1-114. Frequency Sweep for LAeq, 1h Point 1 Vertical Daytime Week..... 266
Table 4.1-115. Frequency Sweep for LAeq, 1h Average Point 1 Daytime Week..... 267
Table 4.1-116. Summary of Measurements Performed to Estimate Leq Point 1 Daytime Week 267
Table 4.1-117. Environmental Noise Results Corrected Point 1 Daytime Week..... 268
Table 4.1-118. Uncertainty Associated with the Estimation of the Measurand (LRAeq). Point 1.... 270
Table 4.1-119. Frequency Sweep for LAeq, 1h Point 2 North Daytime Week 270

Table 4.1-120. Frequency Sweep for LAeq, 1h Point 2 South Daytime Week 271
Table 4.1-121. Frequency Sweep for LAeq, 1h Point 2 East Daytime Week 271
Table 4.1-122. Frequency Sweep for LAeq, 1h Point 2 West Daytime Week 271
Table 4.1-123. Frequency Sweep for LAeq, 1h Point 2 Vertical Daytime Week..... 272
Table 4.1-124. Frequency Sweep for LAeq, 1h Average Point 2 Daytime Week..... 272
Table 4.1-125. Summary of Measurements Performed to Estimate Leq Point 2 Daytime Week 273
Table 4.1-126. Environmental Noise Results Corrected Point 2 Daytime Week..... 273
Table 4.1-127. Uncertainty Associated with the Estimation of the Measurand (LRAeq). Point 2.... 276
Table 4.1-128. Frequency Sweep for LAeq, 1h Point 3 North Daytime Week 276
Table 4.1-129. Frequency Sweep for LAeq, 1h Point 3 South Daytime Week 277
Table 4.1-130. Frequency Sweep for LAeq, 1h Point 3 East Daytime Week 277
Table 4.1-131. Frequency Sweep for LAeq, 1h Point 3 West Daytime Week 277
Table 4.1-132. Frequency Sweep for LAeq, 1h Point 3 Vertical Daytime Week..... 278
Table 4.1-133. Frequency Sweep for LAeq, 1h Average Point 3 Daytime Week..... 278
Table 4.1-134. Summary of Measurements Performed to Estimate Leq Point 3 Daytime Week 279
Table 4.1-135. Environmental Noise Results Corrected Point 3 Daytime Week..... 279
Table 4.1-136. Uncertainty Associated with the Estimation of the Measurand (LRAeq). Point 3.... 282
Table 4.1-137. Frequency Sweep for LAeq, 1h Point 4 North Daytime Week 282
Table 4.1-138. Frequency Sweep for LAeq, 1h Point 4 South Daytime Week 283
Table 4.1-139. Frequency Sweep for LAeq, 1h Point 4 East Daytime Week 283
Table 4.1-140. Frequency Sweep for LAeq, 1h Point 4 West Daytime Week 283
Table 4.1-141. Frequency Sweep for LAeq, 1h Point 4 Vertical Daytime Week..... 284
Table 4.1-142. Frequency Sweep for LAeq, 1h Average Point 4 Daytime Week..... 284
Table 4.1-143. Summary of Measurements Performed to Estimate Leq Point 4 Daytime Week 285
Table 4.1-144. Environmental Noise Results Corrected Point 4 Daytime Week..... 285
Table 4.1-145. Uncertainty Associated with the Estimation of the Measurand (LRAeq). Point 4.... 287
Table 4.1-146. Summary of Environmental Noise Assessment Daytime Week 288
Table 4.1-147. UP identified and percentage distributions. 289
Table 4.1-148. Landscape elements and percentage distributions. 294
Table 4.1-149. Visibility assessment by UP. 296
Table 4.1-150. Assessment of visual fragility by UP. 299
Table 4.1-151. Visual quality assessment by UP. 303
Table 4.1-152. Calculation of the aesthetic potential of the landscape..... 306

4. DESCRIPTION AND ENVIRONMENTAL CHARACTERIZATION OF THE STUDY AREA

The environmental description and characterization of the area includes an identification and characterization of each of the components that comprise the abiotic, biotic, social and environmental zoning environments. For this purpose, it is analyzed separately and according to the following components:

Abiotic environment: Geology, Geomorphology, soil, geotechnics, hydrology, water quality, water uses, hydrogeology, atmosphere and landscape.

Biotic environment: Flora and fauna.

Socioeconomic environment: Participation guidelines, socioeconomic characterization.

4.1 ABIOTIC MEDIUM

Next, the abiotic environment is presented, consisting of the following components: Geology, geomorphology, geotechnics, soil, hydrology, water physicochemical quality, hydrogeology, atmosphere and landscape.

4.1.1 GEOLOGY

Below is a presentation of the regional and local geology, in line with the exploration stage developed by TOUCHSTONE.

4.1.1.1 REGIONAL GEOLOGY

The geological setting in which the 5969 license area is located is conditioned by the presence of the Segovia Diorite (Jds) (See Illustration 4.1-1); this body is located in the northern sector of the Cordillera Central, in its eastern flank, is an elongated body in the direction of the mountain range, with a length of 270 km, a maximum width in its central part of 50 km and a total extension of more than 5,600 km2, are considered some process and related bodies. It extends from the town of San Martín de Loba, in the Department of Bolívar, in the far north, to the Alicante River, in the Department of Antioquia, in the far south (González & Londoño 2002). This unit is the bedrock of the most important vein-type mineralized structures in this part of the country and has been widely recognized for the richness, number and quality of these vein-shaped structures for gold mining.

Lithological units

The lithological units present in the area of influence of the zone of interest include rocks with ages between the Paleozoic and the Quaternary, represented by metamorphic, igneous and sedimentary rocks.

4.1.1.1.1 Metamorphic Rocks

The metamorphic rocks outcropping in the area of influence of the Mining Concession 5969 are grouped in the lithodemic unit called the Cajamarca Complex (Maya & González, 1995).

Gneiss feldspathic quartz

It is the most abundant metamorphic unit on the eastern flank of the Cordillera Central. To the west of the Otú Fault (Feininger et al., 1972). It is constituted by feldspathic and aluminum whose structure varies between schistose and sometimes migmatite, the present wide mineralogical and textural variations, due to both, the metamorphism conditions as to the heterogeneity of the original sediments, the predominant rock is gneissic, well foliated, usually folded and bright gray. Apparently, the located to the west of the Otu Fault are at the same stratigraphic level and correspond to the highest-grade zone of the Cajamarca Complex; the increase of the metamorphic grade would be the cause of the gradation.

These rocks form a mosaic limited by faulty blocks. They are partially covered by younger sediments and are intruded by the Diorite of Segovia, between the Otú fault and the Magdalena river valley, feldspathic quartz predominate in which amphibolite and marble lenses are found (Feininger et al., 1972).

The texture is granular hypidioblastic of medium to coarse size and the predominant composition is quartz, plagioclase and potassium feldspar; in the majority of gneiss biotite and muscovite coexist, the protolith of these gneiss seems to have been varied; in some places they are massive and seem to correspond to metamorphosed felsic plutonic rocks, while in another they are stratified and appear to come from sediments, banded amphibolite lenses of varying thickness, appear associated with the gneiss and seem to correspond to silos of basic rocks metamorphosed to the amphibolite facies.

Quartz-Sericitic Skids (Pzes)

Belonging to the Cajamarca Complex. This unit is presented as a series of graphite shales in which the dark gray or black color predominates; this unit is widely distributed in the complex, they have schistose structure finely laminated in layers of 3 to 5 mm, intensely folded, with veins of milky quartz of variable thicknesses that adapt to the forms caused by the deformation. The course of the schistosity varies between N10 ° E and N20 ° W, with geological dip marked to the East.
The metamorphic paragenesis found indicate regional metamorphism conditions, sometimes with superimposed events of low to medium degree and low pressure in the green schist facies to low amphibolite. The protolith corresponds to pelitic clay sediments with variable content of organic matter (Gonzales, 2001).

Quartzite (Pzq)

Well defined and regionally mapped quartzite groups are found in the different stratigraphic units that compound the Cajamarca Complex, they are interspersed with micaceous schists, it is difficult to separate both lithologies.

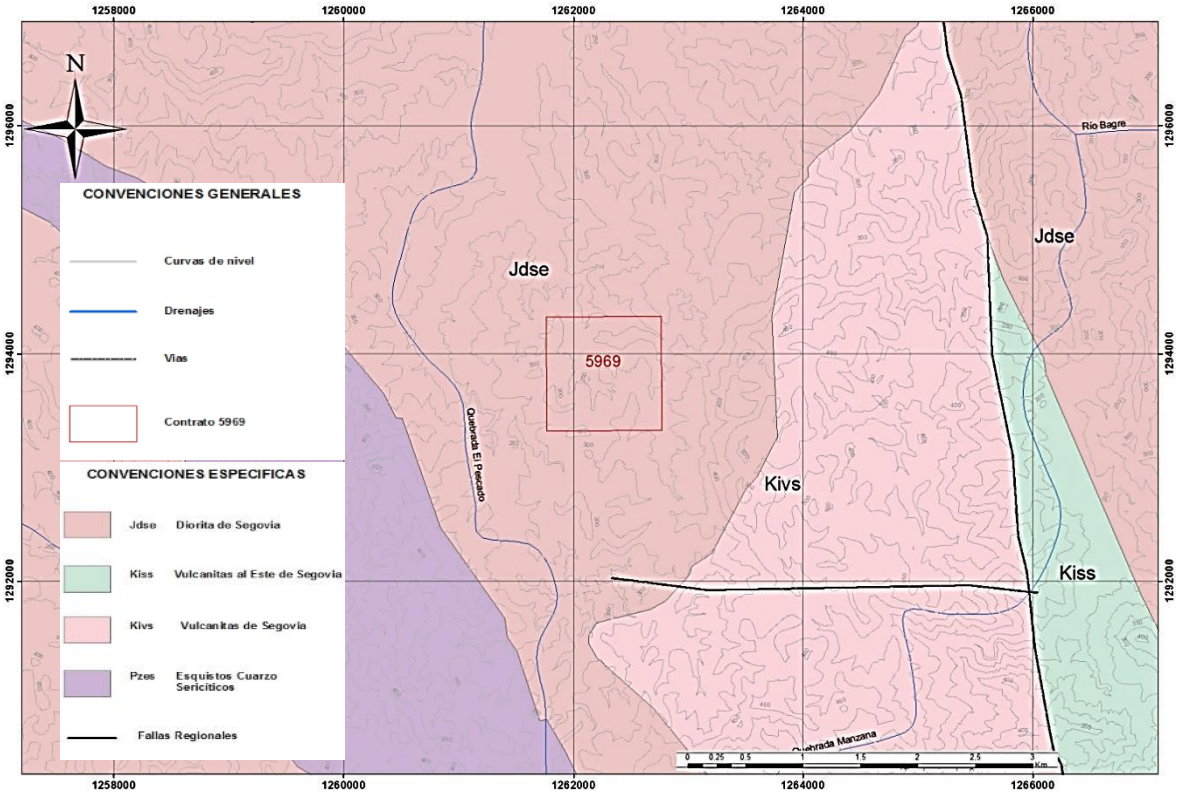

Illustration 4.1-1. Regional Geology.
Source: INGEX, 2015.

The Cajamarca complex in the area of the department of Antioquia contains three series of progressive regional metamorphism, each one characterized by a succession of different facies and mineral zones. The series of lowest degree of metamorphism, is located on the western flank of the central mountain range (Feininger et al., 1972) and is limited by the San Jerónimo fault, the second series comprises most of the metamorphic rocks within the green schist and amphibolite facies and the third comprises the rocks of a relatively higher degree to the west of the Otú fault and are basically feldspathic and aluminum gneiss, these three series are similar and the contacts are transitional, locally affected by thermal effects produced by intrusions.

The quartzite present gradational variations to shale sericitic quartz, marked by the increase in the content of micas and decrease in the content of quartz; this indicates lateral changes in the basin, with an increase in the clay material that is deposited (González 2001).

Paragenesis indicates conditions of low pressure, medium to low degree of metamorphism and are located between high green shale grades to low amphibolite (González, 2001).

4.1.1.1.2 Igneous rocks

The igneous rocks present in the study area are represented by intrusive rocks belonging to the Diorite of Segovia and volcanic rocks belonging to the vulcanite's de Segovia, both located chronologically in the Mesozoic age.

Diorite of Segovia (Jds)

In general, it is about an elongate body in a north-south direction, located east of the Otú-Pericos fault that coincides with the regional tectonic sense, it has a length of 270 km and a width in its central part of 50 km, it is constituted by diorite with textural and compositional gradational variations; these diorites vary from massive too lightly laminated and intrude rocks from the Cajamarca Complex.

More specifically, based on the catalog of stratigraphic units in Colombia (González & Londoño 2002), it is said to constitute a plutonic body of batholithic dimensions, 5,600 km2 with some smaller bodies geographically separated and sometimes located to the west of the tectonic system that it largely controls its location, but due to its petrographic characteristics and relations with metamorphic rocks, it has been considered genetically related; in the northern part, this body is divided into two, separated by a set of metamorphic rocks in tectonic contact, to the east marked by the Palestine Fault and to the west by that of El Bagre (Feininger et al., 1972; Kassem & Arango , 1977).

In the works carried out in the ridge of San Lucas, the oriental body has been called Oriental or Norosí Batholith (Bogotá & Aluja, 1981, Ballesteros, 1983), but it is clear that there is a geographical continuity towards the south with the dioritic body of Segovia (Diorite of Segovia).

It is an elongated body in the north-south direction, in the sense of the regional structures of the Central Cordillera, whose relations with the metamorphic rocks can be both tectonic and intrusive; it shows, in this case, a well-defined contact aureole with the presence of pelitic hornfels of medium degree of metamorphism.

The predominant composition is dioritic to quartz dioritic with local variations to quartz monzonites - granodiorites and gabbro; The most representative part of this pluton is constituted by dioritic and quartz dioritic rocks, massive to slightly laminated and strongly gneissic; laminated rocks are characterized by the presence of bands with diffuse contacts and different proportions of felsic and mafic minerals. Some of the gneissic rocks are cataclastic, although they could be partly protoclastic; near the tectonic contacts with precambrian gneiss are heavily sheared and the original structure has been largely destroyed.

The rock is phaneritic equigranular of medium grain, dark greenish gray color mottled, locally, with pink crystals of potassium feldspar surrounded by a plagioclase crown of cream color and gives a rapakivi structure (La Honda and Alicante rivers, and Pava stream).

Near the Otú fault, there are abundant autoliths of fine granular mafics and the presence of small faults. Irregular melanocratic dykes, sometimes with metamorphic textures, occur locally (González & Londoño 2002).

The Diorite of Segovia is the embedding body of the auriferous quartz veins where the most important and highest yield gold mining operations are carried out in Colombia (Rodríguez & Pernet). The age of this body corresponds to the beginning of the Middle Jurassic based on the isotopic age of 160 ± 7 Ma K/Ar in hornblende reported by Feininger et al. (1972), in a sample from the Montecristo quarry.

Segovia vulcanite (Kivs)

They are elongated bodies east of the Otú fault and limited, largely by the El Bagre fault, east of Remedios and Segovia, are related to sediments located in the east of the Otú fault, between the Nus and El Bagre faults (Feininger et al. al., 1972) east of Segovia, a town in the northeast of the department where the name is assigned; they extend north to the latitude of the Municipality of Zaragoza, Antioquia (González 1992).

The sedimentary-volcanic belt extends for 90 km, with an average width of 6 km and irregularly extends in its northern end. Volcanic rocks are more abundant in the western part of the strip, which is controlled by Fault Nus.

The volcanic rocks are indicated on the map as independent lithological units in those areas where they predominate over sediments, but it is not always possible to make the separation and in the sedimentary unit subordinate vulcanite appear.

There is no known data on the age of these rocks, however their relationship with marine sediments allows them to be assigned an Hauteriviano-Aptiano age (González 1992).

4.1.1.1.3 Sedimentary rocks

The sedimentary rocks that emerge in the area of influence were formed in the marine environment of the Cretaceous.

Sedimentites east of Segovia (kivs)

It is an informal name used to describe some sedimentary rocks related to basic volcanic rocks located east of the Municipality of Segovia and of Otú fault (González 2001); it is a black carbonaceous shale, stratified with siltstones, sandstones, conglomerates, quartz conglomerate ridges, mudstone and basic volcanic rocks; near the Otu fault some lenses of fine granular limestone of gray color appear.

The stratification is from vertical to sub vertical and the stratification planes are micro filled and striated; the fossils observed in this unit (gastropods and pelecypods) locate the unit in the Upper Albian Lower Aptian (Feininger et al., 1972).

Quaternary deposits

Included Quaternary deposits are the result of the recent denudation of the area, such as alluvium, flows, colluviums, torrential flood deposits and ejection cones; these deposits, unbound, are mostly mapped at the local level, yet they are very important because of the information they offer from the surrounding lithologies, the morph dynamic processes acting and the accumulation of materials of economic interest such as gold; In general, it presents particles of varied composition and size, among which are those of diorite and granodiorite, as well as those of rounded quartz with poor selection.

4.1.1.2 REGIONAL STRUCTURAL GEOLOGY

Several authors interpret three deformative phases (See Illustration 4.1-2) with influence in the area of interest, which start from a structure of regional character as the Otu Fault and that concentrates the greatest amount of efforts, this structure presents directions that vary from NNE to NNW and high angles of dip, as well as the extension of hundreds of kilometers on the course and thicknesses of up to hundreds of meters including the shear zone; from there second and third order structures are detached.

The second order structures have a subparallel address to the main structure; These structures have extensions in courses of up to tens of kilometers and are tens of meters thick.

On the other hand, there are structures of third order, subordinated to the previous ones, these structures are oblique to the previous two and harbor most of the mineralization, without ignoring mineralized zones in the second order structures; this type of third order structure has a few kilometers of course and thicknesses of up to several meters; It should be noted that not all third order structures are mineralized and those that are mineralized are not mineralized in their entirety.

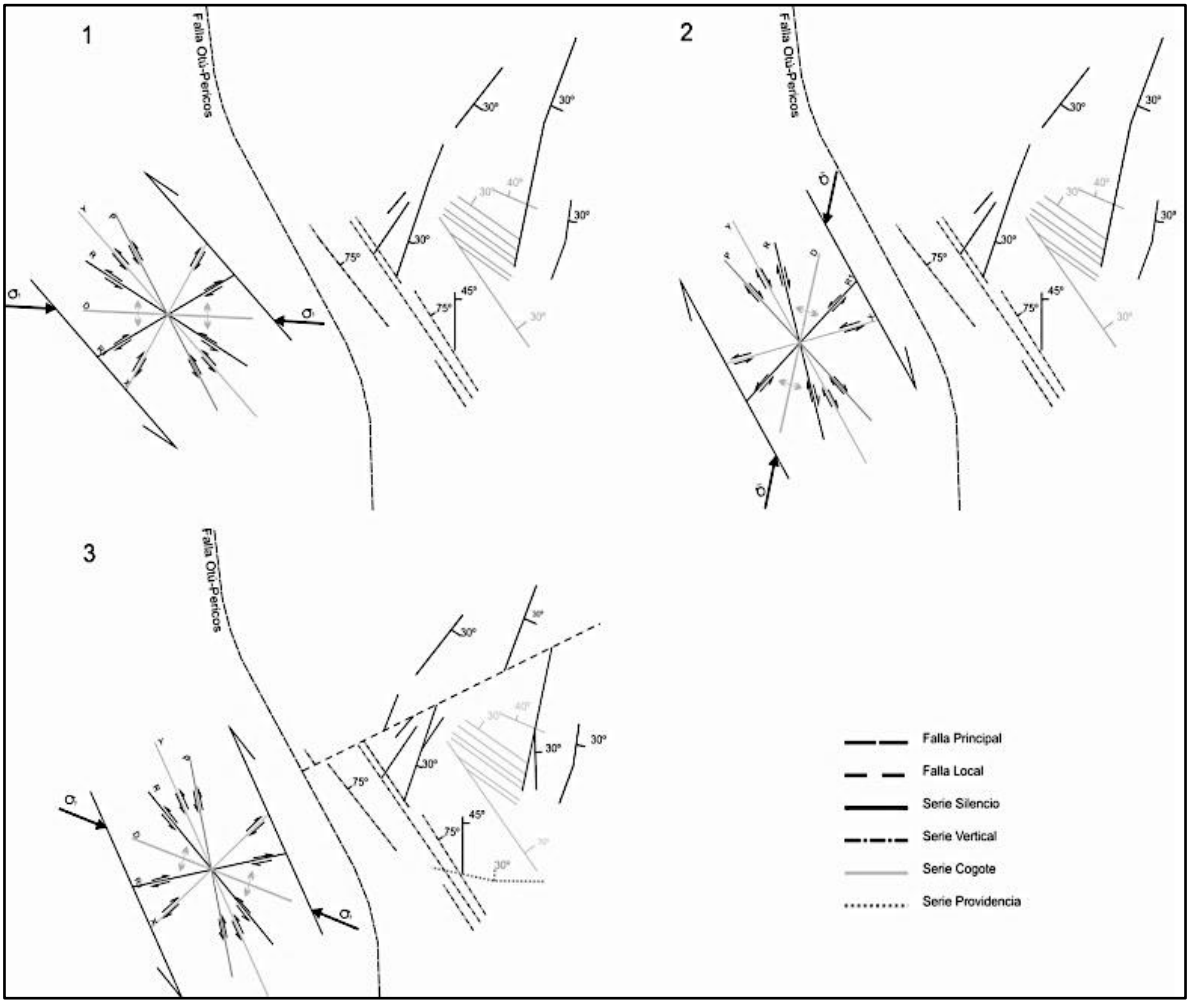

Illustration 4.1-2. Structure formation diagram with the 3 main events.
Source: Echeverry et al., 2009.

4.1.1.3 LOCAL GEOLOGY

Geology is characterized by the presence of a clearly igneous plutonic lithology with dioritic affinity.

With the support of the cartography and the perforations developed in the exploratory stage, it is determined that there is a marked predominance of a plutonic igneous unit correlated with the Diorite of Segovia (Jds); this unit is masked by a thick layer of weathered material that can reach up to 30 meters deep and includes dioritic and granodioritic rock saprolite.

The weathered material varies in shade from yellow-brown to reddish-brown (see Illustration 4.1- 3), this material constantly shows the presence of white veins with low sulfur content; in depth and crossing the deepest weathering limit we can observe the presence of a diorite rock with textural

variations to micro diorite and textural-compositional variations to granodiorite, which in turn is cut by diabase dikes without a clear regularity in the appearance of these dikes; is composed mainly of quartz, plagioclase Na, feldspar K, amphiboles and biotite, as secondary minerals are observed mainly sulfides such as pyrite and chalcopyrite, quartz and oxides. Illustration 4.1-4 shows the local geology of the area.

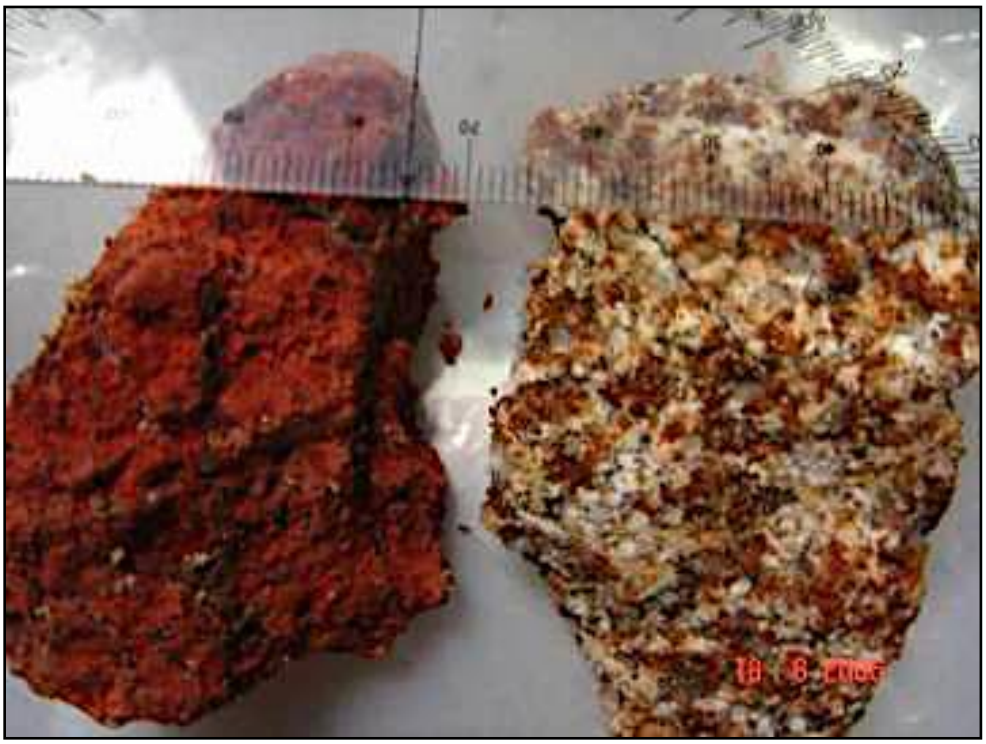

Illustration 4.1-3. Granodiorite hand sample, left weathered, right cooler.
Source: TOUCHSTONE, 2013.

The rock in general presents alterations such as argillic, propylitic, chlorite and potassium. The latter is evidenced by the appearance of secondary biotite, potassium feldspar and the presence of magnetite. The lithological facies in this body do not vary drastically in their mineralogical composition, but rather in the relative proportion of the essential phases, which modifies the petrographic classification; the hydrothermal alteration processes are related to the mineralizing that characterize this body both in its southern part (region of Segovia - Remedios), and in its northern part (south of the Department of Bolivar).

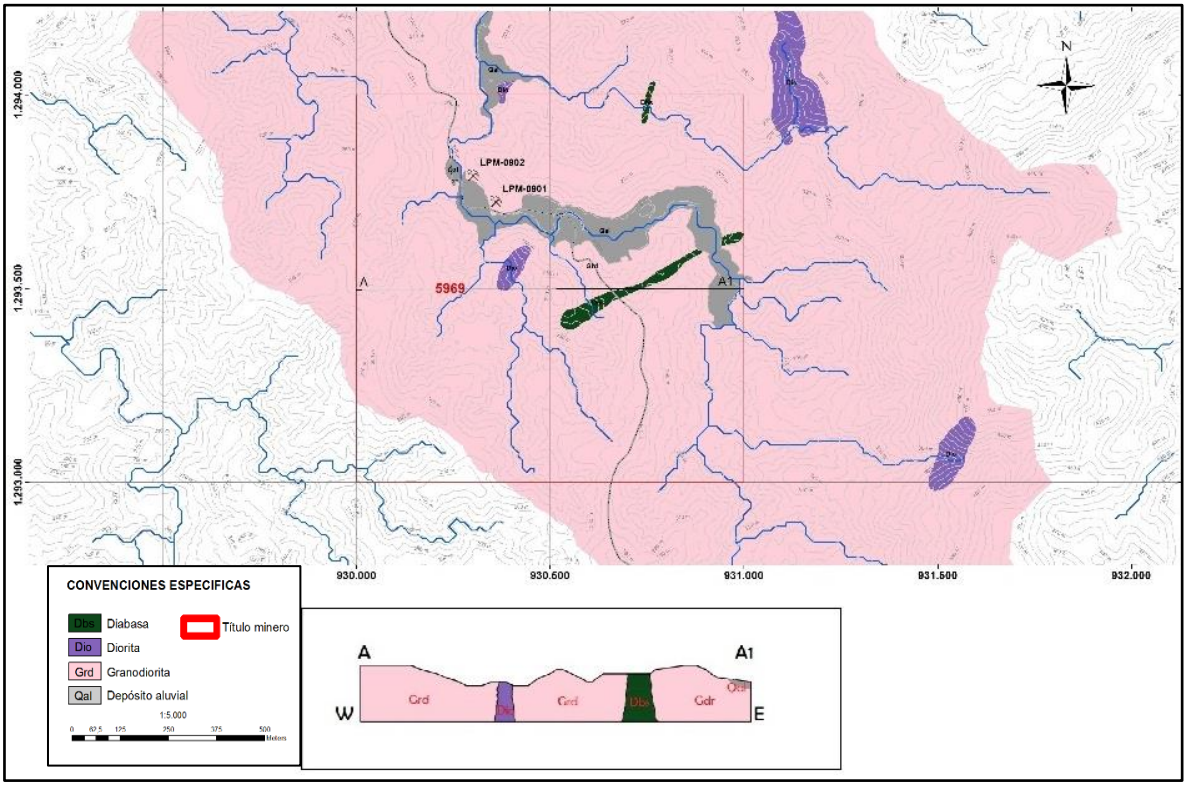

Illustration 4.1-4. Local geology.
Source: INGEX, 2015.

The mineralized structures have NNE, NE and NNW directions, in all cases the vergence is to the W, the angles of dipping vary between 25 and 80 degrees; they are composed of milky quartz in occasions, thicknesses from 1 to maximum 3 meters, in sectors we can see arrangements in druse, the structures present besides accompaniment of sulfides, in special pyrite, in occasions subordinated to marcasite, to a lesser measure chalcopyrite and subordinate galena, arsenopyrite euhedral can also be seen in isolated crystals, these crystals have gold accompanying these associations; the veins' characteristics are essentially mesothermal hydrothermal, although due to the thickness of the structures it cannot be ruled out that 100% of the deposit is orogenic gold type.

Finally, there are some small alluvial deposits formed by gravel, sand and silt; there is no stratigraphic column of the alluvial deposit, there are numerous pebbles of diorite, granodiorite and milky quartz mainly on the surface, with variations from sub angular to rounded, with a medium general sphericity and poor selection, giving the idea of a polymictic deposit.

4.1.1.4 LOCAL STRUCTURAL GEOLOGY

It is located in an area of active tectonic influence, in which the position and movement of both the sin genetic and post-genetic structures play a very important role, given the proximity of the Otu-Pericos and Nus faults, which are located within the Palestinian fault system and which limit the Diorite of Segovia to the east and west.

The interpretations from the structural point of view associated with the Segovia Remedios Mining District (hereinafter DMSR) that are related to the development and characteristics of the mineralized zones and their behavior are valid; the above is made valid in the sector a series of features that certify the influence of the surrounding major structures, especially with regard to the direction of the efforts and movement of the structures of lesser order.

The predominant fractures in the sector present N/S, NNE/SSW and NNW/SSE directions; generalizing, the dipping in most cases is towards the W, the dipping angles are variable and range from 30 to 80 degrees depending on the proximity to some local structure.

In general, based on the observations of underground exploratory galleries and the data taken from the logging process of drill cores, the stresses are dextral and associated with a zone of dilation stress (See Illustration 4.1-5).

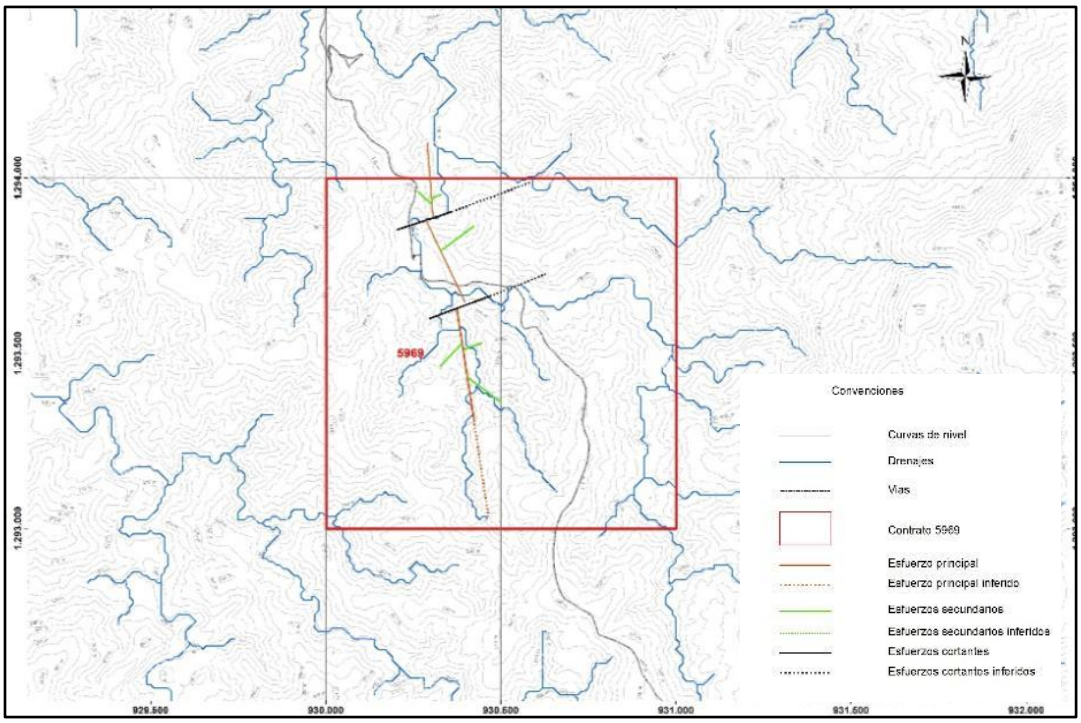

Illustration 4.1-5. Structural local geology.
Source: INGEX, 2015.

4.1.1.5 INDIRECT EXPLORATION

Indirect exploration by geophysics is presented below.

Geophysics

Geophysical studies of induced polarization and resistivity were carried out in order to establish anomalous values in the subsoil from the surface. Subsoil electrical resistivity measurements are common in geophysical surveys; their purpose was to detect and locate geological bodies and structures based on their resistive contrast; the method consists of injecting direct current into the ground by means of a pair of electrodes and determining the difference in potential by means of another pair of electrodes; the magnitude of this measurement depends, among other variables, on the distribution of the resistivity of the subsoil structures, on the distances between the electrodes and on the current injected.

Induced polarization is an electromagnetic method that uses electrodes with time-varying voltages and currents to map the variation in electrical permittivity (dielectric constant) in the subsurface at low frequencies (See Illustration 4.1-6).

Induced polarization is observed when a stationary current passing through two underground electrodes is interrupted, the voltage does not return to zero instantaneously but slowly decays, indicating that the charge has been stored in the rocks; this charge, which accumulates mainly at the interfaces between the clay minerals, is responsible for the IP effect; this effect can be measured in the time domain, by observing the rate of voltage decay, or in the frequency domain by measuring the phase currents between sinusoidal currents and voltages, often used in mineral exploration and sometimes used to distinguish different types of mineralization, the IP method can probe to underground depths of thousands of meters, (Schlumberger Oilfield Glossary).

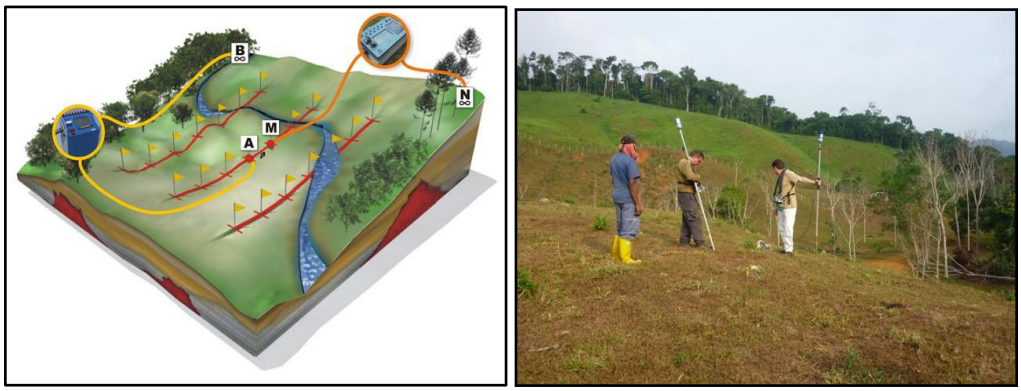

Illustration 4.1-6. Geophysical measurement scheme with the pole-to-pole array (left); field work for electrode placement (right).
Source: TOUCHSTONE, 2013.

The increase in electrode spacing changes the depth of the measurements; the measurement lines were spaced every 50 meters in the W-E direction to obtain measurements perpendicular to the mineralized structures.

The geo-electrical profiles and the area covered by geophysics are shown in Illustration 4.1-9.

4.1.1.6 DIRECT EXPLORATION

Direct exploration, consisting of geochemical sampling, trench and ditch digging, existing wells and galleries, and drilling, is presented below.

4.1.1.6.1 Geochemistry

Within the geochemical analyses, sampling campaigns are presented that included soil, active sediment and surface and ground structure sampling.

Soil sampling was performed in order to apply a geochemical and statistical treatment to the samples obtained and to obtain representative information on possible chemical anomalies in the terrain and to determine targets for the deepest (direct) exploratory phase.

The sampling methodology based on the 43-101 standards involved the use of manual twist drills (See Illustration 4.1-7), with which holes of up to 60 cm were drilled in the soil and a sample was collected at this depth.

The samples obtained were packed and sent to a certified laboratory, taking into account the QA/QC procedures established by the company for this purpose; the samples were analyzed by ICP40B and 1DX3 for multi-element and FAA 313 and G6 fire tests, to determine the Au dispersion circuit in related elements; the results obtained were statistically treated and zones were determined with them.

Illustration 4.1-7. Soil sampling procedure.
Source: TOUCHSTONE, 2013.

The sampling of active sediments was carried out with the objective of establishing the concentration of chemical elements present in the materials that a stream transports and deposits, this to delimit areas of interest that present high anomalies in the concentration of materials, especially metals and in this case as the main objective gold. In this case, a total of 24 active sediment samples were taken and about 80 more were taken in the drains of nearby areas.

The best areas of sand and fine material accumulation were located; with the help of a plastic shovel the sediment was extracted to be passed through a sieve; the material that passed through the mesh of the sieve was dried as far as the field conditions allowed and then deposited in a bag for sediment that allowed the extraction of the remaining water, the sample was packed according to the QA/QC procedures established by the company for the effect; after that it was then sent to a specialized laboratory for geochemical analysis; the results received were statistically processed and evaluated to define areas of anomaly with the greatest interest for further exploration; the summary table with the samples taken is presented below.

4.1.1.6.2 Trench and hoof digging

Trenches were developed to test the continuity in depth of vein-like mineralized structures seen on the surface and to facilitate exposure of fresh rock; the trenches were 1-3 meters deep and up to 20 meters long, in the W-E direction (See Illustration 4.1-8). In general, the findings included white quartz blocks with mild to moderate presence of iron and manganese oxides; the blocks are fractured, with orange coloration in the fractures from the saprolite; the little visible mineralization is composed essentially of pyrite which is mostly oxidized; the results of the sampling corroborate the results of the previous soil anomaly.

Illustration 4.1-8. Trench T39.
Source: TOUCHSTONE, 2013

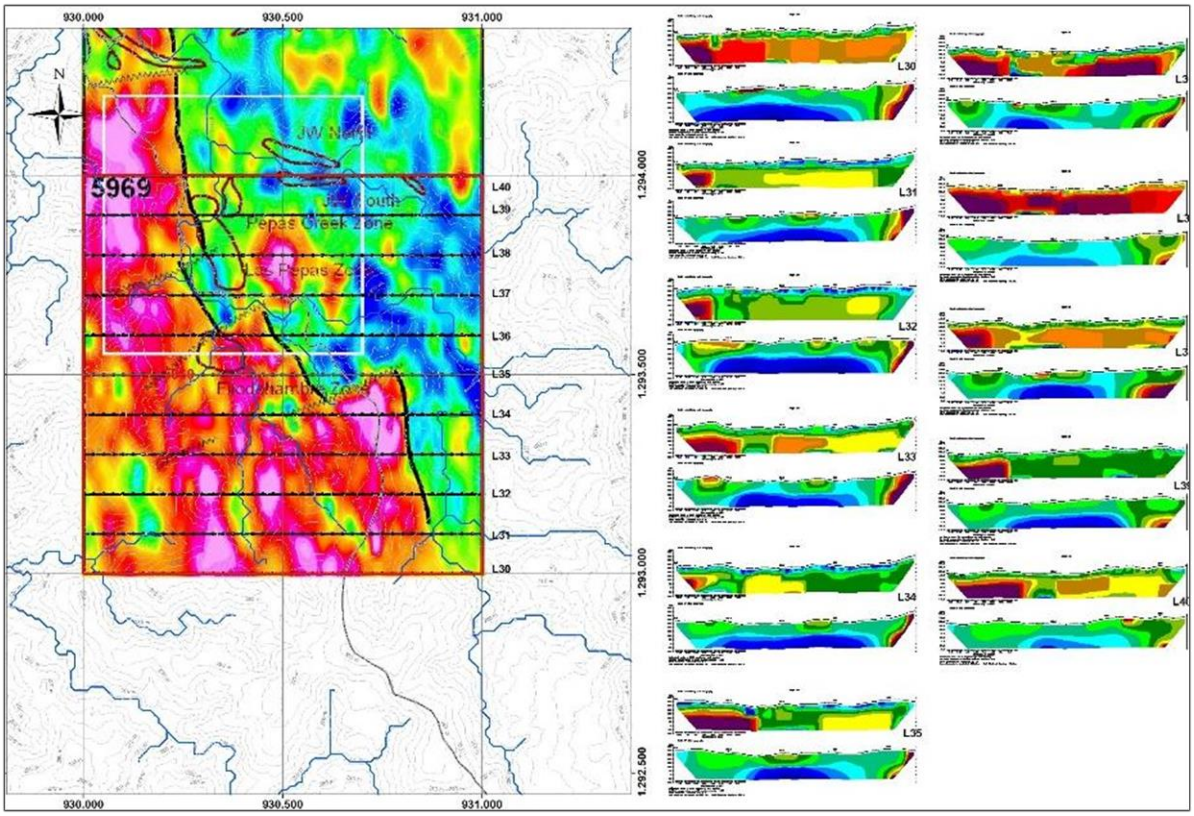

Illustration 4.1-9. Electrical tomography
Source: ARCE GEOFISICOS, 2013

4.1.1.6.3 Existing wells and exploratory galleries

The development of tunnels for underground operation was carried out by the inhabitants of the sector in an artisanal manner. A total of 12 horns were identified; in some cases, these are tasks that are communicated and have a maximum length of up to 50 meters in the guide; it should be noted that 80% of these activities are currently abandoned.

Deep drilling

Between 2003 and 2005 different investment companies carried out drilling campaigns; The drilling process began with the planning of the drilling and its location in the ground according to its predefined target; for the correct location of the drilling platform (See Illustration 4.1-10) The service of the surveying department was used, which, with the help of the total station, located the drill in the exact position to start drilling; the geologist verified the position of the drill, the angle and the azimuth of the drill to ensure the efficient development of the work.

The drilling program allowed for a clear understanding of the lithological units in the subsoil at different depths; these drillings were programmed based on the previous exploration of the delimitation of areas of interest and spatially locates the structures performed in 2003. The purpose of the drilling campaigns was also to cut the mineralized bodies in depth to delimit and even measure them. The location of the holes is shown in Illustration 4.1-13 below.

Illustration 4.1-10. Drilling platform.
Source: TOUCHSTONE, 2013.

The recovery of the cores was carried out by trained personnel; for this purpose, these cores were measured, marked and placed in metal boxes (See Illustration 4.1-11) to move on to the logging process by the geologist; before starting the detailed logging process, a quick logging was done where the most relevant observations of the well were quickly recorded.

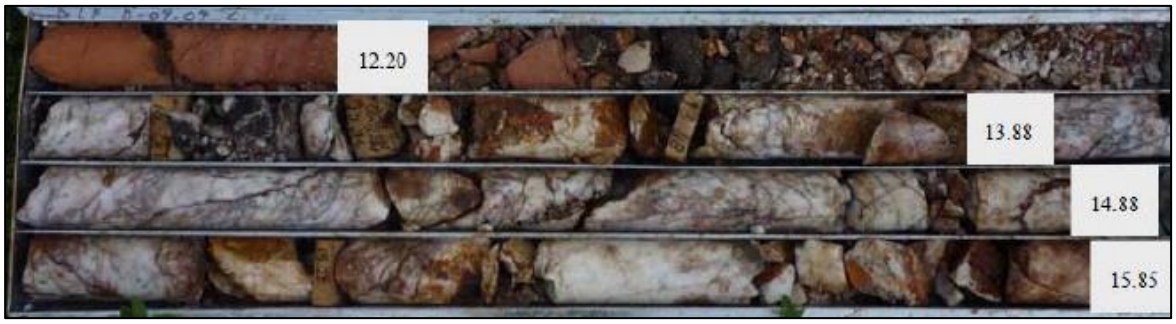

Illustration 4.1-11. Drilling cores ready for the logging process.
Source: TOUCHSTONE, 2013.

Subsequently, the cores were examined in the area of logging (see Illustration 4.1-12 and Illustration 4.1-14) by the geology professional, who recorded his observations in predefined logging format, which was later converted to digital format to take advantage of the information in the elaboration of cartography, modeling and calculation of resources.

Illustration 4.1-12. Logging zone.
Source: TOUCHSTONE, 2013.

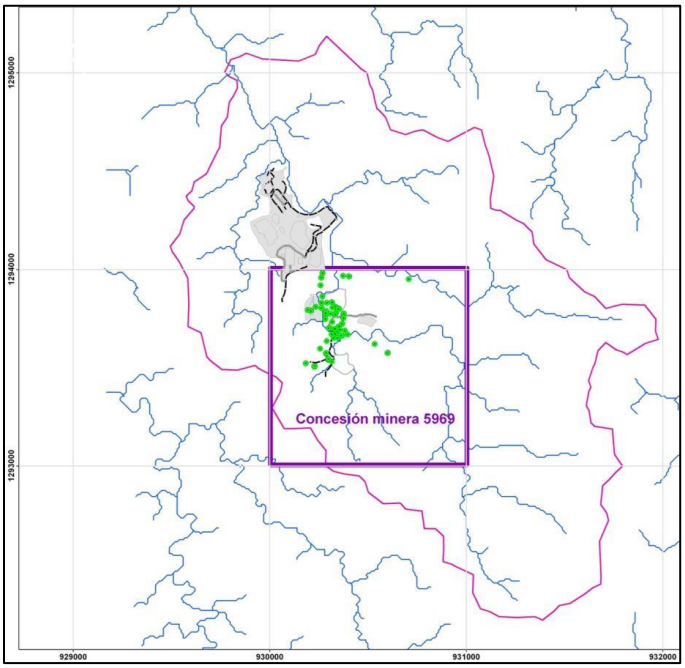

Illustration 4.1-13. Location of perforations (in green).
Source: TOUCHSTONE, 2013.

Illustration 4.1-14. Samples packaged for analysis after cutting.
Source: TOUCHSTONE, 2013.

According to the geologist's criteria, the zones in the well to be sampled were established; with the use of a cutting machine, the cores were divided in the direction indicated by the geologist; later, the sample was packed according to the implemented QA/QC procedures and the other half of the core was left in the box to be preserved as a witness.

These samples (Illustration 4.1-15) were analyzed in certified laboratories and the results analyzed and recorded in databases for use.

Illustration 4.1-15. Quartz vein with sulphides, an outcrop material in the sector.
Source: TOUCHSTONE, 2003.

Quality sampling and analysis

Several samples were taken at the surface and underground exploration stage, each with a specific objective; the underground samples were taken with special interest in the existing artisanal mining tunnels, these samples were taken as a vein channel perpendicular to the structures; this sampling allowed obtaining first-hand geochemical information on the mineralization of the structures, the quality of the elements present and the mineralogical association through a multi-element analysis.

The vein samples analyzed under a reflected light microscope conclude that the mineralization consists of pyrite (with local tags subordination), sphalerite and chalcopyrite in smaller quantities. Free gold with a range of 10 to 100 microns is present, with the presence of base metal sulphosalts and gold telluride. The mineralogy of the gangue is 97 dense quartz, massive and sub crystalline, with ferrous carbonates, chlorite, sericite and kalinite; several generations of quartz are observed, but not all associated with sulfides; sulfides are presented in the form of anhedral masses with quartz.

4.1.2 GEOMORPHOLOGY

The regional and local geomorphology of the study area is presented below.

4.1.2.1 REGIONAL GEOMORPHOLOGY

The study area is located on the eastern flank of the central mountain range. In the eastern part of the department of Antioquia, the relief decreases progressively from west to east towards the Magdalena River, characterized by hills of moderate slopes and sub rounded forms.

Regionally, the area of interest is framed in the foothills of the physiographic unit known as the San Lucas mountain range. The heights do not exceed 2500m.a.s.l.

4.1.2.2 LOCAL GEOMORPHOLOGY

The relief of the study area is characterized by being hilly, with elevations that vary between 170 and 340m.a.s.l. formed on the development of the meteorological profile of plutonic rocks such as granodiorites, diorites and diabase with moderate and gentle slopes.

Local geomorphology, consisting of its geomorphological units, morphometry, morph dynamic processes, and multi-temporal analysis, is presented below.

4.1.2.2.1 Geomorphological Units

For a better understanding of the location of the photographs shown in this chapter, the location of the points where panoramic photographs are taken and directed is shown schematically in Illustration 4.1.16, in order to describe in detail, the different geomorphological units present in the study area.

The flat areas correspond to alluvial terraces of the different drainage systems that run through them and the anthropogenic areas have been the result of the adaptation of the land for the assembly of the existing infrastructure.

Illustration 4.1-17 shows the geomorphological map of the study area, including the area of direct and indirect influence.

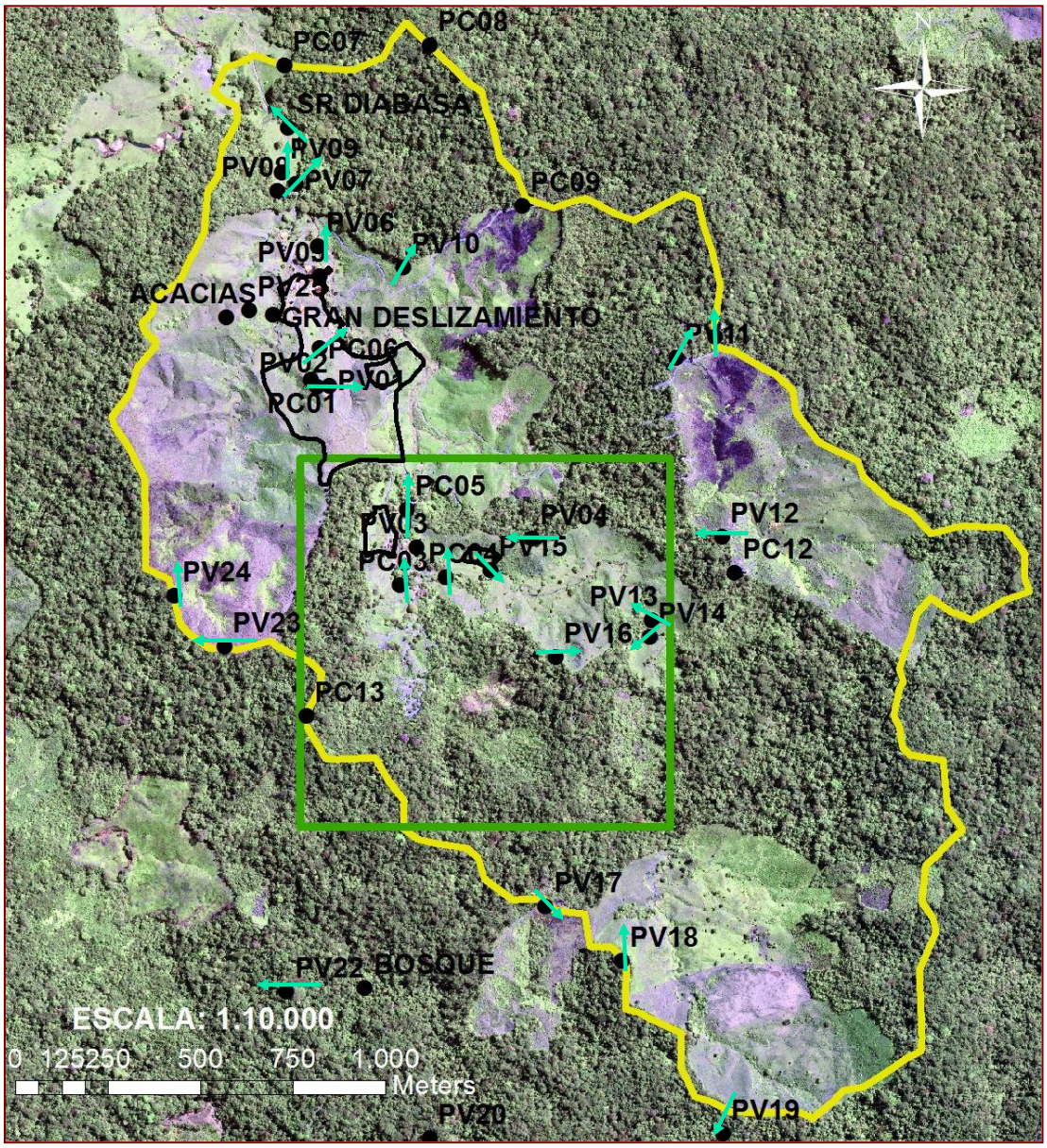

Illustration 4.1-16. Visual points and control points.
Source: INGEX, 2015

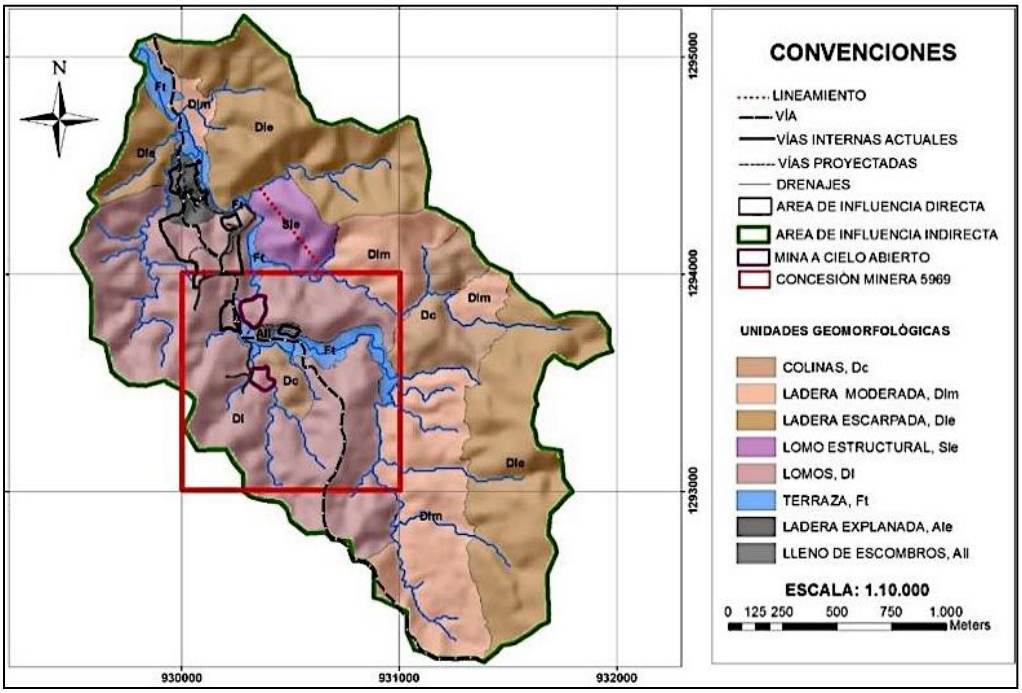

Illustration 4.1-17. Geomorphological units of the study area, scale 1:10000.
Source: INGEX, 2015.

It is highlighted that the geomorphological units' presents in the area of the direct influence correspond to Ridges, Dl. For the denudation unit, four categories were identified which correspond to: ridges, hills, moderate slopes and steep slopes. As for the structural denudation unit, structural ridges were differentiated within failure shoulder pads were observed; in the fluvial unit terraces and active channels were found (Due to the small scale of this unit, it isn't found in the geomorphology map, but its description on this document is found), and in the anthropic unit, open slopes full of debris were identified. These are present within details below.

Denudation Unit

These are geo forms associated with exogenous processes that degrade the relief and tend to level the surface by means of weathering, transport (erosion and mass movements) and sedimentation.

This unit has four (4) categories detailed below.

Hills (Dc)

It represents the 6,11% of the total evaluated areas, correspond to concave rounded surfaces with small to moderate slopes. These hills have moderate heights of less than 100 m, mostly composed of

residual soils. Inside the study areas there are isolated areas surrounded by spines, slopes and alluvial terraces (See Illustration 4.1-18).

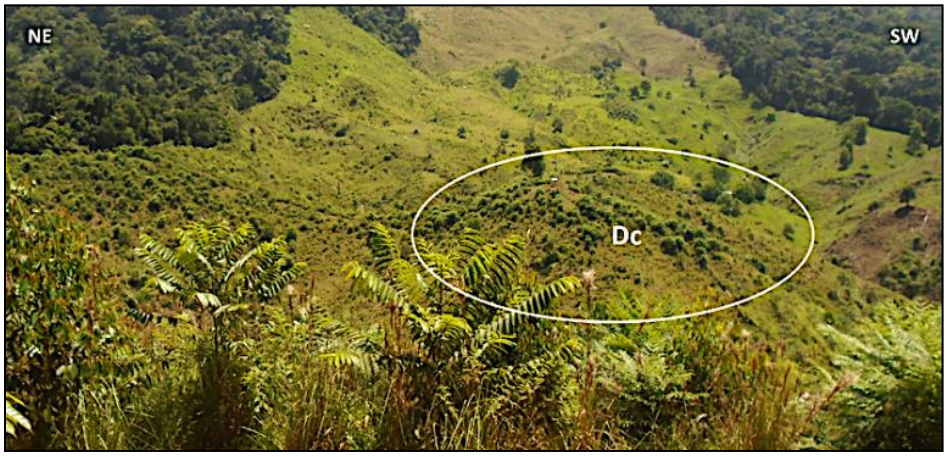

Illustration 4.1-18. The hill (Dc) surrounded by an alluvial terrace.
Source: INGEX, 2015

Ridges (Dl)

They constitute 33.21% of the area evaluated. These geo forms correspond to water dividers, which have semi-rounded, flattened and even flattened crest finishes, with a sub-parallel drainage pattern, limited by short to moderate slopes. These ridges show moderate heights of less than 200 m with an inclination that does not exceed 20° (See Illustration 4.1-19). This category is the one presented in most of the study area.

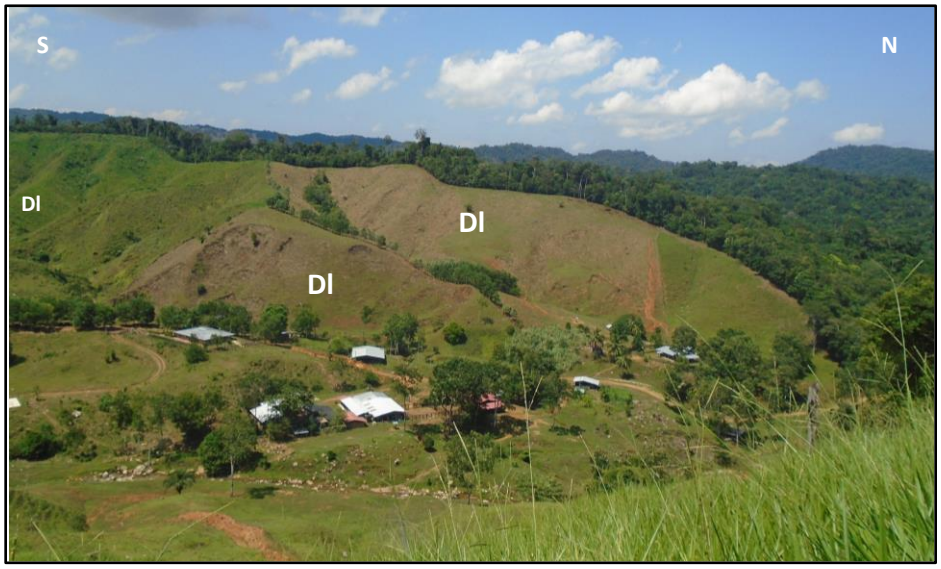

Illustration 4.1-19. Ridges (Dl), composed of residual soil in the western part of the study area (PV 12).
Source: INGEX, 2015

Moderate Slope (Dlm)

It corresponds to 20.09% of the study area. These are elongated, wavy and continuous surfaces located in the south-eastern part of the evaluated area. The slopes are less than 100 m long and can be considered straight to irregular slopes with slopes of no more than 40° formed by denudation processes on the residual soil, very dissected by sub-parallel drains (See Illustration 4.1-20).

Illustration 4.1-20. Moderate slopes (Dlm), on residual soil (PV 11)
Source: INGEX, 2015.

Steep slope (Dle)

They represent 32.28% of the total area evaluated. They correspond to areas whose slopes are steep with slopes equal to or greater than 45°, elongated to straight lines, mostly at the top of the moderate slopes, which include pastures and forest (See Illustration 4.1-21).

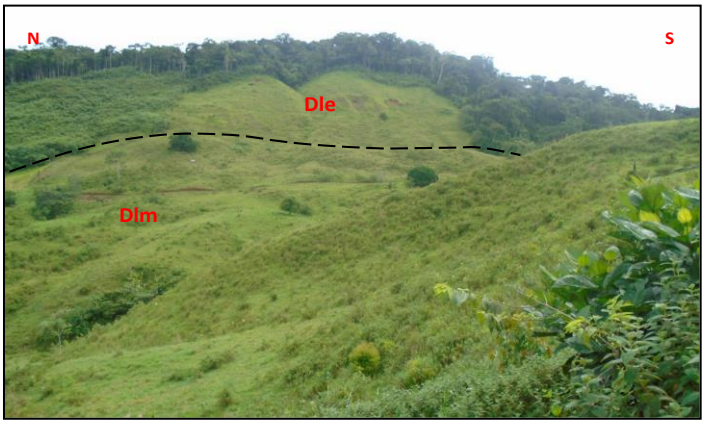

Illustration 4.1-21. Craggy slope (Dle), covered by pastures and forests (PV 14).
Source: INGEX, 2015

Denudation Structural Unit

Geo forms generated from endogenous (internal) and exogenous (external) processes, which form steep and folded expressions of faults, as well as from the arrangement of their layers with respect to the slope of the terrain.

Structural Ridges (Sle)

It corresponds to 3.26% of the study area. These are geoforms associated with elongated hills in a curved or hooked shape (seen from the ground plan), produced by forces associated with faults. These are limited by short to moderate slopes, convex in shape; their peaks can be as broad as thin. These geoforms correspond to a zone of fault shoulder pads that have steps or steps aligned in a preferred N20W direction (See Illustration 4.1-22). They are identified in the southern zone of the direct area of influence.

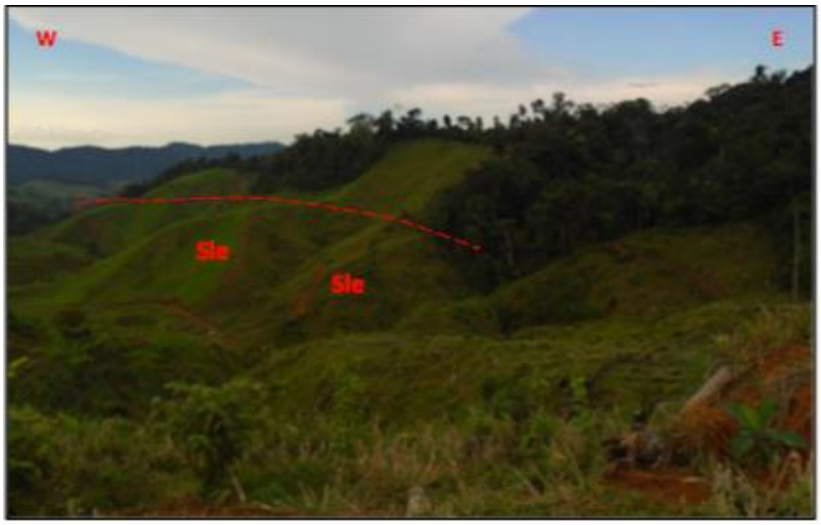

Illustration 4.1-22. Structural Ridges (Sle), the dotted red line indicates the direction of the line (PV 03).
Source: INGEX, 2015.

River Unit

They correspond to those geoforms originated by the erosive action whose predominant agent is the continuous currents of water. They originate in temperate to humid climates and affect any type of rock, particularly those that are soluble and not very cohesive. Active channels and levels of terraces were identified; all of them associated with tributaries of El Pescado Creek, as well as the other tributary channels.

Terrace (Ft)

They occupy 3.49% of the total area evaluated. Morphology flat to slightly wavy, originated by the current rivers or streams, formed by the fluvial or fluvio-torrential dynamics. They are developed in areas near active riverbeds or flooded valleys of rivers and/or streams. These alluvial terraces are easily affected by erosive processes of lateral scour type (See Illustration 4.1-23).

In the study area these terraces reach an average thickness of 2 m and are located mainly on both sides of the riverbed of a tributary of the El Pescado stream.

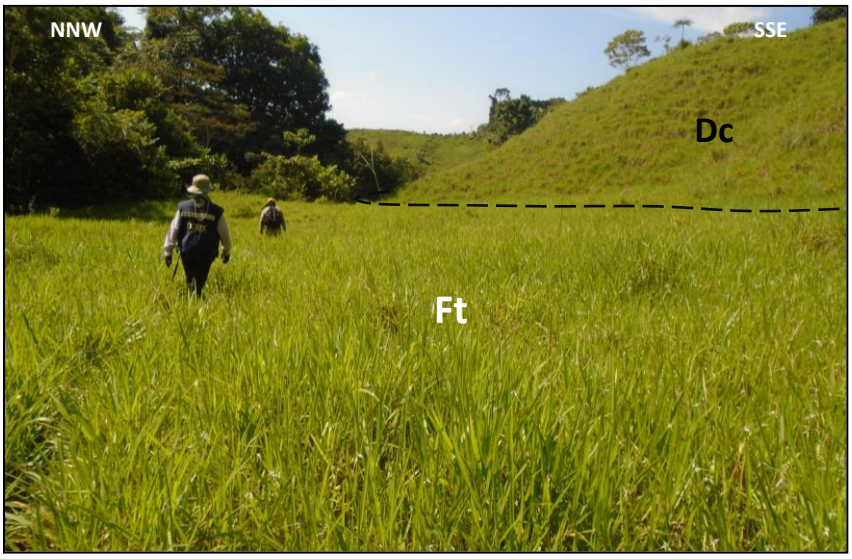

Illustration 4.1-23. Terrace (Ft), the black line indicates the alluvial terrace located on the right bank of a tributary of the El Pescado stream (PV 06).
Source: INGEX, 2015.

Active Channel (Fca)

It corresponds to the frequent mastery of current water flows. At different times of the year, these geoforms may present a variation to the mapped scale, due to the dynamics of the currents, generally presenting a channel with a U-shaped cross-section or caisson, with a width that does not exceed 15.0 m and with gentle slopes of less than 10° (See Illustration 4.1-24). In the study area and at the working scale, it is not possible to present it on the geomorphological map, however, it is considered important to include the description in the document.

Illustration 4.1-24. Active channel (Fca), photograph taken in a tributary of the El Pescado stream.
Source: INGEX, 2015.

Anthropic Unit

These geoforms are the result of human intervention on land for the construction of engineering works, for housing purposes, construction or adaptation of roads, excavations for water accumulation (watering holes or lakes for fish farming), or simply for the disposal of mining debris and organic and inorganic waste. In general, in the study area, they occur locally.

Full of debris (All)

Geo-form that occupies 0.158% of the total area evaluated and is associated with deposits of material from mining excavations which correspond to mounds without compaction, much of its area is covered with vegetation, (See Illustration 4.1-25). In the study area, a small deposit located in the south-west sector was defined, adjacent to a current sinkhole from which material was previously extracted.

Illustration 4.1-25. Full of debris (All), found in the south-west part of the study area.
Source: INGEX, 2015.

Yard Sidehill (Ale)

It constitutes 1.37% of the total area of the study and belongs to slopes that have been esplanaded or terraced in order to adapt them for the construction of infrastructure works. Yard sidehills can be seen in the camp area, roads and surroundings (See Illustration 4.1-26).

Illustration 4.1-26. Yard Sidehill (Ale), current project infrastructure located in the northwest zone (PV 12).
Source: INGEX, 2015.

4.1.2.2.2 Morphometry

The area under study has topography with varying slopes ranging from very gentle to high.

The morphometry of the evaluated area was established from the generation of the slope map. From the topography supplied with contour lines every 10 m, the map was drawn up using five (5) analysis categories (see Table 4.1-1).

Table 4.1-1. Land slope categories and ranges.

CLASS	RANGE	DESCRIPTION
1	0 – 15%	Very soft
2	15% - 30%	Soft
3	30% - 50%	Moderate
4	50% - 100%	high
5	>100%	Very high

Source: INGEX, 2015.

The slope map of the study area can be seen in Illustration 4.1-27.

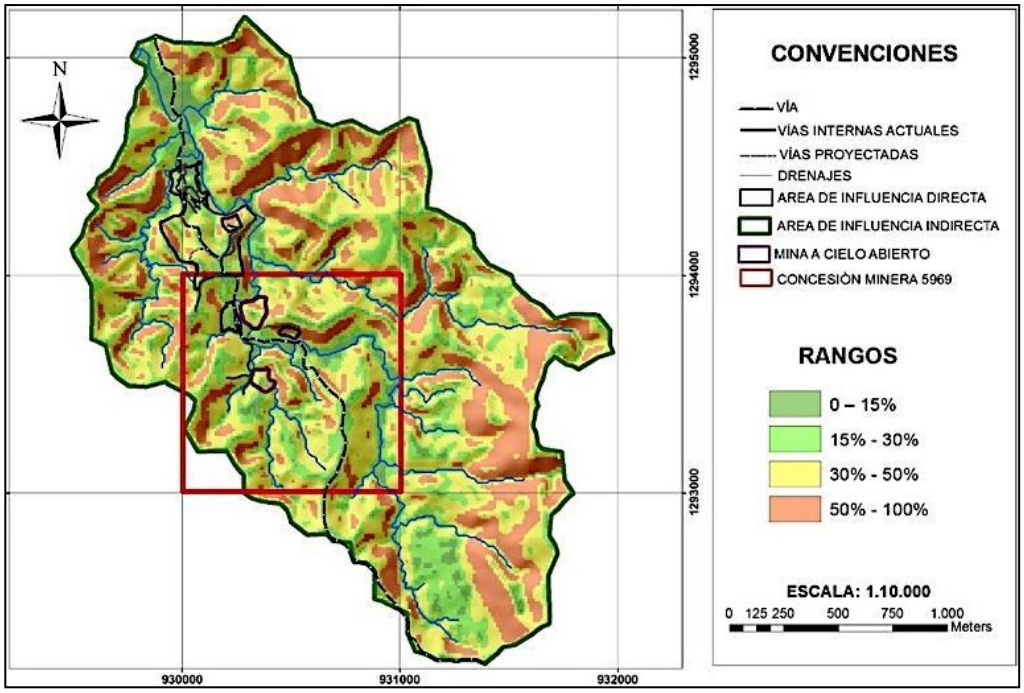

Illustration 4.1-27. Slope map of the study area, scale 1:10000.
Source: INGEX, 2015.

From the generation of the slope map, the slope range histogram is obtained versus the number of pixels as a function of areas. (See Illustration 4.1-28).

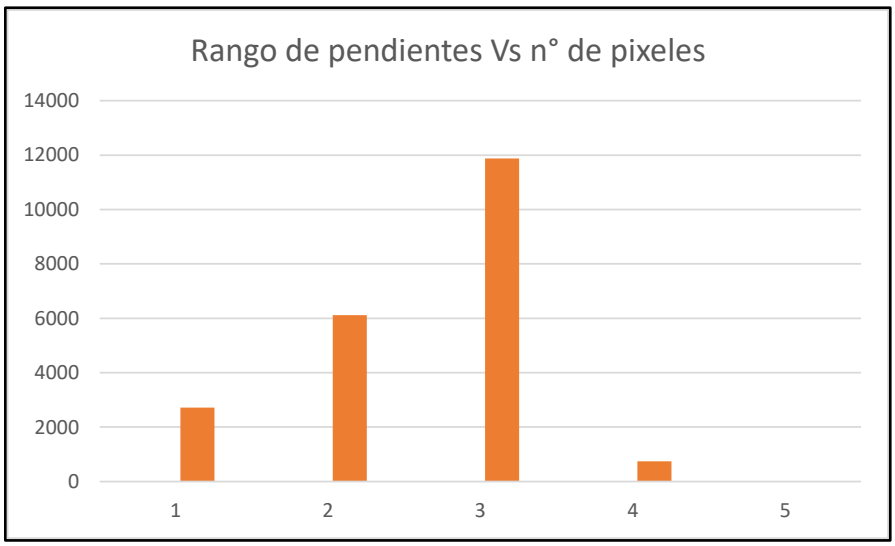

Illustration 4.1-28. Histogram number of pixels Vs range of slopes.
Source: INGEX, 2015.

Table 4.1-2 shows the percentage of each of the slope ranges in the study area.

Table 4.1-2. Percentage each of the ranges.

CATEGORY	TOPOGRAPHICAL SLOPE RANGE (%)	PERCENTAGE (%)	DESCRIPTION
1	0 – 15%	13	Very soft
2	15% - 30%	29	Soft
3	30% - 50%	55	Moderate
4	50% - 100%	3	High
5	>100%	0	Very high

Source: INGEX, 2015.

From the histogram and the summary table, it is established that the greatest number of pixels according to areas corresponds to category 3, which belongs to the moderate slopes (30% to 50%), with representation of 55%.

4.1.2.2.3 Morph dynamic processes

Morph dynamic processes identify areas of greater susceptibility to mass movements, mainly under extreme conditions such as heavy rains or possibly earthquakes.

The identification and description of the morph dynamic processes involved is a fundamental aspect that allows, among other variables, defining the viability of the projected structures according to their magnitude and degree of activity.

The main processes affecting the area are associated with lateral scour movements of the streams, as well as erosive processes such as terracotta and tears. This information can be corroborated in the map of erosion processes and in Annex 4.1 mass movement survey formats.

Lateral undercutting is the removal of material from the bed of a river bed or ravine due to the action of water flow. These materials are undermined in different ways depending on the type of soil: granular soils are quickly eroded because they have little compaction, while clay soils are more resistant to erosion because of their high material compaction.

Landslides involving soils are favored by runoff water and infiltration by secondary porosity, promoting the generation of flows by saturation of geological materials, increasing their natural density and lubricating the contact surfaces between slopes. Illustration 4.1-29 shows the parts and characteristics of a slide. Illustration 4.1-30 shows the special location of erosive processes, most of which are lateral undercutting of streams, which are described in the following sub-items.

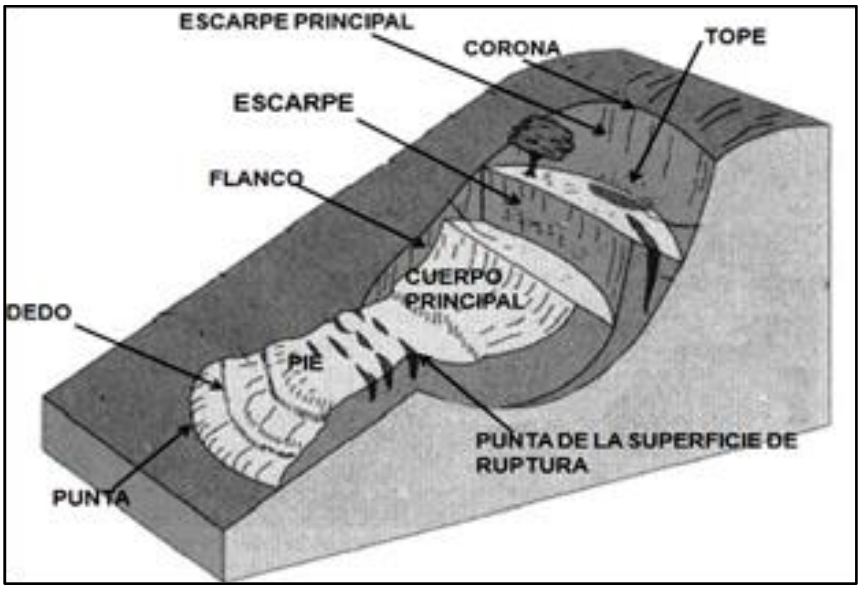

Illustration 4.1-29. The main parts of a slide.
Source: Modified from Gómez y Herrera, 2011.

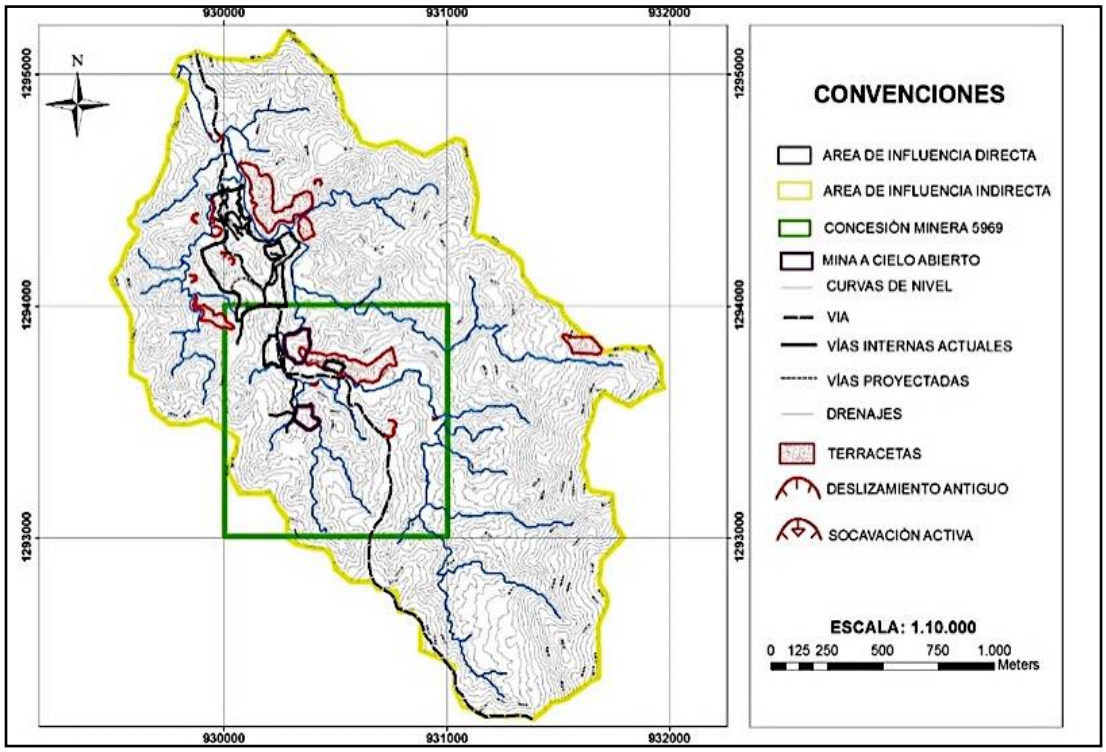

Illustration 4.1-30. Morph dynamic processes map, study area, scale 1:10000.
Source: INGEX, 2015.

Ancient erosive processes (scarred)

In the area corresponding to the mining concession 5969, scars of translational and rotational mass movements were observed. These processes are directly related to the action of gravity and the incidence of runoff water on the soil, where the materials are detached due to their own weight (saturation) and the slope conditions of the land. These crowns vary in length from 30.0 to 80.0 m in length and in some cases scarps of up to 3.0 m are identified (see Illustration 4.1-31). These areas are currently completely covered with vegetation, indicating an inactive state.

Illustration 4.1-31. The red lines indicate some of the crowns of the movements found in the study area (PV 15).
Source: INGEX, 2015.

Undercut processes

In the study area, five erosion type undercut processes were characterized, located on the margins of the tributaries of the El Pescado stream. These processes have crowns with variable lengths between 20.0 m and 50.0 m and heights from 2.5 m to 20.0 m (See Illustration 4.1-31). Generally, the material released corresponds to alluvial deposits; the characteristics of each erosive scour type process are shown in Annex 4.1 mass movement survey formats.

Terraceta erosive processes

Erosion is a physical process of deterioration that occurs on the surface of the earth and constantly changes the shape of the landscape. Mainly this phenomenon is caused by the action of adverse physical factors and accelerated by inadequate human intervention. In the study zone, these processes are observed as terracotta caused by extensive cattle ranching, since the continuous walking of cattle forms cracks and marks in the soil, which help the runoff water to saturate the soil

and, added to this, their weight generates future occurrences of small landslides (See Illustration 4.1-32).

Illustration 4.1-32. Lateral undermining located on the right bank of a tributary of El Pescado Creek with a crown measuring approximately 50m.
Source: INGEX, 2015.

Illustration 4.1-33. The white lines indicate the terracotta on the slopes. PV 06, own register.
Source: INGEX, 2015.

Lamellar Erosion

Laminar erosion is the removal of a thin layer of soil, which is not very noticeable since the total amount of soil removed is small and is formed by the action of water knocking off soil particles. This

type of erosion only drags the top layer of the soil and is favored in soils with steep slopes, almost no vegetation and low organic matter content (see Illustration 4.1-34).

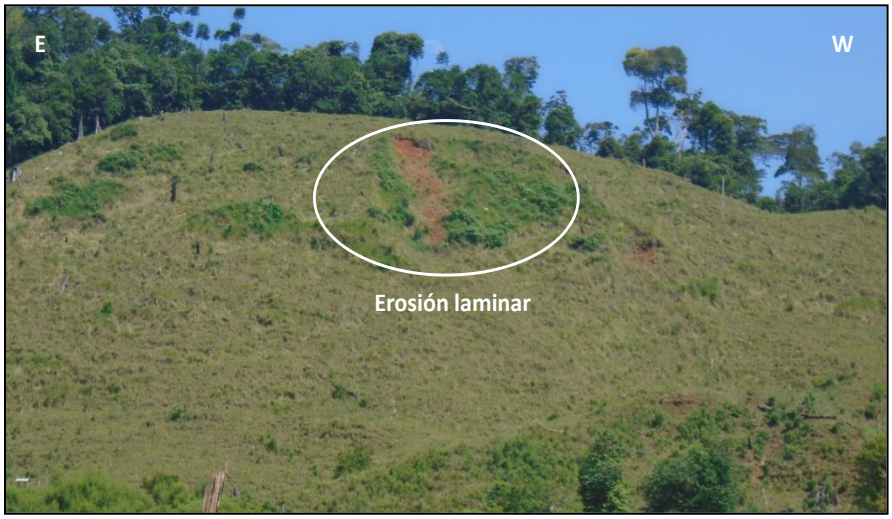

Illustration 4.1-34. The red circle indicates the laminar erosion present on the moderate slopes of the study area (PV 11).
Source: INGEX, 2015.

Multi-temporal analysis

Due to the little information found in the study area for multi-temporal analysis, only the aerial photographs presented in Table 4.1-3 were used:

Table 4.1-3. Land slope categories and ranges.

STRIP No	PHOTOGRAPHY No	SCALE	YEAR
13	181	1:10.200	2005
13	182	1:10.200	2005
13	183	1:10.200	2005
ORTOFOTO			2012

Source: INGEX, 2015.

For the photographs corresponding to strip No. 13, portions of the area without vegetation were identified as a result of the felling of trees, no active or latent morphodynamic processes indicating areas of instability were not identified, nor were any local or regional guidelines or faults identified. Illustration 4.1-35 details the areas resulting from deforestation.

By 2012, deforested areas were identified that cover a larger area than those identified in 2005. In the eastern zone of the area of direct influence, there is a sector with the presence of laminar erosion, which for the current conditions (based on the observations found in the field, 2015) this area is completely recovered. Neither were active erosion processes nor guidelines and faults observed (see Illustration 4.1-36).

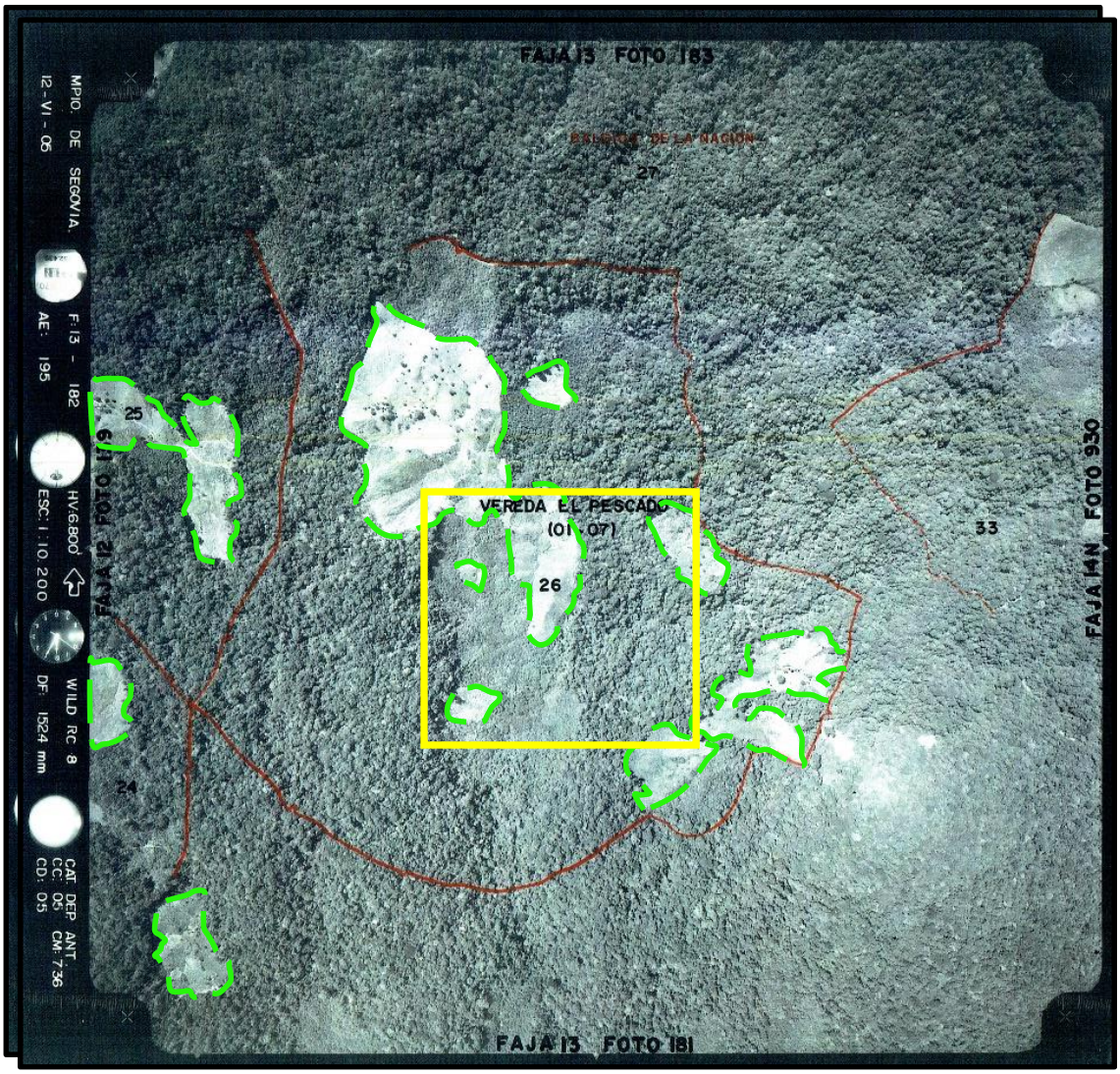

Illustration 4.1-35. Detail of the areas with no green line vegetation, the yellow polygon approaching the mining concession 5969.
Source: INGEX, 2015.

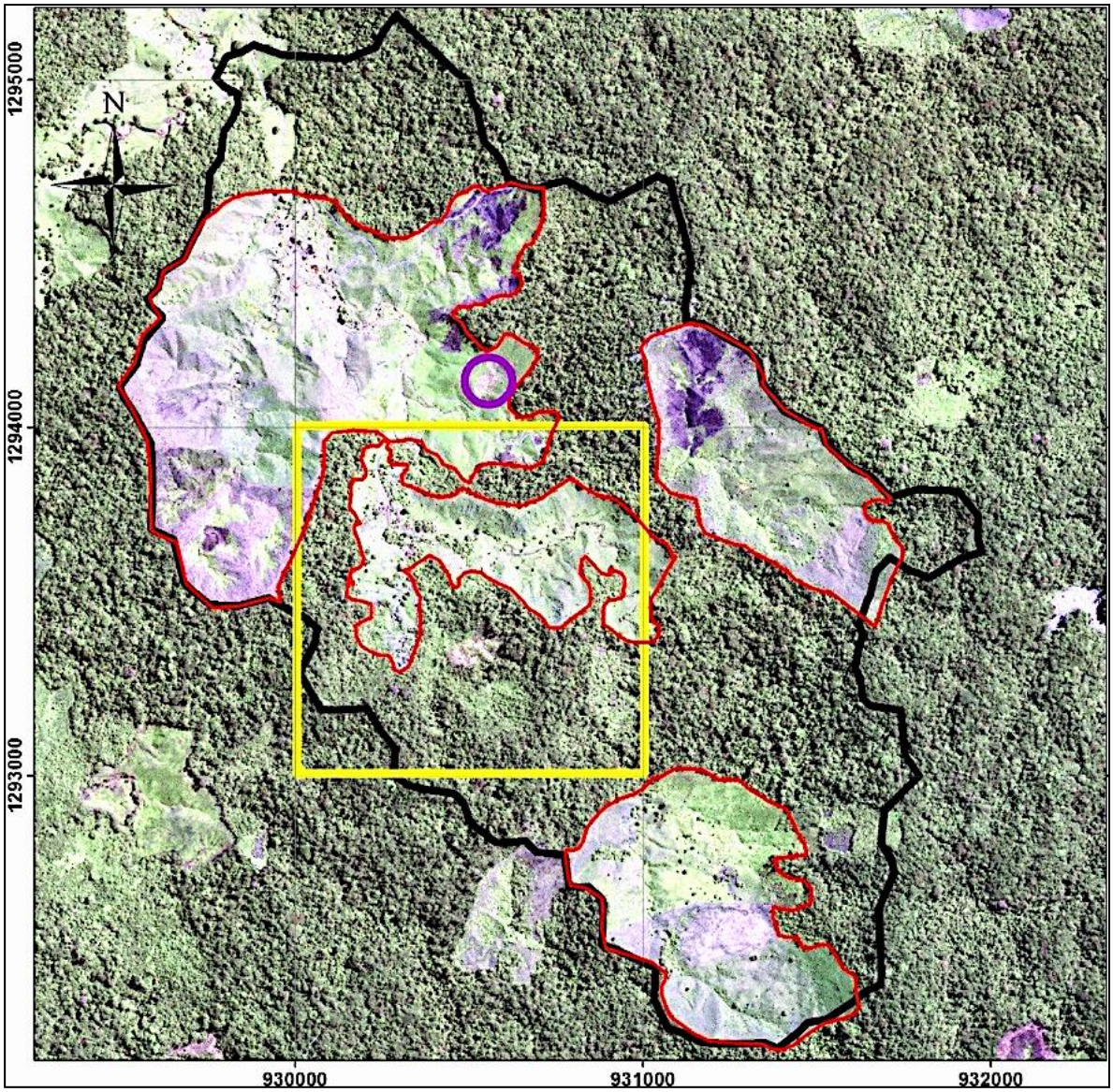

Illustration 4.1-36. Detail of the areas with no red line vegetation, purple circle laminar erosion zone and the yellow polygon mining concession 5969.

4.1.3 GEOTECHNICAL ENGINEERING

In order to identify the different materials, present in the subsoil, in 2005 it was necessary to carry out a direct exploration campaign and, in addition, an indirect campaign in 2015, in accordance with the terms of reference. Each of the explorations carried out in the geotechnical IAs is detailed below.

4.1.3.1 INDIRECT EXPLORATION, SEISMIC METHODS

The main objective of this test is the seismic characterization and complement of direct geotechnical exploration. For the execution of the seismic prospecting test, the methodology described in the standard (ASTM D6429-99, 2011) was used in combination with the manuals and procedures of the equipment manufacturer. Records or readings of surface waves were taken using natural noise or natural field, by executing excitations at different points on the line of geophones. This is for the purpose of advancing the passive Multichannel Analysis of Surface Waves (hereinafter MASW), which provides the depth cut-off wave propagation velocity profile as a result.

The method used is simple, it is done on the surface and manually for shallow drilling (it collects information up to approximately 50 meters), unlike the one applied in the hydrocarbon sector, which is required for deeper depths and to find oil reserves or oil-saturated media, using explosives as a source of wave emission (artificial field), requires access, modifies a change in land use and therefore generates environmental impacts. The following is an account of the applied seismic requirements:

- It does not require machinery, but the reading instruments presented below (see Illustration 4.1-37).
- There is no need for access due to the size of the meters or reading loggers.
- This type of seismic does not require drilling like the artificial field and no physical intervention of the soil or vegetation cover.
- Source of wave emission by means of vibration with a hammer and not by means of explosion shots as is done in the hydrocarbon sector.
- Therefore, it is not an economic activity that implies a change in the use of the land and less one that causes an impact against the environment.

• Seismograph (wave profile plotter). • Geophones (Transforms into an electrical signal analogous to the refractive waves they detect). • Cable connecting the geophones to the seismograph. • Battery. • Wave emission system (Wave emission by vibration application with hammer strike).	

Illustration 4.1-37. Reading instruments.
Source: INGEX, 2016.

The main purpose of the seismic test is to establish a relationship with the geological configuration of the subsoil. The velocity of propagation basically depends on the elastic constants and the density of the medium. Contacts between geological bodies with different seismic wave transmission rates. For indirect exploration, ten (10) seismic refraction lines were executed, distributed in the area of probable geotechnical intervention, through the implementation of infrastructure, cut and fill slopes. (See Illustration 4.1-38 and Illustration 4.1-39).

Illustration 4.1-38. Detail of seismic refraction line J.
Source: INGEX, 2016.

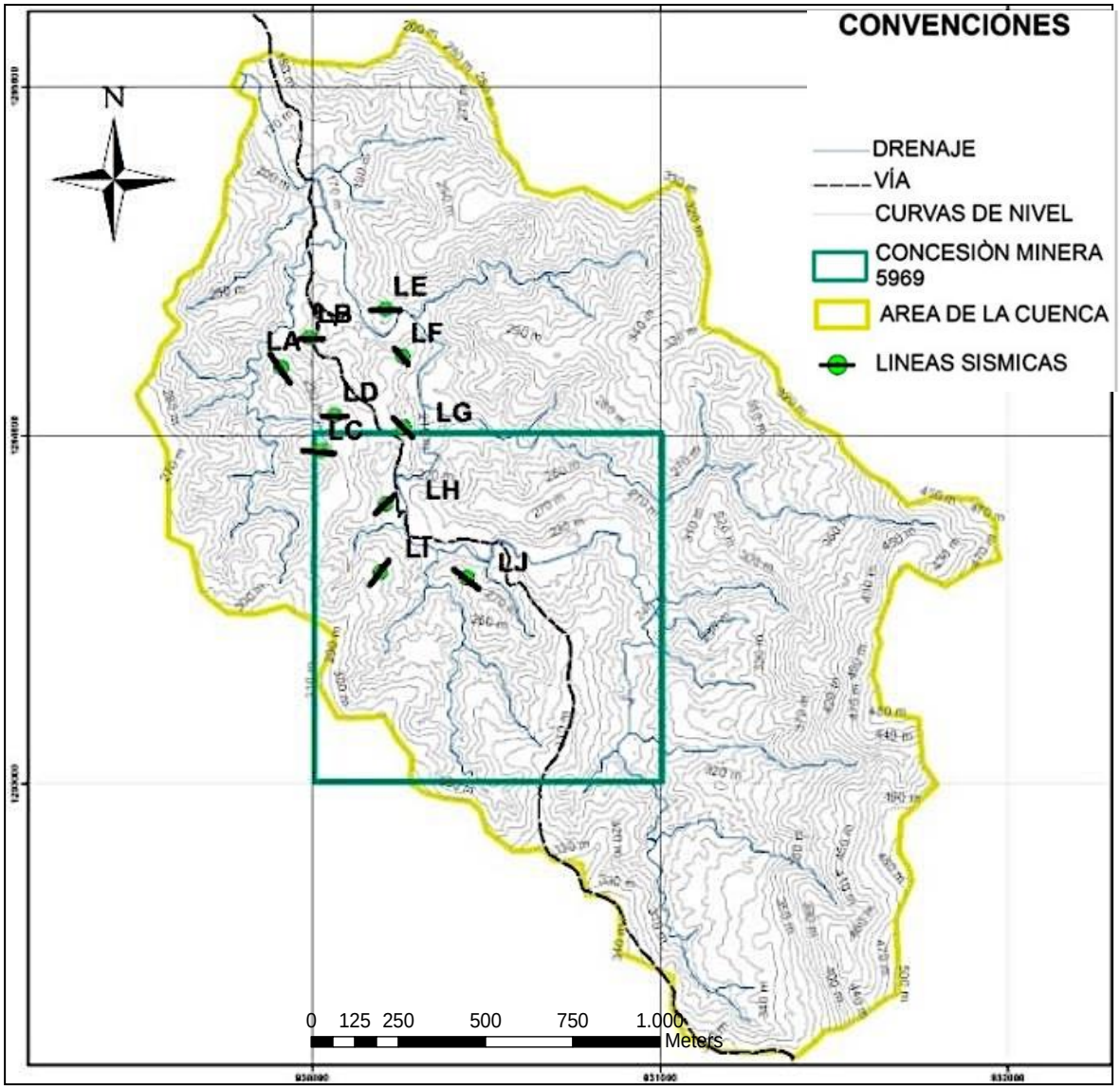

Illustration 4.1-39. Location of the lines of simian refraction.
Source: INGEX, 2016.

Results of seismic refraction lines

The six lines of seismic refraction executed, gave different values in the velocity (Vs, m/s) of wave with respect to the variation in depth (depth, m). The following illustrations graphically show this variation.

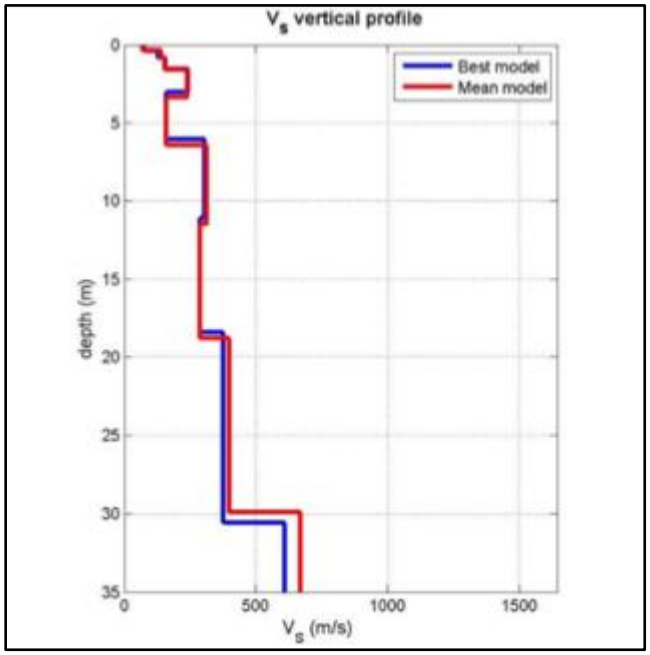

Illustration 4.1-40. Vs variation with respect to depth, seismic refraction line LA (LPS-1).
Source: IN SITU INGENIERÍA S.A.S, 2016.

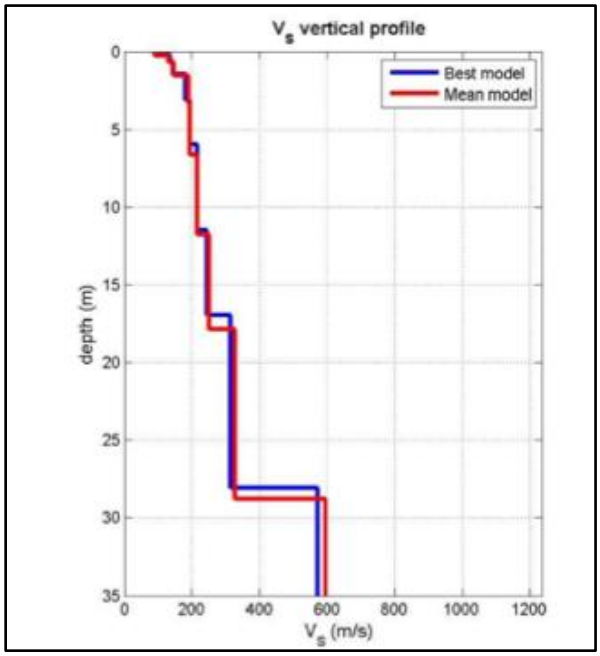

Illustration 4.1-41. Vs variation with respect to depth, seismic refraction line LB (LPS-2).
Source: IN SITU INGENIERÍA S.A.S, 2016.

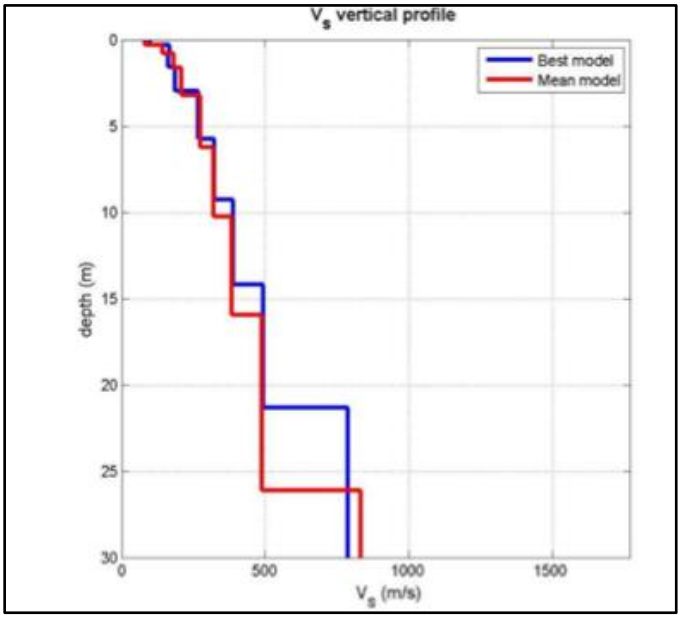

Illustration 4.1-42. Vs variation with respect to depth, seismic refraction line LC (LPS-3).
Source: IN SITU INGENIERÍA S.A.S, 2016.

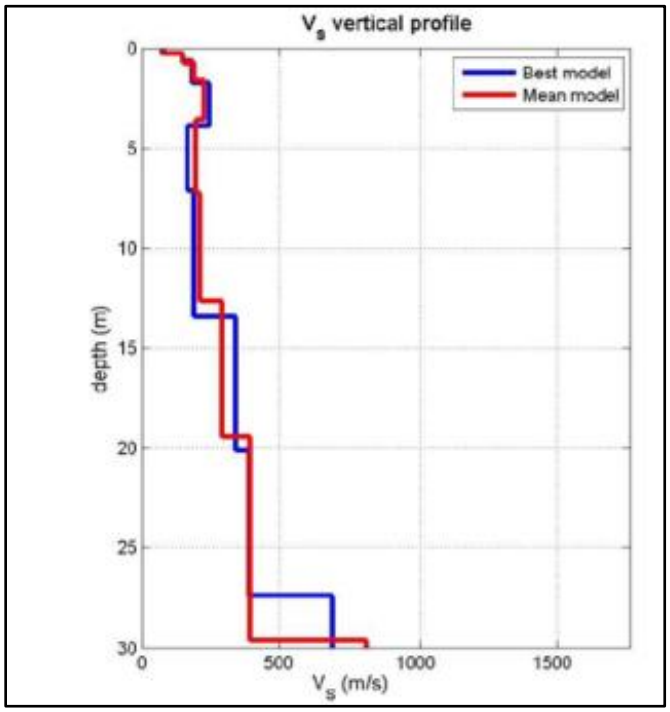

Illustration 4.1-43. Vs variation with respect to depth, seismic refraction line LD (LPS-4).
Source: IN SITU INGENIERÍA S.A.S, 2016.

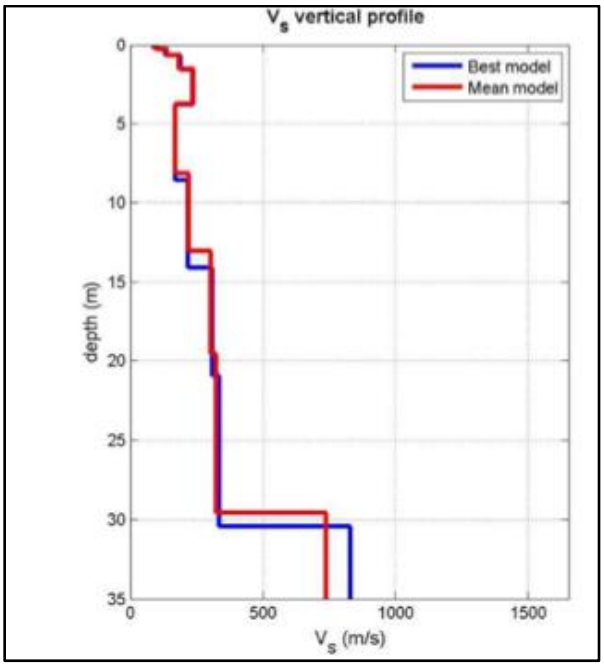

Illustration 4.1-44. Vs variation with respect to depth, seismic refraction line LE (LPS-5).
Source: IN SITU INGENIERÍA S.A.S, 2016.

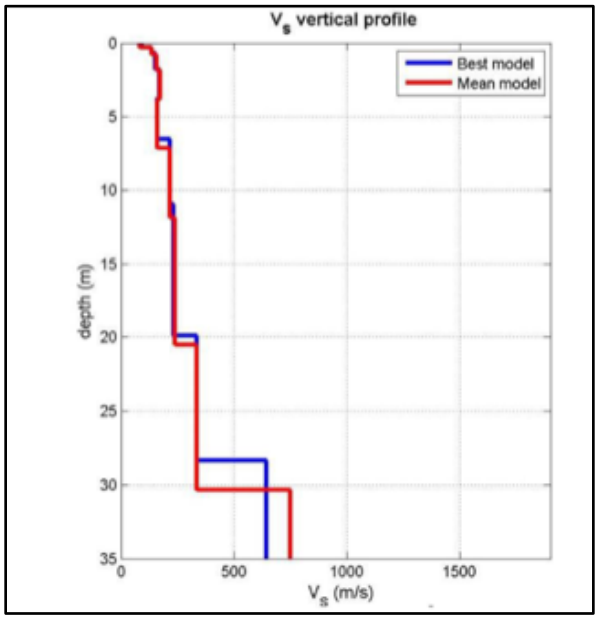

Illustration 4.1-45. Vs variation with respect to depth, seismic refraction line LF (LPS-6).
Source: IN SITU INGENIERÍA S.A.S, 2016.

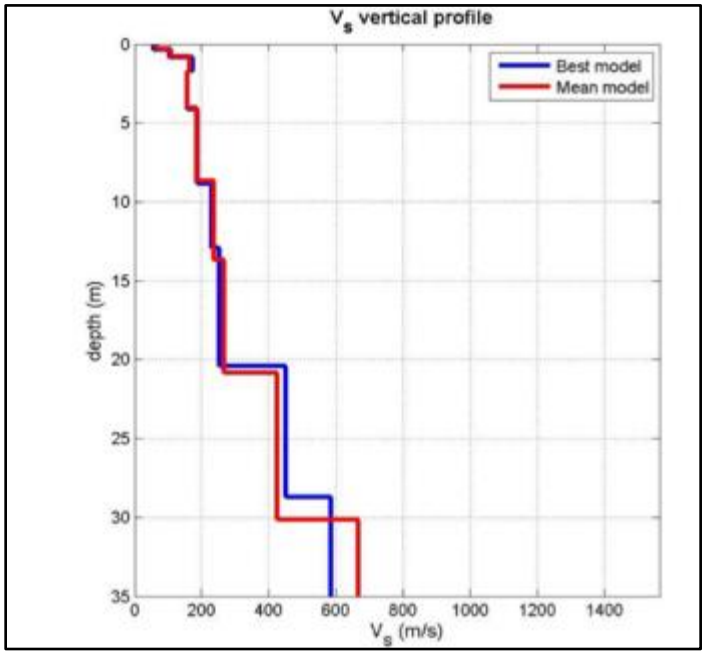

Illustration 4.1-46. Vs variation with respect to depth, seismic refraction line LG (LPS-7).
Source: IN SITU INGENIERÍA S.A.S, 2016.

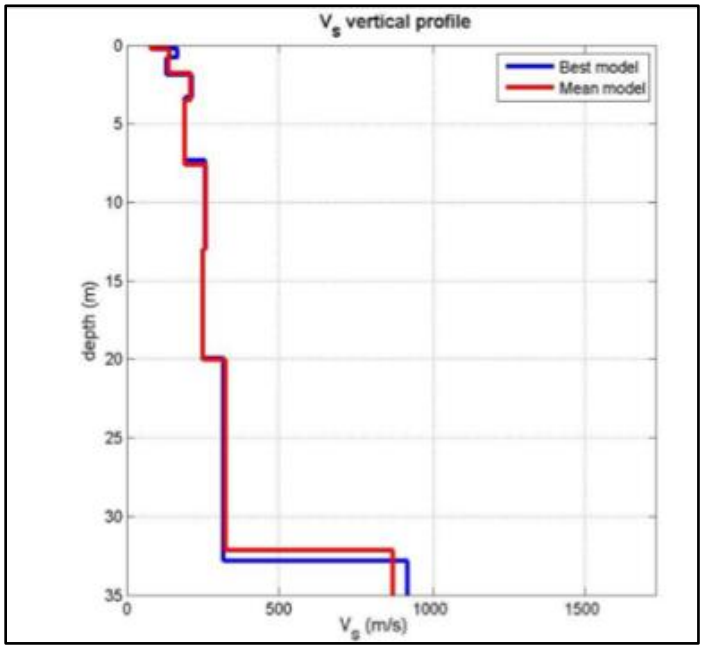

Illustration 4.1-47. Vs Variation relative to depth, seismic refraction line LH (LPS-8)
Source: IN SITU INGENIERÍA S.A.S, 2016.

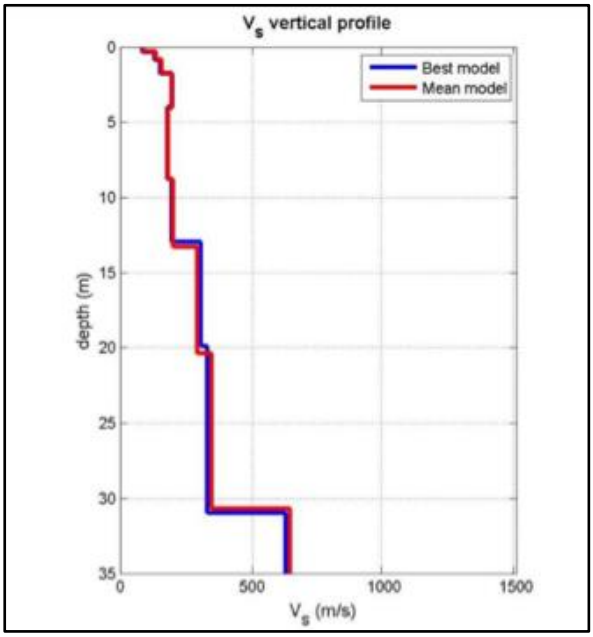

Illustration 4.1-48. Vs variation with respect to depth, seismic refraction line LI (LPS-9).
Source: IN SITU INGENIERÍA S.A.S, 2016.

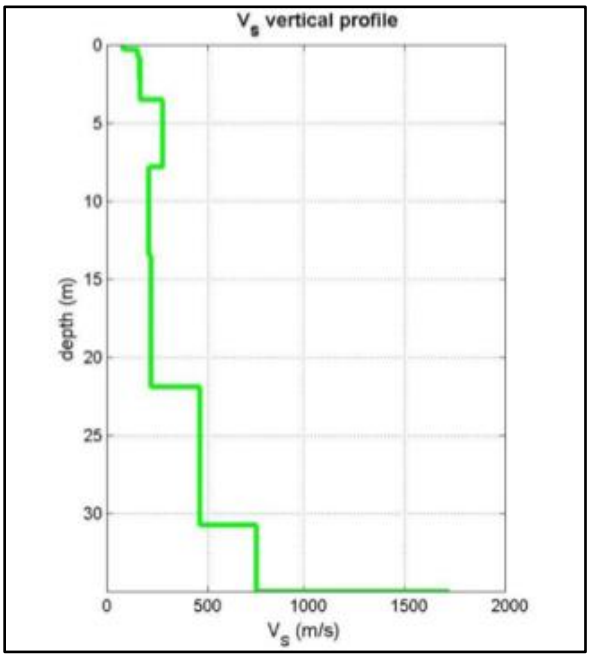

Illustration 4.1-49. Vs variation with respect to depth, seismic refraction line LJ (LPS-10).
Source: IN SITU INGENIERÍA S.A.S, 2016.

From the above graphs it can be deduced that for the first two meters the wave velocities vary between 90 and 200 m/s, from which the Vs value increases progressively to a depth of 30 m, where it reaches values close to 300 m/s. Clearly there is an increase in the wave velocity (700 m/s) at a depth of more than 30.0 m, where the rock is most likely to be in its fresh state. The interpretation of the tests is based on the cut-off wave velocities Vs obtained in the MASW test; Table 4.1 4 shows the relationship between the cut-off wave velocity and the type of soil, as proposed by the National Earthquake Hazards Reduction Program (NEHRP), based on the average cut-off wave velocity in the 30 m surface area (Vs 30).

Table 4.1-4. Seismic characterization of soils, NEHRP 2003.

TYPE	VS30 (M/S)	DESCRIPTION
A	> 1500	Hard rock
B	760 - 1500	Hard rock
C	360 - 760	Soft rock and very dense soil
D	180 - 360	Rigid ground
E	<180	Soft Soil
F	Special soils (liquefiable, collapsible, very plastic clays, organic soils)	

Source: INGEX, 2016.

Table 4.1-5 shows the provisions of Section A.2.4.4 of Title A of NSR-10, highlighting the type of profile to which the subsoil materials correspond.

Table 4.1-5. Detail of the soil profile to which the subsoil materials correspond.

Tipo de perfil	Descripción	Definición
A	Perfil de roca competente	$\bar{v}_s \geq 1500$ m/s
B	Perfil de roca de rigidez media	1500 m/s > $\bar{v}_s \geq 760$ m/s
C	Perfiles de suelos muy densos o roca blanda, que cumplan con el criterio de velocidad de la onda de cortante, o	760 m/s> $\bar{v}_s \geq 360$ m/s
	perfiles de suelos muy densos o roca blanda, que cumplan con cualquiera de los dos criterios	$\bar{N} \geq 50$, o $\bar{s}_u \geq 100$ kPa (≈1 kgf/cm²)
D	Perfiles de suelos rígidos que cumplan con el criterio de velocidad de la onda de cortante, o	360 m/s > $\bar{v}_s \geq 180$ m/s
	perfiles de suelos rígidos que cumplan cualquiera de las dos condiciones	50 > $\bar{N} \geq 15$, o 100 kPa (≈1 kgf/cm²) > $\bar{s}_u \geq 50$ kPa (≈0.5 kgf/cm²)
	Perfil que cumpla el criterio de velocidad de la onda de cortante, o	180 m/s > $\bar{v}_s$
E	perfil que contiene un espesor total **H** mayor de 3 m de arcillas blandas	**IP** > 20 **w** ≥ 40% 50 kPa (≈0.50 kgf/cm²) > $\bar{s}_u$
F	Los perfiles de suelo tipo **F** requieren una evaluación realizada explícitamente en el sitio por un ingeniero geotecnista de acuerdo con el procedimiento de A.2.10. Se contemplan las siguientes subclases: **F1** — Suelos susceptibles a la falla o colapso causado por la excitación sísmica, tales como: suelos licuables, arcillas sensitivas, suelos dispersivos o débilmente cementados, etc. **F2** — Turba y arcillas orgánicas y muy orgánicas (**H** > 3 m para turba o arcillas orgánicas y muy orgánicas). **F3** — Arcillas de muy alta plasticidad (**H** > 7.5 m con Índice de Plasticidad **IP** > 75) **F4** — Perfiles de gran espesor de arcillas de rigidez mediana a blanda (**H** > 36 m)	

Source: NSR-10

4.1.3.2 DIRECT EXPLORATION

The direct explorations of this component are presented as a result of the hydrogeological and geotechnical explorations carried out between 2003 and 2005 by the holders of the concession contract and Ingex Group Miners S.A.S. at that time. Reanalyzed and reinterpreted the analyses and results of the direct explorations mentioned above.

For the corresponding study area, nine (9) exploratory percussion-type soundings were carried out (see Illustration 4.1-50), in order to obtain the number of strokes in the field by means of the Standard Penetration Test (hereinafter SPT) and the physical extraction of samples for subsequent laboratory analysis. The SPT test consisted of measuring the number of strokes required to introduce a very robust bucket (cylindrical and hollow) (external diameter 51 millimeters and internal diameter 35 millimeters, i.e. an area ratio greater than 100) at a given depth. This allowed a sample, naturally altered, to be taken from the inside.

The split barrel sampler is driven into the ground with hammer blows at the top of the drill rod. The weight of the hammer is normalized, as well as the free fall height, being 0.62 kN and 762 mm, respectively (paragraph 5.4.1 of ASTM D 1586-92) (See Illustration 4.1-51).

During the test, the number of strokes required to drive the spoon in the first 150 mm was counted and recorded. Subsequently, it continued to be introduced every 150 mm, until it reached 450 mm, noting the number of strokes required for driving in each 150 mm penetration interval. The test result or standard penetration resistance corresponds (NSPT value) to the number of strokes required to penetrate the bucket (splitbarrelsampler) 305 mm after the initial 150 mm penetration.

If the number of strokes required to deepen in any of these 150 mm intervals is greater than 50, the result of the test is no longer the sum indicated above, but becomes rejection (R), and the length driven in the section in which the 50 strokes have been reached must also be recorded. The SPT test at this point is considered complete when this value is reached. (For example, if 50 strokes have been reached in 120 mm in the interval between 15 and 30 centimeters, the result should be indicated as: N0-15/50 in 120 mm, R.

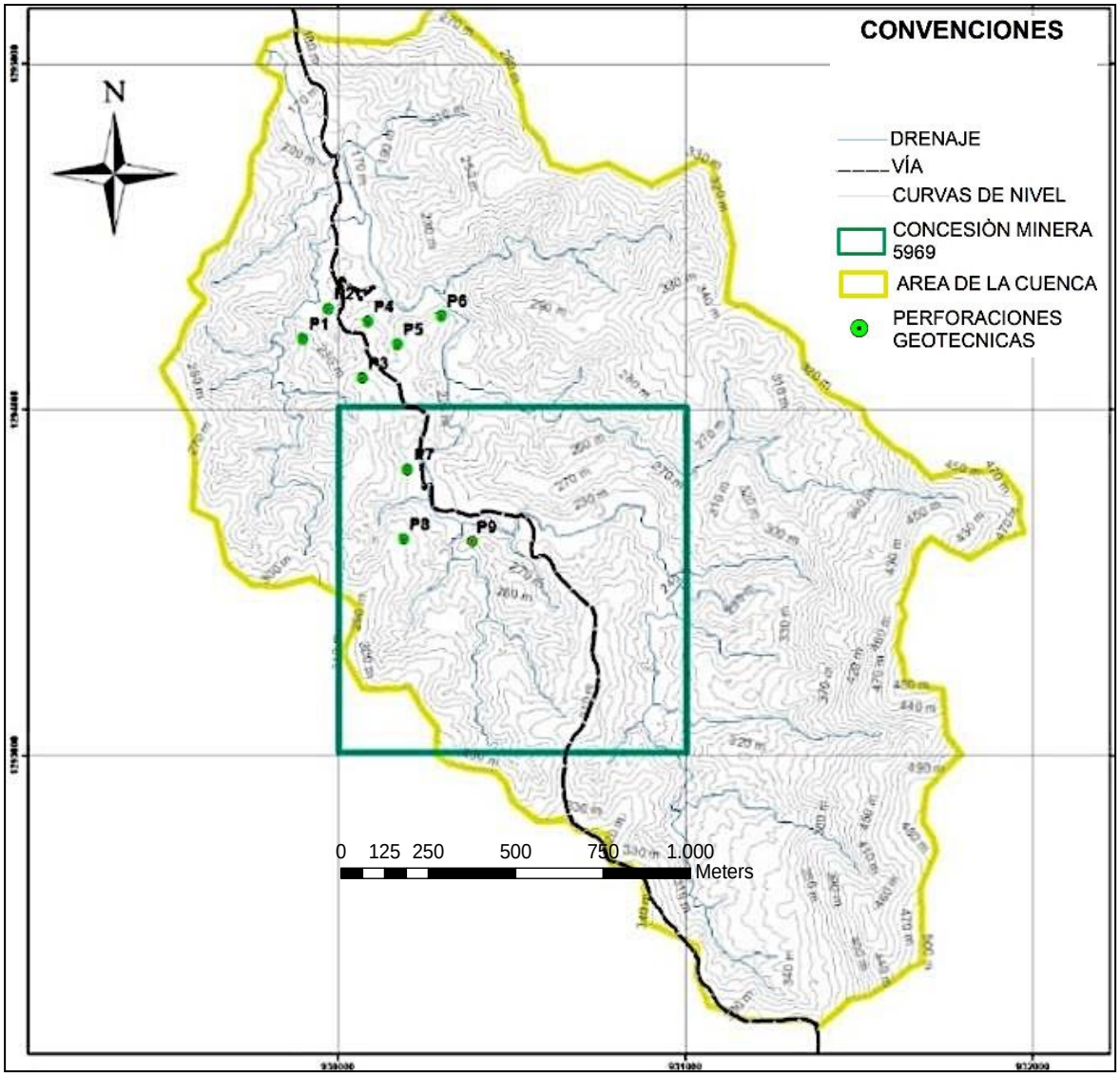

Illustration 4.1-50. Location of geotechnical boreholes, mining title 5969.
Source: Touchstone 2003.

Illustration 4.1-51. Detail of the execution of the SPT test in the field. Survey No. 4.
Source: Touchstone 2003.

4.1.3.2.1 Field penetration test results (spt)

First the value of Nspt was corrected to obtain the N55. From N55 the equivalent angle of friction was calculated using the expressions recommended by Kishida (1970) and JRB (Japan Road Bureau);

Kishida $$\emptyset' eq = 15 + (12{,}5 * N_{45})^{0{,}5}$$

Japan Road Bureau (JRB) $$\emptyset' eq = 15 + (9{,}375 * N_{45})^{0{,}5}$$

Subsequently, the linear regression proposed by González (1988) was carried out to obtain the soil mechanical parameters. From Table 4.1 6 to Table 4.1 14, the equivalent phi values obtained in each of the drillings and the results obtained in each of the mentioned expressions are presented:

Table 4.1-6. Values from Ø' equivalent using Kishida and JRB Vs depth. Drilling 1.

MATERIAL	SAMPLING DEPTH OF THE SAMPLE		STANDARD PENETRATION TEST NSPT	Ø' (JRB) GRADES	Ø' (KISHIDA) GRADES
	INICIAL (m)	FINAL (m)			
Residual soil	1,00	1,5	6	22,44	23,59
	2,0	2,5	14	25,6	27,3
Saprolite	3,0	3,5	15	25,4	26,98
	4,0	4,5	10	23,6	24,88
	5,0	5,5	15	25,0	26,53
	6,0	6,5	24	27,8	29,76
	7,0	7,5	29	28,5	30,59
	8,0	8,5	28	27,8	29,76

MATERIAL	SAMPLING DEPTH OF THE SAMPLE		STANDARD PENETRATION TEST NSPT	Ø' (JRB) GRADES	Ø' (KISHIDA) GRADES
	INICIAL (m)	FINAL (m)			
	9,0	9,5	46	30,8	33,27
	10,0	10,5	36	28,9	31,06
	11,0	11,5	94	36,8	40,17

Source: Modified by Touchstone 2003.

Table 4.1-7. Values from Ø' equivalent using Kishida and JRB Vs depth. Drilling 2.

MATERIAL	SAMPLING DEPTH OF THE SAMPLE		STANDARD PENETRATION TEST NSPT	Ø' (JRB) GRADES	Ø' (KISHIDA) GRADES
	INITIAL (m)	FINAL (m)			
Residual soil	1,0	1,5	26	30,52	32,92
	2,0	2,5	50	35,1	38,2
	3,0	3,5	36	31,1	33,58
	4,0	4,5	53	34,7	37,76
	5,0	5,5	46	32,5	35,21
	6,0	6,5	98	40,9	44,86

Table 4.1-8. Values from Ø' equivalent using Kishida and JRB Vs depth. Drill hole 3.

MATERIAL	SAMPLING DEPTH OF THE SAMPLE		STANDARD PENETRATION TEST NSPT	Ø' (JRB) GRADES	Ø' (KISHIDA) GRADES
	INITIAL (m)	FINAL (m)			
Residual soil	1,0	1,5	12	25,57	27,20
	2,0	2,5	4	20,71	21,59
Saprolite	3,0	3,5	4	20,39	21,22
	4,0	4,5	6	21,67	22,70
	5,0	5,5	20	26,61	28,40
	6,0	6,5	33	30,10	32,43
	7,0	7,5	102	40,50	44,45

Source: Modified byTouchstone 2003.

Table 4.1-9. Values from Ø' equivalent using Kishida and JRB Vs depth. Drill hole 4.

MATERIAL	SAMPLING DEPTH OF THE SAMPLE		STANDARD PENETRATION TEST NSPT	Ø' (JRB) GRADES	Ø' (KISHIDA) GRADES
	INITIAL (m)	FINAL (m)			
Residual soil	1,00	1,5	6	22,44	23,59
	2,0	2,5	14	25,6	27,3
Saprolite	3,0	3,5	15	25,4	26,98
	4,0	4,5	10	23,6	24,88
	5,0	5,5	15	25,0	26,53
	6,0	6,5	24	27,8	29,76
	7,0	7,5	29	28,5	30,59
	8,0	8,5	28	27,8	29,76
	9,0	9,5	46	30,8	33,27
	10,0	10,5	36	28,9	31,06
	11,0	11,5	94	36,8	40,17

Source: Modified by Touchstone 2003.

Table 4.1-10. Values from Ø' equivalent using Kishida and JRB Vs depth. Drill hole 5.

MATERIAL	SAMPLING DEPTH OF THE SAMPLE		STANDARD PENETRATION TEST NSPT	Ø' (JRB) GRADES	Ø' (KISHIDA) GRADES
	INITIAL (m)	FINAL (m)			
Residual soil	1,00	1,5	16	27,17	29,05
	2,0	2,5	10	23,99	25,38
Saprolite	3,0	3,5	8	22,58	23,75
	4,0	4,5	9	23,11	24,37
	5,0	5,5	8	22,29	23,42
	6,0	6,5	16	25,43	27,05
	7,0	7,5	13	24,03	25,43
	8,0	8,5	34	29,07	31,25
	9,0	9,5	96	37,84	41,38

Source: Modified by Touchstone 2003.

Table 4.1-11. Values from Ø' equivalent using Kishida and JRB Vs depth. Drill hole 6.

MATERIAL	SAMPLING DEPTH OF THE SAMPLE		STANDARD PENETRATION TEST NSPT	Ø' (JRB) GRADES	Ø' (KISHIDA) GRADES
	INITIAL (m)	FINAL (m)			
Residual Soil	1,00	1,5	5	21,80	22,86
Saprolite	2,0	2,5	8	23,04	24,29
	3,0	3,5	10	23,47	24,78
	4,0	4,5	10	23,55	24,88
	5,0	5,5	10	23,15	24,41
	6,0	6,5	14	24,76	26,27
	7,0	7,5	16	25,02	26,57
	8,0	8,5	18	25,24	26,82
	9,0	9,5	17	24,61	26,10
	10,0	10,5	87	36,60	39,94

Source: Modified by Touchstone 2003.

Table 4.1-12. Values from Ø' equivalent using Kishida and JRB Vs depth. Drilling 7.

MATERIAL	SAMPLING DEPTH OF THE SAMPLE		STANDARD PENETRATION TEST NSPT	Ø' (JRB) GRADES	Ø' (KISHIDA) GRADES
	INITIAL (m)	FINAL (m)			
Saprolite	1,0	1,5	8	23,61	24,94
	2,0	2,5	20	27,72	29,68
	3,0	3,5	24	28,13	30,16
	4,0	4,5	25	28,52	30,61
	5,0	5,5	30	29,12	31,30
	6,0	6,5	45	32,50	35,20

Source: Modified by Touchstone 2003.

Table 4.1-13. Values from Ø' equivalent using Kishida and JRB Vs depth. Drill hole 8.

MATERIAL	SAMPLING DEPTH OF THE SAMPLE		STANDARD PENETRATION TEST NSPT	Ø' (JRB) GRADES	Ø' (KISHIDA) GRADES
	INITIAL (m)	FINAL (m)			
Residual soil	1,00	1,5	4	21,07	22,01
	2,0	2,5	6	21,94	23,01
Saprolite	3,0	3,5	7	22,05	23,14
	4,0	4,5	8	22,60	23,78
	5,0	5,5	12	23,87	25,24
	6,0	6,5	18	25,98	27,68
	7,0	7,5	18	25,54	27,18
	8,0	8,5	22	26,23	27,96
	9,0	9,5	22	25,84	27,52
	10,0	10,5	29	27,36	29,27
	11,0	11,5	36	28,35	30,41
	12,0	12,5	94	35,95	39,20

Source: Modified by Touchstone 2003.

Table 4.1-14. Values from Ø' equivalent using Kishida and JRB Vs depth. Drill 9.

MATERIAL	SAMPLING DEPTH OF THE SAMPLE		STANDARD PENETRATION TEST NSPT	Ø' (JRB) GRADES	Ø' (KISHIDA) GRADES
	INITIAL (m)	FINAL (m)			
Residual soil	1,00	1,5	4	21,07	22,01
	2,0	2,5	13	25,21	26,79
	3,0	3,5	14	24,97	26,52
Saprolite	4,0	4,5	10	23,50	24,82
	5,0	5,5	10	23,10	24,35
	6,0	6,5	15	25,03	26,58
	7,0	7,5	21	26,39	28,15
	8,0	8,5	24	26,73	28,54
	9,0	9,5	23	26,08	27,80
	10,0	10,5	26	26,70	28,51
	11,0	11,5	96	36,80	40,17

Source: Modified by Touchstone 2003.

In order to obtain a more precise equivalent average value of Φ, all the values obtained in the nine (9) surveys carried out were taken (See Table 4.1-15).

Table 4.1-15. Values from Ø' equivalent using the expressions of Kishida and JRB, for each of the materials.

MATERIAL	Φ JRB EQUIVALENT (DEGREES)	Φ KISHIDA EQUIVALENT (DEGREES)
Residual soil	25,5	32,2
Saprolite	28,0	31,8

Source: Modified by Touchstone 2003.

After performing the linear regression, the equivalent parameter Ø' is obtained using the two methodologies (Kishida and JRB) for each of the defined materials (see Table 4.1-16).

Table 4.1-16. Expressions of the linear regression proposed by González

MATERIAL	Φ EQUIVALENT (DEGREES)
Residual soil	27,7
Saprolite	36,7

Source: Modified by Touchstone 2003.

4.1.3.2.2 Geotechnical laboratory test results

In order to obtain the soil mechanical parameters of materials with a cohesive and frictional behavior, several laboratory tests were carried out, corresponding to the geotechnical classification and the direct cut tests type CU (Consolidated not drained), following the guidelines of the Standards of the National Roads Institute (INVIAS) and the ASTM (American Society for Testing Materials) standards. Table 4.1-17 shows the number of samples, the type of test and the depth from which they were taken from each of the holes.

Table 4.1-17. Tests executed on the samples taken from the different soundings

POLL Nº	SAMPLE	DEPTH (m)	TEST
P1	M1	1,0 – 1,5	Humidity, granulometry, consistency limits
	M2	2,0 – 2,5 (Shelby)	Direct cutting, CU
	M4 y M7	4,0 – 7,5	Humidity, granulometry, consistency limits
P2	M3, M4 y M5	3,0 – 5,5	Humidity, granulometry, consistency limits
P3	M1	1,0 – 1,5	Humidity, granulometry, consistency limits
	M2	2,0 – 2,5 (Shelby)	Direct cutting, CU
	M4, M5 y M6	4,0 - 6,5	Humidity, granulometry, consistency limits
P4	M1	1,0 – 1,5 (Shelby)	Direct cutting, CU
	M2	2,0 – 2,5	Humidity, granulometry, consistency limits
	M7, M8 M9 y M10	7,0 – 10,5	Humidity, granulometry, consistency limits
|P5	M1 y M2	1,0 – 2,5	Humidity, granulometry, consistency limits
	M3	3,0 – 3,5 (Shelby)	Direct cutting, CU
	M6, M7 y M8	6,0 – 8,5	Humidity, granulometry, consistency limits
P6	M1	1,0 – 1,5	Humidity, granulometry, consistency limits
	M3	3,0 – 3,5 (Shelby)	Direct cutting, CU
	M5, M6 y M7	5,0 – 7,5	Humidity, granulometry, consistency limits
P7	M3	3,0 – 3,5 (Shelby)	Direct cutting, CU
	M4, M5 y M6	4,0 – 6,5	Humidity, granulometry, consistency limits
P8	M1 y M2	1,0 – 2,5	Humidity, granulometry, consistency limits
	M5	5,0 – 5,5	Direct cutting, CU
	M10, M11 y M12	10,0 – 12, 5	Humidity, granulometry, consistency limits
P9	M1	1,0 – 1,5	Humidity, granulometry, consistency limits
	M2	2, 0 – 2,5 (Shelby)	Direct cutting, CU
	M8, M9 y M10	8,0 – 10, 5	Humidity, granulometry, consistency limits

Source: Modified by Touchstone 2003.

The results of the geotechnical classification tests are shown below for each of the samples taken (see Table 4.1-18).

Table 4.1-18. Results of geotechnical classification tests.

MATERIAL	POLL	DEPTH	MEDIUM DEPTH	GEOTECHNICAL SORT		% FINES
				AASTHO	ASTM	
Residual soil	P1	1 - 1,5	1,0	A - 4	CL - ML	52,5
	P2	3 - 5,5	4,0	A - 4	ML	51,5
	P3	1 - 1,5	1,0	A - 75	MH	66,6
	P4	2 - 2,5	2,0	A - 5	ML	53,7
	P5	1 - 2,5	1,5	A - 75	MH	40
	P6	1 - 1,5	1,0	A - 75	ML	75,9
	P8	1 - 1,5	2,0	A - 75	MH	57,6
	P9	1 - 1,5	1,0	A - 5	ML	79,1
Saprolite	P1	4 - 7,5	5,5	A - 4	ML	60,6
	P3	4 - 6,5	5,0	A -4	SM	42,8
	P4	7 - 10,5	8,5	A -4	SM	49,6
	P5	6 - 8,50	7,0	A - 5	ML	39
	P6	5 - 7,50	6,0	A - 5	MH	91,2
	P7	4 - 6,50	5,0	A - 4	ML	82,6
	P8	10 -12,50	11,0	A - 4	ML	56,6
	P9	8 - 10,5	9,0	A - 5	MH	56,2

Source: Modified by2233. Direct cutting, CU *Touchstone 2003.*

Below are the results of the direct cutting tests performed on different samples of the different types of material (residual soil and saprolite). The mean and standard deviation values of the soil mechanical parameters were used for the execution of the stability analyses (see Table 4.1-19).

Table 4.1-19. Soil mechanical parameters for materials identified in the field work

MATERIAL	Poll Nº	ɣ (KN/M³)	C (kPa)	ϕ (º)	MEDIA			STANDARD DEVIATION		
					ɣ (KN/M3)	C (kPa)	ϕ (º)	ɣ (KN/M3)	C (kPa)	ϕ (º)
Residual soil	P1	17,15	18,7	33	17,15	27,20	32,80	0,42	11,33	2,60
	P3	16,76	28,6	31,1						
	P4	16,95	18,8	36,4						
	P9	17,74	42,7	30,7						
Saprolite	P7	17,25	28,2	32,2	17,49	30,55	31,95	0,35	3,32	0,35
	P8	17,74	32,9	31,7						

Source: Modified by Touchstone 2003.

It should be noted that the stability analyses were carried out using a statistical method (Monte Carlo), for which reason all the values of the Soil mechanical parameters obtained from all the direct cutting tests carried out were taken in order to obtain a geological/geotechnical model.

4.1.3.2.3 Stability analysis

The stability analyses were performed using the limit equilibrium methodology which is briefly described below:

This stability analysis consists of determining whether there is sufficient strength in the slope soils to withstand the shear stresses that tend to cause failure or slippage. Most of the equilibrium limit methods have the comparison of the forces or moments of resistance and actuation on a given fault surface in common. The main variations of the various methods are the type of fault surface and how the forces act internally on the fault surface. (SUÁREZ, 2006), the results are expressed in terms of safety factors.

This methodology is based on the selection of a theoretical slope breakage surface; the Mohr-Coulomb breakage criterion; and the definition of a safety factor. For the stability analyses carried out in this report, the methods of Spencer, Morgestern & Price and Janbú were used, the latter being the most conservative, since in its mathematical expression it discriminates between the frictional forces between the segments, on the contrary, the Morgestern & Price method takes this force into account, making it a more rigorous method. The SLIDE 6.0 software from Rockscience was used to carry out the stability analyses of the different systems.

Pseudostatic Analysis

Based on the information gathered between the 2004 - 2005 Ingex Grupo Minero S.A.S. reanalyzed the information according to the Earthquake - Colombian Resistant Standard 2010 (hereinafter NSR-10), the municipality of Segovia is framed within an intermediate seismic threat zone.

Based on the provisions of the Standard and for design purposes, effective peak acceleration (Aa) value of 0.11 was used.

For the pseudo static stability analysis, implementing the stability works, a horizontal acceleration coefficient of 0.11g, equivalent to Aa's ¾, was defined for an earthquake with a return period of 475 years.

The Safety Factors were validated based on the permissible limit value criteria for basic safety factors suggested in Chapter H.3 of NSR-10 (see Table 4.1-20 and Table 4.1-21).

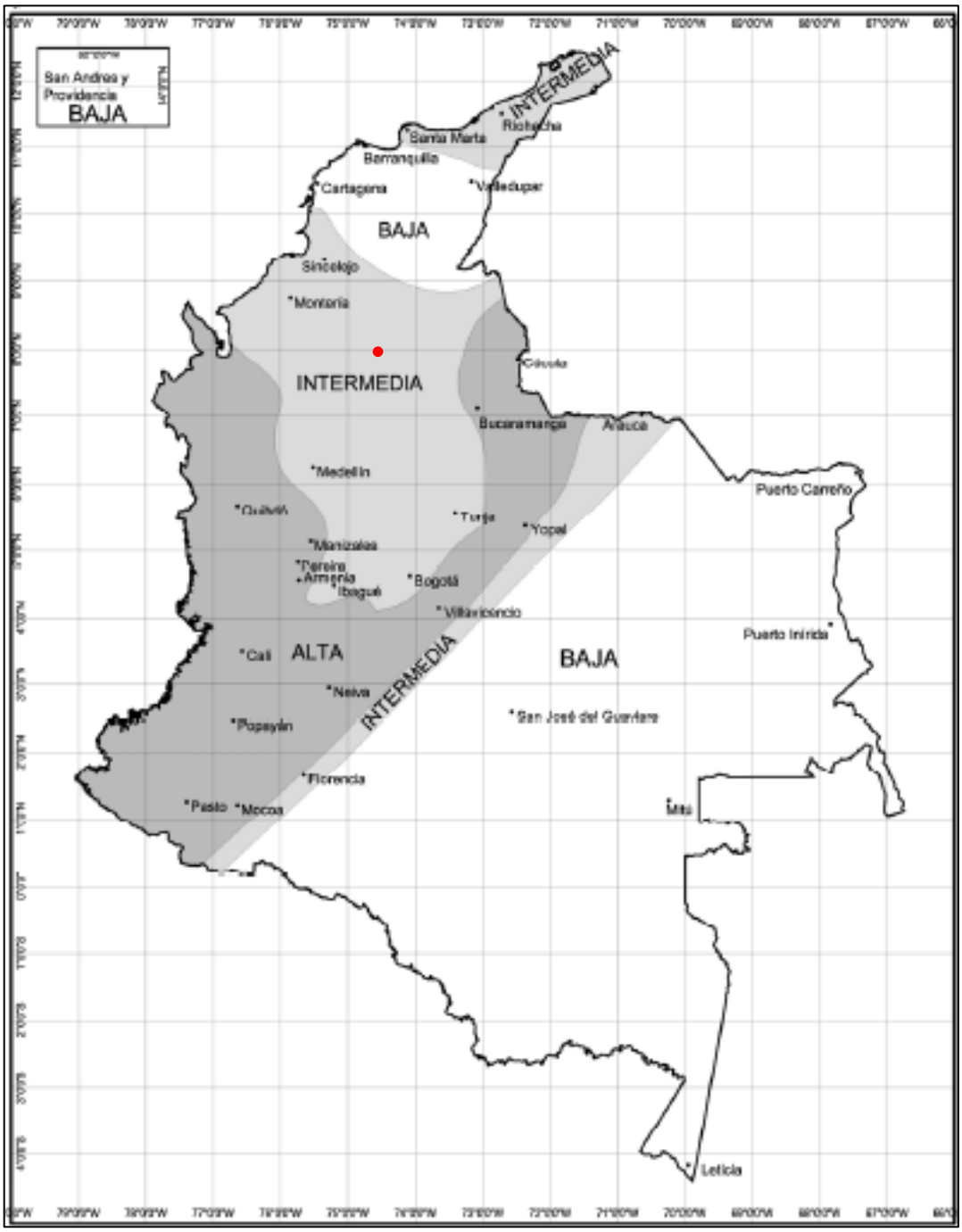

Illustration 4.1-52. Seismic Threat Zones applicable to buildings for NSR-10 at function of Aa and Av. The red dot indicates approximately where the municipality of Segovia Antioquia is located.
Source: Title A NSR-10

Table 4.1-20. Basic safety factors Table H.2.4-1 NSR-10.

CONDITION	DESIGN	CONSTRUCTION
Slope - static situation with normal groundwater.	1.50	1.25
Slope - pseudo-static situation with normal groundwater and design seismic coefficient.	1.05	1.00 (*)
(*)	The pseudo-static seismic construction parameters will be 50% of the design parameters.	

(*) The pseudo-static seismic construction parameters will be 50% of the design parameters. The parameters established within NSR-10 are similar to the Safety Factors presented by USACE 2003.

Table 4.1-21. Safety factor rating ranges for the static and dynamic case (US Army Corps of Engineers, October 2003).

SORTING	F.S. STATIC	F.S. STATIC PSEUDO
Inadmissible	<0.75	<0.5
Very low	0.75 - 1.0	0.50 - 0.75
Low	1.0 – 1.25	0.75 – 1.0
Acceptable	1.25 – 1.50	1.0 - 1.25
Ideal	>1.50	>1.25

Source: INGEX, 2016.

It should be noted that the stability analyses carried out did not use variations in groundwater levels, since in the hydrogeological exploration carried out in the field, no groundwater line was detected.

4.1.3.3 GEOLOGICAL GEOTECHNICAL PROFILES (GEOLOGICAL - GEOTECHNICAL MODEL)

The geotechnical geological profiles were obtained from the definition of five sections within the mining concession 5969. These sections were located in areas with high and very high slopes. Illustration 4.1-53 shows the sections used for the different stability analyses.

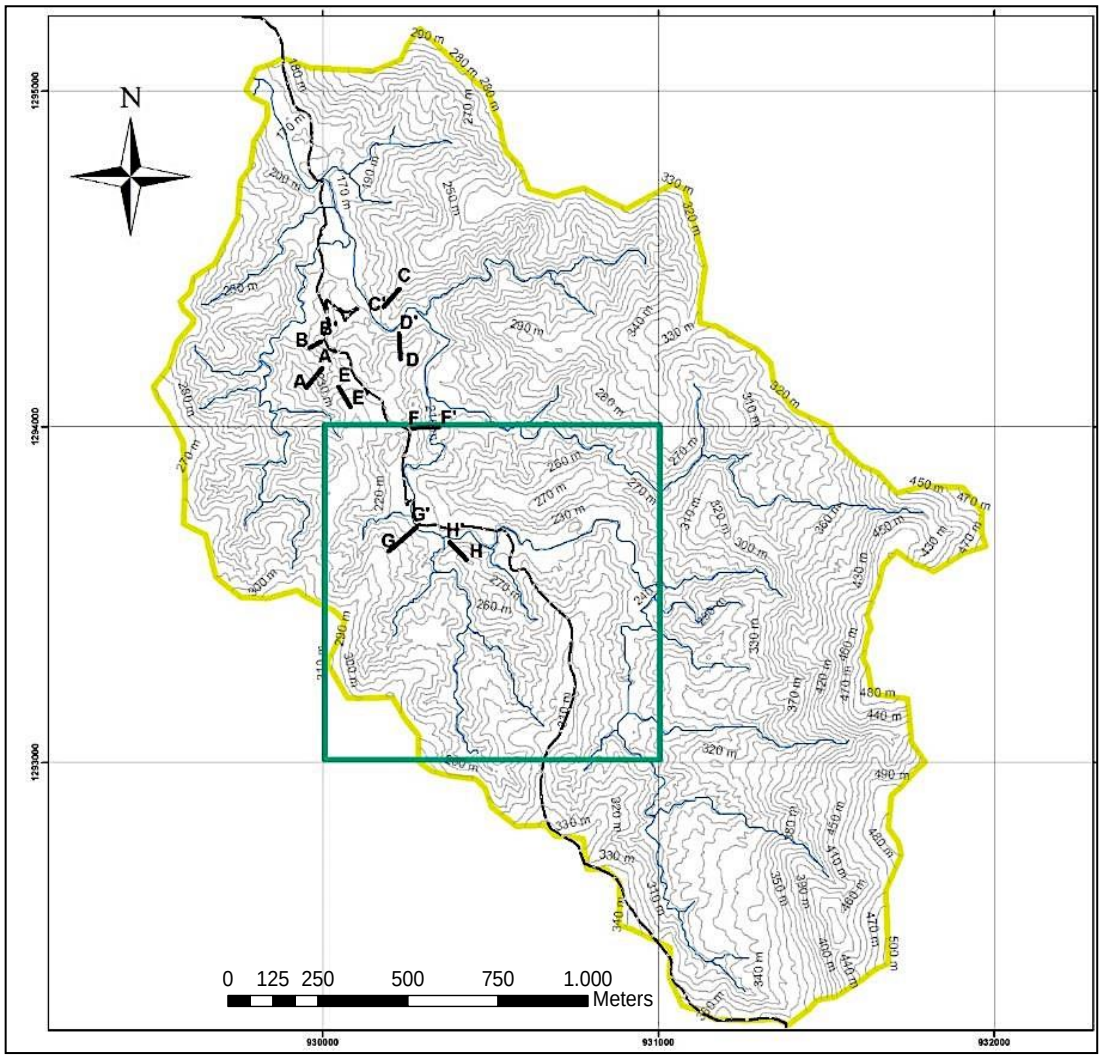

Illustration 4.1-53. Location of the sections, from which the geological-geotechnical profiles were obtained.

Next (See Illustration 4.1-54 to Illustration 4.1-61) the geological-geotechnical profiles corresponding to sections AA, BB, CC, DD, EE, FF, GG and HH are presented, which represent the depths of the residual soils and Saprolite.

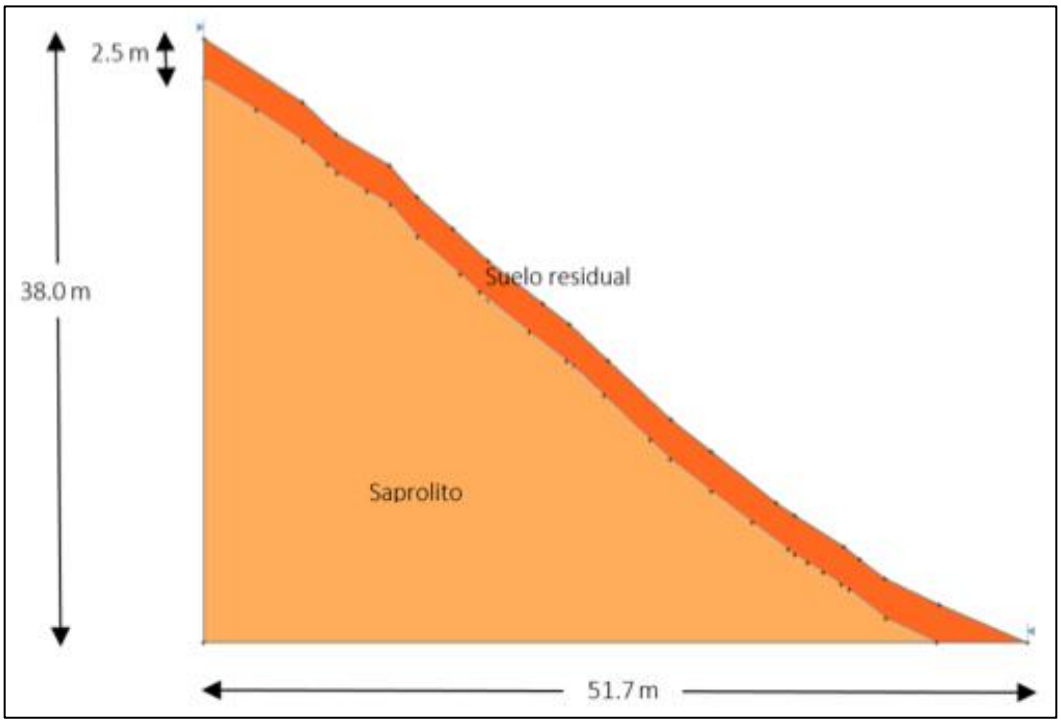

Illustration 4.1-54. Geotechnical geological profile of section AA.
Source: INGEX, 2016.

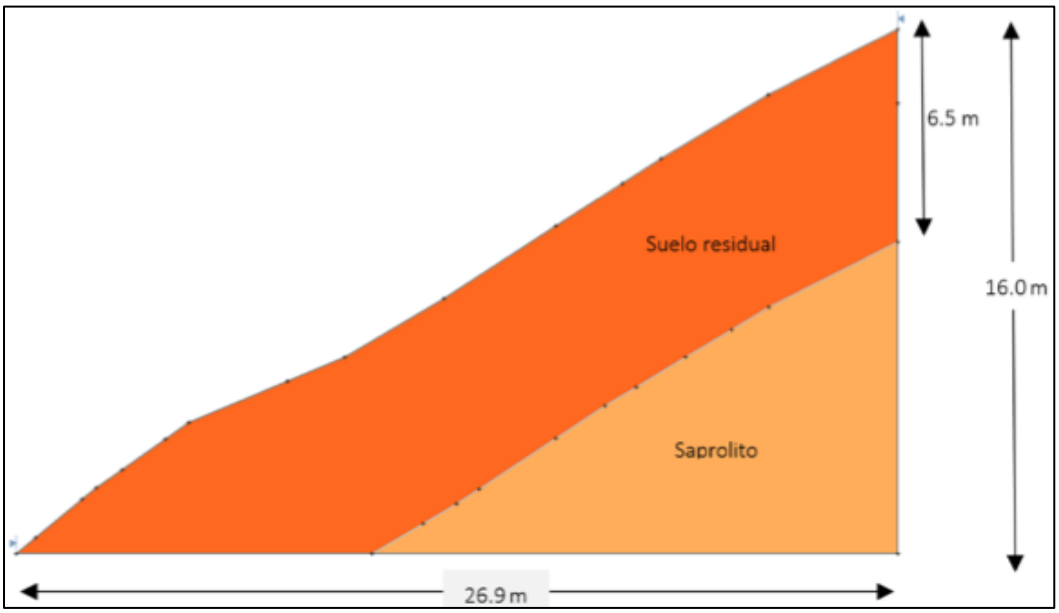

Illustration 4.1-55. Geotechnical geological profile of section BB.
Source: INGEX, 2016.

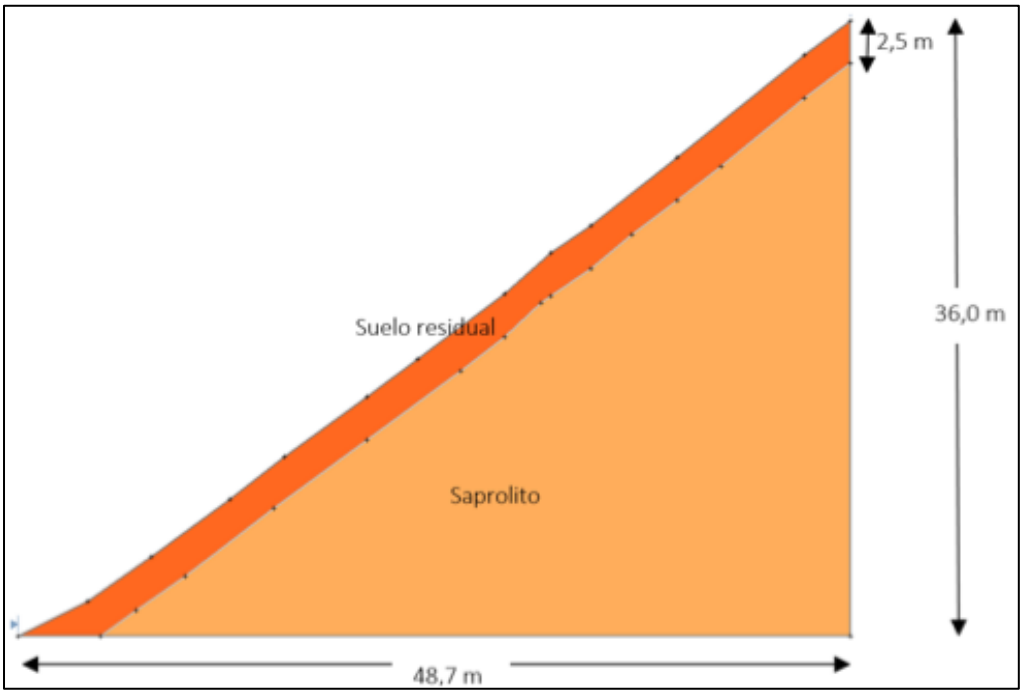

Illustration 4.1-56. Geotechnical geological profile of the CC section.
Source: INGEX, 2016.

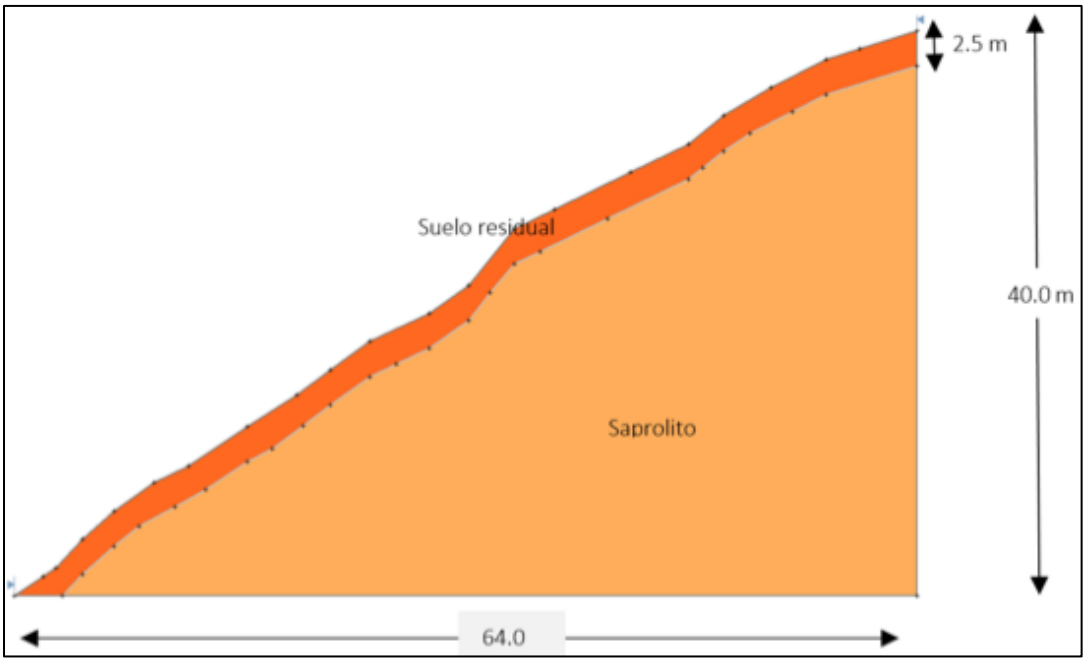

Illustration 4.1-57. Geotechnical geological profile of the DD.
Source: INGEX, 2016.

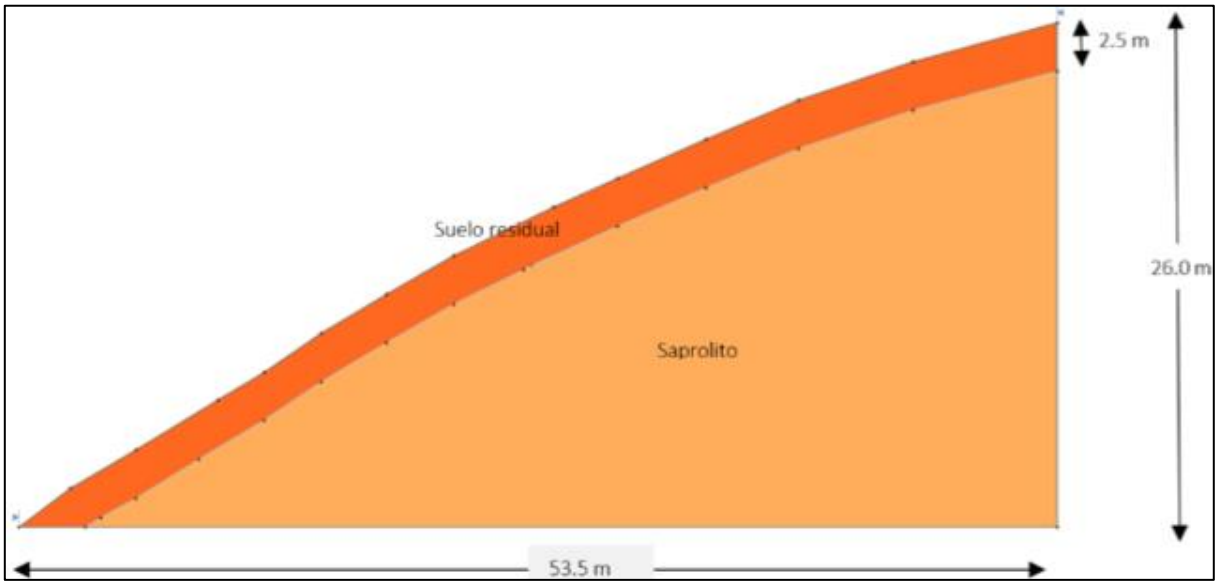

Illustration 4.1-58. Geotechnical geological profile of the U.S. section
Source: INGEX, 2016.

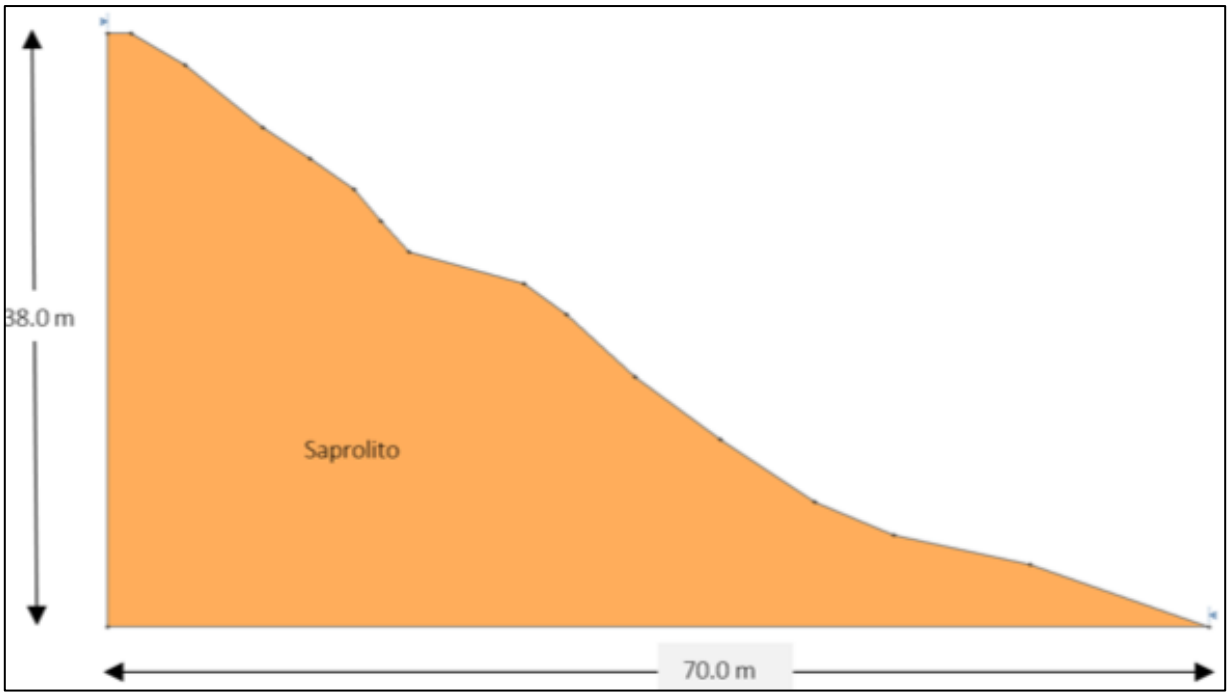

Illustration 4.1-59. Geotechnical geological profile of section FF.
Source: INGEX, 2016.

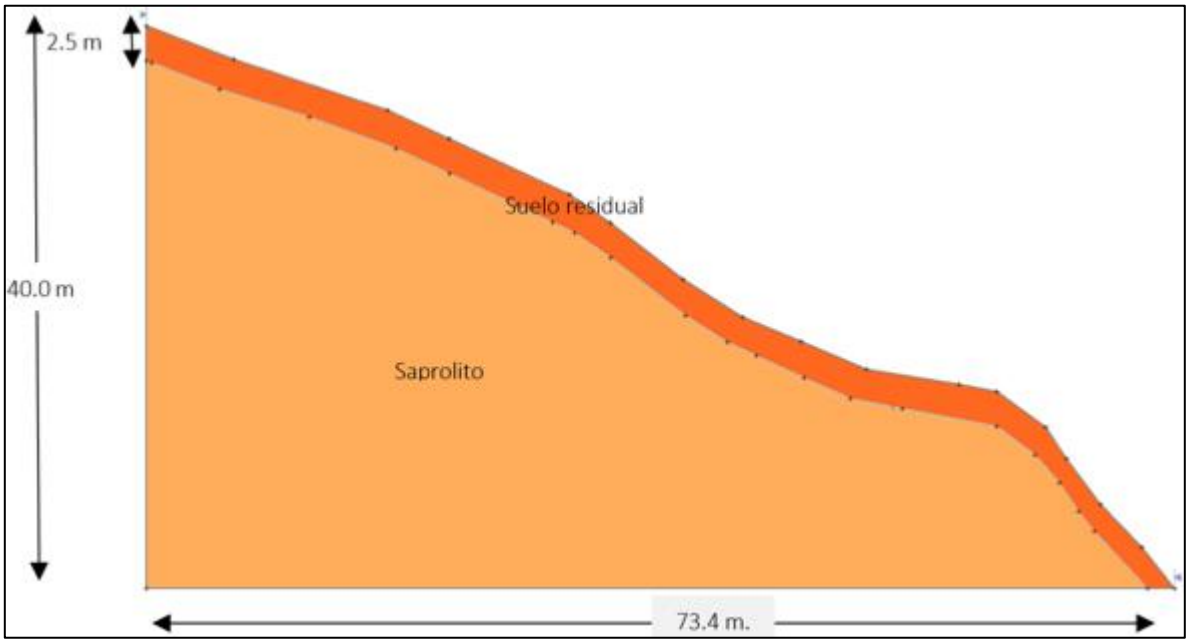

Illustration 4.1-60. Geotechnical geological profile of section GG.
Source: INGEX, 2016.

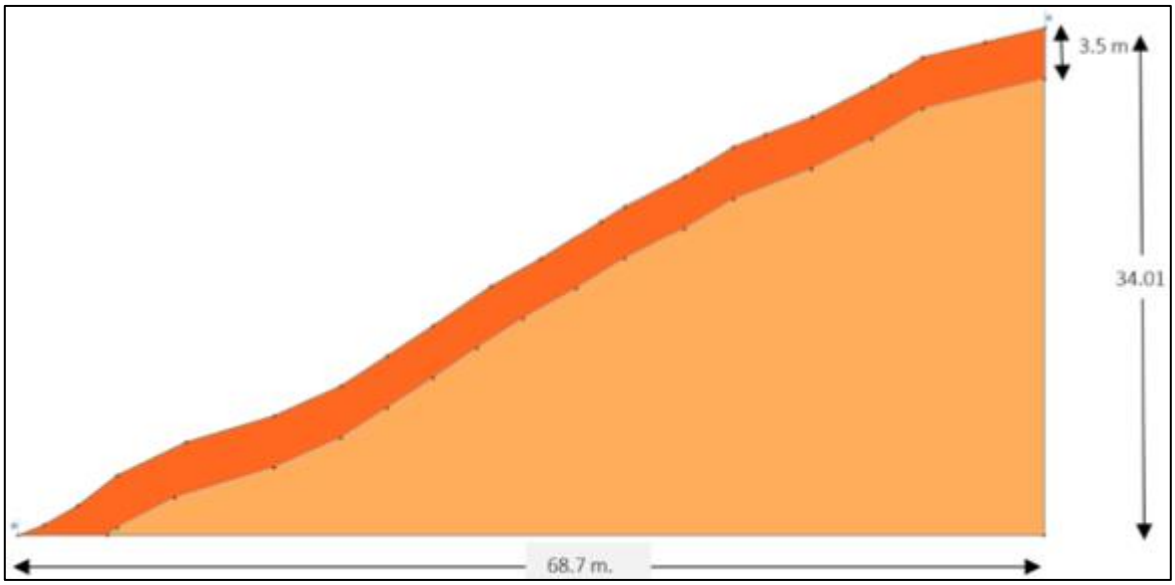

Illustration 4.1-61. Geotechnical geological profile of section HH.
Source: INGEX, 2016.

4.1.3.3.1 Results of stability analysis

Table 4.1-22 shows the results of the safety factors using the Spencer, Morgenstern & and Janbú methods for the three (3) situations: static (normal), pseudostatic (under seismic loading) and with seismic loading and total soil saturation, as well as the probability of failure for each of them.

Table 4.1-22. Safety factor values for each of the conditions evaluated.

CONDITIONS	STATICS				PSEUDO-STATIC				PSEUDOSTATICS AND SATURATION			
METHODS	SPENCER	JANBU	M&P	P.F.	SPENCER	JANBU	M&P	P.F.	SPENCER	JANBU	M&P	P.F.
Profile of AA	1,474	1,373	1,471	0,0%	1,246	1,139	1,245	0,0%	0,596	0,443	0,595	100%
Profile of BB	2,443	2,276	2,442	0,0%	1,994	1,882	1,992	0,0%	1,185	1,032	1,182	46,4%
Profile of CC	1,571	1,452	1,572	0,0%	1,318	1,202	1,319	0,0%	0,655	0,487	0,647	100%
Profile of DD	1,580	1,492	1,579	0,0%	1,296	1,209	1,294	0,0%	0,610	0,503	0,605	100%
Profile of EE	2,105	1,996	2,100	0,0%	1,672	1,575	1,670	0,0%	0,889	0,795	0,884	100%
Profile of FF	1,709	1,575	1,708	0,0%	1,417	1,291	1,418	0,0%	0,727	0,566	0,724	100%
Profile of GG	1,790	1,713	1,789	0,0%	1,430	1,360	1,429	0,0%	0,686	0,603	0,679	100%
Profile of HH	1,925	1,812	1,924	0,0%	1,544	1,438	1,542	0,0%	0,787	0,671	0,780	100%

P.F.: Probability of failure

Source: INGEX, 2016.

4.1.4 SOILS

Following are the soil mapping units, agrological classification and potential uses, current use and land use conflicts.

4.1.4.1 SOIL MAPPING UNITS

In order to carry out the survey of the soil mapping units, a field survey was carried out by means of probes and test pit, at the sites shown in Table 4.1-23 and Illustration 4.1-62).

Table 4.1-23. Geographical location of observation and sampling sites.

POINT	WEST (X)	NORTH (Y)
3	930942,4529	1292661,407
DLM1-2	931209,5614	1292701,741
5	931287,5289	1292778,168
CAJUELADLM2	931287,3078	1292778,058
DLE	931313,5907	1292856,768
7	931179,0416	1292996,638
FOREST	931178,6009	1292997,413
FOREST2	930895,3026	1293149,322
TERRACE1	930922,6833	1293463,385
MONTAIN1	931149,5483	1293797,412
DLM1-2	931295,7527	1293863,46
DLM2--	931217,9333	1294054,681
DLM3	930703,6048	1294050,634
DLM3-1	930731,9961	1293816,679
DLM3-2	930484,2956	1293830,846
SLE1	930442,6892	1294329,704
SLE-2	930397,2236	1294355,537
SLE-2	930396,1191	1294355,428
DL1	930475,8536	1292680,411
DLM11	930968,7106	1292560,837
DLM111	930968,9365	1292564,487
DL2	930235,3453	1292787,693
DL3	930280,5393	1293042,339
DL4	929994,5248	1293303,64
DL- 5 GRASS	929802,2678	1293872,719
DLE3	929812,8838	1294513,071
FT4	929911,468	1294879,789
FT4-2	930041,4746	1294735,829
DLE2	930494,6758	1294864,488
DLE2-2	930245,9119	1294666,53
FH B1	930299,7988	1293311,289

POINT	WEST (X)	NORTH (Y)
FH CALICATA	930347,0812	1293400,144
FH BASIN2	930442,0394	1293543,348
FH BASIN 3	930404,777	1293671,142
FH BASIN3	930268,8105	1293662,04
FH BASIN5	9301ca78,966	1293543,051
FH BASIN-6	930278,1303	1293533,954
FH BA7	930438,7437	1293396,81
FH BASIN8	930399,3719	1293516,753
FH BASIN9	930334,1195	1293768,788
FH CALICATA2	930203,0086	1293836,104
9	930203,449	1293835,108
10	930202,6749	1293834,335
FH BASIN 10	930263,3756	1293962,876
CIELO BARRE11	930358,4085	1293842,413
FH BASIN11	930390,4981	1293966,239
YACIMIENTO NORTE	930341,926	1294061,532
YANO BASIN 1	930365,277	1294175,527
YANO BASIN2	930326,7232	1294327,101
YA NOBASIN3	930266,6118	1294224,88
YANO BASIN4	930229,2481	1294120,638
PBASIN1	930155,7716	1294017,441
PB BASIN2	930017,7622	1293968,417
PB BASIN3	929922,8414	1294010,356
PB BASIN4	929881,3586	1294120,017
PB BASIN5	929951,0649	1294211,938
PB BASIN6	930033,8428	1294174,329
PB BASIN7	930004,3569	1294096,509
YANO BASIN5	930135,2143	1294164,898
YANO BASIN6	930140,1198	1294277,149
YANO BASIN7	930228,9877	1294330,112
PB BASIN 7	929890,4496	1294302,714

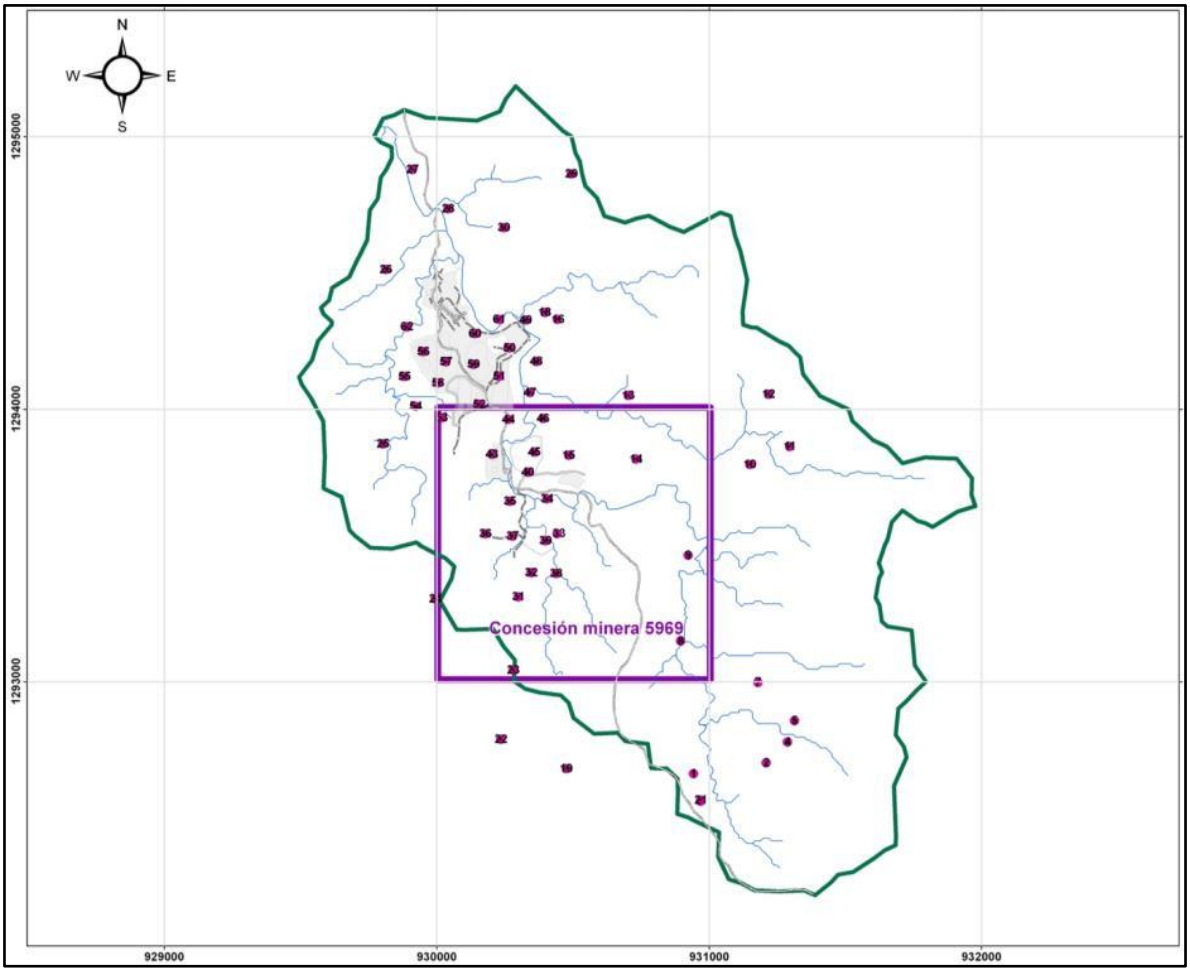

Illustration 4.1-62. Location of control points for lifting floor units, 1: 10,000.
Source: INGEX, 2016.

In the study area, the orders oxisol and tecnosol were identified through the American Soil Taxonomic System (USDA, 2010). Oxisols are mineral soils, highly oxidized and weathered, rich in iron (Fe2O3) and aluminum (Al2O3) sesquioxides with a predominance of 1:1 clays, therefore evolved, commonly found in low latitudes in tropical climates. It may present high leaching and low natural fertility (Ibáñez, 2008). Its diagnostic characteristic is the presence of an oxic horizon within 150 cm of depth.

Whereas technosols are of anthropogenic origin, where the soil has been altered mainly by the deposit of materials. They are called "urban or mining soils", such as roads, mining, garbage dumps, oil spills, coal soot deposits and the like (WRB, 2007). In the new Russian classification system, these are called surface technogenic formations. The pedogenesis or edaphogenesis of techno-soles is strongly affected by materials that include wastes such as landfills, sludge, slag, construction, mining, and ashes; soils with geomembranes, as well as all types of materials made or exposed by human activity that would not otherwise occur on the soil surface and would be affected by surface

formation processes. These materials and their organization give rise to a group of artificial soils, where no horizons are identified, but a mixture of materials; although in ancient technosols, we can begin to see vitreous or Andean properties, or translocation of clays.

Within the technosol group, the spolic subgroup was identified, with a layer 20 cm or thicker within 100 cm of the soil surface, with 20% more artifacts (something recognizable on the ground, made or extracted from the ground by man) containing 35% or more by volume of industrial waste (construction and gold mining waste, dredged materials, debris, etc.).

Table 4.1.24 shows the soil phases, according to the slopes, established by the IGAC (2010), which are also useful for identifying the particular management measures for this resource or component.

Table 4.1-24. Identification of phases of soil associations.

PHASE OR PENDING	CODE
Slightly flat (1% - 3%)	a
Slightly sloping (3 - 7%)	b
Moderately sloping (7 - 12%)	c
Strongly inclined (12 - 25%)	d
Slightly rugged (25 - 50%)	e
Moderately rugged (50 - 75%)	f
Strongly rugged (75 - 100%)	g

Source: INGEX, 2016.

The landscape and attributes, relief and phases, combined in the taxonomic classification of the soil raised in profiles by means of surveys and test pit, are presented in Table 4.1-25 and Illustration 4.1-63.

Table 4.1-25. Taxonomy and other characteristics of the soils characterized in the study area.

LANDSCAPE	LANDSCAPE FEATURE	RELIEF TYPE	PHASES	MAIN CHARACTERISTICS OF SOILS	CARTOGRAPHIC UNIT AND TAXONOMIC COMPONENTS	MODAL PROFILE	SIGN
Hilly	Structural Erosional	Hills	Slopes Moderately sloping (7-12%):	Deep, highly oxidized, weathered, with a scarce horizon A of 0-10cm, horizons B dominate more than 80% in one meter of depth, predominant color 5YR 4/6 (Yellowish Red) abundant minerals of medium and coarse textures, sandy loam (FA) and sandy loam (A). Very fast surface drainage, moderate internal drainage	Typic *Hapludox association*	YANO-DL	LCOTc
			Slopes Strongly inclined (12-25%):				LCOTd
			Slopes Slightly steep (25-50%):				LCOTe
			Moderately steep slopes (50-75%):				LCOTf
			Slopes Strongly rugged (75-100%)				LCOTg
			Slopes Strongly inclined (12-25%):	Soil strongly disturbed by anthropogenic activity, with materials of different mixed sizes, called mining debris,	Tecnosol Spólico Association	FHYP-CA	LCTd

LANDSCAPE	LANDSCAPE FEATURE	RELIEF TYPE	PHASES	MAIN CHARACTERISTICS OF SOILS	CARTOGRAPHIC UNIT AND TAXONOMIC COMPONENTS	MODAL PROFILE	SIGN
				there is an incipient horizon A of different materials, with stains of organic matter and grass roots.			
	Colluvium alluvial	Vallecitos Colluvium alluvial	Slightly sloping terrace (3-7%):	Deep soils, their parent material are alluvial and slope deposits. Variable surface and internal drainage: fast, slow, flooded. Sand and Loam texture (AF). Different colors: yellow, brown, gray and red (5YR, 10YR, 7.5YR)	Typic Hapludox Terraces Association	YANOFT2	**LVAOTb**
			Slightly flat terrace (0-3%):	Soils with alluvial or slope deposits, which do not form a structure, because the particles do not yet have aggregation.	Alluvial and slope deposit association.	PBFT1	**LVADa**

Source: INGEX, 2016

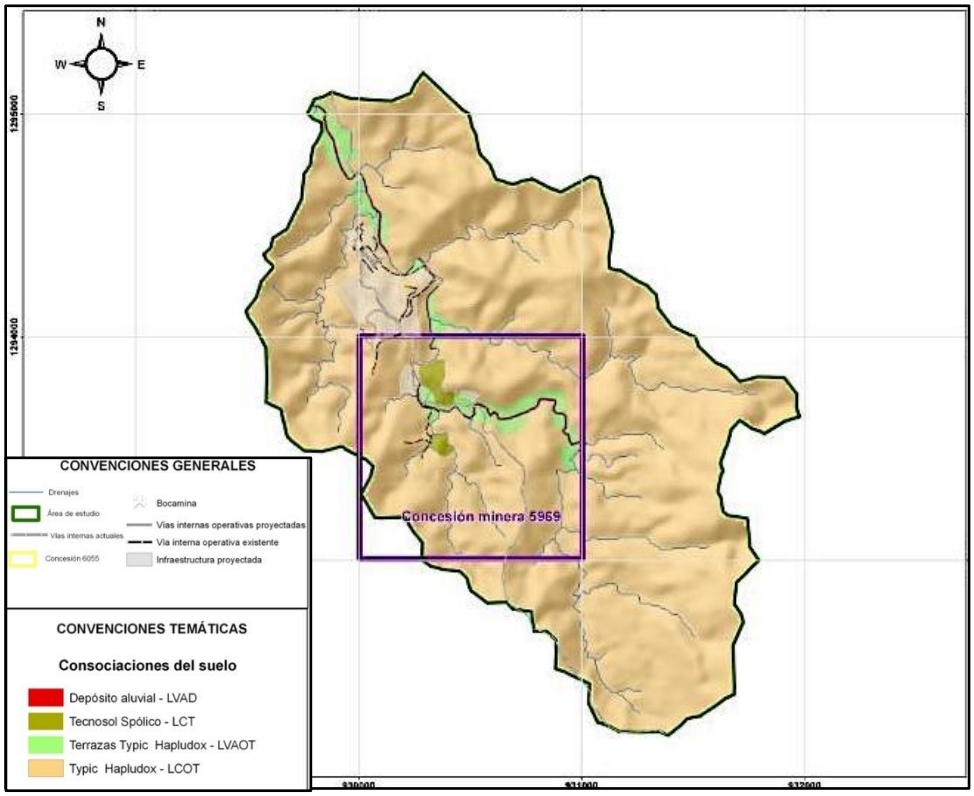

Illustration 4.1-63. Soil associations in the study area.
Source: INGEX, 2016.

According to Illustration 4.1-63, Table 4.1-26 and Illustration 4.1-64, in the area of study there is a domain of the LCOT consociation corresponding to the soil of the Typic Hapludox subclass in 95.48% in the hilly relief and in a 3,29% in the alluvial colluvial valleys, which coincides with the study carried out by the IGAC (2007), where the study area belongs to the Remedios Association (Rem) with this type of soil.

Technosol Spolic is found in a smaller area, representing 0.67% and the alluvial deposit association - LVAD - is found in 0.55%.

Table 4.1-26. Distribution of soil associations in the study area.

SOIL ASSOCIATIONS	AREA (ha)	PERCENTAGE
Typic Hapludox - LCOT	372,88	95,48%
Typic Hapludox Terrace - LVAOT	12,86	3,29%
Tecnosol Spolic - LCT	2,64	0,67%
Alluvial deposit - LVAD	2,14	0,55%
TOTAL	**390,5**	**100,00%**

Source: INGEX, 2016.

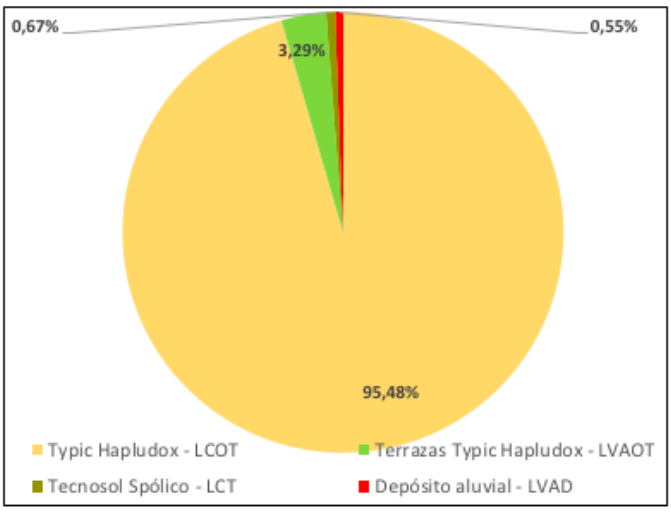

Illustration 4.1-64. Distribution of soil associations
Source: INGEX, 2016.

Of the soil phases and within the LCOT consociation are the LCOTe phases with the largest area in the study basin (See Table 4.1-27, Illustration 4.1-64 and Illustration 4.1-65), with 36.13% of areas on slightly steep slopes (25 - 50%), followed by the LCOTg phase with 32.29% on steeply steep slopes (75 - 100%) and the LCOTf phase with moderately steep slopes (50 - 75%) represented 20.09% of the study area. To a lesser percentage are the LCOTd (6.11%) and LCOTc (1.38%) phases. Therefore, most of the area is on steep and sloping slopes, to a lesser extent, which is a key characteristic in determining the vocation of land use. The other phases, belonging to the remaining soil associations, are in lower percentage LVAOTb (3.29%), LVADa (0.55%) and LCTd (0.16%). These are found on flat,

sloping slopes, which is characteristic of the hilly landscape in which slopes greater than 25% dominate and not areas of low slope.

Table 4.1-27. Distribution of soil phases in the study area.

SOIL PHASE	AREA (ha)	PERCENTAGE
LVAOTb	12,86	3,29%
LCTd	0,62	0,16%
LVADa	2,14	0,55%
LCOTg	126,09	32,29%
LCOTe	141,10	36,13%
LCOTc	5,38	1,38%
LCOTd	23,88	6,11%
LCOTf	78,46	20,09%
TOTAL	**390,5**	**100,00%**

Source: INGEX, 2016

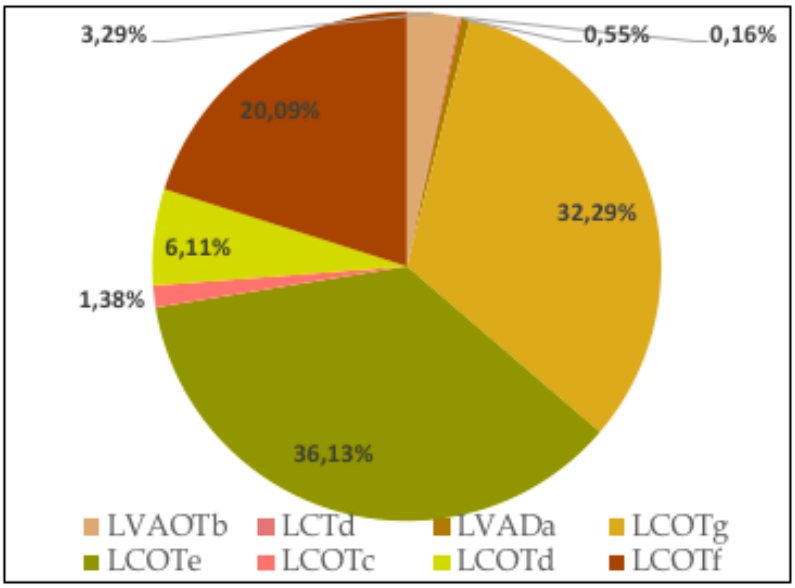

Illustration 4.1-65. Distribution of soil phases in the study area
Source: INGEX, 2016.

Each of the classifications presented in Table 4.1.27 is described in detail below. They are technically supported by the surveying of profiles directly in the field by means of burrow and boreholes, physicochemical and mineralogical analysis of soil samples in laboratories, and secondary information.

Hilly landscape

In the hilly landscape of the hills and valleys of the colluvial alluvium are the reliefs of the alluvial colluvial valleys, presented below.

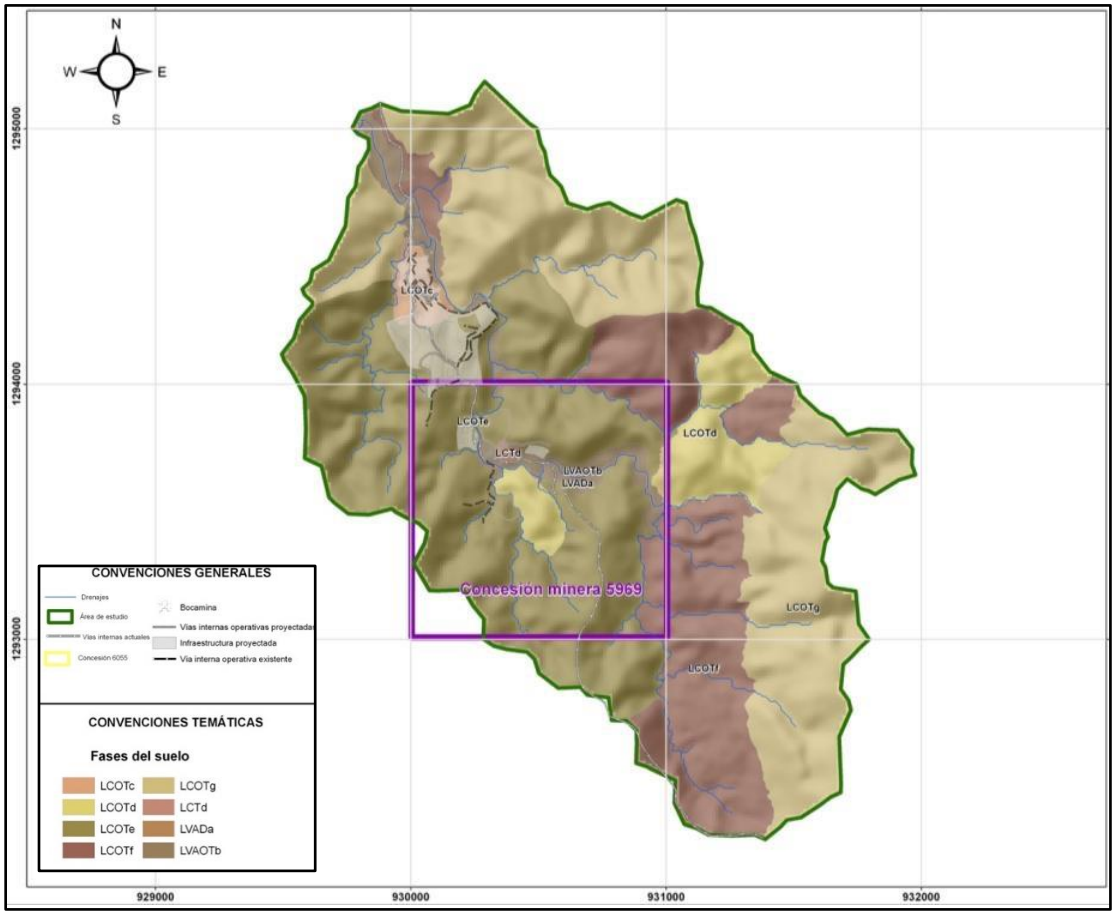

Illustration 4.1-66. Soil phases in the study area.
Source: INGEX, 2016

Hill relief

The parental materials of these hills are igneous rocks (granodiorite, diorite and diabase).

These soils are found on slopes from moderately steep to steeply steep, i.e. between 7% and 75%... The following are the phases identified for this relief based on slope ranges and soil taxonomy (see Table 4.1.28):

- LCOTc: Moderately sloping slopes (7-12%) of consociation Typic Hapludox.
- LCOTd: Heavily sloping slopes (12-25%) of consociation Typic Hapludox.
- LCOTe: Slightly steep slopes (25-50%) of consociation Typic Hapludox.

- LCOTf: Moderately steep slopes (50-75%) of consociation Typic Hapludox.
- LCOTg: Strongly steep slopes (75-100%) of consociation Typic Hapludox.
- LCTd: Heavily sloping slopes (12-25%) of Tecnosol Spólico Association

The following are the characteristics of the Typic Hapludox consociation in the LCOT and Tecnosol Spolic phases in the LCTd phase.

4.1.4.1.1 Typic Hapludox - LCOT

Typic Hapludox type soils are located at heights between 216-349 meters above sea level and are located at the processing plant, campsite, the different deposits and other services or infrastructure on the surface of the project, with pasture vegetation, dense underground forest (Bdbtf) and low secondary vegetation, mainly used as pasture for cattle ranching, fallow and conservation strips. They represent 95.48% of the soil types found in the project.

According to the USDA taxonomic classification (2010), Table 4.1-28 shows their taxonomic classification from order to subgroup:

Table 4.1-28. Taxonomic classification of Typic Hapludox soil.

ORDER	SUBORDER	GREAT GROUP	SUBGROUP
Oxisol	Údox	Hapludox	Typic *Hapludox*

Source: USDA, 2010.

The large Hapludox group presents yellow to red colors, a uniform and deep profile that shows almost no differentiation of horizons and base saturation of less than 35% (CIAT, 1983). The Typic Hapludox according to the USDA (2010) key, are the oxysols where yellow predominates over red and are generally poor in organic matter.

According to the general soil and land zoning study of the department of Antioquia (2007), this subgroup originates from claystones, diorites or diorite quartz. They are deep and morphologically present profiles with a sequence of A-B-C horizons.

Within the study area, the Ap surface horizon is between 0 and 10 cm thick with a colour shade of 7.5 YR and 10 YR, the most common being 7.5 YR 4/4 (Brown).

The horizons B and C have a thickness greater than 40 cm, although more often the horizon B was found up to 100 cm or more depth colors of the shade 5 YR, predominant 5YR 4/6 and 5YR 5/8, corresponding to a yellowish red. The field texture varied from sandy loam (FA) to sandy loam (FArA), coarse to moderately fine in size.

The following is a description and interpretation of the modal profile, physicochemical and mineralogical results of the soil samples collected.

Modal profile

Soil originated from granodiorite rock, with a warm climate, effective surface depth of 40 cm, made up of Ap and B horizons (See Table 4.1 29 and Illustration 4.1 67).

The humidity regime is unique, and the soil temperature is isothermal, with good natural drainage; no epipedons or subsurface horizons were observed, current use in pasture, evidence of erosion and compaction by trampling cattle grazing.

Table 4.1-29. Description of horizons.

HORIZON	DESCRIPTION
Ap (0 - 7cm)	Field texture Clay loam (FAr) and laboratory texture Sand loam (FA); Wet color 7.5 YR 4/4 (Coffee); sub angular, medium sized, friable, weak block structure; soft dry, friable and slightly sticky wet consistency; negative HCl reaction; presence of fine and medium cylindrical pores; evidence of fine grass roots; presence of fine sand sized quartz grains; diffuse horizon boundary. Moderately acidic pH (5.31), low E.C.
B (7 - 100cm)	Field texture FAr and laboratory texture Sandy (A); Wet color 5YR 4/6 (Yellowish Red); Structure of sub angular blocks, medium size, weak; Consistency in dry soft, wet friable and slightly sticky; HCl negative reaction; little evidence of biological activity, scarce presence of roots and absence of large root canals. Little or no staining of decomposed organic matter, with abundant presence of quartz grains of fine sand size. pH moderately acidic (5.19), low E.C.

Source: INGEX, 2016.

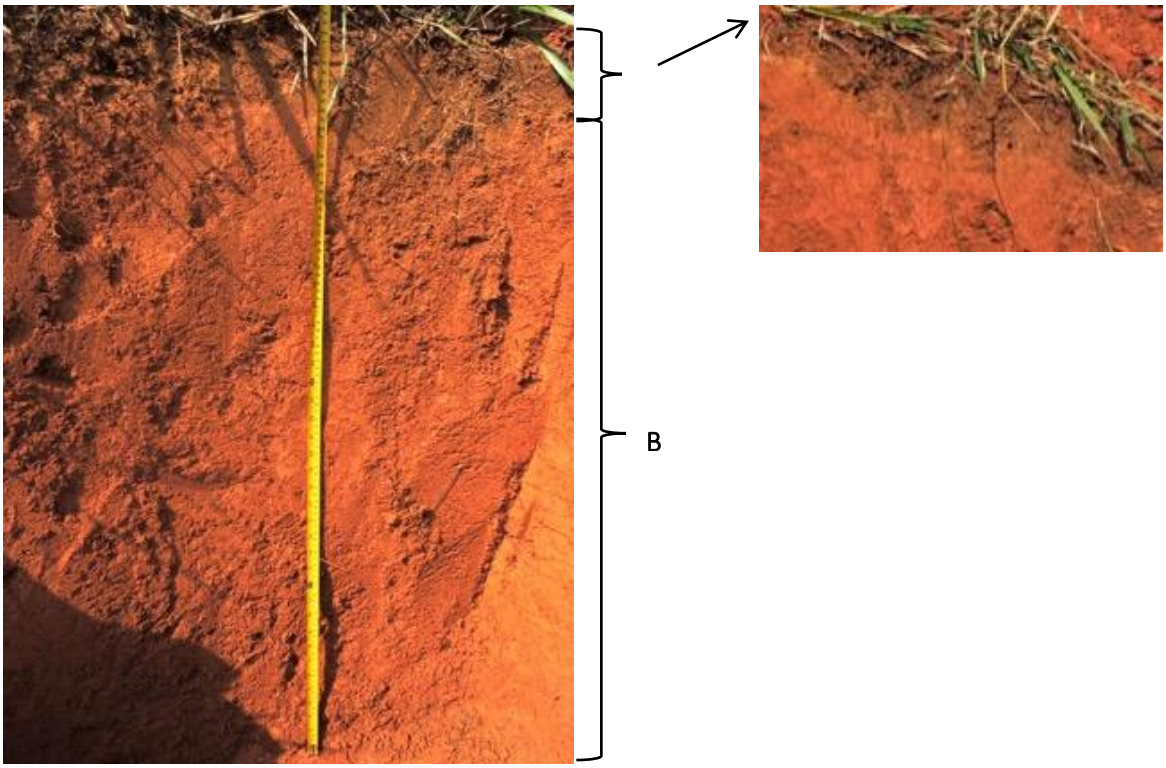

Illustration 4.1-67. DLM Profile, YANO-DL Replica.
Source: INGEX, 2016.

Physical-chemical analysis

The average infiltration of this soil was 5.95cm3*min-1 in the cylinder area (0.0081m2), therefore the theoretical infiltration is 439.99 m3*Ha - 1*hour-1 or 7.3m3Ha - 1*min-1 or 0.73Lt*min-1*m2 (See Illustration 4.1-68). This volume of infiltration can be considered as high, although it should be borne in mind that the field technique used with the double ring (infiltration cylinders) does not allow water to move due to surface runoff, thus generating a vertical flow of income, which in natural conditions does not always occur at this scale, because it can be affected by the slope of the land, the intensity of the rain, the surface litter, the content of clays, silt and sand, among others, therefore this measurement can be interpreted as the capacity of the soil to allow a volume of water to enter over time (theoretical infiltration).

The volume of water entering the soil matrix was favored by the sand contents that predominate in the texture, called as an adequate infiltration for the movement of nutrients and water inside the soil.

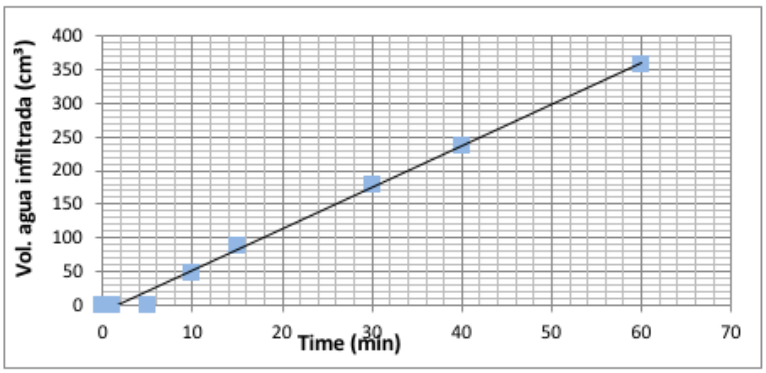

Illustration 4.1-68 YANO-DL infiltration curve.
Source: INGEX, 2016.

The physicochemical results from the laboratory (see Table 4.1-30) show that these soils have a low apparent density, optimum for the textures of this soil, medium porosity and good aeration. The CIC in ranges that favor the exchange that favors the soil-water-plant relationship. The pH is moderately acidic, unsuitable for plant growth, with interchangeable aluminum in low quantities. The EC is low, and the soil is non-saline, which shows a very low number of nutritive electrolytes in the soil solution and a low amount of Na.

Table 4.1-30. Physico-chemical results of the YANO-DL soil profile.

PARAMETER	HORIZONT Ap	HORIZONT B
pH	5.31	5.19
C.E (dS/m)	0.03	0.03
Humidity (%)	22.05	24.67
DAP (g/cm^3)	1.00	0.84
DR (g/cm^3)	2.5	2.08
Porosity (%)	52	50
C.I.C. (meq/100g)	10.00	15.87

PARAMETER	HORIZONT Ap	HORIZONT B
P (di) (ppm)	0.94	0.56
K (meq/100g)	0.34	0.10
Ca (meq/100g)	2.17	1.32
Mg (meq/100g)	0.86	0.37
Na (meq/100g)	0.07	0.07
Fe (di) (ppm)	135	117
Cu (di) (ppm)	0.40	0.60
Al (meq/100g)	0.25	1.73
N Total (%)	0.169	0.086
CO Total (%)	1.58	0.57
Cationic relationships		
Ca/Mg	2.523	3.568
Ca/K	6.38	13.20
Mg/K	2.53	3.70
(Ca+Mg/K)	8.91	16.90
Organic pollutants		
Fats and oils	<0,006 25	<0,006 25
Total hydrocarbons	<0,006 25	<0,006 25
Heavy metals and/or inorganic contaminants		
Manganese (mg/ Kg)	302.547	689.033
Mercury (mg/kg)	0.144	0.108
Cyanide (mg/ Kg)	<0.200	
Copper (mg/ Kg)	<27,5	
Nickel (mg/ Kg)	<42,3	
Silver (mg/ Kg)	<31,0	
Lead (mg/ Kg)	<47,5	

Source: INGEX, 2016.

The Ap horizon has a moisture content of 22.05% and 24.67% in the B horizon, which indicates that dry soil has the capacity to increase its weight in water by 22-24.7%, which can then be released to plants and percolated in the soil matrix. At the agricultural level, this humidity range can be interpreted as a good storage capacity, in case of requiring irrigation systems, the frequency of application would below.
There are low contents of CO and MO (1.02%), Nitrogen, in spite of being in an adequate range, is very close to the limit of presenting deficiency in the case of horizon B. The macro elements P, Ca and Mg are in low amounts, being very notable the deficiency of the first one. The K is only found in the medium-optimal Ap horizon, which is very small. Therefore, the natural fertility conditions of this soil are low.

The levels of iron microelements are very high, contrary to the situation with Cu. In cationic ratios Ca/ Mg and Mg/k, Ca/k and Ca+Mg/k are balanced, only the latter two are unbalanced on horizon A. Although as mentioned above, the amounts of each element are very low.

As for heavy metals (Manganese, Mercury, Copper, Nickel, Silver, Lead and Lead), cyanide, fats and hydrocarbons, they are below the permitted limits in soil according to Louisiana Protocol 29B and those indicated by the EPA (1992).

According to the IGAC, the use of this land, adapted to the initial classification of Klingebiel and Montgomery according to the characteristics of the soils in the country, corresponds to Class VI, i.e. very steep soils suitable for supporting permanent vegetation, which must remain under natural or planted forest. They are not suitable for any type of crop due to erosive processes, shallow effective depth and slopes greater than 25%.

Mineralogy

The Ap and B horizons in the coarse fraction (> 2 mm) are mostly made up of highly weathered parent rock remains (Ap: 50% - B: 60%) (see Table 4.1 31, Table 4.1-32, Illustration 4.1-69 and Illustration 4.1-70), but which still clearly show some of its primary constituents such as Quartz (Ap: 40 % and B: 25%), 8% Garnet on the Ap horizon and secondary constituents such as Limonite (1%) and Hematite (5%) on the B horizon only. Particularly on the Ap horizon is Actinolite (1%).

Table 4.1-31. Mineral count on horizon App.

MINERALS	COARSE FRACTION (>2 mm)	SAND FRACTION (%)	LIMO FRACTION (%)
Rock mother	50		
Quartz	40	96	85
Plagioclase and other feldspar			1
Garnet	8	1	5
Spinel			5
Sericite			Piece
Magnetite		1	3
Limonite			Piece
Others	3 (2% Charcoal and 1% Actinolite		

Source: INGEX, 2016.

Table 4.1-32. Mineral count on horizon B.

MINERALS	COARSE FRACTION (>2 mm)	SAND FRACTION (%)	LIMO FRACTION (%)
Rock mother	60		
Quartz	25	95	75
Plagioclase	Pieces		
Garnet		3	Pieces
Sericite	9	1	Pieces
Magnetite		1	6
Hematite	1		
Limonite	5	1	Pieces

Source: INGEX, 2016.

Illustration 4.1-69. Minerals in circles, present in the soil LCOT, 1: Hyaline abundant quartz
Source: INGEX, 2016.

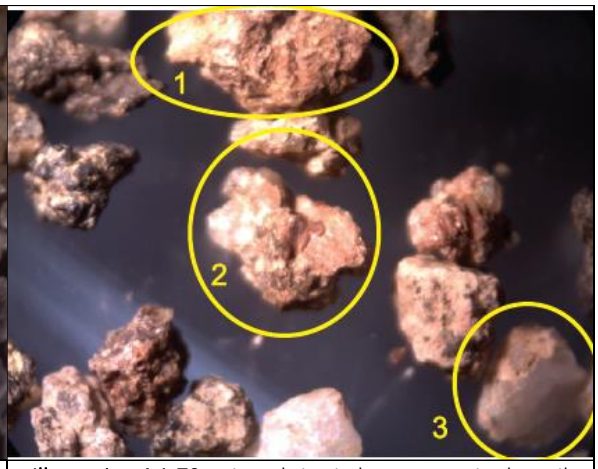

Illustration 4.1-70. Minerals in circles, present in the soil LCOT, 1: Very Weathered Rock, 2: Sericite and 3: Quartz.
Source: INGEX, 2016.

The largest proportion of minerals present in this coarse fraction (See Illustration 4.1-69 and Illustration 4.1-70) corresponded to fragments of weathered rock partially decomposed and completely covered by crusts of secondary minerals such as limonite and goethite, product of surface oxidation.

The sand fraction (2 mm> f> 0.2 mm) (See Illustration 4.1-69 and Illustration 4.1-70), is composed mostly of abrasion and disintegration-resistant minerals such as quartz (Ap: 96% - B: 95 %), observed in Table 4.1-31 and to a lesser extent, Magnetite (1%) and Garnet (Ap: 1% - B: 3%). Traces of other minerals such as Plagioclase and other calcified and altered feldspars are also observed. And secondary at very low levels Sericite (B: 1%), Limonite (B: 1%) and Magnetite (Ap: 1% - B: 1%) in the depth. Therefore, this Arena fraction is composed mostly of quartz fragments, a very stable primary mineral, but which does not provide nutrients.

The sand mineralogy suggests an in-situ weathering under conditions governed by a climate of aggressive characteristics (warm humid), which is why resistant minerals such as quartz and opaque, typical of evolved acid soils, predominate; that they do not possess labile material for a subsequent alteration, therefore, they do not have mineral reserves that supply elements to their fertility. Said composition verifies the classification of these soils as Latosols or Oxisols.

In the Limo Fraction (200 um> F> 20 um) the quartz domain was found (Ap: 85% - B: 75%), and in a smaller proportion Garnet (Ap: 5 - B: 14%), Spinels (Ap: 5%), Magnetite (Ap: 3% - B: 6%), Feldspar (Ap: 1%) and traces of Sericite and Limonite.

The clay fraction is composed primarily of Illita, a non-expansive, phyllosilicate type 2: 1 clay, derived from the sericitization of Muscovite originally present in schists or gneiss as the original parent material of these soils.

4.1.4.1.2 Spolic Tecnosol - LCT

Tecnosol soils are found where there is informal exploitation and deposits of this benefit (See Illustration 4.1-71 and Illustration 4.1-72). The taxonomic identification of this soil was in accordance with WRB because its characteristics did not correspond to any USDA classification (2010).

Modal profile

Soil originated from the deposit mixture of mining material and pre-existing granodiorite rock, constituted by A-B horizons (See Illustration 4.1-73 and Illustration 4.1-74).

It occurs at a height of 231 meters above sea level, the soil moisture regime and the temperature regime of the soil is isothermal; the effective depth is very shallow (20 cm), the erosion is severe due to informal mining, good natural drainage, geomorphological belongs to the loins zone (Dl), the vegetation is stubble without use, the slope is strongly inclined (20-25 %).

In the Table 4.1-33 presents the description by more detailed horizon.

Illustration 4.1-71. Informal exploitation aspect.
Source: INGEX, 2016.

Illustration 4.1-72. Informal exploitation aspect.
Source: INGEX, 2016.

Illustration 4.1-73. Modal profile FHYP-CA.
Source: INGEX, 2016.

Illustration 4.1-74. Anthropic material.
Source: INGEX, 2016.

Table 4.1-33. Description of horizons.

HORIZON	DESCRIPTION
Ap (0-7 cm)	Field texture FArA and laboratory texture Sandy (A), wet color 10 YR ¾ (dark yellowish brown); subangular block structure (see Illustration 4.1-75), medium size, weak grade; Dry consistency soft, friable, slightly sticky; presence of biological activity. Strongly acidic pH (5.19), low EC.
Bsp (7-100cm) Sluice tank	Field and laboratory texture Sandy loam (FA), wet color 2.5YR 4/6 (red); lean, loose, slightly subangular block shape, very fine size and weak grade; soft, wet, friable and slightly sticky dry consistency (see Illustration 4.1-75); negative HCl reaction; mixture of mine materials of different sizes, with rock fragments; mixture of mine materials of different sizes, with rock fragments; and Highly acidic pH (5.40), low EC.

Source: INGEX, 2016.

Illustration 4.1-75. Horizons extracted.
Source: INGEX, 2016.

Physicochemical analysis

The infiltration velocity was calculated at 10.27 cm3.min-1 in 0.0081m2, therefore the theoretical infiltration 760 m3 · Ha-1 * hour-1 or 12.6m3 Ha-1 * min-1 or 1.2Lt * min-1 * m2 (See Illustration 4.1-76). This volume of infiltration, like that obtained in the LOCT infiltration curve, is even higher, and was favored by the sand contents present in the soil matrix, which allows an adequate infiltration for an optimum movement of nutrients and water in the soil. the inside of the floor.

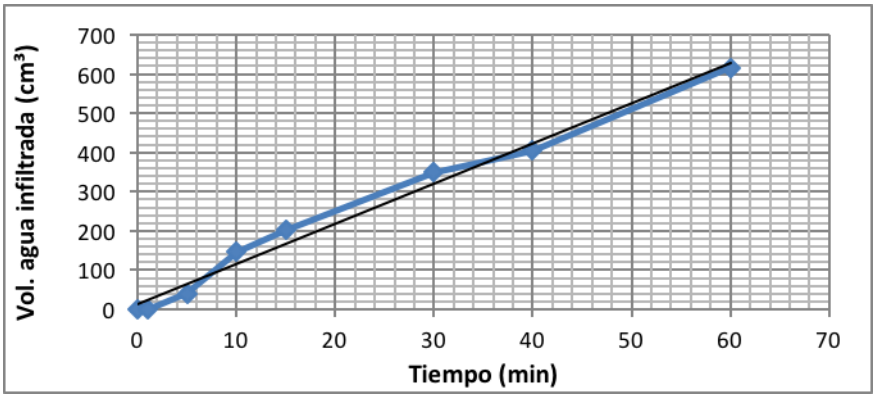

Illustration 4.1-76. Infiltration curve FHYP-CA.
Source: INGEX, 2016.

This soil has a suitable bulk density (<1 g/cm3), slightly higher on the B horizon. The level of porosity (Ap: 48.96 - B: 52.08%) indicates that these soils do not have compaction problems. The CIC is adequate. The pH is strongly acidic and with a high interchangeable Al content in most of the soil, except in horizon A, being a limiting factor for adequate vegetative root growth (see Table 4.1-34).

Table 4.1-34. Physico-chemical laboratory results of the soil profile FHYP-CA.

PARAMETER	HORIZONT Ap	HORIZONT Bsp
pH	5.19	5.40
C.E (dS/m)	0.04	0.06
Humedity (%)	18.37	26.11
DAP (g/cm^3)	0.93	1.05
DR (g/cm^3)	1.92	1.92
Porosity (%)	48.96	52.08
C.I.C. (meq/100g)	13.47	12.63
P (*di*) (ppm)	0.57	0.57
K (meq/100g)	0.16	0.06
Ca (meq/100g)	4.21	1.58
Mg (meq/100g)	0.87	0.31
Na (meq/100g)	0.09	0.09
Fe (di) (ppm)	71	47
Cu (di) (ppm)	0.30	0.50
Al (meq/100g)	0.25	1.96

PARAMETER	HORIZONT Ap	HORIZONT Bsp
N Total (%)	0.17	0.05
CO Total (%)	1.32	0.40
Cationic relationships		
Ca/Mg	4.84	5.10
Ca/K	26.31	26.33
Mg/K	5.44	5.17
(Ca+Mg/K)	31.75	31.50
Organic pollutants		
Fats and oils	<0,006 25	<0,006 25
Total hydrocarbons	<0,006 25	<0,006 25
Heavy metals and/or inorganic contaminants		
Manganese (mg/ Kg)	407.703	1430.61
Mercury (mg/kg)	0.155	< 0.050
Cyanide (mg/ Kg)	8.47	10.74
Copper (mg/ Kg)	<27,5	
Nickel (mg/ Kg)	<42,3	
Silver (mg/ Kg)	<31,0	
Lead (mg/ Kg)	<47,5	

Source: INGEX, 2016.

This soil on the Ap horizon has a moisture content of 18.37% and 26.11% on the Bsp horizon, indicating a difference of 7.74% which represents a higher water storage capacity of the last horizon; this situation could be due to the mixture of materials in the soil matrix which facilitates the displacement of water. In both cases the water storage capacity is medium and suitable for cultivation.

The profile presents low levels of organic matter, being lower in the B horizon, where there are also very low levels of N. This deficient situation is also significant for the elements P, K, Mg, Ca and Cu. The microelement Fe is high on the first horizon and in the depth is suitable. Salinity levels are low. The Ca/Mg ratio is adequate and slightly high for Ca/K, Mg/K and Ca+Mg/k; but although these ratios are balanced, the individual contents of the bases are low.

The Metals Silver, Lead, Manganese, Mercury, Nickel, Copper, Fats and Hydrocarbons are below the limits of the Louisiana 29B Protocol. Cyanide is found at high levels in both horizons because it is an area where the inhabitants work gold mining with the use of this element, thus existing a previous level of contamination.

This soil has adequate physical conditions but poor chemical fertility.

According to the IGAC, the use of this land corresponds to Class IV: Soils with very steep slopes between 25-60%, with limitations for use in crops. They have severe susceptibility to erosion in processes such as furrows, gullies, sol fluxion and mass removal. They are surface soils with little effective depth, low moisture retention and very low natural fertility.

Relief of Valley floodplain alluvial

The parental materials of the colluvial alluvial valleys are alluvial.

These soils have been derived from recent alluvial flooding, in some sectors with colluvial influence, with a flat (0-3%) to slightly sloping (3-7%) slope, warm humid climate, corresponding to the tropical rainforest life zone (bh-T), textures are moderately coarse, and fertility is low The following are the units identified for this relief based on the slope or phase ranges and taxa

LVAOT: Slightly sloping terraces (3-7%) in alluvial rainforest valleys and Typic Hapludox terraces.

LVAD: Slightly flat terraces (0-3%) in alluvial colluvial valleys and alluvial deposit association of slope.

4.1.4.1.3 Typic Hapludox - LVAOT Terraces Association

The Typic Hapludox subgroup was also found in terraces, where the camping area and northern deposit are located, the vegetation corresponds to pasture with the use of cattle ranching, slopes between 0-7%, at altitudes between 192-249 meters above sea level. They represent 0.6% of the soil types found

Modal profile

Soil formed from alluvial deposit parent material at the bottom and shed deposit at the top (see Illustration 4.1-77 and Illustration 4.1-78). Originating from granodiorite or quartz diorite rocks, warm climate, with an effective surface depth, between 30-56 cm, well drained, they are constituted by Ap-Bw-2C horizons (See Illustration 4.1-79). The humidity regime is unique, isothermal soil temperature regime, with good natural drainage, no epipedons or endopedons were observed; current use in pastures, and alluvial mining, evidence of surface erosion by trampling cattle. Table 4.1-35 shows the most detailed description by horizon.

Illustration 4.1-77. Terrace with alluvial deposit.
Source: INGEX, 2016.

Illustration 4.1-78. Lithological discontinuity.
Source: INGEX, 2016.

Physic-chemical analysis

The infiltration rate was calculated at 4.9 cm3.min-1, (0.0081m2), with a theoretical infiltration of 370.2 m3 Ha-1 hour-1 or 6.1m3 Ha- 1*min-1 or 0.6Lt*min-1*m2 (See Illustration 4.1-80). This volume of infiltration is similar to that obtained in the LCOT curve (0.73Lt*min-1*m2) and can also be considered as high and favored by the sand contents.

Illustration 4.1-79. Modal profile YANO FT.
Source: INGEX, 2016.

Table 4.1-35 Description of horizons.

HORIZON	DESCRIPTION
Ap (0 – 11cm) Sluice tank	Clay loam field (FAr) and laboratory texture Sandy; Wet color 10YR 3/4 (dark yellowish brown); angular block structure, very fine; dry consistency loose, wet friable, slightly sticky; HCl negative reaction; presence of fine cylindrical pores; with evidence of fine roots, presence of organic matter and quartz grains of fine and coarse sand size; diffuse horizon boundary. Natural surface drainage good. Moderately acidic pH (5.76), low EC.
Bw (11 - 62cm) Sluice tank	Field texture Sandy clay loam (FArA) and laboratory texture Sandy loam (FA); Wet color 5YR 4/6 (yellowish red); structure in angular blocks, very fine, weak; Dry, wet, friable and slightly sticky consistency; negative HCl reaction; presence of fine cylindrical pores; with little evidence of fine roots, abundant fine sand and medium sized quartz grains. No evidence of erosion Low surface natural drainage. Moderately acidic pH (5.53), low EC.
2C (62-100 cm) Discontinuity	Rocky bedrock with rounded and angular edges, possibly an old bedrock of the river that after changing course made slope deposits, is considered a horizon C (fresh non-weathered rock), without structure.

Source: INGEX, 2016.

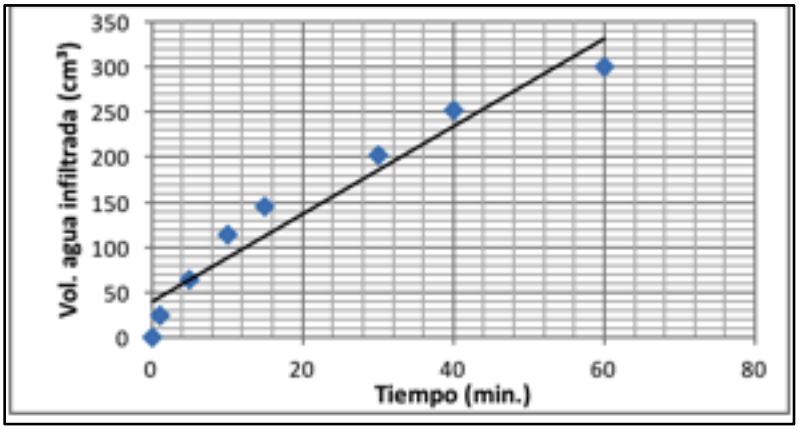

Illustration 4.1-80. Infiltration curve YANO-FT.
Source: INGEX, 2016.

In the analysis of physical results of this soil they show adequate conditions of DAP (<1 g/cm3) and low Dr due perhaps to the fractionation of the minerals, the total porosity is very low in the Ap horizon and very good in the Bw; the CIC is adequate, the pH is moderately acidic and therefore does not present interchangeable Al. This generates suitable physical conditions for plant development. The moisture content (36.9% and 32.13%) represents a high-water storage capacity that could favors plant growth and development (Table 4.1-36).

Table 4.1-36. Physico-chemical results of the YANO-FT soil profile.

PARAMETER	HORIZONT Ap	HORIZONT Bw
pH	5.76	5.53
C.E (dS/m)	0.04	0.02
Humedity (%)	36.90	32.13
DAP (g/cm³)	0.92	0.85
DR (g/cm³)	1.78	1.78
Porosity (%)	35.39	56.18
C.I.C. (meq/100g)	23.28	17.79
P (*di*) (ppm)	0.58	0.58
K (meq/100g)	0.38	0.14
Ca (meq/100g)	9.78	3.96
Mg (meq/100g)	2.08	1.09
Na (meq/100g)	0.10	0.10
Fe (di) (ppm)	149	67
Cu (di) (ppm)	0.30	0.40
Al (meq/100g)	N.A	N.A
N Total (%)	0.31	0.04
CO Total (%)	2.54	0.67
Cationic relationships		
Ca/Mg	4.70	3.63
Ca/K	25.74	28.29
Mg/K	5.47	7.79
(Ca+Mg/K)	31.21	36.07
Organic pollutants		

PARAMETER	HORIZONT Ap	HORIZONT Bw
Fats and oils	<0,006 25	
Total hydrocarbons	<0,006 25	
Heavy metals and/or inorganic contaminants		
Manganese (mg/ Kg)	1277.044	607.464
Mercury (mg/kg)	1.328	0.088
Cyanide (mg/ Kg)	<0.200	
Copper (mg/ Kg)	<27,5	
Nickel (mg/ Kg)	<42,3	
Silver (mg/ Kg)	<31,0	
Lead (mg/ Kg)	<47,5	

Source: INGEX, 2016.

There were high levels of MO and N on the first horizon and very low on the second. In addition, the elements P, Mg and Cu in very deficient quantities; the Ca and K suitable in Ap, but very low in depth. Non-saline soil with high Fe content. Ca/Mg, Ca/K cation ratios are adequate, while Mg/K and Ca+Mg/k ratios are unbalanced. Although the contents of each base are very low. Heavy metals, cyanide, fats and oils and hydrocarbons are below the limits of the Louisiana Protocol 29b. Except for Mercury which is on the Ap horizon at slightly higher levels according to the limits of the EPA (1992).

According to the IGAC, the use of this land corresponds to Class II, suitable for use in agriculture in transitory or perennial crops, it is necessary to establish drainage systems. Erosion management practices are easy to apply. Although it has restrictions in the chemical component that imply the use of fertilizers and correctives.

Mineralogy

The coarse fraction (> 2 mm) in the horizons Ap and Bw, is composed mostly of rock remains (Ap: 65% - B: 40%) very weathered, which hardly show some of its primary constituents such as Quartz (Ap: 15% - Bw: 30%), Garnet (Ap: 1% - Bw: 10%). Amphiboles (Ap: 1%), hematite (Ap: 5%) and Limonite (Ap: 10% - Bw: 5%), and in-depth Sericite (Bw: 15%) (See Table 4.1-37, Table 4.1-38 and Illustration 4.1-81).

Table 4.1-37. Mineral count on Ap horizon.

MINERALS	COARSE FRACTION (>2 mm)	SAND FRACTION (%)	LIMO FRACTION (%)
Mother rock	65		
Quartz	15	95	60
Plagioclase		<1	35
Garnet	1	1	5
Amphiboles	1		
Sericite		2	1
Magnetite		<1	
Hematite	5		
Limonite	10	1	2
Others			Trazas

Source: INGEX, 2016.

Table 4.1-38. Mineral count in horizon Bw.

MINERALS	COARSE FRACTION (>2 mm)	SAND FRACTION (%)	LIMO FRACTION (%)
Mother rock	40	30	
Quartz	30	30	45
Plagioclase		20	40
Garnet	10	2	5 (Garnet and spinel)
Albita		2	
Sericite	15	5	5
Magnetite		1	
Epidote		1	
Limonite	5		5
Epidot and Actinolite		5	

In the sand fraction (2mm> f > 0.2mm) (See Table 4.1-37 and Table 4.1-38), the Ap horizon is dominated by Quartz (95%) with secondary minerals such as Sericite (2%), Garnet (1%) and Limonite (1%) and accessories such as Magnetite (<1%) and Plagioclase (<1%). These quantities of quartz decrease on the Bw horizon to 30% and are found in the same proportions as the parent rock. While the amounts of Plagioclase (20%), Albite (2%), Garnet (2%), Sericite (5%) and Magnetite (1%) are higher and accessory minerals appear.

In the Silt Fraction (200 um > F > 20 um) (See Table 4.1-37 and Table 4.1-38), the following minerals were found: Quartz (Ap: 60%-Bw: 45%) and Plagioclase - Albite (Ap: 35%- Bw: 40%) predominant, and with 5% individual in each Garnet and Sericite horizon, and Limonite in the Bw horizon.

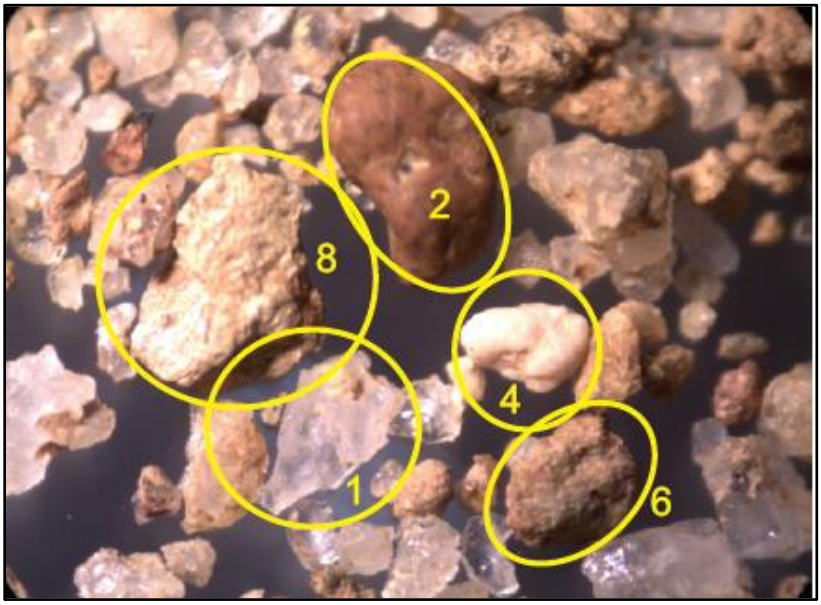

Illustration 4.1-81. In mineral circles present in the YANO-FT profile: 1. Hyaline quartz. 2. Meteorite Metamorphic Rock 4. Albita 6. Garnet 8. Epidot and Actinolite.
Source: INGEX, 2016.

In the fine fraction were very abundant Limonite and some other varieties of iron oxides such as Hematite and Goetite, which provide iron. In these terrace soils Plagioclase was found concentrated in the sand and lime fraction, which gives these soils a special characteristic in the availability of calcium. Garnet was present in almost all of the samples, in concentrations from 1 to 14 %; this is a typical mineral of metamorphic rocks, which speaks of the parent material of the soil. The latter being a name applied to the very finely crystallized Muscovite, constituting a transition between the illite and the Muscovite itself.

4.1.4.1.4 Alluvial alluvial deposit association (LVAD)

Alluvial soils are transported soils, formed by the removal, transport and accumulation of debris in the stream beds. Alluvial deposits composed of coarse fractions (sand and gravel) are good construction materials for pavements, concrete and others, because in the transport process the weakest parts of the fragments have been detached, making them the strongest.

Modal profile

This alluvial deposit is located in the Alluvial Terrace (Ft) geoformation at 190masl, with grass vegetation (See Illustration 4.1-82), used in paddock, slope of 3 % (slightly flat). This soil does not form a structure; therefore, it corresponds to an alluvial and slope deposit, with a mixture of materials contributed by the bodies of water and the slope. The material comes from soil transported from the terrace, wetness of the soil, superficial depth (40cm), good natural drainage, no epipedon, no erosion is evident.

Illustration 4.1-82. Alluvial deposit site.

Source: INGEX, 2016.

In Table 4.1-39, Illustration 4.1-83, Illustration 4.1-84 and Illustration 4.1-85, the description by horizon is presented.

Table 4.1-39. Description by horizons.

HORIZON	DESCRIPTION
B1 (0 – 78cm) Alluvial and watershed deposits	Field texture FArA and laboratory, sandy; color wet 7.5YR 4/6 (strong coffee); non-structured; loose dry consistency; non-sticky wet consistency; negative HCl reaction; presence of abundant fine and medium irregular pores; evidence of fine roots; presence of mixed organic matter in parent material; presence of fine and coarse sand size quartz grains; abrupt boundary between horizons. Moderately acidic pH (5.88), low C.
B2 (78 - 100cm) Weather profile	Sandy field texture (A) and laboratory AF; wet color 10YR 4/4 (dark yellowish brown); no structure; dry and wet consistency loose, wet non-sticky; HCl negative reaction; no evidence of roots at this depth. Moderately acidic pH (5.66), low E.C.

Source: INGEX, 2016.

Illustration 4.1-83. Alluvial deposit profile (PB-FT).
Source: INGEX, 2016.

Illustration 4.1-84. Horizon detail B1.
Source: INGEX, 2016.

Illustration 4.1-85. Detail of horizon B2.
Source: INGEX, 2016.

Physico-chemical analysis

The infiltration rate was calculated at 3.92 cm3.min-1, with a theoretical infiltration of 290.26m3. Ha-1´´ó 0.48Lt min-1*m2 (See Illustration 4.1-86). This volume of infiltration is high and similar to that of the LVAOT soil association, due to the sandy texture and lack of structure of the recent alluvial

deposit, where materials of different sizes have been mixed which do not have a high adhesion between them and favors the movement of water.
The physical analysis (see Illustration 4.1-86) shows a low E.C., without salinity, with adequate apparent density (<1g/cm3), very low porosity in the first horizon and low in the rest of the profile, due to the effect of grazing the cattle. CIC is slightly low, pH, moderately acidic, in a range suitable for plant growth and not having interchangeable aluminum in the soil.

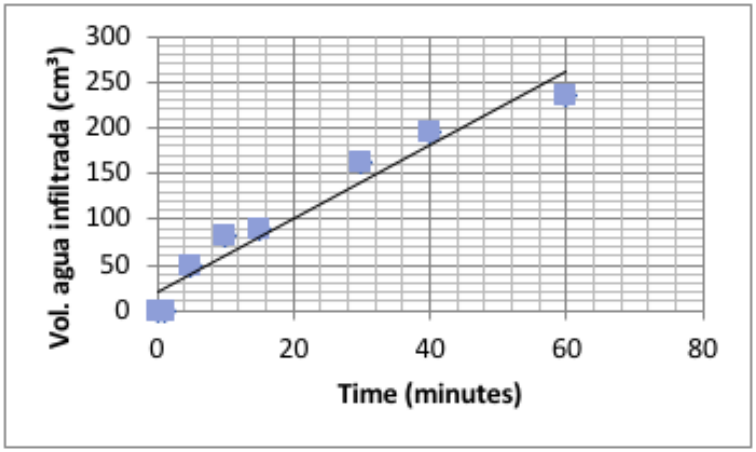

Illustration 4.1-86 Infiltration curve LVAD
Source: INGEX, 2016.

The moisture retention capacity of 15.8% at horizon B1 and 21.5% at horizon B2 represent an average and medium to high water retention, respectively. It correlates with the infiltration capacity obtained in this soil, infiltrating much but storing little water, which means high possibilities of nutrient washing.

Table 4.1-40. Physical results of the PB-FT soil profile.

PARAMETER	HORIZONT B1	HORIZONT B2
pH	5.88	5.66
C.E (dS/m)	0.02	0.03
Humedity (%)	15.80	21.56
DAP (g/cm^3)	0.92	0.88
DR (g/cm^3)	2.08	2.08
Porosity (%)	35.58	40.86
C.I.C. (meq/100g)	7.59	9.76
P (*di*) (ppm)	1.69	11.43
K (meq/100g)	0.14	0.30
Ca (meq/100g)	2.46	2.30
Mg (meq/100g)	1.14	1.29
Na (meq/100g)	0.07	0.10
Fe (di) (ppm)	1345	1346
Cu (di) (ppm)	0.40	0.40
Al (meq/100g)	N. A	N. A

PARAMETER	HORIZONT B1	HORIZONT B2
N Total (%)	0.284	0.060
CO Total (%)	0.15	0.71
Cationic relationships		
Ca/Mg	2.16	1.78
Ca/K	17.57	7.67
Mg/K	8.14	4.30
(Ca+Mg/K)	25.71	11.97
Organic pollutants		
Fats and oils	<0,006 25	
Total hydrocarbons	<0,006 25	
Heavy metals and/or inorganic contaminants		
Manganese (mg/ Kg)	1459.498	814.466
Mercury (mg/kg)	0.175	<0.050
Cyanide (mg/ Kg)	0.200	
Copper (mg/ Kg)	<27,5	
Nickel (mg/ Kg)	<42,3	
Silver (mg/ Kg)	<31,0	
Plomo (mg/ Kg)	<47,5	

Source: INGEX, 2016.

The contents of CO, MO and N are very low. Also, of the macro elements P, Ca and Mg. K is only suitable in the last observed horizon and the microelement Cu is also deficient, while Fe has very high levels, a particular characteristic of Oxysols.

The Ca/Mg ratio is low; the Ca/K ratio is adequate on the first horizon and low on the second. And the cationic ratios Mg/k and Ca+Mg/k are in a suitable range. As a general result, the physical conditions are adequate, but the fertility level in this type of soil is low.

Heavy metals, cyanide, grease and hydrocarbons are below the limits under Louisiana Protocol 29B and EPA (1992).

The classification of this soil according to the IGAC corresponds to Class II, has some limitations for hydraulic or wind erosion that provide new materials, are suitable for agricultural use, in transitory or perennial crops, although the choice of these is not so wide.

Comparison of infiltrations of soil associations

Comparing the infiltration of water in the soil of the soil associations in the study area (See Illustration 4.1-87), it was determined that Tecnosol Spolic (LCT) had the highest infiltration with 760.02 m3.Ha-1 or 1.2Lt min-1*m2, which corresponds to a mixture of materials in the process of pedogenesis; followed by the LCOT association that allowed an infiltration of 439.99 m3 Ha-1 or 0.7Lt min-1*m2 and the LVAOT association with 370.01 m3 Ha-1´´ó 0.6Lt min-1*m2. Finally, there is the LVAD infiltration curve, with 290.26 m3. Ha-1´´ó 0.48Lt min-1*m2, which is consistent with the low porosity of this soil as a measure of the compaction generated by livestock.

The key factor that influences this difference is the texture, aggregation and/or disturbance of the soil material; the TBI is composed of disturbed materials that are mixed by anthropogenic action (informal mining) that facilitate the movement of water. The other associations were in use for grazing with possible compaction due to the trampling of the cattle.

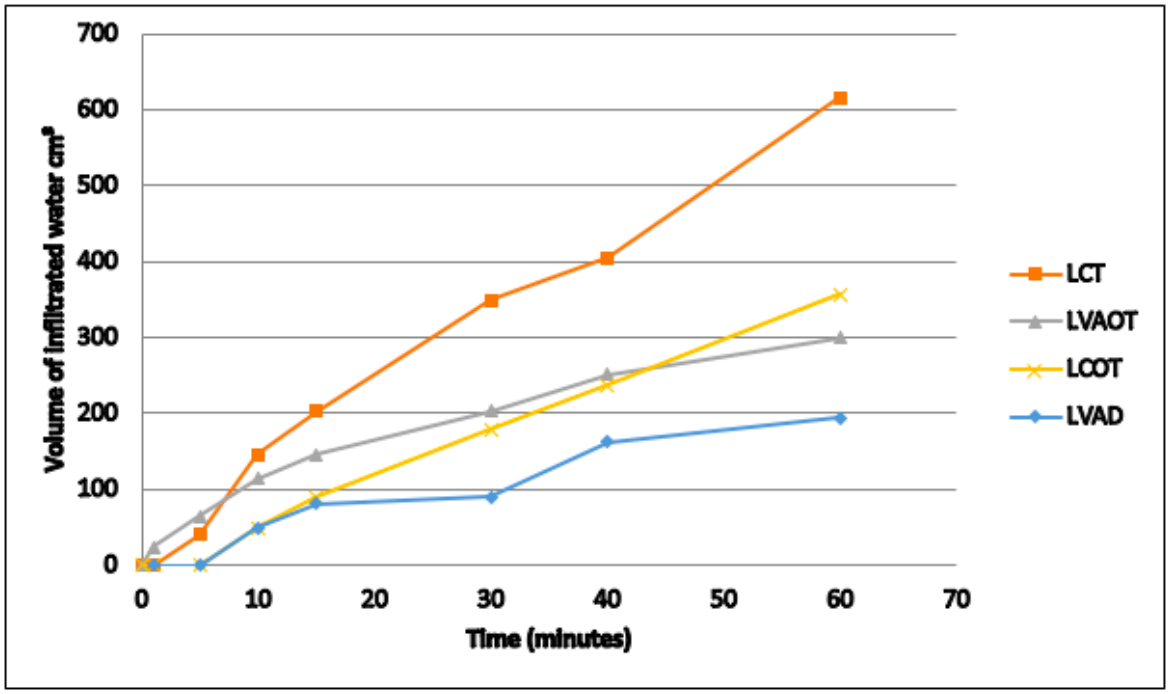

Illustration 4.1-87. Comparison of water infiltrations in the soil for the study area associations.
Source: INGEX, 2016.

4.1.4.2 AGROLOGICAL CLASSIFICATION AND POTENTIAL LAND USES

The agrological classification allows determining the potential use of a soil unit based on soil characteristics (fertility, salinity, effective depth, drainage, moisture retention), relief, slope and climate. This classification, adapted by the IGAC, is represented by a symbol that includes the subclass and management group; the subclass is defined by a Roman number between one and eight (I-VIII), where the limitations or restrictions on the development of agricultural activities are increased until they reach those lands that are restricted to natural conservation and/or recreation. While for the determination of the subclass, the most representative limitations are taken into account, with the following letters representing variables: slope (p), erosion (e), soil (s), humidity (h) and climate (c).

This classification system is structured in such a way that the greater the agrological class, the lower the possibility of agricultural use, reducing the ability to plant various crops, while increasing

management and conservation practices (Guerra, 2014). These vocations for use and recommended management measures are presented in the Table 4.1-41 and Illustration 4.1-88.

Table 4.1-41. Potential land use.

AGROLOGICAL SUBCLASS	SOIL ASSOCIATION	MAIN CHARACTERISTICS	MAIN LIMITATIONS OF USE	RECOMENDED USE	MANAGEMENT PRACTICES RECOMMENDATIONS
IIs	LVAOT	Warm, humid climate, terraced relief, slightly flat and sloping (0-7%), with alluvial and sloping parent material; soil with effective surface depth (30-56cm), texture A and FA, with low nutritional content, moderately acidic pH.	Small areas, due to the fact that the terraces are located at the bottom of slopes, at the foot of slopes with steep to steep slopes. With chemical limitations due to its low macronutrient content. It presents slightly high levels of Mercury in the surface, according to the limits of the EPA (1992), by mining extraction.	Clean subsistence agriculture with transient or perennial crops; crops of low size for the conservation of water resources and flora and fauna.	To plant low bushes and shrubs in the lateral strips of rivers and streams up to 30 m. In the upper part, after 30 m. of the conservation strip, it is recommended to make forest plantations for protection and production, which contribute to the protection of the water; eventually, these reforestation activities can be combined with non-intensive silvopastoral practices.
IVse	LCT	Warm, humid climate, with steeply sloping slopes (12-25%). With a mixture of different types of materials, by the action of man, which have given rise to the Tecnosol type of soil. Soils with low nutritional content for plants.	Soil disturbed by gold mining activities on steeply sloping slopes that could favour erosion processes.	Forestry with protective-productive plantations, and small-scale agriculture of perennial crops such as cocoa, banana, yucca, citrus.	Plant forest plantations and crops with soil conservation management practices such as contour lines. It is required to add chemical synthesis fertilizers and organic fertilizers per sowing site. Agricultural plants must be planted in areas with a lower slope than forest plantations and must respect the conservation strips of water bodies.
VIpe	LCOT	Warm, humid climate, with steeply sloping slopes (>25%). With low nutritional content for plants, moderately acidic pH. Low natural fertility. Soil texture A, FA and FArA.	Chemical limitations by the strongly acidic pH, high content of interchangeable Al and nutritional deficiencies of N, P, K, Mg and Ca	Forestry production-protection with timber plantations on slopes of less than 45%, and protection on slopes of more than 45%, where the native forest is present. Agro-silvopastoral with special pasture management.	To plant timber forest plants in areas that are in cattle ranching, suitable for timber harvesting, must be done with soil conservation practices, fertilizing and liming the planting site. Reforest protection areas with native plants that are easy to propagate or reproduce and allow plant species dispersal factors to repopulate the areas that were intervened. In the case of livestock, make timely rotation of pastures and avoid overloading. And avoid this activity on slopes higher than 45%.

Source: INGEX, 2016.

Each agrological subclass and its potential use is described below.

4.1.4.2.1 Subclass IIs

This subclass was found in the soils of the consociation terraces - LVAOT and alluvial deposit of slope - LVAD, of the hilly landscape and relief Colluvial - alluvial valleys, in terraces, with slightly flat slopes

to inclined (0-7%). The terraces are located at the bottom of the slope, at the foot of the slopes. Therefore, the areas in this subclass are limited in extension; their length ranges from the body of water to the beginning of the slope, varying between 3-20 meters, where there are fresh alluvial deposits subject to natural intervention by flooding and shaped terraces (See Illustration 4.1-89).

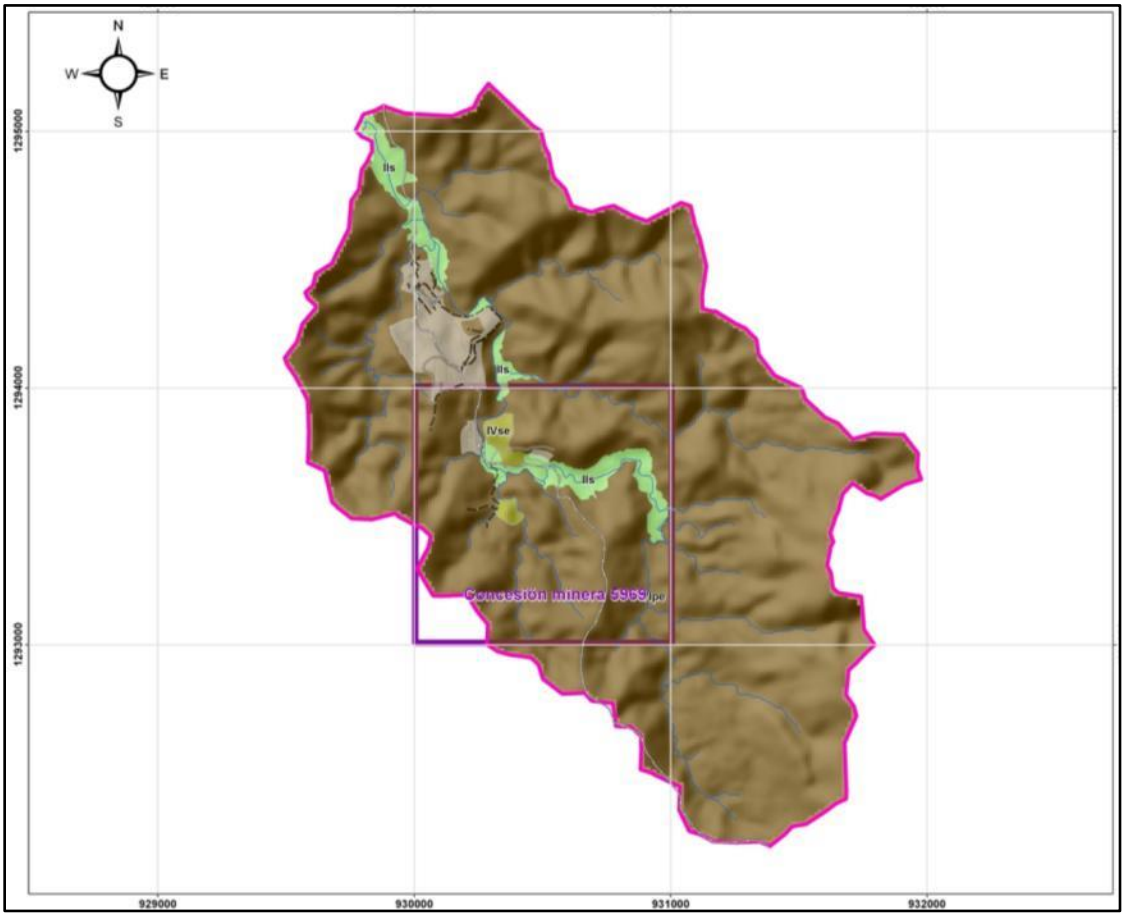

Illustration 4.1-88. Agrologic classes in the study area.
Source: INGEX, 2016.

Illustration 4.1-89. Aspect of category IIs land.
Source: INGEX, 2016.

Potential land use subclass IIs

According to the IGAC, the vocation of use of this land is suitable for agriculture in transitory or perennial crops, being necessary the establishment of drainage and erosion management practices that are easy to apply. Although it has restrictions in the chemical component of the soil where the levels of MO and main and secondary macro elements such as N, P, K, Ca and Mg are so low that they involve the use of fertilizers and corrective measures.

4.1.4.2.2. Subclass IVse

This agrological subclass is presented at the Consociation Tecnosol Spolic (LCT) in the landscape of the hilly erosional structural landscape, relief of hills, with slopes classified as steeply sloping slopes (12-25%). According to the IGAC, this category corresponds to soils with very steep slopes between 25-60%, with limitations for use in crops, as they have severe susceptibility to erosion. They are surface soils with little effective depth, low moisture retention and very low natural fertility. Characteristics corroborated with the chemical analysis of soil where a strongly acidic reaction, high content of interchangeable Al and deficiency of MO and macro elements such as N, P, k, Mg and Ca were found. These two (2) erosion and soil limitations led to its classification in subclass IVse.

Potential land use subclass IVse

The vocation for the use of this land is reforestation with Agroforestry or Agro-silvopastoral activities, combining production-conservation and agricultural forestry activities with semi-permanent and semi-permanent semi intensive crops, such as cocoa, bananas and citrus fruits. Or forestry activities are combined with non-intensive livestock farming. With control measures, mining activities could also be carried out. In addition, it is an area that has been previously used in informal mining.

4.1.4.2.3 Subclass VIpe

This agrologic class was identified in the Typic Hapludox Association (LCOT) of the Hilly erosional structural landscape of hills, on steeply sloping slopes (>25%). According to the IGAC, class VI corresponds to very steep soils (25-50%), suitable for supporting permanent vegetation and/or reforestation, which must remain under natural or planted forest. They are not suitable for any type of crop due to erosive processes, such as furrows, gullies, sol flow and mass removal, with shallow effective depth, low moisture retention and very low natural fertility.

This classification is in accordance with the general study of soils and land zoning in the department of Antioquia, conducted by the IGAC (2007), where the study area belongs to the Remedios Association (Rem), In this study, they were classified as Subclass 6p, with geomorphological zones such as hills and hills of the hilly landscape, steep relief, soils with very strong to strongly acidic reaction and low to very low fertility. As the main limiting factor, they determined the slightly steep slopes. Main use in cattle raising with natural grasses or introduced as grasses and brachiaria. It is susceptible to erosion and mass movements due to steep slopes, rainfall and land use.
Potential land use of subclass VIpe

The purpose of this subclass is to use production-protection forestry, where the areas where the forest has been cut down and burnt down for sowing pastures for livestock (see Illustration 4.1.90) are reforested with timber species; these areas can also be used for clean subsistence crops and specially managed agro-silvopastoral activities. In areas with slopes of more than 45% and in the water protection strips and/or outcrops of these, it should be used as a protective forest with native vegetation, favoring ecological condensation nuclei with the fauna and flora of the area, and protection of the water bodies. For areas with native forest, it is recommended to preserve them and not to carry out these anthropogenic intervention activities.

Results of agrological classes and potential land uses

As shown in Illustration 4.1-91 and Table 4.1-42, the VIpe class is the predominant class (95.49%), according to the steep slope conditions and the susceptibility to erosion that occur in the soil of the LCOT consociation. To a lesser extent, the type IIs classifications refer to the slightly flat lands of the LVAD consociation, and the type IV soils are located in the LCT consociation.

Illustration 4.1-90. Logging and burning of forest, conflict over severe overuse.
Source: INGEX, 2016.

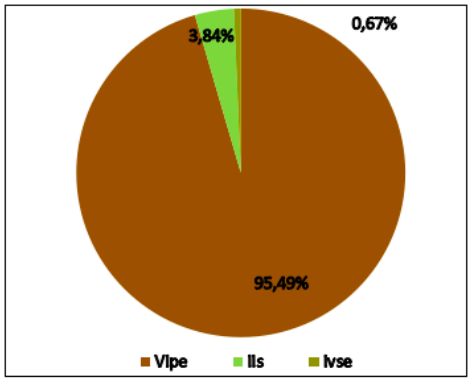

Illustration 4.1-91. Distribution of agrological classes.
Source: INGEX, 2016.

Table 4.1-42. Distribution of agrological classes.

AGROLOGIC CLASS	AREA (ha)	%
VIpe	372,89	95,49%
IIs	14,99	3,84%
IVse	2,64	0,67%
TOTAL	**390,5**	**100,00%**

Source: INGEX, 2016.

Correspondingly with this classification, the vocation or suitability for land use at the crop level (see Illustration 4.1-92, Illustration 4.1-93 and Table 4.1-43), should be 95.49% Production-Protection Forest, complemented with transitory or perennial crops in type IIs soils, 3.84%, and Agro-silvoforestal or agro-silvopastoral in class VIpe soils.

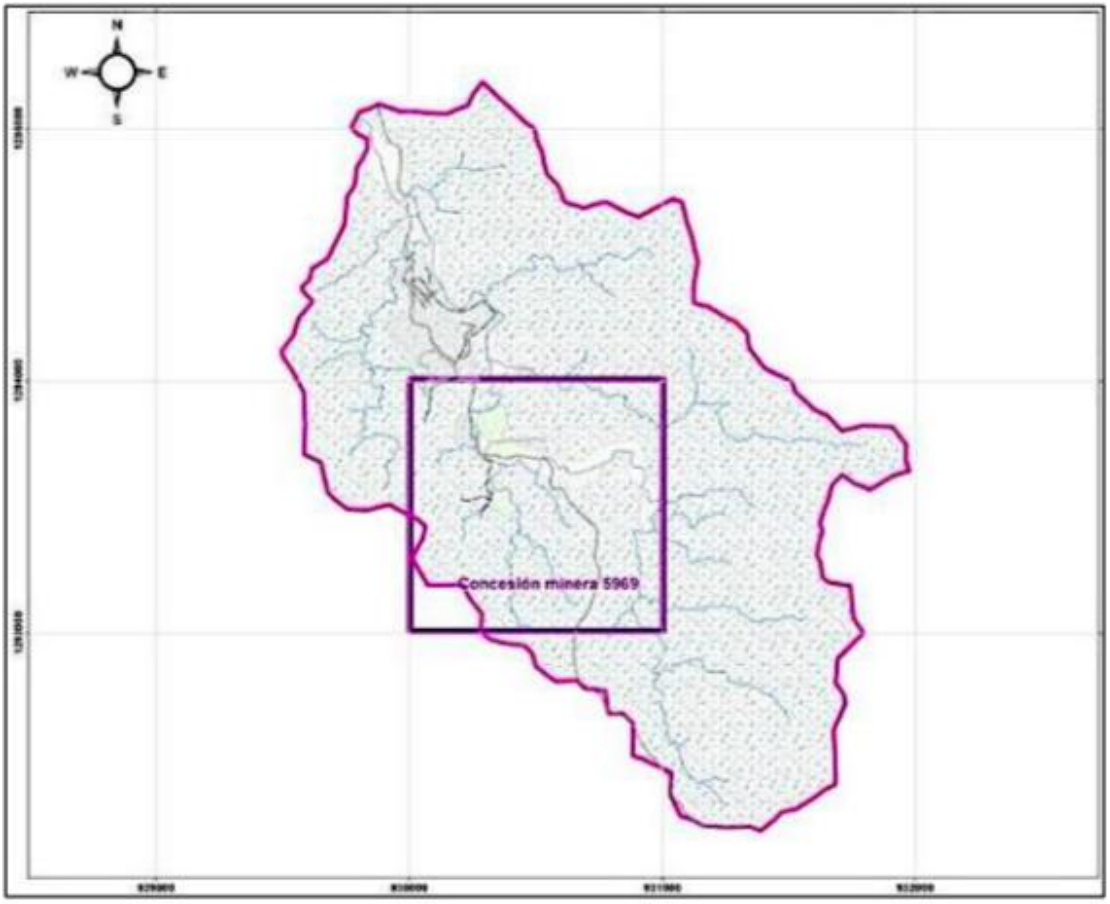

Illustration 4.1-92. Potential land use.
Source: INGEX, 2016.

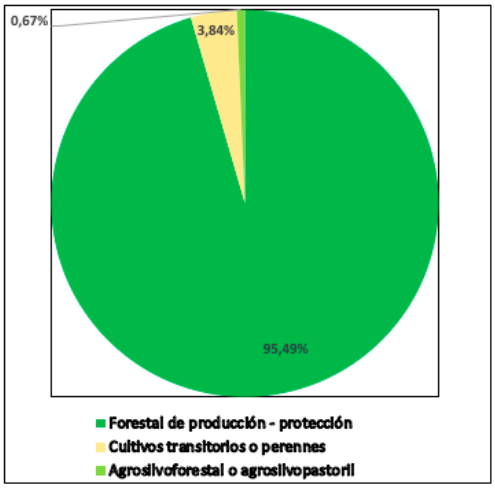

Illustration 4.1-93. Distribution of land use vocation
Source: INGEX, 2016.

Table 4.1-43. Distribution of potential land uses.

POTENTIAL LAND USE	AREA (ha)	%
Production forest - protection	372,89	95,49%
Transient or perennial crops	14,99	3,84%
Agroforestry or agroforestry	2,64	0,67%
TOTAL	**390,5**	**100,00%**

Source: INGEX, 2016.

CURRENT LAND USE

Current land use, referring to human activities on the land resource, was based on the vegetation cover units defined in the flora component and was grouped into the land uses defined in accordance with MADS resolution 1415 of 17 August 2012 (see Table 4.1-44).

Table 4.1-44. Land use classification factors.

Soil Use	Type of use
Agricultural	Intensive transitory crops
	Semi-intensive transient crops
	Semi-permanent and intensive permanent crops
	Semi-permanent and semi-intensive permanent crops
Agro-forestal	Agricultural forestry
	Agro-silvopastoral
	Silvopastoral
Stockbreeder	Intensive and semi-intensive grazing
	Extensive grazing
Forestal	Production
	Production-Protection
	Protection
Conservation	Protective forest
	Water resources
	Recovery

Source: MADS, 2012

The classification of uses by land cover is presented in Table 4.1-45 and Illustration 4.1-94.

Table 4.1-45. Current land use.

ASSOCIATED LAND COVER	SOIL USE	TYPE OF USE	SYMBOL
Dense forest beneath the mainland	Forest Conservation	Production-Protection	Fcpp
Rivers or other bodies of water		Water resources	Crh
Lower secondary vegetation	Livestock Farming Fallow land	Extensive grazing	Gpe
Clean grass			
Banana and Cassava Crops	Agricultural	Transient semi-intensive crops of bread and butter.	Act

ASSOCIATED LAND COVER	SOIL USE	TYPE OF USE	SYMBOL
Cocoa cultivation		Semi-intensive perennial crops	Acp
Mining and infrastructure	Gold mining	Opencast Mining	Ma

Source: INGEX, 2016.

Illustration 4.1-95 shows that the largest use (50.87%) in the study area is for extensive livestock production (GPE), which is characteristic of this mode of production where there is a low animal load on large areas of land. This use is followed by those dedicated to Forest Production - Protection (45.72%) where the existing forest areas and water sources are located. To a lesser extent, the areas dedicated to mining and infrastructure (Ma) and agricultural crops (Acp), with 3.08% and 0.33%, respectively (Table 4.1-46).

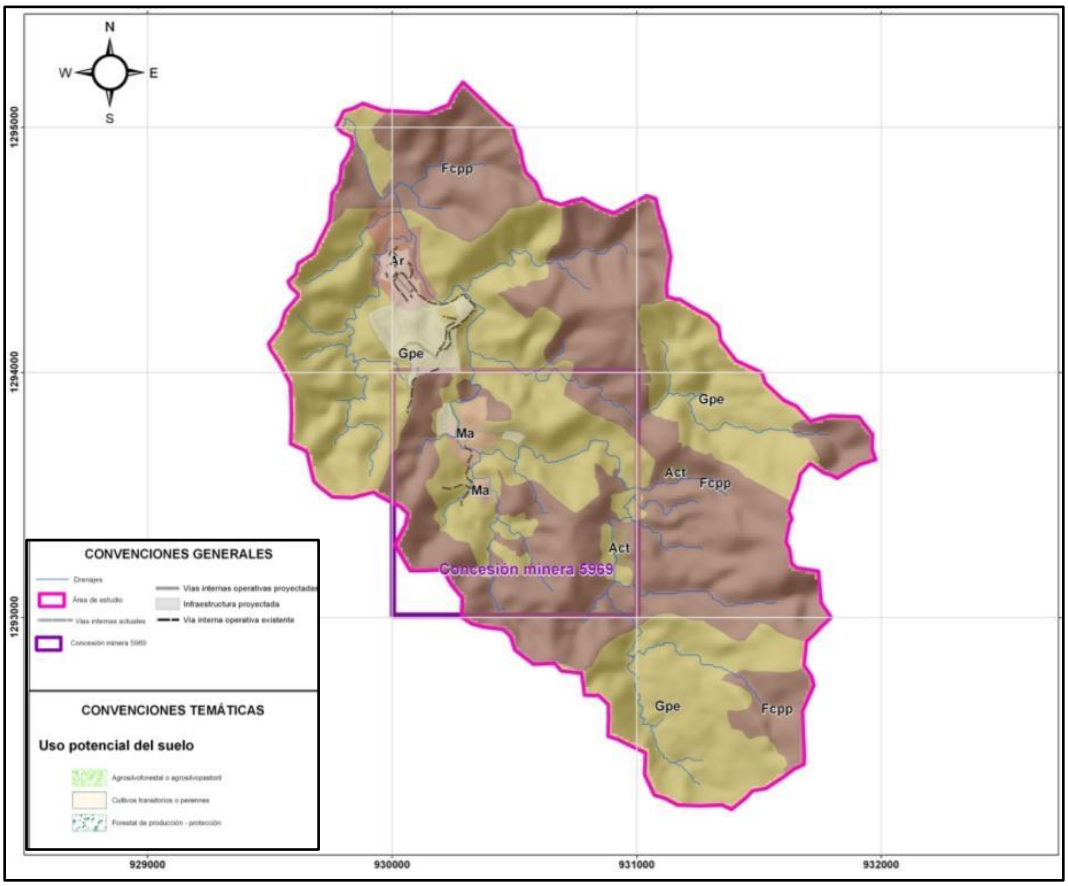

Illustration 4.1-94. Current land use.
Source: INGEX, 2016.

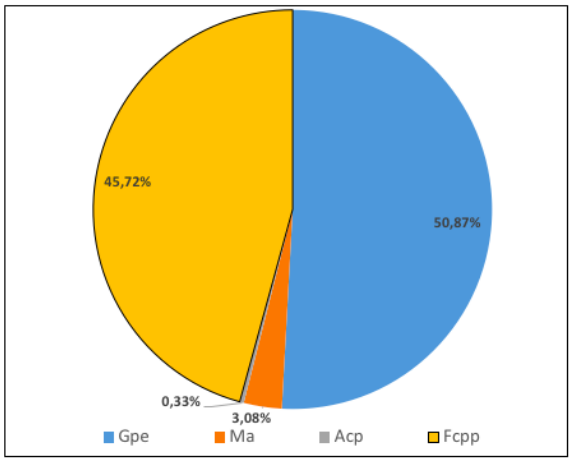

Illustration 4.1-95. Distribution of current land use.
Source: INGEX, 2016.

Table 4.1-46. Distribution of current land use.

CURRENT LAND USE	AREA (ha)	PERCENTAGE
Gpe	198,743557	50,87%
Ma	12,036565	3,08%
Acp	1,297513	0,33%
Fcpp	178,628991	45,72%
TOTAL	**390,7**	**100,00%**

Source: INGEX, 2016.

Each of the categories of uses is described below.

4.1.4.2.4 Soils in conservation

Protected areas such as water bodies, creek protection strips and dense underground forests were classified by means of the existing vegetation cover, which are currently without intervention or a selective intervention that allows them to continue fulfilling their function of conserving the environment, in the protection of existing fauna and flora.

Conservation of water resources (Crh)

Rivers and streams, whose function is the conservation of water resources, are part of this land use.

4.1.4.2.5 Soils in use Production-Protection Forestry (Fcpp)

The dense forest coverings under the mainland dedicated to production-protection forest use were classified, where the wood is used to satisfy the domestic needs of the inhabitants or, in the case of areas with steeper slopes, it is left for conservation.

4.1.4.2.6 Soils in extensive grazing (Gpe)

The use in livestock is the one that mostly occurs in the study area, this is done in the clean grass coverings where grass has been cultivated and in the lower secondary vegetation coverings where the stubble or fallow grass is found. Cattle and calf production is carried out using a low animal load per hectare and large areas of land, eliminating forest areas to turn them into pastures, which makes this activity economically and environmentally inefficient.

4.1.4.2.7 Agricultural Soils

Areas dedicated to the production of transitory and perennial crops in order to generate food for the consumption of the inhabitants. These occur in small areas within the basin.

4.1.4.2.8. Soils in Transitional semi-intensive crops for own consumption (Act)

These are the areas dedicated to the production of crops for the self-consumption of the people of the village, among which are banana and cassava. These crops are grown in small areas and during the year they rotate from transient crops such as corn or rice.

4.1.4.2.9 Soils in semi-intensive perennial crops (Acp)

The perennial crops grown in the area correspond to cocoa areas that are in production although their areas are very small, and the agronomic management is very deficient. Therefore, it does not constitute a significant source of income for the producers of this product.

4.1.4.2.10 Soils in Opencast Mining and Associated Lands (Ma)

In this coverage of mining uses are found the mineral extraction lands by informal people also lands those occupied by houses and dumps. Also transport infrastructure such as roads belong to this coverage.

4.1.4.3 LAND USE CONFLICT

For the definition of land use conflicts, the biophysical supply expressed by the capacity of use and the current use (land demand) was taken into account. The classification of conflicts was made by applying the criteria based on four categories of conflicts according to the categories defined in Resolution 1415 of 17 August 2012 (MADS, 2012) as shown in Table 4.1-47.

Table 4.1-47. Land use conflicts.

AGROLOGICAL SUBCLASS	SOIL ASSOCIATION	POTENTIAL LAND USE	CURRENT LAND USE	USAGE DISPUTES
IIs	LVAOT	Protective agriculture and forestry, agro-silvopastoral	Settlements associated with mining, agriculture, extensive cattle ranching and protective forest, producer.	**Land in Conflict due to moderate overuse**: Due to the fact that the land presents inadequate current uses as it is in settlements, mining and cattle ranching, managed inappropriately, exceeding the capacity of the natural environment to support it. Its potential is in agroforestry and agroforestry activities, with production and protection forests, small-scale crops of cocoa, bananas, cassava, citrus fruits.
IVse VIpe	LCT LCOT	Forest protection - production. Agro-silvopastoral with special pasture management.	Extensive cattle ranching and open pit mining.	**Land in conflict due to severe overuse:** Due to the fact that the land is currently being used inappropriately for livestock without silvopastoral or Fcpp implementation and or in mining areas. These lands are rugged, representing ecological risks by affecting natural resources, such as water, flora and fauna, affecting the natural balance and stability of ecosystems. Due to the current levels of erosion and contamination of soil use with heavy metals, it is not recommended for livestock farming.
VIpe	LCOT	Protected forest - production	Protected forest – production	**Land without use conflict.** They are the used lands according to their vocation.

Source: INGEX, 2016.

As shown in Table 4.1 48, Illustration 4.1-96 and Illustration 4.1-97, the study area is between 50.7% severely overused and 45.4% non-conflicting and used in accordance with its vocation. Only 3.9% is moderately overused. Therefore, activities that are closer to their vocation should be implemented on the land to a severe degree, so that the natural resources of these areas are not further compromised.

Table 4.1-48 Distribution of conflicts in the area of study.

CONFLICT OF USE	AREA (ha)	%
Moderate overuse	15.246629	3.9%
Severe overuse	197.886998	50.7%
No conflict	177.38903	45.4%

Total	390.5	100.0%

Source: INGEX, 2016.

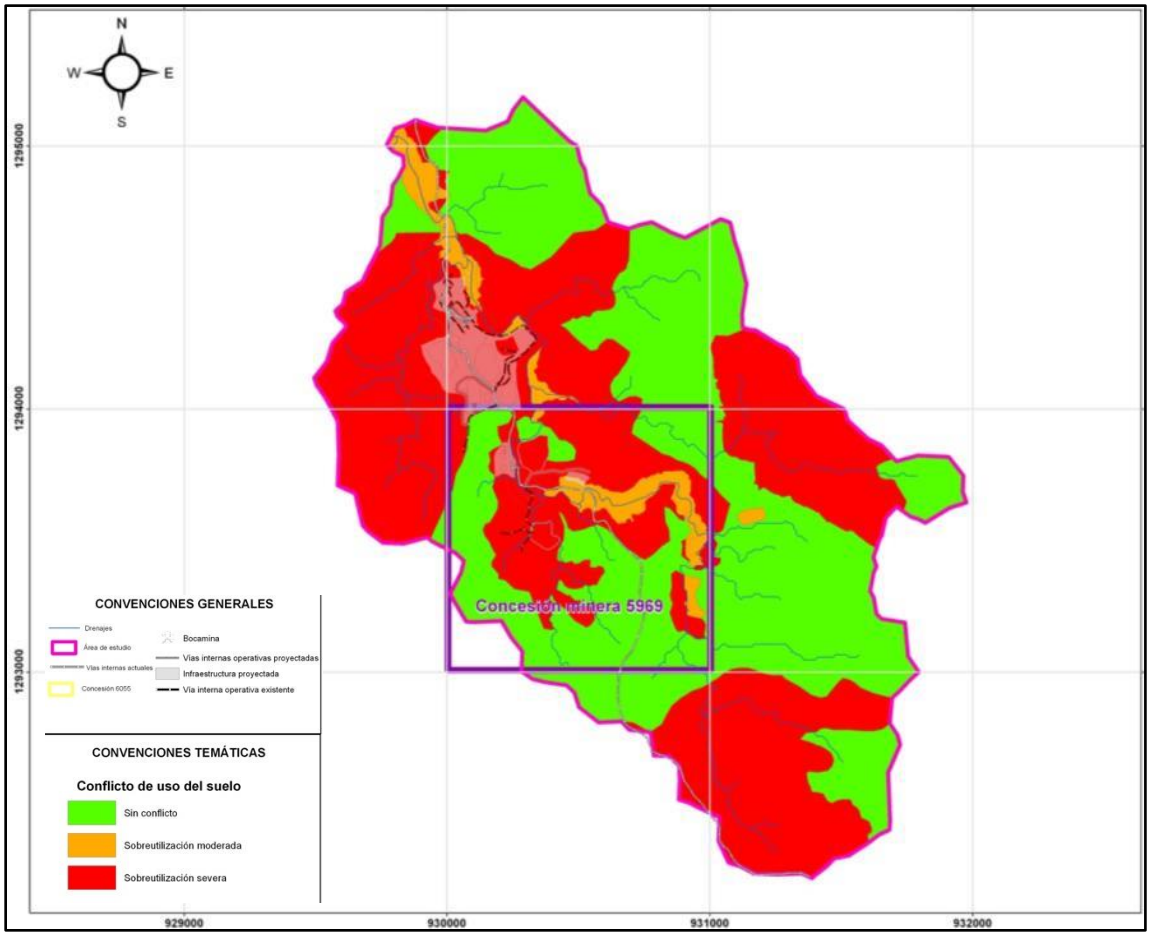

Illustration 4.1-96. Land use conflicts.
Source: INGEX, 2016.

4.1.4.3.1 Land use conflict due to moderate overuse

The type of use it currently presents corresponds to extensive cattle ranching (Gpe) and its vocation of use is for agriculture (2.68%), or is found in lands associated with mining, such as rural settlements, when its aptitude is agricultural or forestry producer.

Due to the above-mentioned differences between the current use and the vocation of the land use, a conflict in the use of the land is identified due to moderate overuse (3.5%), due to the fact that its current use is moderately above the capacity of land use, moderately affecting its sustainable

production, reducing the capacity of soil regeneration, generating losses of flora and fauna associated with this area and possible affectation of the quality and quantity of water bodies.

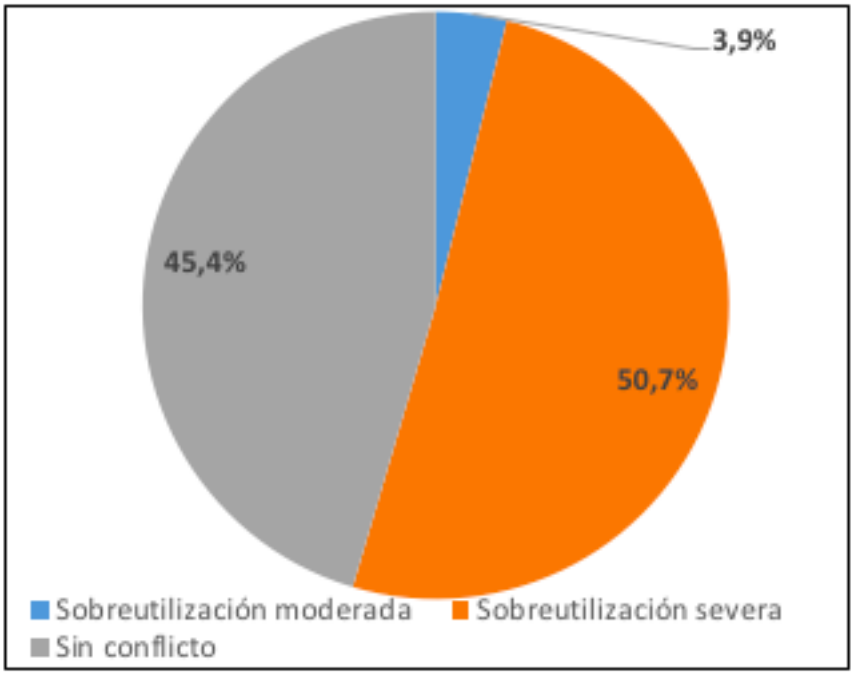

Illustration 4.1-97. Distribution of conflicts in the area of study.
Source: INGEX, 2016.

4.1.4.3.2 Land use conflict due to severe overuse

The type of use that currently occurs is in extensive livestock, alluvial dredging mining, and gold mining in sinkhole and opencast mining, the latter having generated a mixture of materials of different sizes (see Illustration 4.1-98 and Illustration 4.1-99). However, the vocation of use is to conserve water resources through protective-producing forest areas, or in agriculture or agroforestry and livestock in silvopastoral arrangements.

It is susceptible to slope erosion and grazing (cattle trampling), evidence of creeping and mass movement (see Illustration 4.1-100 and Illustration 4.1-101). Due to the differences between the current use and the vocation of use, there is a conflict identified as conflicting lands due to severe overuse (50.7%), due to the fact that the lands present inadequate current uses, contrary to their capacity of use, exceeding the capacity of the natural environment to support them to a severe degree; they present serious ecological risks, which show in some sectors the advanced degradation of the associated natural resources such as water, flora and fauna, affecting the natural balance and stability of the ecosystems.

Illustration 4.1-98. Soil intervened with anthropogenic deposits.

Illustration 4.1-99. Underground Mining

Illustration 4.1-100. Soil erosion processes

Illustration 4.1-101. Moderate and steep slopes.
Source: INGEX, 2016.

4.1.4.3.3 Land without conflict of use

45.4% of the study area is without use conflict since the current use corresponds to its use vocation and therefore there is no deterioration of the soil resources. These lands are presented in the areas whose use and suitability are Forestal Producer-Protector.

4.1.4.4 HYDROLOGY

The hydrography, hydrological and sedimentological regime, water supply, water uses and users (water demand) and scarcity index are presented below.

4.1.4.4.1 Hydrography

The pink basin (see Illustration 4.1-102) with 3.91km², which is limited to the mining project "El Pescado" in concession 5969, is equivalent to the IIA as supported in chapter No. 5969. 3. "Areas of Influence." The main stream is called "No Name #1" (hereinafter SN #1) and is located in the municipality of Segovia - Antioquia.

The main tributaries or main micro-basin channels that make up the SN #1 basin (see Illustration 4.1-103) are: no name #9 (hereinafter SN #9) with an area of 3.05 km2, no name #2 (hereinafter SN #2) with an area of 0.41 km2, the unnamed ravine #4 (hereinafter SN #4) with an area of 0.31 km2, the unnamed stream #5 (hereinafter SN #5) with an area of 0.66 km2, the unnamed stream #8 (hereinafter SN #8) with an area of 1.90 km2, the unnamed stream #6 (hereinafter SN #6) with an area of 0.35 km2 and the unnamed stream #7 (hereinafter SN #7) with an area of 0.081 km2. These are not officially named by the IGAC and were therefore also differentiated in this way.

In the basin or the IIA, according to the climatological study, a monthly average temperature of 24ºC, bimodal rainfall regime, average annual rainfall of 3,800mm/year prevails. Of high hydrological importance, with a yield of 63.18 L/s/km2. The drainage patterns and morphology of the study basins are presented below.

4.1.4.4.2 Drainage patterns

Below are the local drainage patterns and lotic bodies, and the regional drainage hierarchy.

Local drainage patterns and lotic bodies.

In Illustration 4.1-103 and Illustration 4.1-104, the patterns or hierarchies of the drainage network that forms the basin of the main SN # 1 stream and its micro-basins are shown. It is also evident that there are no lentic water bodies, as it is also validated in the hydrogeology component.

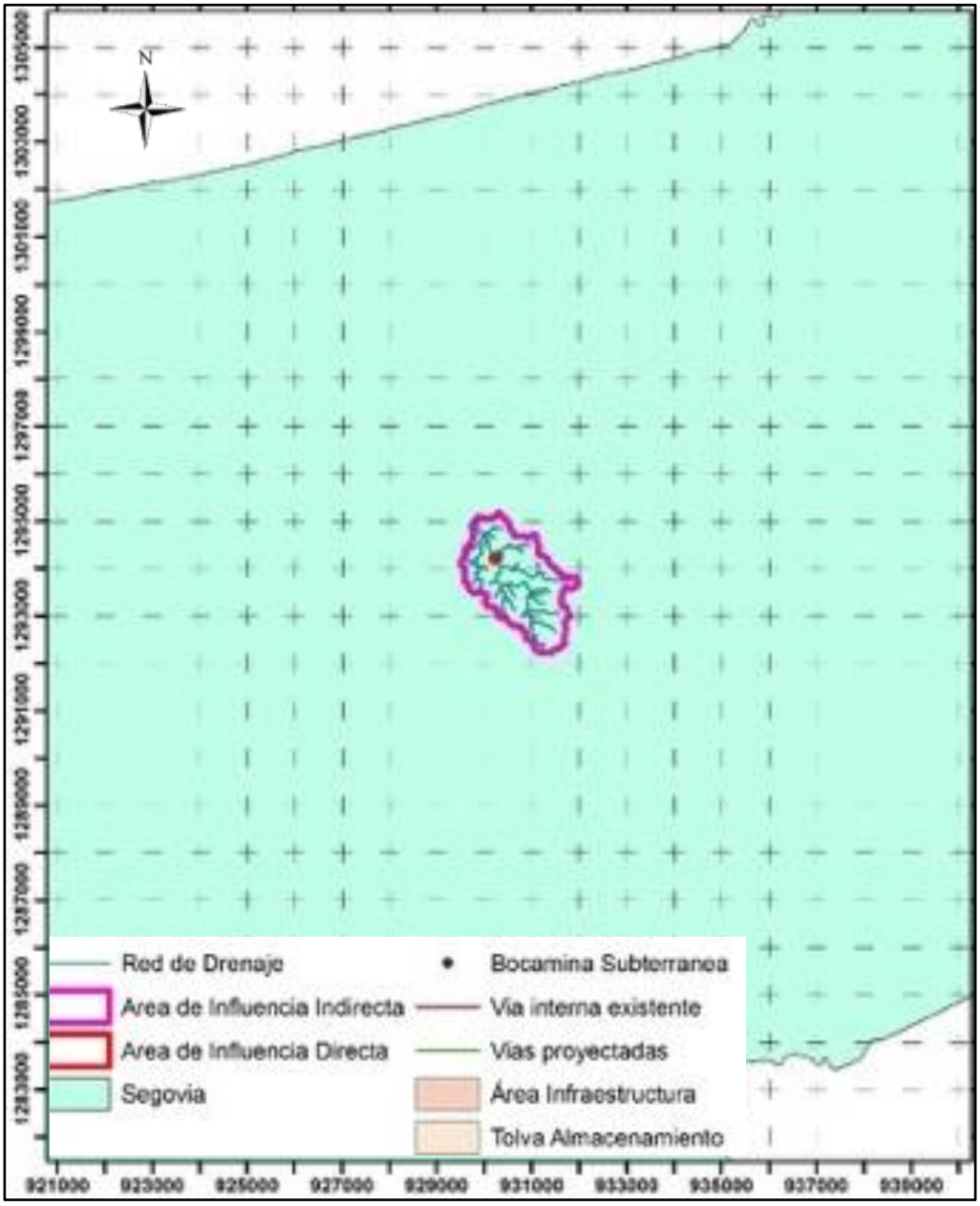

Illustration 4.1-102. Location of the drainage network.
Source: INGEX, 2015.

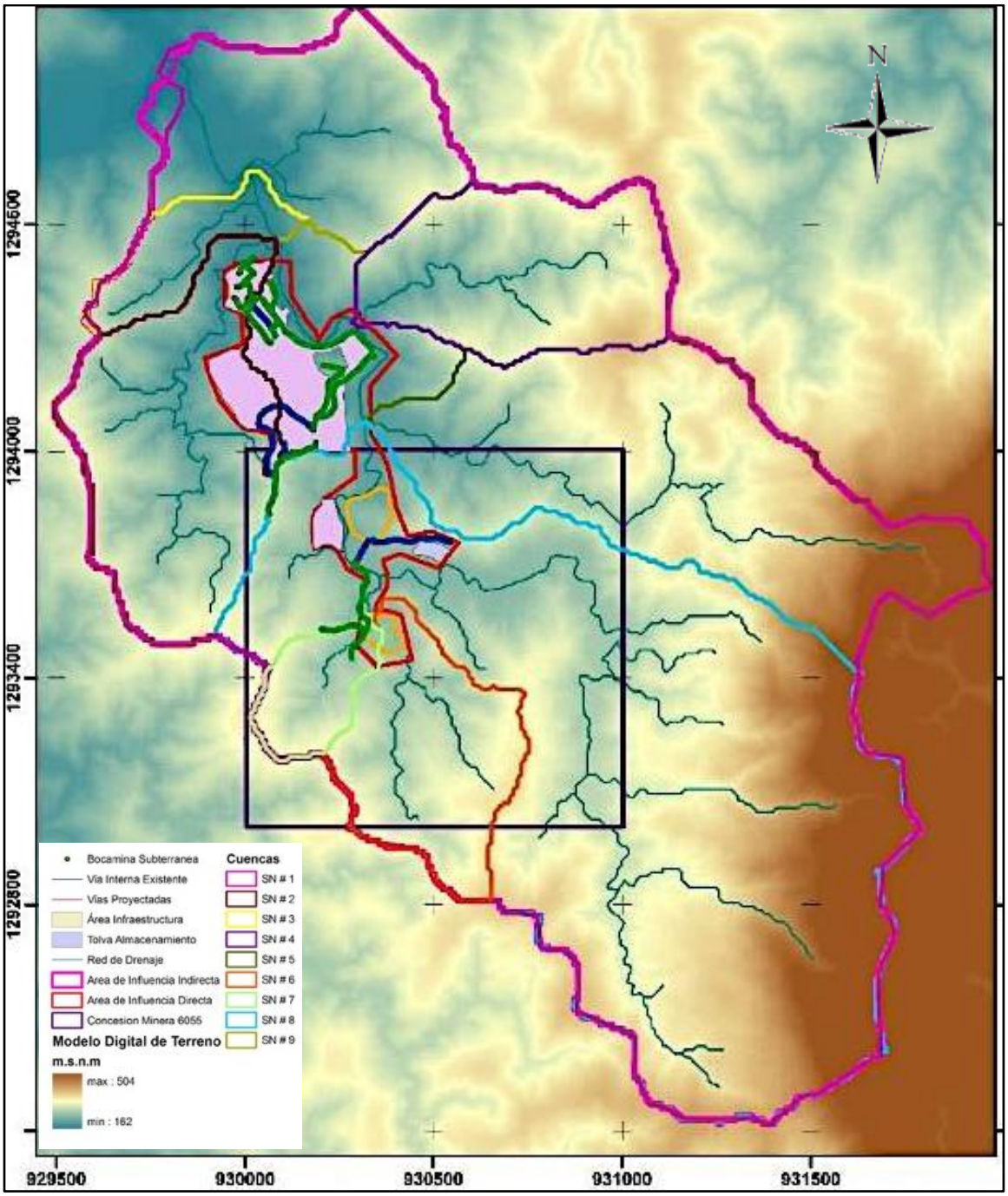

Illustration 4.1-103. Drainage network inside the study area.
Source: INGEX, 2015.

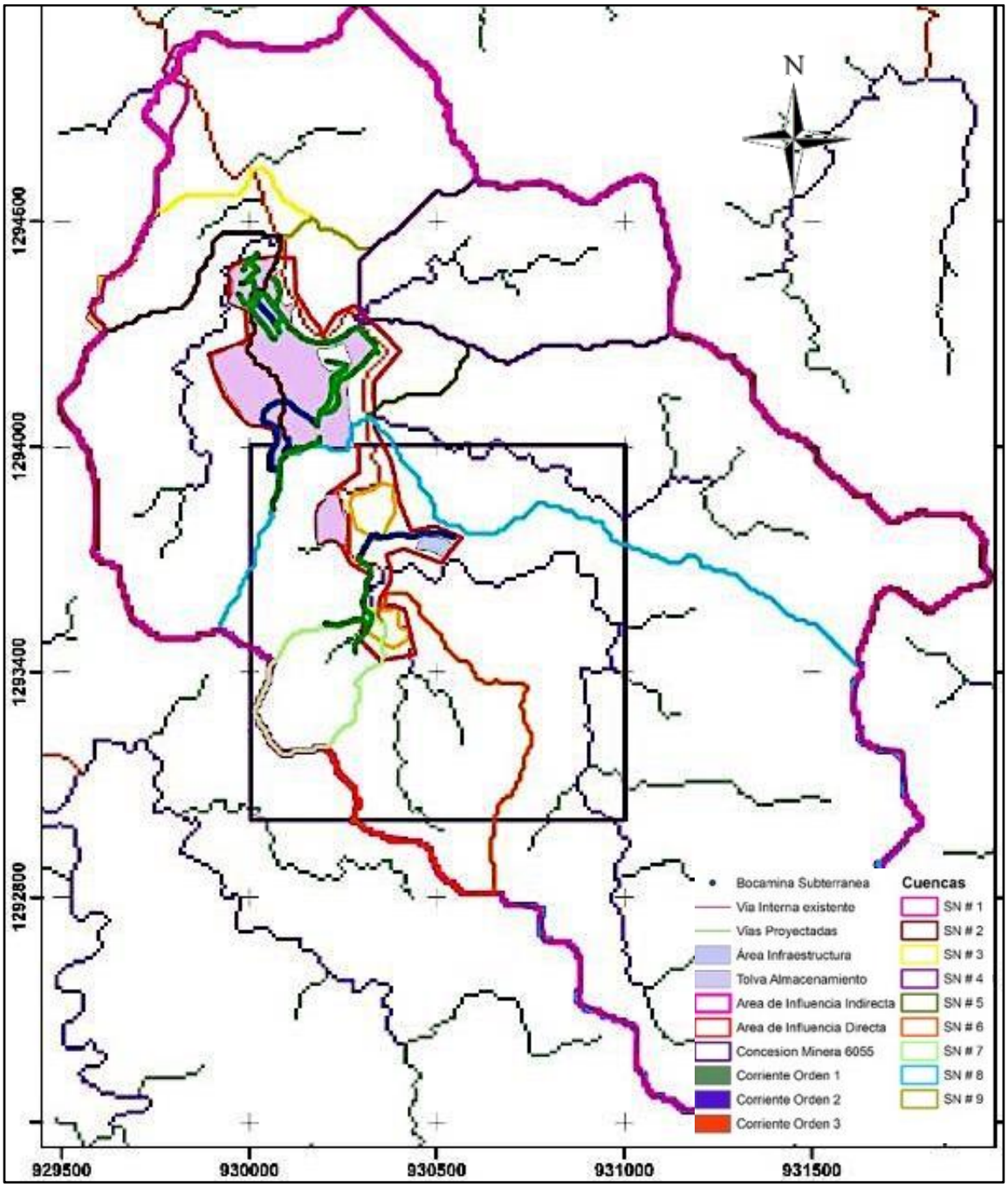

Illustration 4.1-104. Hierarchical order of the drainage network of the study area.
Source: INGEX, 2015.

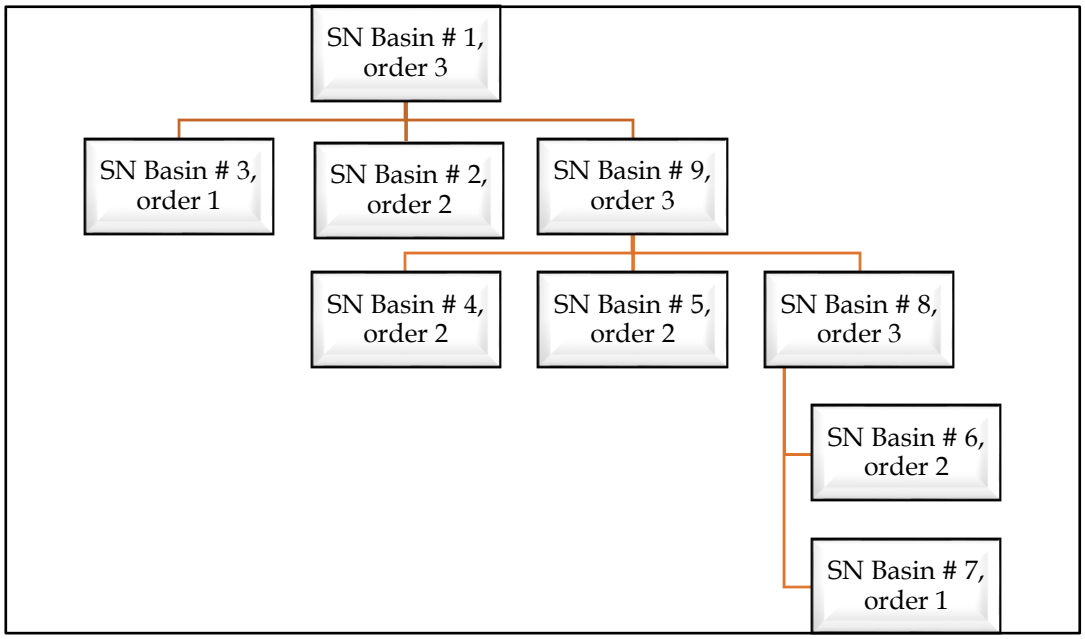

Illustration 4.1-105. Hierarchical order of the drainage network of the study area.
Source: INGEX, 2015.

The drainage pattern of the streams is dendritic, because all the drains are joined to the main stream in all directions. This reflects uniformity in the materials present in the basin, where they start on the slopes and the currents are low.

Regional drainage patterns

According to IDEAM, to ensure systemic management of basin management, it is necessary to define three (3) units that organically make up the system, which are: the hydrological region, the basin itself and the micro-basin as the minimum basic unit. For this purpose, IDEAM developed the codification of basins to facilitate the management exercise, the systematization of information and the spatial concordance of the hydrological models generated. Table 4.1.49 shows the regional drainage pattern of the basins, coded according to IDEAM guidelines, using the Garvellius method (1914), where the largest river is considered to be of order one (1) and the tributaries that reach it are of order two (2) rising successively.

Table 4.1-49. Current order for basins in the study area.

(0)	(1)	(2)	(3)	(4)	(5)	(6)
MAGDALENA - CAUCA	NECHI	BAGRE	Qda El Pescado	No name #1 No name #9 No name #8	No name #2	No name #3 No name #10
					No name #4	
					No name #5	
					No name #6	No name #7

4.1.4.4.3 Morphology of the basin

The slopes of the basin are high; the channel is channeled mainly by the characteristic that it is currently located in the upper part of the basin. For this reason, when the depth of flow is high, this current does not flood many adjacent lands. The flow velocities are high, however, material entrainment is not strong, because the channel is made up of saprolite deposits containing the properties of the parent rock. Below are some geomorphological parameters of the SN #1, SN#9, SN#2, SN #3, SN #4, SN #5, SN #8, #6 and #7 basins (Table 4.1-50 and Table 4.1-51).

Table 4.1-50. Geomorphological parameters of the SN #1, SN#9, SN#2, SN #3, SN #4, SN #5, SN #8, #6 and #7 basins.

PARAMETER	UNITS	SN #1	SN #9	SN #2	SN #3	SN #4	SN #5	SN #8	SN #6	SN #7
Area of the basin	[km^2]	3.91	3.05	0.41	0.073	0.31	0.66	1.90	0.31	0.081
Overall length	[km]	464.41	362.52	49.22	8.92	37.54	79.10	223.04	37.54	9.66
Length of main channel	[km]	5.12	4.46	1.70	0.65	1.31	2.31	3.70	1.31	0.52
Maximum level in the basin	[m]	504.00	504.00	306.00	270.00	348.00	480.00	504.00	348.00	310
Dimension at the start	[m]	164.00	174.16	173.9	170.00	188.00	192.00	192.00	188.00	220
Distance to centroid	[m]	1.60	2.26	0.89	0.29	0.66	1.15	2.16	0.66	0.30
Perimeter	[km]	12.52	10.82	3.66	1.66	2.98	5.64	8.2	2.98	1.52
Average slope	[%]	45.30	56.35	58.11	46.70	67.36	57.93	44.37	67.36	45.99

Source: INGEX, 2015.

Table 4.1-51. Other geomorphological parameters of basins N #1, SN#9, SN#2, SN #3, SN #4, SN #5, SN #8, #6 and #7.

SHAPE PARAMETER	EQUATION	VALUE								
		SN #1	SN #9	SN #2	SN #3	SN # 4	SN # 5	SN #8	SN #6	SN #7
Form Factor (Kf) Interpretation: The value for all basins is close to zero, which shows that the basins are elongated	$K_f = \frac{A_{cuenca}}{L^2}$	0.15	0.15	0.14	0.14	0.18	0.12	0.15	0.24	0.30
Coefficient of Compactness or Gravelius (Kc)	$K_C = 0.2821 \frac{P_{cuenca}}{\sqrt{A_{cuenca}}}$	1.79	1.75	1.61	1.61	1.51	1.96	1.75	1.59	1.51

SHAPE PARAMETER	EQUATION	VALUE								
		SN #1	SN #9	SN #2	SN #3	SN # 4	SN # 5	SN #8	SN #6	SN #7
Interpretation: *Values close to two show elongated basins*										
Maximum length of the basin (Lmax)	--	3.2	2.68	1.12	1.12	0.85	1.72	2.68	0.90	0.46
Maximum basin width (Wmax)	--	0.71	1.55	0.62	0.62	0.45	0.58	1.55	0.39	0.18
Elongation index (Ic) *Interpretation* *It indicates that they are very elongated basins.*	$I_c = \frac{L_{\max}}{W_{\max}}$	2.25	1.73	1.80	1.80	1.89	2.97	1.73	2.31	2.61
A_{VM}	--	2.40	2.11	0.20	0.05	0.16	0.42	2.11	0.19	0.04
A_{vm}	--	1.51	0.94	0.21	0.02	0.15	0.24	0.94	0.15	0.08
Asymmetry Index (Ias) *Interpretation:* *Only the SN #2, #4, #6 and #7 basins are symmetric, the others are asymmetric.*	$I_{as} = \frac{A_{VM}}{A_{Vm}}$	1.59	2.24	0.95	2.17	1.07	1.75	2.24	1.07	1.15
Elongation Ratio (Re) *Interpretation:* Indicates that the basins are elongated	$\mathrm{Re} = 1.128 \frac{\sqrt{A_{cuenca}}}{L_{\max}}$	1.39	0.74	0.64	1.05	0.74	0.53	0.74	0.74	0.70
Circularity ratio (Rci) *Interpretation:* The value is close to zero, so the basins are rectangular in shape	$R_{ci} = 4\pi \frac{A_{cuenca}}{P_{cuenca}^{\ 2}}$	0.31	0.33	0.38	0.33	0.44	0.26	0.33	0.44	0.44

Source: INGEX, 2015.

In the tables above, it can be seen that the basins are elongated and that as the area of these increases, they become more asymmetrical. The SN #1 envelope basin is elongated and does not have a symmetrical drainage.

4.1.4.5 HYDROLOGICAL REGIME

This item is focused on determining the hydrology of the main river basins SN #1, SN#9, SN#2, SN#3, SN #4, SN #5, SN #8, #6 and #7. It consists of the precipitation and evapotranspiration regime, and the flow regime presented below.

4.1.4.5.1 Precipitation and evapotranspiration regime

The annual cycle of the rainfall stations that circumscribe the study area, with data from anomalous years excluded from the validation of information quality, is presented in Table 4.1-52 and Illustration 4.1-106.

Table 4.1-52. Multiannual mean rainfall for nearby stations.

CODE	NAME	P ANUAL (mm/year)	PRECIPITATION (mm/mes)											
			JAN	FEB	MAR	APR	MAY	JUN	JUL	AUG	SEP	OCT	NOV	DEC
27030090	El Bosque	4638.6	127.2	126.6	181.9	380.7	529.1	479.8	452.8	510.9	501.1	558.1	485.9	304.5
27030140	Palma de Coco	3994.7	100.9	112.8	161.3	334.4	456.6	388.8	382.4	452.3	436.9	503.8	412.1	252.5
27030220	El Oriente	3756.6	155.8	177.9	135.2	311.4	359.8	260.6	283.2	351.4	383.0	556.5	440.6	341.1
27011100	Las Brisas	3784.1	101.3	115.3	153.6	314.9	445.1	386.5	366.6	397.6	413.7	436.8	410.0	242.6
27030130	El Londre	3844.2	191.8	179.6	149.0	341.7	344.6	265.4	260.7	359.8	418.0	496.0	462.9	374.8

The rainiest months are May and October (Winter), while the least rainy months are January to March. At the end of the summer between March and May there is an increase in precipitation (from summer to winter), and between May and October the precipitation fluctuates, with a constant high tendency, where rainfall can occur at different intensities. At the end of winter in October until December, rainfall decreases (winter-summer transition).

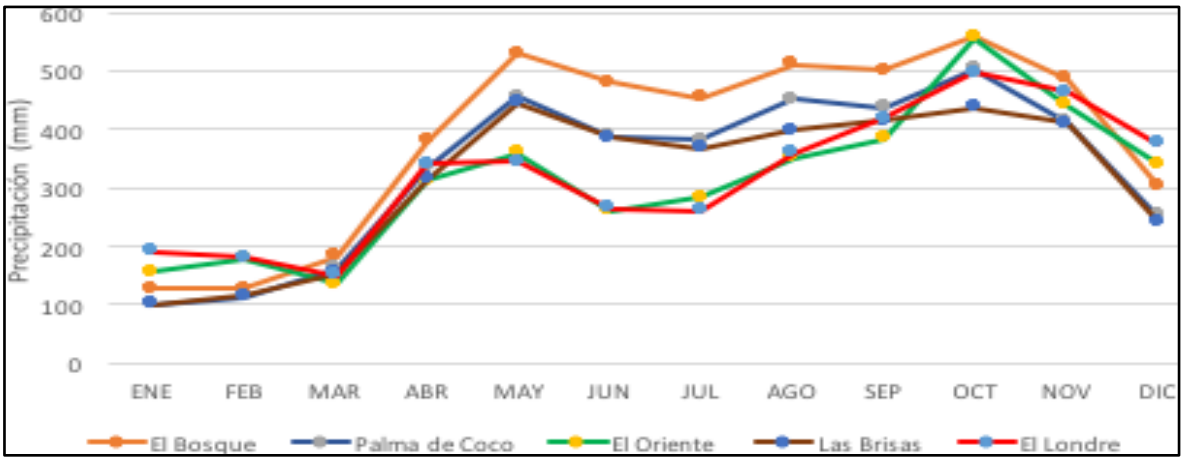

Illustration 4.1-106. Monthly precipitation values.
Source: INGEX, 2015.

Illustration 4.1-107 shows the spatial variation of precipitation, where in the northern areas there are annual precipitation averages much higher than in the southern part. The annual cycle of the stations

with evapotranspiration records, which circumscribe the study area, with data from anomalous years excluded from the validation of information quality, are presented in Table 4.1 53 and Illustration 4.1 108.

Table 4.1-53. Monthly evaporation values for nearby stations.

CODE	NAME	E YEARLY (mm/año)	EVAPORATION (mm/mes)											
			JAN	FEB	MAR	APR	MAY	JUN	JUL	AUG	SEP	OCT	NOV	DEC
27035020	El Boquete	1419.10	104.00	110.70	115.10	120.50	126.40	115.50	134.10	139.90	123.90	121.80	104.20	103.00

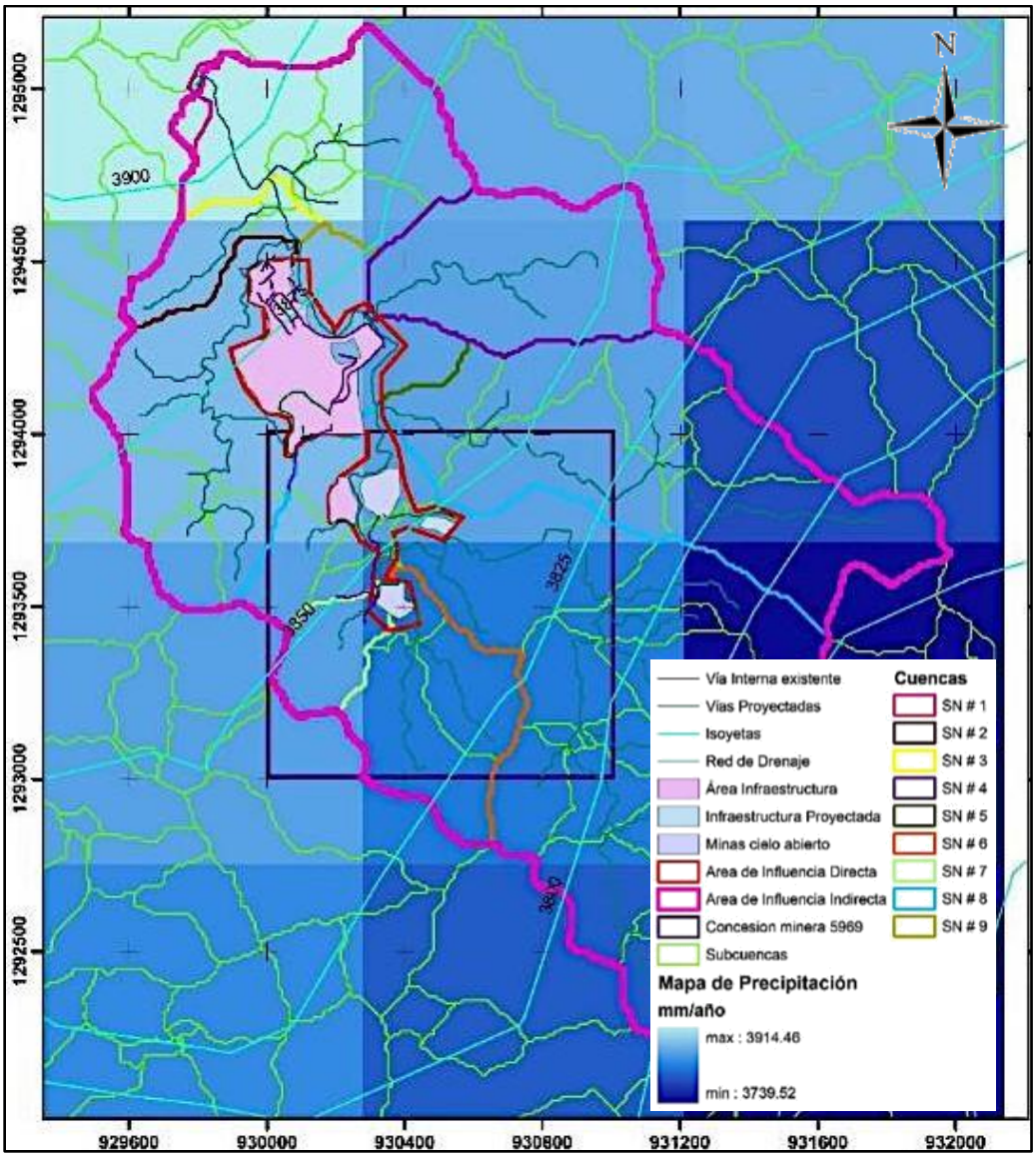

Illustration 4.1-107. Spatial distribution of precipitation
Source: INGEX, 2015.

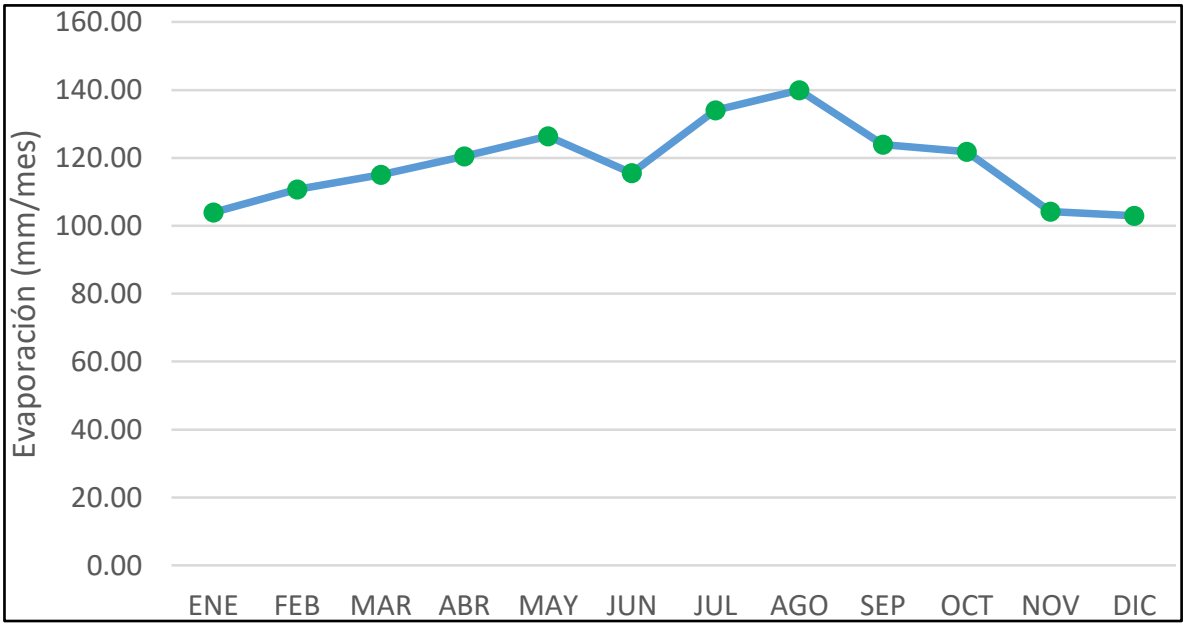

Illustration 4.1-108. Monthly evaporation values.
Source: INGEX, 2015.

Evaporation has a tendency to increase during the months of January to May, coinciding with the increase in precipitation in the study area. This behavior indicates that the water that the basin brings to the system through evaporation tends to return in the form of precipitation. Between August and December evaporation tends to decrease, as does rainfall.

Illustration 4.1-109 shows the spatial variation of evapotranspiration, where evapotranspiration has a high relationship with height, i.e., in the valleys of the currents the highest evapotranspiration values are found and, on the other hand, in the peaks there is less evapotranspiration.

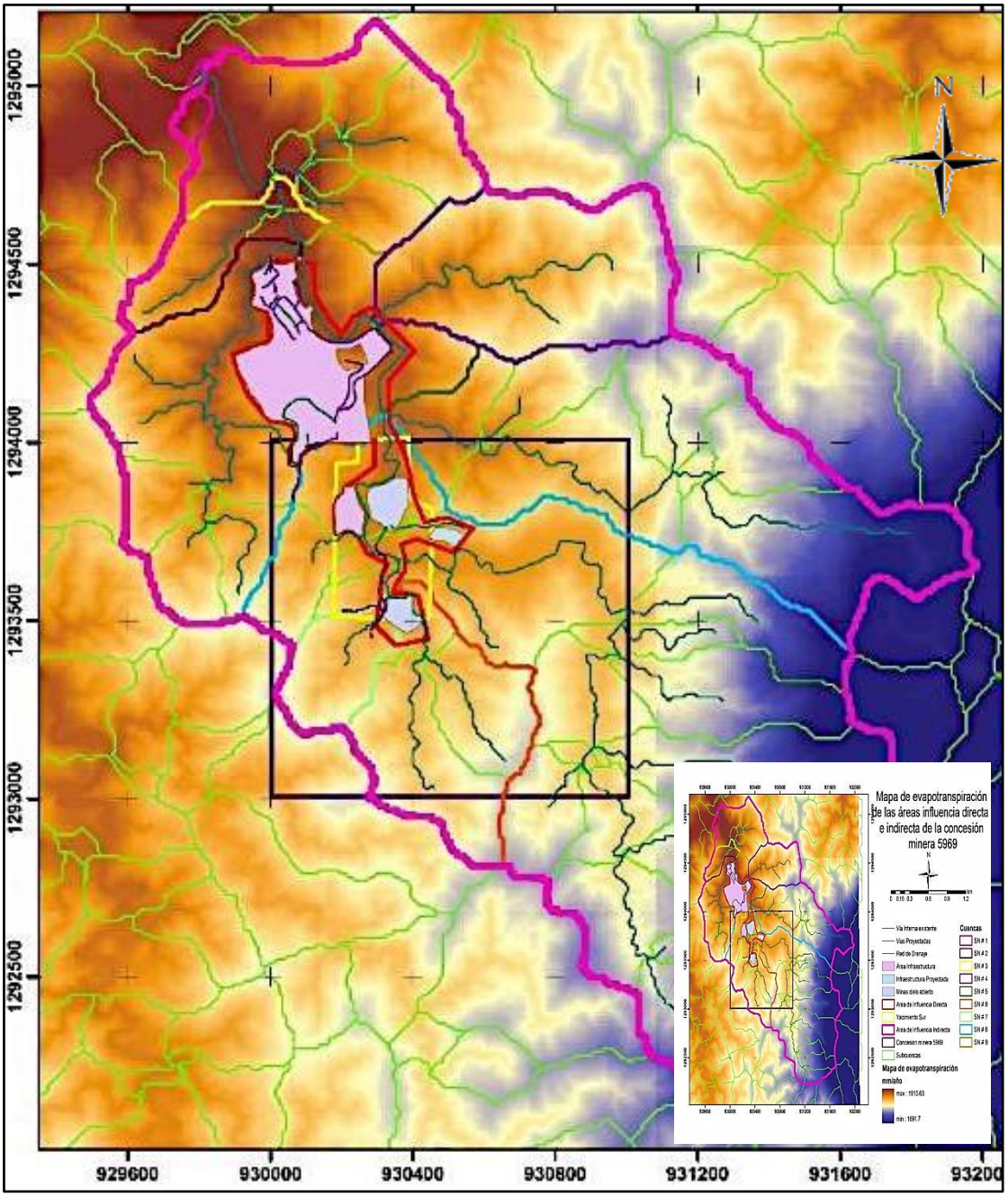

Illustration 4.1-109. Spatial distribution of evapotranspiration.
Source: INGEX, 2015

4.1.4.5.2 Flow Regime

The average, ecological, minimum and maximum flow rates of the study basins are presented below.

4.1.4.5.3 Average flow rates

The water balance needed to calculate the average flows and yields of the basins is presented below.

4.1.4.5.4 Water balance

The hydrological or hydric balance is in a control volume, by means of the mass conservation equations. The volume includes the water and soil columns between the watershed dividing the basin, the upper edge of the atmosphere and an impermeable layer at the bottom of the soil, where the variables involved in the process are: Moisture flow in the atmosphere (F), Precipitation (P), Evaporation (E), Direct runoff (R), storage of water in the atmosphere (W) and storage of water in the soil (S) (See Illustration 4.1-110).

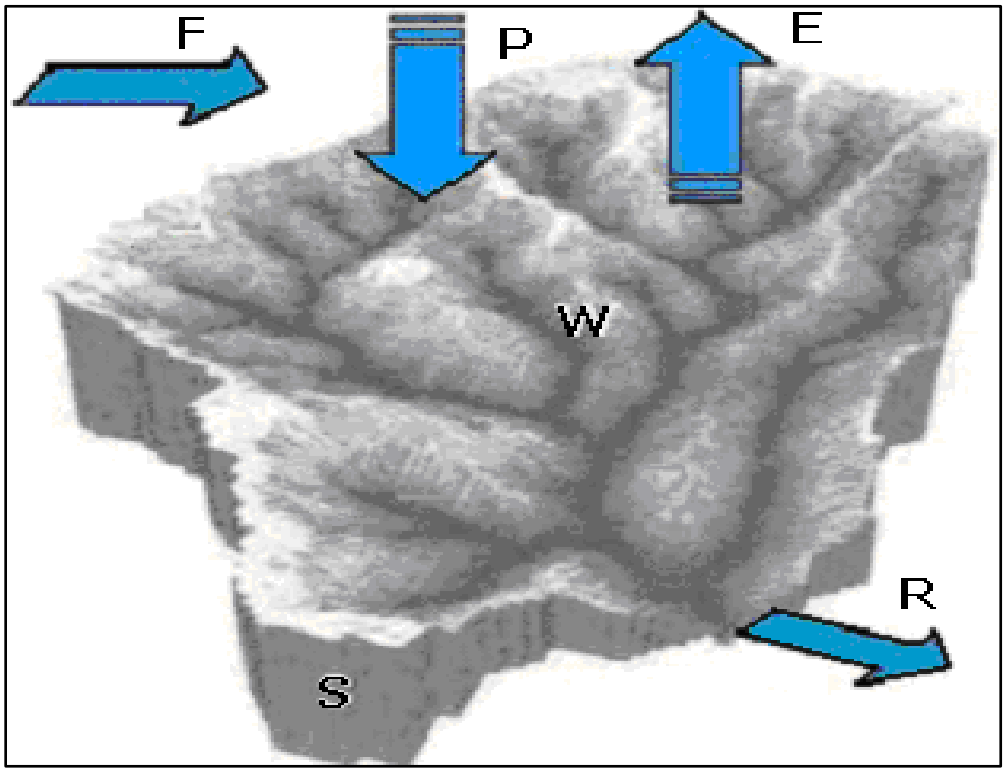

Illustration 4.1-110. Hydrological balance scheme
Source: INGEX, 2015.

The water balance in the atmosphere and in the soil are given by the expressions (1) and (2), respectively.

$$F + E - P = \frac{dW}{dt} \quad (1)$$

$$P - E - R = \frac{dS}{dt} \quad (2)$$

By combining both expressions, equation (3) for the water balance is obtained for the entire control volume:

$$F - R = \frac{d(W + S)}{dt} \quad (3)$$

Considering a long-term balance (of the order of years), changes in the storage of water in the atmosphere (W) and in the storage of water in the soil (S) are negligible, therefore, of the expression (5), it can be said that the atmospheric influx must be equal to the long-run average of the runoff, ie F = R. Thus, the long-term water balance as shown in expression (4).

$$R = P - E \quad (4)$$

Being the variables R, P and E averages taken over a long time and per unit area.

For a given basin, equation (4) is applied in each interior point of the basin, in this case, as is being worked with a Raster Type MDT. In this way, the column of water that it contributes to surface runoff is obtained in each cell. Finally, the average flow is obtained by adding all these contributions from the cells to the surface runoff. These are presented in Table 4.1-54.

Table 4.1-54. Average flows of the basins of the study area.

Parameter	Area of the basin	Average flow rate
Units	[km2]	(m3/s)
CUENCA SN # 1	3.91	0,2475
CUENCA SN #9	3.05	0.1927
CUENCA SN #2	0.41	0.0264
CUENCA SN #3	0.073	0.0046
CUENCA SN #4	0.31	0.0200
CUENCA SN #5	0.66	0.0418
CUENCA SN #8	1.90	0.1188
CUENCA SN #6	0.35	0.0220
CUENCA SN #7	0.081	0.0051

Source: INGEX, 2015.

From the above table, it can be concluded that the most important basin is the one that drains the unnamed stream #1, which has the highest average flow and also collects the waters of the other tributaries mentioned here.

4.1.4.5.5 Monthly water balances

Based on the flow rate information from the Vegachi station, the monthly flow rates for each of the basins were estimated. The procedure consisted of nondimensionalize the flows of the Vegachí station, dividing the monthly values by the average flow of the station and then multiplying them with the average flows of each of the currents studied, obtaining Illustration 4.1-111.

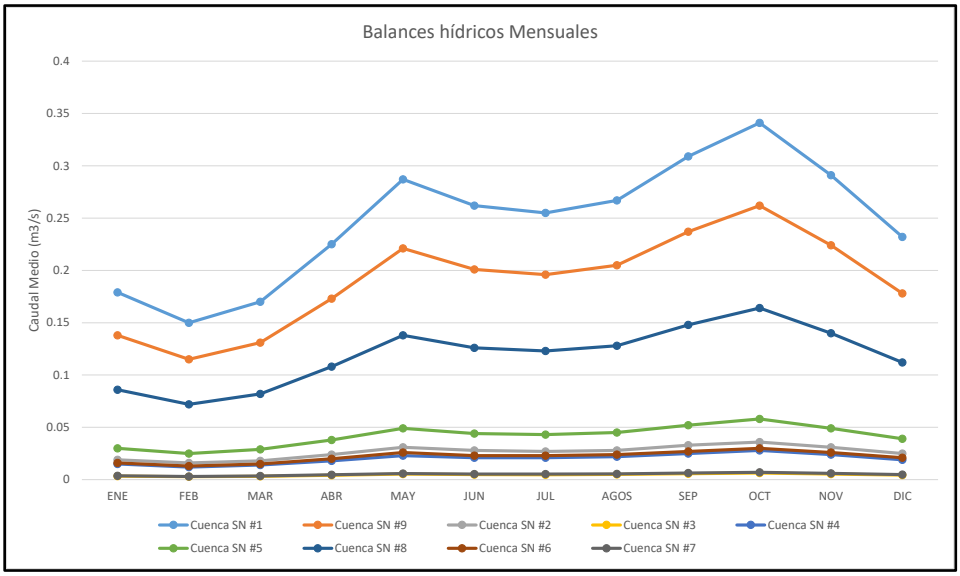

Illustration 4.1-111. Monthly water balances.
Source: INGEX, 2015.

From the above illustration it can be seen that the most critical months in terms of water availability in the streams are January, February and March, while in the months of May, September, October and November the months with a surplus in their flows are had.

Watershed yields

The water yield of the basins is estimated as the division of the average flow in the basin area, to establish what the flow per unit area would be. Table 4.1-55 shows the yields of the basins.

Table 4.1-55. Yields of the basins intervened in the AID and AII of the mining concession 5969.

Parameter	Basin yields
Units	[l/s/km^2]
SN #1 Basin	63.30
SN #9 Basin	63.18
SN #2 Basin	64.39
SN #3 Basin	63.01
SN #4 Basin	64.52
SN #5 Basin	63.33

Parameter	Basin yields
SN #8 Basin	62.52
SN #6 Basin	62.85
SN #7 Basin	62.96

Source: INGEX, 2015

The yield in the river basins in the study area is of the order of 63 l/s/km2, which is important in terms of availability of the resource since the water used will be quickly recovered by the production of the basin.

4.1.4.5.6 Ecological Flow

According to paragraph 3.4-2 of resolution 0865 of 2004, the ecological flow rate is equivalent to 25% of the average flow rate of the driest month. Table 4.1-56 illustrates the flows for currents 1, 6 and 7.

Table 4.1-56. Monthly average flow rates for the unnamed current #1, #6 and #7

Month	Q Medium (m3/s) SN #1	Q Medium (m3/s) SN #9	Q Medium (m3/s) SN #2	Q Medium (m3/s) SN #3	Q Medium (m3/s) SN #4	Q Medium (m3/s) SN #5	Q Medium (m^3/s) SN #8	Q Medium (m^3/s) SN #6	Q Medium (m^3/s) SN #7	Observation
JAN	0.179	0.138	0.019	0.0033	0.015	0.030	0.086	0.016	0.0037	
FEB	0.150	0.115	0.016	0.0028	0.012	0.025	0.072	0.013	0.0031	Drier month
MAR	0.170	0.131	0.018	0.0032	0.014	0.029	0.082	0.015	0.0035	
APR	0.225	0.173	0.024	0.0042	0.018	0.038	0.108	0.020	0.0046	
MAY	0.287	0.221	0.031	0.0053	0.023	0.049	0.138	0.026	0.0059	
JUN	0.262	0.201	0.028	0.0049	0.021	0.044	0.126	0.023	0.0054	
JUL	0.255	0.196	0.027	0.0047	0.021	0.043	0.123	0.023	0.0053	
AUG	0.267	0.205	0.028	0.0050	0.022	0.045	0.128	0.024	0.0055	
SEP	0.309	0.237	0.033	0.0057	0.025	0.052	0.148	0.027	0.0064	
OCT	0.341	0.262	0.036	0.0063	0.028	0.058	0.164	0.030	0.0070	
NOV	0.291	0.224	0.031	0.0054	0.024	0.049	0.140	0.026	0.0060	
DEC	0.232	0.178	0.025	0.0043	0.019	0.039	0.112	0.021	0.0048	

Source: INGEX, 2015.

Thus, based on the flow rate values presented in the table above, the driest month is February, so the ecological flow rate is the next for the currents:

$$Q_{ECOLÓGICO} SN\#1 = 0.150 * 0.25 = 0.0375\, {}^{m^3}/_{s} = 37.5\, {}^{l}/_{s}$$

$$Q_{ECOLÓGICO} SN\#9 = 0.115 * 0.25 = 0.0287\, {}^{m^3}/_{s} = 28.7\, {}^{l}/_{s}$$

$$Q_{ECOLÓGICO} SN\#2 = 0.016 * 0.25 = 0.0040\, {}^{m^3}/_{s} = 4.0\, {}^{l}/_{s}$$

$$Q_{ECOLÓGICO} SN\#3 = 0.0028 * 0.25 = 0.0007\, {}^{m^3}/_{s} = 0.7\, {}^{l}/_{s}$$

$$Q_{ECOLÓGICO} SN\#4 = 0.012 * 0.25 = 0.0030\, {}^{m^3}/_{s} = 3.0\, {}^{l}/_{s}$$

$$Q_{ECOLÓGICO}SN\#5 = 0.025 * 0.25 = 0.0063\, {}^{m^3}/_{s} = 6.3\, {}^{l}/_{s}$$

$$Q_{ECOLÓGICO}SN\#8 = 0.072 * 0.25 = 0.0180\, {}^{m^3}/_{s} = 18.0\, {}^{l}/_{s}$$

$$Q_{ECOLÓGICO}SN\#6 = 0.013 * 0.25 = 0.0033\, {}^{m^3}/_{s} = 3.3\, {}^{l}/_{s}$$

$$Q_{ECOLÓGICO}SN\#7 = 0.0031 * 0.25 = 0.0007\, {}^{m^3}/_{s} = 0.7\, {}^{l}/_{s}$$

Minimum flow rates

With the values obtained for the multiannual mean and standard deviation, the equation proposed by Chow (1951) is used, using the distribution of extreme values type GEV (Heo and Salas, 1996, Chow et al, 1994), i.e. Gumbel, the minimum flow values with an associated return period were obtained for the unnamed stream #1, #6 and #7 (See Illustration 4.1-112 to Illustration 4.1-120).

$$Q(Tr) = \mu_{Q\min} + K(Tr,\gamma) * \sigma_{Q\min}$$

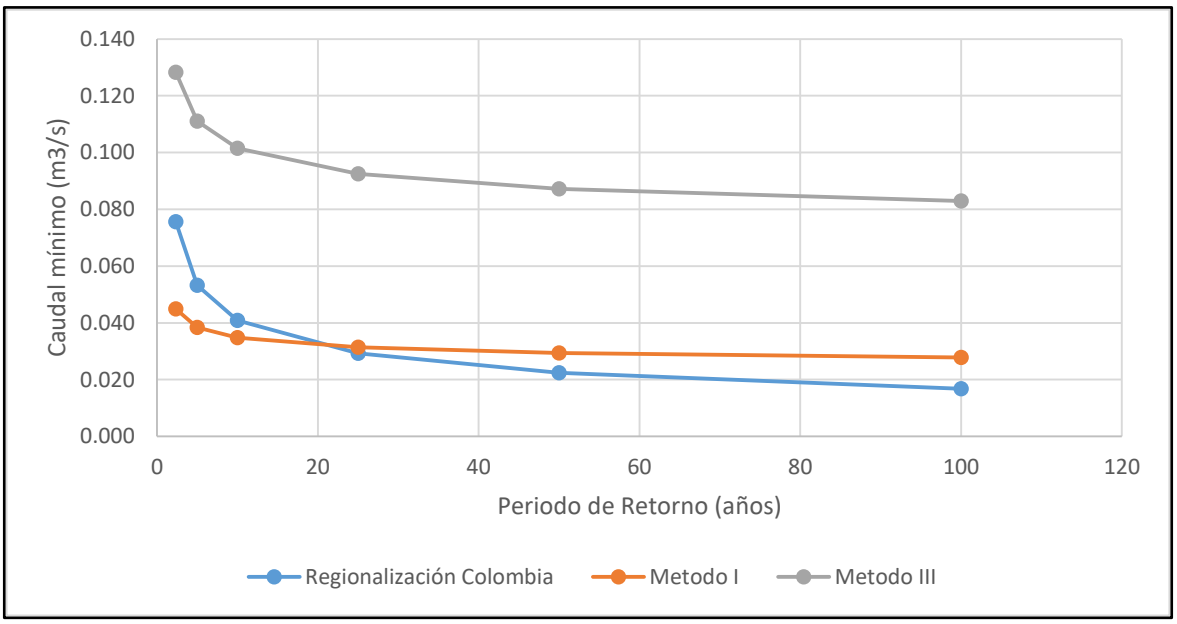

Illustration 4.1-112. Minimum flow rates for the basin of the unnamed stream #1.
Source: INGEX, 2015.

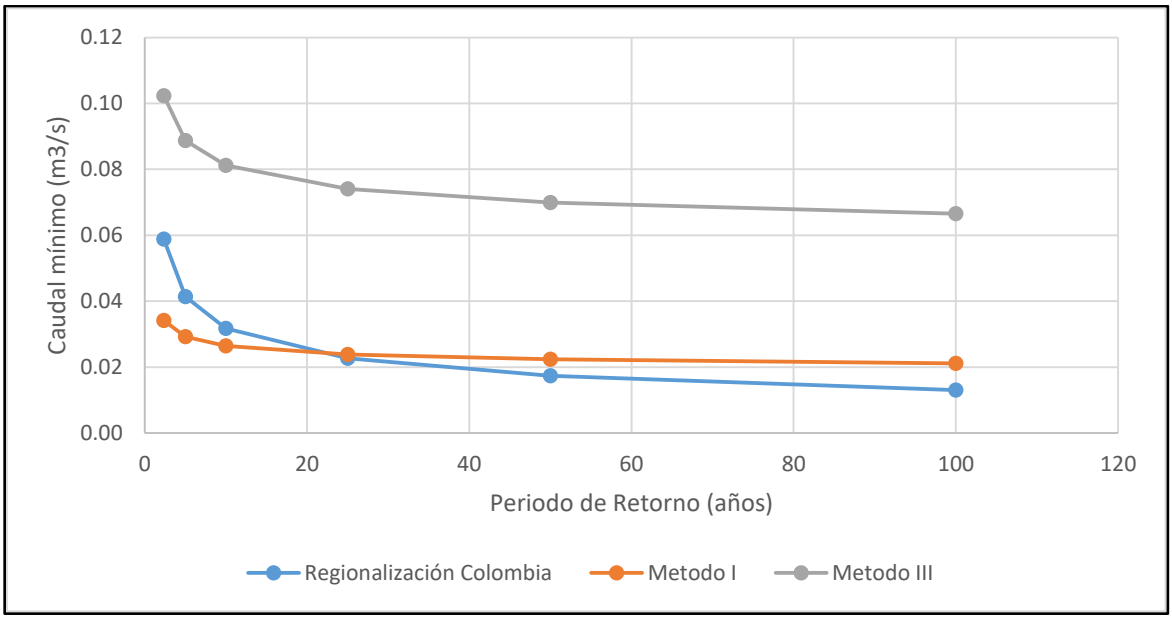

Illustration 4.1-113. Minimum flows for the basin of the unnamed stream #9.
Source: INGEX, 2015.

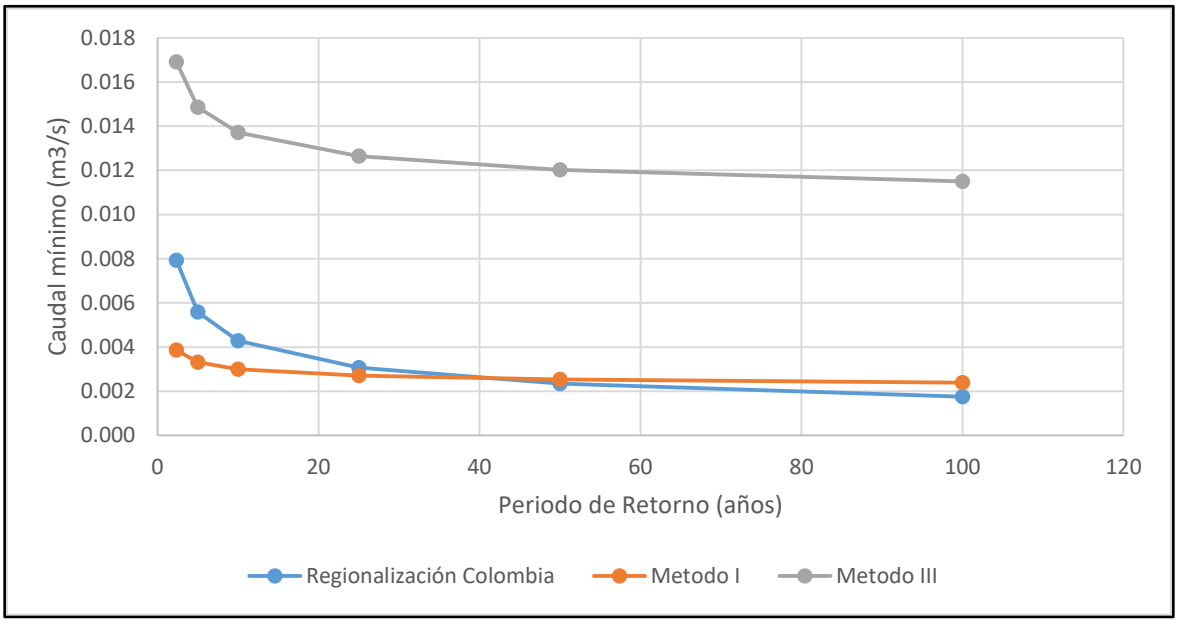

Illustration 4.1-114. Minimum flow rates for the basin of the unnamed #2 stream.
Source: INGEX, 2015.

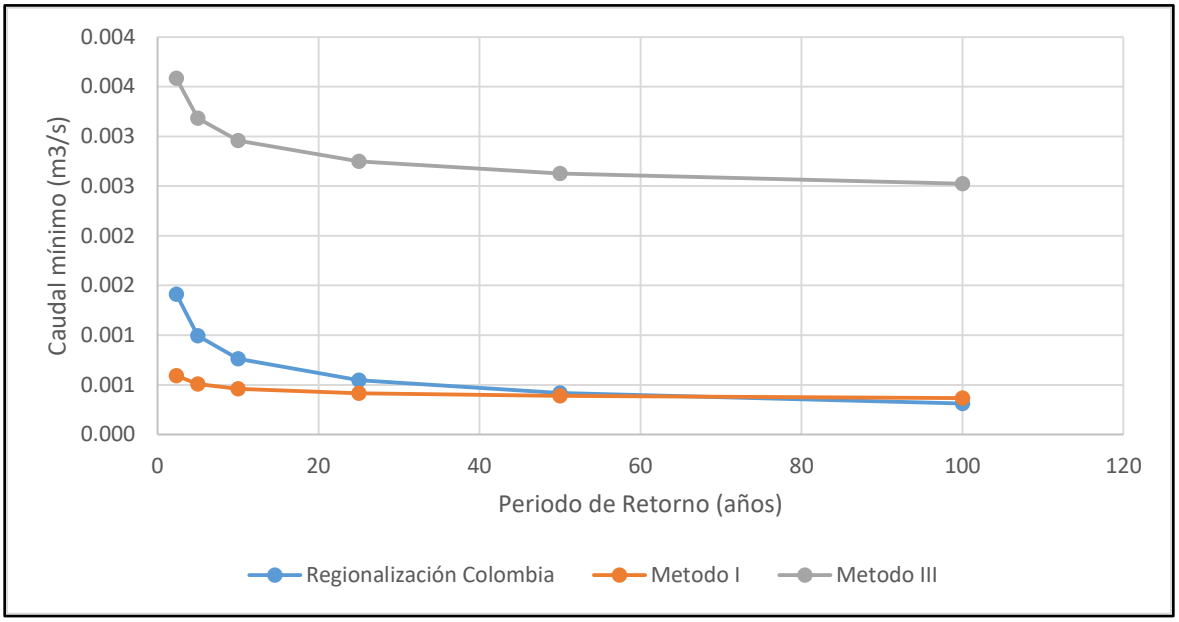

Illustration 4.1-115. Minimum flow rates for the basin of the unnamed stream #3.
Source: INGEX, 2015.

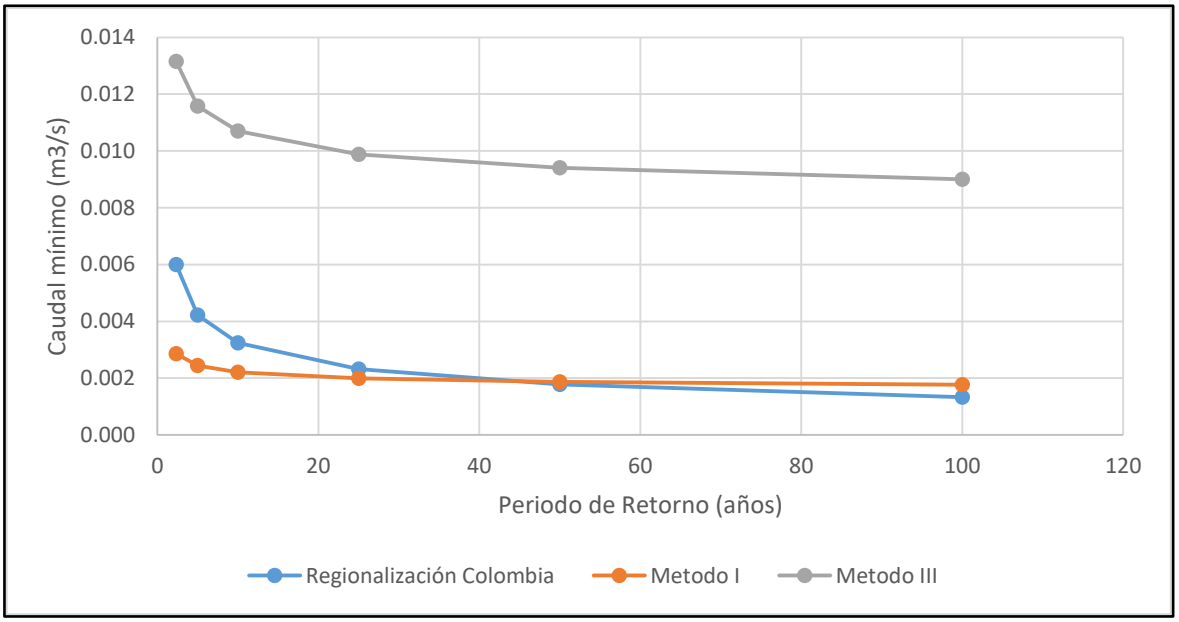

Illustration 4.1-116. Minimum flows for the basin of the unnamed stream #4.
Source: INGEX, 2015.

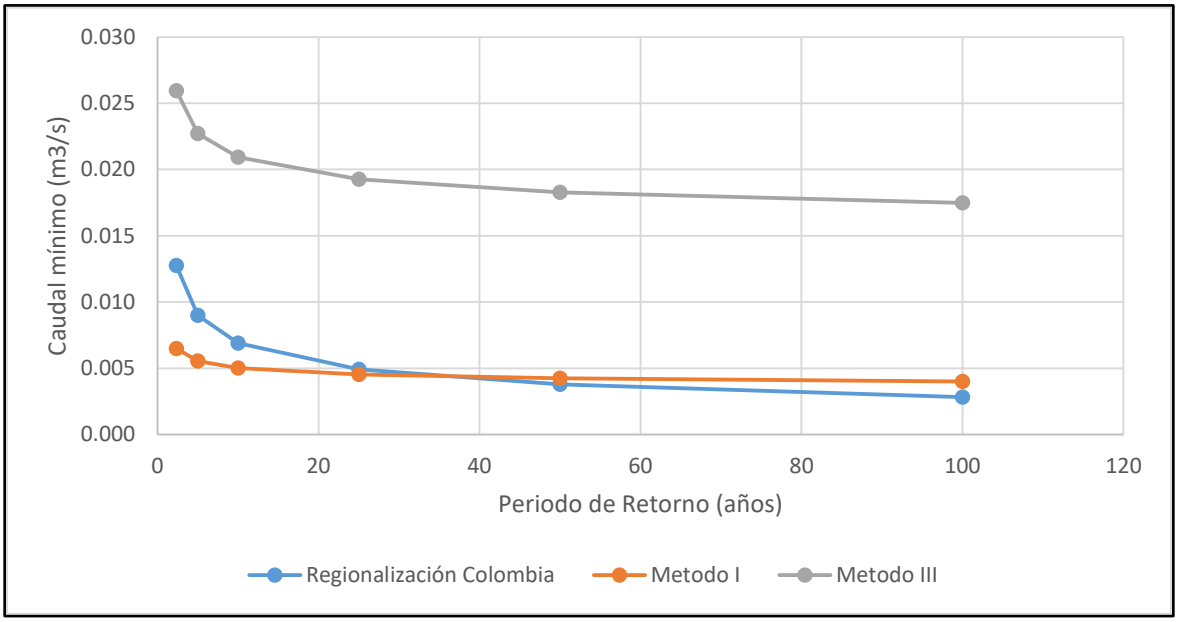

Illustration 4.1-117. Minimum flows for the basin of the unnamed stream #5.
Source: INGEX, 2015.

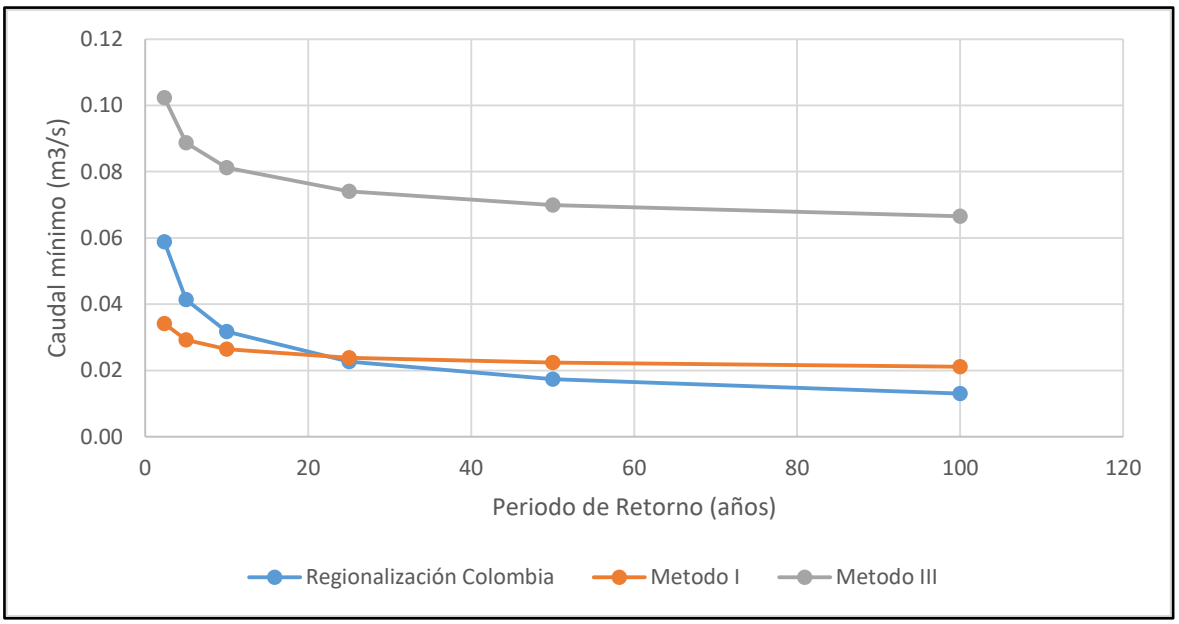

Illustration 4.1-118. Minimum flows for the basin of the unnamed stream #8.
Source: INGEX, 2015.

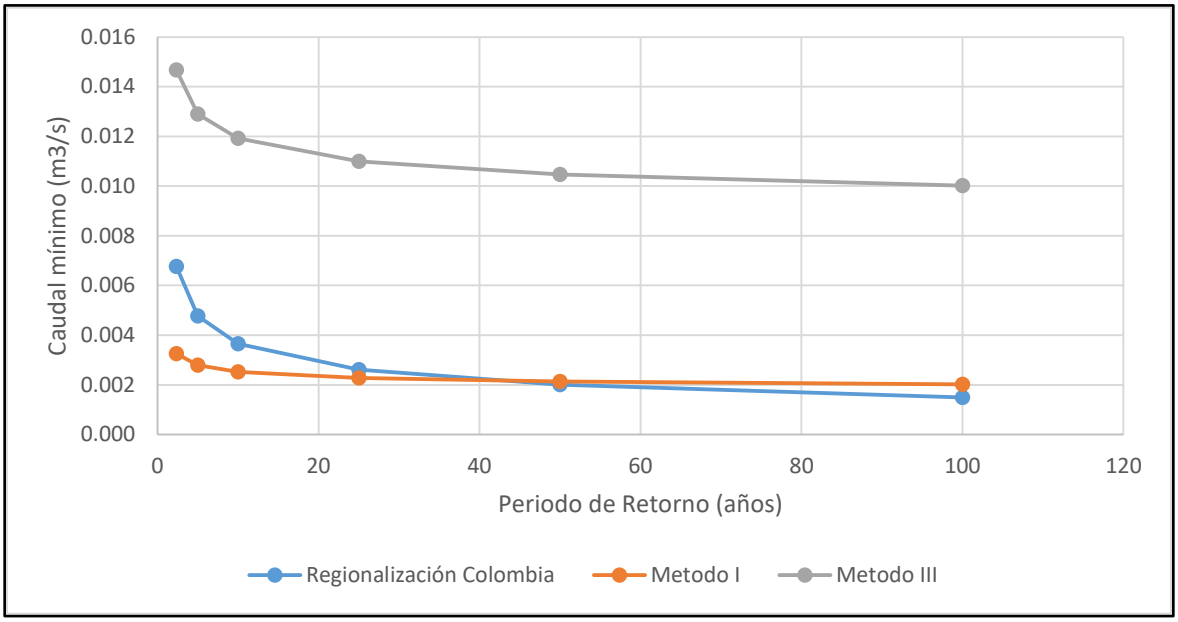

Illustration 4.1-119. Minimum flows for the basin of the unnamed stream #6.
Source: INGEX, 2015.

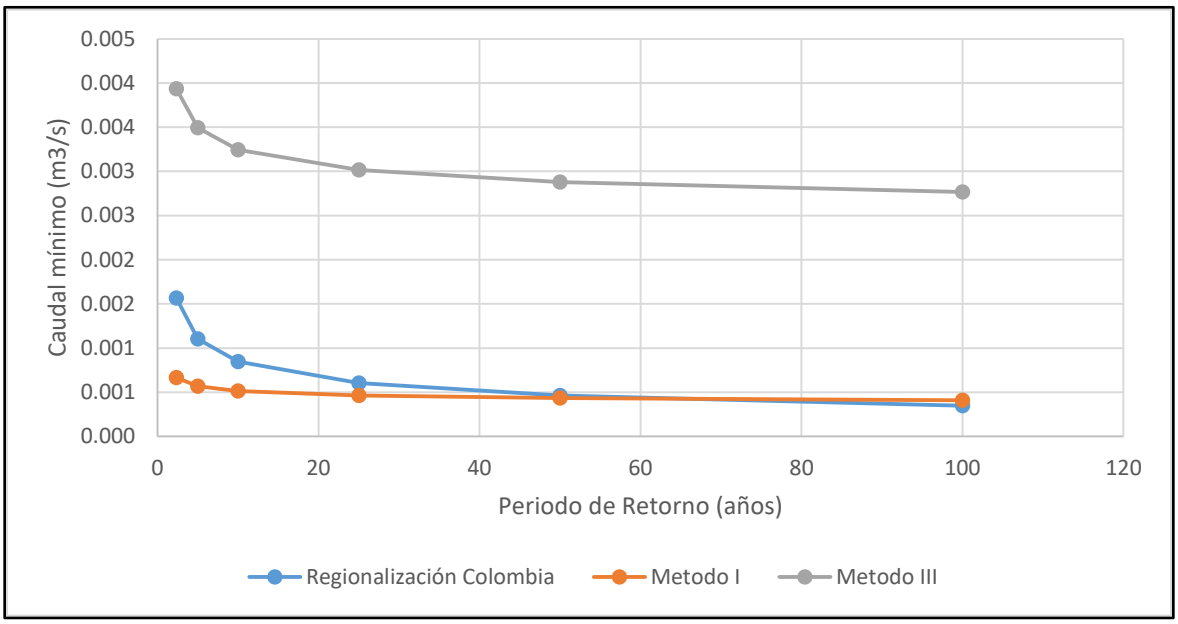

Illustration 4.1-120. Minimum flows for the basin of the unnamed stream #7.
Source: INGEX, 2015.

Maximum flow rates

The following is a calculation of the maximum flow rates of the lotic currents, which were obtained through the rational method, due to the fact that the basin areas are too small to use the unit hydrographic method.

Concentration time

The duration of the rainfall is equal to the time of concentration of the basin, since it is for this duration that the entire basin area is contributing to the runoff process, therefore, it is to be expected that the maximum flows will occur. In the literature there are multiple expressions for the calculation of the time of concentration, among them those proposed by: Temez, William, Kirpich, Johnstone and Cross, California Coulverts Practice, Giandotti, S.C.S., Ventura-Heras. Its theoretical foundations can be reviewed in Campo and Múnera (1997). Due to the different expressions for the calculation of the concentration time, there is a strong variability in the results from one to the other, which makes it necessary to choose appropriately the concentration time and to discard those methods that do not adjust to the local morphometric conditions of the basin.

The expressions used to estimate this parameter were as follows:

- Témez (1978) $T_c = 0.3\left(\frac{L}{S_o^{0.25}}\right)^{0.75}$ (8)

Tc: concentration time in hours.

L: length of the main channel in kilometers.

So: difference of coordinates between the extreme points of the current over L in %.

- Williams (1922) $T_c = \frac{LA^{0.4}}{DS_0^{0.2}}$ (9)

Tc: time of concentration, in hours.

A: area in square miles.

L: distance in a straight line from the site of interest to the highest point of the basin in miles.

So: difference in the coordinates between the extreme points of the basin divided by L, in %.

D: diameter of a circular basin, with area A, in miles.

- Kirpich (1990) $T_c = 0.066\left(\frac{L}{\sqrt{S_0}}\right)^{0.77}$ (10)

Tc: time of concentration, in hours.

L: length from the gauging station to the boundary, following the main channel, in kilometers.

So: difference of coordinates between the end points of the current over L in m/m.

- California Culverts Practice $Tc = 0.01\left(\frac{L^3}{H}\right)^{0,385}$ (11)

Tc: Concentration time in hours

L: length of main channel in kilometers

H: difference in elevation between the point of interest and the dividing line in km.

- Giandiotti $Tc = \frac{4\sqrt{A} + 1,5L}{25,3\sqrt{LS_o}}$ (12)

Tc: Concentration time in hours

Lc: distance from the site of interest to the point at which the main current cuts the divider in km

H: coordinate difference between endpoints of the current in meters S.C.S-Ranser

$T_c = 0.947K^{0.385}$ (13)

$Tc = \frac{L}{72\left(\frac{Ae}{L}\right)^{0.6}}$

$K = \sqrt{\frac{L_c^3}{H}}$ (14)

Tc: time of concentration, in hours.

Lc: distance from the site of interest to the point at which the main current cuts the dividing line, in kilometers.

H: coordinate difference between the endpoints of the current, in feet.

From Table 4.1-57 to Table 4.1-65, the concentration times calculated according to the methodologies described above for each basin are presented.

Table 4.1-57. Concentration times for the unnamed current #1.

Method	Tc (horas)	Tc (min)
Kirpich	0.32	18.98
Kirpich 2	0.00	0.20
Temez	0.72	43.00
Ventura-Heras	0.72	43.02
Giandiotti	1.06	63.44
Bransby-Williams	1.24	74.37
Johnstone	0.48	28.59

Source: INGEX, 2015.

Table 4.1-58. Concentration times for unnamed current #9.

Method	Tc (horas)	Tc (min)
Kirpich	0.26	15.68
Kirpich 2	0.00	0.20
Temez	0.63	37.96
Ventura-Heras	1.50	90.02
Giandiotti	0.94	56.42
Bransby-Williams	4.26	255.57
Johnstone	0.42	25.26

Source: INGEX, 2015.

Table 4.1-59. Concentration times for the unnamed current #2.

Method	Tc (horas)	Tc (min)
Kirpich	0.12	7.37
Kirpich 2	0.00	0.28
Temez	0.30	18.25
Ventura-Heras	0.62	36.96
Giandiotti	0.56	33.35
Bransby-Williams	1.52	91.14
Johnstone	0.25	15.21

Source: INGEX, 2015.

Table 4.1-60. Concentration times for unnamed current #3.

Method	Tc (horas)	Tc (min)
Kirpich	0.06	3.83
Kirpich 2	0.01	0.32
Temez	0.13	7.81
Ventura-Heras	0.13	7.81
Giandiotti	0.26	15.42
Bransby-Williams	0.18	10.92
Johnstone	0.11	6.69

Source: INGEX, 2015.

Table 4.1-61. Concentration times for the unnamed current #4.

Method	Tc (horas)	Tc (min)
Kirpich	0.09	5.70
Kirpich 2	0.00	0.26
Temez	0.23	13.79
Ventura-Heras	0.49	29.20
Giandiotti	0.41	24.85
Bransby-Williams	1.13	67.74
Johnstone	0.18	10.65

Source: INGEX, 2015.

Table 4.1-62. Concentration times for the unnamed current #5.

Method	Tc (horas)	Tc (min)
Kirpich	0.16	9.35
Kirpich 2	0.00	0.21
Temez	0.35	21.01
Ventura-Heras	0.83	49.83
Giandiotti	0.49	29.67
Bransby-Williams	2.20	131.85
Johnstone	0.23	14.00

Source: INGEX, 2015.

Table 4.1-63. Concentration times for the unnamed current #8.

Method	Tc (horas)	Tc (min)
Kirpich	0.25	14.89
Kirpich 2	0.00	0.20
Temez	0.54	32.20
Ventura-Heras	0.54	32.52
Giandiotti	0.78	46.97
Bransby-Williams	0.91	54.52
Johnstone	0.36	21.54

Source: INGEX, 2015.

Table 4.1-64. Concentration times for the unnamed current #6.

Method	Tc (horas)	Tc (min)
Kirpich	0.10	6.28
Kirpich 2	0.00	0.29
Temez	0.22	13.40
Ventura-Heras	0.53	31.78
Giandiotti	0.48	28.52
Bransby-Williams	1.30	77.97
Johnstone	0.19	11.27

Source: INGEX, 2015.

Table 4.1-65. Concentration times for the unnamed current #7.

Method	Tc (horas)	Tc (min)
Kirpich	0.05	3.25
Kirpich 2	0.01	0.33
Temez	0.11	6.48
Ventura-Heras	0.26	15.37
Giandiotti	0.25	15.19
Bransby-Williams	0.56	33.34
Johnstone	0.09	5.66

Source: INGEX, 2015.

To select the time of concentration, an average of the results obtained with the previous methodologies was performed, for this purpose the highest and lowest value was eliminated in order to focus the result.

4.1.4.5.7 Rainfall intensity

It is assumed for the estimation of hydrological events of a certain magnitude in the basin, that the occurrence of the design flow rate is equal in frequency to the design storm. To determine rainfall intensity, the Intensity-Duration-Frequency (IDF) curves are used, which relate their duration to the intensity associated with different return periods.

The study basin does not have hydrological records that allow the determination of the IDF curve; for this reason, it is necessary to infer them from neighboring basins by means of regional analyses. To determine the precipitation histories over this basin, the precipitation records of the Palma de Coco station (27030140) are used.

The design intensity for the basin of interest was determined from the Palma de Coco station, once the IDF curve was constructed based on the maximum monthly rainfall records of that station (Wilches, 2001). Table 4.1-66 and Illustration 4.1-121 show the reported intensities for a rainfall duration equal to the time of basin concentration.

Table 4.1-66. Intensities for different return periods.

Return Period (years)	I (mm/h) duration 45 minutes	I (mm/h) duration 25 minutes	I (mm/h) duration 20 minutes
2.33	85.07	115.3	193.9
5	96.61	131.0	220.2
10	108.45	147.0	247.2
25	126.34	171.2	288.0
50	141.81	192.2	323.3
100	159.18	215.8	362.8

Source: INGEX, 2015.

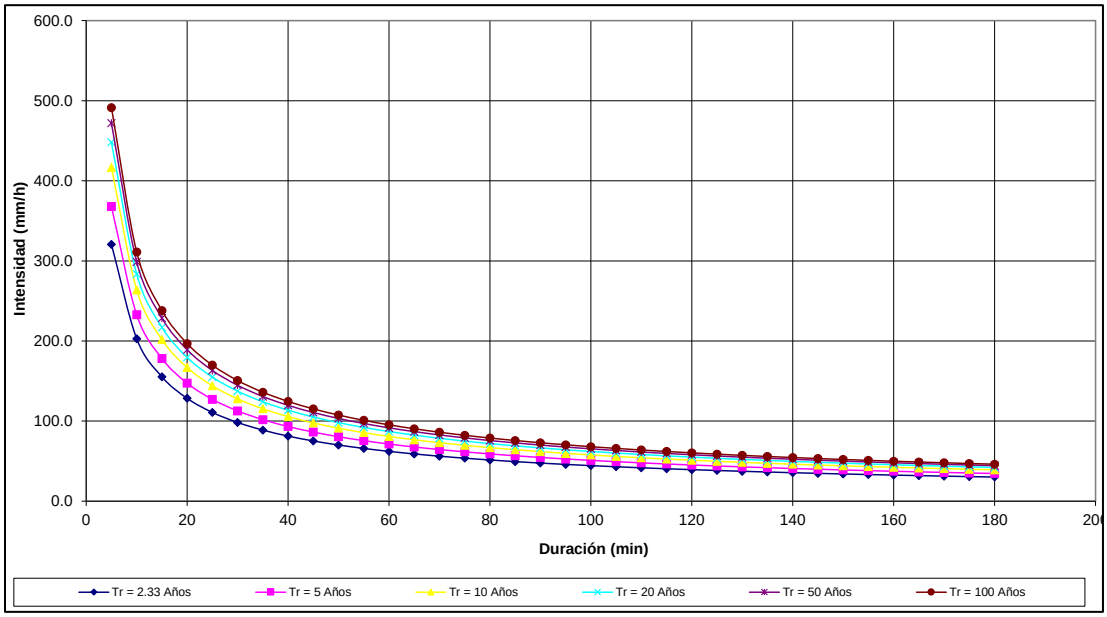

Illustration 4.1-121. Intensity - frequency - duration curve for the Palma de Coco season.
Source: INGEX, 2015.

Rational method

The method assumes that runoff is directly proportional to effective precipitation and although this is not true in reality, the errors in such small basins (less than 8 km²) are not significant.

With this method the flow rate can be found with the following expression:

$$Q = \frac{C * i * A}{3.6}$$

Where A is the basin area km², i is the rainfall intensity in mm/h which depends on the return period as well as the runoff coefficient C and 3.6 is a unit conversion value. The value of the runoff coefficient for each proposed return period for a watershed with forests and wooded forests with slopes greater than 7% into which the study sub-basins can be classified is presented in Table 4.1-67 (Chow, 1994).

Table 4.1-67. Runoff coefficients.

Tretorno (years)	2.33	5	10	25	50	100
Runoff	0.35	0.39	0.41	0.45	0.48	0.52

Source: INGEX, 2015.

The information collected is used to estimate the maximum flow in the basin, which is shown in Table 4.1-68.

Table 4.1-68. Maximum flow rates.

Period of return (years)	SN #1	SN #9	SN #2	SN #3	SN #4	SN #5	SN #8	SN #6	SN #7
2.33	26.06	18.55	3.89	1.38	3.48	6.26	15.71	3.92	1.53
5	32.98	23.48	4.92	1.74	4.40	7.92	19.89	4.97	1.93
10	38.92	27.70	5.81	2.06	5.19	9.35	23.47	5.86	2.28
25	49.76	35.42	7.42	2.63	6.64	11.95	30.01	7.49	2.92
50	59.58	42.41	8.89	3.15	7.94	14.31	35.93	8.97	3.49
100	72.45	51.57	10.81	3.83	9.66	17.40	43.69	10.91	4.25

Source: INGEX, 2015.

4.1.4.6 SEDIMENTOLOGICAL REGIME

In order to carry out an adequate morphological classification of the basin, which would allow us to infer how the transport processes in the basin are, we used the proposal of Flores et al. (2006), in which 4 basic types of bed classification are established: cascade, step - pool, plane bed, pool-riffle. The results are shown in Illustration 4.1.122, from which it can be seen that in the basin there are two dominant geomorphological types: waterfalls and wells, and rapids and wells. These results show that the basin as such does not have deposition zones, therefore in the long term it is expected that all sediments produced by erosive processes in the basin will be evacuated from it.

4.1.4.6.1 Estimate of the annual denudation of the study area

The average annual rate of soil loss from laminar erosion is estimated based on the Universal Soil Loss Equation:

$$E = RKLSCP$$

Where:

E is the loss of soil per unit area [T (m2 per year)-1]].

R is the erosion factor of rainfall [MJ mm (m2 h)-1]].

K is the soil erodibility factor [T m2 h (m2 MJ h)-1]].

LS is the topographical[dimensionless] factor

C is the coverage factor for handling[dimensionless].

P is a factor for conservation practice[dimensionless].

This equation describes the relationship between laminar erosion due to rainfall and the main factors that control it.

The erosion factor, R, evaluates the potential capacity of rainfall to produce erosion in given circumstances. According to Pérez (2001), the rainfall erodability factor for Colombia can be calculated according to the following expression:

$$R = 1.193 \times 10^{-8}\, PMA^{1.70148}$$

Where PMA is the average annual rainfall[mm/year] and R is the erosion factor of rainfall [MJ mm (m2 h)-1]. For the basin defined up to the catchment site, values for R ranging from 1.54×10-2 to 1.40×10-2[T m2 h (m2 MJ h)-1] were estimated.

The soil erodibility factor, K, represents the degree of natural resistance that the soil offers when other erosive factors act. The value of this factor was taken from the Hydrological Atlas of Colombia (Poveda et al., 2007). In this study, a K map was obtained for the entire Colombian territory with a resolution of 120 arc seconds (pixels of approximately 3.7 km), depending on the soil texture. It should be borne in mind that for the preparation of this map only a small number of textures were taken into account for soil classification and the scale of the information used was 1:3'400 000, however, due to the absence of data, it was decided to work with this information. For the study area a K-value of 7,192×10-2[T m2 h (m2 MJ h)-1] was estimated.

The LS factor is the product of the slope length (L) and slope (S) sub-factors, which are calculated using the following expressions (McCool et al., 1987 and 1989 and Foster et al., 1977, cited by Barrios, 2000):

$$L = (\lambda / 22.13)^m$$

$$m = \beta / (1 + b)$$

$$\beta = \{(sen\theta / 0.0896) / [3.0(sen\theta)^{0.8} + 0.56]\} \times r$$

$S = 10.8 sen\theta + 0.03$; para $p < 9\%$

$S = 16.8 sen\theta - 0.50$; para $p > 9\%$

Where:

λ length of slope (m)

m variable exponent according to β

β relationship between furrow erosion and furrow erosion

θ Ground angle of inclination

p slope of the land (%)

r coefficient equal to: 0.5 in forest or pasture land; 1.0 in agricultural land; and 2.0 in construction sites.

The spatial distribution of λ within the basin was estimated using the MDE according to the CALSITE model (Bolton et al., 1995, cited by Barrios, 2000):

$$\lambda = (A/\pi)^{0.5}$$

Where A is the accumulated drainage area. Finally, the coverage resulting from applying the equation (2.15) was updated to consider λ = 0 in the pixels corresponding to the drainage network of the basin.

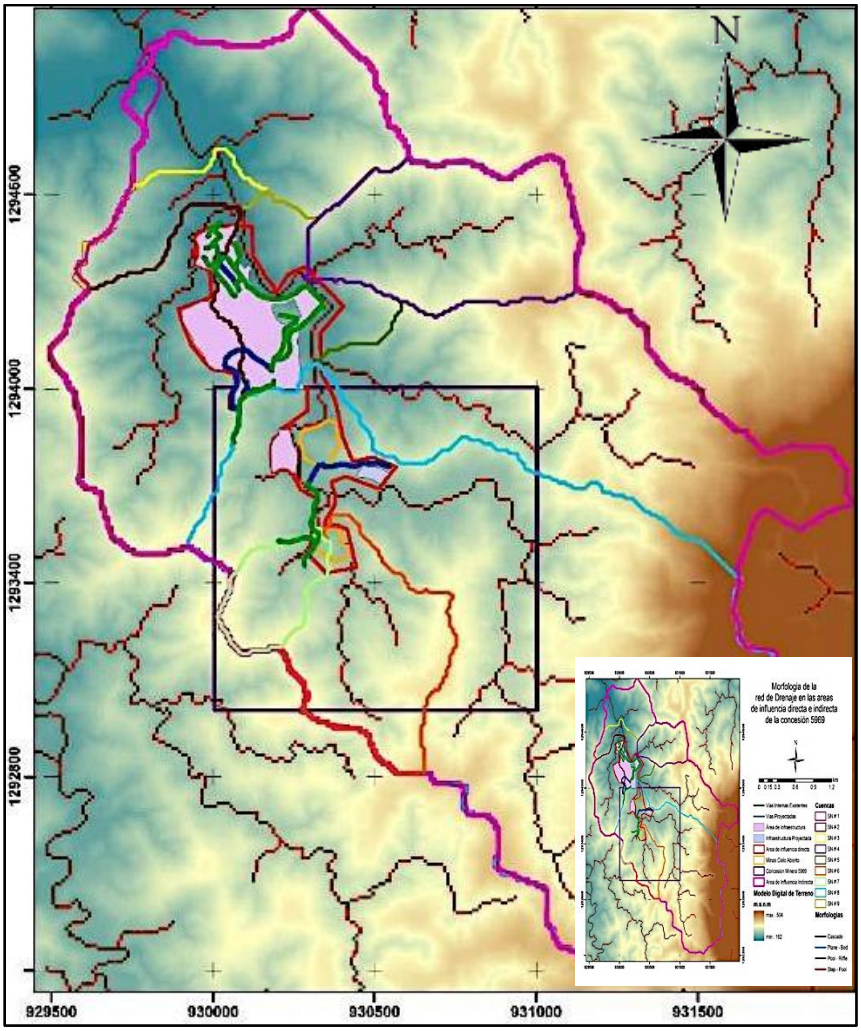

Illustration 4.1-122. Morphological classification of currents.
Source: INGEX, 2015.

Factor C has been defined as the relationship between the loss of soil from a plot under certain use and management, and the losses corresponding to uncultivated soil. A large number of tables have been prepared to determine the value of the C coefficient depending on the type and coverage of the vegetation cover. Considering that the land use in the analyzed basin corresponds mainly to forests and grasslands and taking as a reference the classification proposed in the Hydrological Atlas of Colombia (Poveda et al., 2007), a value of 0.12 was assumed for the study area.

To obtain the values due to conservation practices, P, the parameters of the slope map have been used (the factor P varies according to the slope), since there is no information on the direct measurement of this variable. The values have been assigned by dividing the slope in the ranges presented in Table 4.1 69

Table 4.1-69. Values assigned to P according to the slope.

Slope value	Value assigned to P
0% a 20%	0,35
20% a 40%	0,5
40% a 60%	0,6
60% a 80%	0,7
80% a 100%	0,8

Source: INGEX, 2015.

Having the rasterized basin, the average annual rate of soil loss due to laminar erosion was calculated for each cell as the product of the five factors described above. Illustration 4.1-123 shows the laminar erosion map obtained for the basin associated with the catchment area.
By integrating the laminar erosion map in the direction of flow, it is obtained that the annual rate of sediments produced in the currents within the area of direct and indirect influence by laminar erosion is shown in Table 4.1-70

Table 4.1-70. Laminar erosion in each of the currents.

Current	Laminar Erosion (T/year)
SN #1	34.90
SN #9	25.87
SN #2	3.88
SN #3	0.083
SN #4	3.28
SN #5	5.69
SN #8	15.30
SN #6	2.83
SN #7	0.70

Source: INGEX, 2015.

It should be taken into account that within the estimate made, no important processes in the production of sediments were considered, such as the formation of gullies and furrows in the upper parts of the basin, erosion in the banks of the river beds and mass removal.

4.1.4.6.2 Flood temporal and spatial relationship

Flooding only affects flat areas adjacent to rivers such as meadows and overgrown areas. Because the currents found in the area of direct and indirect influence are in the upper part of the basin, where the valleys are canyoned and where there are no flood plains, the risk of this type of event is very low. In addition, there are no major infrastructure projects in this area susceptible to flood damage.

4.1.4.7 WATER SUPPLY

The total water supply is defined by the modal value of the annual average flow or modal flow. This magnitude represents the most likely average annual flow rate and is extracted from the probability density curve (hereinafter referred to as the PDC) of the annual flows. This series is constructed from the registers at the hydrometric stations that measure the flow of water from the supply source.

Since the country does not have municipal punctual hydrological information, it is proposed to use UNESCO's methodology (1979) to extract these values from hydrological regionalizations, modal iso-efficiency maps or modeling exercises that comply with all stages of hydrological modeling protocols, especially with the validation of the performance of the proposed models (Domínguez, 2000).

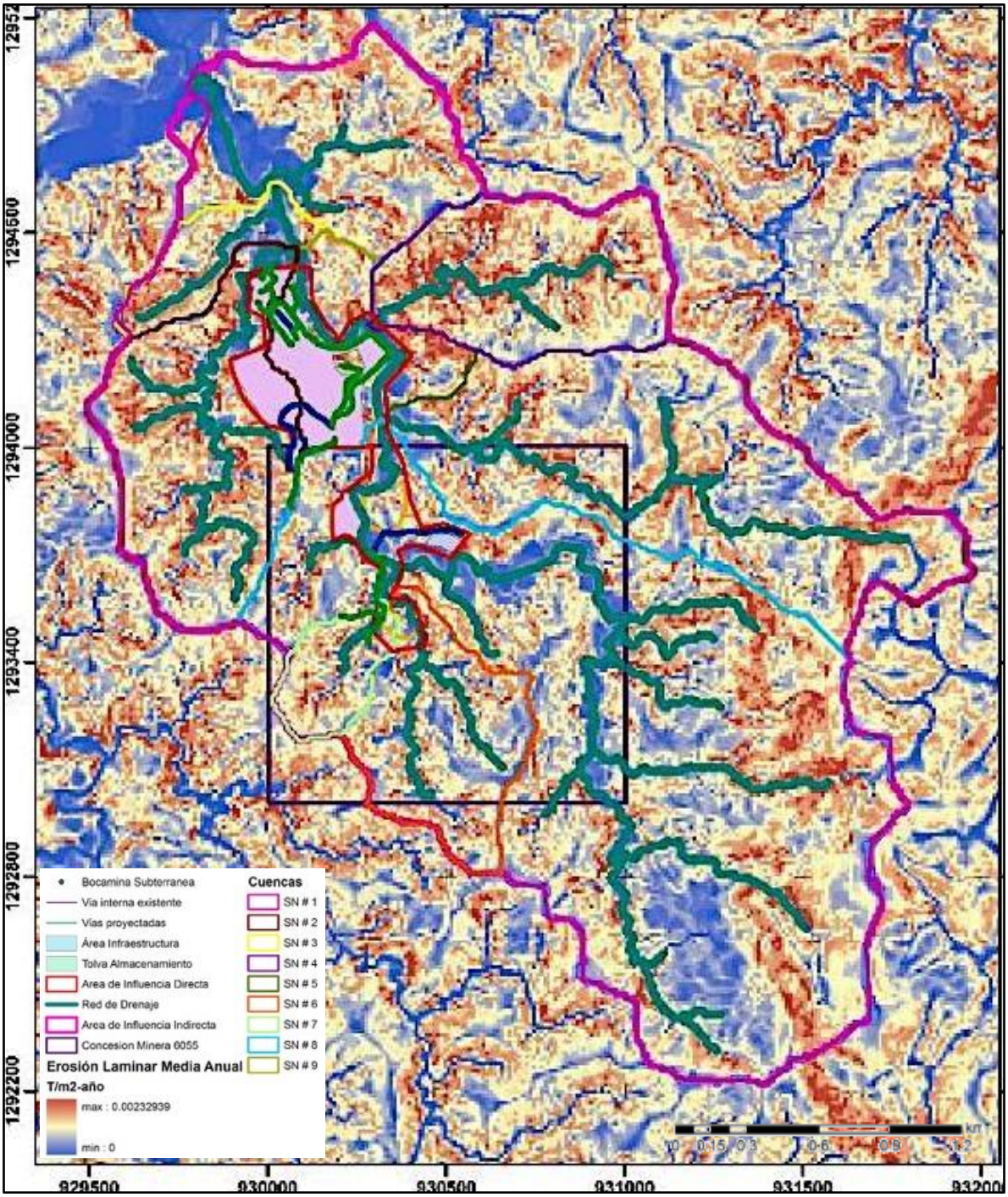

Illustration 4.1-123. Laminar erosion map in the study area.
Source: INGEX, 2015.

The net surface water supply results from the following expression:

$$O_n = O_t \; x \left(1 - (R_e + R_{it})\right)$$

Where:

Ot: Total surface water supply[m3].

Re: Reduction factor to maintain the low water regime.

Rit; Reduction factor for temporary irregularity in water supply.

The total offer is expressed as:$O_t = Q_o * T$

Where: Qo- modal flow rate at the supply source[m3/s] and T is the number of seconds in the aggregate interval of the water scarcity index.

To define Re, the probabilistic distribution function (hereinafter FDP) of the low water flow rates (p(Qmin)) is constructed. The low water flow rate is obtained from the FDP with a 97.5% probability of excess %5,97 Qmin, so that the reduction to maintain the low water regime of the source would be equal to:

$$R_e = \frac{Q_{min\,97.5\%}}{Q_o}$$

The reduction due to temporary irregularity of the water supply should be a function of the coefficients of variation (CV) and asymmetry of the annual average flow rates (CS) and of the correlation radius of the daily flow rate autocorrelation function (D). The latter represents the temporary memory of the flow rate regime. In plain rivers the correlation radius is greater than in Mountain Rivers. The greatest Rit reduction occurs in currents where the annual modal flow is low, the coefficient of variation is high, the positive asymmetry and the correlation radius is tending to 0.

Conversely in rivers where CV → 0, CS <<< 0, D >> 0 and the annual modal flow is high this reduction will be minimal.

However, due to limitations such as the short length of the annual and low water flow series (30 years on average) and the complexity of parameter D, as a first approximation to obtain R_{it} it is recommended to apply the tabulation presented in Table 4.1-71.

Table 4.1-71. Scale of reductions for temporary irregularity in water supply.

Cv	R_{it}, {%}
0 - 0.2	15
0.2 - 0.3	25
0.3 - 0.4	35
0.4 - 0.6	40
> 0.6	2

Source: INGEX, 2015.

From the non-dimensional flow duration curve constructed with the information from the Vegachí station, the modal flow of each of the sources and the flow was obtained with a probability of exceeding 97.5%. The modal flow rate according to the probabilistic density curve of the flows is 0.8 times the average flow rate of the source to intervene, while the value that is exceeded 97.5% of the time is 0.4 times the average flow rate of each of the currents (See Illustration 4.1-124 and Illustration 4.1-125). Table 4.1-72 illustrates the water supply of the streams under study.

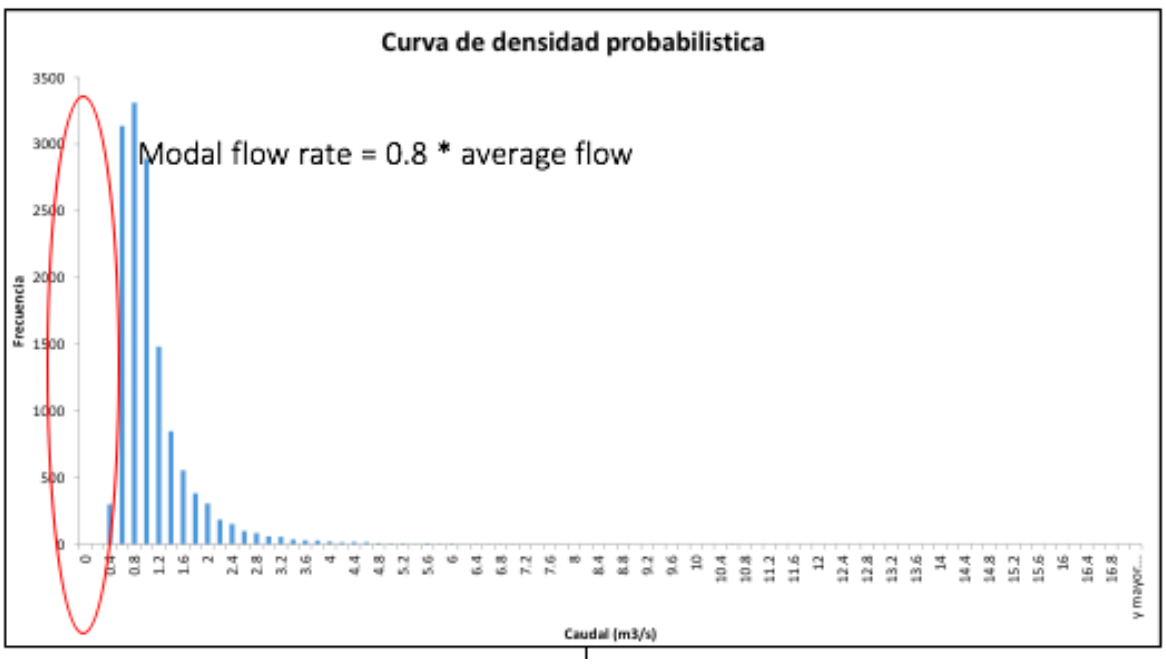

Illustration 4.1-124. Probabilistic density curve.
Source: INGEX, 2015.

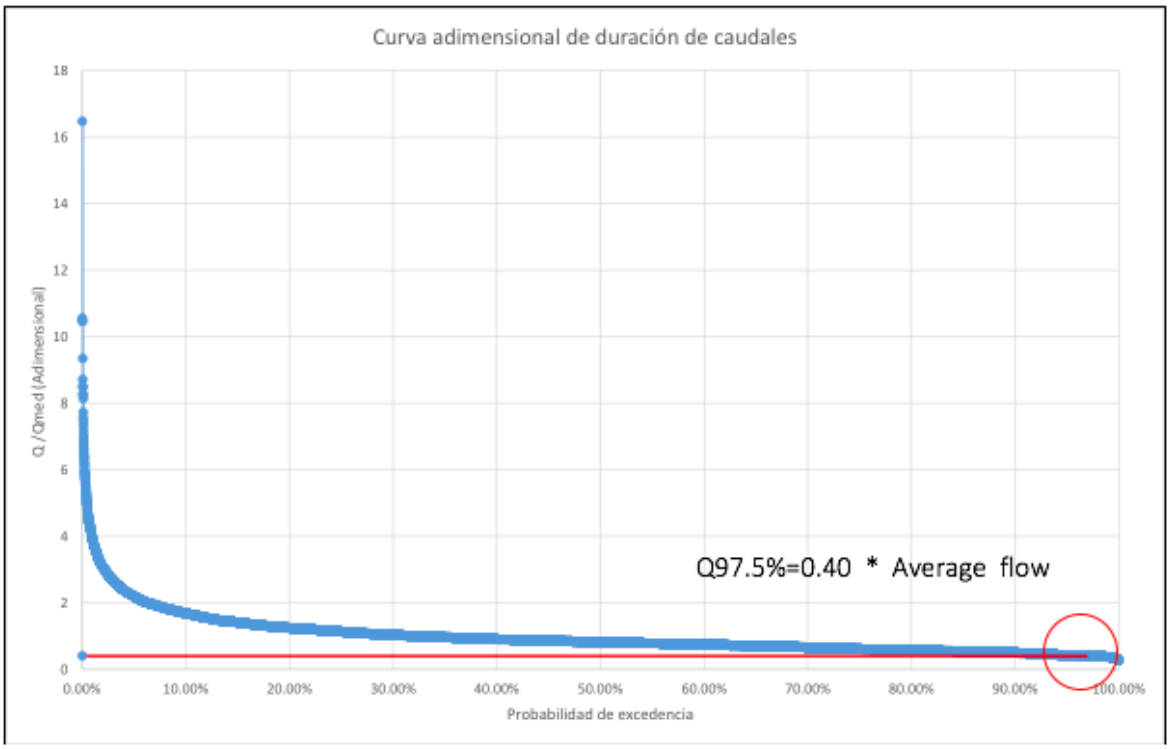

Illustration 4.1-125. Dimensionless flow duration curve.
Source: INGEX, 2015.

Table 4.1-72. Water supply of the currents under study.

CURRENT	MEDIUM FLOW (m^3/s)	MODAL FLOW (m^3/s) (0.8 * MEDIUM FLOW)	Q97.5% (m^3/s)	OFFER (m^3/day)
SN #1	0,248	0,198	0,100	8132,335
SN #9	0,193	0,154	0,078	6331,721
SN #2	0,026	0,021	0,011	867,449
SN #3	0,0046	0,004	0,002	167.575
SN #4	0,020	0,016	0,008	657,158
SN #5	0,042	0,033	0,017	1373,461
SN #8	0.119	0.095	0.048	3903.521
SN #6	0.022	0.018	0.009	722.874
SN #7	0.005	0.004	0.002	167.575

Source: INGEX, 2015.

4.1.4.8 WATER USES AND USERS (WATER DEMAND)

Below is the water demand balance by watershed (see Illustration 4.1-126), based on the quantitative inventory of water uses and users. Fundamental input to determine the shortage rate and adequately manage the use of the resource by the project, avoiding affecting the quality and quantity of water for these users, and the natural water balance.

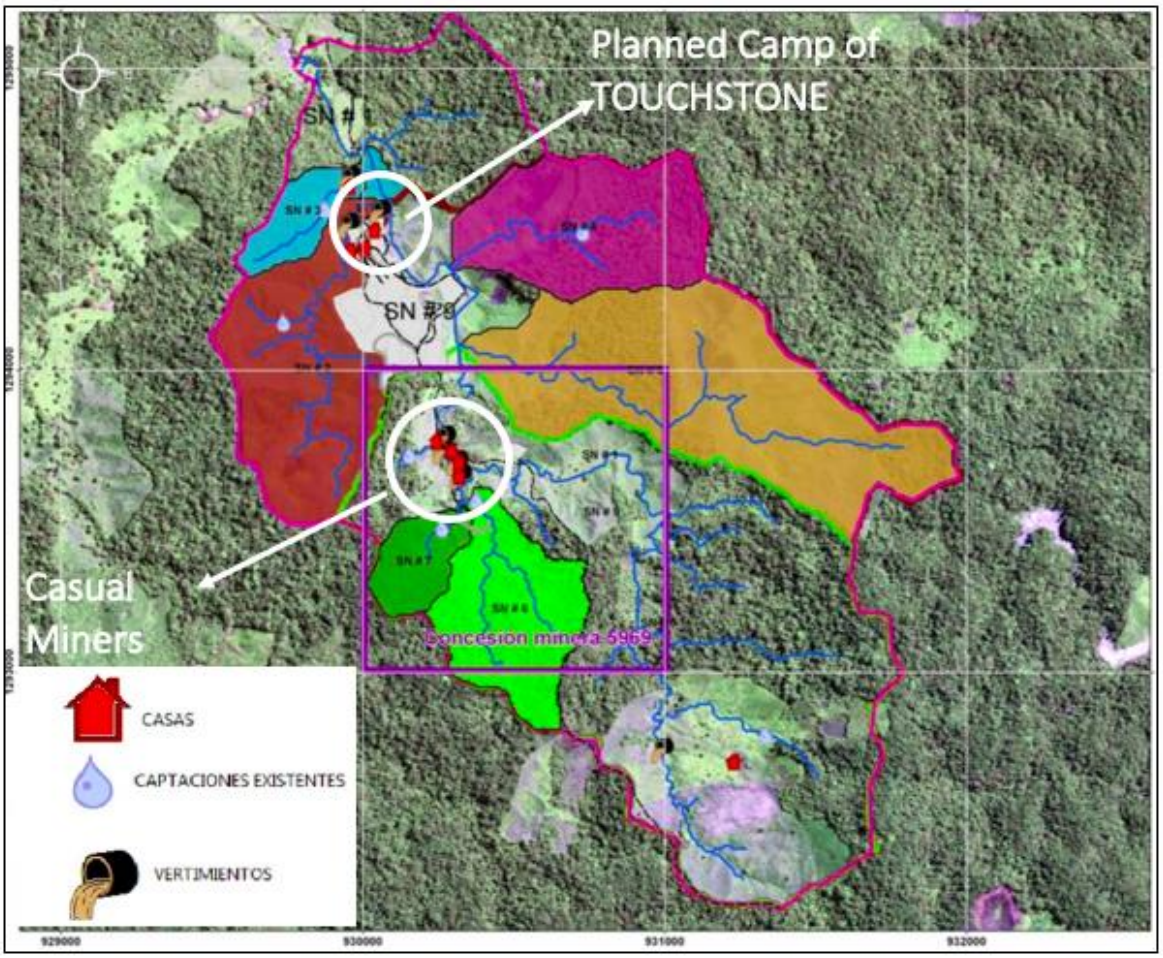

Illustration 4.1-126. Quantitative inventory of uses and users.
Source: INGEX, 2015.

User catchments are located upstream in independent basins, i.e. in SN#2, SN#3, SN#4, SN#6, SN#7 and in two (2) births of SN#8 (See Table 4.1-73). These do not receive direct anthropic intervention effects in terms of quality by previous discharges and/or quantity by other previous catchments.

Table 4.1-73. Hydrographic location of catchments and user dumping.

USER	PROJECTED CAPTURE LOCATION	TYPE OF DISCHARGE	DUMPING LOCATION
House of Gustavo Salazar	Upstream of SN#3	Untreated Domestic	Downstream of SN#3
Projected TOUCHSTONE Camp	Upstream of SN#2	Domestic with treatment	Downstream 1 of SN#2
	Upstream of SN#4	Domestic with treatment	Downstream 2 of SN#2
House of Gustavo Salazar	Upstream from birth 1 of SN#8	Untreated Domestic	Downstream 1 of SN#8
Gold Processing Plants and Informal Mines	Upstream of SN#6 and Upstream of SN#7	Industrialist	Downstream 2 of SN#8
		Industrialist	Downstream 3 of SN#8

USER	PROJECTED CAPTURE LOCATION	TYPE OF DISCHARGE	DUMPING LOCATION
		Industrialist	Downstream 4 of SN#8
Torres family dwelling	Upstream of SN#6	Untreated Domestic	Downstream 5 of SN#8
Bernardo Salazar House	Upstream from birth 2 of SN#8	Untreated Domestic	Downstream of birth 3 SN#8

Source: INGEX, 2015.

However, the quality of the resource in the area is affecting its supply or availability, through the direct reception of downstream discharges from the SN#2, SN#3 and SN#8 basins and indirectly by converging the quality of these sources on the main channel of the SN#8, SN#9 and SN#1 basins of greater hierarchy.

This is due to the fact that 66.66% and 100% of domestic and 100% of industrial discharges (Informal Miners' Benefit Plants), respectively, are discharged to these surface water sources without prior treatment.

Table 4.1-74 below presents in detail the inventory of the uses and users of the abiotic environment study basin.

Table 4.1-74. Inventory of uses and users.

USER	COORD. PREDIO	HAB	COORD. CAPTURE	WATER SUPPLY BASIN	TYPE OF SIS. TREATMENT	CONSUMPTION (M^3/DÍA)	LANDFILL USE AND GENERATION ACTIVITIES	COORD. DUMPING
House of Gustavo Salazar	929960 1294610	4	929874 1294537	Upstream of SN#3	None	0.525	Domestic Activities (Personal grooming, food preparation, laundry)	Downstream of SN#3: 929958 - 1294636
TOUCHSTONE Camp	930010 1294408 929962 1294399 930042 1294466	29	930728 1294461 929787 1294273	Upstream of SN#2	Filtration and degradation with macrophytes.	3.81	Domestic Activities (Personal grooming, food preparation, laundry)	Downstream 1 of SN#2: 930058 - 1294524 Downstream 2 of SN#2: 929954 - 1294480
House of Gustavo Salazar	930247 1293767	3	930154 1293722	Upstream from birth 1 of SN#8	None	0.393	Domestic Activities (Personal grooming, food preparation, laundry)	Downstream 1 of SN#8: 930267 - 1293761
Gold Processing Plant and Informal Mine	930296 1293734	-	930263 1293480	Upstream of SN#6	None	5.74	Shredding, material washing, cyanidation and mercury handling.	Downstream 2 and 3 SN#8: 930268 - 1293730 930273 - 1293775

USER	COORD. PREDIO	HAB	COORD. CAPTURE	WATER SUPPLY BASIN	TYPE OF SIS. TREATMENT	CONSUMPTION (M^3/DÍA)	LANDFILL USE AND GENERATION ACTIVITIES	COORD. DUMPING
Gold Processing Plant and Informal Mine	930322 1293650	-	930376 1293572	Upstream of SN#7	None	5.74	Shredding, material washing, cyanidation and mercury handling.	Downstream 4 of SN#8: 930325 - 1293650
Torres family dwelling	930322 1293697	6	930376 1293572	Upstream of SN#6	None	0.788	Domestic Activities (Personal grooming, food preparation, laundry)	Downstream 5 of SN#8: 930314 - 1293693
Bernardo Salazar House	931232 1292704	4	931334 1292793	Upstream from birth 2 of SN#8	None	0.525	Domestic Activities (Personal grooming, food preparation, laundry)	Downstream from birth 3 SN#8: 930994 - 1292740

Source: INGEX, 2015.

The global water demand by sub-basin and global water demand according to the inventory, and the water footprint, are presented below.

4.1.4.8.1 Calculation of the overall water demand of the SN#1 basin

From the surveys carried out in each dwelling or economic activity, the variables necessary to determine the demand of the enveloping or higher hierarchy basin, i.e. SN#1, were synthesized and calculated in Table 4.1-75.

Table 4.1-75. Basin water demand SN#1.

Water use	Human consumption Livestock Miner
Supply system	Surface water catchments
HUMAN CONSUMPTION	
Total population (Hab)	46
Level of complexity of the system	Bajo
Minimum crew (L*inhabit/day)	100
Maximum crew (L*hab/day)	150
Net provision (L*inhabit/day)	100
Climate effects	15%
Conduction and adduction losses	-10%
Gross provision (based on average) (L*inhab/day)	127.8
Current average daily flow rate "QMD" (L/s)	0.068

Maximum daily consumption coefficient, k1	1.3
Maximum hourly consumption coefficient, k2	1.6
Current maximum hourly flow rate "QMH" (L/s)	0.142
Current total population demand (L/day)	**12228**
Total current population demand (m3/month)	**367**
LIVESTOCK CONSUMPTION	
Beef cattle	473
Average livestock head consumption (L*cab/day)	78.5
Pigs	8
Average adult pig consumption (L*cab/day)	18
Poultry	60
Consumption per poultry (L*ave/day)	0.27
Current livestock demand (L/day)	**37291**
Current livestock demand (m3/month)	**1119**
INFORMAL MINING CONSUMPTION	
Demand in the primary sector (profit plants) (L/day)	**1920**
Demand in the primary sector (profit plants) (m3/month)	**57.6**
TOTAL WATER DEMAND	
Current global demand (L/day)	51439
Current global demand (m3/day)	51.44
Current global demand (m3/month)	1543

Source: INGEX, 2015.

In Table 4.1-76 and Illustration 4.1-127, it can be seen that the highest demand is found in livestock consumption with 72% of total water use, followed by human and mining consumption with 24% and 4% respectively.

Table 4.1-76. Total water demand within the SN#1 watershed.

CONSUMPTION		TOTAL INDIVIDUALS	CONSUMPTION(L*Ind/day)	DEMAND (L/day)	DEMAND (m^3/day)
Human		46	265.824	12227.9	12.228 (24%)
Livestock	Bovine animals	473	78.5	37130.5	37.291 (72%)
	Pigs	8	18	144	
	Birds	60	0.27	16.2	
Informal mining		2	960	1920	1.92 (4%)
TOTAL WATER DEMAND (L/day)					51.44 (100%)

Source: INGEX, 2015.

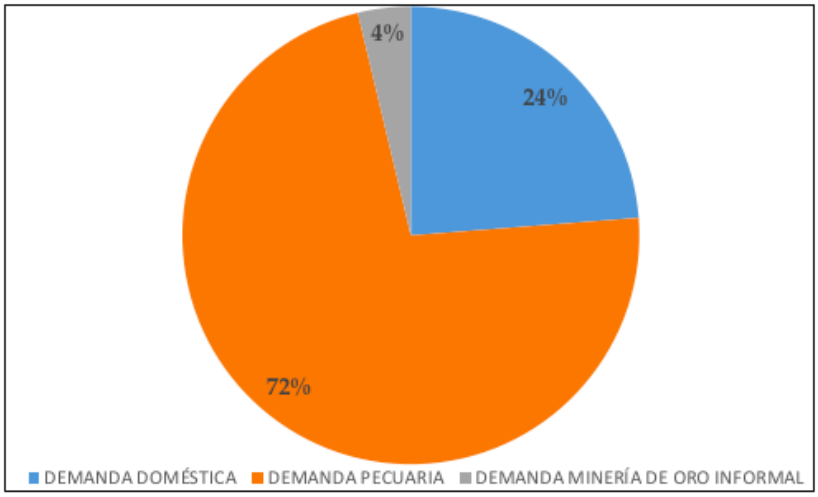

Illustration 4.1-127. Percentage distribution of water demands in the SN#1 basin.
Source: INGEX, 2015.

According to the above, it can be concluded that the greatest use in the microbasin is due to the livestock sector with an approximate consumption of 37.3m3/day (See Table 4.1-76).

The calculations and considerations are presented below by demands for the SN#1 basin.

Domestic demand

It presents the human or domestic consumption of forty-six (46) inhabitants, including inhabitants of the TOUCHSTONE camp, informal miners and local residents. These provide the basic needs for food and water, personal hygiene and housekeeping with water.

For this consumption, there are no water and sewerage networks. For this reason, the inhabitants use the surface water system to discharge domestic greywater without prior treatment and in some cases also to dispose of solid waste inadequately.

Human consumption for the existing population in the SN#1 basin was calculated in accordance with Title B of the Technical Regulation of the Potable Water and Basic Sanitation Sector (hereinafter RAS 2000), which defines the maximum hourly flow (hereinafter QMH) corresponding to temporary peaks, in order to guarantee water supply. In line with the following considerations of the level of complexity of the system, net provisioning, climate correction and losses.

The demand for water for the hydro-sanitary units, food, personal hygiene and housing hygiene, required by the population, is primarily conditioned by the level of complexity of the system. Where the RAS 2000 establishes minimum and maximum values in the net endowment (See Table 4.1-76).

Table 4.1-77. Net provision according to the level of complexity of the system.

LEVEL OF COMPLEXITY OF THE SYSTEM	MINIMUM NET DOWNLOAD (L/person/day)	MAXIMUM NET DOWNLOAD (L/person/day)
Bass	100	150
Medium	120	175
Medium high	130	-
High	150	-

Source: RAS, 2000.

The level of complexity is low for this water system because the number of inhabitants is 46, a much lower value than an aqueduct of thousands of people as municipal headwaters; therefore, the net daily endowment corresponds to the minimum, i.e. 100 L / inhabitant day.

With respect to the net endowment chosen, paragraph B.2.4.4.4.2 of the SAR 2000 was corrected for climate by means of proportionality percentages due to the effects of climate on the net endowment or on water supply. Taking into account the level of complexity and the warm climate of the basin, the climate correction is + 15% (see Table 4.1-78).

Table 4.1-78. Effect of climate on net provisioning.

SYSTEM COMPLEXITY LEVEL	WARM CLIMATE (MORE THAN 28°C)	TEMPERATURE WEATHER (BETWEEN 20°C and 28°C)	COLD WEATHER (LESS THAN 20°C)
Low	+ 15 %	+ 10%	No Weather Correction Supported
Medium	+ 15 %	+ 10 %	
Medium high	+ 20 %	+ 15 %	
High	+ 20 %	+ 15 %	

Source: RAS, 2000

Taking into account the above table, the value of the climate corrected net endowment was calculated as follows:

$$\text{Endowment neat}_{\text{Corrected}} = \text{Endowment}_{\text{Neat}} * (1 + \text{Endowment}_{\text{weather}})$$

$$\text{Endowment neat}_{\text{Corrected}} = 100\ \text{L/hab·day} * 1.15 = 115\ \text{L/hab·day}$$

$$\text{Endowment neat}_{\text{Corrected}} = 115\ \text{L/hab·day}$$

In accordance with the provisions of paragraph B.2.6 of the RAS 2000, the gross endowment is equivalent to:

$$D_{\text{gross}} = D\ \text{neat}_{\text{corrected}} / (1 - \%p)$$

Being:

Gross D = Gross allocation.

Corrected net D = Corrected neat provision

p = Percentage of losses.

According to the above, a percentage of losses of 10% is established due to the individual adduction and conduction system that transports the flow to the homes and economic activities.

$$D_{gross} = 115 \text{ L/hab·day} / (1- 0.1) = 127.8 \text{ L/hab·day}$$

$$D_{gross} = 127.8 \text{ L/hab·day}$$

According to the value of the gross endowment and the inhabitants, the average daily flow according to paragraph B.2.7.1 of the RAS 2000 is equal to:

$$Q_{md}= P^* d_{gross}/ 86400$$

Being:

Qmd = Average daily flow rate

P = Population

D Gross= Gross provision

Then the result of the average daily flow is:

$$Q_{md}= (46*127.8. \text{ L/hab-day})/86400 \text{ s}= 0.068 \text{ L/s}$$

$$Q_{md}= 0.068 \text{ L/s}$$

Finally, to determine the water demand of the inhabitants or human consumption, the maximum daily consumption coefficient (K1) (See Table 4.1-79) and the maximum hourly consumption coefficient (K2) (See Table 4.1-80) are taken into account. Where K1 is obtained from the ratio of the highest daily consumption to the average daily consumption, while K2 is the ratio of the maximum hourly consumption to the maximum daily consumption (RAS, 2000).

Table 4.1-79. Maximum daily consumption coefficient, k1, according to the System Complexity Level

COMPLEXITY LEVEL	K1
Low	1,30
Medium	1,30
Medium High	1,20
High	1,20

Table 4.1-80. Maximum hourly consumption coefficient, k2, depending on the System Complexity Level and the distribution network type.

COMPLEXITY LEVEL	MINOR DISTRIBUTION NETWORK	SECONDARY NETWORK	MATRIX NETWORK
Low	1,60	--	--
Medium	1,60	1,50	--
Medium High	1,50	1,45	1,40
High	1,50	1,45	1,40

Source: RAS, 2000.

With respect to the aforementioned tables, human consumption or domestic demand is equivalent to:

$$D_{habitants} = k1 * k2 * D_{gross\ total}$$

$$D_{habitants} = 1.3 * 1.6 * 0.068\ L/s$$

$$D_{habitants} = 0.142\ L/s = 12228\ L/day$$

Livestock demand

Water consumption is presented for 473 cattle, 8 pigs and 60 poultry that demand this resource. This consumption or use is considered the predominant in the area because it is the main economic activity.

However, it influences deforestation and evapotranspiration, affecting the water balance of the basin. There is also a probability of contamination of organic matter in the hydrological system by cattle feces.

In the same way for the determination of water demand, for the livestock zone the estimations of the 2014 National Water Study (hereinafter ENA, 2014) were followed. Calculating a livestock consumption or demand of 37.3 m3 / day, as presented in the following equation.

$$Cp = Consumption_{Bovines} + Consumption_{pigs} + Consumption_{poultry}$$

$$Cp = (473\ ind * 78.5\ L/day*ind) + (8\ ind * 18\ L/day*ind) + (60\ ind * 0.27\ L/day*ind)$$

$$Csp = 37291\ L/day$$

$$Csp = 37.3\ m^3/day$$

Demand for informal mining

Corresponds to water consumption for two (2) gold beneficiation plants and informal mines.

They also use the surface water system to discharge industrial sewage with cyanide, solids and mercury, without prior treatment, and in some cases also inadequate disposal of solid waste such as sterile or contaminated tailings. The profit plants have 16 ball mills or "Cocos" each. A "Coco" has an approximate consumption of 60 liters of water during a grinding process of 16 hours a day. Next, the water demand of informal mining is calculated.

$$C_{casual\ mining} = (60\ L/\ (1\ day * grinder)) * 16\ grinders$$

$$C_{miner} = 960\ L/day$$

$$C_{casual\ mining} = 960\ L/day * 2\ benefit\ plant = 1920\ L/day$$

$$C_{casual\ mining} = 57.6\ m^3/day$$

Calculation of water demand by sub-basins

The balance of domestic, livestock and informal mining demands is also presented for each sub-basin in terms of flows and percentages on basin SN # 1 (See Table 4.1-81 and Illustration 4.1-28), to then determine the remaining water availability while conserving the ecological flow.

Table 4.1-81. Water demand by basin.

BASINS	DOMESTIC DEMAND (m3 / day)	LIVESTOCK DEMAND (m3 / day)	INFORMAL MINING DEMAND (m3 / day)	TOTAL HYDRATION DEMAND (m3 / day)	TOTAL HYDRAULIC DEMAND ON BASIN SN # 1 (%)
SN # 6	1,594944	0,0054	0,96	2,560344	5
SN # 7	0	0	0,96	0,96	2
SN # 8	3,455712	9,5093	1,92	14,885012	29
SN # 2	2,392416	9,42	0	11,81241600	23
SN # 4	5,31648	12,56	0	17,87648	35
SN # 5	0	5,652	0	5,652	11
SN # 9	11,164608	37,2853	1,92	50,369908	98
SN # 3	1,063296	0,0054	0	1,068696	2
SN#1	12,227904	37,2907	1,92	51,438604	100

Source: INGEX, 2015.

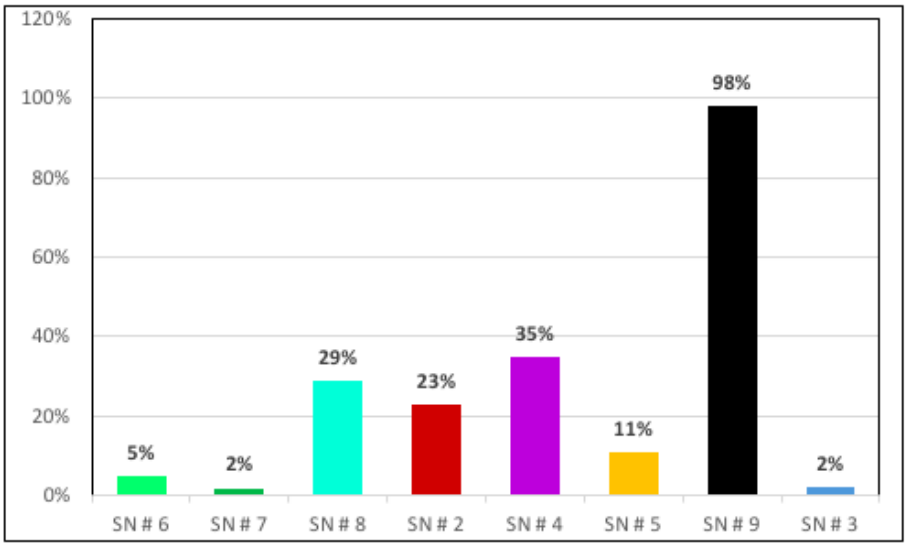

Illustration 4.1-128. Percentage distribution of water demand by sub-basin over 100% of demand of the SN#1 basin.
Source: INGEX, 2015.

The basin with the greatest demand over the total of the global basin is SN # 9 with 98% (50.37m3/day) to receive or include the rest of the sub-basins and therefore demands, with the exception of SN # 3. In second place is the SN # 4 with 35% (17.87 m3/day), which unlike the previous one, directly presents the greatest water use and demand. Third, SN # 8 (29% = 14.88m3/day)

presents a case similar to SN # 9. In fourth place of direct water demand is SN # 2 with 23% (11.81m3/day). The rest of the basins present demands of less than 11% of the total global demand.

Water footprint

The water footprint reflects the territorial impact of water use in terms of water availability, in quantity or quality, from a determined anthropic process (IDEAM - MADS, ENA 2014) (See Illustration 4.1-129).

Human appropriation of water occurs through one or more of the following processes: incorporation into a product, evaporation in the process and transfer between basins. The water footprint offers an innovative vision that incorporates the blue, green and gray footprint, presented below (IDEAM - MADS, ENA 2014).

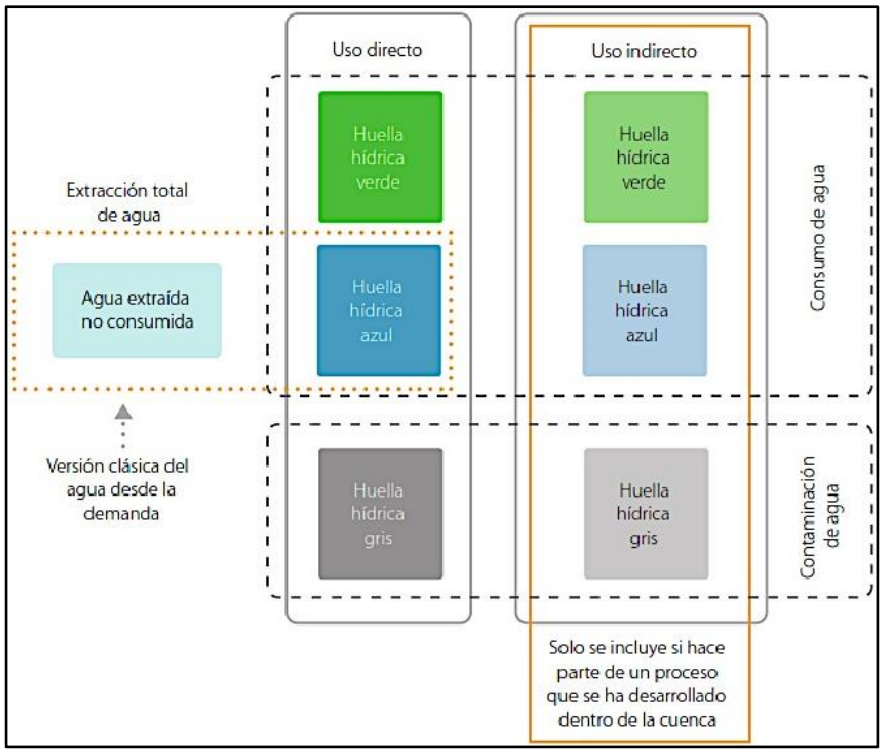

Illustration 4.1-129. Components of the water footprint within the microbasin
Source: ENA, 2014.

Blue footprint

The blueprint refers to the human appropriation of water (rivers, lakes, and aquifers) (IDEAM - MADS, ENA 2014).

For the area or study basin of the abiotic environment, the blue water footprint is associated with the current water demand. A high value of the water footprint in relation to the available supply is considered as an indicator of vulnerability, even more so when the limit of the ecological flow is exceeded (IDEAM - MADS, ENA 2014).

Starting from the previous concept, the supply balanced with the demand and the ecological flow, Table 4.1-82 determines the flow available for new additional activities such as this mining project and also the magnitude of the blueprint. Guaranteeing the conservation of the ecological flows of the basins required for the maintenance of the ecosystem, the flora and fauna of the water currents (Numeral 3.4.2 of resolution 0865 of 2004).

Table 4.1-82. Water supply available for new activities.

BASINS	HYDRAULIC OFFER (m3 / day)	CURRENT HYDRAULIC DEMAND (m3 / day)	FLOW ECOLOGICAL (m3 / day)	WATER SUPPLY AVAILABLE FOR NEW ACTIVITIES (m3 / day)
SN # 6	722,874	2,560344	285,12	435,193656
SN # 7	167,575	0,96	60,48	106,135
SN # 8	3903,521	14,885012	1555,2	2333,435988
SN # 2	867,449	11,81241600	345,6	510,036584
SN # 4	657,158	17,87648	259,2	380,08152
SN # 5	1373,461	5,652	544,32	823,489
SN # 9	6331,721	50,369908	2479,68	3801,671092
SN # 3	167,575	1,068696	60,48	106,026304
SN#1	8132,335	51,438604	3240	4840,896396

Source: INGEX, 2015.

Table 4.1-82 and Illustration 4.1-130 show that currently the basins do not present pressures in the water supply, due to the fact that less than 3% are used. The availability of water for new users or activities in these basins is greater than 57% of the water supply, guaranteeing the conservation of ecological flows (<40%) and sustaining current demand in the area.

According to the above, it can be concluded that the system does not present a degree of vulnerability of the water resource in the basins.

Green footprint

The green footprint refers to the human appropriation of green water (stored in the ground). It is quantified by estimating evapotranspirated water by vegetation associated with an anthropic process (crops) that does not originate from irrigation water (rain-fed agriculture) (IDEAM - MADS, ENA 2014).

For the study basin, as there are no active crops, this footprint is equivalent to zero.

Gray footprint

It is defined as the volume of fresh water necessary to assimilate and dilute the polluting load discharged to a receiving body so that water quality conditions are guaranteed for the environment, people and human activities, in accordance with current regulations. Due to the limitation of information on water quality at the national level and the methodological advance of the subject, the decision is made to include the gray water footprint at the concept level and exclude it in terms of calculation and analysis of results, so that postpones the quantification and subsequent evaluation (IDEAM - MADS, ENA 2014).

This footprint corresponds to the affectations in the quality of the water supply or availability, by the direct reception of discharges downstream of basins SN # 2, SN # 3 and SN # 8, and indirect when the quality of these sources converges. the main channel of the highest basins SN # 8, SN # 9 and SN # 1. This is due to the fact that 66.66% and 100% of the domestic and industrial discharges (beneficiary plants of informal miners), respectively, are discharged to these superficial water sources without previous treatment. The only domestic discharges treated are those of the TOUCHSTONE exploration camp corresponding to 33.4% (2 discharges) (See Illustration 4.1-130).

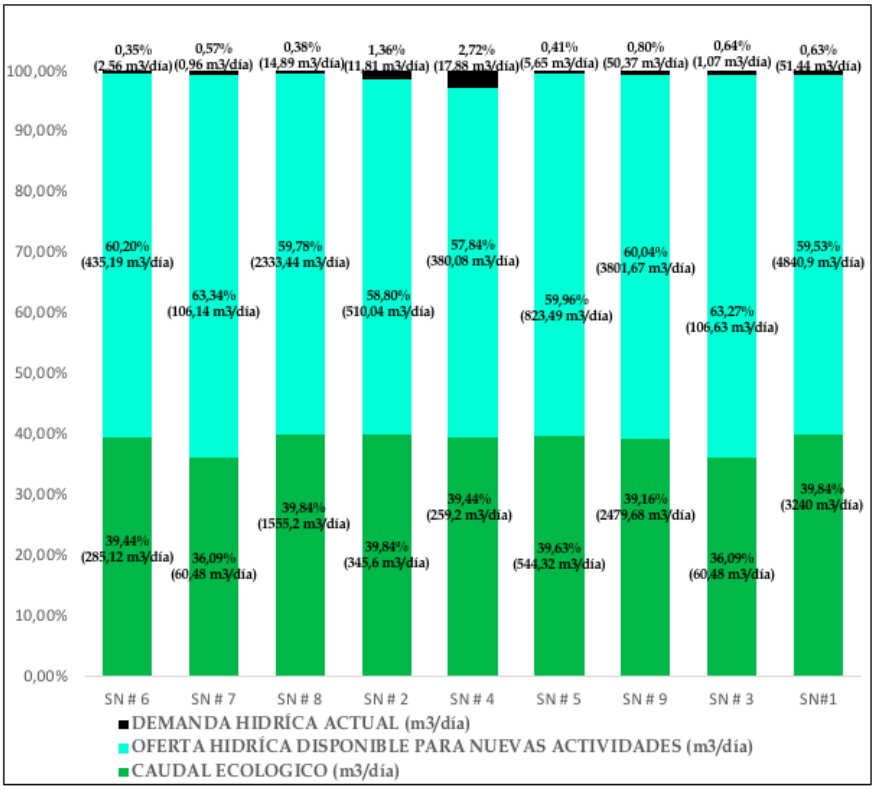

Illustration 4.1-130. Distribution of current water demand, available water supply and ecological flow.
Source: INGEX, 2015.

4.1.4.9 SCARCE INDEX

Water is a vital element for the existence of human beings, and for the well-being of the environmental environment in which they develop their social and productive activities. The development of these activities influences, directly or indirectly, the sources supplying water. The exaggerated exploitation of a source can have effects on the characteristics of the water quality offered and alter its flow dynamics, by taking it from some supply sources and pouring them, most of the time, contaminated in other bodies of water. Finally, excessive pressure on a water source can lead to its disappearance. In this sense, it is important for the tasks of sustainable resource planning to know the amount of available water offered by the source, the levels of demand and the restrictions of use necessary to maintain the health of the supply source. That is, in addition to providing water for human consumption and supply of productive activities, it is necessary that the current permanently maintain a remnant of water to meet other environmental goods and services, offered by the current as water supply ecosystems associated, shelter of aquatic biodiversity and recreation, among others. Although sometimes insufficient, this restriction is generally met by letting the minimum historical flow through the channel, thus reducing the real supply available for water consumption.

Other factors affect the actual availability of water, among them the variability of the hydrological regime of the supplying sources and the quality of it. A current with a highly variable hydrological regime is unreliable as a source of water supply, so the temporary irregularity of the source must be taken into account when estimating the supply of a water current.

For the above reasons it is convenient to define two types of offer: a) total offer that reflects the water circulating through the supply source and b) net offer that defines the amount of water offered by the source after having discounted the amount of water that must stay in it for the purpose of maintaining the dynamics of low water (low water or minimum flows) and to take into account the adverse effects of the temporary irregularity of supply. Taking these definitions into account, the scarcity index is established as the following relationship (Table 4.1 83):

$$I_e = \frac{D}{O_n} \, x \, 100\%$$

Where: Ie- Shortage index [%], D - Water demand [m3], On- Net surface water supply [m3].

Table 4.1-83. Water supply of the currents under study.

CURRENT	FLOW MEDIUM (m3 / s)	MODAL FLOW (m3 / s) (0.8 * MEDIUM FLOW)	Q97.5% (m^3/s)	OFFER (m3 / day)	DEMAND (m^3/día)	SCARCE INDEX
SN #1	0,248	0,198	0,100	8132,335	51,438604	0.6
SN # 9	0,193	0,154	0,078	6331,721	50,369908	0.8
SN #2	0,026	0,021	0,011	867,449	11,812416	1.4
SN #3	0,001	0,001	0,001	167.575	1,068696	0.6
SN #4	0,020	0,016	0,008	657,158	17,87648	2.7
SN #5	0,042	0,033	0,017	1373,461	5,652	0.4
SN # 8	0.119	0.095	0.048	3903.521	14,885012	0.4

SN #6	0.022	0.018	0.009	722.874	2,560344	0.4
SN #7	0.005	0.004	0.002	167.575	0,96	0.6

Source: INGEX, 2015.

According to the results obtained from the scarcity index of the analyzed basins, it can be seen that all of them are below 3%, which means that there are no pressures on the water resource.

4.1.4.9.1 Water quality

Table 4.1-84 and Illustration 4.1-131 show the location of the water quality monitoring points, located on the study drainage network.

Table 4.1-84. Geographic location of the sampling stations.

MONITORING POINT	EAST(X)	WEST (Y)
P-01	929897	1293967
P-02	929835	1294248
P-03	929988	1294547
P-04	930350	1293575
P-05	930973	1293276
P-06	930621	1293966
P-07	930353	1294082
P-08	930337	1293999
P-09	930180	1294290
P-10	930100	1294551
P-11	929963	1294706

Source: INGEX, 2015.

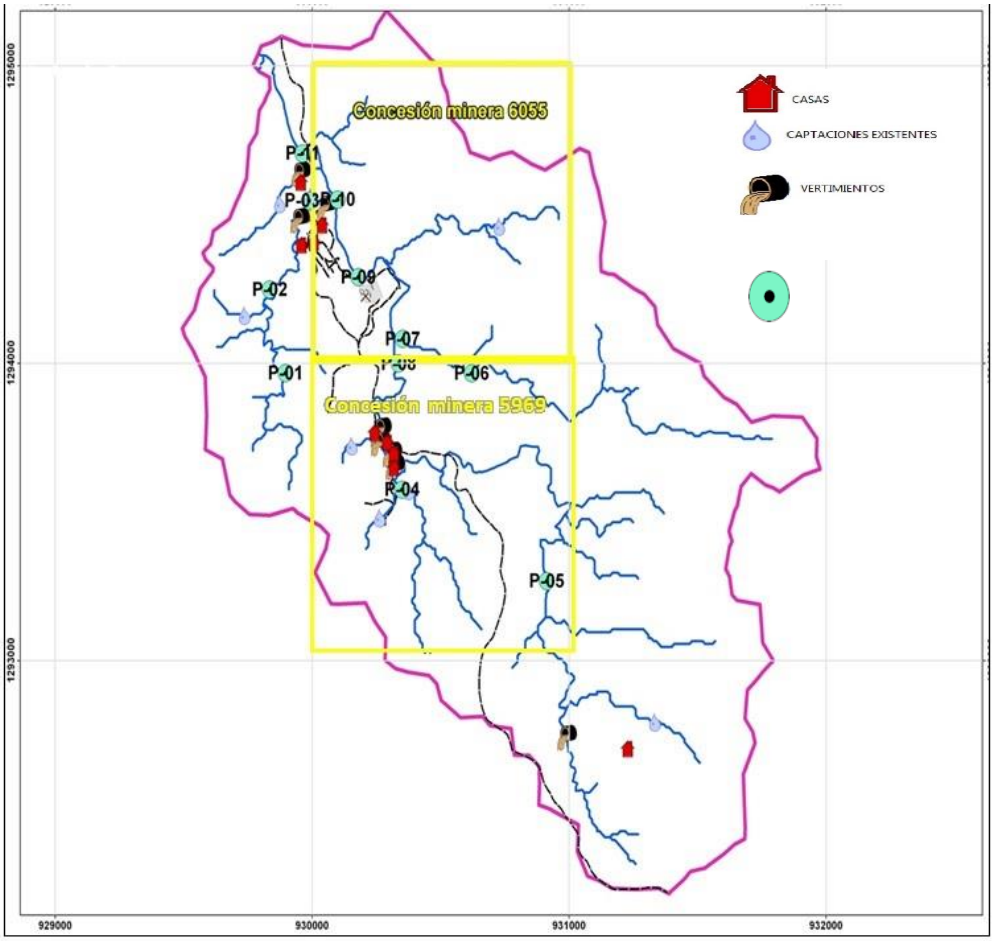

Illustration 4.1-131. Location of water quality monitoring stations.
Source: INGEX, 2015.

The above, with the dual purpose of measuring the quality downstream and upstream, with respect to the discharges of existing users in the area and also the sites of the planned mining infrastructure that may be discharged. Obtaining a baseline of the quality of the representative water resource before starting the operation of this project.

In Table 4.1-85, the variables monitored at these points are presented, in accordance with the terms of reference and the maximum permissible limits for water use according to Decree 1594 of 1984.

Table 4.1-85. Maximum permissible limits of variables evaluated.

PARAMETER	HUMAN CONSUMPTION AND / OR DOMESTIC USE		AGRICULTURAL USE	LIVESTOCK USE	USE RECREATIONAL PURPOSES, PRIMARY CONTACT	USE RECREATIONAL PURPOSES, SECONDARY CONTACT	USE AESTHETIC PURPOSES	USE PRESERVATION OF FLORA AND FAUNA
	Article 38 Conventional pretreatment	**Article 39 Previous disinfection**	**Article 40**	**Article 41**	**Article 42**	**Article 43**	**Article 44**	**Article 45**
Organoleptic	--	--	--	--	No floating	No floating	No floating	--
Ambient Temperature (ºC)	--	--	--	--	--	--	--	--
Water temperature (ºC)	--	--	--	--	--	--	--	--
Dissolved oxygen (mg O2 / L)	--	--	--	--	--	--	--	>4,0
% Oxygen saturation	--	--	--	--	70	70	--	--
pH (pH units)	5,0-9,0	6,5-8,5	4,5-9,0	--	5,0-9,0	5,0-9,0	--	4,5-9,0
Total COD (mg O2 / L)	--	--	--	--	--	--	--	--
Total BOD5 (mg O2 / L)	--	--	--	--	--	--	--	--
Suspended solids (mg / L)	--	--	--	--	--	--	--	--
Dissolved solids (mg / L)	--	--	--	--	--	--	--	--
Solids sedimentables (mg / L)	--	--	--	--	--	--	--	--
Total Solids (mg / L)	--	--	--	--	--	--	--	--
Electrical conductivity (µs / cm)	--	--	--	--	--	--	--	--
Turbidity (NTU)	--	10	--	--	--	--	--	--
Total organic carbon (mgC / L)	--	--	--	--	--	--	--	--
Bicarbonates (mgCaCO3 / L)	--	--	--	--	--	--	--	--
Chlorides (mgCl- / L)	250	250	--	--	--	--	--	--
Sulfates (mgSO4 2- / L)	400	400	--	--	--	--	--	--
Organic phosphorus (mgP / L)	--	--	--	--	--	--	--	--
Inorganic phosphorus (mgP / L)	--	--	--	--	--	--	--	--
Phosphates (Orthophosphates) (mg (PO4) 3-))	--	--	--	--	--	--	--	--
Total phosphorus (mgP / L)	--	--	--	--	--	--	--	--
Nitrites (mgNO2-N / L)	10	10	--	10	--	--	--	--
Nitrates (mgNO3-N / L)	10	10	--	--	--	--	--	--
Ammoniacal nitrogen (mgNH3-N / L)	1	1	--	--	--	--	--	--
Total Iron (mg FeE / L)	--	--	5	--	--	--	--	--
Total Calcium (mgCa / L)	--	--	--	--	--	--	--	--
Total Magnesium ((mgMg / L))	--	--	--	--	--	--	--	--
Sodium (mgNa / L)	--	--	--	--	--	--	--	--
Total Chromium (mg Cr / L)	--	--	--	--	--	--	--	--

PARAMETER	HUMAN CONSUMPTION AND / OR DOMESTIC USE		AGRICULTURAL USE	LIVESTOCK USE	USE RECREATIONAL PURPOSES, PRIMARY CONTACT	USE RECREATIONAL PURPOSES, SECONDARY CONTACT	USE AESTHETIC PURPOSES	USE PRESERVATION OF FLORA AND FAUNA
	Article 38 Conventional pretreatment	**Article 39 Previous disinfection**	**Article 40**	**Article 41**	**Article 42**	**Article 43**	**Article 44**	**Article 45**
Total Cadmium (mg Cd / L)	0,01	0,01	0,01	0,05	--	--	--	--
Total Copper (mg Cu / L)	1	1	0,02	0,5	--	--	--	--
Total Mercury (mg Hg / L)	0,002	0,002	--	0,01	--	--	--	--
Total Nickel (mg Ni / L)	--	--	0,2	--	--	--	--	--
Total Silver (mg Ag / L)	0,05	0,05	--	--	--	--	--	--
Total Lead (mgPb / L)	0,05	0,05	5	0,1	--	--	--	--
Total Zinc (mgZn / L)	15	15	2	25	--	--	--	--
Total Arsenic (mg As / L)	0,05	0,05	0,1	0,2	--	--	--	--
Total barium (mg Ba / L)	1	1	--	--	--	--	--	--
Hexavalent chromium (Cr6 +)	0,05	0,05	0,1	1	--	--	--	--
Potassium (mgK / L)	--	--	--	--	--	--	--	--
SAAM (mg / L)	0,5	0,5	--	--	0,5	0,5	--	--
Antimony	--	--	--	--	--	--	--	--
Fats and oils (mg / L)	Sin película visible	Sin película visible	--	--	Without visible film	Without visible film	Without visible film	--
Total phenols (mg / L)	0,002	0,002	--	--	0,002	--	--	--
Total hydrocarbons (mg / L)	--	--	--	--	--	--	--	--
Total Alkalinity (mgCaCO3 / L)	--	--	--	--	--	--	--	--
Acidity (mgCaCO3 / L)	--	--	--	--	--	--	--	--
Fecal coliforms (NMP / 100mL)	2000	--	1000	--	200	--	--	--
Total coliforms (NMP / 100mL)	20000	1000	5000	--	1000	5000	--	--
Total Cyanides (mg CN- / L)	0,2	0,2	--	--	--	--	--	--
Free and dissociable cyanide (mg CN- / L)	--	--	--	--	--	--	--	--
Total Hardness (mgCaCO3 / L)	--	--	--	--	--	--	--	--

Source: INGEX, 2015.

Next, in Table 4.1-86 and in Annex 4.2, the laboratory results of the variables evaluated in the different monitoring stations are presented.

Table 4.1-86. Results of monitored physicochemical parameters.

PARAMETERS	UNITS	SAMPLING STATIONS										
		P-01	P-02	P-03	P-04	P-05	P-06	P-07	P-08	P-09	P-10	P-11
Suspended solids Total	mg/L	< 7	< 7	9	< 7	< 7	< 7	< 7	11	9	< 7	< 7
Dissolved solids Total	mg/L	60	76	63	75	79	76	73	79	68	67	77
Sedimentable solids	mL/L-h	<0,10	<0,10	<0,10	<0,10	<0,10	<0,10	<0,10	<0,10	<0,10	<0,10	<0,10
Total Solids	mg/L	72	86	80	85	89	91	86	97	89	91	91
Electrical conductivity	µs/cm	117	115	114	102	124	117	118	127	121	120	122
pH	Und de pH	6,62	6,79	6,8	6,48	6,75	6,8	6,8	7,8	6,91	7,14	6,56
Ambient temperature	ºC	30	26	25	25	34	28	34	31	29	31	30
Water temperature	ºC	28	26	25	24	27	26	28	29	29	26	28
Turbidity	NTU	1	1,97	5,89	1,6	0,918	0,941	1,56	4,49	1,72	1,46	1,36
Dissolved oxygen	mgO_2/L	6,4	5,3	6,2	5,8	5,6-6,1	7	7,1	6,8	6,7	6,7	6,4
Saturation	%Sat	88,0	72,8	82,4	75,8	78,3	94,7	94,4	93,5	93,7	93,7	85,1
DBO	mgO2/L	< 2,00	< 2,00	< 2,00	< 2,00	< 2,00	< 2,00	< 2,00	< 2,00	< 2,00	< 2,00	< 2,00
DQO	mgO2/L	< 12,0	< 12,0	< 12,0	< 12,0	< 12,0	< 12,0	< 12,0	< 12,0	< 12,0	< 12,0	< 12,0
Total organic carbon	mgC/L	0,757	1,102	1,111	1,073	0,786	0,821	0,824	1,18	1,086	8,608	1,231
Total alkalinity	mgCaCO3/L	59,6	59	58,4	51,8	59,6	57,8	56,8	64	58,8	58,9	59,8
Acidity	mgCaCO3/L	16,8	12,1	13,5	10,9	13,9	9,3	12,3	10,5	9,1	10,3	10,3
Total hardness	mgCaCO3/L	56,20	52,90	58,00	44,70	61,40	64,20	55,30	64,50	59,80	56,40	55,20
Bicarbonates	mgCaCO3/L	61	59	59	52	60	58	56	61	58	58	59
Chlorides	mgCl-/L	< 1,50	< 1,50	< 1,50	< 1,50	< 1,50	< 1,50	< 1,50	< 1,50	< 1,50	< 1,50	< 1,50
Nitrites	mgNO2-N/L	< 0,003	< 0,003	< 0,003	< 0,003	< 0,003	< 0,003	< 0,003	< 0,003	< 0,003	< 0,003	< 0,003
Nitrates	mgNO3-N/L	< 1,50	< 1,50	< 1,50	< 1,50	< 1,50	< 1,50	< 1,50	< 1,50	< 1,50	< 1,50	< 1,50
Ammoniacal nitrogen	mgNH3-N/L	< 1,00	< 1,00	< 1,00	< 1,00	< 1,00	< 1,00	< 1,00	< 1,00	< 1,00	< 1,00	< 1,00
Organic phosphorus	mgP/L	< 0,025	< 0,025	< 0,025	< 0,025	< 0,025	< 0,025	< 0,025	< 0,025	< 0,025	< 0,025	< 0,025
Inorganic phosphorus	mgP/L	0.038	< 0,025	< 0,025	< 0,025	0,038	0,052	0,061	< 0,025	< 0,025	< 0,025	0,028
Total Phosphorus	mgP/L	0.039	< 0,025	< 0,025	< 0,025	0,038	0,053	0,062	< 0,025	< 0,025	< 0,025	0,029
Phosphates (orthophosphates)	mg(PO4)3-	< 0,153	< 0,153	< 0,153	< 0,153	< 0,153	< 0,153	< 0,153	< 0,153	< 0,153	< 0,153	< 0,153
Total Iron	mgFe/L	< 0,050	0,069	0,264	0,11	0,052	0,085	0,105	0,216	0,067	0,053	< 0,050
Total Calcium	mgCa/L	10,9	10,5	11,1	8,99	13	11,2	11,5	13,2	12,7	13,4	12,2
Total Magnesium	mg Mg/L	5,62	5,31	5,18	4,32	5,9	5,65	5,32	5,9	5,62	5,21	5,51
Total Sodium	mg Na/L	6,63	7,93	7,89	7,92	6,95	6,29	7,28	6,81	7,5	6,74	7,54
Potassium	mg K/L	0,512	0,444	0,614	0,125	0,132	0,505	0,599	0,98	0,433	0,503	0,506
Total chromium	mgCr/L	<0,010	<0,010	<0,010	<0,010	<0,010	<0,010	< 0,010	< 0,010	< 0,010	< 0,010	< 0,010
Total Cadmium	mgCd/L	< 0,003	< 0,003	< 0,003	< 0,003	< 0,003	< 0,003	< 0,003	< 0,003	< 0,003	< 0,003	< 0,003
Total copper	mgCu/L	< 0,050	< 0,050	< 0,050	< 0,050	< 0,050	< 0,050	< 0,050	< 0,050	< 0,050	< 0,050	< 0,050
Total mercury	mgHg/L	<0,001	<0,001	<0,001	< 0,001	< 0,001	<0,001	< 0,001	< 0,001	< 0,001	< 0,001	< 0,001
Total Nickel	mgNi/L	< 0,020	< 0,020	< 0,020	< 0,020	< 0,020	< 0,020	< 0,020	< 0,020	< 0,020	< 0,020	< 0,020
Total silver	mgAg/L	< 0,100	< 0,100	< 0,100	< 0,100	< 0,100	< 0,100	< 0,100	< 0,100	< 0,100	< 0,100	< 0,100
Total lead	mgPb/L	< 0,010	< 0,010	< 0,010	< 0,010	< 0,010	< 0,010	< 0,010	< 0,010	< 0,010	< 0,010	< 0,010
Zinc	mgZn/L	<0,050	<0,050	< 0,050	< 0,050	< 0,050	<0,050	< 0,050	< 0,050	< 0,050	< 0,050	< 0,050
Antimony	mg Sb/L	<0,521	<0,521	<0,521	<0,521	<0,521	<0,521	<0,521	<0,521	<0,521	<0,521	<0,521
Total Arsenic	mg As/L	< 0,010	<0,010	< 0,010	< 0,010	< 0,010	<0,010	< 0,010	< 0,010	< 0,010	< 0,010	< 0,010
Total barium	mg Ba /L	< 0,090	< 0,090	< 0,090	< 0,090	< 0,090	< 0,090	< 0,090	< 0,090	< 0,090	< 0,090	< 0,090
Hexavalent chromium	mg Cr6+/L	< 0,020	<0,020	< 0,020	< 0,020	< 0,020	<0,020	< 0,020	< 0,020	< 0,020	< 0,020	< 0,020
SAAM	mgSAAM/L	< 0,100	<0,100	< 0,100	< 0,100	< 0,100	<0,100	< 0,100	< 0,100	< 0,100	< 0,100	< 0,100
Fats and oils	mg Grasas/L	3,1	< 3,0	8	3,9	6,7	4,2	< 3,0	5	3,9	12,5	13,3
Phenols	mgFenoles/L	1,2	< 0,050	< 0,050	< 0,050	< 0,050	< 0,050	< 0,050	< 0,050	< 0,050	< 0,050	< 0,050
Total hydrocarbons	mg/L	< 0,040	<0,040	< 0,040	< 0,040	< 0,040	<0,040	< 0,040	< 0,040	< 0,040	< 0,040	< 0,040
Free and separable cyanide	mgCN-/L	< 0,050	< 0,050	< 0,050	< 0,050	< 0,050	< 0,050	< 0,050	< 0,050	< 0,050	< 0,050	< 0,050
Total cyanide	mgCN-/L	< 0,050	< 0,050	< 0,050	< 0,050	< 0,050	< 0,050	< 0,050	0,195	0,577	< 0,050	< 0,050

PARAMETERS	UNITS	SAMPLING STATIONS										
		P-01	P-02	P-03	P-04	P-05	P-06	P-07	P-08	P-09	P-10	P-11
Total coliforms	NMP/100mL	12997	17329	24196	17329	12033	14136	8230	24196	11199	8664	15531
Faecal coliforms	NMP/100mL	201	122	17329	110	198	644	108	5475	305	1354	4884
Sulphates	mgSO4 2/L	< 10,0	< 10,0	< 10,0	< 10,0	< 10,0	< 10,0	< 10,0	< 10,0	< 10,0	< 10,0	< 10,0

Source: UPB – UDEA – SGS - CORANTIOQUIA, 2015.

Below is the interpretation of results and indices of quality and contamination.

4.1.4.9.2 Interpretation of results

According to the information obtained in the field from the organoleptic variables (odor, turbidity and color) in the different seasons, it was determined that the eleven (11) sampling points do not represent any type of alteration to the odorless, colorless and crystalline characteristics. Considering normal conditions in this body of water. In general, the results, according to Roldán & Ramírez (2008) are characteristic of surface waters in the Colombian Andean region with some exceptions, as detailed below.

4.1.4.9.3 Total Suspended Solids (TSS)

TSS is distinguished as the material that is in the solid phase in water in the form of colloids or fine particles, which produce turbidity. The higher the content of OSH, the higher the degree of turbidity (Rocha, 2000). According to the recorded values of OSH (see Table 4.1-86 and Illustration 4.1-132) in the basin, the water can be categorized as good quality for all sampling stations. Stations P-01, P-02, P-04, P-05, P-06, P-07, P-10 and P-11, are below the detection method (gravimetric method) with a value < 7 mg/L (Ramírez & Viña, 1998). Stations P-03, P-08 and P-09 were able to detect and present values between 9 and 11 mg/L, also indicating a low presence of TSS composed of organic and inorganic material. Where the organic material consists mainly of algae or microorganisms and the inorganic material of clays, silicates and feldspars.

The maximum permissible limit value of this parameter is not established in the Colombian regulations in force for surface waters or for other Latin American regulations with similar climatic conditions.

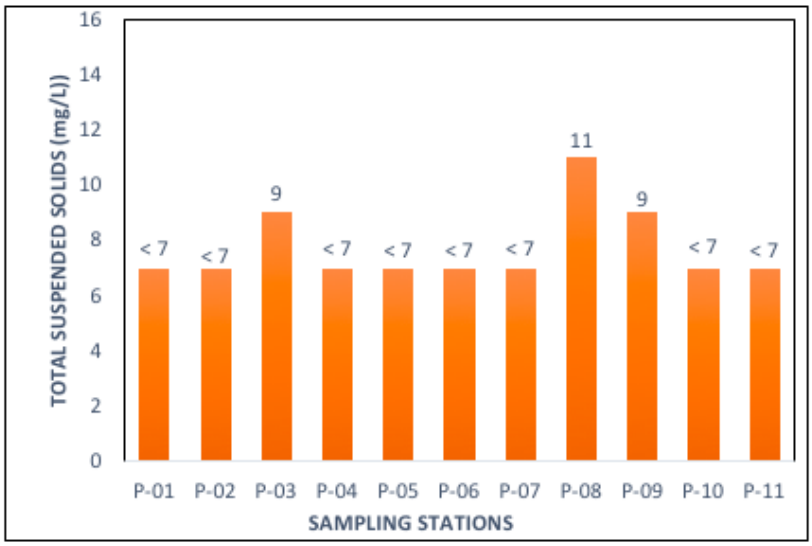

Illustration 4.1-132. Total suspended solids values.
Source: INGEX, 2015.

4.1.4.9.4 Total Dissolved Solids (TDS)

TDS is the combined content of all inorganic and organic substances contained in a liquid in molecular, ionized or micro-granular suspension form (sun colloid). These cannot be separated from the liquid by any physical means (sedimentation, filtration, etc.). Dissolved solids are not detectable to the naked eye, i.e. you may have completely crystalline water with a high content of dissolved solids (Rocha, 2000).

The TDS (see Illustration 4.1-133) recorded values between 60 and 79mg/L, indicating the presence of organic matter and dissolved inorganic salts (mainly calcium, magnesium, potassium, sodium, bicarbonates, chlorides and sulphates).

The average SDT established for rivers at the international level has been estimated at about 120mg/L (Livingston, 1963).

For Colombian regulations, this parameter is not regulated. But with Mexico's nom-127-ssa1-1994 regulations, these values are below the maximum limit of 1000 mg/L.

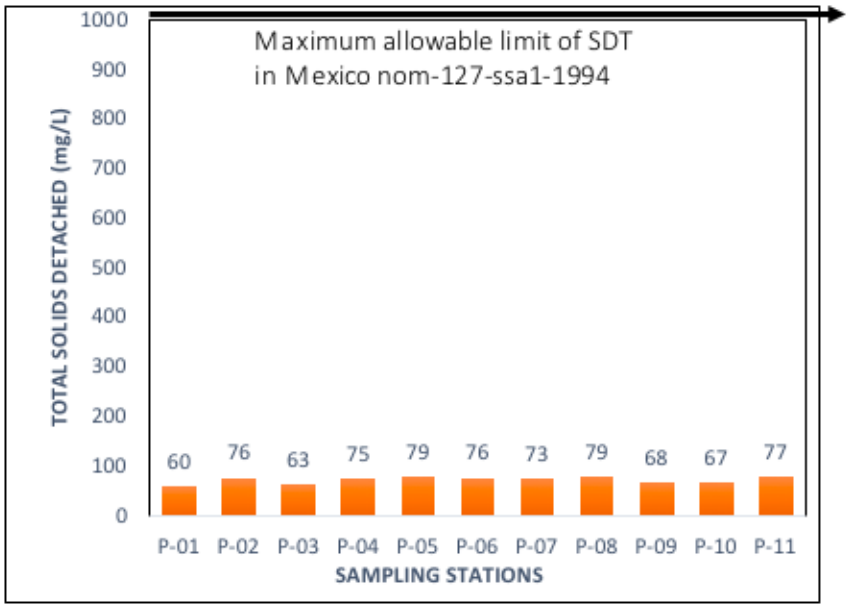

Illustration 4.1-133. Total dissolved solids values.
Source: INGEX, 2015.

4.1.4.9.5 Sediment solids (SSED)

The SSEDs recorded at the different sampling stations were below the method stop limit (SM-2540F) with values less than 0.1 ml/L-h. For this reason, no transport of this type of particles in the drains is inferred.
The maximum permissible limit value of this parameter is not established in the Colombian regulations in force for surface waters or for other Latin American regulations with similar climatic conditions.

4.1.4.9.6 Total Solids (TS)

The average value of the STs at the eleven (11) study stations was 87 mg/L, ranging from 72 to 97 mg/L (See Illustration 4.1-134). The concentrations of ST recorded are considered normal for these surface water bodies. This parameter has a higher incidence of TDS in the balance of solids than TSS and SSED.

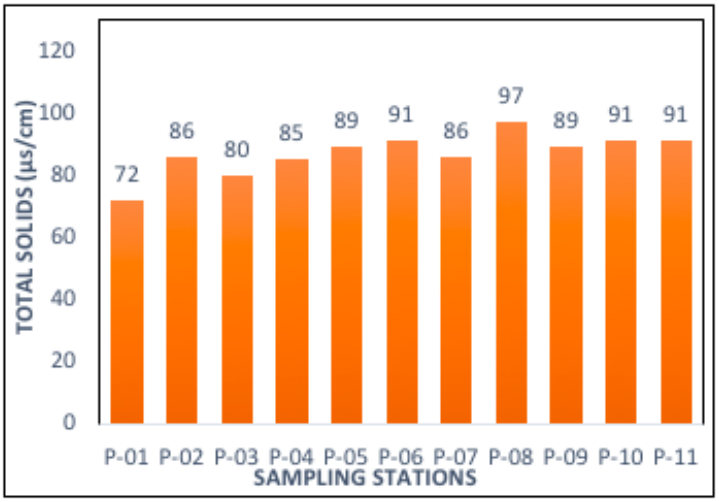

Illustration 4.1-134. Total solids values.
Source: INGEX, 2015.

The maximum permissible limit value of this parameter is not established in the Colombian regulations in force for surface waters or for other Latin American regulations with similar climatic conditions.

4.1.4.10 ELECTRICAL CONDUCTIVITY

The electrical conductivity records showed similar behavior as shown in Illustration 4.1-135. Where the average measured conductivity in surface waters was 118µS/cm, with a range of variation from 102 to 127µS/cm, a trend similar to the reported dissolved solids.

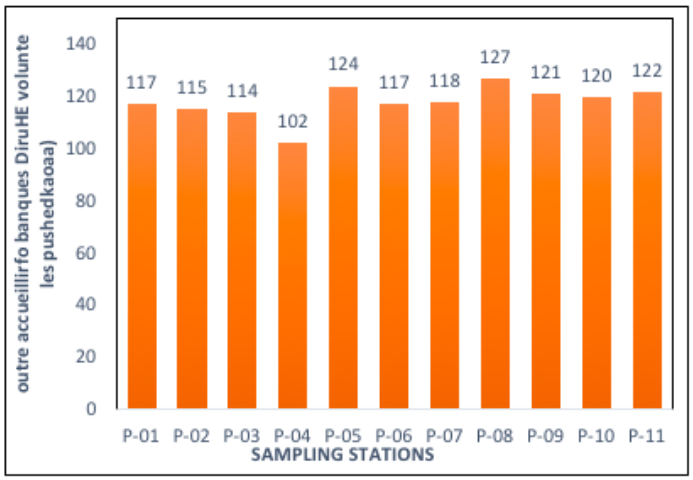

Illustration 4.1-135. Electrical conductivity values.
Source: INGEX, 2015.

This is because electrical conductivity is a measure of the ability of water to conduct an electrical current; that is, variations in dissolved solids (soluble salts) increase the conductivity of water. For this reason, the presence of dissolved ions in the water was moderated according to the average result of the conductivity (118 µS/cm), which was corresponding to the dissolved solids (87 mg/L). The permissible limit value of this parameter is not established in the Colombian regulations in force for surface waters or for other Latin American regulations with similar climatic conditions.

4.1.4.10.1 Hydrogen potential (pH)

pH is a characteristic of water that is involved in most of the biochemical and biological processes that take place in this system. pH can be defined as a measure that expresses the degree of acidity or basicity of a solution on a scale ranging from 0 to 14. It is an important variable to measure in aquatic ecosystems because the magnitude of this variable indicates the acid or alkaline characteristics of a body of water, given that high fluctuations can influence the different reactions that occur there, altering natural cycles of each ecosystem. It is worth mentioning that the pH varies according to temperature, salinity, pressure and depth (Cifuentes et al., 2009).

In Illustration 4.1-136, the pH is recorded showing acceptable values at all monitoring stations, for all uses of Decree 1594 of 1984, with the exception of point P-04, which for 2 decimal places, does not comply only with potable use with prior disinfection.

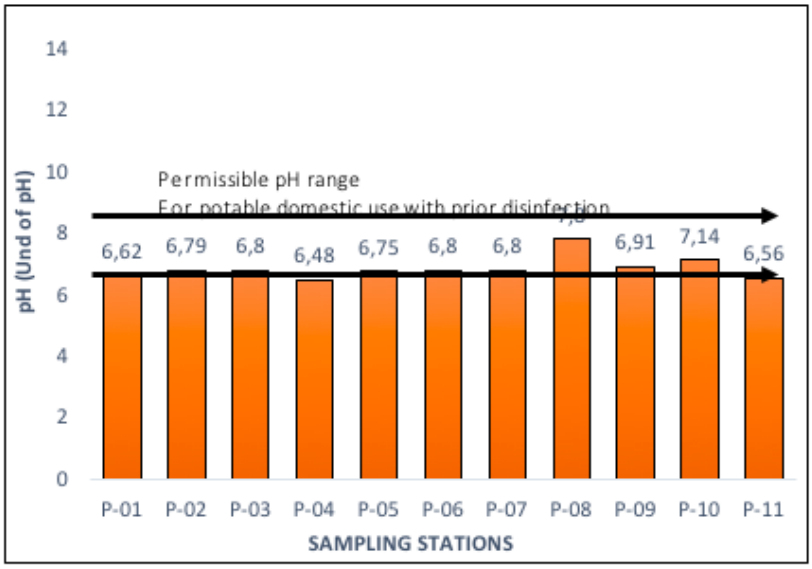

Illustration 4.1-136. pH values.
Source: INGEX, 2015.

Likewise, a low variation of the pH in the basin was observed, inferring that there is no affectation of aquatic life; therefore, a high stability of this aquatic system (Machado & Roldán 1981). This can be

seen in the high presence of organisms from the benthic, fish and planktonic communities collected and observed in this body of water.

4.1.4.10.2 Ambient temperature

The highest values were presented at stations P-06 and P-08 with 34ºC (see Illustration 4.1-137). On the other hand, stations P-04 and P-05 showed the lowest temperature at 25ºC. The basin is in the range of 25 to 34ºC. These values are adjusted to the study area, where there is a predominance of a warm climate of the Andean zone.

4.1.4.10.3 Water temperature

Temperature is a physical variable of great importance for hydrological ecosystems. This is due to the fact that if the temperature increases, there is a decrease in the concentration of dissolved oxygen, which can cause the death of aquatic species, especially ichthyofaunal. Also, thermal pollution can cause disturbances in aquatic ecosystems, because in some cases the temperature range restricts the productivity and reproduction of aquatic communities (Rocha, 2000).

Similar values were observed for the stations, between 24 and 29ºC, indicating that there is no effect on the environment by this variable. However, the water temperature was more sensitive during sampling, showing higher values at stations P-01, P-02, P-08, P-09 and P-10, this being a phenomenon related to the time of measurement (12 a.m. to 3:00 pm) (See Illustration 4.1-138).

Although the temperature does not present quality criteria in the current environmental regulations of Colombia and Latin America, the values recorded are adequate, because they allow the development of aquatic communities that develop in this type of ecosystems.

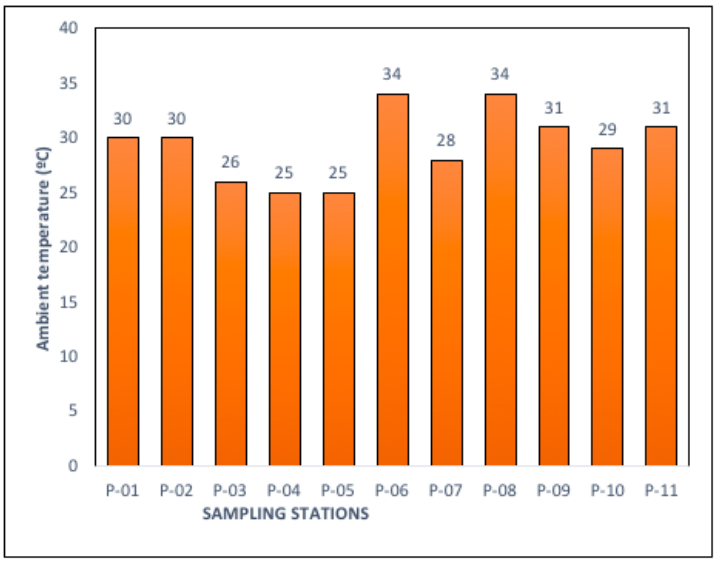

Illustration 4.1-137. Ambient temperature values.
Source: INGEX, 2015

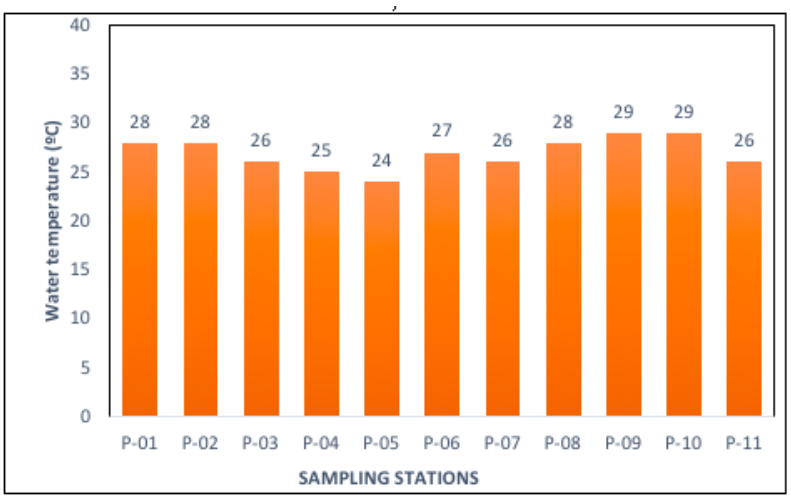

Illustration 4.1-138. Water temperature values.
Source: INGEX, 2015.

4.1.4.10.4 Turbidity

Turbidity is a characteristic related to the content of finely divided solids in water. It is also an extremely important parameter not only because it is a characteristic of purity in water, but also because it interferes with water treatment processes such as disinfection with chemical agents or ultraviolet radiation, generating a decrease in biocide effectiveness (Rocha, 2000).

The results are in the range of 5.89 to 0.941 NTU (Neophelometric Turbidity Units) (See Illustration 4.1-139).

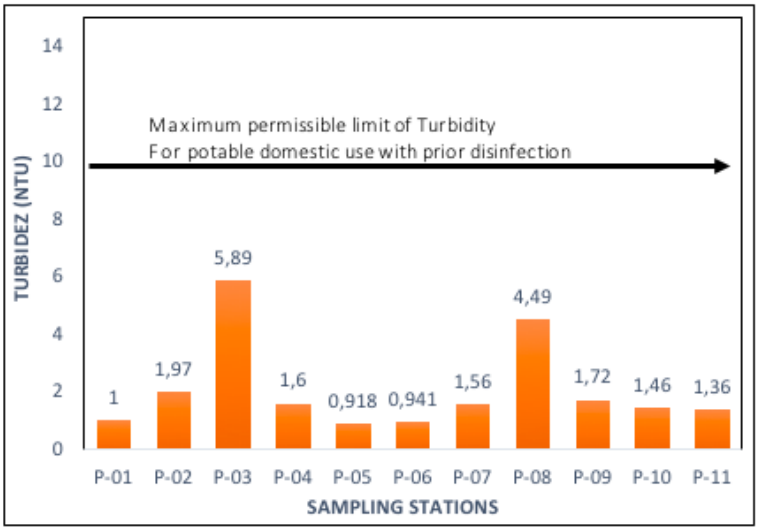

Illustration 4.1-139. Turbidity results.
Source: INGEX, 2015.

Stations P-03 and P-08 had the greatest contribution of turbidity, coming from the presence of suspended materials, clays, organic colloids, plankton and microscopic organisms caused mainly by anthropogenic activities (discharges of organic matter, artisanal mining and livestock) developed in this study area. While the rest of the sampling stations were below 2 NTU, optimal value for human consumption (Estupiñan & Avila, 2010).

These results are below the maximum value allowed in Colombia for potable human consumption with prior disinfection.

4.1.4.10.5 Dissolved Oxygen (DO)

The DO has been one of the most studied non-conservative constituents (its concentration is variable) in aquatic ecosystems (Packard, et al., 1969). This is an essential nutritional requirement for most living organisms because of their dependence on the aerobic breathing process for energy generation and mobilization of carbon in the cell. In addition, OD is important in the processes of photosynthesis, oxidation-reduction, solubility of minerals and decomposition of organic matter (Packard, et al., 1969).

The OD showed a homogeneous behavior among the different sampling stations (See Illustration 4.1-140) being the minimum of 5.3mg/L in the P-02 station and the maximum of 7.1mg/L in the P-07 station.

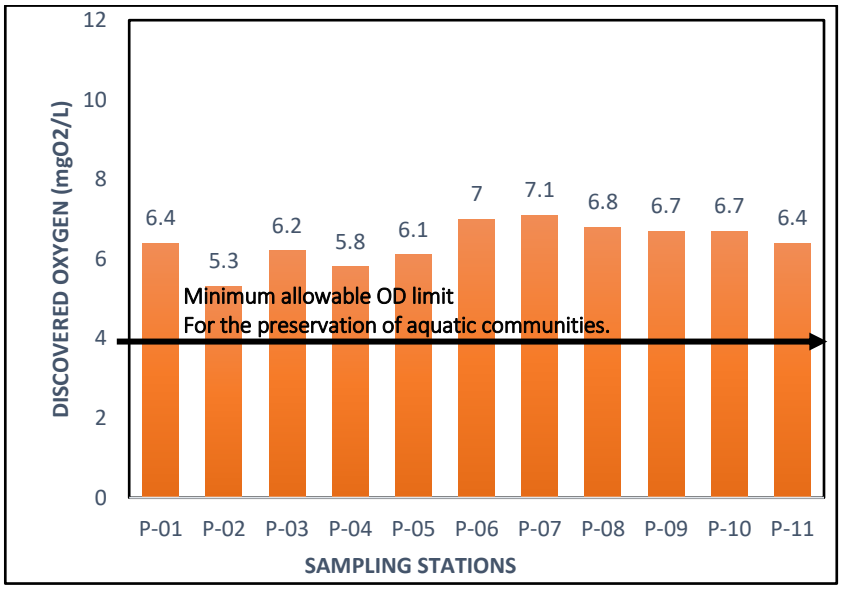

Illustration 4.1-140. Dissolved Oxygen Results
Source: INGEX, 2015.

According to Table 4.1-87, the seasons are acceptable, i.e. OD suitable for the life of the vast majority of species and other aquatic organisms.

Table 4.1-87. Dissolved oxygen concentration ranges and frequent ecosystem consequences.

[OD] mg/L	Condition	Consequences
0	Anoxia	Massive death of aerobic organisms
0-5	Hypoxia	Disappearance of susceptible organisms and species
5-8	Agreeable	[OD] suitable for the lives of the vast majority of fish species and other aquatic organisms.
8-12	Good	
>12	Supersaturated	Systems in full photosynthetic production

Stations P-01, P-02, P-03, P-04, P-05 and P-11 had values below the recommended limit of 6.5 to 8.5 mg/L (Roldan, 1992). However, dissolved oxygen levels were normal in the basin, above the minimum permissible limit for flora and fauna preservation purposes established by the regulations. Likewise, the DO presents in all cases superior values required for life to exist for benthic, icthyc, peripheral, planktonic and macrophytes communities, according to González et al. (2013).

The DO has been estimated as a good indicator of the level of saprobiity or organic matter content in natural waters. Therefore, the dissolved oxygen values obtained in the study area are related to good quality environments.

4.1.4.10.6 Percentage of dissolved oxygen saturation (% Sat)

The percentage of dissolved oxygen saturation recorded high values (see Illustration 4.1-141), ranging from 72.8% to 94.7% saturation, with homogeneity at all sampling stations. This situation can be attributed to the topographic formation of the basin and the rocky-sandy formation of this body of water.

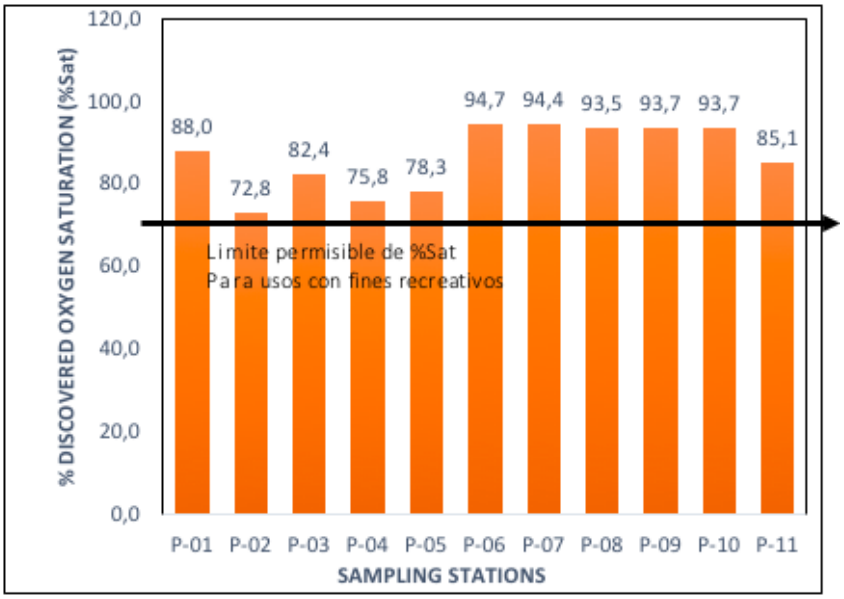

Illustration 4.1-141. Results of % dissolved oxygen saturation.
Source: INGEX, 2015.

However, if the saturation were less than 40%, the basin would be in poor environmental condition. Similarly, if saturation levels were above 110%, i.e. oversaturation and eutrophication. This variable is above the minimum permissible limit for recreational use.

Biochemical Oxygen Demand (BOD)

BOD is defined as the amount of oxygen required by bacteria to stabilize biodegradable organic matter under aerobic conditions. By biodegradable matter, it is understood as the organic matter that serves as food for microorganisms and provides energy as a result of its oxidation (Rocha, 2000). Natural waters, on the other hand, generally have very low BOD values.

The BOD is below the detection limit (2 mg O2/L) in the different sampling stations, indicating the normal presence of organic matter in the water body, due to the fact that levels higher than 8 mg O2/L indicate contamination processes due to the presence of organic matter (Roldan, 1992). The maximum permissible limit value of this parameter is not established in the Colombian regulations in force for surface waters or for other Latin American regulations with similar climatic conditions.

Chemical oxygen demand (COD)

COD is the amount of oxygen in mg/L consumed in the oxidation of reducing substances in water. This means the amount of oxygen needed to degrade low-biodegradable material.
The COD showed values below 12.0 mg O2/L at all sampling stations, similar to the BOD results. Therefore, the surface waters of the basin present good quality conditions with a low content of biodegradable and non-biodegradable organic matter.

The maximum permissible limit value of this parameter is not established in the Colombian regulations in force for surface waters or for other Latin American regulations with similar climatic conditions.

Total Organic Carbon (TOC)

Illustration 4.1-142 shows how the TOC presented a maximum value of 8.608 mg C/L at the P-10 station and a minimum of 0.757 mg C/L at the P-01 station.

These TOC values are contributed to different substances, from natural compounds to synthetic compounds present in human activities such as detergents, pesticides, fertilizers, etc. However, lower TOCs < 10 mg C/L are considered normal for natural waters such as the 11 sampling stations.

The maximum permissible limit value of this parameter is not established in the Colombian regulations in force for surface waters or for other Latin American regulations with similar climatic conditions.

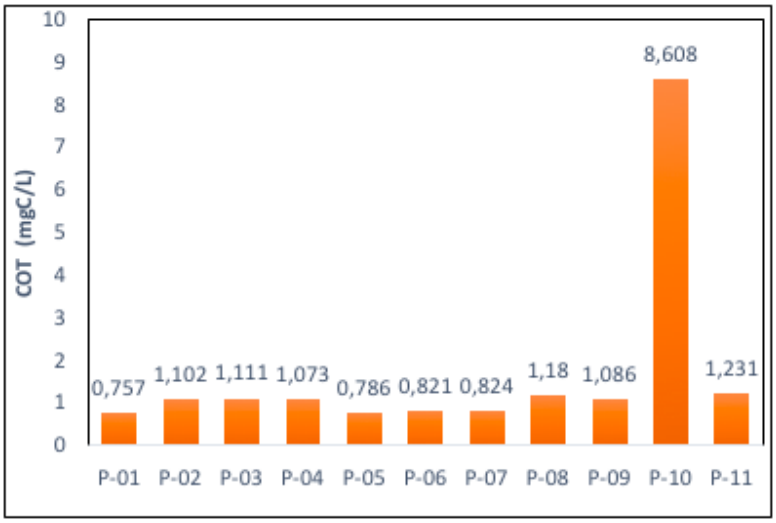

Illustration 4.1-142. Total organic carbon (TOC) results.
Source: INGEX, 2015.

Total Alkalinity

Total alkalinity is a parameter that determines the ability of water to neutralize acidic and basic effects, mainly salts of weak acids or strong bases. For natural waters the alkalinity is mainly due to bicarbonate ions (HCO3-), carbonates (CO3-2) and hydroxides (OH-) which come from minerals found in the form of carbonates and bicarbonates (Rocha, 2000). Another case of alkalinity occurs when there are strong base spills such as caustic soda, which are common in the paper industry.

The total alkalinity showed an interval of 51.8 to 64mg/L CaCO3 (Illustration 4.1-143), showing a high similarity between the eleven (11) sampling stations.

These values are higher than acceptable for aquatic life (20 mg/L CaCO3). Similarly, it is related to the content of dissolved solids obtained, inferring in an inorganic carbon source, therefore, in a buffer measure for sudden changes in pH (acidification).

Based on the above, and according to Roldán & Ramírez (2008), it can be considered that the total alkalinity reported for the eleven sampling stations in the basin is normal, due to the fact that they present values in accordance with the Colombian Andean zone. As for current Colombian and Latin American regulations, this parameter is not found in water quality legislation.

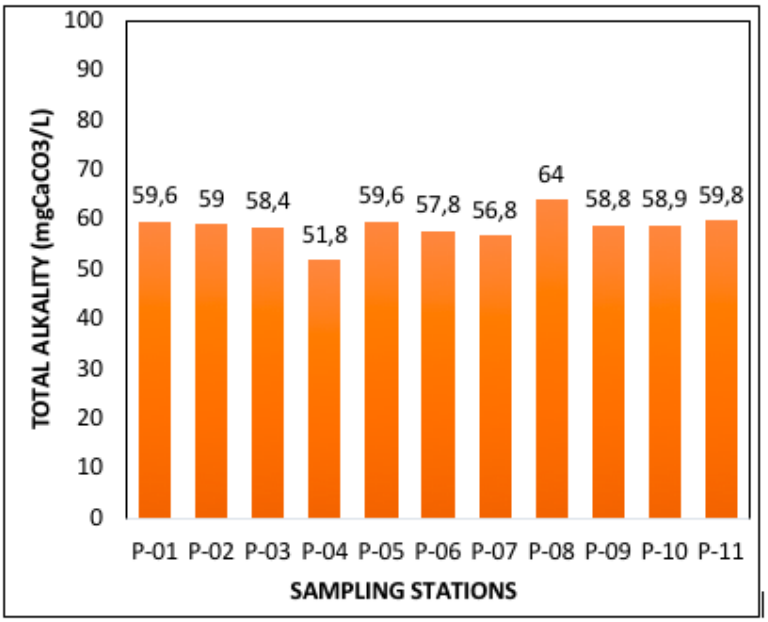

Illustration 4.1-143. Total alkalinity results.
Source: INGEX, 2015.

Acidity

The acidity of the water samples collected in the eleven (11) sampling stations presents concentrations between 9.1 and 16.8 mg CaCO3 (see Illustration 4.1-144).

These concentrations can be produced by CO2, by the presence of free H+ ions, by the presence of mineral acidity from strong acids such as sulfuric, nitric, and hydrochloric, among others.

According to the above and based on the pH levels found in the waters of the basin, the acidity of the system is considered to be the product of the presence of CO2 and mineral acidity. Due to the oxidation of organic matter and sulphides from rocks.

The maximum permissible limit value of this parameter is not established in the Colombian regulations in force for surface waters or for other Latin American regulations with similar climatic conditions.

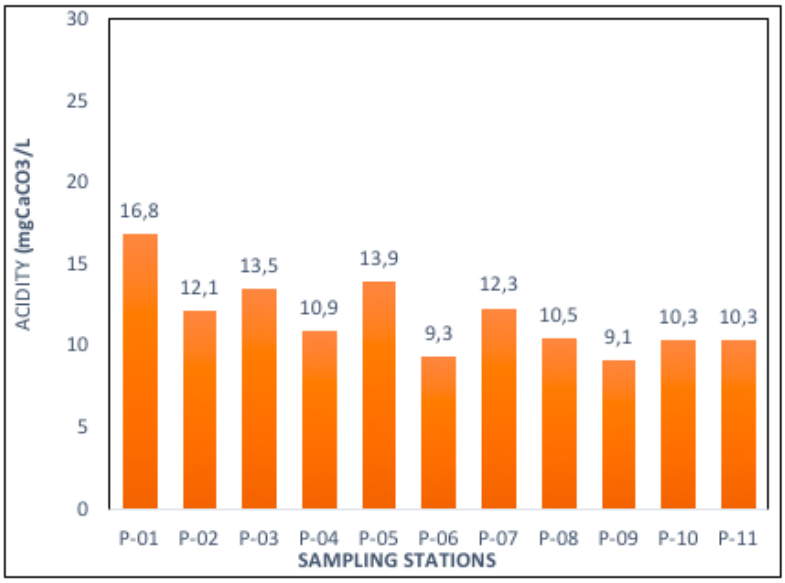

Illustration 4.1-144. Acidity results.
Source: INGEX, 2015.

Total hardness

The oscillation of total surface water hardness in the basin is shown in Illustration 4.1-145.

Station P-04 had the lowest hardness concentration (44.7 mg CaCO3/L) while station P-08 had the highest concentration (64.5 CaCO3/L). These concentrations are due to the presence of cations such as Magnesium, Calcium, Strontium, Barium, and other metals, which are present in the form of dissolved solids. Of these, calcium and magnesium are the most abundant since hardness is closely related to these two elements.

Total hardness levels in natural waters are classified as soft waters (< 75 mg/L total hardness as CaCO3) (Roldán & Ramírez, 2008).

As for the current regulations in Colombia, this parameter is not found in water quality legislation. However, for Peruvian regulations, a maximum permissible value of 500 mg CaCO3/L is established, so this parameter complies with this regulation.

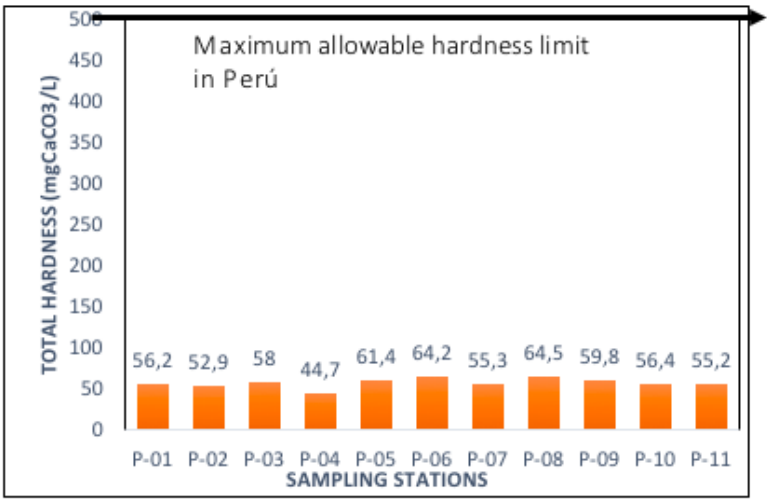

Illustration 4.1-145. Total hardness results.
Source: INGEX, 2015.

Bicarbonates

The bicarbonates were found between 52 and 61 mg CaCO3/L (Illustration 4.1-146), according to the hardness, alkalinity and pH results reported at the different sampling stations. Bicarbonates represent the largest contribution to alkalinity in natural waters, through wear and tear and dissolution of rocks in the basin containing carbonates such as limestone. The maximum permissible limit value of this parameter is not established in the Colombian regulations in force for surface waters or for other Latin American regulations with similar climatic conditions.

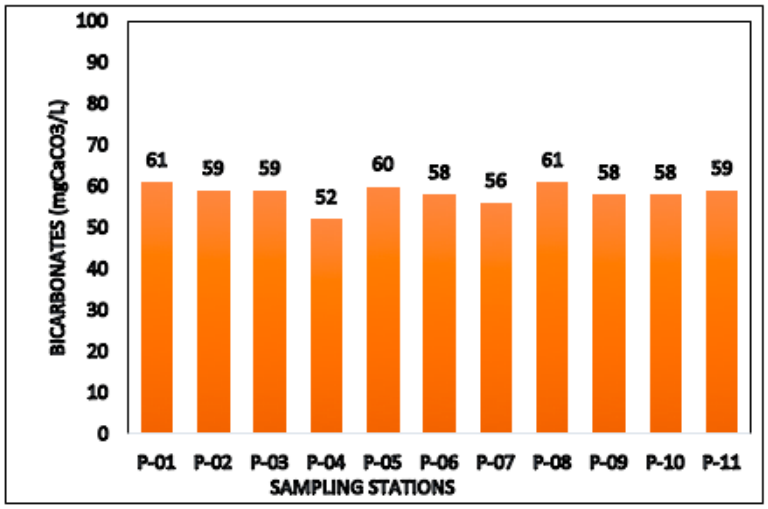

Illustration 4.1-146. Bicarbonate results.
Source: INGEX, 2015.

Chlorides

The chlorides evaluated showed similar behavior between the different sampling stations, below the stop limit (<1.5 mg Cl-/L). These values are considered normal according to Roldan & Ramírez (2008) who testify that these types of water bodies have very low chloride contents of less than 5 mg Cl-/L. Also, Osorio et al. (2000) states that in natural waters, typical chloride concentrations are in the range of 1 to 100 mg Cl-/L.

In rivers, the concentration of chlorides increases along the course of the riverbed from its source. For this reason, it can be concluded that the low presence of chlorides in this basin is due to the proximity of the sampling points to the different births of this study area.

In relation to current environmental regulations in Colombia, a maximum value of 250 mg Cl-/L is established for use for human consumption and/or domestic use. Therefore, these points meet the maximum allowable concentrations.

Nitrites

The nitrites recorded in the eleven sampling stations were below <0.003 mg NO2-/L. This is due to the fact that nitrites are very reactive and can act as oxidizing and reducing agents, therefore they are only found in appreciable quantities in low oxygenation conditions, due to frequent fecal contamination (intensive and extensive and rudimentary livestock) and extensive agricultural crops. For this reason, the presence of a low concentration indicates normal levels, which in surface waters do not usually exceed 0.100 mg NO2-/L.

As for the current environmental regulations, nitrites were found within the standard, therefore there is no suspicions that allow considering any type of affectation in the study area due to the effects of this nitrogenous compound.

Nitrates

Similarly, the concentration of nitrates is observed below the stop limits (<1.5 mg NO3-/L). According to Roldan (1992), the values are considered normal for these bodies of water because concentrations equal to or greater than 5 mg NO3-/L indicate contamination by domestic waste, animal waste or the presence of fertilizers.

With respect to the levels of nitrates recorded at the different sampling stations, full compliance with current environmental regulations in Colombia is established, where the maximum permissible value of nitrates permitted for human consumption and/or domestic use is 10 mg NO3-/L.

Ammoniacal nitrogen

Ammoniacal nitrogen is one of the momentary components in water, because it is part of the nitrogen cycle and is intervened by biological activity. In water it can appear in molecular form or as

ammonium ion, depending on pH. The presence of free ammonia or ammonium ion in surface waters is considered as a chemical proof of contamination.

The concentrations of ammoniacal nitrogen in the stations are below the stop limit (<1 mgNH3-N/L), these values are in accordance with current environmental regulations, which state that the maximum permissible value for use for human consumption and/or domestic use should not exceed 1 mgNH3-N/L. It should be noted that high concentrations of this ion can have serious ecological implications, causing losses to the aquatic community (Roldán, 1992; Ramírez et al., 1998, Roldán & Ramírez, 2008).

Organic Phosphorus

On the other hand, the organic phosphorus recorded in the basin showed concentrations below the stop limit (<0.025 mgP/L) in the different monitoring stations. These results according to Roldan & Ramírez (2008) are considered normal for natural waters, given that phosphorus is a limiting macronutrient and in high concentrations can be used negatively by dominant species, favoring the growth of algae and other organisms.

The maximum permissible limit value of this parameter is not established in the Colombian regulations in force for surface waters or for other Latin American regulations with similar climatic conditions.

Inorganic phosphorus

Illustration 4.1-147 shows the results obtained from inorganic phosphorus.

This parameter showed moderately higher concentrations of organic phosphorus in the stations P-01 (0.038mg P/L), P-05 (0.038mg P/L), P-06(0.052mg P/L), P-07 (0,061mg P/L) and P-11 (0.028mg P/L), this behavior of inorganic phosphorus differs from organic, since it constitutes 25% of total phosphorus compared to 75% of organic, This suggests a possible predominance of biosynthesis processes over the mineralization of phosphorous organic matter, and also possible precipitation losses over inorganic phosphorus sediments as a consequence of high photosynthetic activity (Díaz et al., 2007; Cortes & Ga

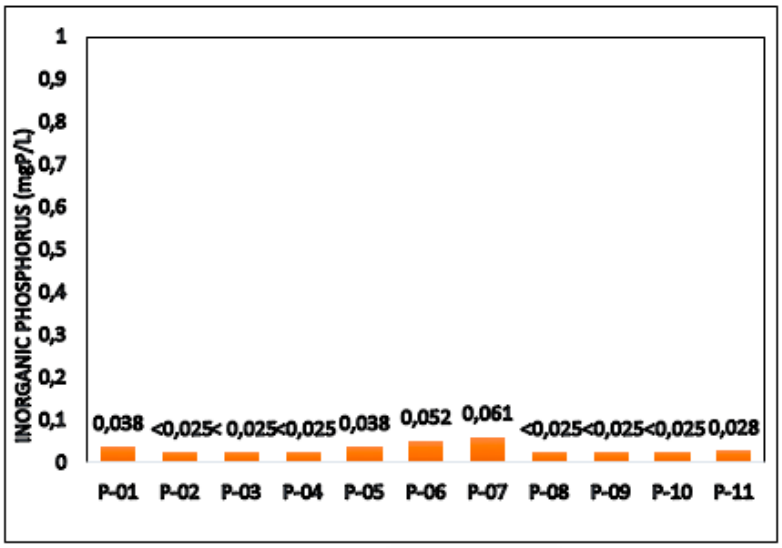

Illustration 4.1-147. Result of inorganic phosphorus.
Source: INGEX, 2015.

The maximum permissible limit value of this parameter is not established in the Colombian regulations in force for surface waters or for other Latin American regulations with similar climatic conditions.

Total phosphorus

Phosphorus is an essential element in the growth of plants and animals. Currently considered as one of the nutrients that control algae growth, this parameter is found in natural and waste water. Where it is considered a critical variable in water quality due to its influence on the eutrophication process (Arboleda, 2000).

The oscillation in the concentrations of total phosphorus (organic phosphorus + inorganic phosphorus) in the surface water of the basin is shown in Illustration 4.1-148.

Most of the sampling sites were characterized by values below the stop limit (<0.025mgP/L). However, stations P-01, P-05, P-05, P-06, P-07 and P-11 showed concentrations in the range of 0.029 to 0.062 mg P/L. These concentrations reflect a moderate nutrient content in the basin indicating a eutrophic system.

The maximum permissible limit value of this parameter is not established in the Colombian regulations in force for surface waters or for other Latin American regulations with similar climatic conditions.

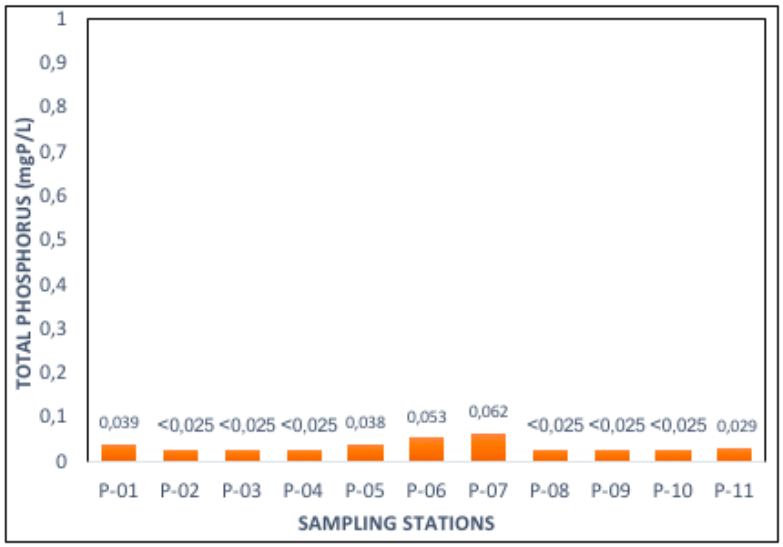

Illustration 4.1-148. Result of total match.
Source: INGEX, 2015.

Phosphates

The phosphates showed similar values in the eleven sampling stations, being below the stop limit (<0.153 mg (PO4)3-/L). These phosphates may be soluble as debris particles or in the bodies of aquatic organisms. It is common to find phosphates in water as they are nutrients of aquatic life and limit the growth of aquatic plants. However, the presence of phosphates in natural water bodies is mainly attributed to processes of decomposition of organic matter, runoff or soil washing, industrial and domestic discharges (Holmes, 1996); since in uncontaminated natural waters they are found in low concentrations allowing chemical and biological processes (Roldán, 2003).

The maximum permissible limit value of this parameter is not established in the Colombian regulations in force for surface waters or for other Latin American regulations with similar climatic conditions.

Total iron

The presence of iron in surface and ground water causes problems in water systems, modifying the organoleptic characteristics of water (smell, taste and color), as well as problems associated with microbiological corrosion caused by "iron bacteria" in water collection and conveyance systems for different uses.

The iron levels (see Illustration 4.1-149) found in the basin presented values between <0.05 to 0.264 mg Fe/L, where the highest values were found in P-03 and P-08, where anthropogenic activities are mainly carried out (organic matter discharge and artisanal mining). However, the total iron found at

all sampling stations has concentrations with natural surface water characteristics, which vary with concentrations typically between 0.01 to 0.03 mg Fe/L (Marin, 2003).

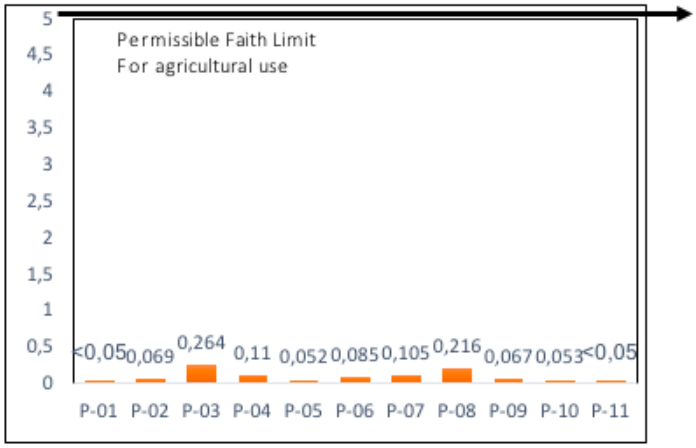

Illustration 4.1-149. Result of total iron.
Source: INGEX, 2015.

On the other hand, iron was found to be at normal levels according to current environmental regulations, where a maximum value of 5 mg Fe/L is established for the use of irrigation for agricultural purposes.

Total Calcium

Calcium is a chemical element and is found in water in a greater quantity than magnesium, these compounds are characterized by being metallic ions that intervene in the hardness of water. The total calcium concentration found in the basin was between 8.99 and 13.4 mg Ca/l (See Illustration 4.1-150).

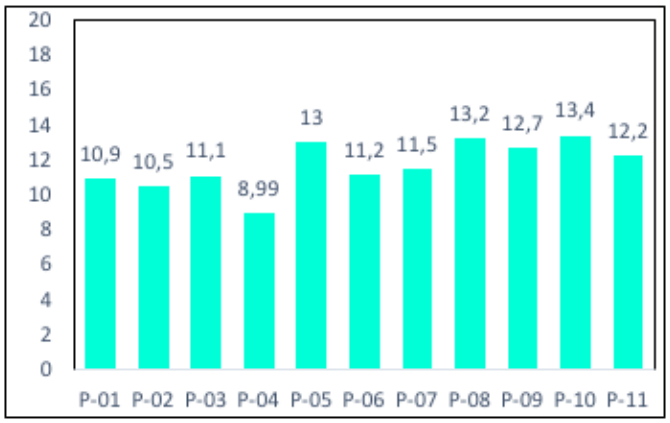

Illustration 4.1-150. Calcium result.
Source: INGEX, 2015.

These values showed normal levels for surface water, inferring that the system is not in any kind of alteration due to the presence of this ion. The maximum permissible limit value of this parameter is not established in the Colombian regulations in force for surface waters or for other Latin American regulations with similar climatic conditions.

Total Magnesium

Likewise, the magnesium reported in the monitored basin (see Illustration 4.1-151) was below the calcium ion discussed above. Presenting a minimum value at station P-03 (4.32 mg Mg/L) and a maximum value at stations P-05 and P-08 (5.9 mg Mg/L). These are normal values in relation to the hardness of the water detected in the basin and to the characteristics in surface water bodies.

The presence of this ion is important in aquatic ecosystems for primary productivity because magnesium is the nucleus of the chlorophyll molecule (Roldan & Ramírez, 2008).

The maximum permissible limit value of this parameter is not established in the Colombian regulations in force for surface waters or for other Latin American regulations with similar climatic conditions.

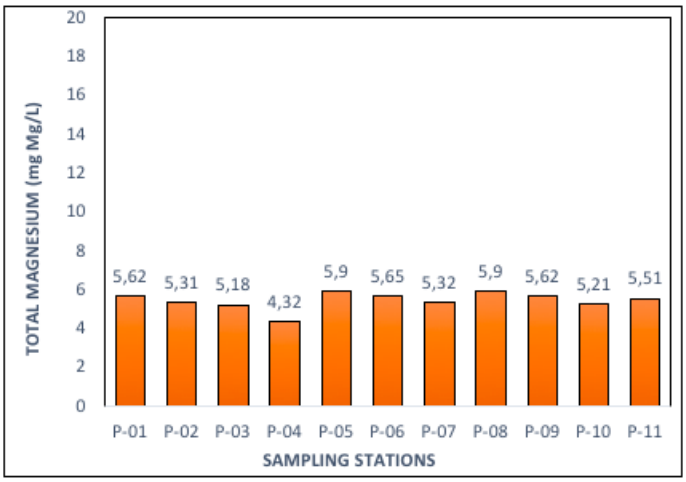

Illustration 4.1-151. Magnesium result.
Source: INGEX, 2015.

Total sodium

Sodium is found in nature in the form of silicates such as albite and nephelite. The most common form is found in halite. High concentrations of sodium salts create an osmotic barrier for most organisms (Roldán and Ramírez, 2008). In freshwater, the highest levels of sodium are found in lowland rivers and groundwater, while in the highlands, the content of this relatively low element.

With respect to the results recorded for sodium in Illustration 4.1-152, it is observed that there is no significant range of difference between sampling stations within the basin, being between 6.29 and 7.92 mg Na/L.

Likewise, these values can be related to normal environments since sodium is one of the major metals in natural waters and is found in concentrations of less than 1 to 300 mg Na/L (Pan American Health Organization. 1988). It should be noted that when the concentration of sodium or potassium is higher than that of calcium, magnesium or bicarbonates, the water is considered to have a low mineralization as occurs in the ratio of sodium to magnesium.

The maximum permissible limit value of this parameter is not established in current Colombian regulations for surface water. However, the laws of Peru and Mexico regulate that for human consumption the maximum permissible level is 200 mg Na/l. Therefore, this parameter is below the maximum levels allowed in the regulations of these countries.

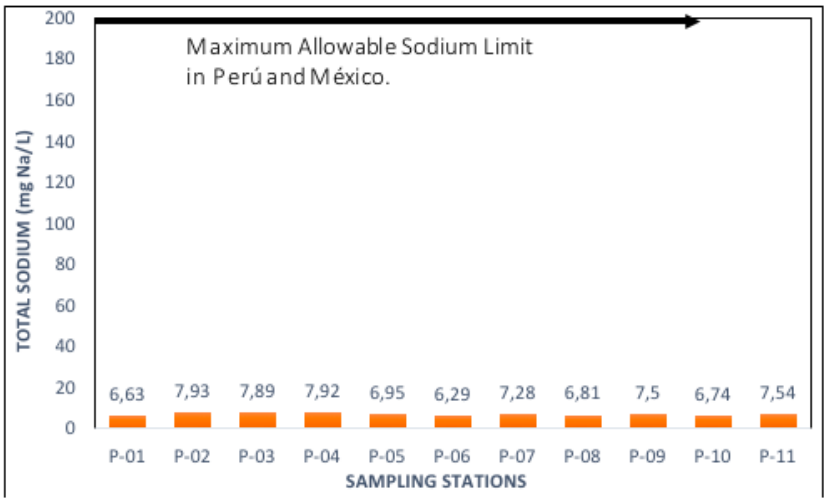

Illustration 4.1-152. Total sodium result.
Source: INGEX, 2015.

Potassium

In natural waters the concentration of potassium is always lower than sodium. It is found in nature in the form of leucite, wild and volcanic rocks. As can be seen in Illustration 4.1-153, potassium is in the range of 0.125 to 0.98 mg K/L for the different sampling stations. It should be noted that the maximum potassium concentration for this type of surface water is 10 mg K/L, although it can be increased by atmospheric deposits, runoff from agricultural land and the influence of grey water drainage. Given its importance for plant nutrition, its presence in water is beneficial.

According to the above, the basin presented low values for potassium, however these concentrations are indicative of water bodies with little intervention of human activities.

The maximum permissible limit value of this parameter is not established in the Colombian regulations in force for surface waters or for other Latin American regulations with similar climatic conditions.

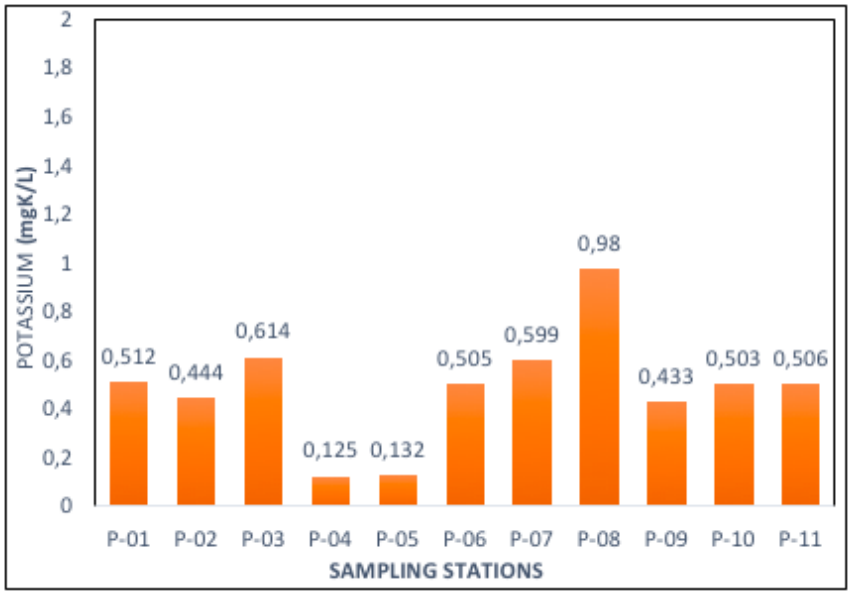

Illustration 4.1-153. Total Potassium Result.
Source: INGEX, 2015.

Metals

Considering the metals evaluated (total chromium, total cadmium, total copper, total mercury, total nickel, total silver, total lead, total zinc, antimony, total arsenic, total barium and hexavalent chromium), these showed concentrations below the stop limit.

According to the above, any alteration of the surface waters in the basin by these analyzed metals can be ruled out. It can also be concluded that these parameters comply with the current environmental regulations of Decree 1594 of 1984.

Methylene blue active substances (SAAM)

For SAAMs registered in the basin, values below the limit of detection (< 0.1 mg/L) were obtained at the different sampling stations. Indicating that there is a low presence of detergents (with phosphates) produced by domestic discharges. On the other hand, current environmental regulations state that the maximum permissible value for SAAM in uses for consumption and/or domestic and recreational purposes should not exceed 0.5 mg/L. Therefore, these concentrations comply with Decree 1594 of 1984.

Fats and Oils

As shown in Illustration 4.1-154, fats and oils were found with varying concentrations ranging from < 0.3 to 13.3mg/L at the different sampling stations. It is worth mentioning that the data presented a growth trend with respect to the flow. On the other hand, the presence of fats and oils in water can alter its aesthetic quality, smell, taste and appearance, as well as the life of aquatic communities because it limits the gain of dissolved oxygen with the atmosphere. However, the levels of fats and oils present in the basin did not limit the oxygen concentrations in this body of water as can be seen in this parameter analyzed. For this reason, any alteration of the resource due to the presence of fats and oils in this study area can be ruled out.

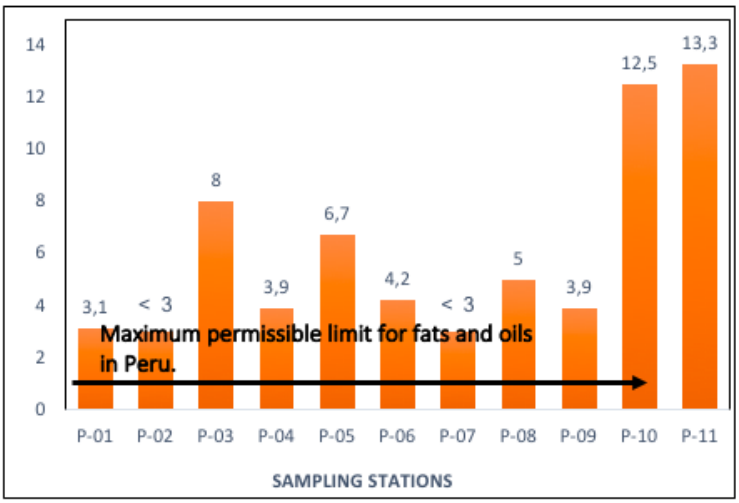

Illustration 4.1-154. Result of fats and oils.
Source: INGEX, 2015.

Current environmental regulations do not define the concentration of fats and oils, but rather determine the absence of visible film to comply with this standard. Therefore, the use of this resource for human consumption and/or domestic use is not restricted since none of the sampling stations showed a visible film of fats and oils. On the other hand, Peruvian regulations established that the maximum value allowed for fats and oils is 0.5 mg/L. With respect to the above, it is concluded that none of the eleven sampling stations meet these criteria in terms of water quality for human consumption in Peruvian regulations.

Phenols

Most of the sampling stations had values below the stop limit (< 0.05 mg/L) for phenols. However, station P-01 showed an outlier of 1.2 mg/L. Three possible explanations for this increase in phenol concentration at this station could be: (i) Decomposition of organic matter due to the presence of dead animals or significant amounts of decomposing plant material, (ii) areas rich in humic matter, or (iii) origin linked to mining effluents. This last explanation seems unlikely since this sampling area

has no presence of artisanal mining and no exploitation. The second explanation also loses strength when considering that if humic substances were present in stations P-02 and P-03 they would also present an increase in the concentration of phenols. On the other hand, the regulations stipulate that the maximum permissible concentration of phenols is 0.002 mg/l. which means that only station P-01 does not comply.

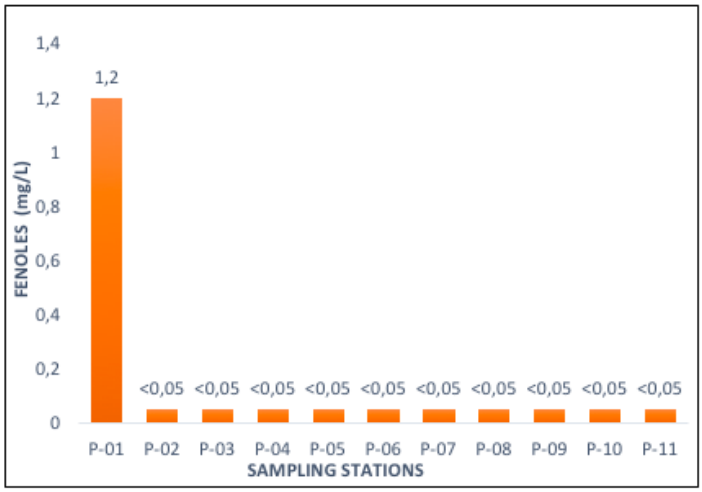

Illustration 4.1-155. Result of phenols.
Source: INGEX, 2015.

Total hydrocarbons

Most of the total hydrocarbons found in surface water bodies are toxic, causing health problems both for aquatic communities and for human and domestic use. The concentrations found in the basin in the eleven (11) sampling stations did not exceed the stop limit by the analysis technique used by the laboratory for its evaluation being below < 0.04 mg/L.

Therefore, the total hydrocarbon concentrations contemplated in current environmental regulations are in full compliance.

Free cyanide

Free cyanide is the term used to describe the cyanide ion (CN-) that dissolves in water as hydrogen cyanide (HCN) that forms in the solution. Most of the free cyanide in water is found as HCN when there are abundant hydrogen ions which allow it to volatilize and disperse in the air (Logsdon et al, 2001). The free cyanide form is considered to be the most toxic cyanide that can be found.

Concentrations were below the stop limits at the different sampling stations within the basin, i.e. < 0.05 mg/L.

The maximum permissible limit value of this parameter is not established in the Colombian regulations in force for surface waters or for other Latin American regulations with similar climatic conditions.

Total cyanide

With regard to total cyanide (see Illustration 4.1-156), most values below the detection level of less than 0.05mg/L were reported at the different sampling stations, except for stations P-08 and P-09, which had concentrations between 0.195mg/L and 0.577mg/L respectively. These values are due to artisanal gold mining activities that occur in the study area where cyanide residues can be found in these stations, due to the fact that they are found downstream of the mining mills.

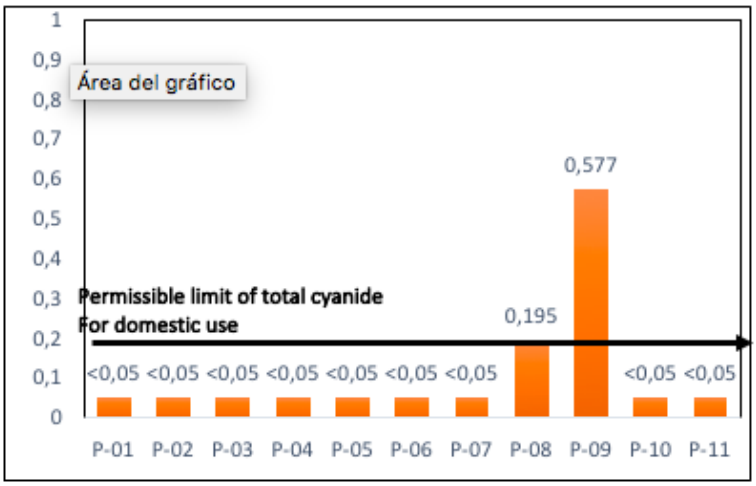

Illustration 4.1-156. Total cyanide result.
Source: INGEX, 2015.

Similarly, the values defined in current environmental regulations establish that the maximum permissible value for human and domestic use must not exceed 0.2 mg/L. Accordingly, stations P-08 and P-09 do not comply with the regulations.

Total coliforms

Total coliform values were recorded from 8230 to 24196 MPN/100ml (See Illustration 4.1-157).

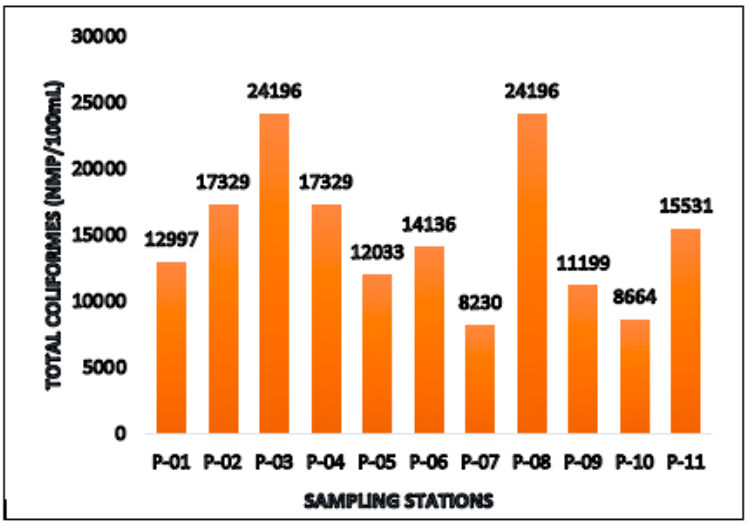

Illustration 4.1-157. Result of total coliforms.
Source: INGEX, 2015.

The highest concentration levels were found in P-03 and P-08, with the highest levels of anthropogenic activities. However, in all the sampling stations high levels of total coliforms were found due to the presence of cattle in the entire study area and domestic dumping. According to the above, it can be concluded that the basin presents a degree of contamination which can affect aquatic life. According to current environmental regulations, none of the stations comply with the maximum parameters established for the different uses of this water resource.

Fecal coliforms

Fecal coliforms (see Illustration 4.1-158) showed the same tendency to increase at the same sampling stations as total coliforms. Where the highest concentration of fecal coliforms occurred in P-03 (17329 NMP/100ml) followed by P-08 (5475 NMP/100ml), these being the seasons with the greatest human activity in the area.

With respect to current environmental regulations, the content of fecal coliforms presents high values in stations P-01, P-03, P-06, P-08, P-09, P-10 and P-11, therefore, there is no compliance with it in the maximum permissible limits of recreational use, domestic and agricultural consumption.

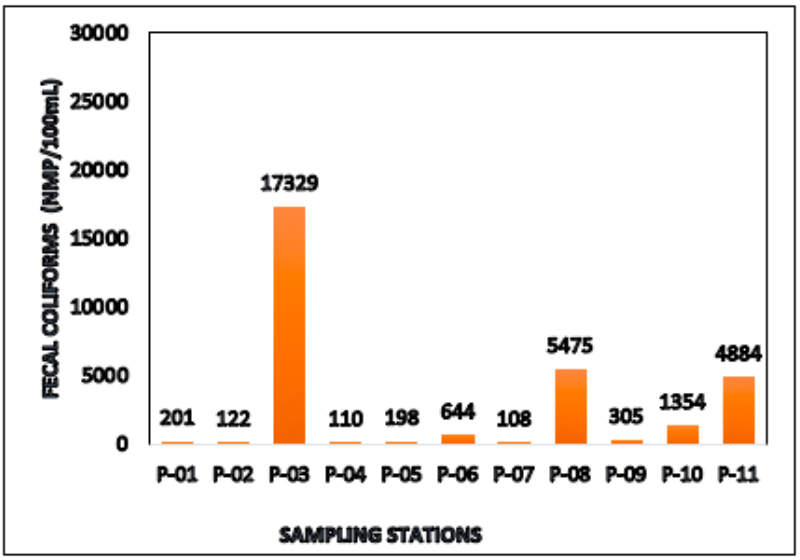

Illustration 4.1-158. Result of fecal coliforms
Source: INGEX, 2015.

Sulphates

Sulphates recorded in the basin had a concentration below the stop limit (< 10 mg/L) at all sampling stations. These results according to Roldan & Ramírez (2008) are typical values of natural waters, because they usually occur in a range of 2 to 10 mg/L.

With regard to current environmental regulations, it defines a maximum permissible limit of 400 mg/L for the use of the resource for human and/or domestic water consumption, none of the stations has any type of non-compliance with regulations. It should be noted that high levels of this parameter do not present toxicity to aquatic life but do present problems for water quality and use.

4.1.4.11 PHYSICAL-CHEMICAL AND MICROBIOLOGICAL INDICES

Table 4.1-88 shows the results obtained from the water quality indices (hereinafter ICA) and the pollution indices (hereinafter ICO), recorded in the different sampling stations to evaluate the physicochemical variables in the basin.

Table 4.1-88. ICAs and ICOs by sampling stations.

STATIONS	ICA INDICE	ICO INDICES					
		ICOMI	ICOMO	ICOSUS	ICOpH	ICOTRO	
P-01	76,63	0,14	0,33	0,00	0,00	Eutrophic	0.039
P-02	74,93	0,13	0,40	0,00	0,00	Oligotrophic	< 0,025
P-03	70,71	0,13	0,39	0,00	0,00	Oligotrophic	< 0,025
P-04	75,17	0,10	0,39	0,00	0,00	Oligotrophic	< 0,025
P-05	76,21	0,15	0,35	0,00	0,00	Eutrophic	0,038
P-06	75,73	0,15	0,31	0,00	0,00	Eutrophic	0,053

STATIONS	ICA INDICE	ICO INDICES					
		ICOMI	ICOMO	ICOSUS	ICOpH	ICOTRO	
P-07	78,79	0,13	0,27	0,00	0,00	Eutrophic	0,062
P-08	72,95	0,17	0,35	0,01	0,02	Oligotrophic	< 0,025
P-09	77,68	0,15	0,30	0,00	0,00	Oligotrophic	< 0,025
P-10	75,39	0,14	0,28	0,00	0,00	Oligotrophic	< 0,025
P-11	71,41	0,14	0,35	0,00	0,00	Eutrophic	0,029
ICA quality ranges: 100-91 Excellent, 90-71 Good, 70-51 Fair, 50-26 Poor and 25-0 Very Poor ICO contamination ranges: 0-0.2 None, >0.2-0.4 Low, >0.4-0.6 Medium, >0.6-0.8 High and >0.8-1.0 Very High							

Source: INGEX, 2015.

ICA

In general terms, the ICA results were in accordance with the physicochemical characteristics discussed above (see Table 4.1-88 and Illustration 4.1-159). In other words, they have good water quality.

Pollution Indexes (ICO)

In general terms, the surface waters in the basin presented low levels of contamination, expressed through the different ICOs (See Illustration 4.1-160 and Table 4.1-88).

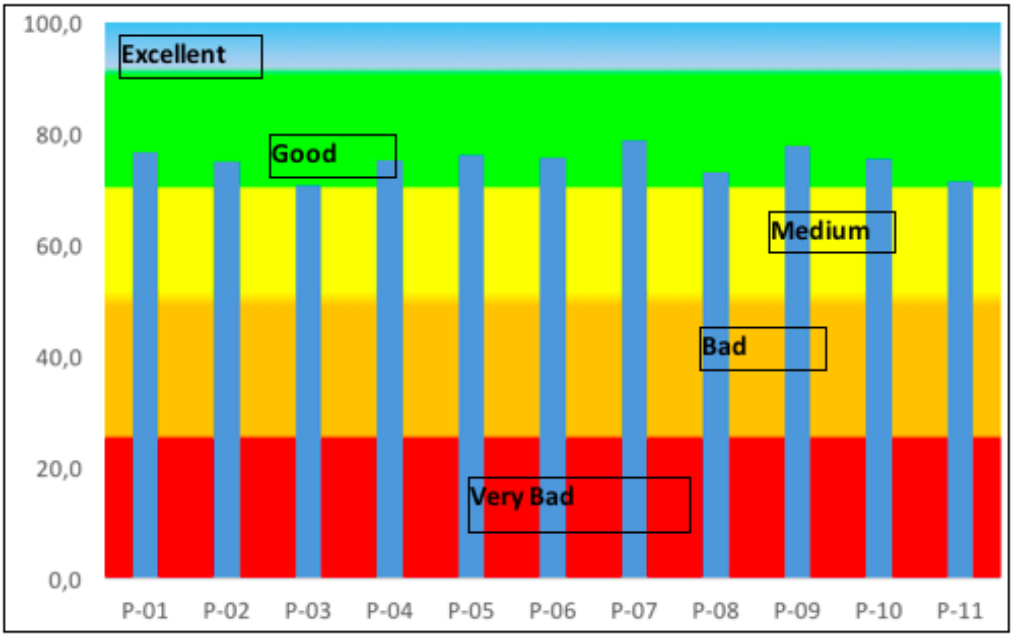

Illustration 4.1-159. Water quality index (WQI) values.
Source: INGEX, 2015.

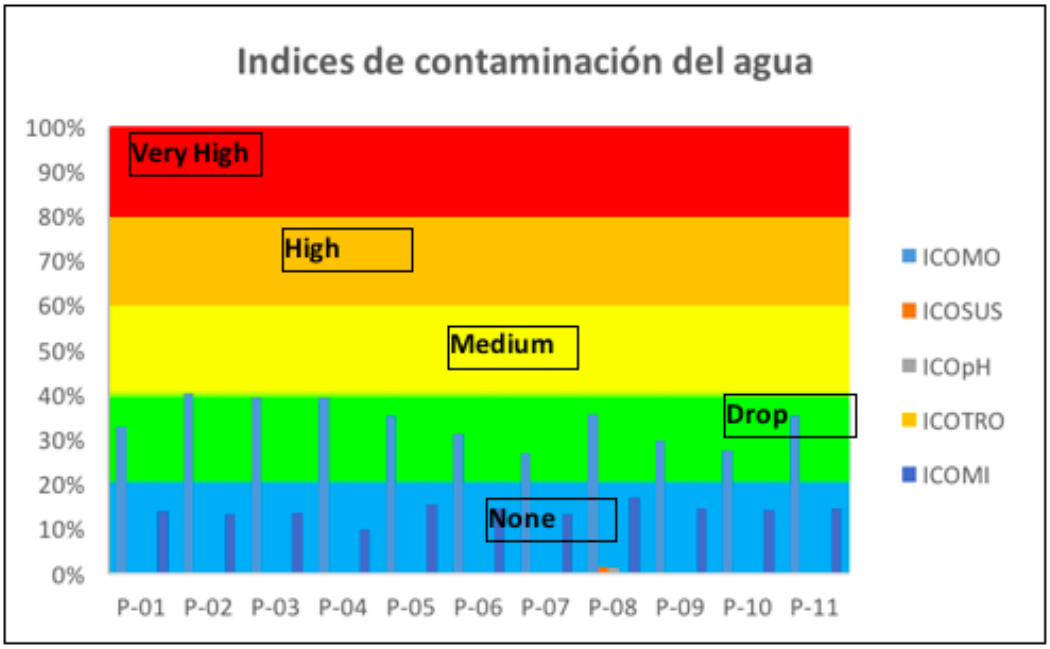

Illustration 4.1-160. Pollution index values (ICO).
Source: INGEX, 2015.

Particularly, ICOMI showed a stable behavior in all the sampling stations, between 0.10 and 0.17, which did not present any degree of contamination by mineralization.

ICOMO has low organic matter contamination for all seasons.

ICOSUS exhibited irrelevant (none) degrees of contamination. This is due to the low concentration of suspended solids.

The ICOpH presented extremely low values (none) in the eleven (11) sampling stations, due to the fact that no alteration is observed in this body of water due to pH variation effects (acidification or alkalinization).

Finally, the ICOTRO index presents conditions ranging from oligotrophy (P-02, P-03, P-04, P-08, P-09 and P-10) to eutrophy (P-01, P-05, P-06, P-07 and P-11), although in general terms the conditions regarding water quality in these stations are adequate, because this slight eutrophication is due to normal conditions of these natural waters of the basin and therefore no nutrient pollution processes are determined. Likewise, the rest of the stations that reported levels of oligotrophy are a normal condition for these water bodies (Ramírez et al., 1999).

Potential Water Quality Indicator (IACAL)

The IACAL indicates the pollutants discharged into the different surface water systems (organic matter, suspended solids and nutrients) affecting the conditions of these bodies of water (IDEAM, 2010). This is found in the information from the 2014 ENA (see Illustration 4.1-161).
This index involves the hydrographic zone of a system over a period of time, evaluated for a water supply, where it covers different physicochemical variables such as: COD, BOD, SST, total nitrogen, total phosphorus and water supply.

With respect to the above and to the area of hydrology studied, where fundamentally the largest water system in the basin corresponds to a tributary of the Bagre River, which is a tributary of the Nechí River lower part (tributary of the Cauca River middle part).

Therefore, the results obtained from the IACAL reported in the ENA 2010-2014 indicate that in the lower zone of the Nechí River (where the basin is located) a very low probability of contamination is determined, where the total load discharged is estimated for the BOD is 1235 tons/year, for COD 1085 tons/year and for SST 2648 tons/year. These results are very low for this hydrographic zone according to the IACAL.

The above discussed, on the IACAL, is in accordance with the results obtained for the ICA and ICO calculated in the different sampling stations within the characterized basin. This reflects that although the IACAL index is a generality for this hydrographic zone of the Nechí river, it can be supported by the monitoring carried out for the evaluated basin, where the quality of the water is good, condition that is supported with the physicochemical and microbiological results that were reported, as well as the ICA and ICO indexes estimated from these variables.

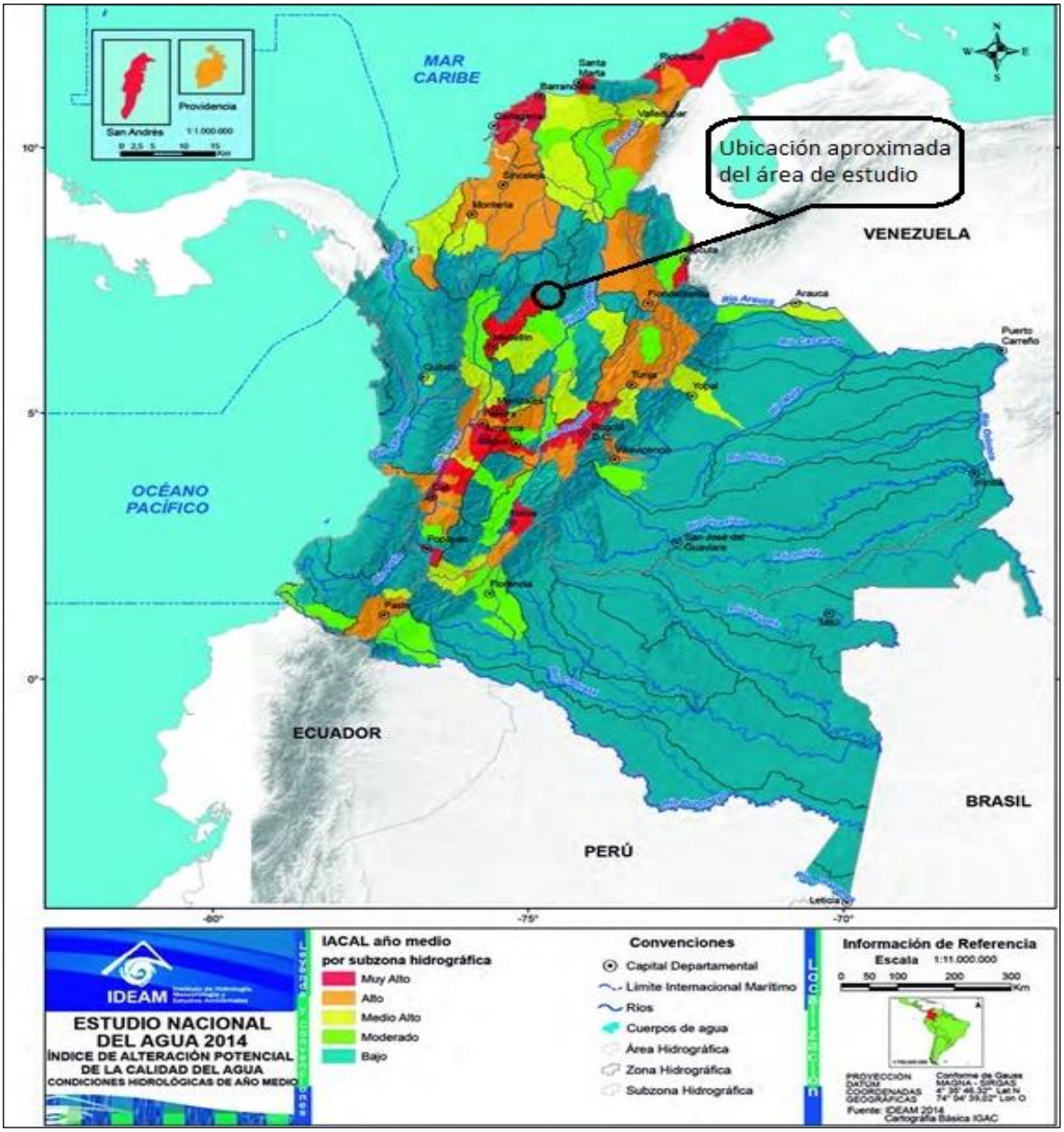

Illustration 4.1-161. IACAL at mid-year conditions for 309 hydrographic sub-areas
Source: Taken and modified from ENA, 2014.

4.1.5 HYDROGEOLOGY

The following are presented below: regional hydrogeology, inventory of water points, hydrogeological units, infiltration analysis, geophysics, conceptual hydrogeological model, hydrogeochemical model, intrinsic vulnerability, hydraulic parameters, numerical hydrogeological model and monitoring well network.

4.1.5.1 REGIONAL HYDROGEOLOGY

No regional aquifer systems are identified in the study area, due to the low hydrogeological potential of the region identified in macro-geological studies, developed by the Colombian Geological Service (hereinafter SGC) and IDEAM.

In the department of Antioquia, two (2) large areas with a good chance of finding a high aquifer potential are identified. The aquifer zone of the Lower Cauca sub-region is located 42 km to the northwest and the aquifer zone of the Middle Magdalena sub-region is located 60 km to the southeast (see Illustration 4.1-162); these are delimited in the map of homogeneous hydrogeological zones of Colombia (IDEAM, 2002).

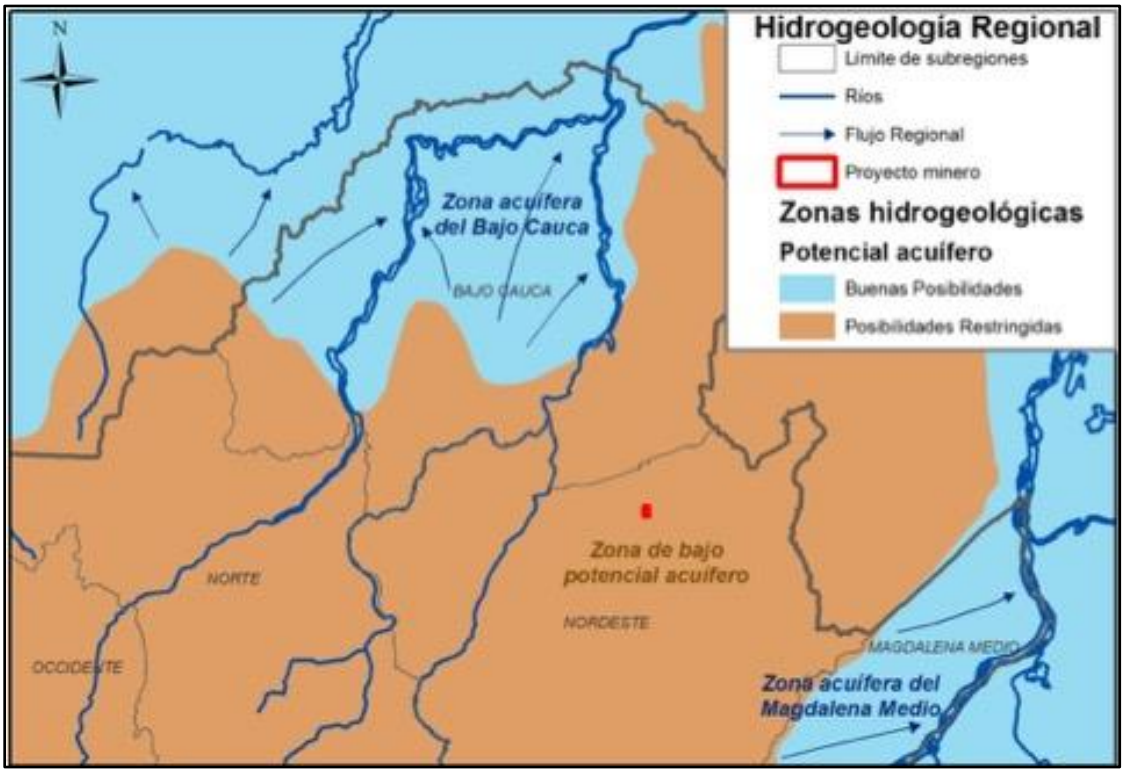

Illustration 4.1-162. Map of homogeneous hydrogeological zones in Antioquia.
Source: IDEAM, 2002.

Illustration 4.1-162 shows the study area as a low potential aquifer zone and the regional flow of groundwater from the Lower Cauca and Middle Magdalena aquifers, plotted by arrows indicating the preferential direction towards the main surface water streams where groundwater is finally discharged to maintain the base flow of these streams.

The delimitation of these aquifer zones is based on the identification and grouping of sedimentary rock units, mainly from the tertiary zone, and recent deposits from the quaternary zone, which have shown a high potential for groundwater production in the country, such as the aquifer zones of the lower Cauca and middle Magdalena regions.

Aquifers present in areas with high hydrogeological potential have a variable recharge area depending on the materials considered and the particular characteristics of the soil.

For tertiary rocks, such recharge areas may be spatially limited to upwelling sites of permeable strata if they are confined or semi-confined aquifers. On the other hand, for quaternary deposits that generally correspond to free aquifers, their recharge area may be the entire exposed surface area, with the main limitation being the morphological configuration of the terrain, for which there will be greater potential for recharge in low slope terrain.

However, there are other regions such as the area of study, which, due to their lithological characteristics, exhibit low or restricted hydrogeological potential, that is, little or no possibility of finding important groundwater producing aquifers, or that the water associated with these units is so scarce that it is not economically profitable to make use of the resource.

This is because it is located on igneous rocks with zero primary porosity and for this reason it is framed within an area of low groundwater potential in the northeastern subregion of Antioquia.

Betancur, et al (2009) and Arismendy, et al (2004), provide further details on hydrogeological models for the Lower Cauca and Middle Magdalena aquifers, respectively. On the other hand, and as a consequence of the low hydrogeological potential in the Northeast of Antioquia, groundwater exploration work in that sub region is not found in the literature. However, in hard rocks (igneous and metamorphic), the secondary porosity given by structures such as diaclases or faults allows water to flow through rocks to underground or surface reservoirs, even to be stored within the same structures. For this, the capacity of the unaltered hard rocks to store water depends basically on the degree of interconnection that exists between the fracture system, since it is not enough that there are fractures in the massif, they must be connected to each other to facilitate the flow (UNESCO, 1985).

Therefore, fracture or fault systems of hard rocks can be of hydrogeological importance, both as storage and groundwater flow pipes, depending on the permeability conditions they present.

On the other hand, hard rocks may have some degree of weathering even if they do not have fracture systems. The processes of physical and chemical alteration generated by the effects of climate and

vegetation can cause local modifications, both in the healthy rock and in the fracture systems they possess, generating increases or decreases in secondary porosity and in permeability (UNESCO, 1985). In general terms, hard rocks are compact, so their primary porosity is negligible; however, the important thing to analyze is their secondary porosity, that generated by weathering and fracture systems.

4.1.5.2 INVENTORY OF WATER POINTS

A groundwater point is a place where there is a natural emergence of groundwater or a site where civil works (wells or cisterns) allow access to it (MADS, 2014).

As mentioned above, in the area of study a low aquifer potential is identified according to the regional geological configuration, evidence of this is the non-existence of groundwater collection works such as wells and cisterns, which are commonly built by local people in regions with high aquifer potential. However, in order to have information on the status of the water resource in the area, an inventory of the perennial surface water flow births in the study area was carried out.

In total, 23 births were identified (see Table 4.1-89 and Illustration 4.1-163), where only one (1) is currently used by the inhabitants of the area by means of an intake located on the bed of the river.

All these births have their origin in the geological unit of the Batholit of Segovia, towards the highest parts of the basin. It is important to note that all the births identified have a very high elevation, close to the watershed of the hydrographical basin, which is a possible indicator of the degree of impermeability of the soil, since it does not favor the infiltración in the upper part of the basin and then give rise to the births in a low elevation más, but, on the contrary, it favors the superficial runoff direct from the upper parts of the basin where the births are located and where the currents originate.

Table 4.1-89. Points of birth of water currents.

NAME	NORTH	EAST	ELEVATION
PAC-001	1294275	929773	217
NAC-01	1293877	929739	237
NAC-02	1293701	929769	240
NAC-03	1293701	929944	247
NAC-04	1292316	931274	314
NAC-05	1292468	931300	328
NAC-06	1292609	931530	403
NAC-07	1293035	931685	442
NAC-08	1293265	931448	405
NAC-09	1293439	931448	399
NAC-10	1293623	931811	445
NAC-11	1294442	931059	289

NAME	NORTH	EAST	ELEVATION
NAC-12	1293985	931428	321
NAC-13	1294167	931242	315
NAC-14	1294185	930760	287
NAC-15	1295006	930238	229
NAC-16	1294811	930495	254
NAC-17	1293553	930062	255
NAC-18	1293309	930146	265
NAC-19	1292925	930524	289
NAC-20	1292934	930721	304
NAC-21	1293177	930596	303
NAC-22	1294367	929653	238

Source: INGEX, 2015.

Illustration 4.1-163. Inventory of surface water sources.
Source: INGEX, 2015.

4.1.5.3 HYDROGEOLOGICAL UNITS

Based on the local geology identified, within the study area there are four (4) geological units (see Illustration 4.1-164): granodiorite, diorite, diabase and alluvial deposits.

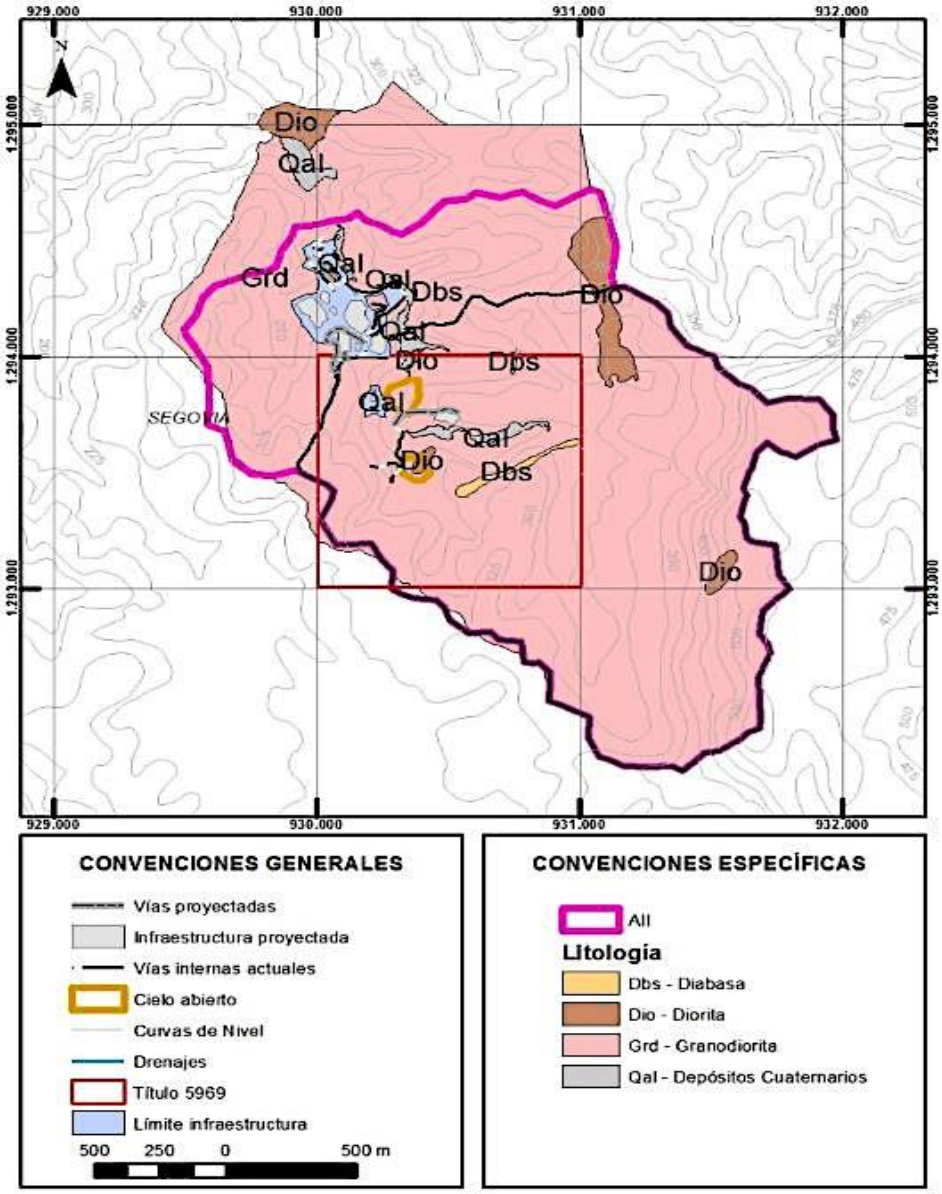

Illustration 4.1-164. Local geology.
Source: INGEX, 2015.

The important features of these units for hydrogeological analysis are the following:

- The granodiorite has a moderate to strong degree of weathering, generating a residual soil whose texture is clayey to clayey silt.

- Diorite has moderate weathering and generates residual soils with a silty texture.

- The diabase has a moderate degree of weathering and develops residual soils with a silty texture.

- Alluvial deposits are spatially limited to the margins of some streams and are located mainly at the bottom of the micro-basins. They are composed of gravel and pebbles at the base and fine sand and clay at the top. The clasts are composed of granodiorites, diorites and diabases, indicating that they come from the same igneous units mentioned above. Because they are sedimentary bodies of little thickness and extension, in addition to forming isolated bodies, this unit has little importance from the hydrogeological point of view and for this reason, within the classification of the hydrogeological units it will be incorporated into the unit of the residual soils and the saprolite developed by weathering.

- On the other hand, due to the scarcity of outcrops in the area, it was only possible to identify some sites where fractures with preferential N-S and NE directions with 60°W dipping were present. The outcrops of these structures are spatially limited and preferential fractures in one direction only, their ability to significantly influence groundwater flow is estimated to be negligible as the fracture density is low which implies little connectivity between the systems, and they are very locally located in the area. For these reasons, the structures for the construction of the conceptual hydrogeological model are not taken into account.

- The study area is mainly located on the geological unit of the Batolito de Segovia (Jdcs), corresponding to the granodiorite unit described above, which, due to the effects of weathering, has developed a residual soil and a saprolite with variable thicknesses towards the surface of the ground. Underlying these is the fresh rock of the batolith. The other units such as the diorite and diabase are small in size in the area of interest and will not be intervened by the mining project. Based on this geological context, a classification of two (2) hydrogeological units (see Illustration 4.1-165 and Table 4.1-90) has been made from the theoretical hydraulic characteristics of each one according to its textural and structural composition. These hydrogeological units are described below.

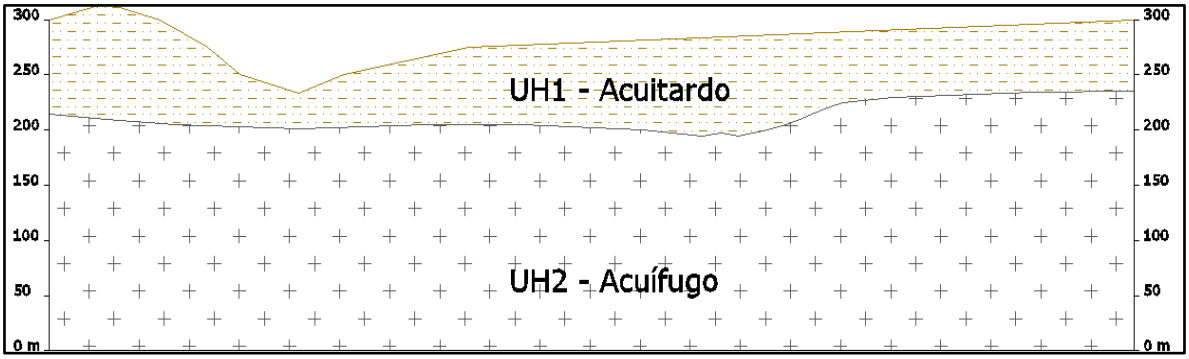

Illustration 4.1-165. Profile of hydrogeological units (W-E orientation).
Source: INGEX, 2015

Table 4.1-90. Theoretical permeability values.

MATERIAL	PERMEABILITY (M/DÍA)	DEGREE OF PERMEABILITY	TYPE OF TRAINING
Clean gravel	1000	Very good	Permeable
Clean coarse sand	10 – 1000	Good to very good	Permeable
Mixture of sand	5 – 10	Bad	Semi permeable
Fine sand	1 – 5	Bad	Semi permeable
Waxy sand	0.1 – 2	Bad	Semi permeable
Silt	0.001 – 0.5	Bad	Semi permeable
Clay	< 0.001	Bad	Impermeable

Source: Universidad Nacional de Colombia, Medellín, 2009, in MADS, 2014.

4.1.5.3.1 Hydrogeological Unit 1 (UH1 - Aquitard)

The direct exploration developed mainly on the UH1 - Aquitard, has been based on the inspection of old abandoned tunnels, developed by artisanal mining and exploratory drilling, evidencing the absence of the hydrogeological resource.

It is formed by the grouping of residual soil and saprolite, as well as the isolated bodies of alluvial deposits, which constitute a porous medium. According to field observations, this unit contains materials with variable granulometry, from fine to medium with clay and silt contents, and in some parts of sands in silt-clay matrix. These characteristics give the unit a low permeability (between 0.5 and 1.8 m/day according to the infiltration tests carried out) (see Illustration 4.1-165 and Table 4.1-90) and it is classified as an aquitard, which corresponds to a semi-permeable hydrogeological unit that can store a negligible amount of water and also transmits it at very low speeds by means of the phenomenon known as dripping.

4.1.5.3.2 Hydrogeological Unit 2 (UH2 - Aquifuge)

It is formed by the fresh igneous rocks of granodiorite, diorite and diabase, which by their characteristics constitute an impermeable medium which prevents the flow of water through it. This unit is classified as an aquifer, which corresponds to a hydrogeological unit that does not have the

capacity to store water and therefore cannot transmit it (permeability <0.001 m/d) (See Illustration 4.1-165 and Table 4.1-90).

UH2 has not been able to obtain detailed information on the existence and attitude of tectonic structures such as faults and diaclases due to the absence of fresh rock outcrops; for this reason, and considering that there are no regional structures in the area according to the geological cartography of the SGC, for purposes of simplifying the hydrogeological model, the hypothesis is established that this unit is generally healthy in the study area.

Based on the previous identification of hydrogeological units, it is determined that only the UH1 would have the possibility of presenting a hydraulic connection with the surface water currents, since these run over the unit, being able to provide water as infiltration or receive water as a base flow; however, this can only be verified by direct exploration (drilling and search in old artisanal mining tunnels) and indirect (electric tomography).

4.1.5.4 INFILTRATION ANALYSIS

The infiltration corresponds to that portion of rainwater that can enter the soil, rather than run off over it in the form of direct surface runoff. There are mainly two (2) scenarios (see Illustration 4.1-166) in which water infiltration into the soil is encouraged, considering in advance that soils are sufficiently permeable as those composed of gravel and clean sand.

- Low slope areas.
- Areas with vegetation.

For the area of study, an analysis is performed to determine the potential for infiltration of the soil, based on the morphology it exhibits, for this purpose a slope map is prepared from the topography. The method to be implemented considers that the potential for infiltration in the soil depends both on the permeability of the soil and its slope; thus, the mathematical formula to be used is: (Essig et al., 2009; Philip, 1991; Chow et al., 1988).

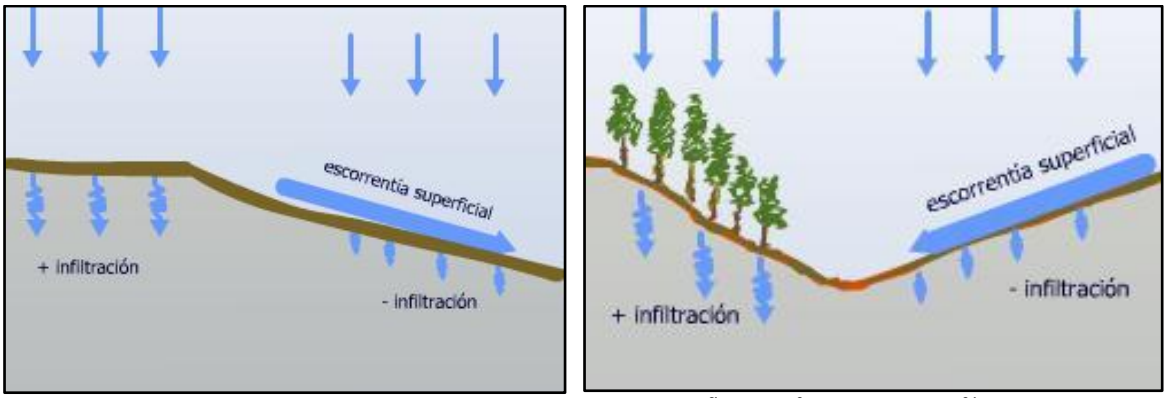

Influence of soil slope on infiltration

Influence of vegetation on infiltration.

Illustration 4.1-166. Scenarios that favor infiltration.

Retrieved from: ***http://pendientedemigracion.ucm.es/info/diciex/proyectos/agua/esc_sub_infiltracion.html***

$$\boldsymbol{Infiltration\ potential = Ks * cos(\gamma)}$$

Where Ks are the hydraulic conductivity of the saturated soil expressed in mm/year, and γ is the slope of the soil in sexagesimal degrees measured from the horizontal. In this way, the infiltration potential is also expressed in mm/year.

The hydrogeological unit UH1 - Aquitard is the only porous medium of the two (2) identified hydrogeological units that could allow water to infiltrate the soil. Thus, for the analysis of the infiltration potential in this unit, an average permeability value of 0.25 mm/d is established from the theoretical data considered, equivalent to 91.4 mm/year. This permeability combined with the slope map of the terrain allows a zoning (see Illustration 4.1-167) of the permeability potential to be found according to the method described above.

The potential infiltration map is calculated under the hypothesis that the porous medium is in a steady flow regime, this implies that it remains constantly saturated with water and that its conditions do not change over time. This is a hypothesis that is not close to reality, since the UH1 - Aquitard, is subject to the changes of stationary periods existing throughout the hydrological year for the region. Thus, the way of interpreting the previous map is that the infiltration values presented in mm/year show the maximum capacity of the soil, given the slope of the land, to allow water to infiltrate once it has reached its saturation point. The actual infiltration capacity is less than the potential capacity given the seasonality of the climate.

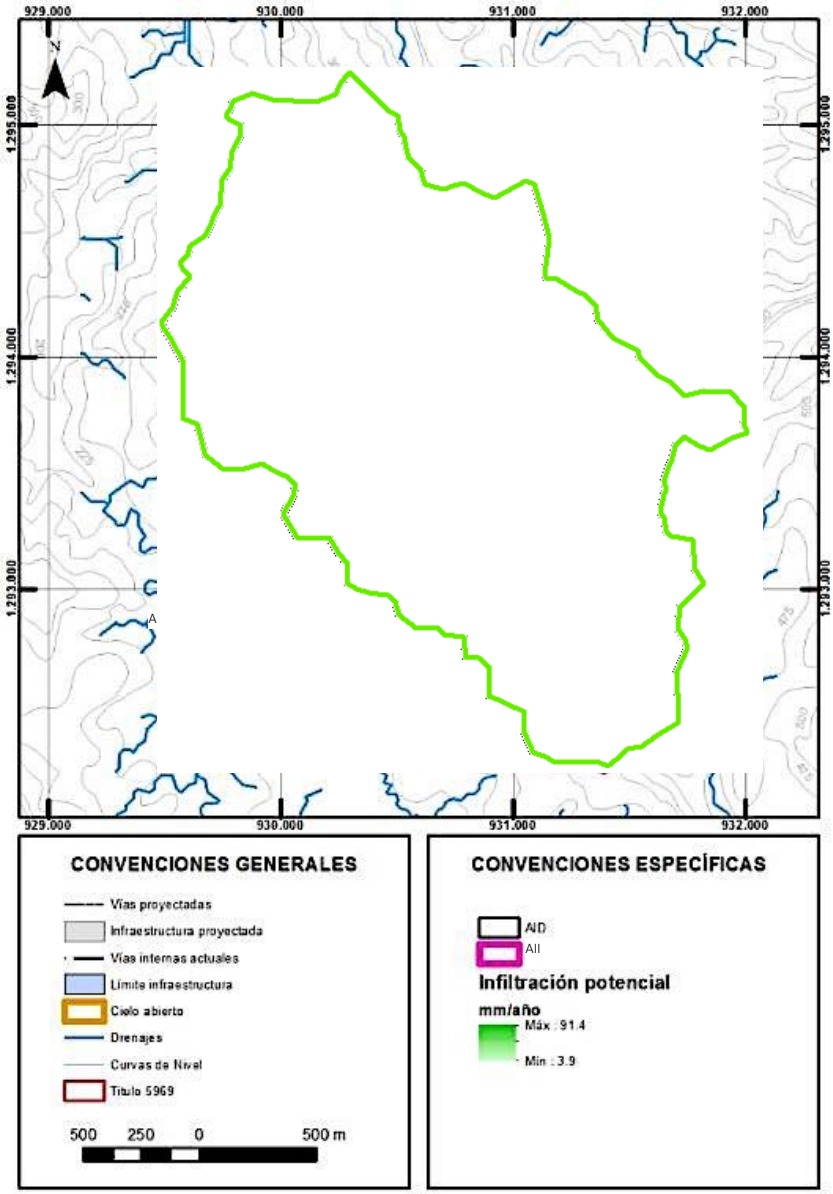

Illustration 4.1-167. Potential infiltration in mm/year.
Source: INGEX, 2015.

The areas with the greatest potential for infiltration are those with flat areas, both in the upper part of the basin and in the lower parts associated with the drainage channel. However, this infiltration potential is not homogeneous over the entire area due to the variation of the slopes. An average potential infiltration value for the entire area of influence is approximately 17.8 mm/year; however, this value is restricted to a very small percentage of the total area, while the most likely potential infiltration value is approximately 8 mm/year (See Illustration 4.1-168).

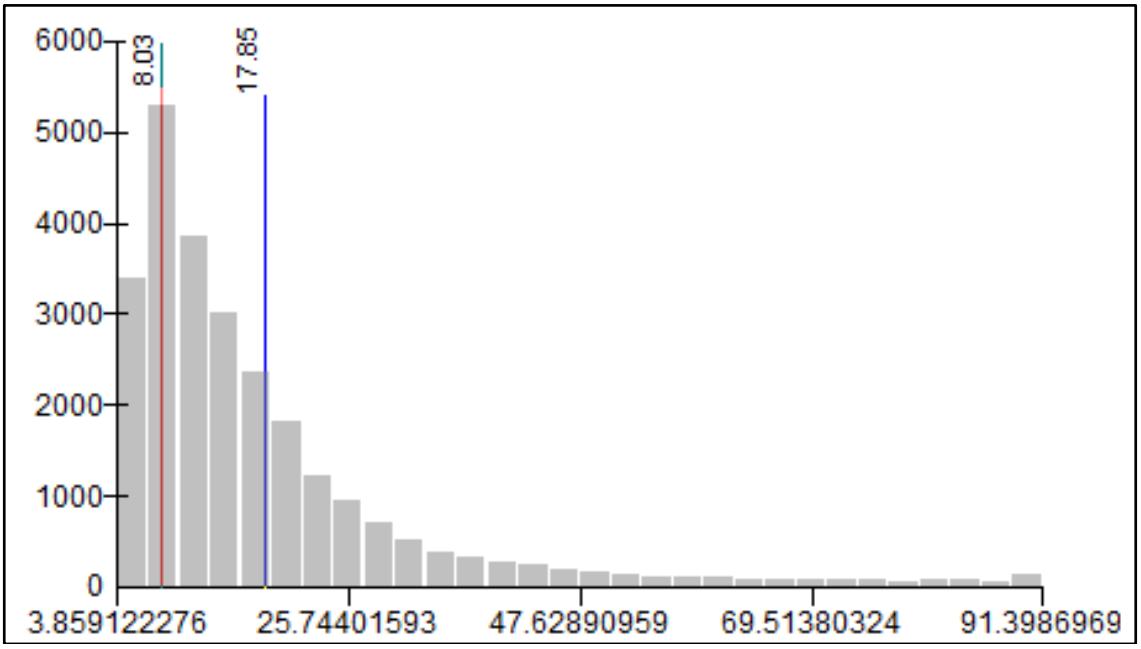

Illustration 4.1-168. Histogram of infiltration potential (mm/year).
Source: INGEX, 2015.

This indicates that the soil, according to the hypotheses, has a low potential for infiltration if compared to the average annual rainfall that falls in the area of 3,500 mm/year, or 0.23% of the average annual rainfall.

4.1.5.5 INDIRECT GROUNDWATER EXPLORATION (GEOPHYSICS)

In the area of study, a geoelectrical campaign was carried out consisting of 16 electric tomography lines (see Illustration 4.1-169), a geophysics tool for the study of the subsoil that consists of determining the distribution of a characteristic physical parameter within a limited spatial scope, from a very high number of measurements taken from the surface.

This multielectrode resistivity method is based on 2D modelling of the soil resistivity, usually using profiles. It consists of obtaining a series of apparent resistivity measurements with a determined tetra electric micro-device and with a constant separation between electrodes; and varying the distances between the transmitter-receiver electrode pairs by multiples of a value, so that the final result is a section or cut with test pit at various levels of depth.

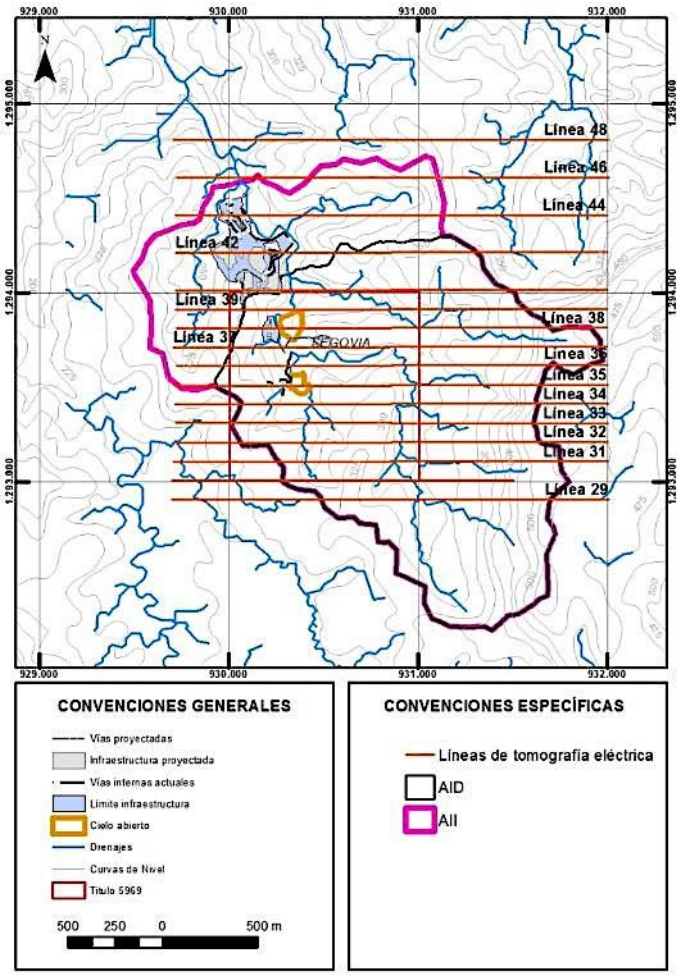

Illustration 4.1-169. Location of the electrical tomography lines.
Source: INGEX, 2015.

This technique provides both lateral and in-depth information. The system consists of a central unit consisting of a resistivity meter or basic unit, an electrode selector and a set of multi-connector cables that allow the use of electrodes that can be switched fully automatically via the electrode selector and controlled by the basic control unit.

When electric current is introduced into the ground, it can propagate in three (3) different ways through the subsoil: dielectric conduction, electronic conduction and electrolytic conduction. Electrolytic conduction is the most important mode of propagation, and on which resistivity methods are based.

If an electrical current of I amps is passed through an object, and the power is reduced by V volts, the object's resistance R is calculated by Ohm's law.

R = resilience

U= measured voltage

I = transmitted current

K= geometric factor

ρ= resistivity

ρ_a= apparent resistivity

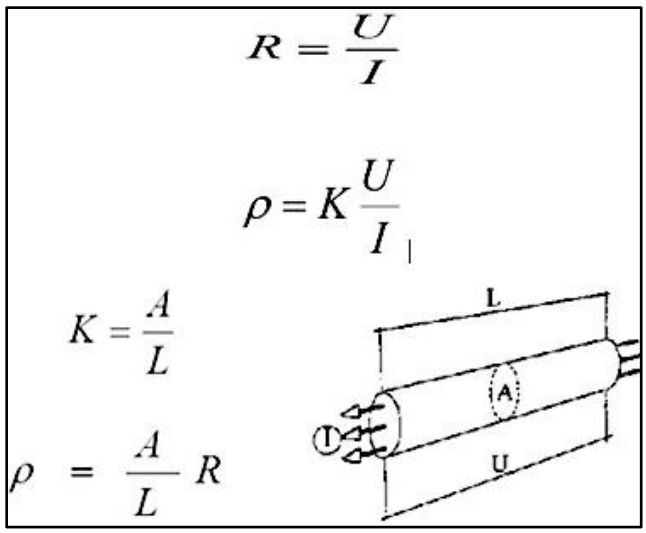

Illustration 4.1-170. Ohm's Law.

The specific electrical resistance of each material to resist the passage of an electric current is measured in ohms per meter (Ω*m). It is equal to the resistance by the constant K which is the geometric factor that depends on the shape of the object and the arrangement of the electrodes used to pass the current and measure the voltage, thus K is the penetration factor or coefficient of the device and depends on the spacing between electrodes, varying its value in each type of acquisition arrangement (Wenner, Schlumberger, dipole-dipole, dipole-pole, pole-pole, gradient, etc.). The calculated resistivity will correspond to the apparent resistivity of the soil and not to the actual resistivity. This is because the subsoil is generally made up of different materials, so that the electric field introduced into the ground will affect several layers simultaneously, so that the resistivity measured will correspond to an intermediate value of all of them. Only for homogeneous soils or for very shallow depths of investigation will the measured resistivity value coincide with that of the actual resistivity. Since apparent resistivity values are obtained, the use of inversion software is required to obtain the real resistivity values and also to include the topographic values for this inversion. The software used is Res2dinv version 3.59.115.

Electrical resistivity is a parameter that varies according to the characteristics of the soil.

Some of the factors that influence it are:

- The degree of saturation of the soil.
- The temperature.
- Porosity and the shape of the pores.
- The salinity of the fluid.
- The type of rock.
- The geological processes that affect materials.
- The presence of clayey materials with high cation exchange capacity.

It is precisely this close relationship between electrical resistivity and the degree of soil saturation that allows these resistivity methods to be used in the search for sources of water filtration in the ground. In this sense, increases in the water content of the soil will cause decreases in resistivity.

With regard to the other factors, it should be noted that the salinity of the fluid, the porosity of the soil, and the temperature (although this is a minor factor), show a behavior similar to that of the degree of humidity. A curious case is that of salt, which behaves as an excellent insulator in the dry state, while in solution it gives the soil a high level of conductivity.

The data acquisition was performed using a multi-electrode method and the configuration used is the so-called Dipole-Dipole (see Illustration 4.1-171).

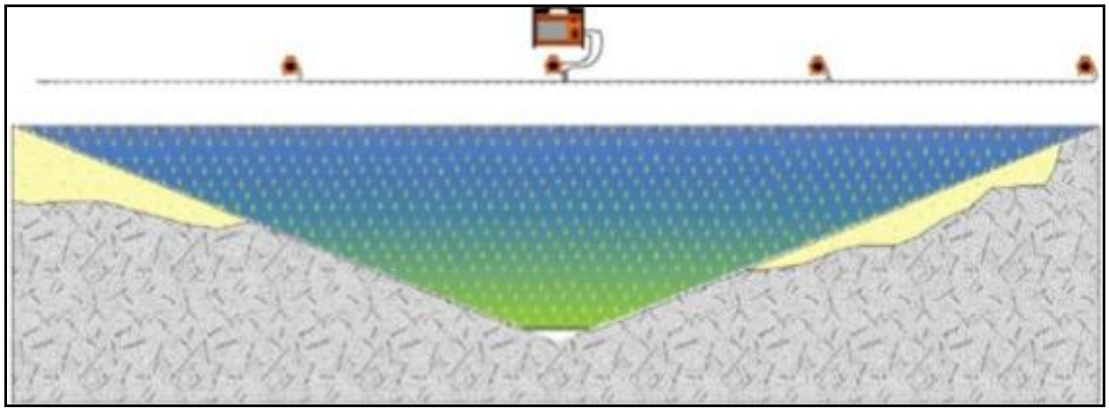

Illustration 4.1-171. Acquisition diagram with the Dipole-Dipole type configuration.
Source: ARCE GEOFISICOS, 2013.

It is not only the factory characteristics of the rock hat determine its resistivity, factors such as the presence of water give a substantial change in the measurement as well as weakness planes such as fractures, faults or stratigraphic contacts, can show resistivity of apparent totally vertical layers. In igneous or metamorphic units in which zones of infiltration or saturation are present, the method may not show unity per unit (gneiss, shales, quartzite, diorites, granodiorites, etc.), but rather a contrast between the values of high, medium and low resistivity (product of possible saturation).

For the interpretation of the tomography, the different factors on which the resistivity of the rocks depends are taken into account, although the rocks have geo-electrical properties depending on their factory, they are susceptible to presenting anomalous values at the moment of being measured, either by water saturation, salt saturation, dryness, among others. The following illustration shows different resistivity values for different lithology. After the process of reversing the apparent resistivity data, an interpretation of the results obtained is made, the resistivity values are delimited looking for contrasts in each tomography, and special care was taken with the existing geological information (Illustration 4.1-172).

The total penetration of the geo-electrical method is proportional to the geometry of the surface array, in other words the total depth of investigation depends on the total length of the acquisition line, in this sense the described lines reached maximum penetrations of up to 300 m, with a separation between electrodes of 50 m. Separation between electrodes also limits or conditions the minimum depth of investigation, although the type of array used allowed for large depths of resistivity data to be reached (mainly for hydrothermal deposits or reservoirs Hunger Edge and Pepes), in turn causing a portion of the surface (Saprolite) to be unmeasured due to the way in which the equipotential lines travel in depth; under normal conditions, an information blind zone of approximately half of the electrode gap is generated.

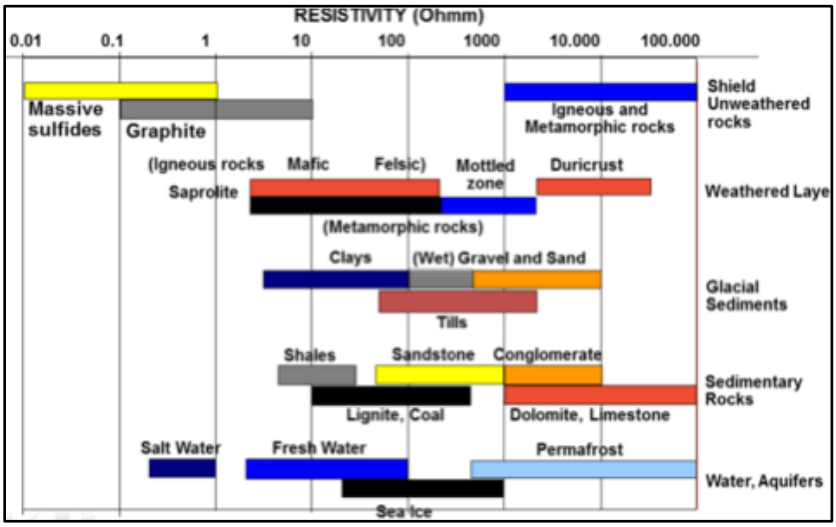

Illustration 4.1-172. Resistivity values for different lithologies.
Source: Palacky, 1987.

The above indicates that for each scan on average no information was taken between the first 20 to 25 meters and it is this area that generally corresponds to the area saprolitized. However, in this area it was confirmed that there is no water present, through drilling and surveying of abandoned old mining tunnels (direct exploration) (See Illustration 4.1-173).

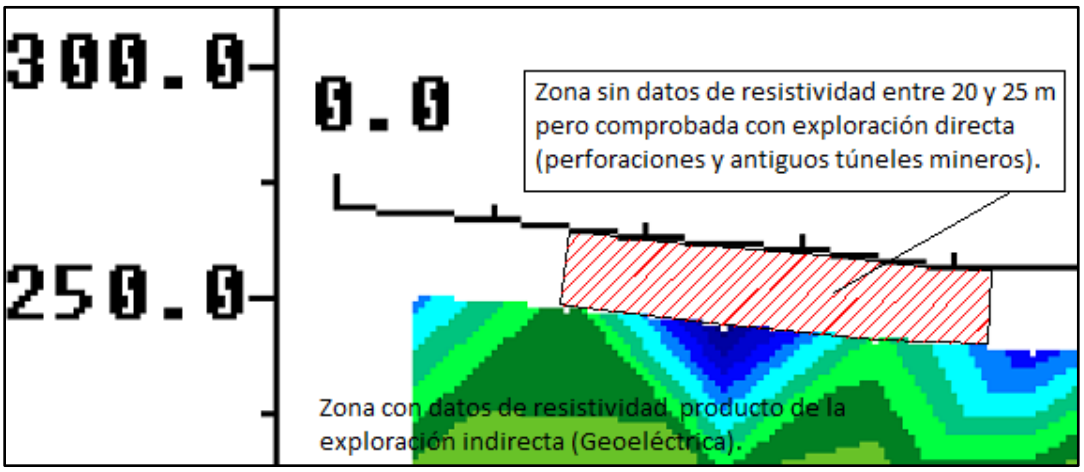

Illustration 4.1-173. Zones of loss or acquisition of information associated with the separation between electrodes.
Source: ARCE GEOFISICOS, 2013.

The following illustrations correspond to the iso-resistivity profiles obtained from the electrical tomography (See Illustration 4.1-174 to Illustration 4.1-189).

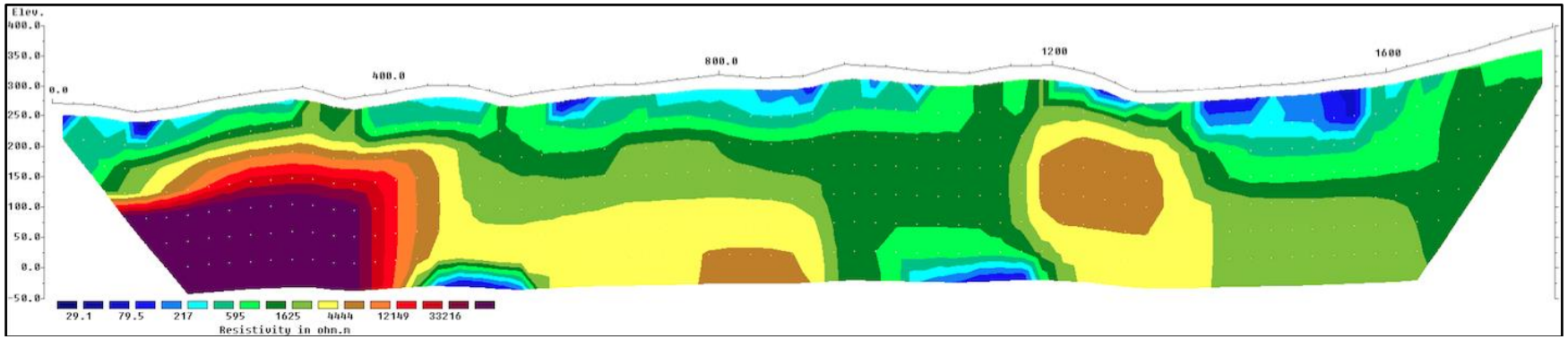

Illustration 4.1-174. Profile No. 29 iso-resistivity.
Source: ARCE GEOFISICOS, 2013.

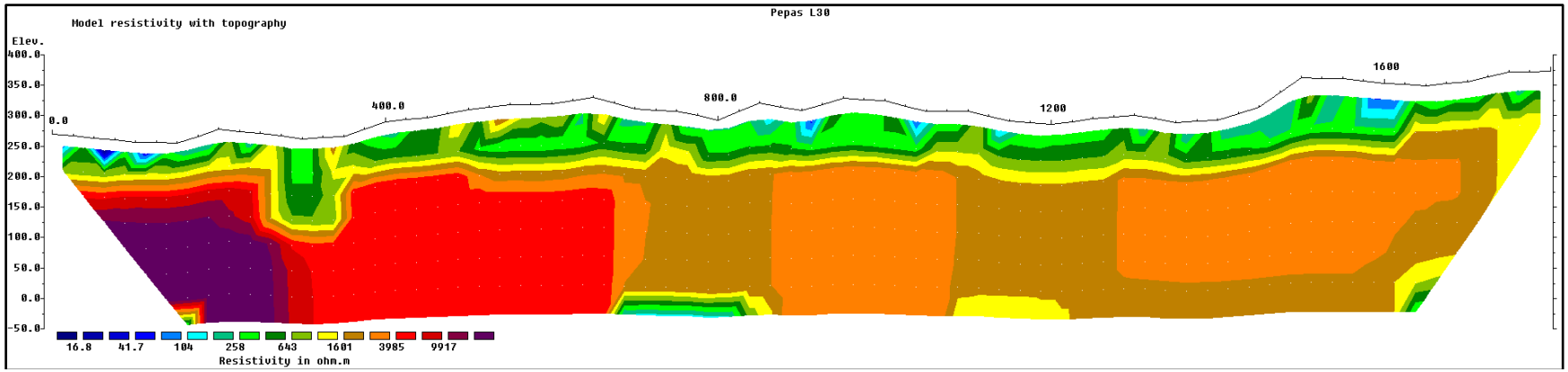

Illustration 4.1-175. Profile No. 30 iso-resistivity.
Source: ARCE GEOFISICOS, 2013.

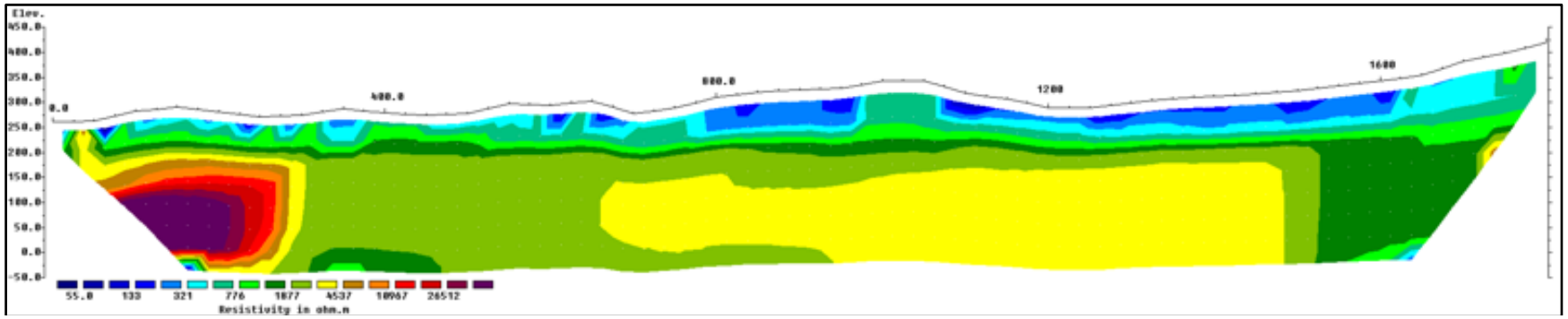

Illustration 4.1-176. Profile No. 31 iso-resistivity.
Source: ARCE GEOFISICOS, 2013.

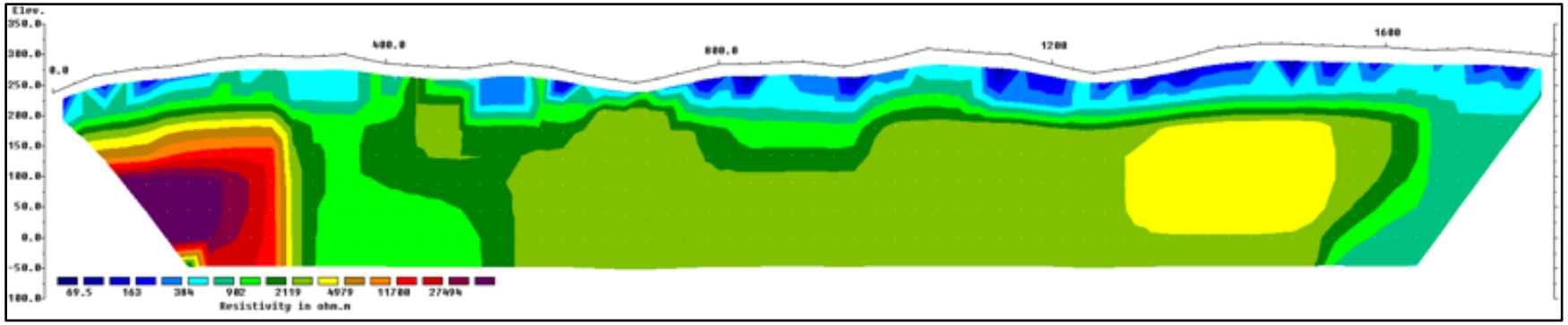

Illustration 4.1-177. Profile No. 32 iso-resistivity.
Source: ARCE GEOFISICOS, 2013.

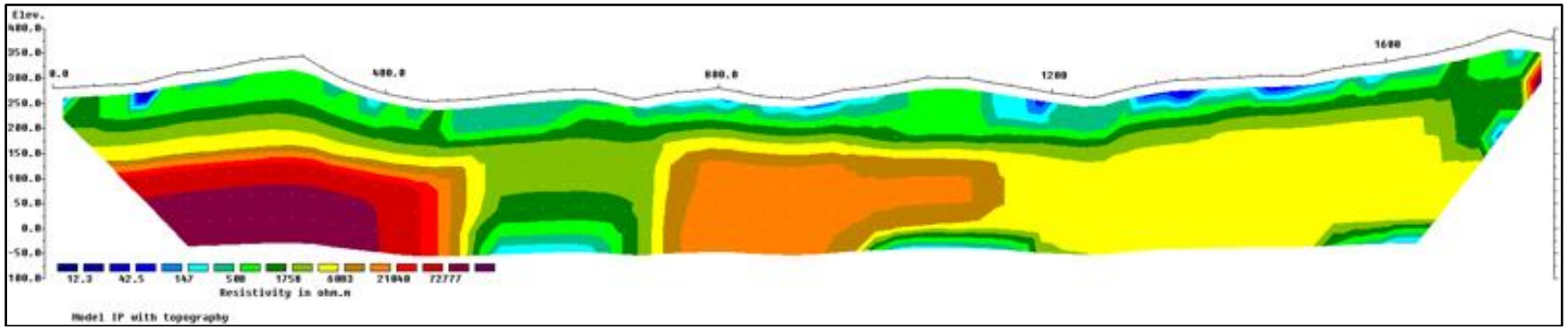

Illustration 4.1-178. Profile No. 33 iso-resistivity.
Source: ARCE GEOFISICOS, 2013.

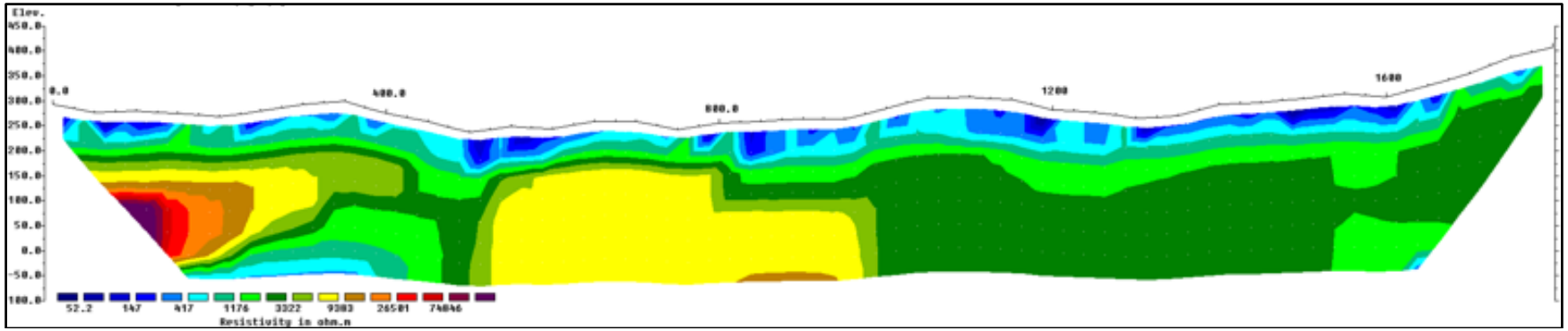

Illustration 4.1-179. Profile No. 34 iso-resistivity.
Source: ARCE GEOFISICOS, 2013.

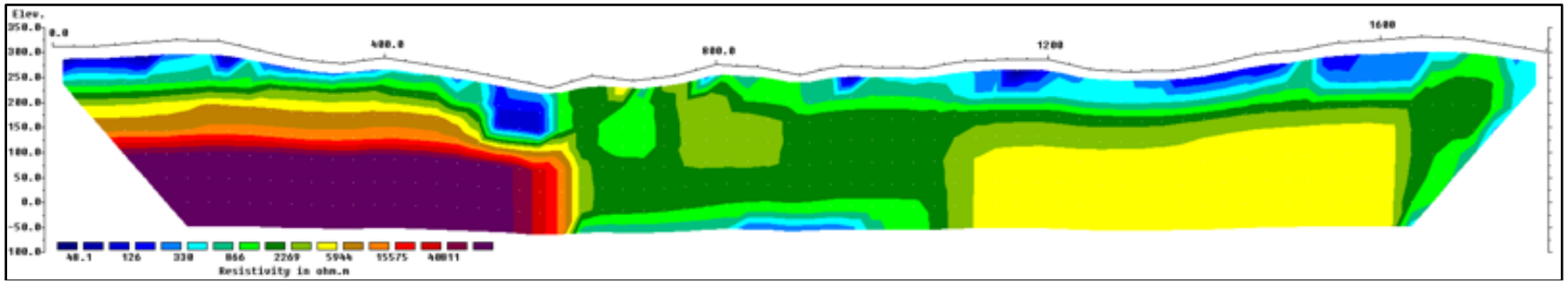

Illustration 4.1-180. Profile No. 35 iso-resistivity.
Source: ARCE GEOFISICOS, 2013.

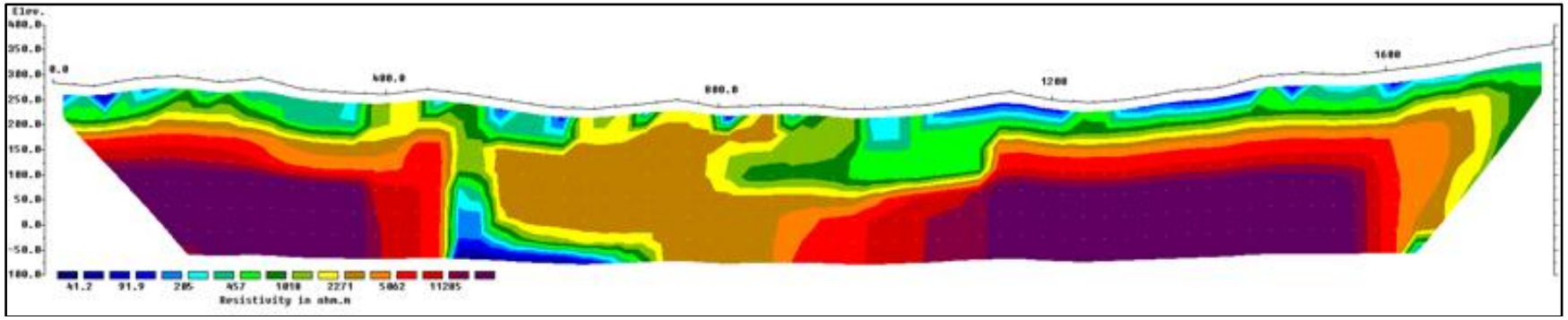

Illustration 4.1-181. Profile No. 36 iso-resistivity.
Source: ARCE GEOFISICOS, 2013.

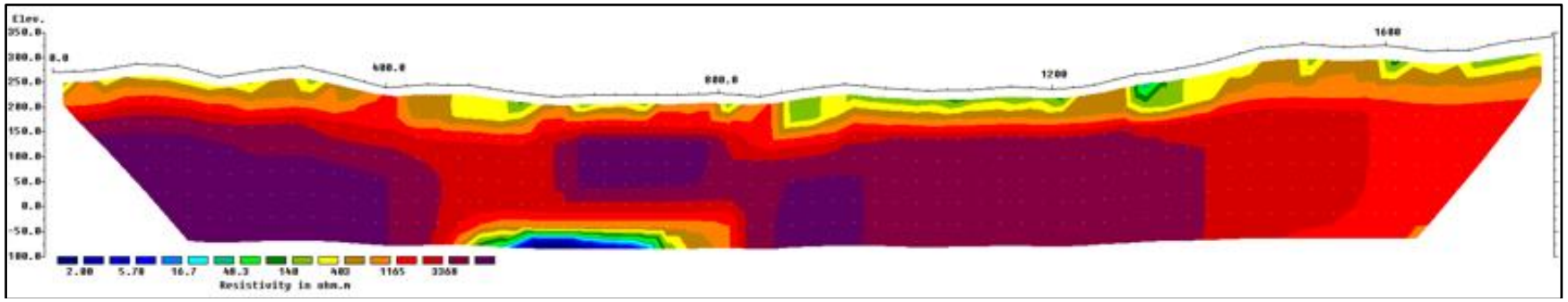

Illustration 4.1-182. Iso-resistivity profile No. 37.
Source: ARCE GEOFISICOS, 2013.

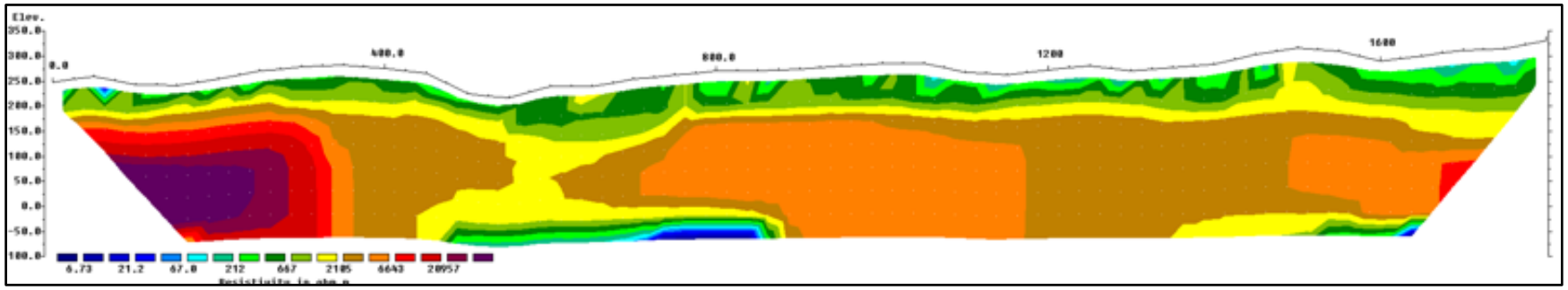

Illustration 4.1-183. Profile No 38 iso-resistivity.
Source: ARCE GEOFISICOS, 2013.

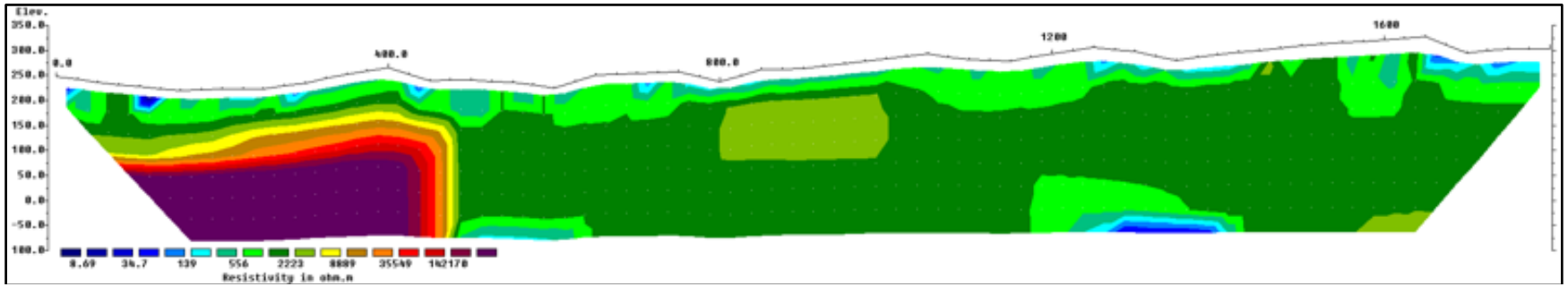

Illustration 4.1-184. Profile No. 39 iso-resistivity.
Source: ARCE GEOFISICOS, 2013.

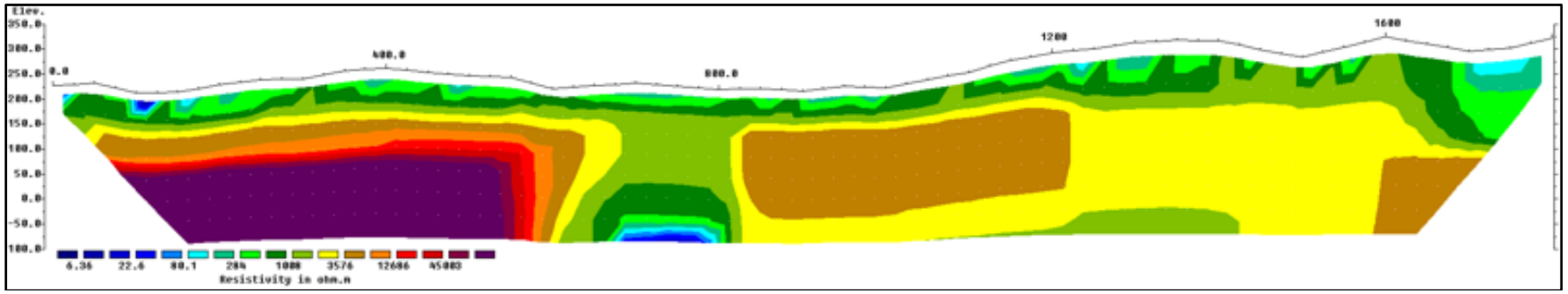

Illustration 4.1-185. Profile No. 40 iso-resistivity.
Source: ARCE GEOFISICOS, 2013.

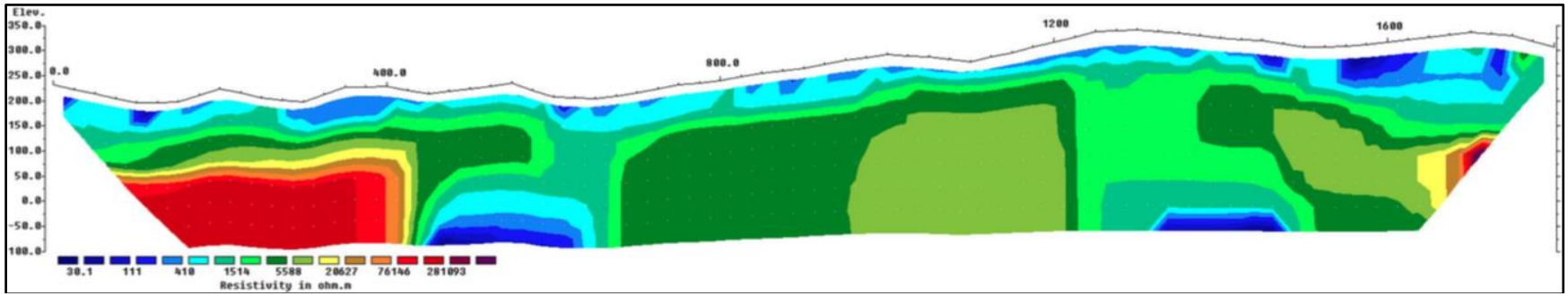

Illustration 4.1-186. Profile No. 42 iso-resistivity.
Source: ARCE GEOFISICOS, 2013.

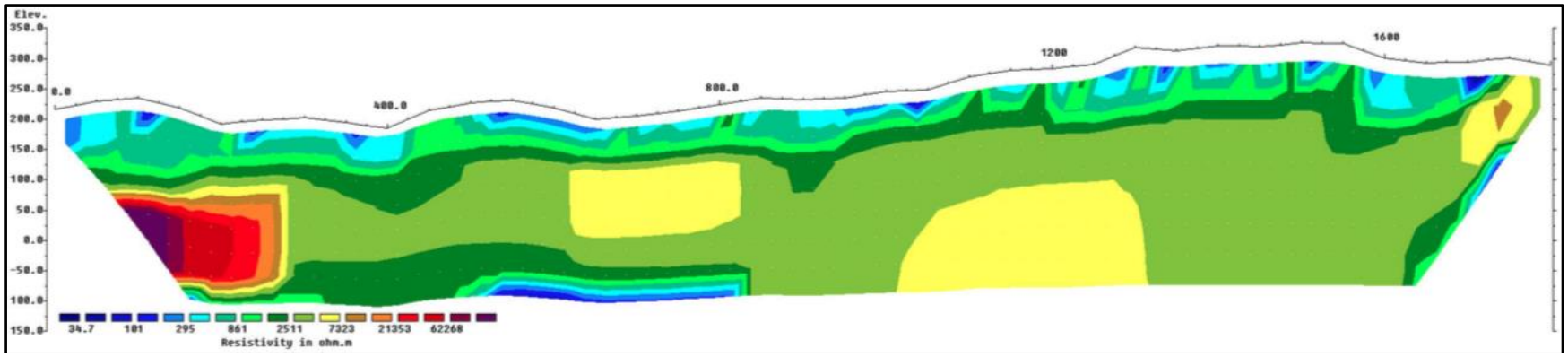

Illustration 4.1-187. Iso-resistivity profile No 44.
Source: ARCE GEOFISICOS, 2013.

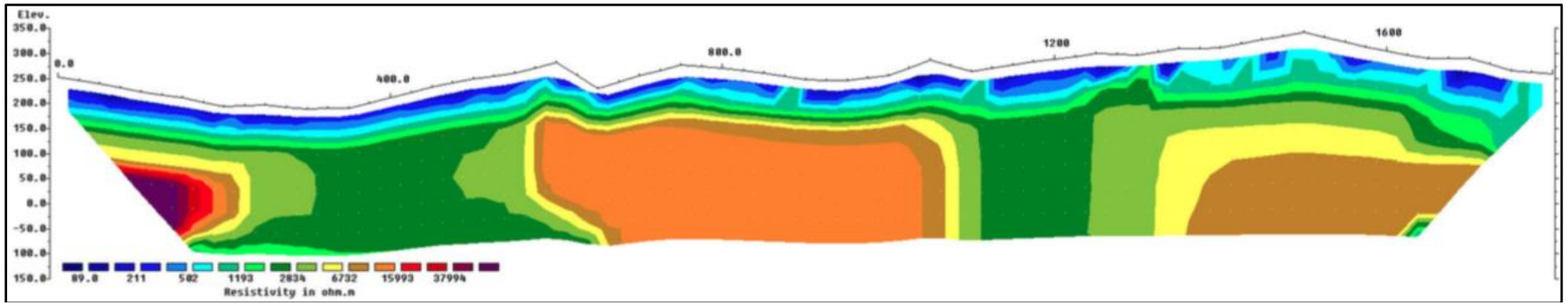

Illustration 4.1-188. Profile No 46 iso-resistivity.
Source: ARCE GEOFISICOS, 2013.

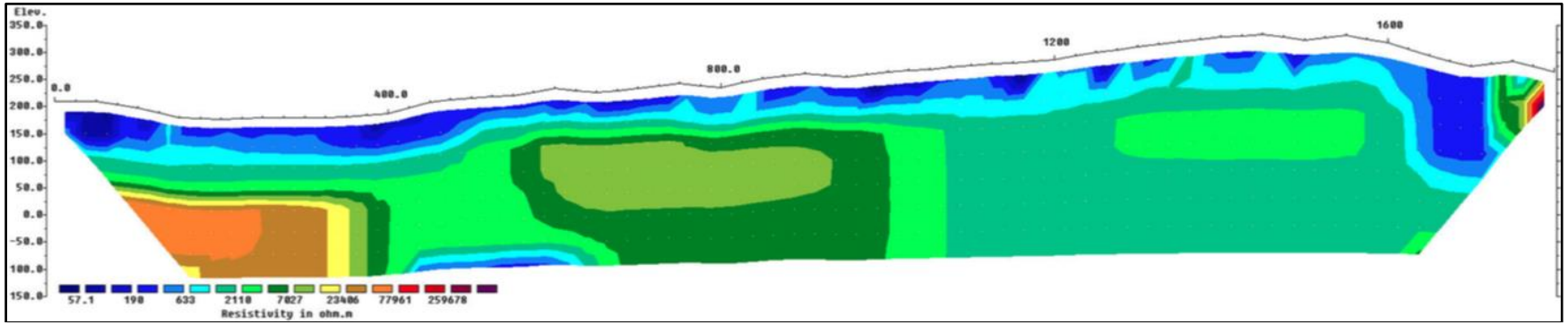

Illustration 4.1-189. Profile No 48 iso-resistivity.
Source: ARCE GEOFISICOS, 2013.

The following shows the set of geo-electrical profiles interpreted (Illustration 4.1-90 to Illustration 4.1-205). These profiles have been assigned two colors, the area of red dotted coloring corresponds mainly to the fresh granodiorite which is clearly the predominant geological unit in the subsoil, On the other hand, there is the blue dotted coloration area, which corresponds mainly to areas whose materials are very fine, as is the case of the superficial part of the profiles where the saprolite is registered and part of the residual soil; At the same time, these blue areas can indicate a lithological change, especially towards the bottom of the profiles, and can even be interpreted as the presence of fault zones, as in the case of lines 36, 42 and 48, which generate a plane of discontinuity in the rock which favors its weathering by altering minerals such as feldspars to clayey materials.

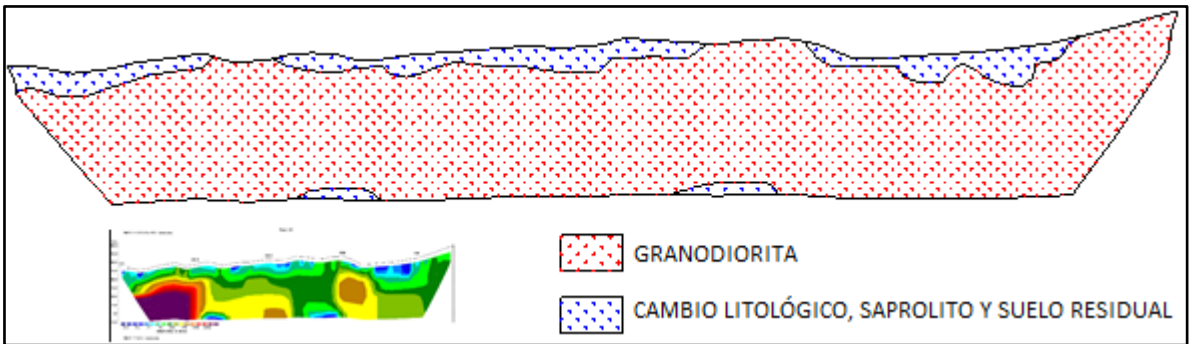

Illustration 4.1-190. Profile No. 29 iso-resistivity, interpreted applied to hydrogeology.
Source: INGEX, 2015.

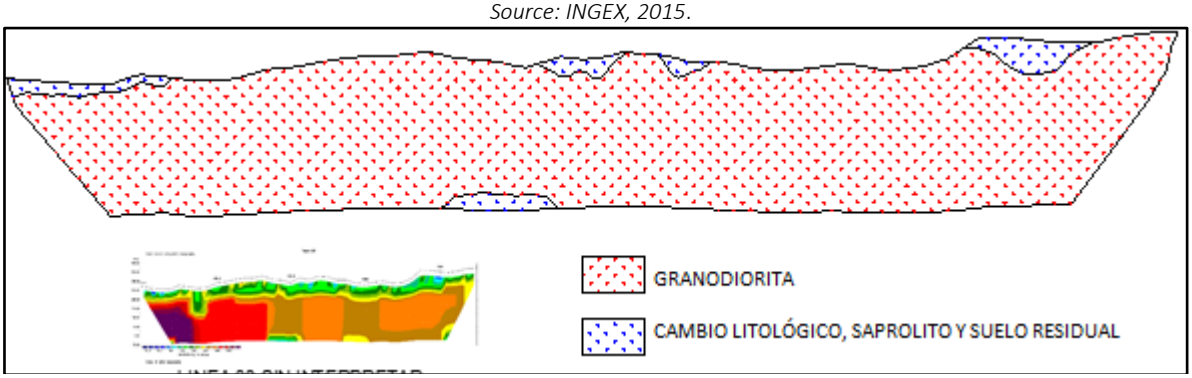

Illustration 4.1-191. Profile No. 30 iso-resistivity, interpreted applied to hydrogeology.
Source: INGEX, 2015.

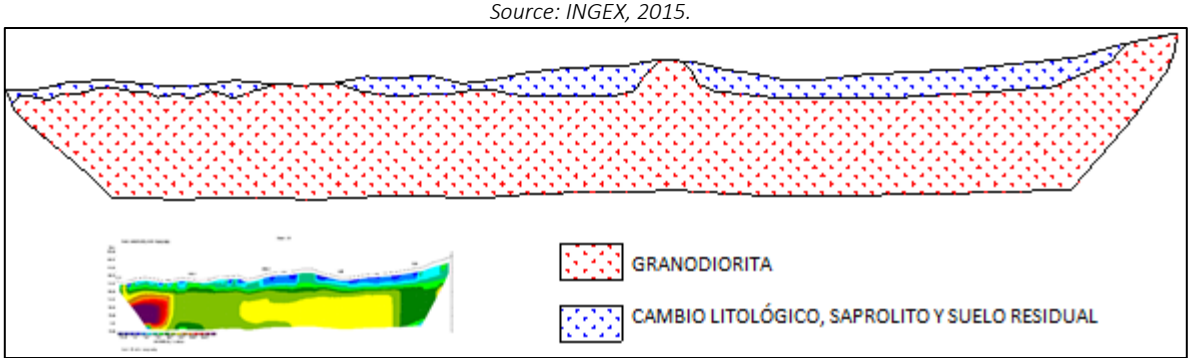

Illustration 4.1-192. Profile No. 31 iso-resistivity, interpreted applied to hydrogeology.
Source: INGEX, 2015.

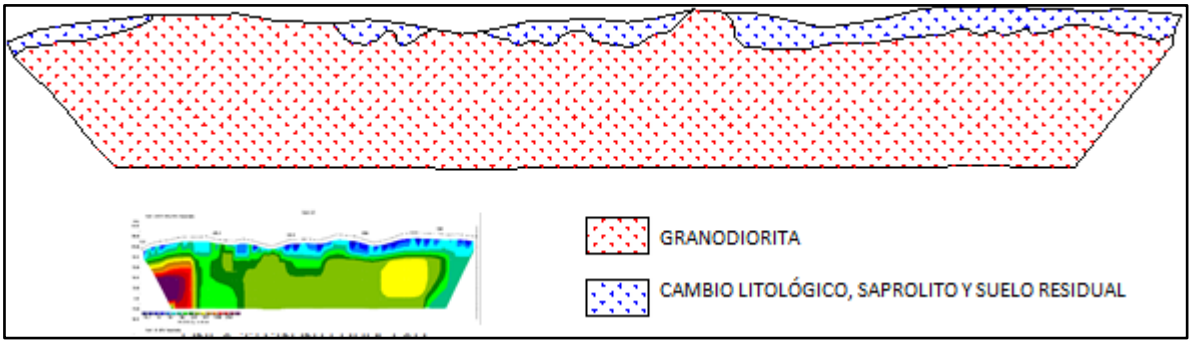

Illustration 4.1-193. Profile No. 32 iso-resistivity, interpreted applied to hydrogeology.
Source: INGEX, 2015.

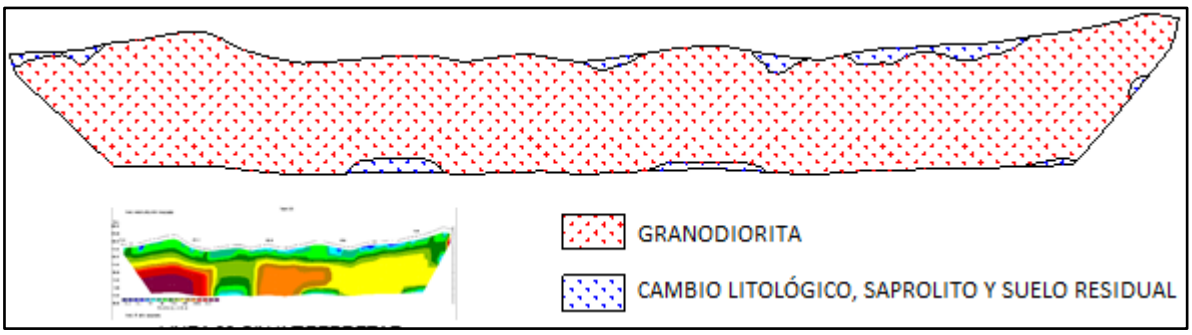

Illustration 4.1-194. Profile No. 33 iso-resistivity, interpreted applied to hydrogeology.
Source: INGEX, 2015.

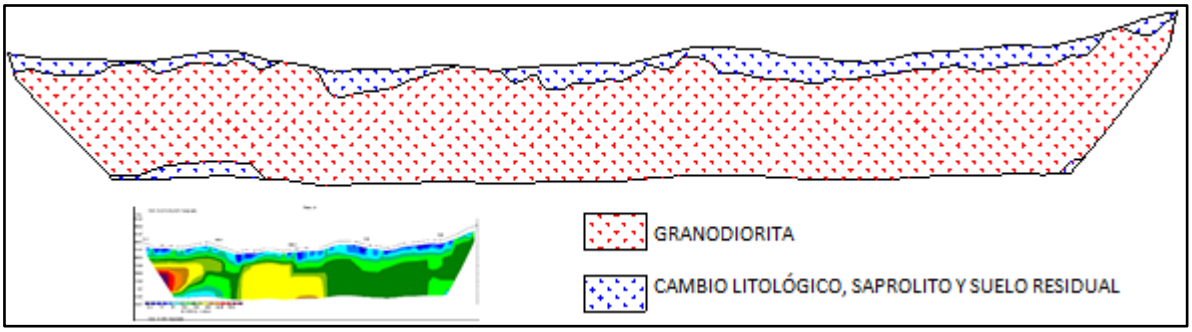

Illustration 4.1-195. Profile No. 34 iso-resistivity, interpreted applied to hydrogeology.
Source: INGEX, 2015.

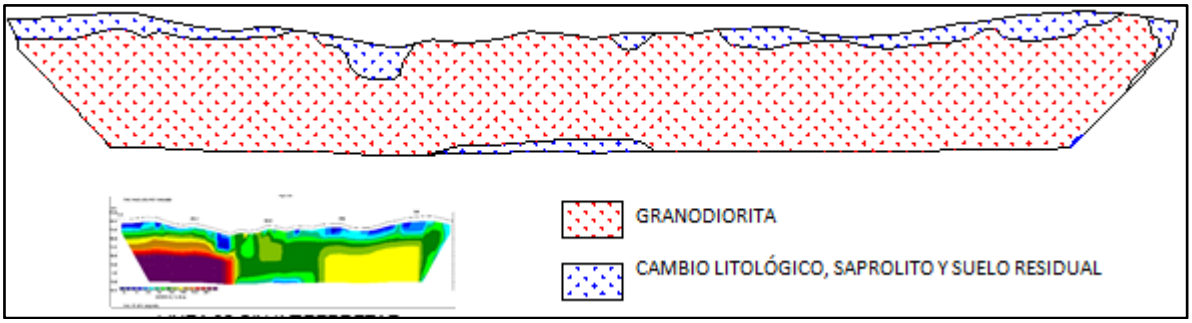

Illustration 4.1-196. Profile No. 35 iso-resistivity, interpreted applied to hydrogeology.
Source: INGEX, 2015.

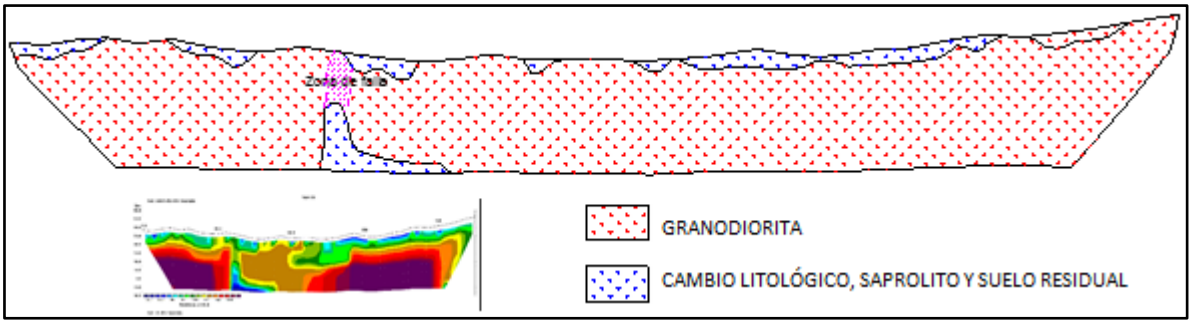

Illustration 4.1-197. Profile No. 36 iso-resistivity, interpreted as applied to hydrogeology.
Source: INGEX, 2015.

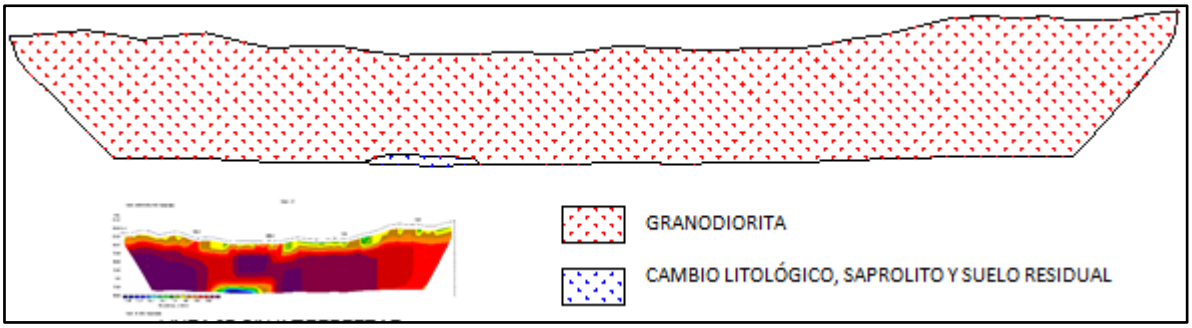

Illustration 4.1-198. Profile No. 37 iso-resistivity, interpreted as applied to hydrogeology.
Source: INGEX, 2015.

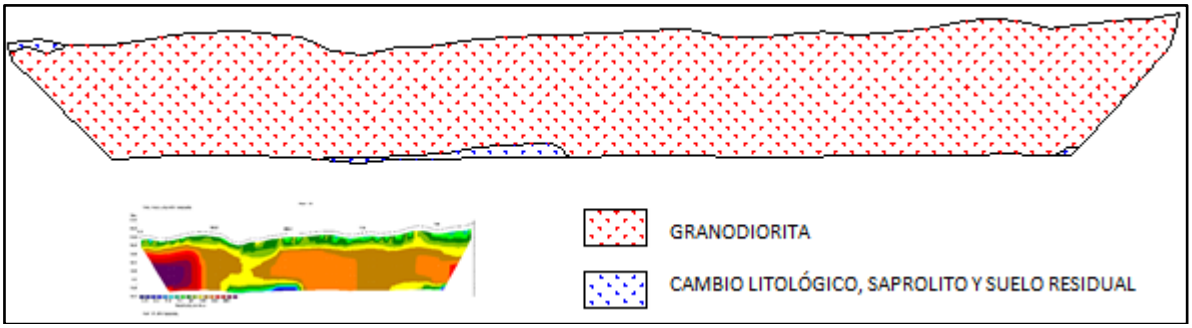

Illustration 4.1-199. Profile No. 38 iso-resistivity, interpreted applied to hydrogeology.
Source: INGEX, 2015.

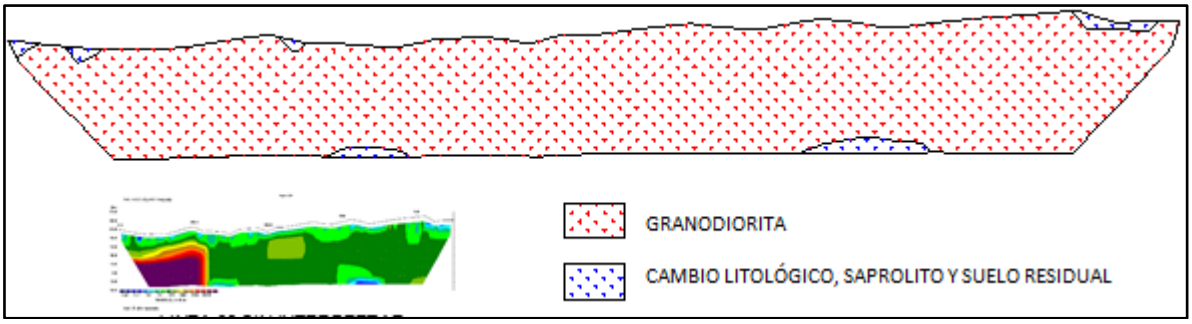

Illustration 4.1-200. Profile No. 39 iso-resistivity, interpreted as applied to hydrogeology.
Source: INGEX, 2015.

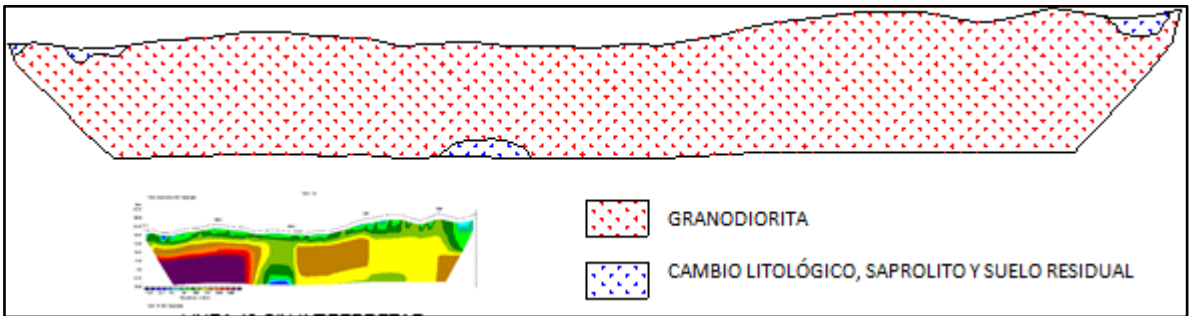

Illustration 4.1-201. Profile No. 40 iso-resistivity, interpreted applied to hydrogeology.
Source: INGEX, 2015.

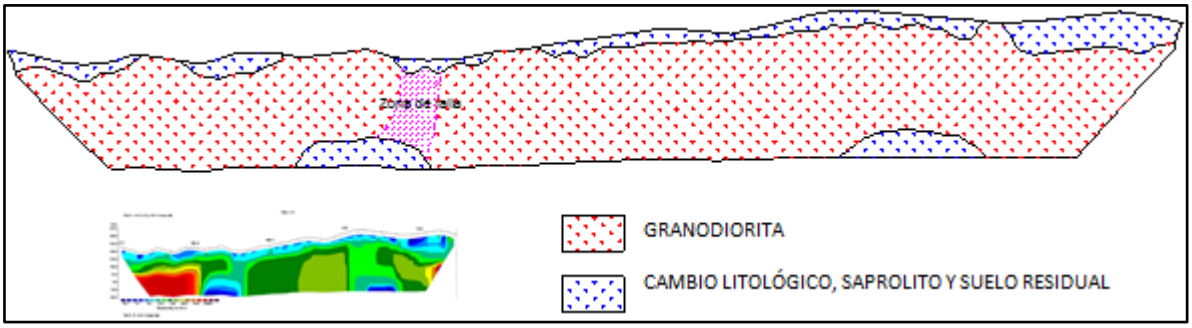

Illustration 4.1-202. Profile No. 42 iso-resistivity, interpreted applied to hydrogeology.
Source: INGEX, 2015.

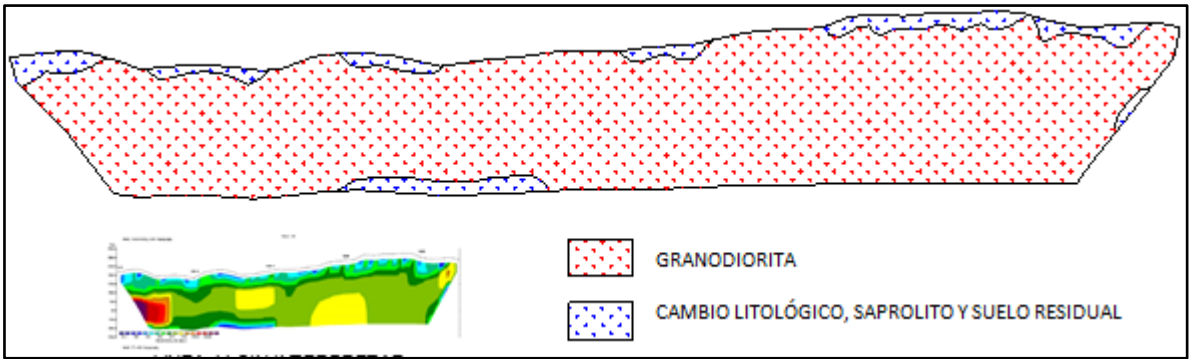

Illustration 4.1-203. Profile No. 44 iso-resistivity, interpreted as applied to hydrogeology.
Source: INGEX, 2015.

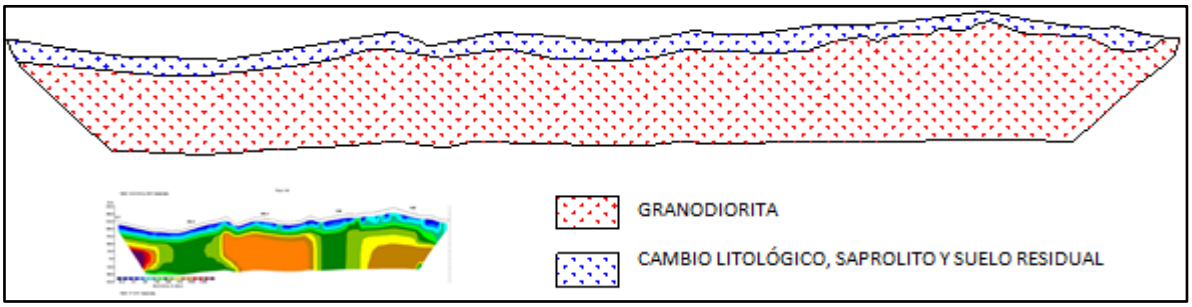

Illustration 4.1.204. Profile No. 46 iso-resistivity, interpreted as applied to hydrogeology.
Source: INGEX, 2015.

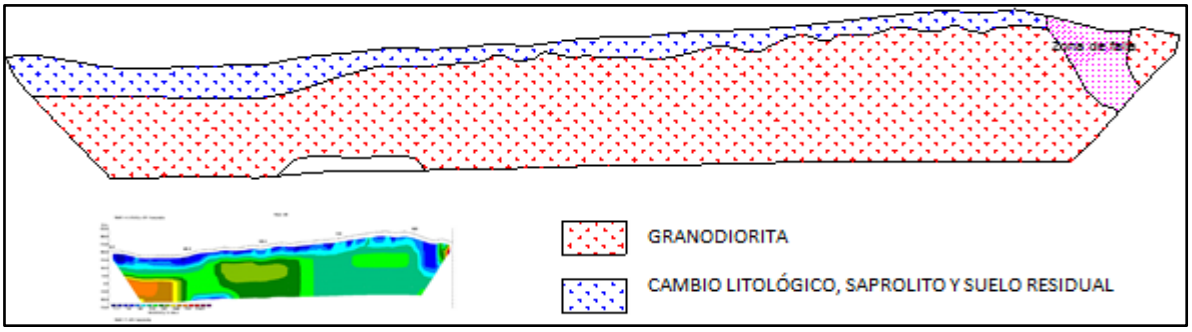

Illustration 4.1-205. Profile No. 48 iso-resistivity, interpreted as applied to hydrogeology.
Source: INGEX, 2015.

As a result of the above profiles interpreted, the following model of lithology blocks and absence of saturated zone (Absence of groundwater verified by direct exploration, lithological change, residual soil and saprolite) was constructed in different views (See Illustration 4.1-206 and Illustration 4.1-207).

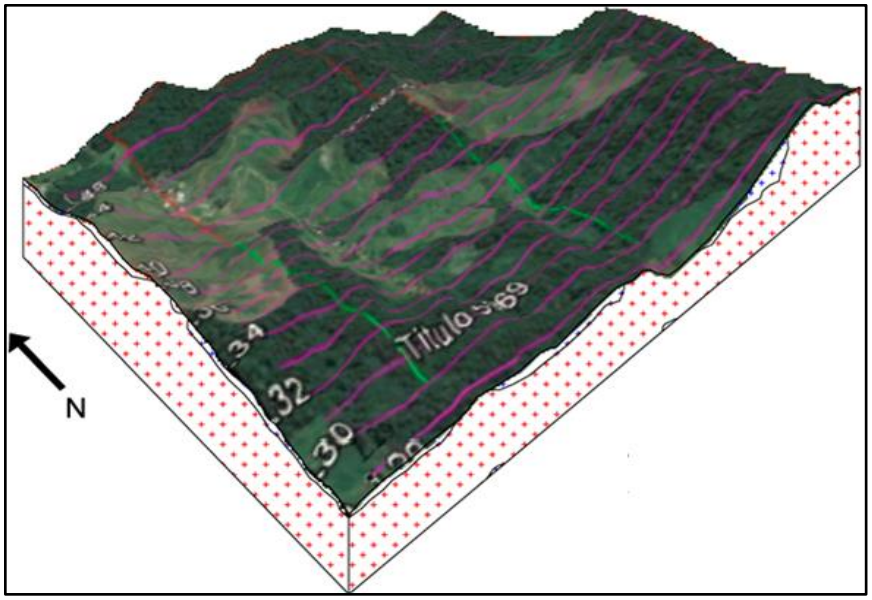

Illustration 4.1-206. Block diagrams of the geo-electric interpretation of the terrain, view No. 1.
Source: INGEX, 2015.

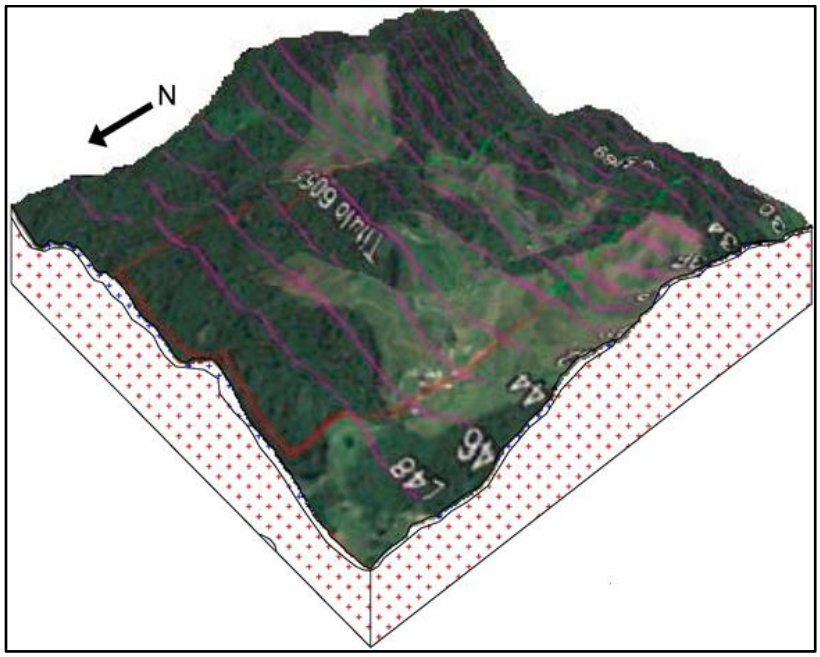

Illustration 4.1-207. Block diagrams of the geo-electric interpretation of the terrain, view No. 2.
Source: INGEX, 2015

The resistivity obtained in the tomography scans are adjusted with acceptable levels of reliability, as verified in the field geology.

The high resistivity values found correspond to typical values for igneous units, in addition to this resistivity values were found associated with areas of fine materials which may have some negligible moisture content, as shown by the soil in the soil.

The approximate thickness found for the saprolite and transition zone to fresh rock was 50 m maximum, with a notable decrease between lines 37 and 40, where the thickness of these units is not greater than 25 m.

4.1.5.6 CONCEPTUAL HYDROGEOLOGICAL MODEL

A hydrogeological model is a descriptive and graphical representation of a system of hydrogeological units that incorporates an interpretation of geological and hydraulic conditions and their interrelationship with associated systems, thereby reducing the physical problem and aquifer dominance to a simplified version of reality. A conceptual hydrogeological model is dynamic because it is constructed from temporal variables such as climatological and hydrological variables and therefore, as new information becomes available or existing information is re-evaluated, it is susceptible to adjustment (MADS, 2014).

Based on the geological model and the information gathered, it was clearly established that most of the study area is dominated by the lithology of the Batholith of Segovia. This batholith, which together with the other unaltered igneous rocks forms the UH2 - Aquifuge, by means of the weathering that has been suffered, has originated the residual soil and has contributed to the alluvial deposits of the UH1 - Aquitard. As mentioned in the classification of the hydrogeological units, the Aquitard is the only porous medium through which there could be a flow of water; however, field observations show that this unit is dry, this is evidenced by three (3) factors:

- The first of these is the exploration drilling campaign for the ore body, which was carried out to calculate gold mining reserves. These perforations did not intercept the existence of any water table in the residual soil and saprolite (UH1 - Aquitard), and in the unaltered igneous rocks (UH2 - Aquifuge).

- The second factor corresponds to the dual-purpose drilling campaign (geotechnical and hydrogeological drilling) that was carried out for the development of the stability model, nor did such drilling intercept any water table in the residual soil (UH1 - Aquitard).

Illustration 4.1-208. Detail of the execution of the SPT test in the field, sounding No. 1.
Source: INGEX, 2015.

Illustration 4.1-209. Detail of dry saprolite, sounding No. 1.
Source: INGEX, 2015.

Illustration 4.1-210. Detail of the execution of the SPT test in the field, sounding No. 6.
Source: INGEX, 2015.

Illustration 4.1-211. Detail of dry saprolite, sounding No. 6.
Source: INGEX, 2015.

The third factor is the tunnels built by inhabitants of the Segovia area, on the unit in question, to develop artisanal mining work (See Illustrations). The tunnels developed in the residual soil have reached the depth where the soil ends and the fresh rock of the batholith begins, and even at this depth, there was no presence of groundwater level indicating in a decisive way that the UH1 - Aquitard does not store groundwater.

Illustration 4.1-212. Dry residual soil or without underground water in an artisanal mining tunnel, in (UH1 - Aquitard).
Source: INGEX, 2015.

Illustration 4.1-213. Dry residual soil from artisanal mining tunnel without underground water (UH1 - Aquitard).
Source: INGEX, 2015.

Illustration 4.1-214. Artisanal mining tunnel, transfer of residual soil to saprolite (UH1 - Aquitard).
Source: INGEX, 2015.

Illustration 4.1-215. Artisanal mining tunnel, transfer of residual soil to saprolite (UH1 - Aquitard).
Source: INGEX, 2015.

In addition to the evidence of the non-existence of groundwater in UH1, the analysis of the potential for soil infiltration must be taken into consideration, which establishes that in the study area the average value of annual infiltration is 17.8 mm/year, with a more probable value of 8 mm/year, compared with the average annual precipitation of approximately 3 mm/year.500 mm/year, corresponds to approximately 0.2%, i.e. of every 1,000 mm of precipitation, only 2 mm have a high potential to infiltrate the soil (under ideal conditions or with 100% potential) according to their current conditions, therefore infiltration under non-ideal or practical conditions can be much less than 0.2% or 8 mm/year, thus being considered negligible.

This infiltration/precipitation ratio is very low. This explains why there is no groundwater in the residual soil, and also allows us to understand why the springs of the water systems are at topographic heights close to the watershed, since the water does not have the possibility of infiltrating the upper zones of the basin, so it must drain superficially, giving rise to an early origin, in terms of its course over the basin, of the water currents.

From the above, it is conclusive that UH1 is not a groundwater storage unit, and due to its low permeability, it hinders the flow of water through it, mainly favoring direct surface runoff in areas of high slope, and little infiltration into the low slope highlands and then discharged into the headwaters of the surface water streams by shallow subsurface flow (See Illustration 4.1-216 and Illustration 4.1-217).

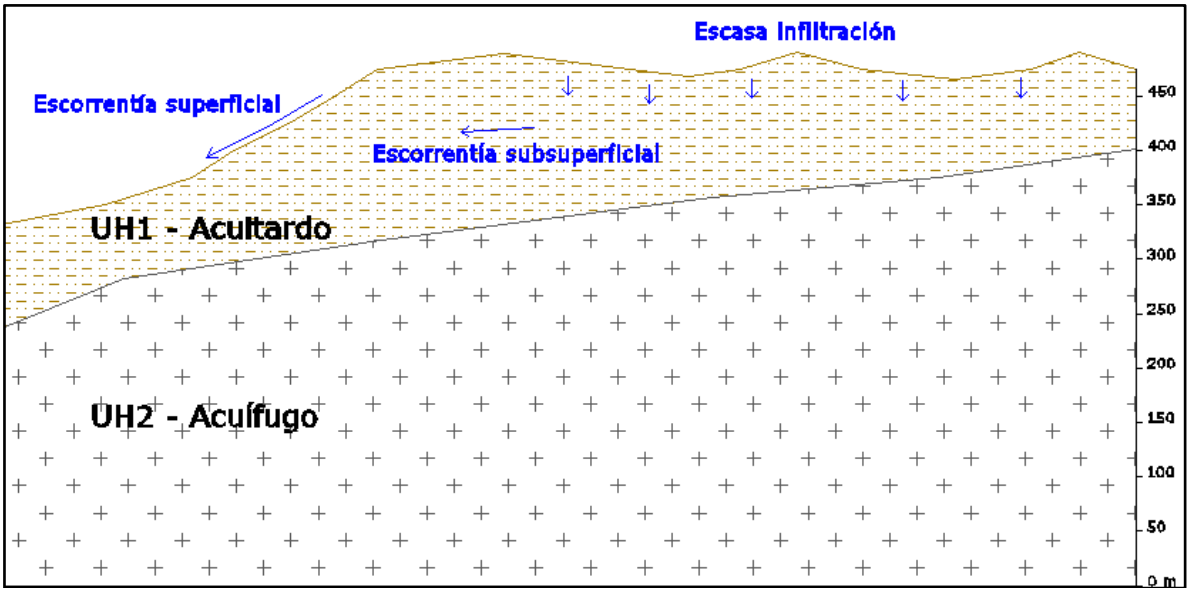

Illustration 4.1-216. Schematic profile of the water flow system in the waste soil.
Source: INGEX, 2015.

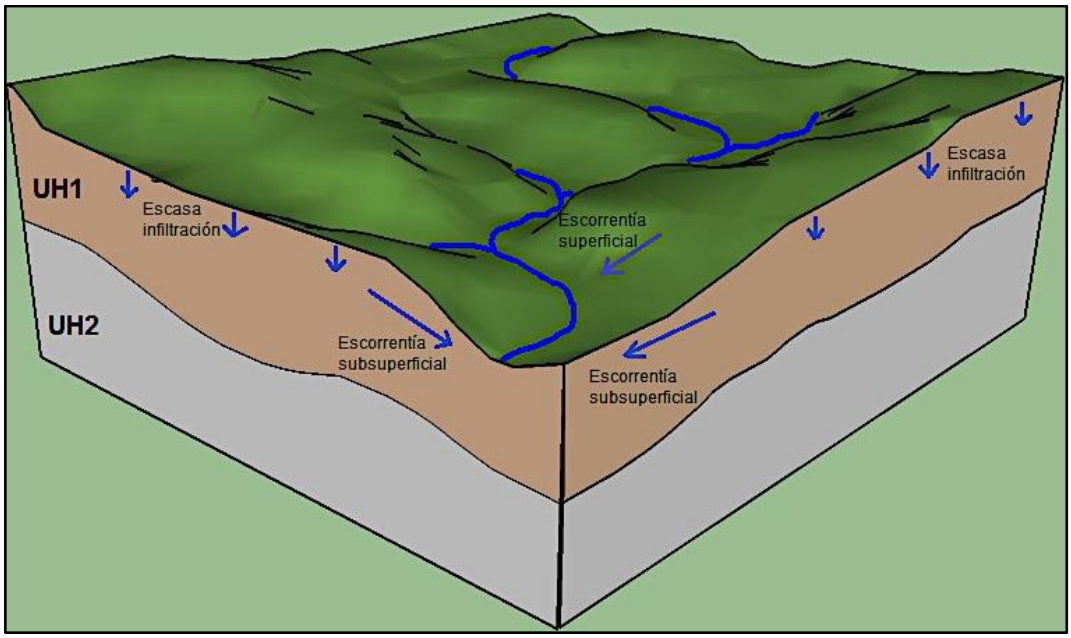

Illustration 4.1-217. Block diagram of the water flow system in the waste soil.
Source: INGEX, 2015.

4.1.5.7 OTHER CONSIDERATIONS ON HYDROGEOLOGY

The hydrogeological analysis carried out above tries to comply with the content required in the terms of reference for the elaboration of the environmental baseline; however, due to the hydrogeological conditions of the study area, due to the absence of groundwater in the porous environment, it is not possible to analyze the remaining items for the following reasons:

4.1.5.7.1 Hydrochemical analysis of groundwater

Because no groundwater was found in the porous medium within the study area, no hydrochemical sampling or analysis of the water resource was performed.

4.1.5.7.2 Intrinsic vulnerability of the aquifer to pollution

Similarly, the other existing methods take into account the variable depth of the groundwater or aquifer from the ground surface. But for this particular case study, since there is no presence of groundwater, there is no element susceptible to contamination, therefore no method of analysis of intrinsic vulnerability to contamination is applicable.

4.1.5.7.3 Pumping test and determination of hydraulic parameters

In order to obtain direct information from an aquifer, it is necessary to drill wells or special piezometers that allow groundwater to be pumped and to measure withdrawal and recovery levels in order to determine the hydraulic parameters of the aquifer. This work was planned in conjunction with the geotechnical exploration which collected soil samples. The intention was to use drilling for two purposes, to extract cores from the soil for geotechnical testing and to determine the existence of the groundwater level for pumping tests; however, no groundwater level was intercepted during drilling, so that the pumping tests could not be carried out and the hydraulic parameters of the hydrogeological unit known as the aquitard could not be determined.

4.1.5.7.4 Numerical hydrogeological model

The purpose of the numerical hydrogeological model is to simulate the behavior of the groundwater resource by determining the position of the groundwater table at a given time and its variation according to the development of mining activities that could affect it. This modeling is developed based on the numerical modeling protocol proposed by Anderson & Woessner (2002) and using computer software that can implement finite element or finite difference numerical methods, depending on the modeler's preference. However, due to the results obtained in the conceptual hydrogeological model, it is not appropriate to implement a numerical model for a semi-permeable hydrogeological unit in whose system there are no aquifer units or groundwater saturation levels in the subsoil.

4.1.5.7.5 Monitoring Wells network

As mentioned above, the geotechnical-hydrogeological dual-purpose drilling did not find the groundwater level and therefore it was not possible to form the well network for pumping testing and groundwater monitoring.

4.1.6 ATMOSPHERE

The climate component is presented below.

4.1.6.1 WEATHER

Below are the annual cycles and/or spatial results of precipitation, evapotranspiration, relative humidity, temperature, brightness and solar radiation, atmospheric pressure, cloudiness and aridity index.

4.1.6.1.1 Precipitation

The annual cycle of the rainfall stations that circumscribe the study area, with data from anomalous years excluded from the data quality validation, is presented in Table 4.1-91 and Illustration 4.1-218.

Table 4.1-91. Multiannual mean rainfall for nearby stations.

CODE	NAME	ANNUAL RAINFALL (mm/año)	RAINFALL (mm/mes)											
			JAN	FEB	MAR	APR	MAY	JUN	JUL	AGO	SEP	OCT	NOV	DEC
27030090	The Forest	4638.6	127.2	126.6	181.9	380.7	529.1	479.8	452.8	510.9	501.1	558.1	485.9	304.5
27030140	Coconut Palm	3994.7	100.9	112.8	161.3	334.4	456.6	388.8	382.4	452.3	436.9	503.8	412.1	252.5
27030220	The West	3756.6	155.8	177.9	135.2	311.4	359.8	260.6	283.2	351.4	383.0	556.5	440.6	341.1
27011100	The Breezes	3784.1	101.3	115.3	153.6	314.9	445.1	386.5	366.6	397.6	413.7	436.8	410.0	242.6
27030130	The Londre	3844.2	191.8	179.6	149.0	341.7	344.6	265.4	260.7	359.8	418.0	496.0	462.9	374.8

Source: INGEX, 2015.

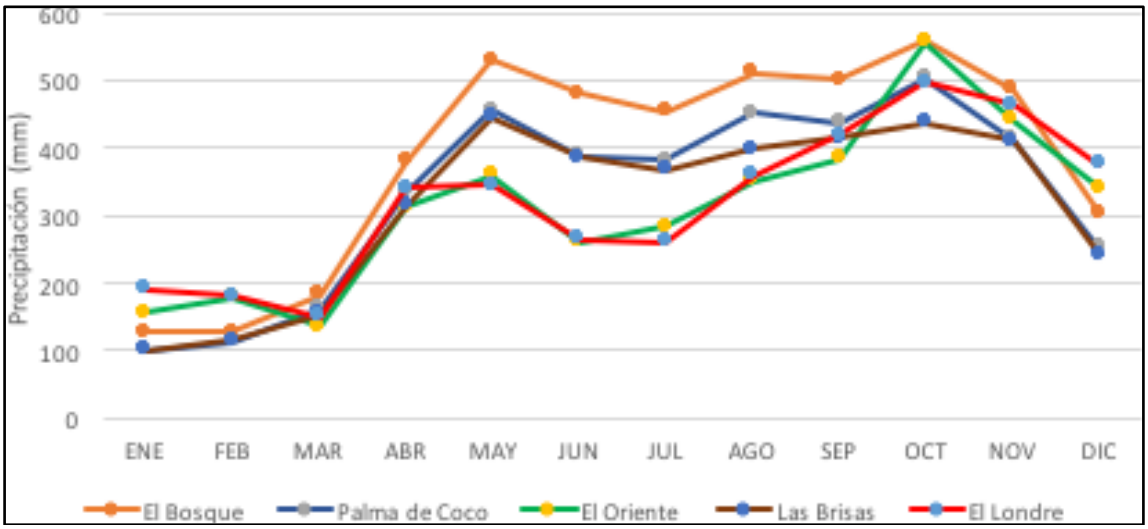

Illustration 4.1-218. Monthly precipitation values.
Source: INGEX, 2015.

The rainiest months are May and October (Winter), while the least rainy months are January to March. At the end of summer between March and May there is an increase in precipitation (from summer to winter), and between May and October precipitation fluctuates, with a constant high trend, where rainfall can occur at different intensities. Ending the winter in October until December decreases rainfall (Winter-Summer Transition).

Illustration 4.1-219 shows the spatial variation of precipitation, where in the northern areas there are annual precipitation averages much higher than in the southern part.

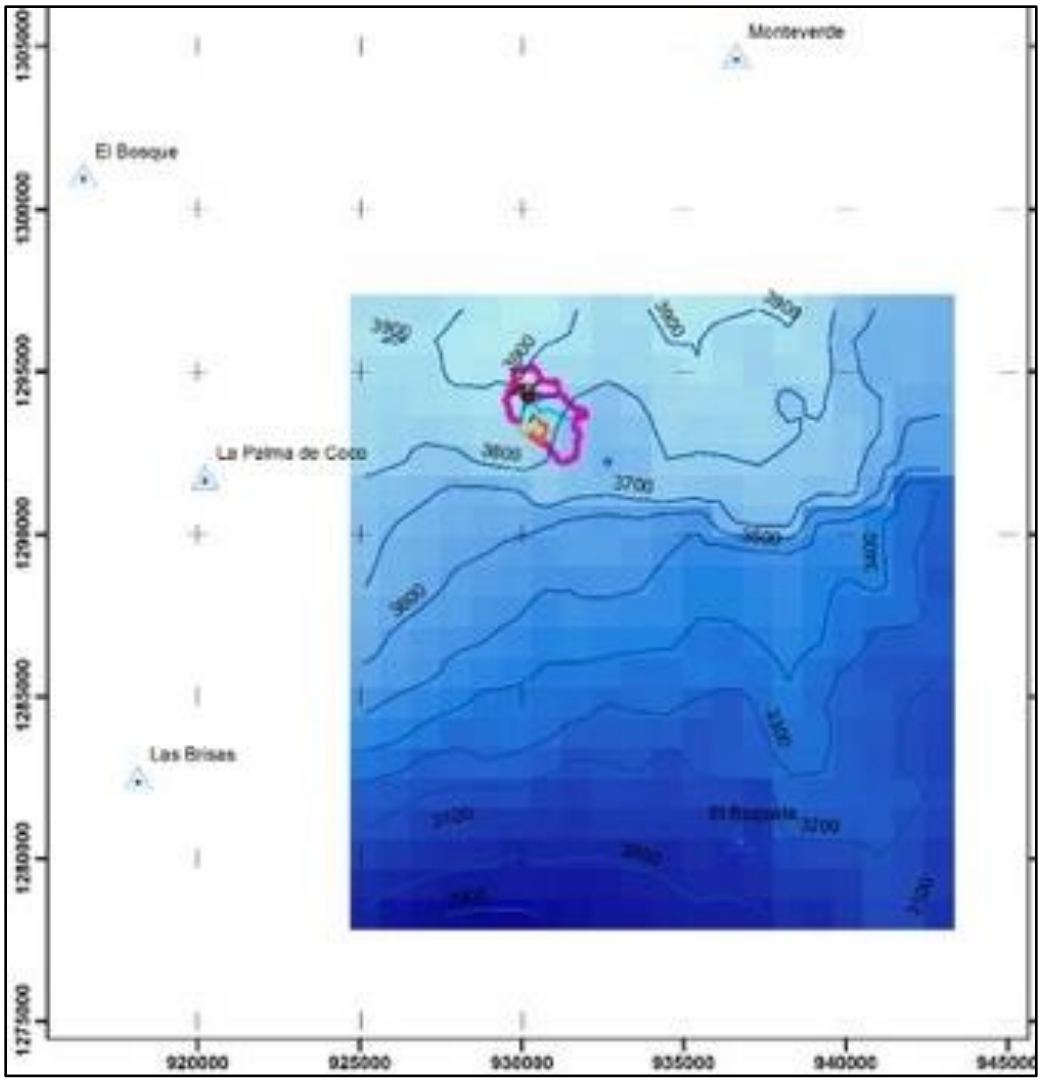

Illustration 4.1-219. Spatial distribution of precipitation.
Source: INGEX, 2015.

4.1.6.1.2 Evapotranspiration

The annual cycle of the stations with evapotranspiration records, which circumscribe the study area, with data from anomalous years excluded from the validation of information quality, are presented in Table 4.1-92 and Illustration 4.1-220.

Table 4.1-92. Monthly evaporation values for nearby stations.

CODE	NAME	annual evaporation (mm/year)	EVAPORATION (mm/year)											
			JAN	FEB	MAR	APR	MAY	JUN	JUL	AGO	SEP	OCT	NOV	DEC
27035020	El Boquete	1419.10	104.00	110.70	115.10	120.50	126.40	115.50	134.10	139.90	123.90	121.80	104.20	103.00

Source: INGEX, 2015.

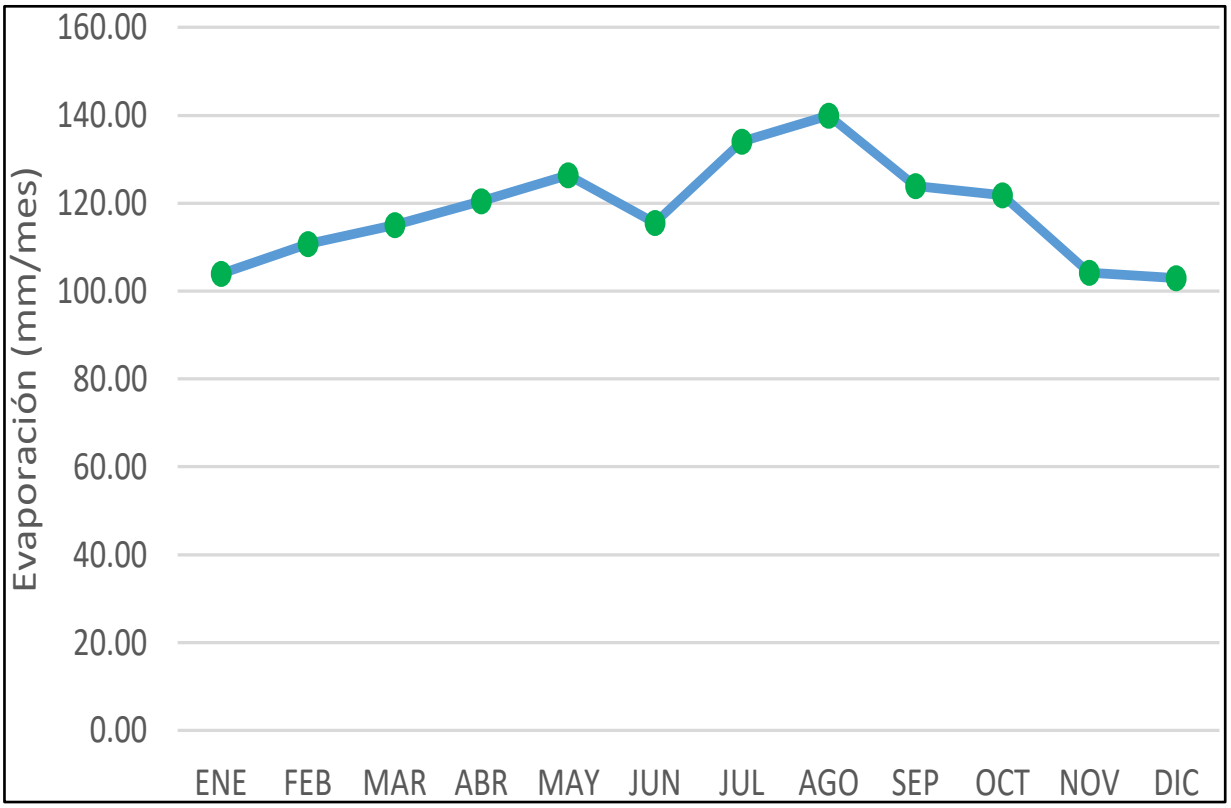

Illustration 4.1-220. Monthly evaporation values.
Source: INGEX, 2015.

Evaporation has a tendency to increase during the months of January to May, coinciding with the increase in precipitation in the study area. This behavior indicates that the water that the basin brings to the system through evaporation tends to return in the form of precipitation. Between August and December evaporation tends to decrease, as does rainfall.

Illustration 4.1-221 shows the spatial variation of evapotranspiration, where evapotranspiration has a high relationship with height, i.e., in the stream valleys the highest evapotranspiration values are found and, on the other hand, the lowest evapotranspiration values are found at the tops.

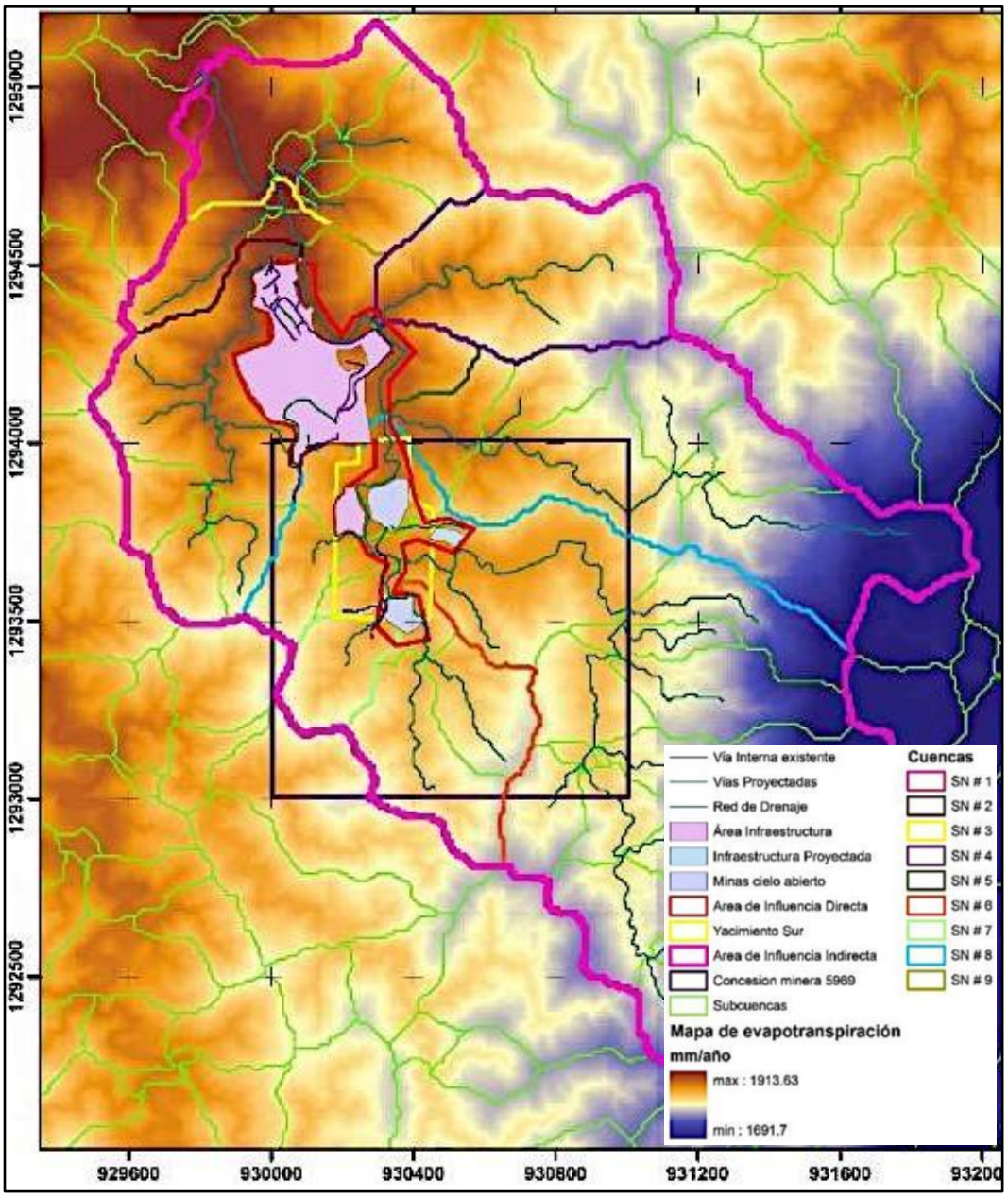

Illustration 4.1-221. Spatial distribution of evapotranspiration.
Source: INGEX, 2015.

The value of evapotranspiration is 1883.23mm/year, while for the area of indirect influence it is 1826.17mm/year.

4.1.6.1.3 Relative humidity

The annual cycle of the stations with relative humidity records, which circumscribe the study area, with data from anomalous years excluded from the data quality validation, are presented in Table 4.1 93 and Illustration 4.1-222.

Table 4.1-93. Monthly relative humidity values for nearby stations.

CODE	NAME	Rh (%)	RELATIVE HUMIDITY (%)											
			JAN	FEB	MAR	APR	MAY	JUN	JUL	AGO	SEP	OCT	NOV	DEC
27035020	El Boquete	84.9	84	83	84	84	85	85	84	85	86	86	87	86

Source: INGEX, 2015.

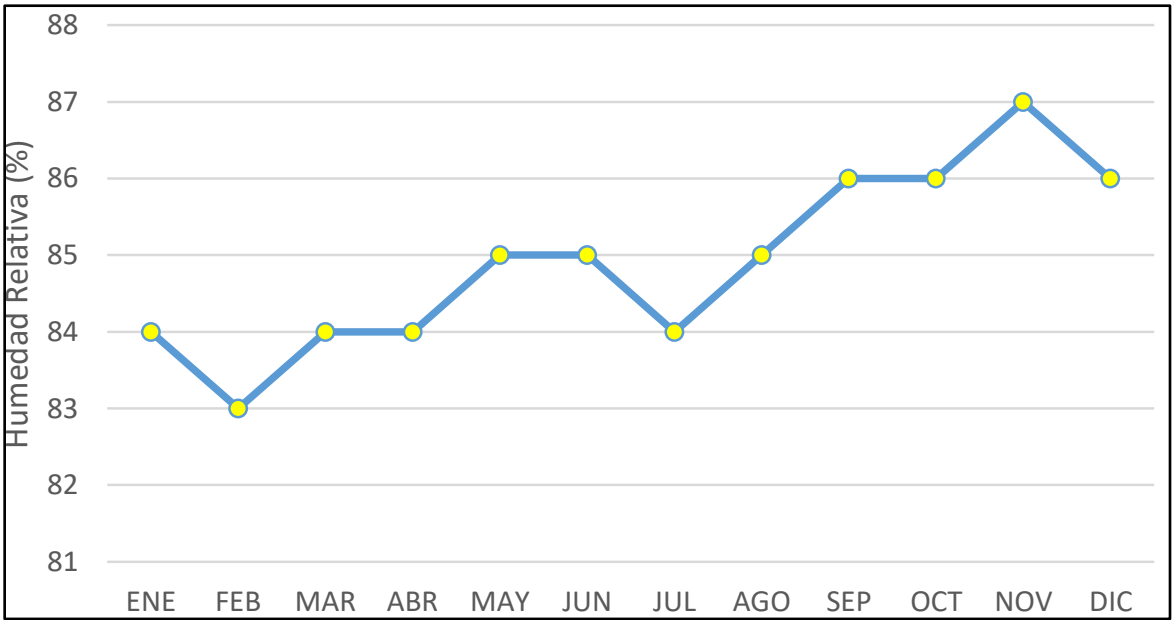

Illustration 4.1-222. Monthly relative humidity values.
Source: INGEX, 2015.

The relative humidity increases as the rainfall in the study area increases, and this increase is more marked towards the second half of the year, when the highest precipitation values are obtained.

4.1.6.1.4 Temperature

Illustration 4.1-223 shows the spatial distribution of the mean annual temperature in the study area. It is observed that the lowest temperatures correspond to the zone of the highest altitude, reaching up to 24.6°C, while the highest temperatures are associated with the river valleys, reaching 26.6°C.

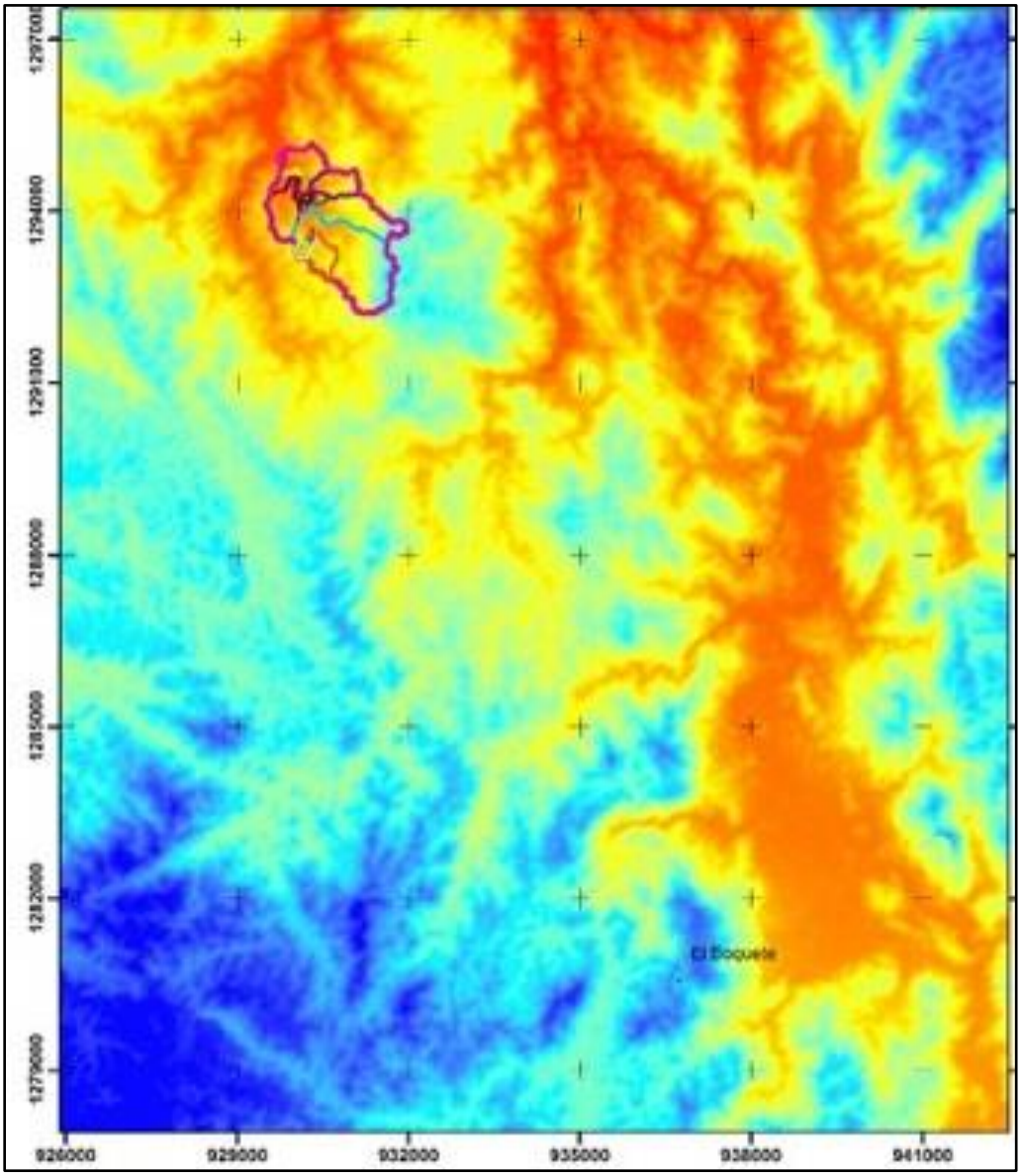

Illustration 4.1-223. Spatial temperature variation.
Source: INGEX, 2015.

4.1.6.1.5 Solar Brightness

The annual cycle of the stations with sunshine records, which circumscribe the study area, with data from anomalous years excluded from the validation of information quality, are presented in Illustration 4.1-224.

CODE	NAME	Solar Brightness (hours)	Solar Brightness (hours)											
			JAN	FEB	MAR	APR	MAY	JUN	JUL	AGO	SEP	OCT	NOV	DEC
27035020	The Boquete	160.0	190.4	171.4	141.2	143.0	158.0	129.9	163.6	183.6	148.0	146.3	170.9	173.9

Source: INGEX, 2015.

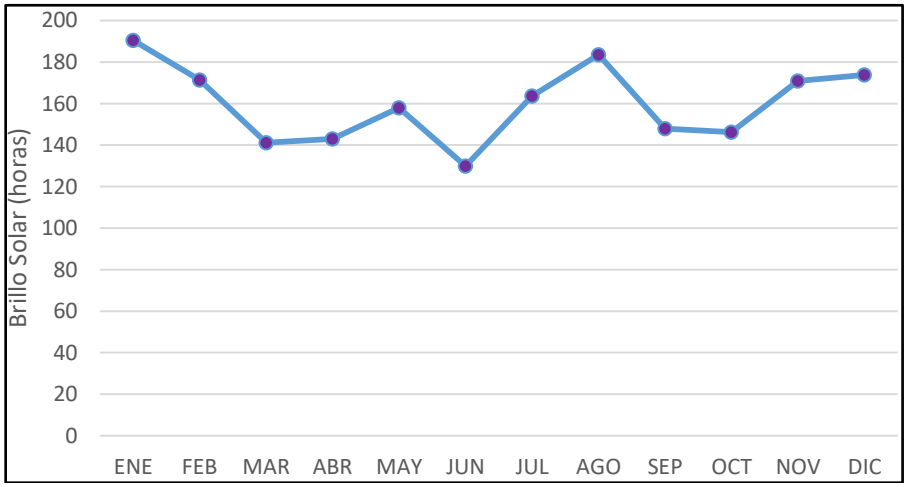

Illustration 4.1-224. Monthly values of solar brightness.
Source: INGEX, 2015.

The values of solar brightness for the study area are uniform throughout the year, with the minimums of solar brightness coinciding with the maximums of precipitation. This is because during this time, clouds decrease the amount of sunshine that reaches the earth's surface.

4.1.6.1.6 Solar radiation

From the solar radiation information, extracted from the NCEP/NCAR reanalysis, the annual cycle of this variable was estimated and its behavior throughout the year was analyzed.

Table 4.1-94 and Illustration 4.1-225 show the average solar radiation value and the annual cycle. The solar radiation is maximum during the spring and autumn equinoxes, due to the proximity of the sun to the earth, while in the winter and summer solstices the solar radiation is less.

Table 4.1-94. Monthly solar radiation values for the NCEP/NCAR point.

CODE	NAME	Solar radiation (kWh/m^2)	SOLAR RADIATION (kWh/m2)											
			JAN	FEB	MAR	APR	MAY	JUN	JUL	AGO	SEP	OCT	NOV	DEC
N/A	Solar radiation Point 1	3.8	3.1	3.5	4.1	4.3	4.1	3.9	3.9	4.0	4.0	4.0	3.6	3.2

Source: INGEX, 2015.

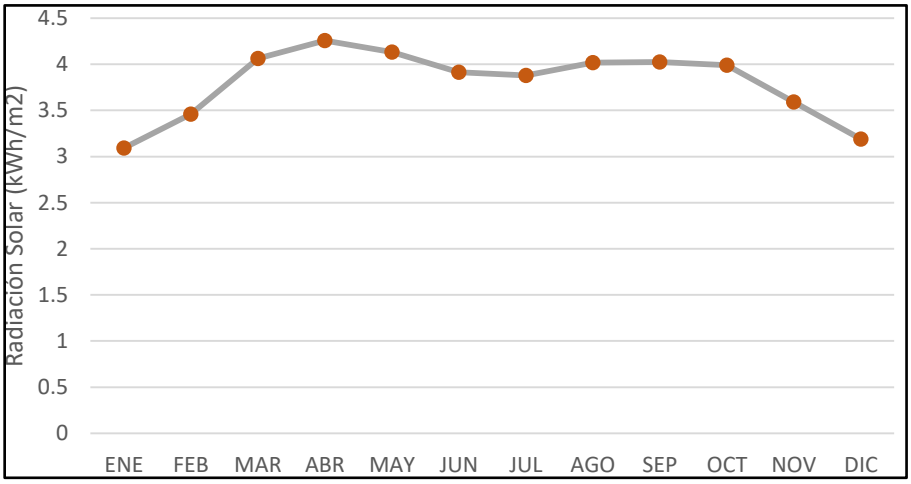

Illustration 4.1-225. Monthly solar radiation values.
Source: INGEX, 2015.

4.1.6.1.7 Atmospheric pressure

From the atmospheric pressure information, extracted from the NCEP/NCAR reanalysis, the annual cycle of this variable was estimated and its behavior throughout the year was analyzed.

Table 4.1-95 and Illustration 4.1-226 show the average air pressure value and the annual cycle. The atmospheric pressure presents a unimodal cycle with peaks in the middle of the year, and minimums at the end and beginning of the year.

Table 4.1-95. Monthly atmospheric pressure values at NCEP/NCAR point.

CODE	NAME	Atmospheric Pressure (mbar)	ATMOSPHERIC PRESSURE (mbar)											
			JAN	FEB	MAR	APR	MAY	JUN	JUL	AGO	SEP	OCT	NOV	DEC
N/A	Atmospheric Pressure Point 1	912.5	911.9	912.0	912.1	912.3	912.8	913.0	913.2	913.1	913.1	912.8	912.0	912.1

Source: INGEX, 2015.

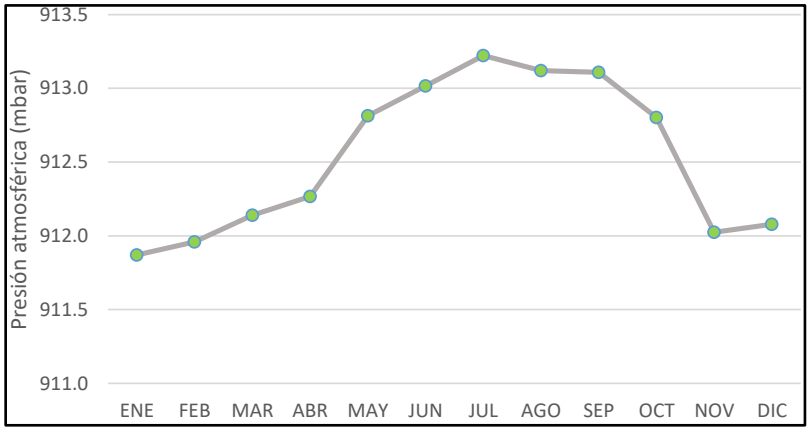

Illustration 4.1-226. Monthly values of atmospheric pressure.
Source: INGEX, 2015.

4.1.6.1.8 Cloud cover

From the cloudiness information, extracted from the NCEP/NCAR reanalysis, the annual cycle of this variable was estimated and its behavior throughout the year was analyzed. Table 4.1.96 and Illustration 4.1.227 show the value of the average cloud cover and the annual cycle in the east. In this area, cloud cover is around 73% throughout the year, with cloud cover peaking in the rainy months.

Table 4.1-96. Monthly cloudiness values for the reanalysis point.

CODE	NAME	Cloudiness (%)	CLOUDINESS (%)											
			JAN	FEB	MAR	APR	MAY	JUN	JUL	AGO	SEP	OCT	NOV	DEC
N/A	Cloudiness point 1	73.4	70.5	74.4	77.4	76.2	74.8	72.6	71.7	72.3	70.2	74.6	74.5	72.1

Source: INGEX, 2015.

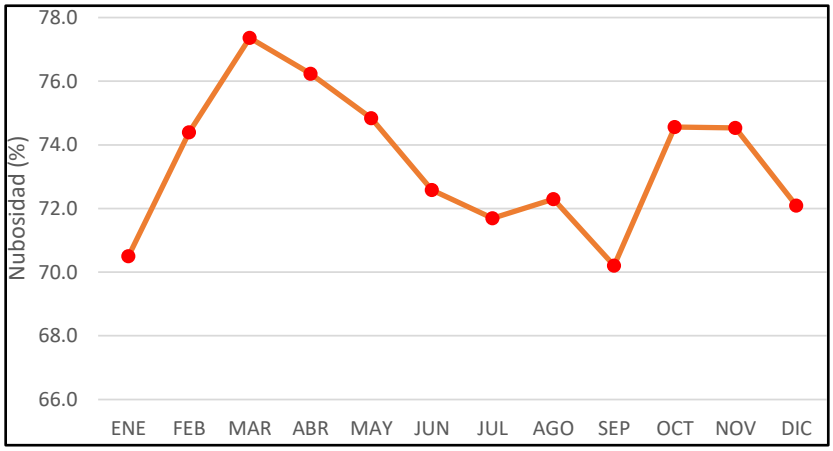

Illustration 4.1-227. Monthly cloud cover values.
Source: INGEX, 2015.

4.1.6.1.9 Aridity index

The spatial variation of the aridity index of the study area is shown below. Result of the relationship between the mean multiannual precipitation and the potential evapotranspiration of the study area. From Illustration 4.1-228 it can be seen that the area does not have a desert value and therefore a good indication of humidity.

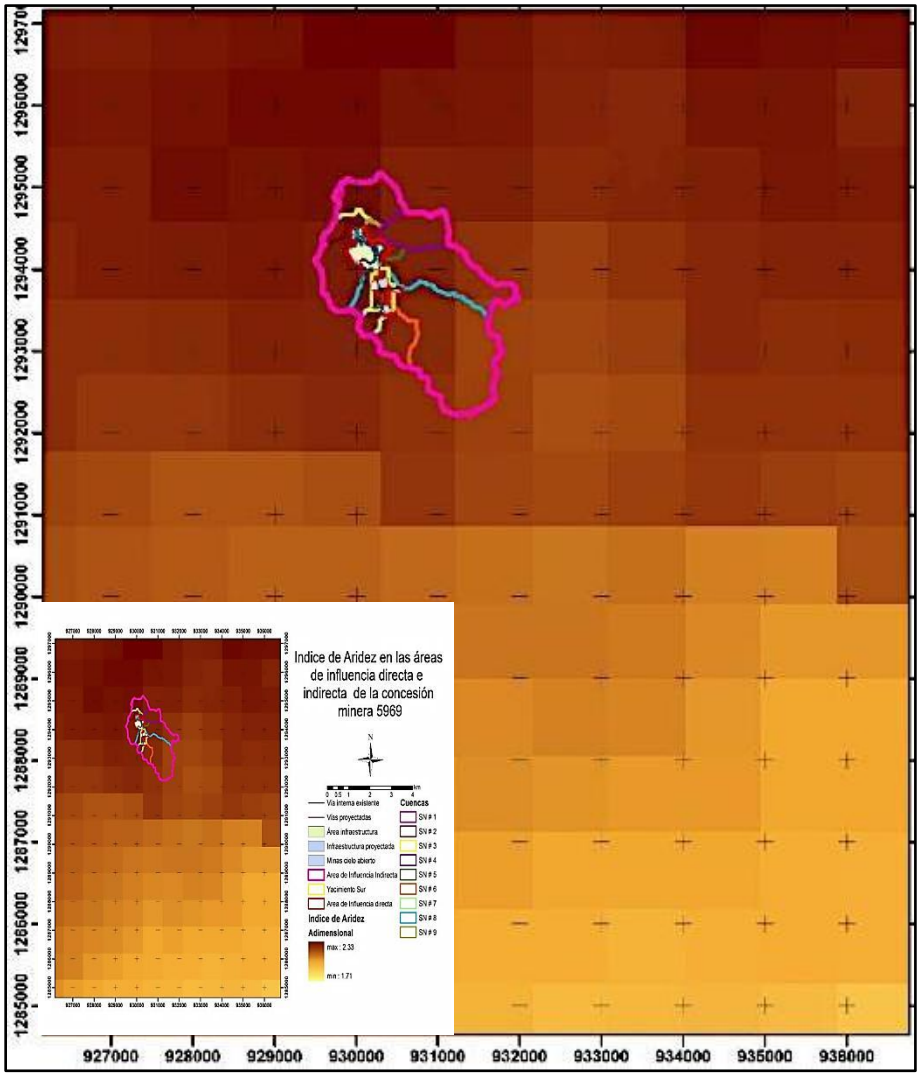

Illustration 4.1-228. Spatial variation of the aridity index.
Source: INGEX, 2015.

4.1.6.2 AIR QUALITY

Air is one of the basic elements of every living thing. The lungs filter about 15 kg of atmospheric air daily, while the human body absorbs only 2.5 kg of water and less than 1.5 kg of food.

For this reason, since ancient times, man has been aware of the danger posed by a polluted atmosphere such as that created naturally, for example by a volcanic eruption. Subsequently, with the advent of the industrial era, the problem of pollution and atmospheric pollution took on all its magnitude and has become a growing concern in urban and industrial areas.

In order to know the air quality in the vicinity of the mining project "El Pescado" in Segovia- Antioquia, where Ingex Grupo Minero S.A.S. carries out the mining exploration phase, the company Especialista en Ingeniería, Medio Ambiente y Servicios S.A.S. was sub-contracted, who, through the Public Health Laboratory of the University of Antioquia, conducted the respective air quality assessments. The Laboratory is accredited by the Instituto de Hidrología, Meteorología y Estudios Ambientales de Colombia (IDEAM) under Resolution 2448 of October 3, 2012, by which accreditation is granted to the Public Health Laboratory attached to the Extension Center of the National School of Public Health "Héctor Abad Gómez" of the University of Antioquia, to produce quantitative, physical and chemical information for the environmental studies or analyses required by the competent Environmental Authorities.

4.1.6.2.1 Results and Analysis

The evaluations carried out are compared with Resolution 610 of 2010 of the Ministry of Environment, Housing and Territorial Development, now the Ministry of Environment and Sustainable Development. The permissible limit values are corrected to the reference conditions of the municipality of Segovia Antioquia, in which the permissible limits are observed and the Norm that dictates them. It is important to note that they are taken as base values for correction at reference conditions of 760 mmHg and 25 °C.

Table 4.1-97. Exposure limit values for evaluated contaminants.

POLLUTANT	LIMIT VALUE FOR REFERENCE CONDITIONS	LAW
Particles smaller than 10µ (PM_{10})	Annual Exposure 50 µg/m^3 Daily Exposure 100 µg/m^3	Resolution 610 of March 2010 of the Ministry of Environment, Housing and Territorial Development, now, Ministries of Environment and Sustainable Development.
Sulphurous Anhydride (SO_2)	Annual Exposure 80 µg/m^3 Daily Exposure 250 µg/m^3	
Nitrogen Dioxide (NO_2)	Annual Exposure 100 µg/m^3 Daily Exposure 150 µg/m^3	

Source: Ingex, 2016

4.1.6.2.1.1 Air quality results point

4.1.6.2.1.1.1 PM_{10} Point 1 Evaluation

PM_{10} Point 1 evaluations were performed with mass flow equipment, in the time period from November 24 to December 12, 2015. The Table 4.1-98 displays weather conditions and data at the time of equipment calibration.

Teble 4.1-98. Equipment PM_{10} Point 1 calibration

m	b	r	Pa (mmHg)	Ta (K)	SSP (CFM)		
1,005394	0,02160	0,999986	723,3	300,55	36,98		
CALIBRATION							
Orifice	H (inH_2O)	IC (CFM)	IC_t ($CFM*K^{0,5}/mmHg^{0,5}$)	Q_{a_orif} (m^3/min)	Q_a_Curve (m^3/min)	Dif (m^3/min)	Fulfilled
18	3,4	39	25,140	1,204	1,205	0,001	Yes
13	3,2	38	24,495	1,168	1,168	0,001	Yes
10	3	37	23,851	1,132	1,131	0,001	Yes
7	2,8	36	23,206	1,094	1,094	0,001	Yes
5	2,6	35	22,561	1,055	1,057	0,001	Yes
m_1		($CFM*K^{0,5}/mmHg^{0,5}$)/(m^3/min)		17,37403	1) Dif <0,04 m^3/min, all points		Yes
b_1		$CFM*K^{0,5}/mmHg^{0,5}$		4,20486	2) 4 de 5 points within the range		Yes
r_1				0,99980	3)Correlation coefficient r>=0,99		Yes

Source: Ingex, 2016

STANDARDS:

1. Difference for all points ≤ 0.04 m^3/min.
2. 4 of the 5 points must be within the working range, for PM_{10} [1.02-1.24] m^3/min.
3. Correlation coefficient r ≥ 0.99.

The criteria described above are met YES

Table 4.1-99 presents the results of the PM_{10} evaluations carried out under Point 1. It can be seen that in the period evaluated the exposure limits stipulated by Resolution 610 of 2010 of the Ministry of Environment, Housing and Territorial Development, now the Ministry of Environment and Sustainable Development, were not exceeded for this pollutant; finding that concentrations are in the range of 2.3µg/m^3 to 22.6µg/m^3 and with an arithmetic average of 8.2µg/m^3.

Table 4.1-99 PM_{10} Point 1 results

Date	Outflow (m^3/min)	Time (min)	Pollutant Mass (µg)	Concentration PM_{10} (µg/m^3)		
2015/11/24	1,0937	1466,4	2,3023E+04	15,21	+/-	1,08
2015/11/25	1,0195	1420,2	3,1667E+03	2,32	+/-	0,18
2015/11/26	1,0937	1422,0	6,8367E+03	4,66	+/-	0,34
2015/11/28	1,0937	1439,4	1,1860E+04	7,98	+/-	0,57
2015/11/29	1,1308	1255,2*	1,5620E+04		+/-	
2015/11/30	1,0937	1435,8	6,8667E+03	4,63	+/-	0,34
2015/12/01	1,0937	1428,6	5,6800E+03	3,85	+/-	0,28
2015/12/02	1,0937	1429,8	6,9767E+03	4,73	+/-	0,34
2015/12/03	1,0937	1433,4	1,6473E+04	11,13	+/-	0,79
2015/12/04	1,0937	1439,4	1,0213E+04	6,87	+/-	0,49
2015/12/05	1,0937	1438,8	7,1667E+03	4,82	+/-	0,35
2015/12/06	1,0195	1429,2	9,9533E+03	7,24	+/-	0,54
2015/12/07	1,0937	1433,4	6,8633E+03	4,64	+/-	0,34
2015/12/08	1,0937	424,2*	8,8533E+03		+/-	
2015/12/09	1,0937	1435,8	2,2113E+04	14,92	+/-	1,06
2015/12/10	1,0566	1431,6	1,1213E+04	7,85	+/-	0,57
2015/12/11	1,1679	1416,0	3,5250E+04	22,58	+/-	1,56
2015/12/12	0,0	0,0*			+/-	

Source: Ingex, 2016

Illustration 4.1-229 shows a comparison between PM_{10} concentrations and the current standard in Point 1.

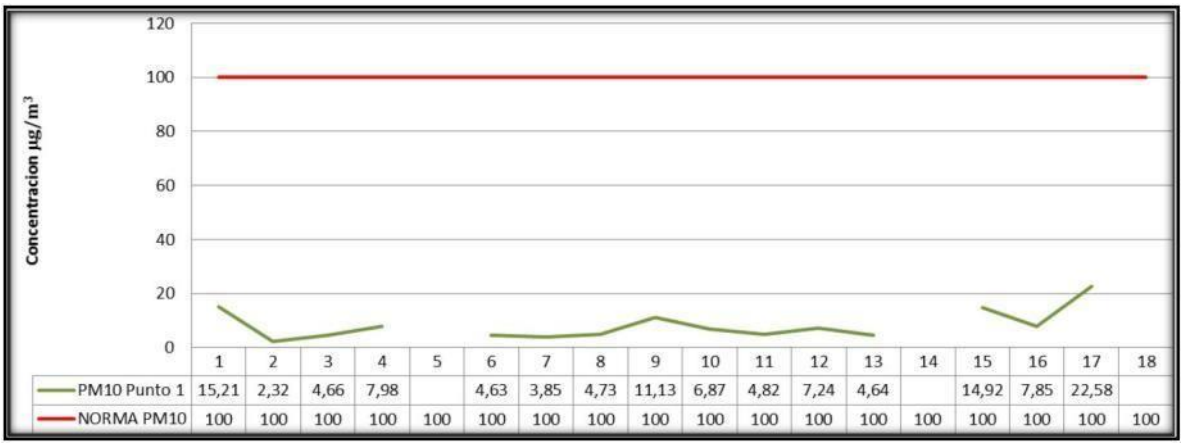

Illustration 4.1-229. Concentration of PM_{10} vs. standard Point 1

Source: Ingex, 2016

4.1.6.2.1.1.2. SO_2 and NO_2 evaluation Point 1

The NO_2 and SO_2 evaluations performed, were carried out simultaneously with those of particles in the period of time between November 24 and December 12, 2015.

Table 4.1-100 presents the data for the monitoring flow rate calibration of the equipment according to the calculations described in the sampling methodology. It is specified that the calibration was performed with dry gas equipment, so no adjustment is made for moisture.

Table 4.1-100. RAC3 fumes calibration Point 1

T_{ref} (K)	P_{ref} (mmHg)	T_m(K)	P_m (mmHg)
298,15	760,00	303,95	723,30
Q_{ref} (l/min)		%Var perm	
0,2000		10%	
Q_m (l/min)			
0,2142			
LOWER BOUND		UPPER BOUND	
0,1928		0,2357	
HR	STANDARD TYPE CALIBRATION		
0,650	DRY CALIBRATOR		
CONSTANTS P_{H2O}		P_{H2O} (mmHg)	
A	18,6008	0,0000	
B	3998,977		
C	38,9974		

Source: Ingex, 2016

Table 4.1-101 and Table 4.1-102 show the results found in the concentrations of SO_2 and NO_2 at Point 1. All results are below the maximum permissible standards of Colombian regulations for these contaminants.

Table 4.1-101. SO_2 Concentrations Point 1

Date	Outflow (m^3/min)	Time (min)	Pollutant Mass (µg)	Concentration PM_{10} (µg/m^3)		
2015/11/24	0,2105	1466	8,0000E-01	< 2,75**	+/-	< 0,43
2015/11/25	0,2109	1420	8,0000E-01	< 2,83**	+/-	< 0,44
2015/11/26	0,2126	1422	8,0000E-01	< 2,80**	+/-	< 0,44
2015/11/28	0,2120	1439	8,0000E-01	< 2,78**	+/-	< 0,43
2015/11/29	0,2133	1255*	8,0000E-01	< 3,16**	+/-	< 0,49
2015/11/30	0,2133	1436	8,0000E-01	< 2,77**	+/-	< 0,43
2015/12/01	0,2129	1429	8,0000E-01	< 2,79**	+/-	< 0,43
2015/12/02	0,2131	1430	8,0000E-01	< 2,78**	+/-	< 0,43
2015/12/03	0,2123	1433	8,0000E-01	< 2,78**	+/-	< 0,43
2015/12/04	0,2112	1439	8,0000E-01	< 2,79**	+/-	< 0,43
2015/12/05	0,2105	1439	8,0000E-01	< 2,80**	+/-	< 0,44
2015/12/06	0,2109	1429	8,0000E-01	< 2,81**	+/-	< 0,44
2015/12/07	0,2126	1433	8,0000E-01	< 2,78**	+/-	< 0,43

2015/12/08	0,2120	424*	8,0000E-01	< 9,42**	+/-	< 1,47
2015/12/09	0,2133	1436	8,0000E-01	< 2,77**	+/-	< 0,43

*Samples outside the valid sampling time 24h ±1.
**Samples below the detection limit of the technique.

Source: Ingex, 2016

Illustration 4.2-230 shows a comparison between the concentrations of SO_2 and the current Standard in force in Point 1.

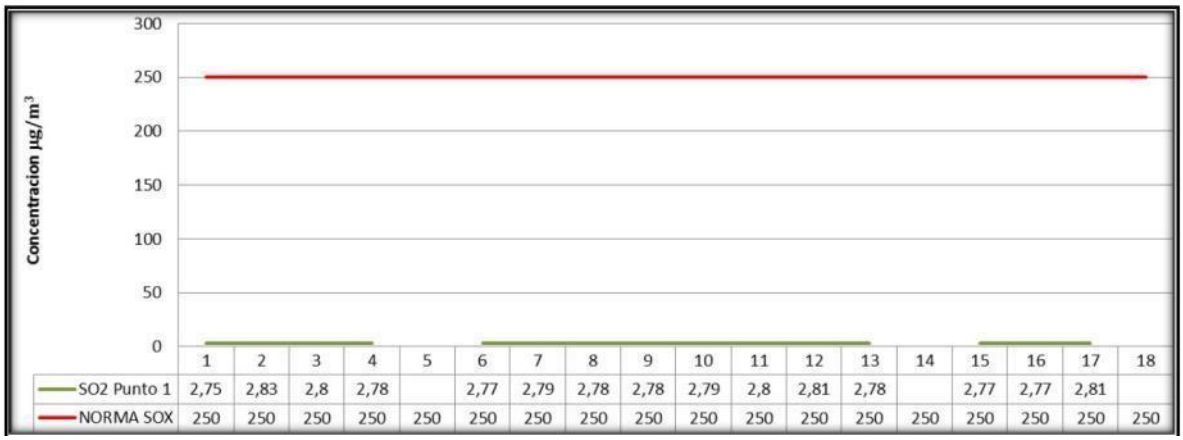

Illustration 4.1-230. SO_2 vs Standard Comparison Point 1
Source: Ingex, 2016

Table 4.1-102. NO_2 Concentrations Point 1.

Date	Outflow (m^3/min)	Time (min)	Pollutant Mass (µg)	Concentration PM_{10} (µg/m^3)		
2015/11/24	0,2114	1466	4,4000E-01	< 1,50**	+/-	< 0,23
2015/11/25	0,2114	1420	4,4000E-01	< 1,55**	+/-	< 0,24
2015/11/26	0,2114	1422	1,6490E+00	5,81	+/-	0,84
2015/11/28	0,2112	1439	4,4000E-01	< 1,53**	+/-	< 0,24
2015/11/29	0,2112	1255*	4,4000E-01	< 1,76**	+/-	< 0,27
2015/11/30	0,2118	1436	4,4000E-01	< 1,53**	+/-	< 0,24
2015/12/01	0,2114	1429	1,5450E+00	5,42	+/-	0,80
2015/12/02	0,2112	1430	4,4000E-01	< 1,54**	+/-	< 0,24
2015/12/03	0,2117	1433	4,4000E-01	< 1,54**	+/-	< 0,24
2015/12/04	0,2119	1439	4,4000E-01	< 1,53**	+/-	< 0,24
2015/12/05	0,2114	1439	4,4000E-01	< 1,53**	+/-	< 0,24
2015/12/06	0,2114	1429	4,4000E-01	< 1,54**	+/-	< 0,24
2015/12/07	0,2114	1433	1,8560E+00	6,49	+/-	0,92
2015/12/08	0,2112	424*	4,4000E-01	< 5,20**	+/-	< 0,81
2015/12/09	0,2112	1436	4,4000E-01	< 1,54**	+/-	< 0,24
2015/12/10	0,2118	1432	4,4000E-01	< 1,54**	+/-	< 0,24
2015/12/11	0,2114	1416	4,4000E-01	< 1,56**	+/-	< 0,24

2015/12/12	0,2112	0*			+/-	

*Samples outside the valid sampling time 24h ±1.
**Samples below the detection limit of the technique.

Source: Ingex, 2016

Illustration 4.1-231 shows a comparison between NO_2 concentrations and the current Standard in force in Point 1.

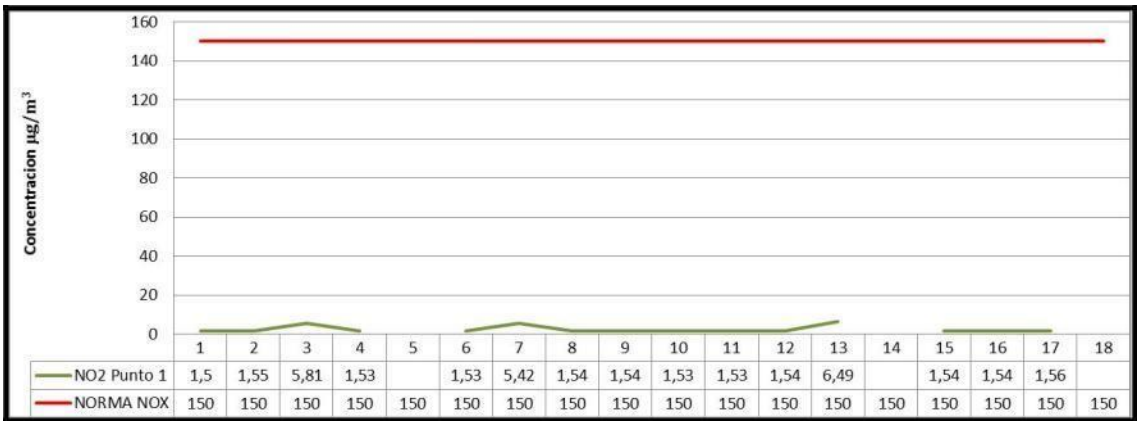

Illustration 4.1-231. NO_2 Comparison Standard Point 1
Source: Ingex, 2016

4.1.6.2.1.2 Air quality results Point 2

4.1.6.2.1.2.1 PM_{10} Point 2 Evaluation

The following are the results of the PM_{10} evaluations conducted under Point 2. Before sampling was started, the equipment was calibrated using a calibration kit for high-volume equipment, Table 4.1-103 shows the values reported in the calibration.

Table 4.1-103. PM_{10} Point 2 Calibration

m	b	r	P_a (mmHg)	T_a (K)	SSP(CFM)		
1,005394	0,02160	0,999986	737	305,15	37,81		
CALIBRATION							
Orifice	H(inH_2O)	IC (CFM)	IC_t (CFM*$K^{0,5}$/mmHg^{0,5})	Q_{a_orif} (m^3/min)	Q_{a_Curva} (m^3/min)	Dif (m^3/min)	Fulfilled
18	3,3	40	25,738	1,184	1,176	0,008	YES
13	3,1	39	25,095	1,148	1,155	0,007	YES
10	3	38	24,452	1,130	1,134	0,004	YES
7	2,9	37	23,808	1,111	1,113	0,001	YES
5	2,6	34	21,878	1,053	1,049	0,004	YES

m_1	$(CFM*K^{0,5}/mmHg^{0,5})/(m^3/min)$	30,38330	1) Diff <0,04 m^3/min all points.	YES
b_1	$CFM*K^{0,5}/mmHg^{0,5}$	-10,00119	2)4 de 5 points within the range.	YES
r_1		0,99248	3) Correlation Coefficient r>=0,99	YES

Source: Ingex, 2016

STANDARDS:

1. Difference for all points ≤ 0.04 m^3/min.
2. 4 of the 5 points must be within the working range, for PM_{10} [1.02-1.24] m^3/min.
3. Correlation coefficient r ≥ 0.99.

The criteria described above are met YES

The results of the PM_{10} evaluations carried out in Point 2 can be seen in the Table 4.1-104. It can be observed that the exposure limits stipulated by the Colombian regulations were not exceeded during the period evaluated; finding that the concentrations in the range of 2.6µg/m^3 to 16.9µg/m^3 and with an arithmetic average of 9.5µg/m^3.

Table 4.1-104. PM_{10} Point 2 Results.

Date	Outflow (m^3/min)	Time (min)	Pollutant Mass (µg)	Concentration PM_{10} (µg/m^3)		
2015/11/24	1,0916	1498,2	2,6267E+04	16,95	+/-	3,58
2015/11/25	1,0916	1411,2	1,5663E+04	10,73	+/-	2,27
2015/11/26	1,1339	1384,2	1,0497E+04	7,06	+/-	1,46
2015/11/28	1,1339	1423,8	1,2853E+04	8,40	+/-	1,74
2015/11/29	1,1339	1383,6	2,0567E+04	13,84	+/-	2,87
2015/11/30	1,1339	1431,6	8,7900E+03	5,71	+/-	1,19
2015/12/01	1,0492	1441,2	3,7300E+03	2,60	+/-	0,56
2015/12/02	1,0916	1438,8	1,1610E+04	7,80	+/-	1,65
2015/12/03	1,0916	1423,8	1,9123E+04	12,99	+/-	2,74
2015/12/04	1,1339	1438,8	1,5610E+04	10,10	+/-	2,09
2015/12/05	1,1128	1438,2	1,0857E+04	7,16	+/-	1,50
2015/12/06	1,0916	1435,8	1,0540E+04	7,10	+/-	1,50
2015/12/07	1,1233	1404,6	6,4033E+03	4,28	+/-	0,89
2015/12/08	1,1339	422,4*	2,3100E+03		+/-	
2015/12/09	1,0916	1434,6	1,8967E+04	12,78	+/-	2,70
2015/12/10	1,1339	1439,4	1,8137E+04	11,73	+/-	2,43
2015/12/11	1,0916	1425,0	1,8937E+04	12,85	+/-	2,71
2015/12/12	1,1339	105,6*	6,0000E+03		+/-	

*Samples outside the valid sampling time 24h ±1.

Source: Ingex, 2016

Illustration 4.1-232 shows a comparison between PM_{10} concentrations and the current standard in Point 2.

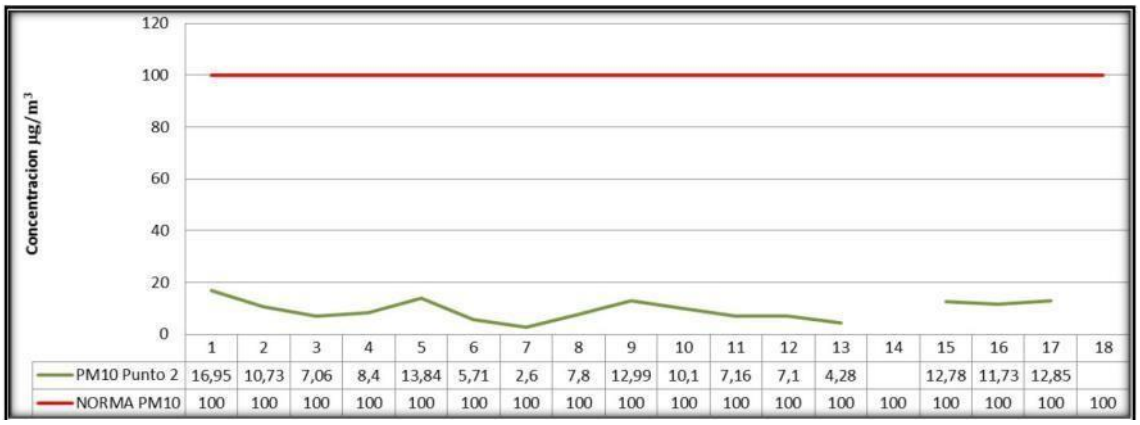

Illustration 4.1-232. Comparison PM_{10} vs Standard Point 2
Source: Ingex, 2016

4.1.6.2.1.2.2. SO_2 and NO_2 evaluation Point 2.

Table 4.1-106 and Table 4.1-107 present the concentrations found in the time period from 24 November to 12 December 2015, for the pollutants SO_2 and NO_2 in Point 2. All results are below the maximum permissible standards of Colombian regulations for these contaminants.

Additionally, Table 4.1-106 shows the data for the calibration of the monitoring flow rate of the equipment according to the calculations described in the sampling methodology.

Table 4.1-105. Calibration data RAC3 fumes Point 2.

T_{ref} (K)	P_{ref} (mmHg)	T_m (K)	P_m (mmHg)
298,15	760,00	305,15	737,00
Q_{ref} (l/min)		%Var perm	
0,2000		10%	
Q_m (l/min)			
0,2111			
LOWER BOUND		UPPER BOUND	
0,1900		0,2322	
HR	STANDARD TYPE CALIBRATION		
0,650	DRY CALIBRATOR		
CONSTANTS P_{H20}		P_{H20} (mmHg)	
A	18,6008	0,0000	
B	3998,977		
C	38,9974		

Source: Ingex, 2016

Table 4.1-106. SO_2 Concentrations Point 2.

Date	Outflow (m^3/min)	Time (min)	Pollutant Mass (µg)	Concentration PM_{10} (µg/m^3)		
2015/11/24	0,2094	1498	8,0000E-01	< 2,69**	+/-	< 0,42
2015/11/25	0,2073	1411	8,0000E-01	< 2,89**	+/-	< 0,45
2015/11/26	0,2054	1384	8,0000E-01	< 2,97**	+/-	< 0,46
2015/11/28	0,2035	1424	8,0000E-01	< 2,91**	+/-	< 0,45
2015/11/29	0,2036	1384	8,0000E-01	< 3,00**	+/-	< 0,47
2015/11/30	0,2025	1432	8,0000E-01	< 2,91**	+/-	< 0,45
2015/12/01	0,2021	1441	8,0000E-01	< 2,90**	+/-	< 0,45
2015/12/02	0,2020	1439	8,0000E-01	< 2,91**	+/-	< 0,45
2015/12/03	0,2029	1424	8,0000E-01	< 2,92**	+/-	< 0,46
2015/12/04	0,2018	1439	8,0000E-01	< 2,91**	+/-	< 0,45
2015/12/05	0,2094	1438	8,0000E-01	< 2,80**	+/-	< 0,44
2015/12/06	0,2073	1436	8,0000E-01	< 2,84**	+/-	< 0,44
2015/12/07	0,2054	1405	8,0000E-01	< 2,93**	+/-	< 0,46
2015/12/08	0,2035	422*	8,0000E-01		+/-	
2015/12/09	0,2036	1435	8,0000E-01	< 2,89**	+/-	< 0,45
2015/12/10	0,2025	1439	8,0000E-01	< 2,90**	+/-	< 0,45
2015/12/11	0,2021	1425	8,0000E-01	< 2,93**	+/-	< 0,46
2015/12/12	0,2020	106*	8,0000E-01		+/-	

*Samples outside the valid sampling time 24h ±1.
**Samples below the detection limit of the technique.

Source: Ingex, 2016

Illustration 4.1-223 shows a comparison between SO_2 concentrations and the current Standard in force in Point 2.

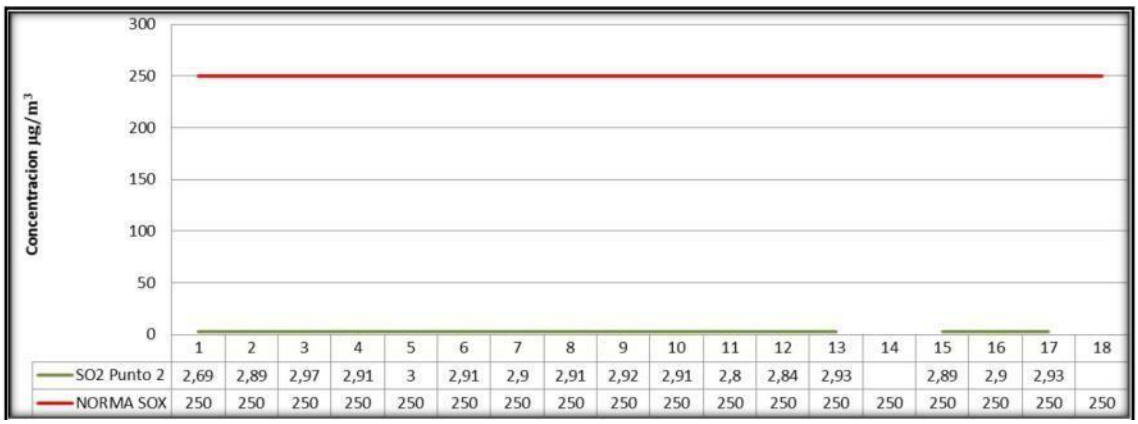

Illustration 4.1-233. SO_2 vs Standard Comparison Point 2.
Source: Ingex, 2016

Table 4.1-107. NO_2 Concentrations Point 2.

Date	Outflow (m^3/min)	Time (min)	Pollutant Mass (µg)	Concentration PM_{10} (µg/m^3)		
2015/11/24	0,2032	1498	1,5450E+00	5,36	+/-	0,79
2015/11/25	0,2042	1411	2,7890E+00	10,21	+/-	1,36
2015/11/26	0,2049	1384	1,6490E+00	6,14	+/-	0,89
2015/11/28	0,2041	1424	1,5450E+00	5,61	+/-	0,82
2015/11/29	0,2040	1384	4,4000E-01	< 1,65**	+/-	< 0,26
2015/11/30	0,2044	1432	4,4000E-01	< 1,59**	+/-	< 0,25
2015/12/01	0,2040	1441	4,4000E-01	< 1,58**	+/-	< 0,25
2015/12/02	0,2041	1439	1,5450E+00	5,55	+/-	0,82
2015/12/03	0,2038	1424	4,4000E-01	< 1,60**	+/-	< 0,25
2015/12/04	0,2042	1439	4,4000E-01	< 1,58**	+/-	< 0,25
2015/12/05	0,2032	1438	4,4000E-01	< 1,59**	+/-	< 0,25
2015/12/06	0,2042	1436	4,4000E-01	< 1,58**	+/-	< 0,25
2015/12/07	0,2049	1405	4,4000E-01	< 1,61**	+/-	< 0,25
2015/12/08	0,2041	422*	4,4000E-01		+/-	
2015/12/09	0,2040	1435	4,4000E-01	< 1,59**	+/-	< 0,25
2015/12/10	0,2044	1439	4,4000E-01	< 1,58**	+/-	< 0,25
2015/12/11	0,2040	1425	4,4000E-01	< 1,60**	+/-	< 0,25
2015/12/12	0,2041	106*	4,4000E-01		+/-	0,79

*Samples outside the valid sampling time 24h ±1.
**Samples below the detection limit of the technique.

Source: Ingex, 2016

Illustration 4.1-234 shows a comparison between NO_2 concentrations and the current Standard in Point 2.

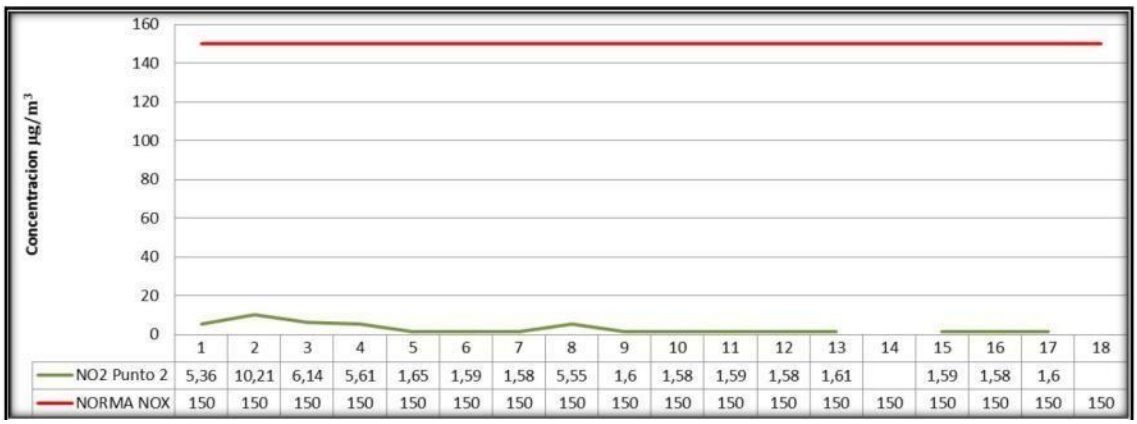

Illustration 4.1-234. Comparison NO_2 vs Standard point 2
Source: Ingex, 2016

4.1.6.2.2 Wind Rose

In order to determine the wind direction and wind speed conditions during the air quality sampling period, meteorological data for 2014 were acquired for the study area.

The results allow us to conclude that 5.5% of the time is calm and the dominant wind speed is the one in the range of 2.1 m/s to 3.6 m/s in 52.6% of the time evaluated. See Illustration 4.1-235.

Regarding the direction of the winds, there is a marked incidence of winds coming from the Northwest with north-westerly winds. See Wind Rose Illustration 4.1-236.

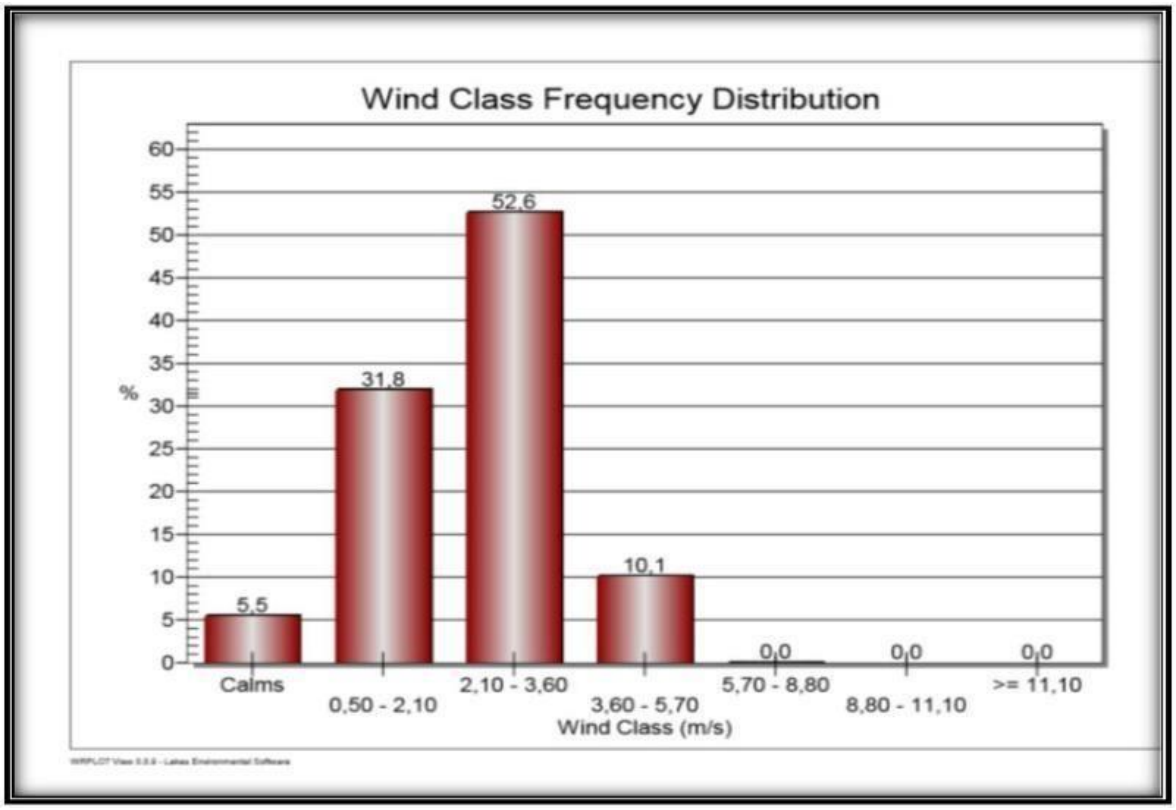

Illustration 4.1-235. Wind speed distribution.
Source: Ingex, 2016

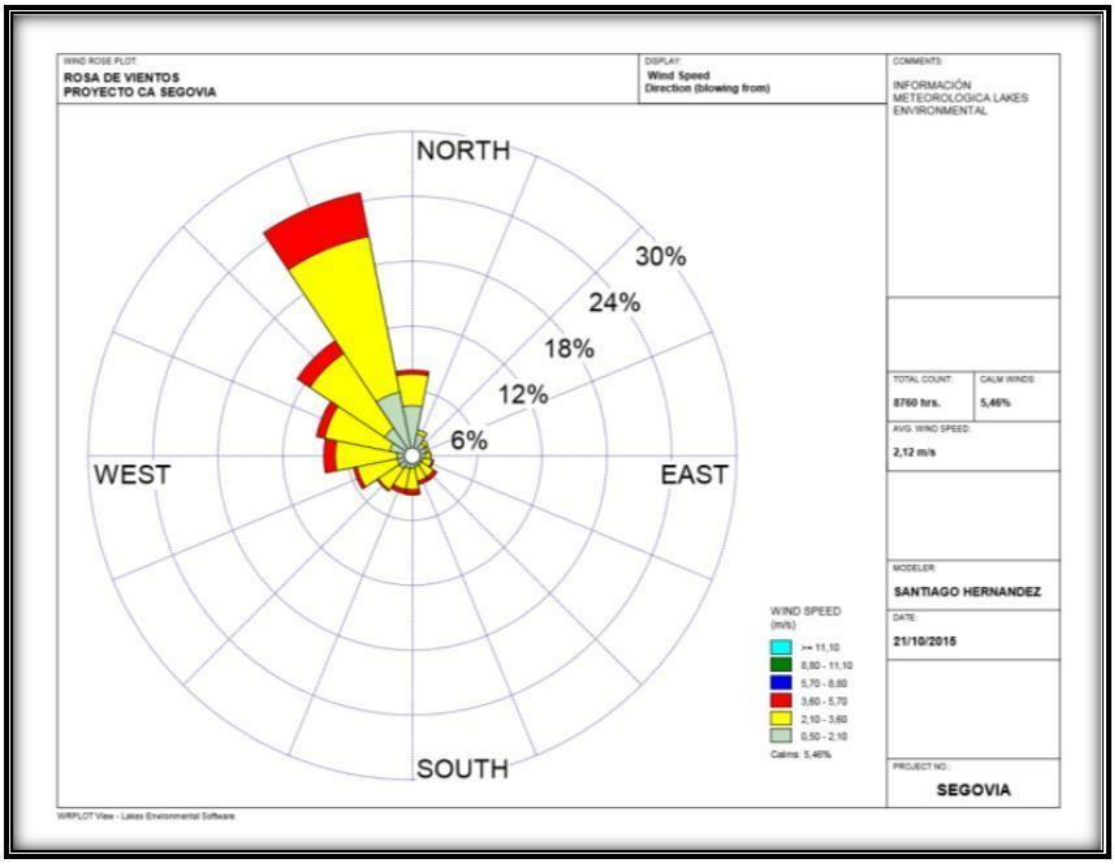

Illustration 4.1-236. Wind Rose Sampling Point Segovia
Source: Ingex, 2016

4.1.6.2.3 Conclusions

The concentrations of particles less than 10 microns (PM_{10}) in the environment, evaluated in the Zone, according to Resolution 610 of 2010 Ministry of Environment, Housing and Territorial Development, now the Ministry of Environment and Sustainable Development, do not exceed the maximum permissible limits for this contaminant for 24-hour periods at the two monitored points; If the trend for the period under assessment is to be maintained, the maximum annual arithmetic average of 50 µg/m^3 per year allowed for this pollutant shall not be exceeded at any of the points under assessment. Illustration 4.1-237 shows a comparison of the assessments made at each sampling point.

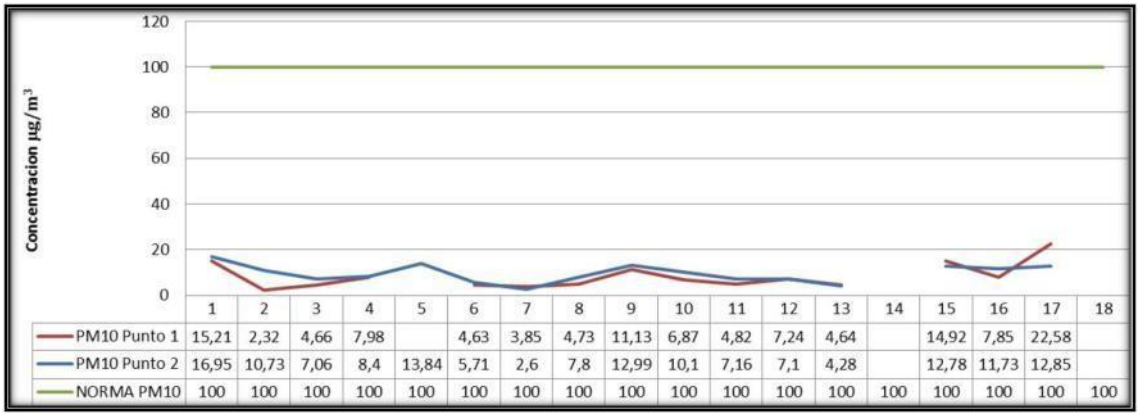

	1	2	3	4	5	6	7	8	9	10	11	12	13	14	15	16	17	18
PM10 Punto 1	15,21	2,32	4,66	7,98		4,63	3,85	4,73	11,13	6,87	4,82	7,24	4,64		14,92	7,85	22,58	
PM10 Punto 2	16,95	10,73	7,06	8,4	13,84	5,71	2,6	7,8	12,99	10,1	7,16	7,1	4,28		12,78	11,73	12,85	
NORMA PM10	100	100	100	100	100	100	100	100	100	100	100	100	100	100	100	100	100	100

Illustration 4.1-237. PM_{10} comparison between evaluated points
Source: Ingex, 2016

The concentrations of Sulfur Dioxides (SO_2) and Nitrogen Dioxides (NO_2) evaluated in the Zone, according to Resolution 610 of 2010 Ministry of Environment, Housing and Territorial Development, now Ministry of Environment and Sustainable Development, do not exceed the maximum permissible limits for these pollutants for 24-hour periods. Illustration 4.1-238 and Illustration 4.1-239 show a comparison between the assessments made at each sampling point.

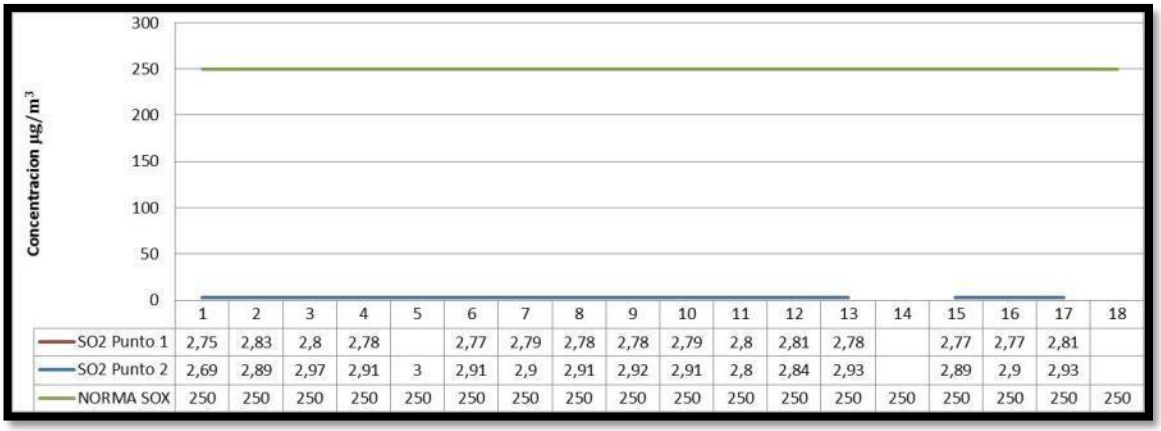

	1	2	3	4	5	6	7	8	9	10	11	12	13	14	15	16	17	18
SO2 Punto 1	2,75	2,83	2,8	2,78		2,77	2,79	2,78	2,78	2,79	2,8	2,81	2,78		2,77	2,77	2,81	
SO2 Punto 2	2,69	2,89	2,97	2,91	3	2,91	2,9	2,91	2,92	2,91	2,8	2,84	2,93		2,89	2,9	2,93	
NORMA SOX	250	250	250	250	250	250	250	250	250	250	250	250	250	250	250	250	250	250

Illustration 4.1-238. Comparison of SO_2 between evaluated points.
Source: Ingex, 2016

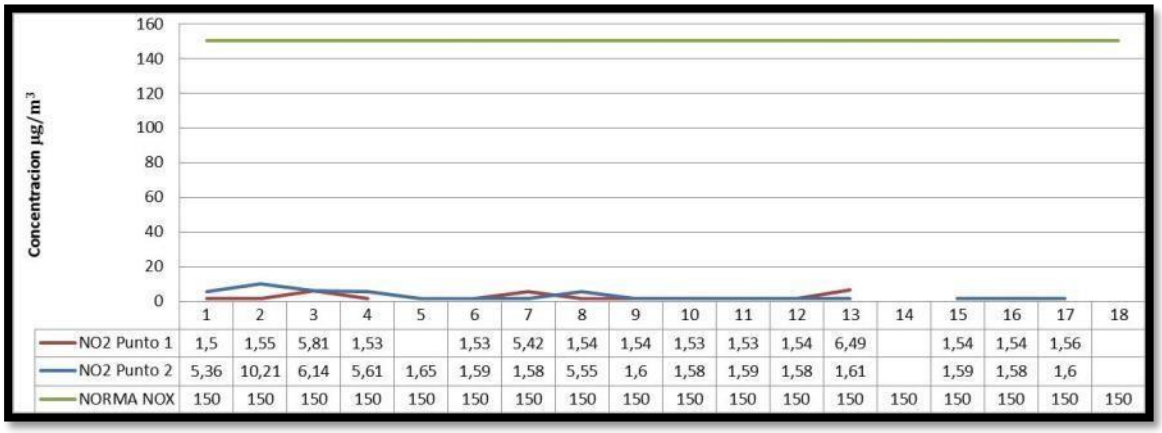

	1	2	3	4	5	6	7	8	9	10	11	12	13	14	15	16	17	18
NO2 Punto 1	1,5	1,55	5,81	1,53		1,53	5,42	1,54	1,54	1,53	1,53	1,54	6,49		1,54	1,54	1,56	
NO2 Punto 2	5,36	10,21	6,14	5,61	1,65	1,59	1,58	5,55	1,6	1,58	1,59	1,58	1,61		1,59	1,58	1,6	
NORMA NOX	150	150	150	150	150	150	150	150	150	150	150	150	150	150	150	150	150	150

Illustration 4.1-239. Comparison of NO_2 between evaluated points.
Source: Ingex, 2016

4.1.6.3 NOISE

4.1.6.3.1 Sampling Sites

For the environmental noise evaluations, four (4) fixed measurement points were taken in the vicinity of the mining project "El Pescado", municipality of Segovia - Antioquia. The following table shows the location of the monitoring points.

Table 4.1-108. Location Monitoring Points

POINT	COORDINATES	
Point 1	07º15'40,9" N	074º44´42,2" O
Point 2	07º16'07,2" N	074º43´00,0" O
Point 3	07º15'09,6" N	074º42´33,3" O
Point 4	07º14'30,7" N	074º42´00,1" O

Source: Ingex, 2016

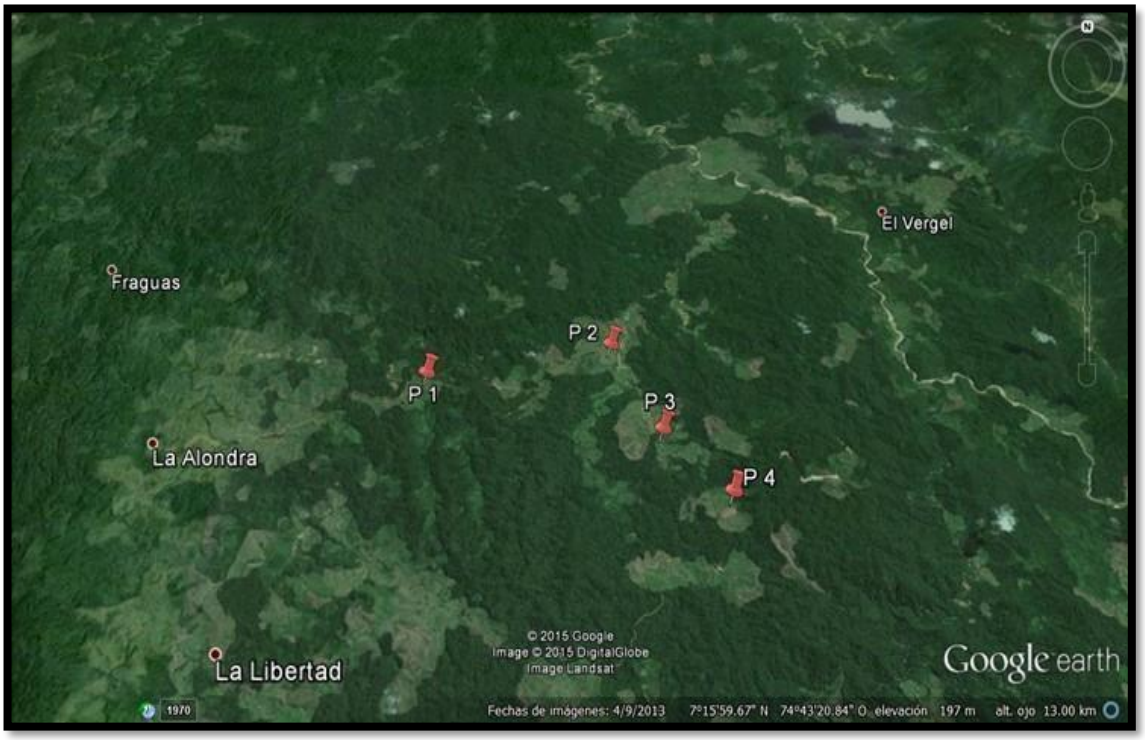

Illustration 4.1-240. Location Sampling points, within the mining project "El Pescado".
Source: Google Earth 2015

4.1.6.3.2 Presentation of results and analysis

The following are the results found, Annex 2 shows the field formats provided by the company CONINTEGRAL S.A.S. for every point and hour of monitoring. Sampling was carried out at the points described above during the week, during daylight hours.

Table 4.1-109. Weather Conditions Daytime Week

POINT	WIND SPEED (m/s)	WIND DIRECTION	RAIN	TEMPERATURE (ºC)	BAROMETRIC PRESSURE (mmHg)	HUMIDITY (%)
1	2.3	W.S	NO	28.8	731.4	65
2	0.7	N.W	NO	25.0	737.0	74
3	0.4	W.S	NO	29.5	725.3	70
4	1.2	E.S	NO	30.5	723.3	68

Source: Ingex, 2016

Illustration 4.1-241. Environmental Noise Assessment Daytime Point 1.
Source: Ingex, 2016

Illustration 4.1-242. Environmental Noise Assessment Daytime Point 2.
Source: Ingex, 2016

Illustration 4.1-243. Environmental Noise Assessment Daytime Point 3.
Source: Ingex, 2016

Illustration 4.1-244. Environmental Noise Assessment Daytime Point 4.
Source: Ingex, 2016

4.1.6.3.2.1 Environmental Noise Point 1 Daytime Week

Below are the values found for the calculation of environmental noise in Point 1 during the daytime period, the evaluation was carried out on December 14, 2015.

Table 4.1-110. Frequency Sweep for LAeq, 1h Point 1 North Daytime Week

	TONAL COMPONENT 20-125											TONAL COMPONENT 160-400				
f (Hz)	12	16	20	25	32	40	50	63	80	100	125	160	200	250	315	400
dB (A)	0,0	0,0	19,3	23,3	26,8	29,7	31,9	33,6	34,4	35,0	34,9	34,1	33,1	32,9	31,6	31,0
$L=L_t-L_S$			0,0	0,0	0,0	0,0	0,0	0,0	0,0	0,4	0,0	0,0	0,0	0,0	0,0	0,0
			No tonal component (20 – 125 Hz)									No tonal component (160-400 Hz)				
			KT =0									KT=0				
	Tonal Component 500-20000																
f (Hz)	500	630	800	1000	1250	1600	2000	2500	3200	4000	5000	6300	8000	10000	12500	16000	20000
dB (A)	32,7	35,5	38,3	38,3	36,6	35,5	37,9	30,6	29,9	28,5	27,0	31,7	35,5	21,6	21,4	20,4	9,5
$L=L_t-L_S$	0,0	0,0	0,0	0,0	0,0	0,0	4,9	0,0	0,0	0,0	0,0	0,0	8,9	0,0	0,0	0,0	
	There is a strong tonal component (500 – 16000 Hz)																
	KT = 6																

Source: Ingex, 2016

Table 4.1-111. Frequency Sweep for LAeq, 1h Point 1 South Daytime Week

	TONAL COMPONENT 20-125											TONAL COMPONENT 160-400				
f (Hz)	12	16	20	25	32	40	50	63	80	100	125	160	200	250	315	400
dB (A)	0,0	0,0	9,0	12,6	15,4	17,0	18,0	18,0	18,3	19,1	19,6	19,4	19,5	20,0	19,4	21,5
$L=L_t-L_S$			0,0	0,0	0,0	0,0	0,0	0,0	0,0	0,4	0,0	0,0	0,0	0,0	0,0	0,0
			No tonal component (20 – 125 Hz)									No tonal component (160-400 Hz)				
			KT =0									KT=0				
	Tonal Component 500-20000																
f (Hz)	500	630	800	1000	1250	1600	2000	2500	3200	4000	5000	6300	8000	10000	12500	16000	20000
dB (A)	24,7	20,9	22,2	22,7	22,5	25,0	23,6	22,7	27,5	24,3	24,6	34,9	37,3	19,5	20,9	20,7	7,6
$L=L_t-L_S$	3,5	0,0	0,0	0,3	0,0	2,0	0,0	0,0	4,0	0,0	0,0	0,0	10,1	0,0	0,8	0,0	
	There is a strong tonal component (500 – 16000 Hz)																
	KT = 6																

Source: Ingex, 2016

Table 4.1-112. Frequency Sweep for LAeq, 1h Point 1 East Daytime Week

	TONAL COMPONENT 20-125											TONAL COMPONENT 160-400				
f (Hz)	12	16	20	25	32	40	50	63	80	100	125	160	200	250	315	400
dB (A)	0,0	0,0	14,5	18,0	21,2	23,8	25,3	25,9	25,8	25,4	25,7	25,3	25,1	24,7	24,4	24,4
$L=L_t-L_S$			0,0	0,0	0,0	0,0	0,0	0,3	0,0	0,4	0,3	0,0	0,0	0,0	0,0	0,0
			No tonal component (20 – 125 Hz)									No tonal component (160-400 Hz)				
			KT =0									KT=0				

	Tonal Component 500-20000																
f (Hz)	500	630	800	1000	1250	1600	2000	2500	3200	4000	5000	6300	8000	10000	12500	16000	20000
dB (A)	24,8	24,3	25,5	26,1	26,7	27,9	28,5	27,0	32,3	30,8	29,7	38,9	42,1	20,5	21,7	19,7	13,5
$L=L_t-L_S$	0,4	0,0	0,0	0,0	0,0	0,0	1,1	0,0	3,4	0,0	0,0	0,0	12,4	0,0	1,6	0,0	
	There is a strong tonal component (500 – 16000 Hz)																
	KT = 6																

Source: Ingex, 2016

Table 4.1-113. Frequency Sweep for LAeq, 1h Point 1 West Daytime Week

	TONAL COMPONENT 20-125											TONAL COMPONENT 160-400				
f (Hz)	12	16	20	25	32	40	50	63	80	100	125	160	200	250	315	400
dB (A)	0,0	0,0	-4,9	-3,7	-2,8	-1,6	-0,4	1,5	1,7	4,7	5,7	7,7	12,1	12,6	14,4	18,6
$L=L_t-L_S$			0,0	0,0	0,0	0,0	0,0	0,0	0,0	0,0	0,0	0,0	0,0	0,0	0,0	0,0
			No tonal component (20 – 125 Hz)									No tonal component (160-400 Hz)				
			KT =0									KT=0				

	Tonal Component 500-20000																
f (Hz)	500	630	800	1000	1250	1600	2000	2500	3200	4000	5000	6300	8000	10000	12500	16000	20000
dB (A)	19,5	20,3	23,2	26,4	32,0	38,4	37,3	30,2	37,1	39,4	34,6	47,4	46,3	19,5	20,8	16,4	13,0
$L=L_t-L_S$	0,0	0,0	0,0	0,0	0,0	3,8	0,0	0,0	0,0	3,6	0,0	7,0	0,0	0,0	2,9	0,0	
	There is a strong tonal component (500 – 16000 Hz)																
	KT = 6																

Source: Ingex, 2016

Table 4.1-114. Frequency Sweep for LAeq, 1h Point 1 Vertical Daytime Week

	TONAL COMPONENT 20-125											TONAL COMPONENT 160-400				
f (Hz)	12	16	20	25	32	40	50	63	80	100	125	160	200	250	315	400
dB (A)	0,0	0,0	-5,3	-2,4	-1,2	1,4	3,6	4,0	4,3	4,9	6,0	4,8	7,3	11,2	10,0	12,2
$L=L_t-L_S$			0,0	0,0	0,0	0,0	0,0	0,0	0,0	0,0	1,2	0,0	0,0	2,6	0,0	0,0
			No tonal component (20 – 125 Hz)									No tonal component (160-400 Hz)				
			KT =0									KT=0				

	Tonal Component 500-20000																
f (Hz)	500	630	800	1000	1250	1600	2000	2500	3200	4000	5000	6300	8000	10000	12500	16000	20000
dB (A)	17,6	23,5	26,0	27,7	21,5	24,1	19,3	21,1	17,9	19,9	28,3	31,7	38,1	37,8	22,8	13,9	-2,0
$L = L_t - L_S$	0,0	0,0	0,0	4,0	0,0	3,7	0,0	2,5	0,0	0,0	0,0	0,0	3,4	0,0	0,0	0,0	
	There is a strong tonal component (500 – 16000 Hz)																
	KT = 6																

Source: Ingex, 2016

Table 4.1-115. Frequency Sweep for LAeq, 1h Average Point 1 Daytime Week

	TONAL COMPONENT 20-125												TONAL COMPONENT 160-400			
f (Hz)	12	16	20	25	32	40	50	63	80	100	125	160	200	250	315	400
dB (A)	0,0	0,0	13,9	17,7	21,1	23,9	25,9	27,4	28,1	28,6	28,5	27,8	26,9	26,8	25,7	25,5
$L=L_t-L_S$			0,0	0,0	0,0	0,0	0,0	0,0	0,0	0,3	0,0	0,0	0,0	0,0	0,0	0,0
			No tonal component (20 – 125 Hz)										No tonal component (160-400 Hz)			
			KT =0										KT=0			

	Tonal Component 500-20000																
f (Hz)	500	630	800	1000	1250	1600	2000	2500	3200	4000	5000	6300	8000	10000	12500	16000	20000
dB (A)	27,2	29,3	32,0	32,2	31,4	33,7	34,0	27,8	32,3	33,4	30,2	41,4	41,7	31,1	21,6	18,9	10,6
$L = L_t - L_S$	0,0	0,0	0,0	0,5	0,0	0,0	3,3	0,0	0,0	2,2	0,0	0,0	5,5	0,0	0,0	0,0	
	There is a strong tonal component (500 – 16000 Hz)																
	KT = 6																

Source: Ingex, 2016

Table 4.1-116. Summary of Measurements Performed to Estimate Leq Point 1 Daytime Week

Measurement	Ti min	LAeq,Ti dB(A)	KTi dB(A)	KIi dB(A)	KSi dB(A)	KMax,i dB(A)	LRAeq,Ti dB(A)
1	15,00	48,00	6	0	0	6	54,00
2	15,00	40,90	6	0	0	6	46,90
3	15,00	45,40	6	0	0	6	51,40
4	15,00	51,00	6	0	0	6	57,00
5	15,00	42,50	3	0	0	6	48,50
T --->	75,00						
K Average --->			6,00	0,00	0,00	LRAeq,T--->	53,05
KMAX,G --->			6,00				
LAeq,T --->		47,05	LRAeq,T --->	53,05			

Source: Ingex, 2016

Table 4.1-117. Environmental Noise Results Corrected Point 1 Daytime Week.

Results
L_{RAeq}
53,05±3,67

Source: Ingex, 2016

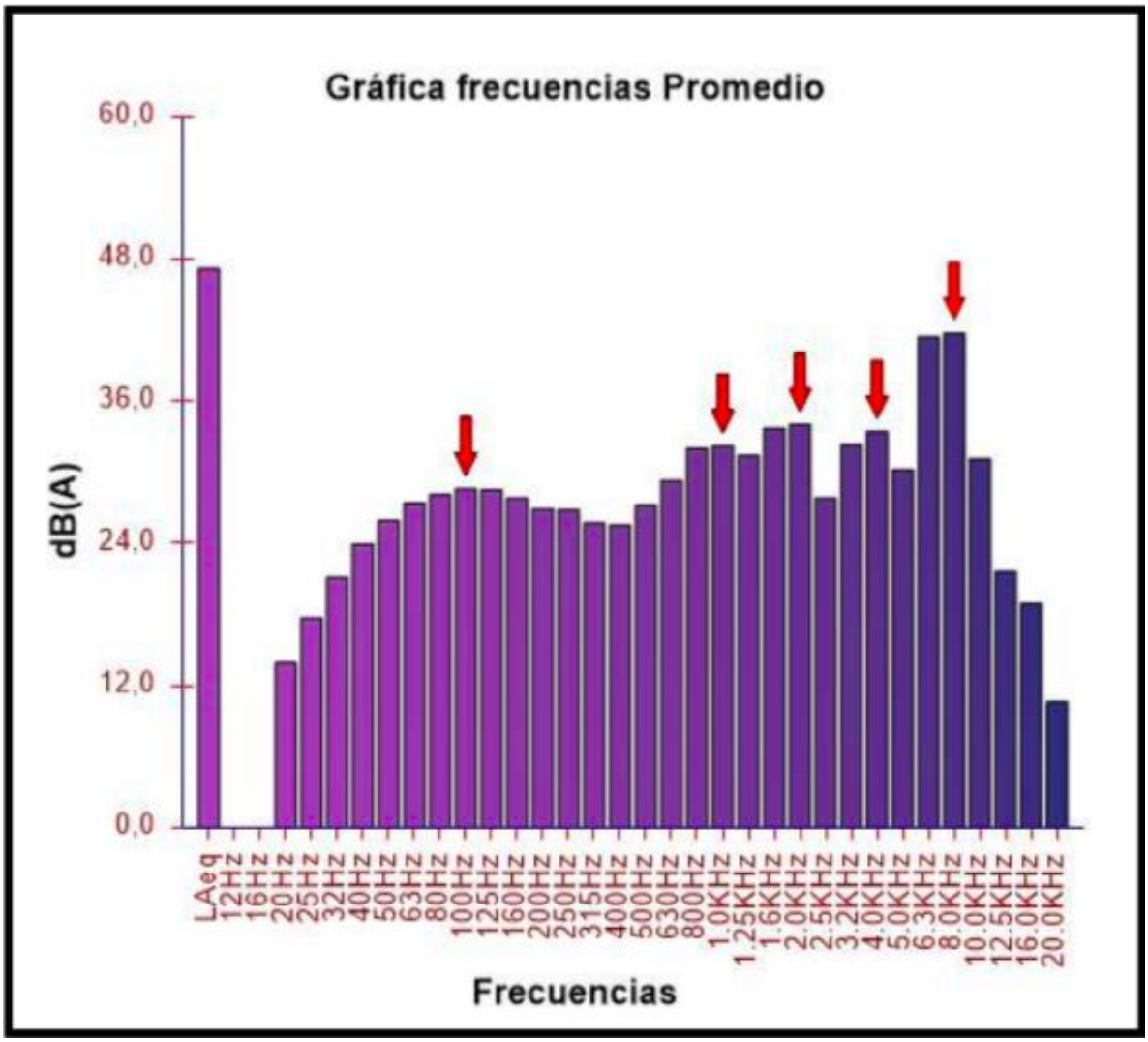

Illustration 4.1-245. Frequency sweep Average Point 1 Daytime Week.
Source: Ingex, 2016

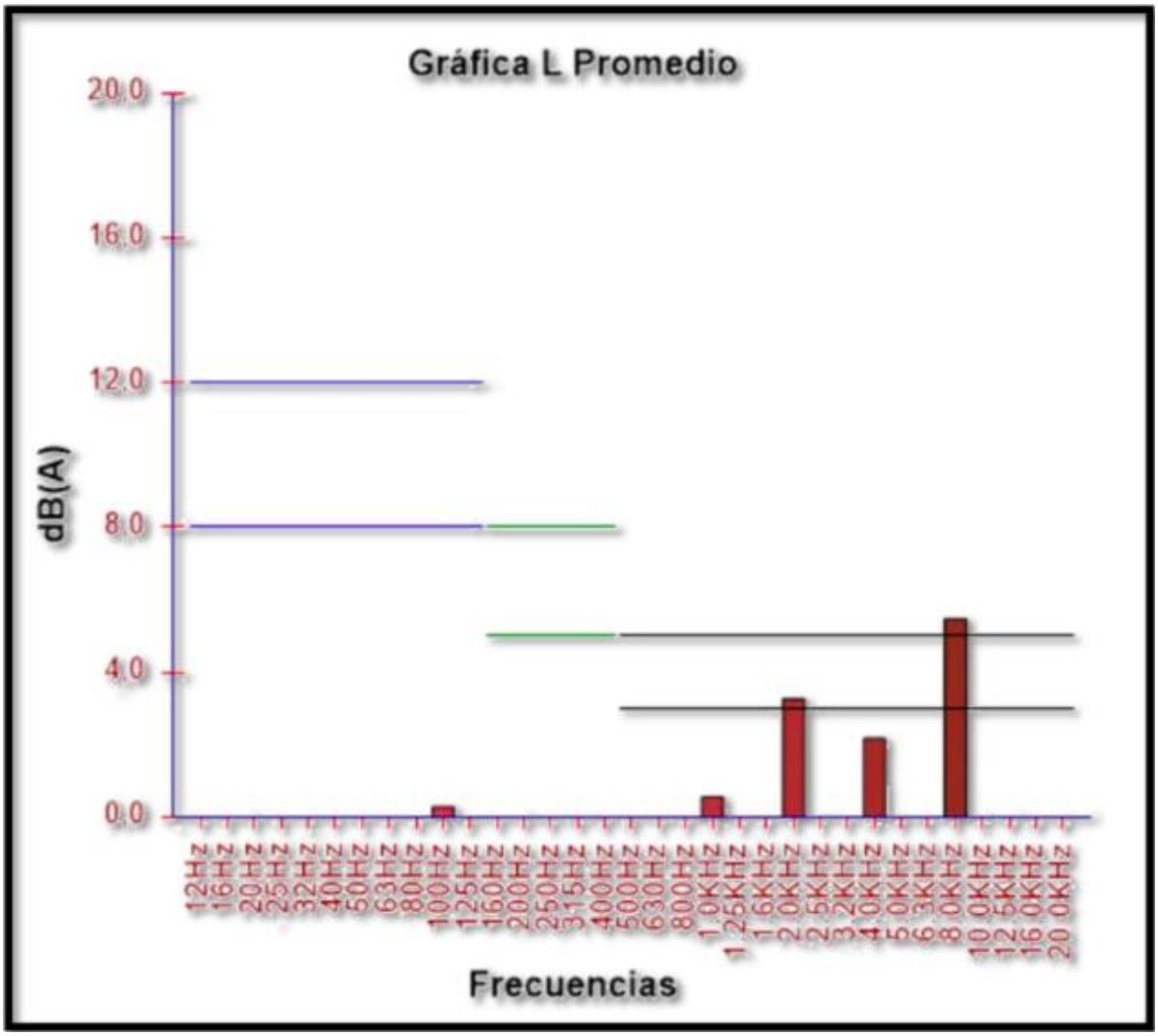

Illustration 4.1-246. Hue Adjustments Point 1 Daytime Week.
Source: Ingex, 2016

4.1.6.3.2.2 Uncertainty Evaluation Point 1 Daytime Week

The following table summarizes the n sources that contribute to the estimate of the measurand, the last row shows the combined uncertainty.

Table 4.1-118. Uncertainty Associated with the Estimation of the Measurand (LRAeq). Point 1.

Source	Unit	y	µ	V	ci	Ct (%)	p (%)	k ó tp (ef)	U
W	dB	0,0000	0,2043	â^ž	1,0000	1,2370	95,4500	2,0000	±0,4086
X	dB	0,0000	1,8255	â^ž	1,0000	98,7630	95,4500	2,0000	±3,6511
Y	dB	0,0000	0,0000	â^ž	1,0000	0,0000	95,4500	2,0000	±0,0000
LRAeq	dB	53,0543	1,8369	â^ž	1,0000	100,0000	95,4500	2,0000	±3,6739

Source: Ingex, 2016

Where:
y = Value for the source
µ = Standard uncertainty
V = Degrees of freedom
ci = Sensitivity coefficient
Ct (%)= Percentage contribution to total uncertainty.
p (%)= The degree of confidence with which you want to estimate the coverage factor. k or tp(ef) = Coverage factor
U= Expanded uncertainty

4.1.6.3.2.3 Environmental Noise Point 2 Daytime Week

Below are the values found for the calculation of environmental noise in Point 2 during the daytime period, the evaluation was carried out on December 15, 2015.

Table 4.1-119. Frequency Sweep for LAeq, 1h Point 2 North Daytime Week

	TONAL COMPONENT 20-125											TONAL COMPONENT 160-400				
f (Hz)	12	16	20	25	32	40	50	63	80	100	125	160	200	250	315	400
dB (A)	0,0	0,0	-7,9	-7,5	-6,5	-4,7	-0,8	4,5	9,9	11,8	15,0	15,2	23,1	25,0	23,3	25,7
$L=L_t-L_S$			0,0	0,0	0,0	0,0	0,0	0,0	0,0	0,0	0,0	0,0	0,0	1,8	0,0	0,0
			No tonal component (20 – 125 Hz)									No tonal component (160-400 Hz)				
			KT =0									KT=0				
	Tonal Component 500-20000															
f (Hz)	500	630	800	1000	1250	1600	2000	2500	3200	4000	5000	6300	8000	10000	12500	16000	20000
dB (A)	27,5	29,6	30,5	31,3	31,7	36,9	34,5	36,8	37,4	34,8	32,6	41,8	51,8	26,3	15,2	21,8	-1,5
$L=L_t-L_S$	0,0	0,0	0,0	0,0	0,0	3,8	0,0	0,0	1,6	0,0	0,0	0,0	17,8	0,0	0,0	15,0	
	There is a strong tonal component (500 – 16000 Hz)																
	KT = 6																

Source: Ingex, 2016

Table 4.1-120. Frequency Sweep for LAeq, 1h Point 2 South Daytime Week

	TONAL COMPONENT 20-125											TONAL COMPONENT 160-400				
f (Hz)	12	16	20	25	32	40	50	63	80	100	125	160	200	250	315	400
dB (A)	0,0	0,0	-7,9	-7,6	-6,7	-3,8	1,0	5,1	9,7	11,1	14,1	17,3	25,1	26,5	21,3	26,6
$L=L_t-L_S$			0,0	0,0	0,0	0,0	0,0	0,0	0,0	0,0	0,0	0,0	0,0	3,3	0,0	0,0
			No tonal component (20 – 125 Hz)									No tonal component (160-400 Hz)				
			KT =0									KT=0				

	Tonal Component 500-20000																
f (Hz)	500	630	800	1000	1250	1600	2000	2500	3200	4000	5000	6300	8000	10000	12500	16000	20000
dB (A)	27,9	31,3	32,0	31,3	32,7	36,5	33,7	33,2	35,1	34,6	32,4	43,6	51,4	24,0	16,8	22,0	-2,6
$L=L_t-L_S$	0,0	0,0	0,7	0,0	0,0	3,3	0,0	0,0	1,2	0,0	0,0	0,0	17,6	0,0	0,0	14,9	
	There is a strong tonal component (500 – 16000 Hz)																
	KT = 6																

Source: Ingex, 2016

Table 4.1-121. Frequency Sweep for LAeq, 1h Point 2 East Daytime Week

	TONAL COMPONENT 20-125											TONAL COMPONENT 160-400				
f (Hz)	12	16	20	25	32	40	50	63	80	100	125	160	200	250	315	400
dB (A)	0,0	0,0	-7,6	-7,1	-6,8	-7,0	-5,7	-4,0	-2,2	-1,3	1,6	7,1	9,0	9,8	9,8	11,7
$L=L_t-L_S$			0,0	0,0	0,3	0,0	0,0	0,0	0,0	0,0	0,0	0,0	0,0	3,3	0,0	0,0
			No tonal component (20 – 125 Hz)									No tonal component (160-400 Hz)				
			KT =0									KT=0				

	Tonal Component 500-20000																
f (Hz)	500	630	800	1000	1250	1600	2000	2500	3200	4000	5000	6300	8000	10000	12500	16000	20000
dB (A)	13,2	13,7	24,2	27,6	37,6	47,8	47,2	24,9	39,1	41,2	35,6	46,5	44,5	25,2	19,9	9,2	-2,6
$L=L_t-L_S$	0,0	0,0	0,0	0,0	0,0	5,4	0,0	0,0	0,0	3,9	0,0	6,5	0,0	0,0	0,0	0,0	
	There is a strong tonal component (500 – 16000 Hz)																
	KT = 6																

Source: Ingex, 2016

Table 4.1-122. Frequency Sweep for LAeq, 1h Point 2 West Daytime Week

	TONAL COMPONENT 20-125											TONAL COMPONENT 160-400				
f (Hz)	12	16	20	25	32	40	50	63	80	100	125	160	200	250	315	400
dB (A)	0,0	0,0	-7,9	-7,2	-6,0	-2,3	1,9	5,6	12,6	15,4	19,0	20,9	25,2	25,6	25,6	28,1
$L=L_t-L_S$			0,0	0,0	0,0	0,0	0,0	0,0	0,0	0,0	0,0	0,0	0,0	0,0	0,0	0,0
			No tonal component (20 – 125 Hz)									No tonal component (160-400 Hz)				
			KT =0									KT=0				

	Tonal Component 500-20000																
f (Hz)	500	630	800	1000	1250	1600	2000	2500	3200	4000	5000	6300	8000	10000	12500	16000	20000
dB (A)	28,7	29,7	31,6	35,0	31,6	33,4	31,5	28,6	29,3	29,3	30,2	41,2	52,3	26,7	16,5	22,1	-2,7
$L = L_t - L_S$	0,0	0,0	0,0	3,4	0,0	1,9	0,0	0,0	0,0	0,0	0,0	0,0	18,4	0,0	0,0	15,2	
	There is a strong tonal component (500 – 16000 Hz)																
	KT = 6																

Source: Ingex, 2016

Table 4.1-123. Frequency Sweep for LAeq, 1h Point 2 Vertical Daytime Week

	TONAL COMPONENT 20-125											TONAL COMPONENT 160-400				
f (Hz)	12	16	20	25	32	40	50	63	80	100	125	160	200	250	315	400
dB (A)	0,0	0,0	-8,0	-7,8	-7,2	-5,9	-4,5	0,2	0,8	2,8	6,2	13,3	21,3	25,3	21,5	25,2
$L=L_t-L_S$			0,0	0,0	0,0	0,0	0,0	0,0	0,0	0,0	0,0	0,0	0,0	3,9	0,0	0,0
			No tonal component (20 – 125 Hz)									No tonal component (160-400 Hz)				
			KT =0									KT=0				
	Tonal Component 500-20000																
f (Hz)	500	630	800	1000	1250	1600	2000	2500	3200	4000	5000	6300	8000	10000	12500	16000	20000
dB (A)	27,0	29,5	33,4	30,6	33,4	42,1	32,6	32,7	38,5	33,8	31,0	43,6	52,1	24,8	16,3	22,7	-2,6
$L = L_t - L_S$	0,0	0,0	3,4	0,0	0,0	9,1	0,0	0,0	5,3	0,0	0,0	0,0	17,9	0,0	0,0	15,9	
	There is a strong tonal component (500 – 16000 Hz)																
	KT = 6																

Source: Ingex, 2016

Table 4.1-124. Frequency Sweep for LAeq, 1h Average Point 2 Daytime Week

	TONAL COMPONENT 20-125											TONAL COMPONENT 160-400				
f (Hz)	12	16	20	25	32	40	50	63	80	100	125	160	200	250	315	400
dB (A)	0,0	0,0	-7,9	-7,4	-6,6	-4,4	-0,7	3,5	8,9	11,2	14,5	16,7	23,0	24,7	22,4	25,6
$L=L_t-L_S$			0,0	0,0	0,0	0,0	0,0	0,0	0,0	0,0	0,0	0,0	0,0	2,0	0,0	0,0
			No tonal component (20 – 125 Hz)									No tonal component (160-400 Hz)				
			KT =0									KT=0				
	Tonal Component 500-20000																
f (Hz)	500	630	800	1000	1250	1600	2000	2500	3200	4000	5000	6300	8000	10000	12500	16000	20000
dB (A)	26,9	29,1	31,2	31,8	34,1	42,5	40,9	32,9	37,0	36,5	32,8	43,8	51,1	25,5	17,3	21,2	-2,4
$L = L_t - L_S$	0,0	0,0	0,0	0,0	0,0	5,0	0,0	0,0	2,2	0,0	0,0	0,0	16,5	0,0	0,0	13,8	
	There is a strong tonal component (500 – 16000 Hz)																
	KT = 6																

Source: Ingex, 2016

Table 4.1-125. Summary of Measurements Performed to Estimate Leq Point 2 Daytime Week

Measurement	Ti min	LAeq,Ti dB(A)	KTi dB(A)	KIi dB(A)	KSi dB(A)	KMax,i dB(A)	LRAeq,Ti dB(A)
1	15,00	52,80	6	0	0	6	58,80
2	15,00	52,60	6	0	0	6	58,60
3	15,00	52,50	6	0	0	6	58,50
4	15,00	52,90	6	0	0	6	58,90
5	15,00	53,40	6	0	0	6	59,40
T --->	75,00						
K Average --->			6,00	0,00	0,00	LRAeq,T--->	58,85
KMAX,G --->			6,00				
LAeq,T --->		52,85	LRAeq,T --->	58,85			

Source: Ingex, 2016

Table 4.1-126. Environmental Noise Results Corrected Point 2 Daytime Week

Results
L_{RAeq}
58,85±0,45

Source: Ingex, 2016

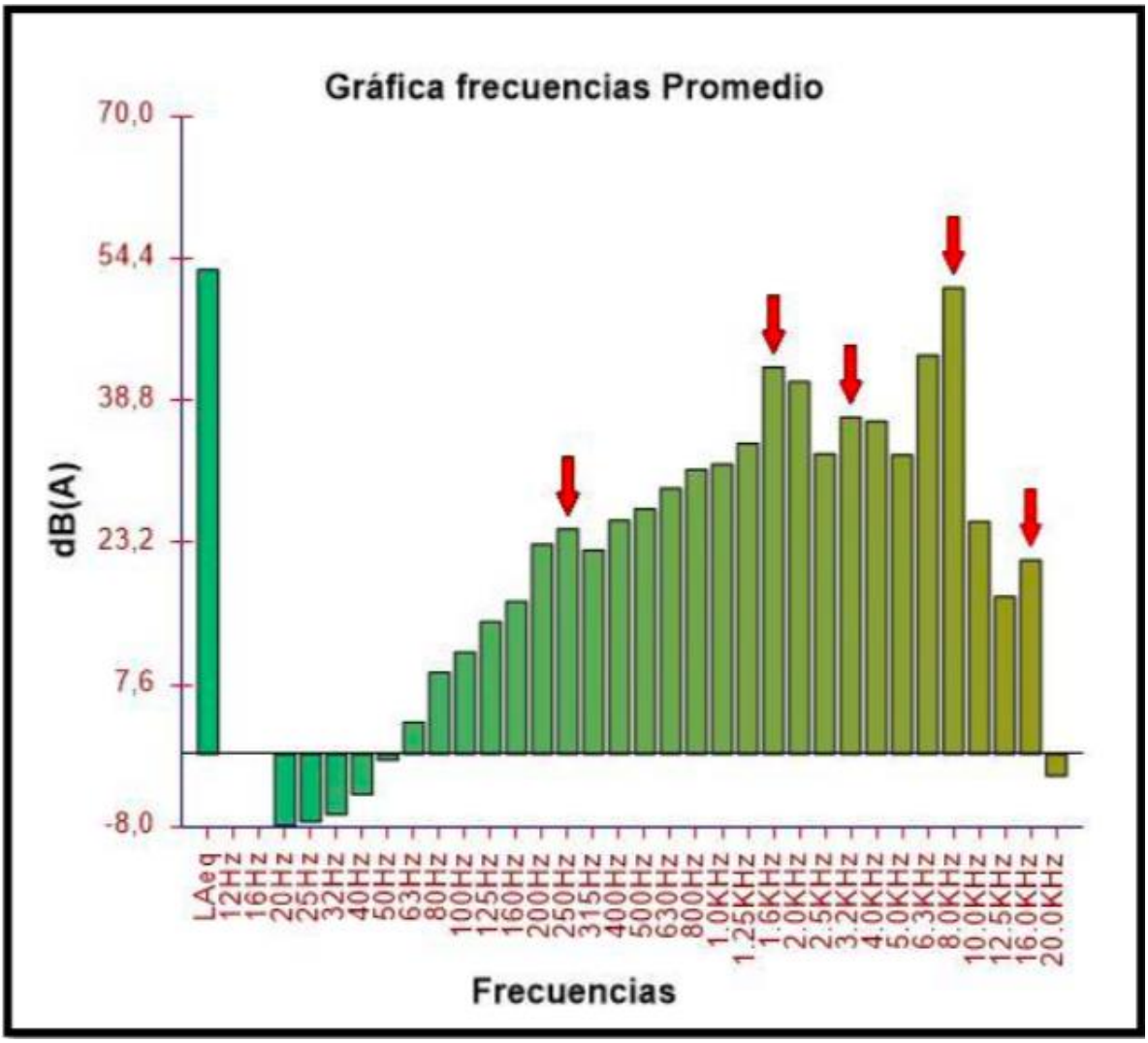

Illustration 4.1-247. Frequency sweep Average Point 2 Daytime Week.
Source: Ingex, 2016

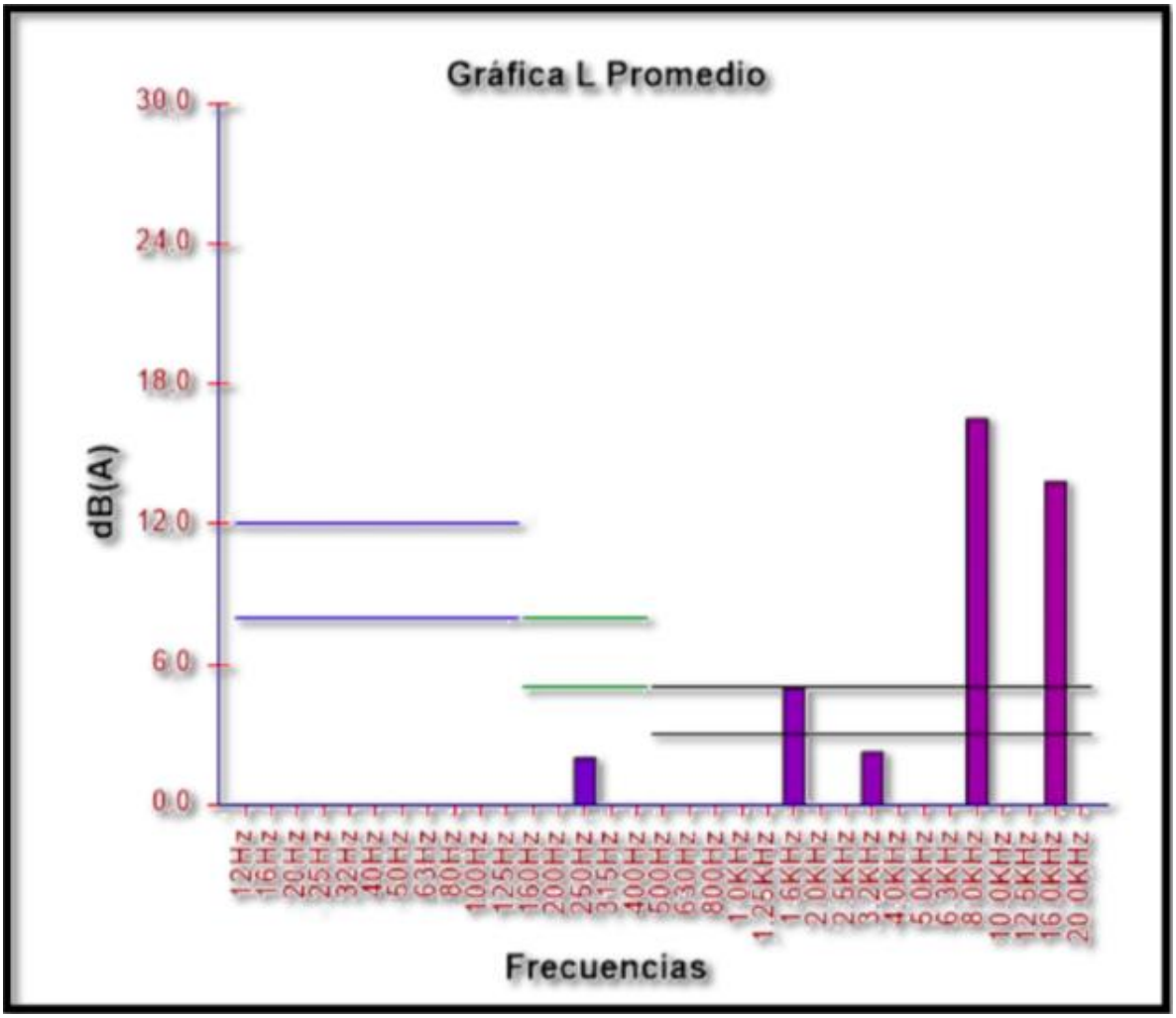

Illustration 4.1-248. Hue Adjustments Point 2 Daytime Week.
Source: Ingex, 2016

4.1.6.3.2.4 Uncertainty Evaluation Point 2 Daytime Week

The following table summarizes the n sources that contribute to the estimate of the measurand, the last row shows the combined uncertainty.

Table 4.1-127. Uncertainty Associated with the Estimation of the Measurand (LRAeq). Point 2.

Source	Unit	y	µ	V	ci	Ct (%)	p (%)	k ó tp (ef)	U
W	dB	0,0000	0,1585	â^ž	1,0000	50,5408	95,4500	2,0000	±0,3171
χ	dB	0,0000	0,1568	â^ž	1,0000	49,4592	95,4500	2,0000	±0,3137
γ	dB	0,0000	0,0000	â^ž	1,0000	0,0000	95,4500	2,0000	±0,0000
LRAeq	dB	58,8515	0,2230	â^ž	1,0000	100,0000	95,4500	2,0000	±0,4460

Source: Ingex, 2016

Where:
y = Value for the source
µ = Standard uncertainty
V = Degrees of freedom
ci = Sensitivity coefficient
Ct (%)= Percentage contribution to total uncertainty.
p (%)= The degree of confidence with which you want to estimate the coverage factor. k or tp(ef) = Coverage factor
U= Expanded uncertainty

4.1.6.3.2.5 Environmental Noise Point 3 Daytime Week

Below are the values found for the calculation of environmental noise in Point 2 during the daytime period, the evaluation was carried out on December 15, 2015.

Table 4.1-128. Frequency Sweep for LAeq, 1h Point 3 North Daytime Week

	TONAL COMPONENT 20-125											TONAL COMPONENT 160-400				
f (Hz)	12	16	20	25	32	40	50	63	80	100	125	160	200	250	315	400
dB (A)	0,0	0,0	-1,7	2,2	5,7	8,9	11,6	15,4	17,8	20,2	23,2	25,6	28,1	30,4	31,6	34,5
$L=L_t-L_S$			0,0	0,0	0,0	0,0	0,0	0,0	0,0	0,0	0,0	0,0	0,0	0,0	0,0	0,0
			No tonal component (20 – 125 Hz)									No tonal component (160-400 Hz)				
			KT =0									KT=0				

	Tonal Component 500-20000																
f (Hz)	500	630	800	1000	1250	1600	2000	2500	3200	4000	5000	6300	8000	10000	12500	16000	20000
dB (A)	34,5	36,8	41,2	43,3	43,1	47,0	44,1	42,8	39,5	37,9	38,0	42,1	48,5	36,6	28,1	22,8	15,3
$L=L_t-L_S$	0,0	0,0	0,0	1,1	0,0	3,4	0,0	0,0	0,0	0,0	0,0	0,0	9,2	0,0	0,0	15,9	
	There is a strong tonal component (500 – 16000 Hz)																
	KT = 6																

Source: Ingex, 2016

Table 4.1-129. Frequency Sweep for LAeq, 1h Point 3 South Daytime Week

	TONAL COMPONENT 20-125											TONAL COMPONENT 160-400				
f (Hz)	12	16	20	25	32	40	50	63	80	100	125	160	200	250	315	400
dB (A)	0,0	0,0	-7,8	-7,8	-7,3	-6,2	-3,9	0,5	4,2	10,1	15,2	18,1	20,5	22,8	24,4	26,2
$L=L_t-L_S$			0,0	0,0	0,0	0,0	0,0	0,0	0,0	0,0	0,0	0,0	0,0	0,0	0,0	0,0
			No tonal component (20 – 125 Hz)									No tonal component (160-400 Hz)				
			KT =0									KT=0				

	Tonal Component 500-20000																
f (Hz)	500	630	800	1000	1250	1600	2000	2500	3200	4000	5000	6300	8000	10000	12500	16000	20000
dB (A)	30,2	32,1	32,7	32,7	34,1	34,3	35,3	36,2	37,3	36,8	37,7	40,8	47,8	37,2	23,8	15,4	-1,1
$L=L_t-L_S$	0,0	0,0	0,0	0,0	0,0	0,0	0,0	0,0	0,8	0,0	0,0	0,0	8,8	0,0	0,0	0,0	
	There is a strong tonal component (500 – 16000 Hz)																
	KT = 6																

Source: Ingex, 2016

Table 4.1-130. Frequency Sweep for LAeq, 1h Point 3 East Daytime Week

	TONAL COMPONENT 20-125											TONAL COMPONENT 160-400				
f (Hz)	12	16	20	25	32	40	50	63	80	100	125	160	200	250	315	400
dB (A)	0,0	0,0	-7,9	-7,9	-7,6	-7,1	-4,7	-2,0	3,2	10,2	14,4	15,8	19,8	21,5	24,2	26,6
$L=L_t-L_S$			0,0	0,0	0,0	0,0	0,0	0,0	0,0	0,0	0,0	0,0	0,0	0,0	0,0	0,0
			No tonal component (20 – 125 Hz)									No tonal component (160-400 Hz)				
			KT =0									KT=0				

	Tonal Component 500-20000																
f (Hz)	500	630	800	1000	1250	1600	2000	2500	3200	4000	5000	6300	8000	10000	12500	16000	20000
dB (A)	29,1	34,5	34,9	35,6	41,4	39,4	39,6	36,8	36,6	35,6	36,4	41,5	47,2	35,8	22,2	14,1	-2,1
$L=L_t-L_S$	0,0	0,0	0,0	0,0	3,9	0,0	1,5	0,0	0,8	0,0	0,0	0,0	8,6	0,0	0,0	0,0	
	There is a strong tonal component (500 – 16000 Hz)																
	KT = 6																

Source: Ingex, 2016

Table 4.1-131. Frequency Sweep for LAeq, 1h Point 3 West Daytime Week

	TONAL COMPONENT 20-125											TONAL COMPONENT 160-400				
f (Hz)	12	16	20	25	32	40	50	63	80	100	125	160	200	250	315	400
dB (A)	0,0	0,0	-8,0	-7,9	-7,6	-7,1	-5,0	-1,9	3,0	9,6	13,9	15,7	19,7	21,4	23,6	26,4
$L=L_t-L_S$			0,0	0,0	0,0	0,0	0,0	0,0	0,0	0,0	0,0	0,0	0,0	0,0	0,0	0,0
			No tonal component (20 – 125 Hz)									No tonal component (160-400 Hz)				
			KT =0									KT=0				

	Tonal Component 500-20000																
f (Hz)	500	630	800	1000	1250	1600	2000	2500	3200	4000	5000	6300	8000	10000	12500	16000	20000
dB (A)	28,8	31,4	32,3	33,1	34,5	33,9	34,4	34,4	35,2	35,8	36,5	40,9	46,2	34,9	21,8	12,5	-2,4
$L = L_t - L_S$	0,0	0,0	0,0	0,0	1,0	0,0	0,0	0,0	0,0	0,0	0,0	0,0	8,3	0,0	0,0	0,0	
	There is a strong tonal component (500 – 16000 Hz)																
	KT = 6																

Source: Ingex, 2016

Table 4.1-132. Frequency Sweep for LAeq, 1h Point 3 Vertical Daytime Week

	TONAL COMPONENT 20-125											TONAL COMPONENT 160-400				
f (Hz)	12	16	20	25	32	40	50	63	80	100	125	160	200	250	315	400
dB (A)	0,0	0,0	-6,7	-5,4	-2,4	3,5	7,3	8,6	13,7	16,4	20,5	21,0	23,7	26,6	26,8	26,9
$L=L_t-L_S$			0,0	0,0	0,0	0,0	0,0	0,0	0,0	0,0	0,0	0,0	0,0	0,0	0,0	0,0
			No tonal component (20 – 125 Hz)									No tonal component (160-400 Hz)				
			KT =0									KT=0				
	Tonal Component 500-20000																
f (Hz)	500	630	800	1000	1250	1600	2000	2500	3200	4000	5000	6300	8000	10000	12500	16000	20000
dB (A)	27,5	29,8	33,4	33,5	38,6	41,5	42,6	43,9	39,6	38,4	39,5	42,9	48,1	37,3	30,4	24,2	14,5
$L = L_t - L_S$	0,0	0,0	0,0	0,0	1,0	0,0	0,0	2,8	0,0	0,0	0,0	0,0	8,0	0,0	0,0	0,0	
	There is a strong tonal component (500 – 16000 Hz)																
	KT = 6																

Source: Ingex, 2016

Table 4.1-133. Frequency Sweep for LAeq, 1h Average Point 3 Daytime Week

	TONAL COMPONENT 20-125											TONAL COMPONENT 160-400				
f (Hz)	12	16	20	25	32	40	50	63	80	100	125	160	200	250	315	400
dB (A)	0,0	0,0	-5,6	-3,1	-0,2	3,3	6,2	9,5	12,6	15,5	19,1	21,0	23,7	26,1	27,3	29,7
$L=L_t-L_S$			0,0	0,0	0,0	0,0	0,0	0,0	0,0	0,0	0,0	0,0	0,0	0,0	0,0	0,0
			No tonal component (20 – 125 Hz)									No tonal component (160-400 Hz)				
			KT =0									KT=0				
	Tonal Component 500-20000																
f (Hz)	500	630	800	1000	1250	1600	2000	2500	3200	4000	5000	6300	8000	10000	12500	16000	20000
dB (A)	30,8	33,6	36,4	37,9	39,7	41,9	40,7	40,4	38,0	37,0	37,8	41,7	47,6	36,5	26,6	20,3	11,1
$L = L_t - L_S$	0,0	0,0	0,0	0,0	0,0	1,7	0,0	2,8	0,0	0,0	0,0	0,0	8,5	0,0	0,0	0,0	
	There is a strong tonal component (500 – 16000 Hz)																
	KT = 6																

Source: Ingex, 2016

Table 4.1-134. Summary of Measurements Performed to Estimate Leq Point 3 Daytime Week

Measurement	Ti min	LAeq,Ti dB(A)	KTi dB(A)	KIi dB(A)	KSi dB(A)	KMax,i dB(A)	LRAeq,Ti dB(A)
1	15,00	54,30	6	0	0	6	60,30
2	15,00	50,50	6	0	0	6	56,50
3	15,00	51,10	6	0	0	6	57,10
4	15,00	49,30	6	0	0	6	55,30
5	15,00	52,60	6	0	0	6	58,60
T --->	75,00						
K Average --->			6,00	0,00	0,00	LRAeq,T--->	57,92
KMAX,G --->			6,00				
LAeq,T --->		51,92	LRAeq,T --->	57,92			

Source: Ingex, 2016

Table 4.1-135. Environmental Noise Results Corrected Point 3 Daytime Week

Results
L_{RAeq}
57,92±1,77

Source: Ingex, 2016

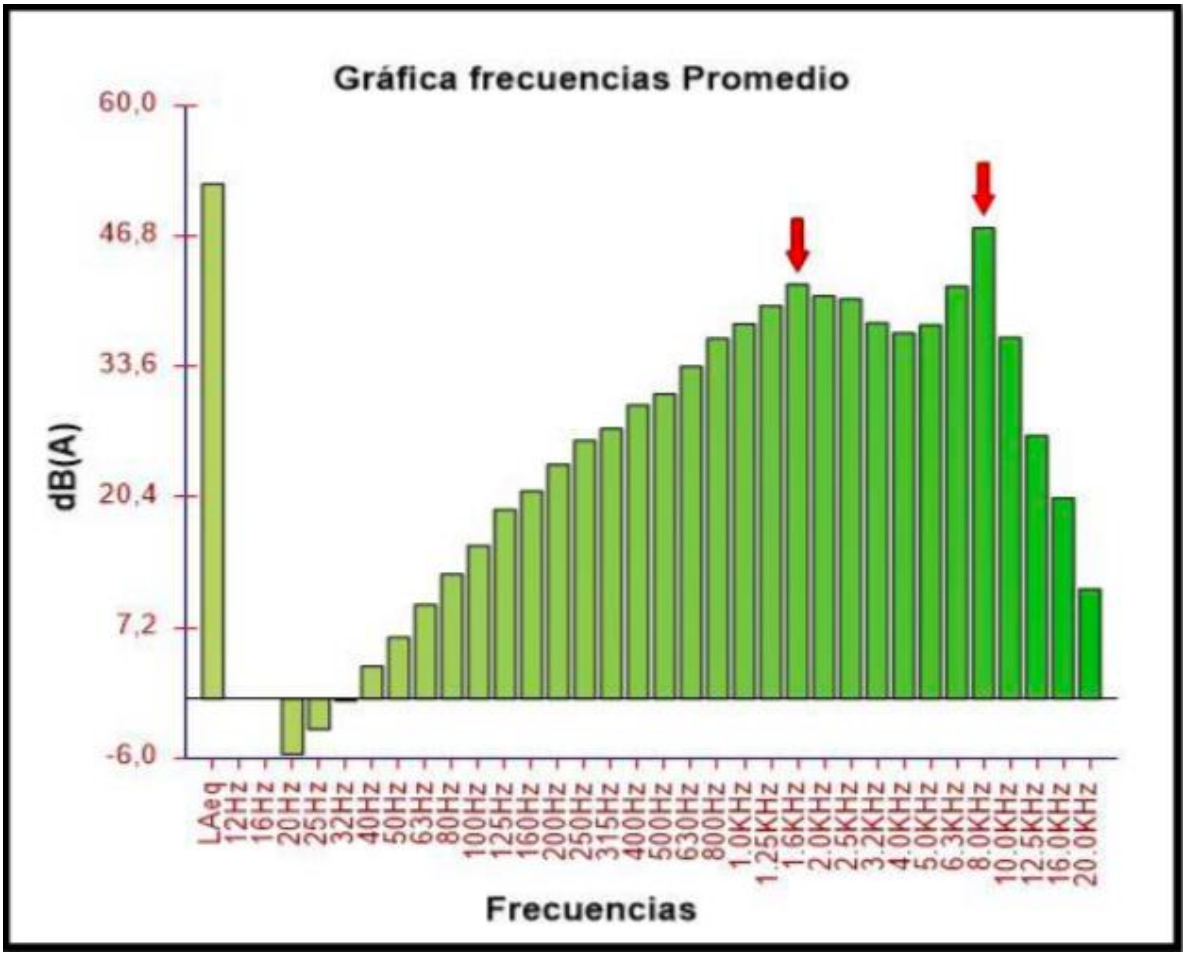

Illustration 4.1-249. Frequency sweep Average Point 3 Daytime Week.
Source: Ingex, 2016

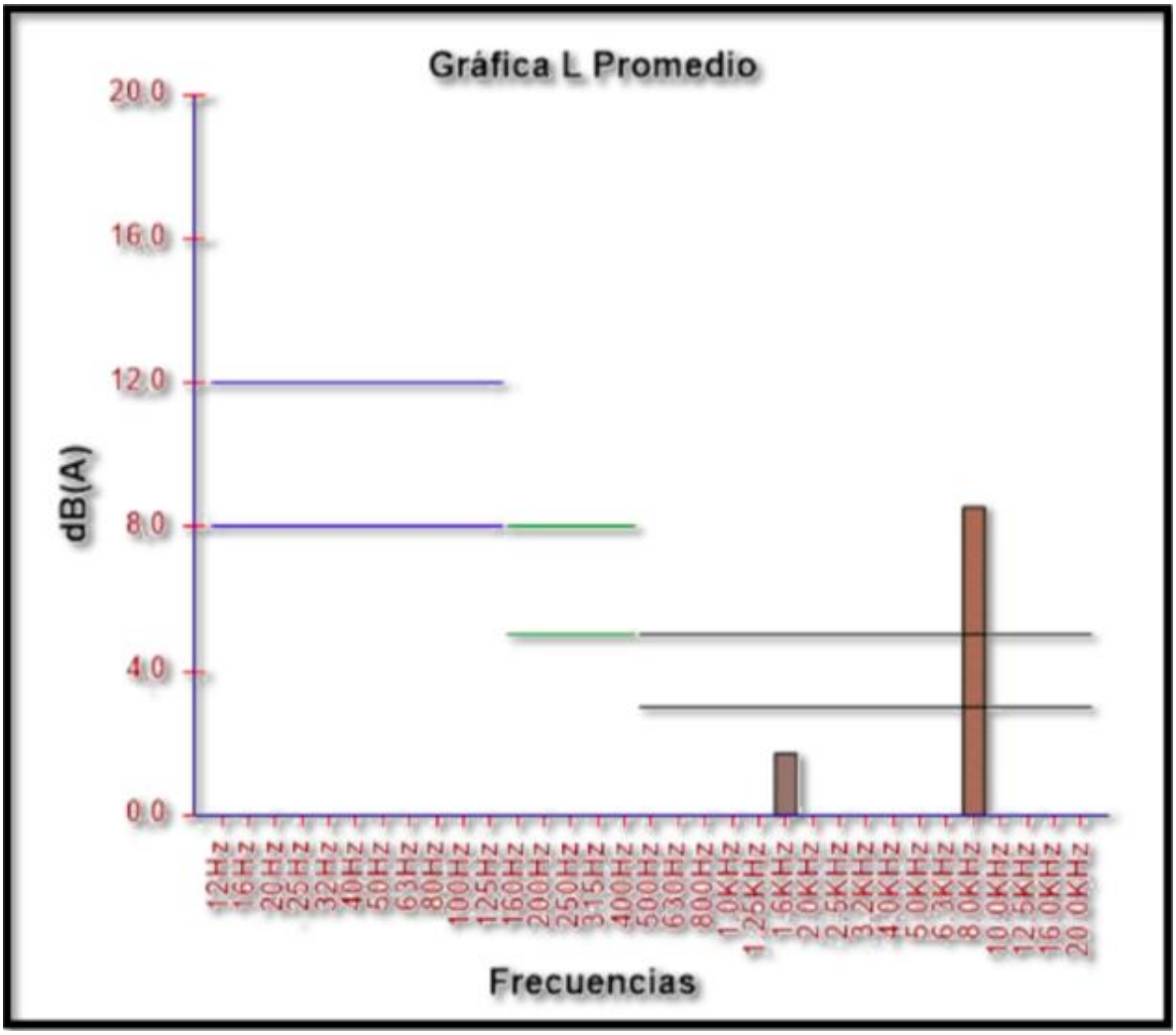

Illustration 4.1-250. Hue Adjustments Point 3 Daytime Week.
Source: Ingex, 2016

4.1.6.3.2.6 Uncertainty Evaluation Point 3 Daytime Week

The following table summarizes the n sources that contribute to the estimate of the measurand, the last row shows the combined uncertainty.

Table 4.1-136. Uncertainty Associated with the Estimation of the Measurand (LRAeq). Point 3.

Source	Unit	y	µ	V	ci	Ct (%)	p (%)	k ó tp (ef)	U
W	dB	0,0000	0,1714	â^ž	1,0000	3,7617	95,4500	2,0000	±0,3428
χ	dB	0,0000	0,8669	â^ž	1,0000	9,2383	95,4500	2,0000	±1,7339
γ	dB	0,0000	0,0000	â^ž	1,0000	0,0000	95,4500	2,0000	±0,0000
LRAeq	dB	57,9160	0,8837	â^ž	1,0000	100,0000	95,4500	2,0000	±1,7675

Source: Ingex, 2016

Where:
y = Value for the source
µ = Standard uncertainty
V = Degrees of freedom
ci = Sensitivity coefficient
Ct (%)= Percentage contribution to total uncertainty.
p (%)= The degree of confidence with which you want to estimate the coverage factor. k or tp(ef) = Coverage factor
U= Expanded uncertainty

4.1.6.3.2.7 Environmental Noise Point 4 Daytime Week

Below are the values found for the calculation of environmental noise in Point 4 during the daytime period, the evaluation was carried out on December 15, 2015.

Table 4.1-137. Frequency Sweep for LAeq, 1h Point 4 North Daytime Week

	TONAL COMPONENT 20-125											TONAL COMPONENT 160-400				
f (Hz)	12	16	20	25	32	40	50	63	80	100	125	160	200	250	315	400
dB (A)	0,0	0,0	-2,6	1,1	4,3	6,8	10,9	13,6	16,4	20,2	24,9	20,4	21,0	22,8	23,0	25,3
$L=L_t-L_S$			0,0	0,0	0,0	0,0	0,0	0,0	0,0	0,0	4,6	0,0	0,0	0,0	0,0	0,0
			No tonal component (20 – 125 Hz)									No tonal component (160-400 Hz)				
			KT =0									KT=0				

	Tonal Component 500-20000																
f (Hz)	500	630	800	1000	1250	1600	2000	2500	3200	4000	5000	6300	8000	10000	12500	16000	20000
dB (A)	28,3	30,8	32,9	32,2	31,6	32,5	32,1	30,3	31,1	29,7	30,1	32,3	41,9	36,3	21,5	16,3	6,5
$L=L_t-L_S$	0,0	0,0	1,4	0,0	0,0	0,6	0,0	0,0	1,1	0,0	0,0	0,0	7,6	0,0	0,0	0,0	
	There is a strong tonal component (500 – 16000 Hz)																
	KT = 6																

Source: Ingex, 2016

Table 4.1-138. Frequency Sweep for LAeq, 1h Point 4 South Daytime Week

	TONAL COMPONENT 20-125											TONAL COMPONENT 160-400				
f (Hz)	12	16	20	25	32	40	50	63	80	100	125	160	200	250	315	400
dB (A)	0,0	0,0	-2,6	1,1	4,3	6,8	10,9	13,6	16,4	20,2	24,9	20,4	21,0	22,8	23,0	25,3
$L=L_t-L_S$			0,0	0,0	0,0	0,0	0,0	0,0	0,0	0,0	4,6	0,0	0,0	0,0	0,0	0,0
			No tonal component (20 – 125 Hz)									No tonal component (160-400 Hz)				
			KT =0									KT=0				

	Tonal Component 500-20000																
f (Hz)	500	630	800	1000	1250	1600	2000	2500	3200	4000	5000	6300	8000	10000	12500	16000	20000
dB (A)	28,3	30,8	32,9	32,2	31,6	32,5	32,1	30,3	31,1	29,7	30,1	32,3	41,9	36,3	21,5	16,3	6,5
$L=L_t-L_S$	0,0	0,0	1,4	0,0	0,0	0,6	0,0	0,0	1,1	0,0	0,0	0,0	7,6	0,0	0,0	0,0	
	There is a strong tonal component (500 – 16000 Hz)																
	KT = 6																

Source: Ingex, 2016

Table 4.1-139. Frequency Sweep for LAeq, 1h Point 4 East Daytime Week

	TONAL COMPONENT 20-125											TONAL COMPONENT 160-400				
f (Hz)	12	16	20	25	32	40	50	63	80	100	125	160	200	250	315	400
dB (A)	0,0	0,0	-1,5	4,6	7,3	8,3	10,7	10,7	11,4	13,9	11,9	10,6	10,7	10,3	12,7	12,0
$L=L_t-L_S$			0,0	0,0	0,0	0,0	0,0	0,0	0,0	2,3	0,0	0,0	0,3	0,0	1,6	0,0
			No tonal component (20 – 125 Hz)									No tonal component (160-400 Hz)				
			KT =0									KT=0				

	Tonal Component 500-20000																
f (Hz)	500	630	800	1000	1250	1600	2000	2500	3200	4000	5000	6300	8000	10000	12500	16000	20000
dB (A)	14,4	19,3	27,1	30,1	28,4	27,5	29,5	30,9	21,0	20,8	29,5	32,5	38,5	35,5	18,8	14,4	-2,1
$L=L_t-L_S$	0,0	0,0	0,0	2,4	0,0	0,0	0,0	5,7	0,0	0,0	0,0	0,0	4,5	0,0	0,0	0,0	
	There is a strong tonal component (500 – 16000 Hz)																
	KT = 6																

Source: Ingex, 2016

Table 4.1-140. Frequency Sweep for LAeq, 1h Point 4 West Daytime Week

	TONAL COMPONENT 20-125											TONAL COMPONENT 160-400				
f (Hz)	12	16	20	25	32	40	50	63	80	100	125	160	200	250	315	400
dB (A)	0,0	0,0	0,5	4,1	6,7	8,8	10,6	12,1	13,4	15,8	16,3	14,8	13,2	17,5	13,3	15,2
$L=L_t-L_S$			0,0	0,0	0,0	0,0	0,0	0,0	0,0	0,0	1,0	0,0	0,0	4,3	0,0	0,0
			No tonal component (20 – 125 Hz)									No tonal component (160-400 Hz)				
			KT =0									KT=0				

	Tonal Component 500-20000																
f (Hz)	500	630	800	1000	1250	1600	2000	2500	3200	4000	5000	6300	8000	10000	12500	16000	20000
dB (A)	18,3	18,7	21,9	21,7	26,4	27,0	28,5	27,7	26,3	25,9	29,1	30,6	34,0	34,7	19,9	16,3	-1,8
$L = L_t - L_S$	0,0	0,0	1,7	0,0	0,0	0,0	1,2	0,0	0,0	0,0	0,0	0,0	7,8	0,0	0,0	0,0	
	There is a strong tonal component (500 – 16000 Hz)																
	KT = 6																

Source: Ingex, 2016

Table 4.1-141. Frequency Sweep for LAeq, 1h Point 4 Vertical Daytime Week

	TONAL COMPONENT 20-125											TONAL COMPONENT 160-400				
f (Hz)	12	16	20	25	32	40	50	63	80	100	125	160	200	250	315	400
dB (A)	0,0	0,0	-2,6	1,1	4,3	6,8	10,9	13,6	16,4	20,2	24,9	20,4	21,0	22,8	23,0	25,3
$L=L_t-L_S$			0,0	0,0	0,0	0,0	0,0	0,0	0,0	0,0	4,6	0,0	0,0	0,0	0,0	0,0
			No tonal component (20 – 125 Hz)									No tonal component (160-400 Hz)				
			KT =0									KT=0				

	Tonal Component 500-20000																
f (Hz)	500	630	800	1000	1250	1600	2000	2500	3200	4000	5000	6300	8000	10000	12500	16000	20000
dB (A)	28,3	30,8	32,9	32,2	31,6	32,5	32,1	30,3	31,1	29,7	30,1	32,3	41,9	36,3	21,5	16,3	6,5
$L = L_t - L_S$	0,0	0,0	1,4	0,0	0,0	0,6	0,0	0,0	1,1	0,0	0,0	0,0	7,6	0,0	0,0	0,0	
	There is a strong tonal component (500 – 16000 Hz)																
	KT = 6																

Source: Ingex, 2016

Table 4.1-142. Frequency Sweep for LAeq, 1h Average Point 4 Daytime Week

	TONAL COMPONENT 20-125											TONAL COMPONENT 160-400				
f (Hz)	12	16	20	25	32	40	50	63	80	100	125	160	200	250	315	400
dB (A)	0,0	0,0	-1,6	2,7	5,6	7,6	10,8	12,9	15,2	18,8	22,9	18,7	19,1	21,1	21,1	23,3
$L=L_t-L_S$			0,0	0,0	0,0	0,0	0,0	0,0	0,0	0,0	4,2	0,0	0,0	1,0	0,0	0,0
			No tonal component (20 – 125 Hz)									No tonal component (160-400 Hz)				
			KT =0									KT=0				

	Tonal Component 500-20000																
f (Hz)	500	630	800	1000	1250	1600	2000	2500	3200	4000	5000	6300	8000	10000	12500	16000	20000
dB (A)	26,3	28,8	31,2	30,9	30,4	31,1	31,1	30,0	29,5	28,2	29,8	32,1	40,5	35,9	20,8	16,0	4,7
$L = L_t - L_S$	0,0	0,0	1,3	0,0	0,0	0,6	0,6	0,0	1,1	0,0	0,0	0,0	6,5	0,0	0,0	0,0	
	There is a strong tonal component (500 – 16000 Hz)																
	KT = 6																

Source: Ingex, 2016

Table 4.1-143. Summary of Measurements Performed to Estimate Leq Point 4 Daytime Week

Measurement	Ti min	LAeq,Ti dB(A)	KTi dB(A)	KIi dB(A)	KSi dB(A)	KMax,i dB(A)	LRAeq,Ti dB(A)
1	15,00	45,70	6	0	0	6	51,70
2	15,00	45,70	6	0	0	6	51,70
3	15,00	42,70	6	0	0	6	48,70
4	15,00	40,40	6	0	0	6	46,40
5	15,00	45,70	6	0	0	6	51,70
T --->	75,00						
K Average --->			6,00	0,00	0,00	LRAeq,T--->	50,50
KMAX,G --->			6,00				
LAeq,T --->		44,50	LRAeq,T --->	50,50			

Source: Ingex, 2016

Table 4.1-144. Environmental Noise Results Corrected Point 4 Daytime Week

Results
L_{RAeq}
50,50±2,19

Source: Ingex, 2016

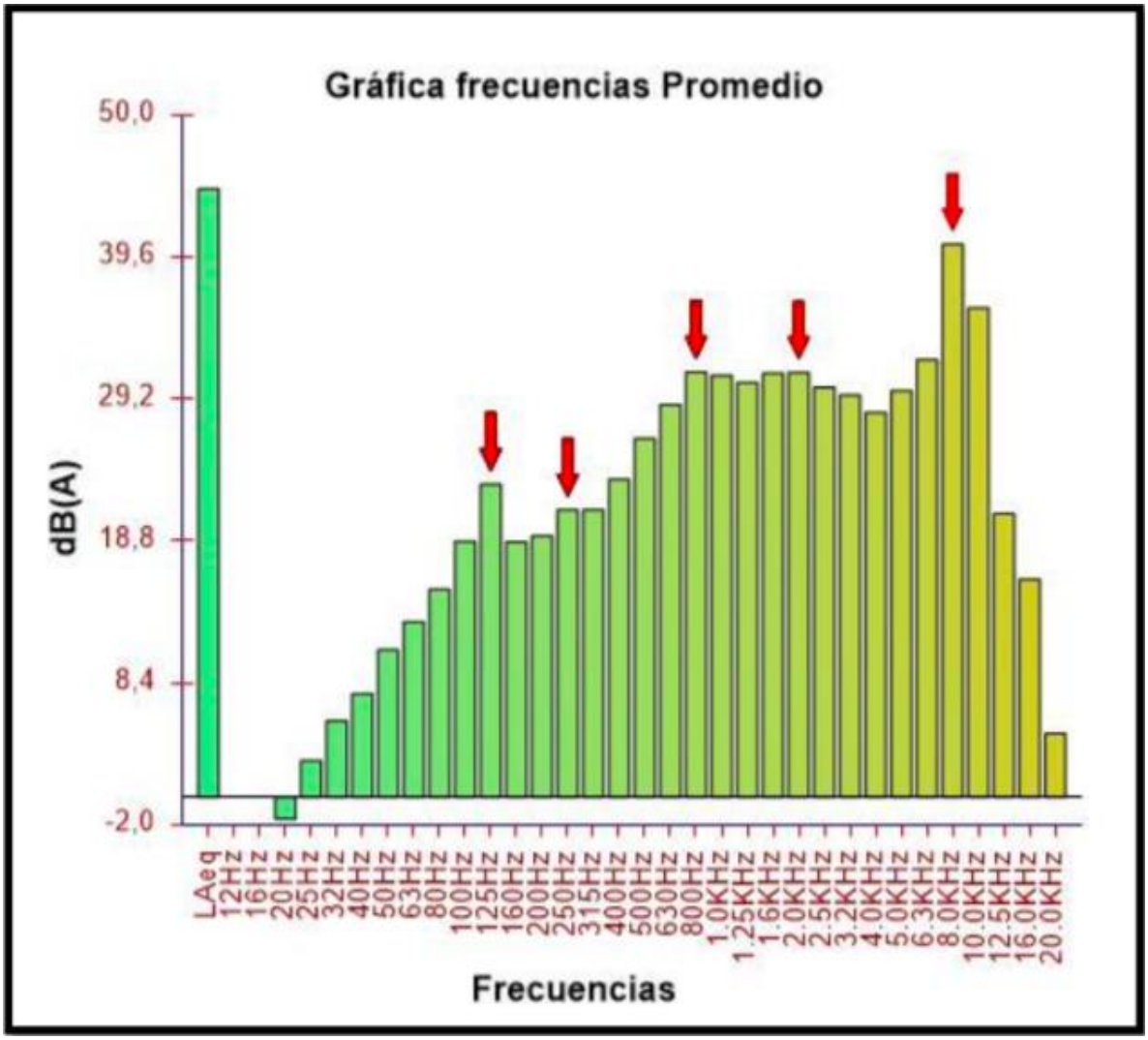

Illustration 4.1-251. Frequency sweep Average Point 4 Daytime Week.
Source: Ingex, 2016

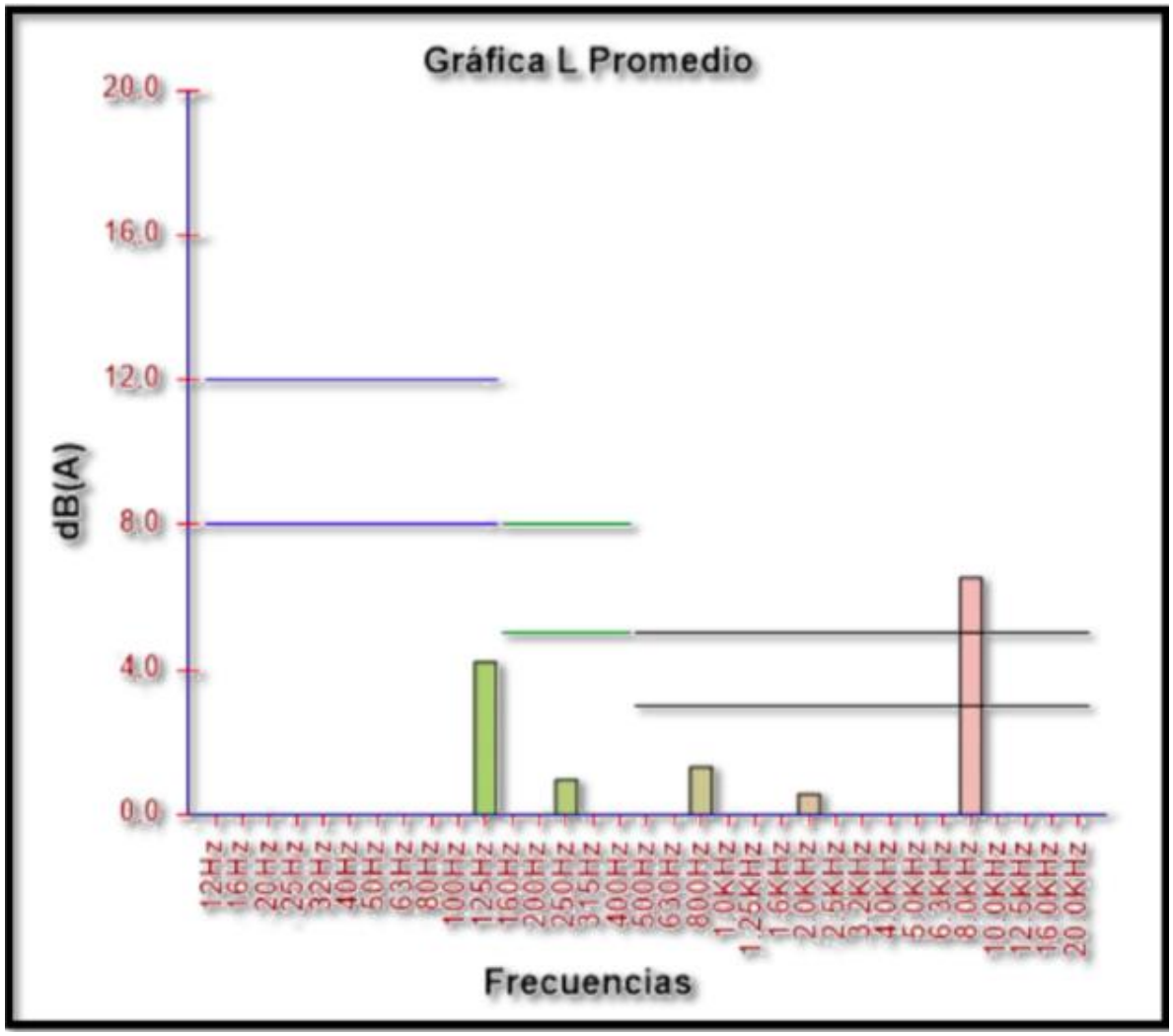

Illustration 4.1-252. Hue Adjustments Point 4 Daytime Week.
Source: Ingex, 2016

4.1.6.3.2.8 Uncertainty Evaluation Point 4 Daytime Week

The following table summarizes the n sources that contribute to the estimate of the measurand, the last row shows the combined uncertainty.

Table 4.1-145. Uncertainty Associated with the Estimation of the Measurand (LRAeq). Point 4.

Source	Unit	y	µ	V	ci	Ct (%)	p (%)	k ó tp (ef)	U
W	dB	0,0000	0,1702	â^ž	1,0000	2,4238	95,4500	2,0000	±0,3403

χ	dB	0,0000	1,0796	â^ž	1,0000	97,5762	95,4500	2,0000	±2,1593
γ	dB	0,0000	0,0000	â^ž	1,0000	0,0000	95,4500	2,0000	±0,0000
LRAeq	dB	50,5039	1,0930	â^ž	1,0000	100,0000	95,4500	2,0000	±2,1859

Source: Ingex, 2016

Where:
y = Value for the source
μ = Standard uncertainty
V = Degrees of freedom
ci = Sensitivity coefficient
Ct (%)= Percentage contribution to total uncertainty.
p (%)= The degree of confidence with which you want to estimate the coverage factor. k or tp(ef) = Coverage factor
U= Expanded uncertainty

4.1.6.3.3 Conclusions

The environmental noise evaluations carried out on the four (4) points of influence of the mining project El Pescado located in Segovia - Antioquia, in accordance with Resolution 0627 of 2006 of the Ministry of the Environment, Housing and Territorial Development, now the Ministry of the Environment and Sustainable Development, show that the values of Point 1 (53,05 dB(A) ± 3,67 dB(A)) and Point 4 (50,50 dB(A) ± 2,19 dB(A)) comply with the above mentioned standard, unlike the values evaluated in Point 2 (58,85 dB(A) ± 0,45 dB(A)) and Point 3 (57,92 dB(A) ± 1,77 dB(A)), which do not meet the maximum permissible standards of ambient noise levels in dB(A) for the suburban or rural sector D for quietness and moderate noise established in Table 2 of Article 17 of Resolution 0627 of 2006 which is set at 55 dB(A).

Below is a summary of the Environmental Noise results calculated in the area described.

Table 4.1-146. Summary of Environmental Noise Assessment Daytime Week

Point	Coordinates		Environmental Noise Evaluated dB (A)	Maximum standard daylight time allowed dB(A)
Point 1	07°15'40,9"N	074°44'42,2"O	53,05 ± 3,67*	55
Point 2	07°16'07,2"N	074°43'00,0"O	58,85 ± 0,45*	55
Point 3	07°15'09,6"N	074°42'33,3"O	57,92 ± 1,77*	55
Point 4	07°14'30,7"N	074°42'00,1"O	50,50 ± 2,19*	55

* These results are valid for the day and time of measurement.
Source: Ingex, 2016

4.1.7 LANDSCAPE

Following are the units and elements of landscape, and visual analysis.

4.1.7.1 LANDSCAPE UNITS

The process of mapping algebra between the geomorphology and flora themes, managed to obtain thirty-two (32) landscape units (hereinafter UP), formed by vegetation coverings settled in geomorphological units and the access road as an existing anthropic intervention of the landscape devoid of vegetation (See Table 4.1-147 and illustrations).

Table 4.1-147. UP identified and percentage distributions.

#	UNITY OF LANDSCAPE (UL)	PERCENTAGE QUANTITY PER UNIT OF LANDSCAPE	PERCENTAGE DISTRIBUTION OF UPSTREAM AREAS OF UL
1	Dense forest beneath the mainland in hills (Dfbm – Dc)	2,25%	1,89%
2	Dense forest under the mainland on back (Dfum – Dl)	3,37%	12,76%
3	Dense underground forest on steep slopes on the mainland (Duf– Dle)	6,74%	21,22%
4	Dense lowland forest on moderate slope (Dlf – Dlm)	4,49%	8,84%
5	Dense under-ground forest on the terrace (Duf – Ft)	4,49%	0,39%
6	Dense underground forest on structural spine (Duf – Sle)	2,25%	0,63%
7	Cocoa on a hill (Ch – Dc)	1,12%	0,13%
8	Caco on moderate slope (Ch – Dlm)	1,12%	0,20%
9	Moderate slope grass (gr –Dlm)	4,49%	0,35%
10	Pasto en terraza (Pa – Ft)	2,25%	0,61%
11	Clean grass on an esplanade slope (Cgr – Ale)	1,12%	0,26%
12	Clean grass on a hill (Cgr – Dc)	3,37%	3,16%
13	Clean grass on back (Cgr– Dl)	6,74%	18,15%
14	Clean grass on steep slopes (Cgr – Del)	5,62%	9,27%
15	Clean grass on moderate slope (Cgr– Dlm)	6,74%	10,38%
16	Clean grass on the terrace (Cgr – Ft)	6,74%	2,15%
17	Clean grass on structural spine (Cgr – Sle)	1,12%	2,48%
18	Discontinuous urban fabric on an esplanade slope (Duf – Ale)	1,12%	1,06%
19	Urban discontinuous spine fabric (Udf – Dl)	6,74%	0,22%
20	Discontinuous urban fabric on steep slopes (Duf – Dle)	3,37%	0,34%
21	Urban fabric discontinuous on moderate slope (Ufd – Dlm)	1,12%	0,02%
22	Discontinuous urban fabric on terrace (Duf – Ft)	3,37%	0,74%
23	Road on an esplanade slope (R – Ale)	1,12%	0,05%
24	Roadway full of debris (R – All)	1,12%	0,01%
25	Loin track (L – Dl)	1,12%	0,20%
26	Road on steep slope (R – Dle)	1,12%	0,00%
27	Moderate slope road (R – Dlm)	1,12%	0,11%
28	Road on the terrace (R – Ft)	1,12%	0,09%
29	Secondary low hill vegetation (Sv – Dc)	1,12%	0,53%
30	Secondary low back vegetation (Sv – Dl)	3,37%	2,27%

#	UNITY OF LANDSCAPE (UL)	PERCENTAGE QUANTITY PER UNIT OF LANDSCAPE	PERCENTAGE DISTRIBUTION OF UPSTREAM AREAS OF UL
31	Secondary low vegetation on steep slopes (Sv – Dle)	2,25%	1,33%
32	Secondary low vegetation on moderate slopes (Sv – Dlm)	6,74%	0,15%

Source: INGEX, 2015.

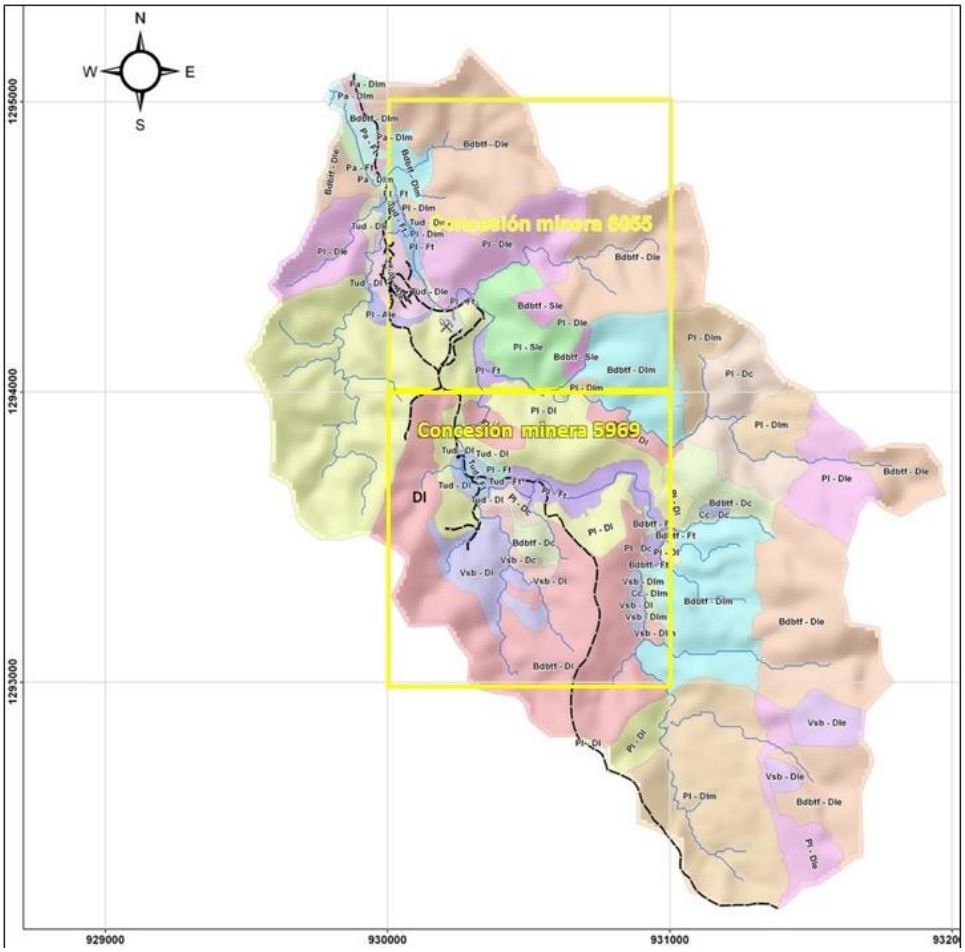

Illustration 4.1-253. Landscape units.
Source: INGEX, 2015.

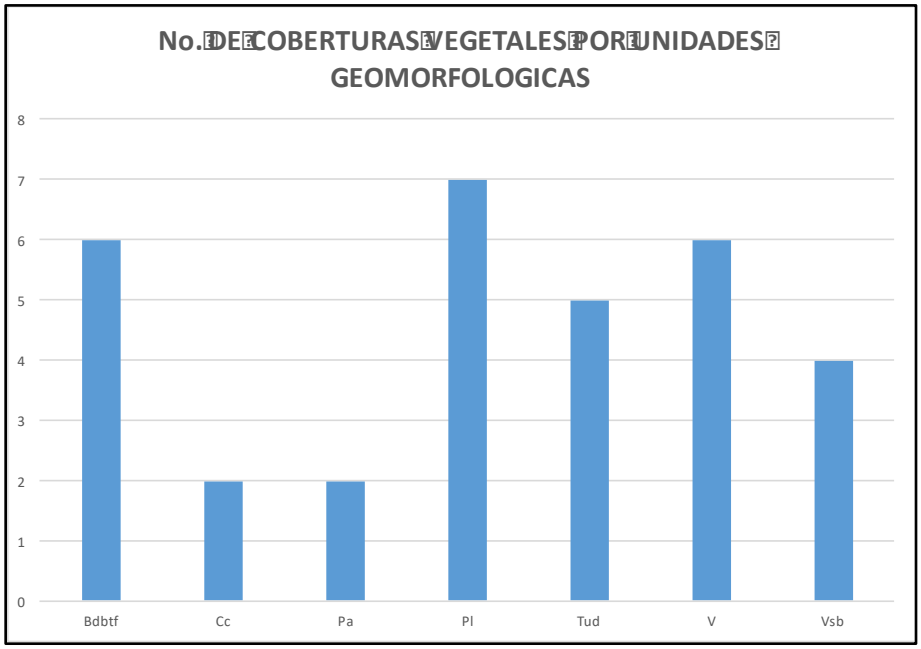

Illustration 4.1-254. No. of plant coverings by geomorphological units.
Source: INGEX, 2015.

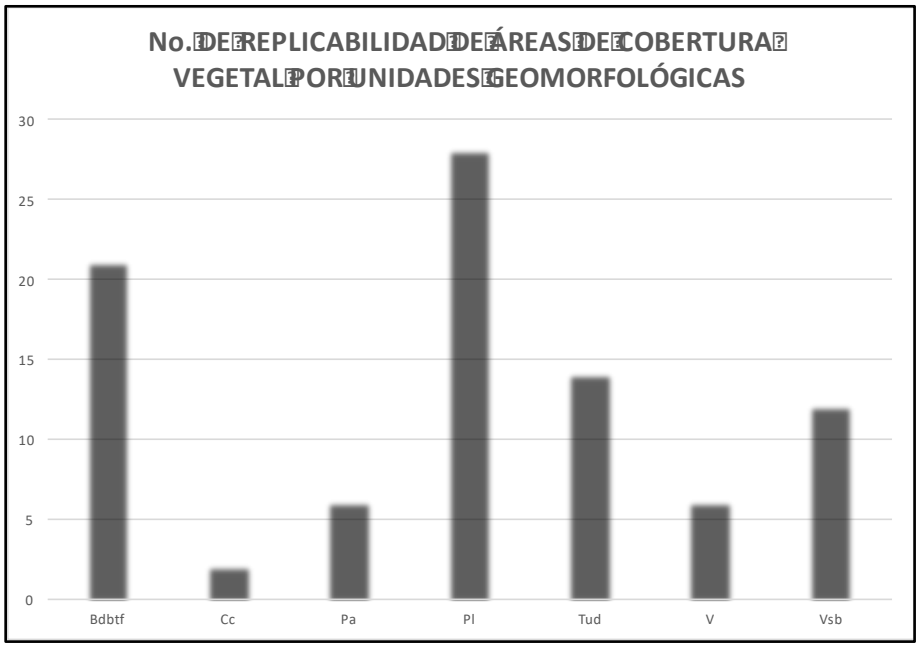

Illustration 4.1-255. No. of replicability of vegetation cover areas by geomorphological units.
Source: INGEX, 2015.

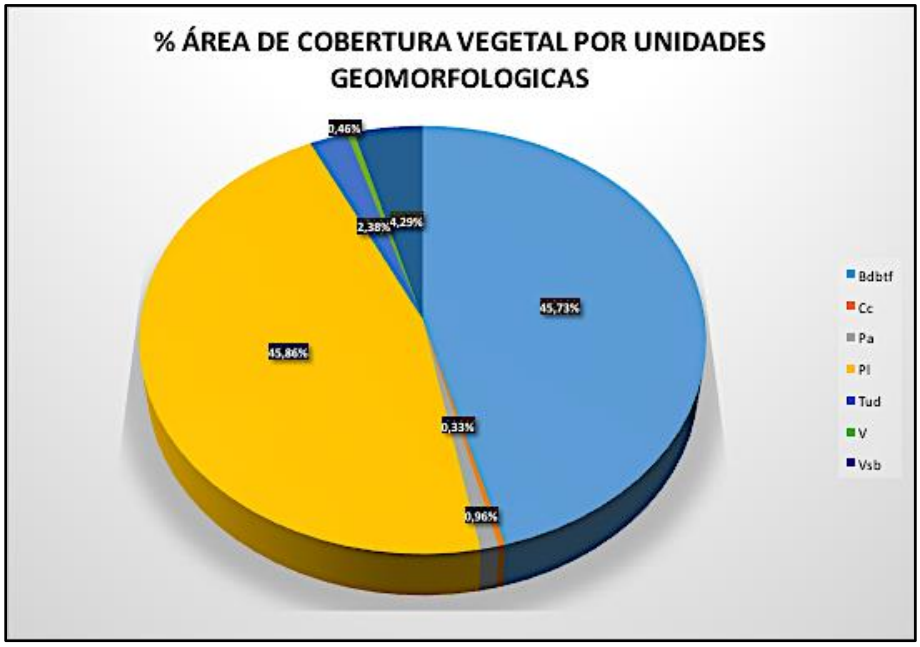

Illustration 4.1-256. Percentage of vegetative cover area by geomorphological units.
Source: INGEX, 2015.

The coverage of clean grass is 7 UP (See Illustration 4.1-254), in 28 areas (See Illustration 4.1-255) and representing 45.73% (See Illustration 4.1-256) in the basin area.

The dense forest under the mainland makes up 6 UP in 21 areas and represents 45.86% of the basin area.

Then, in descending order, there are the following coverages:

Discontinuous urban fabric with 5 UP, 14 areas and 2.38% in the basin area.

Secondary low vegetation with 4 UPs and 12 areas. But with a higher percentage of the basin area than the discontinuous urban fabric (4.29%).

Grass with 2 UP, 6 areas and 0.96% in the basin area.

Way with 6 UP, 6 areas and 0.46% in the basin area.

Crops with 2 UP, 2 areas and 0.33% in the basin area.

By unifying the categories of grass (Pa) with clean grass (Pl) and the others resulting from anthropogenic interventions (Crops, Discontinuous urban weaving, low secondary road and

vegetation), anthropism predominates with 54% and dense forest under the mainland with 46% (See Illustration 4.1-257).

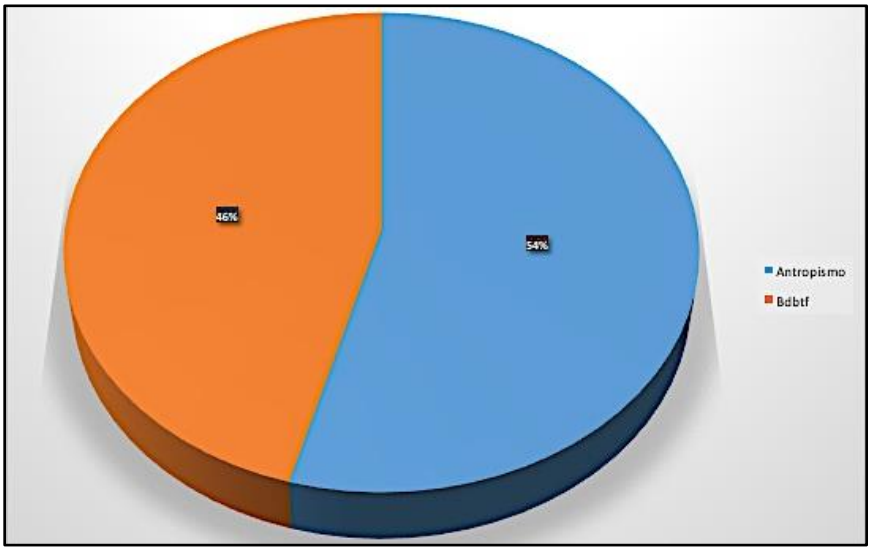

Illustration 4.1-257. Percentage distribution of anthropism and dense underground forest.
Source: INGEX, 2015.

The landscape units; Pl-Dl and Pl-Dlm have 6 areas each, so they are the most disaggregated and/or replicable of the clean grass cover. Secondarily, Bdbtf - Dle, Tud - Dl and Vsb - Dlm are more replicable (see Illustration 4.1-258).

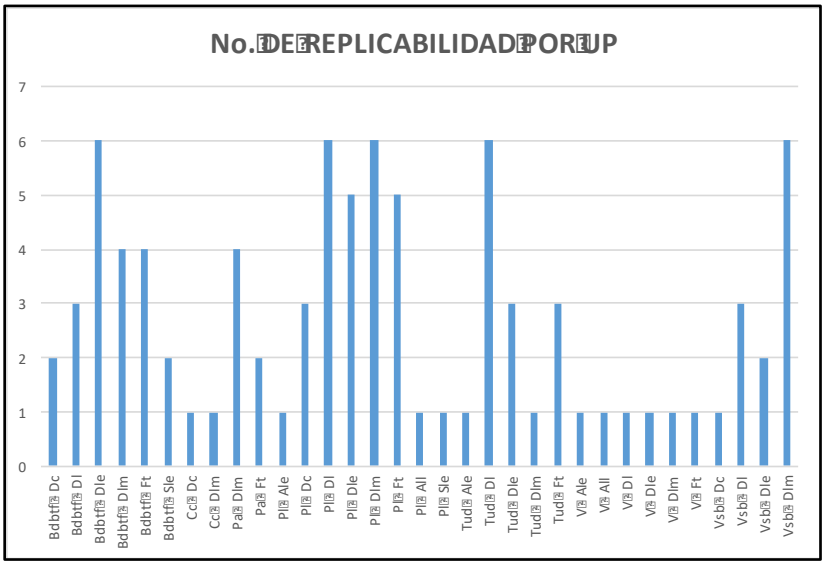

Illustration 4.1-258. No. of replicability by UP.
Source: INGEX, 2015.

The UP with the highest percentage of area is Bdbtf - Dle, with 21.20% and followed in descending order by Pl - Dl (18.13%), Bdbtf - Dl (12.75%), Pl - Dlm (10.37%), Pl - Dle (9.26%) and Bdbtf - Dlm (8.83%), as shown in Illustration 4.1-259.

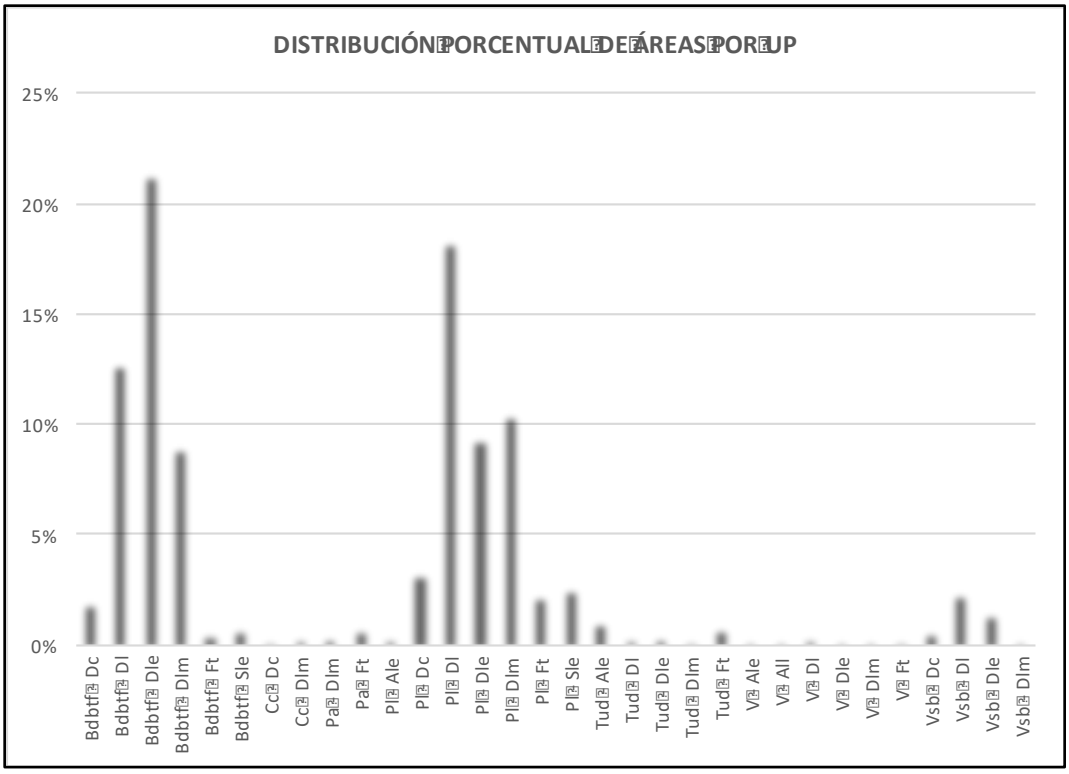

Illustration 4.1-259. Percentage distribution of areas by UP.
Source: INGEX, 2015.

4.1.7.2 LANDSCAPE ELEMENTS

Table 4.1-98 shows the identified landscape elements (see Illustration 4.1-259 and Illustration 4.1-260).

Table 4.1-148. Landscape elements and percentage distributions.

LANDSCAPE ELEMENT	PERCENTAGE DISTRIBUTION OF AREAS
Matrix	50,10%
Remaining patch	0,58%
Environmental Resource Patch	45,07%
Green Corridor or Connector and Remaining Patch	4,26%
TOTAL	**100,00%**

Source: INGEX, 2015.

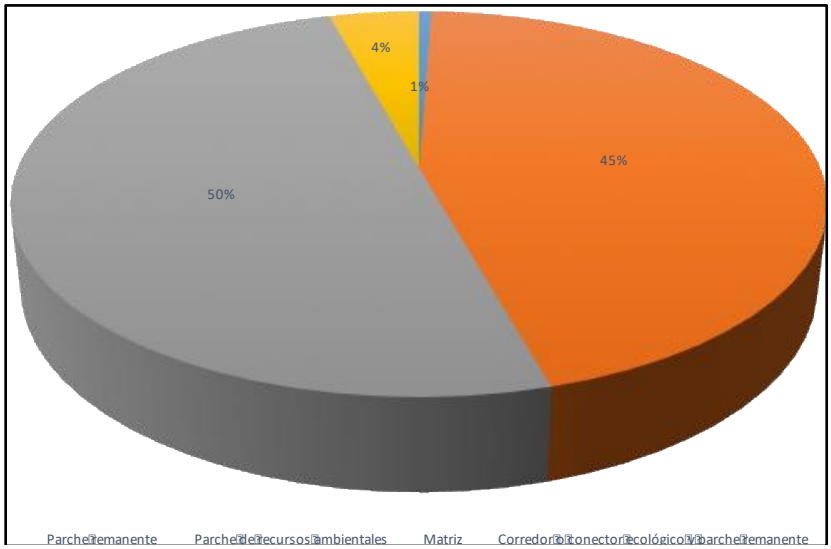

Illustration 4.1.260. Landscape elements and percentage distributions.
Source: INGEX, 2015.

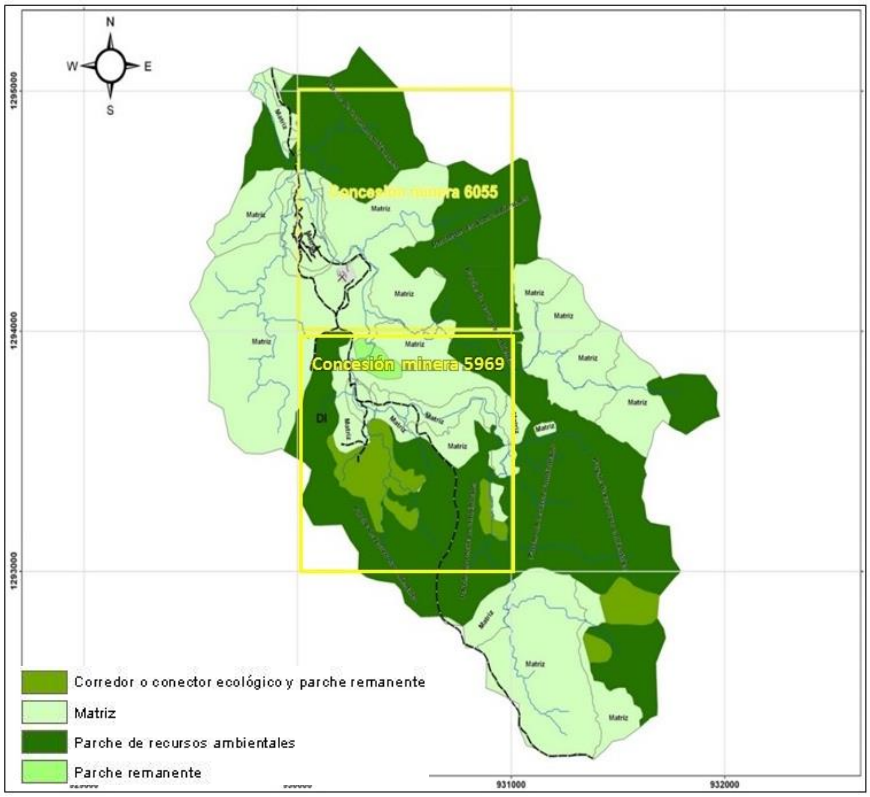

Illustration 4.1-261. Landscape elements.
Source: INGEX, 2015.

The matrix corresponds to the region dominated by anthropism with the exception of the lower secondary vegetation which is the ecological connector of the forests and the remaining patches depending on the location. While the dense forest under the mainland is a patch of environmental resources.

4.1.7.3 VISUAL LANDSCAPE ANALYSIS

In addition to landscape analysis from the perspective of vegetation cover, geomorphology and anthropism. In this item, it is presented from a visual perspective through visibility, aesthetic potential, quality and visual fragility.

Visibility

They were evaluated from the visual basins (observation points), each one of the UPs. This assessment resulted in the levels of visibility presented in Table 4.1-149 and illustrations.

Table 4.1-149. Visibility assessment by UP.

#	UP	VISIBILITY
1	Bdbtf - Dc	Nearby
2	Bdbtf - Dc	Nearby
3	Bdbtf - Dl	Nearby
4	Bdbtf - Dl	Nearby
5	Bdbtf - Dl	Nearby
6	Bdbtf - Dl - T	Nearby
7	Bdbtf - Dle	Nearby
8	Bdbtf - Dle	Nearby
9	Bdbtf - Dle	Nearby
10	Bdbtf - Dle	Nearby
11	Bdbtf - Dle	Nearby
12	Bdbtf - Dle	Nearby
13	Bdbtf - Dle - T	Nearby
14	Bdbtf - Dlm	Nearby
15	Bdbtf - Dlm	Nearby
16	Bdbtf - Dlm	Nearby
17	Bdbtf - Dlm	Nearby
18	Bdbtf - Ft	Nearby
19	Bdbtf - Ft	Nearby
20	Bdbtf - Ft	Nearby
21	Bdbtf - Ft	Nearby
22	Bdbtf - Sle	Nearby
23	Bdbtf - Sle	Nearby
24	Cc - Dc	faraway

#	UP	VISIBILITY
25	Cc - Dlm	faraway
26	Pa - Dlm	Nearby
27	Pa - Dlm	Nearby
28	Pa - Dlm	Nearby
29	Pa - Dlm	Nearby
30	Pa - Ft	Nearby
31	Pa - Ft	Nearby
32	Pl - Ale	Nearby
33	Pl - All	Nearby
34	Pl - Dc	Nearby
35	Pl - Dc	Nearby
36	Pl - Dc	Nearby
37	Pl - Dl	Nearby
38	Pl - Dl	Nearby
39	Pl - Dl	Nearby
40	Pl - Dl	Nearby
41	Pl - Dl	Nearby
42	Pl - Dl	Nearby
43	Pl - Dl - T	Nearby
44	Pl - Dl - T	Nearby
45	Pl - Dle	Nearby
46	Pl - Dle	Nearby
47	Pl - Dle	Nearby
48	Pl - Dle	Nearby

#	UP	VISIBILITY
49	Pl - Dle	Nearby
50	Pl - Dle - T	Nearby
51	Pl - Dle - T	Nearby
52	Pl - Dlm	Nearby
53	Pl - Dlm	Nearby
54	Pl - Dlm	Nearby
55	Pl - Dlm	Nearby
56	Pl - Dlm	Nearby
57	Pl - Dlm	Nearby
58	Pl - Dlm - T	Nearby
59	Pl - Dlm - T	Nearby
60	Pl - Ft	Nearby
61	Pl - Ft	Nearby
62	Pl - Ft	Nearby
63	Pl - Ft	Nearby
64	Pl - Ft	Nearby
65	Pl - Ft - T	Nearby
66	Pl - Ft - T	Nearby
67	Pl - Ft - T	Nearby
68	Pl - Sle	Nearby
69	Pl - Sle - T	Nearby
70	Tud - Ale	Medium
71	Tud - Dl	Medium
72	Tud - Dl	Medium
73	Tud - Dl	Medium
74	Tud - Dl	Medium
75	Tud - Dl	Medium
76	Tud - Dl	Medium
77	Tud - Dle	Medium
78	Tud - Dle	Medium
79	Tud - Dle	Medium
80	Tud - Dlm	Medium
81	Tud - Dlm - T	Medium
82	Tud - Ft	Medium
83	Tud - Ft	Medium
84	Tud - Ft	Medium
85	Tud - Ft - T	Medium
86	V - Ale	Medium
87	V - All	Medium
88	V - Dl	Medium

#	UP	VISIBILITY
89	V - Dle	Medium
90	V - Dlm	Medium
91	V - Ft	Medium
92	Vsb - Dc	Medium
93	Vsb - Dl	Medium
94	Vsb - Dl	Medium
95	Vsb - Dl	Medium
96	Vsb - Dle	Medium
97	Vsb - Dle	Medium
98	Vsb - Dlm	Medium
99	Vsb - Dlm	Medium
100	Vsb - Dlm	Medium
101	Vsb - Dlm	Medium
102	Vsb - Dlm	Medium
103	Vsb - Dlm	Medium

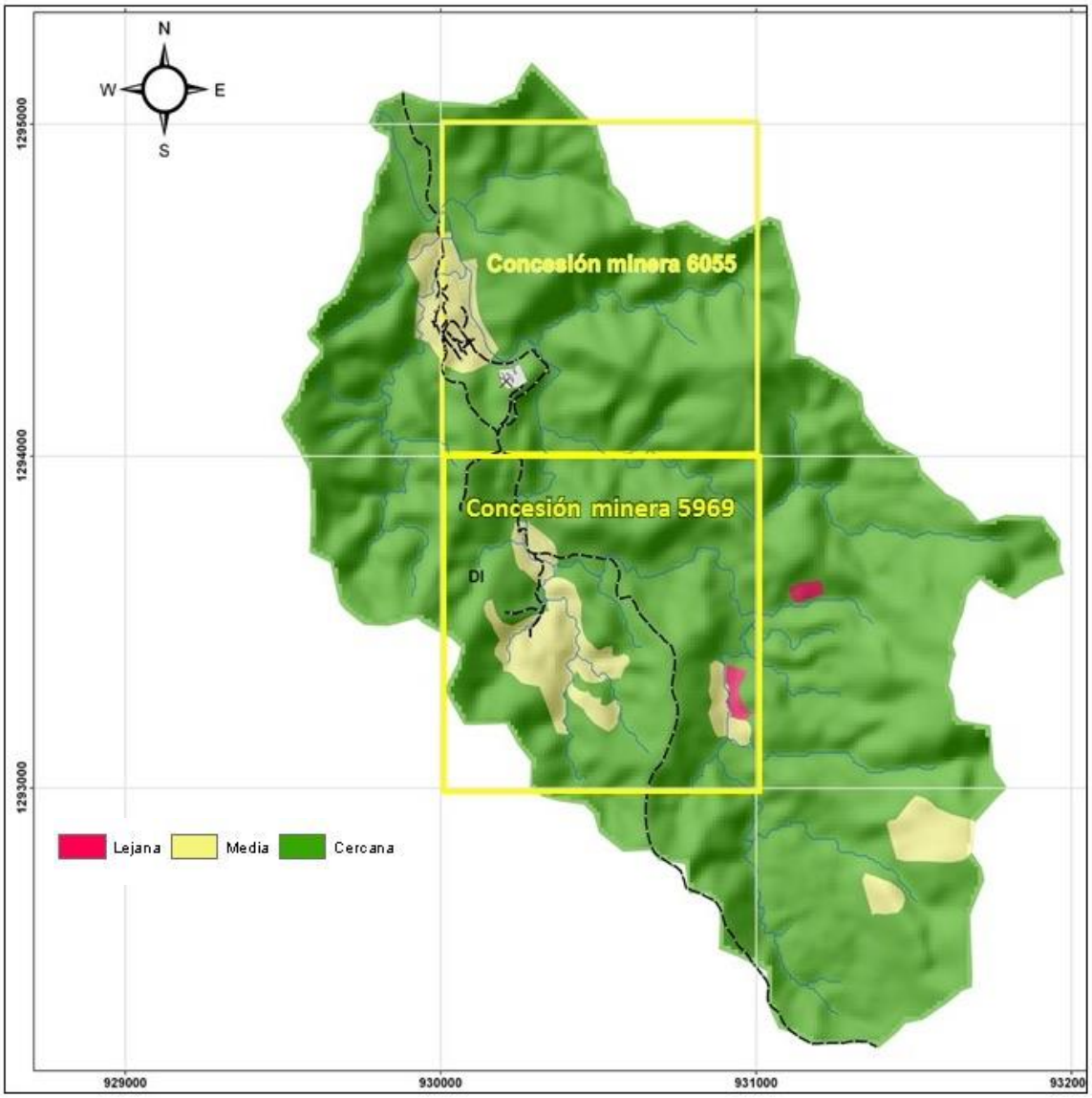

Illustration 4.1-262. Landscape visibility.
Source: INGEX, 2015.

65% of the area has close or short visibility (see Illustration 4.1-263), which is closely related to UPs with grassland and forest cover. The 33% is of medium visibility corresponding to the UPs with secondary vegetation coverings and discontinuous urban fabrics due to their size and location on the banks of the streams. While 2% corresponds to the coverages of abandoned crops that due to their small size and being immersed in the rest of the coverings are not notable.

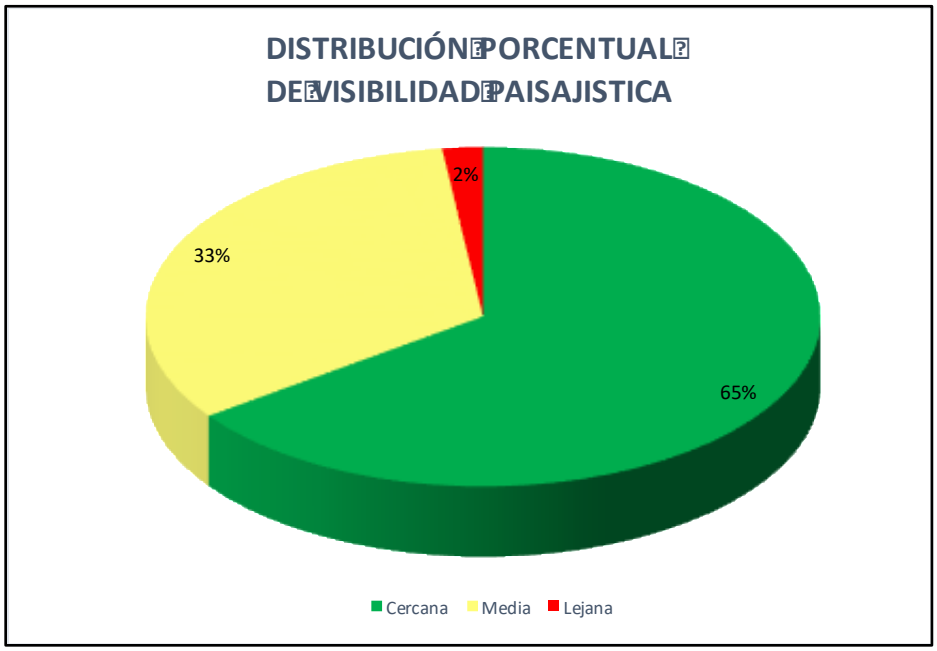

Illustration 4.1-263. Percentage distribution of landscape visibility.
Source: INGEX, 2015.Visual fragility - visual absorption capacity

The assessment of visual absorption capacity is shown in Table 4.1-150 and illustrations.

Table 4.1-150. Assessment of visual fragility by UP.

#	UP	PENDING	PLANT DIVERSITY	SOIL STABILITY AND ERODIBILITY	AESTHETIC POTENTIAL	HUMAN PERFORMANCE	COLOUR CONTRAST	CLASS
1	Bdbtf - Dc	2	3	3	2	1	2	MODERATE
2	Bdbtf - Dc	2	3	3	2	1	2	MODERATE
3	Bdbtf - Dl	2	3	3	2	1	2	MODERATE
4	Bdbtf - Dl	2	3	3	2	1	2	MODERATE
5	Bdbtf - Dl	2	3	3	2	1	2	MODERATE
6	Bdbtf - Dl - T	2	3	3	2	1	2	MODERATE
7	Bdbtf - Dle	2	3	3	2	1	2	MODERATE
8	Bdbtf - Dle	2	3	3	2	1	2	MODERATE
9	Bdbtf - Dle	2	3	3	2	1	2	MODERATE
10	Bdbtf - Dle	2	3	3	2	1	2	MODERATE
11	Bdbtf - Dle	2	3	3	2	1	2	MODERATE
12	Bdbtf - Dle	2	3	3	2	1	2	MODERATE
13	Bdbtf - Dle - T	2	3	3	2	1	2	MODERATE
14	Bdbtf - Dlm	2	3	3	2	1	2	MODERATE
15	Bdbtf - Dlm	2	3	3	2	1	2	MODERATE
16	Bdbtf - Dlm	2	3	3	2	1	2	MODERATE
17	Bdbtf - Dlm	2	3	3	2	1	2	MODERATE
18	Bdbtf - Ft	3	3	3	2	1	2	HIGH
19	Bdbtf - Ft	3	3	3	2	1	2	HIGH
20	Bdbtf - Ft	3	3	3	2	1	2	HIGH
21	Bdbtf - Ft	3	3	3	2	1	2	HIGH
22	Bdbtf - Sle	3	3	3	2	1	2	HIGH

#	UP	PENDING	PLANT DIVERSITY	SOIL STABILITY AND ERODIBILITY	AESTHETIC POTENTIAL	HUMAN PERFORMANCE	COLOUR CONTRAST	CLASS
23	Bdbtf - Sle	3	3	3	2	1	2	HIGH
24	Cc - Dc	2	1	3	2	3	1	MODERATE
25	Cc - Dlm	2	1	3	2	3	1	MODERATE
26	Pa - Dlm	2	1	3	2	3	1	MODERATE
27	Pa - Dlm	2	1	3	2	3	1	MODERATE
28	Pa - Dlm	2	1	3	2	3	1	MODERATE
29	Pa - Dlm	2	1	3	2	3	1	MODERATE
30	Pa - Ft	3	1	3	2	3	1	MODERATE
31	Pa - Ft	3	1	3	2	3	1	MODERATE
32	Pl - Ale	3	1	3	2	3	1	MODERATE
33	Pl - Dc	2	1	3	2	3	1	MODERATE
34	Pl - Dc	2	1	3	2	3	1	MODERATE
35	Pl - Dc	2	1	3	2	3	1	MODERATE
36	Pl - Dl	2	1	3	2	3	1	MODERATE
37	Pl - Dl	2	1	3	2	3	1	MODERATE
38	Pl - Dl	2	1	3	2	3	1	MODERATE
39	Pl - Dl	2	1	3	2	3	1	MODERATE
40	Pl - Dl	2	1	3	2	3	1	MODERATE
41	Pl - Dl	2	1	3	2	3	1	MODERATE
42	Pl - Dl - T	2	1	3	2	3	1	MODERATE
43	Pl - Dl - T	2	1	3	2	3	1	MODERATE
44	Pl - Dle	2	1	3	2	3	1	MODERATE
45	Pl - Dle	2	1	3	2	3	1	MODERATE
46	Pl - Dle	2	1	3	2	3	1	MODERATE
47	Pl - Dle	2	1	3	2	3	1	MODERATE
48	Pl - Dle	2	1	3	2	3	1	MODERATE
49	Pl - Dle - T	2	1	3	2	3	1	MODERATE
50	Pl - Dle - T	2	1	3	2	3	1	MODERATE
51	Pl - Dlm	2	1	3	2	3	1	MODERATE
52	Pl - Dlm	2	1	3	2	3	1	MODERATE
53	Pl - Dlm	2	1	3	2	3	1	MODERATE
54	Pl - Dlm	2	1	3	2	3	1	MODERATE
55	Pl - Dlm	2	1	3	2	3	1	MODERATE
56	Pl - Dlm	2	1	3	2	3	1	MODERATE
57	Pl - Dlm - T	2	1	3	2	3	1	MODERATE
58	Pl - Dlm - T	2	1	3	2	3	1	MODERATE
59	Pl - Ft	3	1	3	2	3	1	MODERATE
60	Pl - Ft	3	1	3	2	3	1	MODERATE
61	Pl - Ft	3	1	3	2	3	1	MODERATE
62	Pl - Ft	3	1	3	2	3	1	MODERATE
63	Pl - Ft	3	1	3	2	3	1	MODERATE
64	Pl - AII	3	1	3	2	3	1	MODERATE
65	Pl - Ft - T	3	1	3	2	3	1	MODERATE
66	Pl - Ft - T	3	1	3	2	3	1	MODERATE
67	Pl - Ft - T	3	1	3	2	3	1	MODERATE
68	Pl - Sle	3	1	3	2	3	1	MODERATE
69	Pl - Sle - T	3	1	3	2	3	1	MODERATE
70	Tud - Ale	3	1	3	2	3	1	MODERATE
71	Tud - Dl	2	1	3	2	3	1	MODERATE
72	Tud - Dl	2	1	3	2	3	1	MODERATE
73	Tud - Dl	2	1	3	2	3	1	MODERATE
74	Tud - Dl	2	1	3	2	3	1	MODERATE
75	Tud - Dl	2	1	3	2	3	1	MODERATE
76	Tud - Dl	2	1	3	2	3	1	MODERATE
77	Tud - Dle	2	1	3	2	3	1	MODERATE

#	UP	PENDING	PLANT DIVERSITY	SOIL STABILITY AND ERODIBILITY	AESTHETIC POTENTIAL	HUMAN PERFORMANCE	COLOUR CONTRAST	CLASS
78	Tud - Dle	2	1	3	2	3	1	MODERATE
79	Tud - Dle	2	1	3	2	3	1	MODERATE
80	Tud - Dlm	2	1	3	2	3	1	MODERATE
81	Tud - Dlm - T	2	1	3	2	3	1	MODERATE
82	Tud - Ft	3	1	3	2	3	1	MODERATE
83	Tud - Ft	3	1	3	2	3	1	MODERATE
84	Tud - Ft	3	1	3	2	3	1	MODERATE
85	Tud - Ft -T	3	1	3	2	3	1	MODERATE
86	V - Ale	3	1	3	2	3	1	MODERATE
87	V - All	3	1	3	2	3	1	MODERATE
88	V - Dl	2	1	3	2	3	1	MODERATE
89	V - Dle	2	1	3	2	3	1	MODERATE
90	V - Dlm	2	1	3	2	3	1	MODERATE
91	V - Ft	3	1	3	2	3	1	MODERATE
92	Vsb - Dc	2	3	3	2	2	2	MODERATE
93	Vsb - Dl	2	3	3	2	2	2	MODERATE
94	Vsb - Dl	2	3	3	2	2	2	MODERATE
95	Vsb - Dl	2	3	3	2	2	2	MODERATE
96	Vsb - Dle	2	3	3	2	2	2	MODERATE
97	Vsb - Dle	2	3	3	2	2	2	MODERATE
98	Vsb - Dlm	2	3	3	2	2	2	MODERATE
99	Vsb - Dlm	2	3	3	2	2	2	MODERATE
100	Vsb - Dlm	2	3	3	2	2	2	MODERATE
101	Vsb - Dlm	2	3	3	2	2	2	MODERATE
102	Vsb - Dlm	2	3	3	2	2	2	MODERATE
103	Vsb - Dlm	2	3	3	2	2	2	MODERATE

Source: INGEX, 2015.

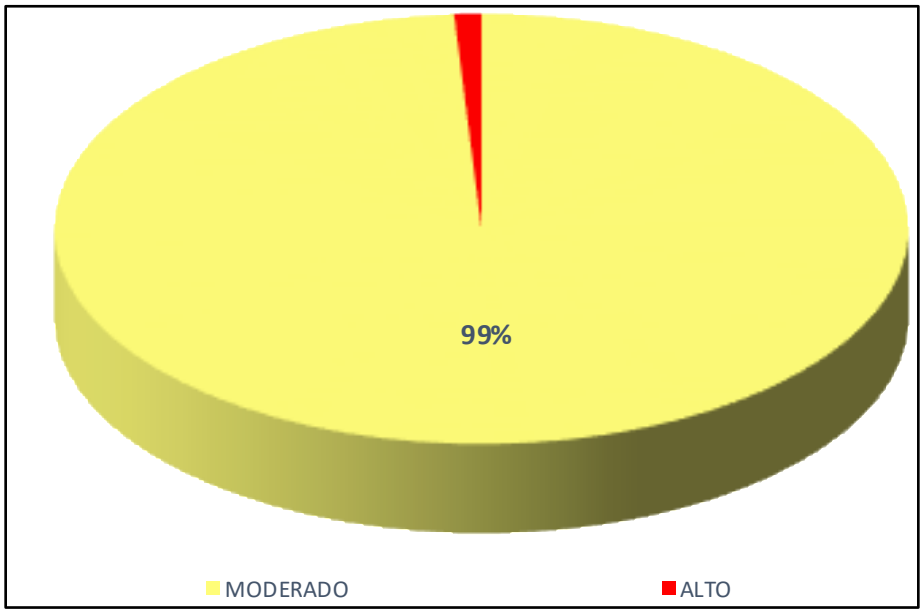

Illustration 4.1-264. Percentage distribution of visual fragility or absorption capacity.
Source: INGEX, 2015

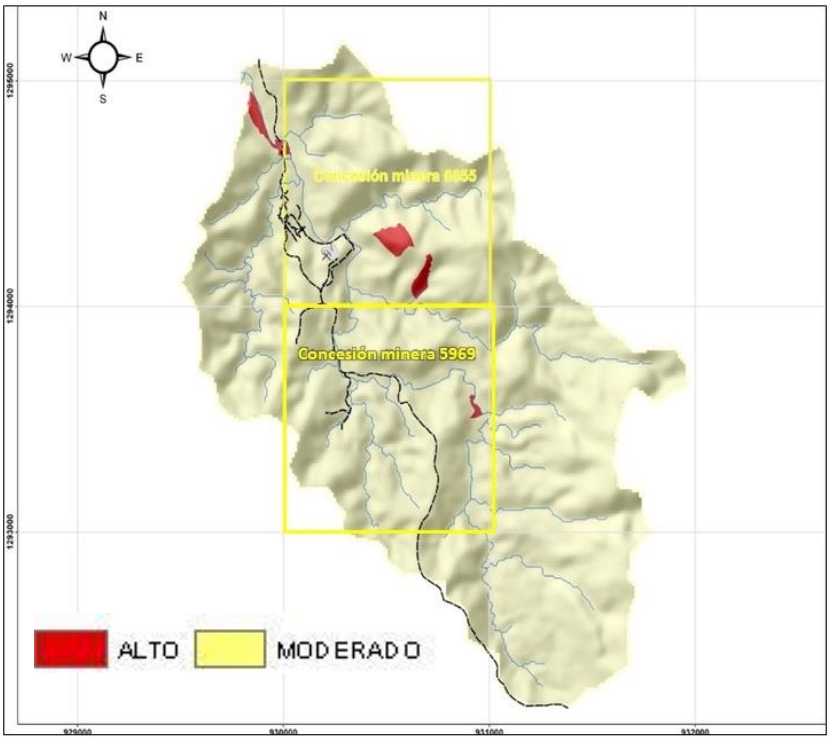

Illustration 4.1-265. Fragility or visual absorption capacity of the landscape.
Source: INGEX, 2015.

According to the above illustrations, 99% of the watershed has moderate visual fragility or absorption capacity. The 1% is high in the UPs with dense lowland forests located on alluvial terraces and on protruding structural ridges.

4.1.7.3.1 Visual quality of the landscape

The assessment of landscape visual quality is shown in Table 4.1-151 and illustrations.

Table 4.1-151. Visual quality assessment by UP.

#	UP	MORPHOLOGY	VEGETATION	WATER	COLOR	SCENIC BACKGROUND	RARITY	HUMAN PERFORMANCE	CLASS
1	Bdbtf - Dc	1	5	3	5	5	2	2	A
2	Bdbtf - Dc	1	5	3	5	5	2	2	A
3	Bdbtf - Dl	3	5	5	5	5	2	2	A
4	Bdbtf - Dl	3	5	5	5	5	2	2	A
5	Bdbtf - Dl	3	5	5	5	5	2	2	A
6	Bdbtf - Dl - T	3	5	5	5	5	2	2	A
7	Bdbtf - Dle	5	5	0	5	5	2	2	A
8	Bdbtf - Dle	5	5	0	5	5	2	2	A
9	Bdbtf - Dle	5	5	0	5	5	2	2	A
10	Bdbtf - Dle	5	5	0	5	5	2	2	A
11	Bdbtf - Dle	5	5	0	5	5	2	2	A
12	Bdbtf - Dle	5	5	0	5	5	2	2	A
13	Bdbtf - Dle - T	5	5	0	5	5	2	2	A
14	Bdbtf - Dlm	3	5	5	5	5	2	2	A
15	Bdbtf - Dlm	3	5	5	5	5	2	2	A
16	Bdbtf - Dlm	3	5	5	5	5	2	2	A
17	Bdbtf - Dlm	3	5	5	5	5	2	2	A
18	Bdbtf - Ft	1	5	5	5	5	2	2	A
19	Bdbtf - Ft	1	5	5	5	5	2	2	A
20	Bdbtf - Ft	1	5	5	5	5	2	2	A
21	Bdbtf - Ft	1	5	5	5	5	2	2	A
22	Bdbtf - Sle	3	5	5	5	5	2	2	A
23	Bdbtf - Sle	3	5	5	5	5	2	2	A
24	Cc - Dc	1	1	3	1	3	1	0	C
25	Cc - Dlm	3	1	5	1	3	1	0	B
26	Pa - Dlm	3	3	5	1	3	1	0	B
27	Pa - Dlm	3	3	5	1	3	1	0	B
28	Pa - Dlm	3	3	5	1	3	1	0	B
29	Pa - Dlm	3	3	5	1	3	1	0	B
30	Pa - Ft	1	3	5	1	3	1	0	B
31	Pa - Ft	1	3	5	1	3	1	0	B
32	Pl - Ale	1	1	0	1	3	1	0	C
33	Pl - Dc	1	1	3	1	3	1	0	C
34	Pl - Dc	1	1	3	1	3	1	0	C
35	Pl - Dc	1	1	3	1	3	1	0	C
36	Pl - Dl	3	1	5	1	3	1	0	B
37	Pl - Dl	3	1	5	1	3	1	0	B
38	Pl - Dl	3	1	5	1	3	1	0	B
39	Pl - Dl	3	1	5	1	3	1	0	B
40	Pl - Dl	3	1	5	1	3	1	0	B
41	Pl - Dl	3	1	5	1	3	1	0	B
42	Pl - Dl - T	3	1	5	1	3	1	0	B
43	Pl - Dl - T	3	1	5	1	3	1	0	B
44	Pl - Dle	5	1	0	1	3	1	0	C

#	UP	MORPHOLOGY	VEGETATION	WATER	COLOR	SCENIC BACKGROUND	RARITY	HUMAN PERFORMANCE	CLASS
45	Pl - Dle	5	1	0	1	3	1	0	C
46	Pl - Dle	5	1	0	1	3	1	0	C
47	Pl - Dle	5	1	0	1	3	1	0	C
48	Pl - Dle	5	1	0	1	3	1	0	C
49	Pl - Dle - T	5	1	0	1	3	1	0	C
50	Pl - Dle - T	5	1	0	1	3	1	0	C
51	Pl - Dlm	3	1	5	1	3	1	0	B
52	Pl - Dlm	3	1	5	1	3	1	0	B
53	Pl - Dlm	3	1	5	1	3	1	0	B
54	Pl - Dlm	3	1	5	1	3	1	0	B
55	Pl - Dlm	3	1	5	1	3	1	0	B
56	Pl - Dlm	3	1	5	1	3	1	0	B
57	Pl - Dlm - T	3	1	5	1	3	1	0	B
58	Pl - Dlm - T	3	1	5	1	3	1	0	B
59	Pl - Ft	1	1	5	1	3	1	0	B
60	Pl - Ft	1	1	5	1	3	1	0	B
61	Pl - Ft	1	1	5	1	3	1	0	B
62	Pl - Ft	1	1	5	1	3	1	0	B
63	Pl - Ft	1	1	5	1	3	1	0	B
64	Pl - All	1	1	5	1	3	1	0	B
65	Pl - Ft - T	1	1	5	1	3	1	0	B
66	Pl - Ft - T	1	1	5	1	3	1	0	B
67	Pl - Ft - T	1	1	5	1	3	1	0	B
68	Pl - Sle	3	1	5	1	3	1	0	B
69	Pl - Sle - T	3	1	5	1	3	1	0	B
70	Tud - Ale	1	1	3	1	3	1	0	C
71	Tud - Dl	3	1	0	1	3	1	0	C
72	Tud - Dl	3	1	0	1	3	1	0	C
73	Tud - Dl	3	1	0	1	3	1	0	C
74	Tud - Dl	3	1	0	1	3	1	0	C
75	Tud - Dl	3	1	0	1	3	1	0	C
76	Tud - Dl	3	1	0	1	3	1	0	C
77	Tud - Dle	5	1	0	1	3	1	0	C
78	Tud - Dle	5	1	0	1	3	1	0	C
79	Tud - Dle	5	1	0	1	3	1	0	C
80	Tud - Dlm	3	1	5	1	3	1	0	B
81	Tud - Dlm - T	3	1	5	1	3	1	0	B
82	Tud - Ft	1	1	5	1	3	1	0	B
83	Tud - Ft	1	1	5	1	3	1	0	B
84	Tud - Ft	1	1	5	1	3	1	0	B
85	Tud - Ft -T	1	1	5	1	3	1	0	B
86	V - Ale	1	1	0	1	3	1	0	C
87	V - All	1	1	5	1	3	1	0	B
88	V - Dl	3	1	5	1	3	1	0	B
89	V - Dle	5	1	0	1	3	1	0	C
90	V - Dlm	3	1	5	1	3	1	0	B
91	V - Ft	1	1	5	1	3	1	0	B
92	Vsb - Dc	1	3	5	3	5	1	0	B
93	Vsb - Dl	3	3	5	3	5	1	0	A
94	Vsb - Dl	3	3	5	3	5	1	0	A
95	Vsb - Dl	3	3	5	3	5	1	0	A
96	Vsb - Dle	5	3	0	3	5	1	0	B
97	Vsb - Dle	5	3	0	3	5	1	0	B
98	Vsb - Dlm	3	3	5	3	5	1	0	A
99	Vsb - Dlm	3	3	5	3	5	1	0	A

#	UP	MORPHOLOGY	VEGETATION	WATER	COLOR	SCENIC BACKGROUND	RARITY	HUMAN PERFORMANCE	CLASS
100	Vsb - Dlm	3	3	5	3	5	1	0	A
101	Vsb - Dlm	3	3	5	3	5	1	0	A
102	Vsb - Dlm	3	3	5	3	5	1	0	A
103	Vsb - Dlm	3	3	5	3	5	1	0	A

Source: INGEX, 2015.

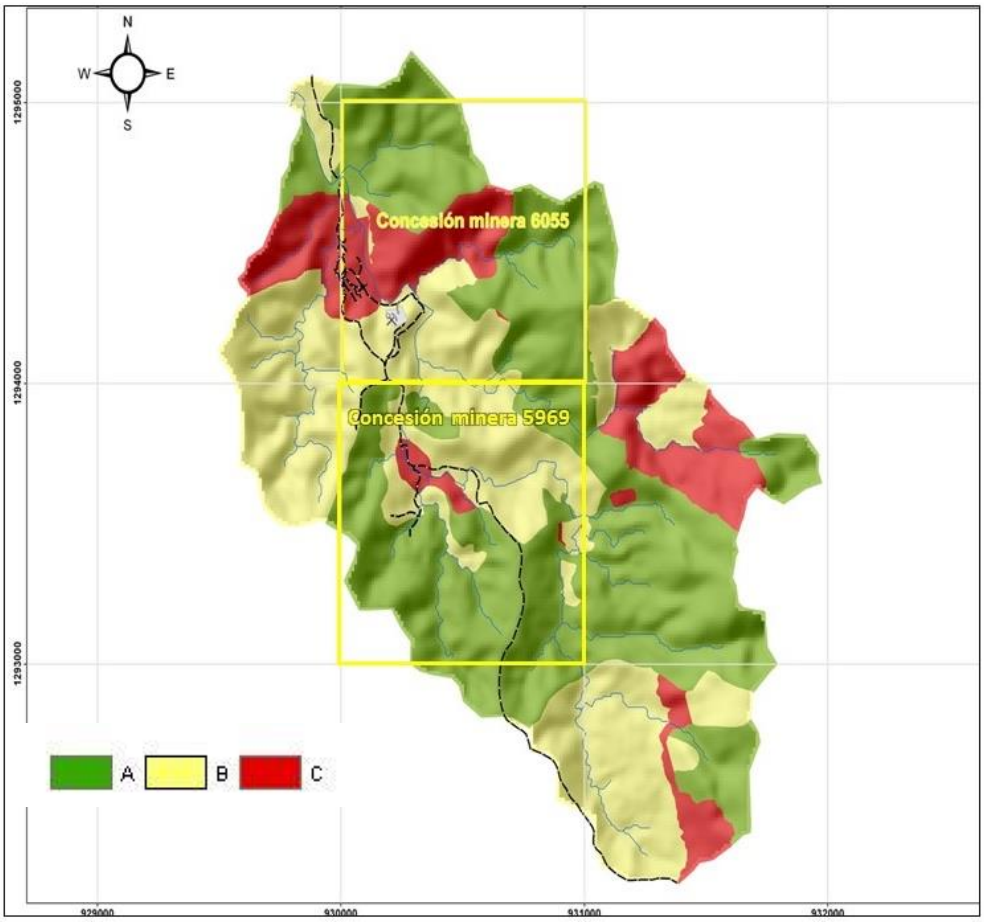

Illustration 4.1-266. Landscape visual quality.
Source: INGEX, 2015.

The areas in which the highest quality (Class A) is appreciated (48%) are those natural landscapes, which have a richness in their composition and density of elements that make this a propitious habitat for wildlife. Whereas in the basin there is a medium quality (Class B) with 37% and a low quality (Class C) with 15% in the UPs with anthropic intervention. Therefore, in the basin, the landscape quality is predominant between medium and low, due to the anthropogenic interventions.

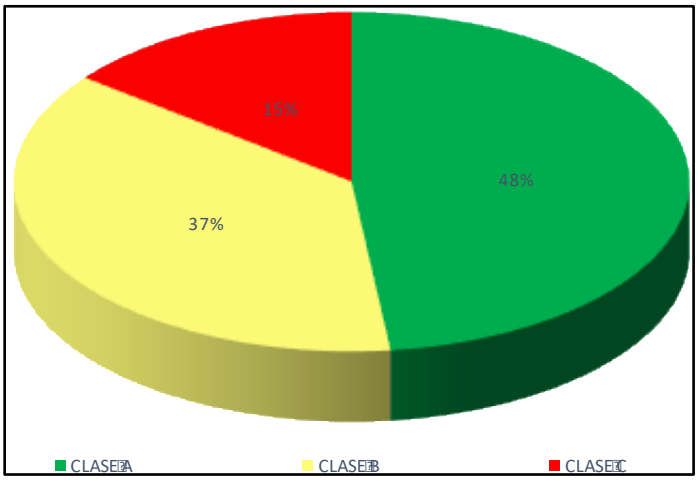

Illustration 4.1-267. Percentage distribution of landscape visual quality.
Source: INGEX, 2015.

4.1.7.3.2 Overall aesthetic potential of the landscape

The assessment of biophysical and architectural components is presented in Table 4.1-152.

Table 4.1-152. Calculation of the aesthetic potential of the landscape.

COMPONENT	WEIGHT	VALOR	POTENTIAL
BIOPHYSICAL COMPOSITION COMPONENTS			
Shape of the terrain (relief) (Morphology)	3	3	9
Soil and rock	1	0	0
Fauna	5	5	25
Water	5	5	25
Vegetation	5	5	25
Anthropic performance (Human performance)	0	0	0
Weather	1	1	1
Total biophysical composition			**85**
ARCHITECTURAL COMPOSITION COMPONENTS			
Shape	3	3	9
Axes-línea	3	3	9
Texture	3	2	6
Scale-space	1	0	0
Color	3	3	9
Fund escénico	3	3	9
Total architectural composition			**42**
Aesthetic potential			**63,5**

Because the average is 63.5, it is in the category of overall aesthetic potential of the average landscape. This coincides with the fact that visibility and fragility are also moderate, and quality is predominantly low to medium.